CT CORONARY ANGIOGRAPHY: VALIDATION AND CLINICAL IMPLEMENTATION

CT coronair angiografie: validatie en klinische implementatie

Carlos A.G. Van Mieghem

Financial support for the publication of this thesis was generously provided by:

Abbott Vascular
Boston Scientific
Bristol-Myers Squibb
Medtronic
Merck Sharpe & Dohme BV
Novartis Pharma B.V.
Pfizer bv
Radi Medical Systems BV
Servier Nederland B.V.
Siemens Nederland N.V.
Volcano

Design cover : A.W. Everaers and C.A.G. Van Mieghem
Layout : A.W. Everaers
Printed by : Optima
ISBN : 978-90-8559-454-3

CT CORONARY ANGIOGRAPHY: VALIDATION AND CLINICAL IMPLEMENTATION

CT coronair angiografie:
validatie en klinische implementatie

PROEFSCHRIFT

ter verkrijging van de graad van doctor aan de
Erasmus Universiteit Rotterdam
op gezag van de
rector magnificus

Prof.dr. S.W.J. Lamberts

en volgens besluit van het College voor Promoties.

De openbare verdediging zal plaatsvinden op
21 januari 2009 om 15.45 uur

door

CARLOS AMEDEE GEORGETTE VAN MIEGHEM
geboren te Wynberg, Zuid-Afrika

PROMOTIECOMMISSIE

Promotores:	Prof.dr. P.J. de Feyter
	Prof.dr. P.W.J.C. Serruys
Co-promoter:	Dr. N.R. Mollet
Overige leden:	Prof.dr. G.P. Krestin
	Prof.dr. W.J. Niessen
	Prof.dr. A.F.W. van der Steen

Financial support by the Netherlands Heart Foundation for the publication of this thesis is greatfully acknowledged.

Financial support by the Department of Radiology of Erasmus MC University Medical Centre Rotterdam for the publication of this thesis is greatfully acknowledged.

Dankzij Tine

TABLE OF CONTENTS

PART I

PREFACE

1

Introduction and Outline of the Thesis

INTRODUCTION AND OUTLINE OF THE THESIS

Coronary heart disease is the most frequent cause of death in the Western society.[1] Coronary arteriography, a technique to visualize morphologic characteristics of the coronary arteries, has provided an objective basic standard of diagnosis and fundamentally changed our approach to the patient with suspected coronary artery disease.

The advent of conventional coronary angiography towards the end of the 1950s allowed in-vivo assessment of coronary stenoses due to atherosclerosis.[2] The introduction of this diagnostic technique allowed the development of rational treatment modalities such as coronary artery bypass surgery (CABG) and, subsequently, percutaneous coronary intervention, roughly one and two decades later respectively.[3-5] The timeline and introduction of conventional coronary angiography in clinical practice including some landmark clinical studies is shown in Figure 1.[2,3,5-9]

Until the end of the 1980s the general belief prevailed that acute myocardial infarction or unstable angina pectoris were the consequence of high-grade coronary stenoses, lesions that could be depicted by conventional coronary angiography. However, several data occasioned a reassessment of this central dogma of clinical cardiology. Angiographic studies obtained before acute myocardial infarction and those obtained during the infarction revealed that the atherosclerotic lesions that gave rise to occlusive thrombosis did not cause high-grade stenoses in many cases.[10-12] A number of "regression trials" in the early 1990s showed that lipid lowering therapy had a minimal effect on the degree of high-grade coronary stenoses. Yet, these studies revealed a consistent decrease in acute coronary events.[13] Autopsy studies among patients with sudden cardiac death have shown that the vast majority of these acute clinical events occur as a result of plaque rupture at sites with noncritical luminal narrowing.[14-16] Finally, in patients with stable angina pectoris percutaneous revascularization of high-grade coronary stenoses in addition to optimal medical therapy does not reduce the rates of death and myocardial infarction as compared to optimal medical therapy alone.[17]

Non-invasive imaging of the coronary arteries has been an important challenge over the last 15 years and started off in the early 1990s using magnetic resonance imaging and electron beam computed tomography (EBCT).[18-20] The introduction of multislice CT technology in 1998 set the stage for a rapid technological development that resulted in a significant improvement in image quality, thereby favoring computed tomography coronary angiography (CTCA) as the preferred technique for noninvasive coronary artery imaging.[21] CTCA avoids catheter-related complications, is less costly and importantly helps us to refocus our eyes on the central manifestation of coronary artery disease, atherosclerotic involvement of the coronary artery wall.[22] The subsequent improvements in multi-slice CT technology and the first

CTCA studies reporting on the natural history of coronary artery disease are summarized on the same timeline in Figure 1.[23]

The aims of this thesis are multiple: first, to validate CTCA as a diagnostic technique to identify and characterize coronary atherosclerotic plaque using intravascular ultrasound and optical coherence tomography as reference intravascular imaging tests; second, to explore the spectrum of patients with possible native vessel coronary artery disease in whom CTCA might be clinically useful; third, to assess the clinical value of CTCA in patients who underwent previous coronary artery stenting.

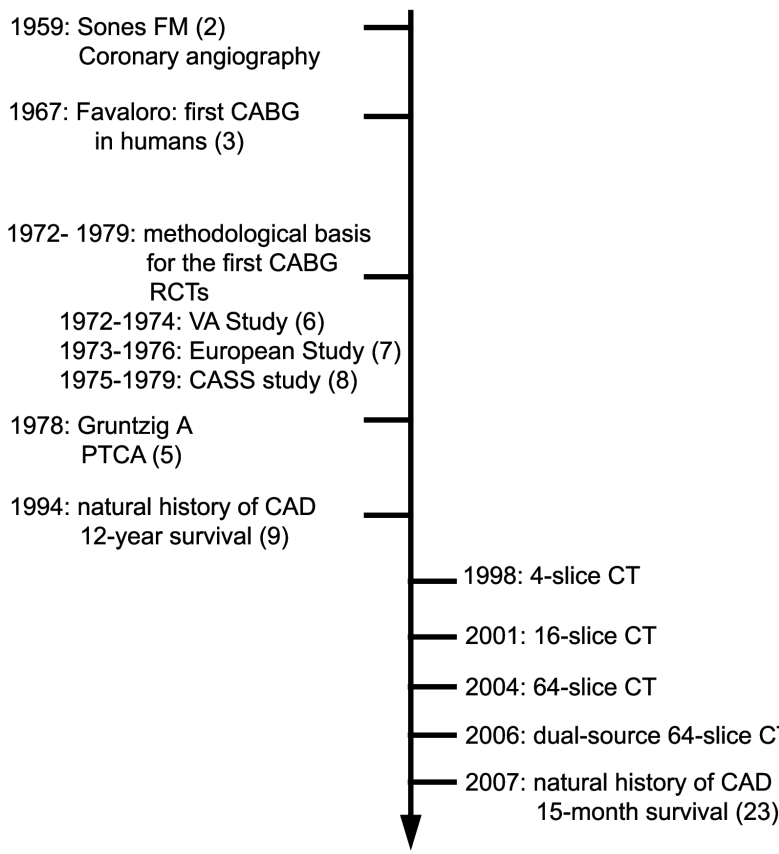

Figure 1. Historical overview: the development of coronary angiography. Invasive and non-invasive assessment. The numbers in between brackets are referring to the references in the text. PTCA denotes percutaneous transluminal coronary angioplasty; RCT denotes randomized clinical trial.

Part 1 addresses the role of CTCA in the diagnostic work-up of patients with suspected coronary artery disease, illustrates the potential of CTCA to overcome the inherent limitations of

conventional coronary angiography and highlights how the information provided by CTCA can aid in planning or performing coronary and non-coronary intervention (Chapter 2). Part 2 addresses the potential of CTCA to visualize the early stages of coronary artery disease where " luminographic" involvement is still absent or minimal. The design and the results of the Integrated Biomarker and Imaging Study (IBIS), a multimodality imaging and biomarker study that aimed to characterize subclinical coronary atherosclerotic disease, are discussed (Chapters 3-5). Part 3 describes the diagnostic performance of 64-slice CTCA to detect obstructive coronary artery disease in a wide clinical spectrum of patients, ranging from those presenting with stable angina pectoris to patients admitted with acute coronary syndrome without ST-segment elevation (Chapters 6 and 7, interlude 2). Of particular value is the diagnostic performance of 64-slice CTCA in patients with a low-to-intermediate pretest likelihood of significant CAD (Chapters 8 and 9). There are two fundamentally different approaches to assess coronary artery disease, anatomical and functional. We address this important topic by combining anatomical information, using CTCA, with functional data (Chapters 10 and 11, interlude 3). Angiographic assessment of complex coronary pathology such as bifurcation lesions and chronic total occlusions is sometimes suboptimal and might be a reason to refer a patient for an alternative imaging technique. We evaluated the value of CTCA in these lesion subsets (Chapters 12 and 13, interlude 4). In addition, we provide our initial experience with the integration of CT data in the cathlab for the purpose of percutaneous coronary interventions using magnetic navigation (Chapter 14). Part 4 deals with in-vivo CT coronary stent imaging. Both the technical knowledge required to obtain good visualisation of the lumen inside the stent as well as the possible clinical application are discussed. Part 5 summarises the current findings and touches upon the future steps that are being taken to accommodate CTCA as a diagnostic tool in clinical cardiology.

REFERENCES

1 Rosamond W, Flegal K, Friday G, et al. Heart disease and stroke statistics--2007 update: a report from the American Heart Association Statistics Committee and Stroke Statistics Subcommittee. Circulation 2007; 115:e69-171

2 Sones FM, Shirey EK, Proudfit WL, et al. Cine coronary arteriography. Circulation 1959; 20:773-775

3 Favaloro RG, Effler DB, Groves LK, et al. Myocardial revascularization by internal mammary artery implant procedures. Clinical experience. J Thorac Cardiovasc Surg 1967; 54:359-370

4 Spencer FC, Green GE, Tice DA, et al. Surgical therapy for coronary artery disease. Curr Probl Surg 1970:3-49

5 Gruntzig A. Transluminal dilatation of coronary-artery stenosis. Lancet 1978; 1:263

6 Eleven-year survival in the Veterans Administration randomized trial of coronary bypass surgery for stable angina. The Veterans Administration Coronary Artery Bypass Surgery Cooperative Study Group. N Engl J Med 1984; 311:1333-1339

7 Coronary-artery bypass surgery in stable angina pectoris: Survival at two years. European Coronary Surgery Study Group. Lancet 1979; 1:889-893

8 Coronary artery surgery study (CASS): a randomized trial of coronary artery bypass surgery. Survival data. Circulation 1983; 68:939-950

9 Emond M, Mock MB, Davis KB, et al. Long-term survival of medically treated patients in the Coronary Artery Surgery Study (CASS) Registry. Circulation 1994; 90:2645-2657

10 Hackett D, Davies G, Maseri A. Pre-existing coronary stenoses in patients with first myocardial infarction are not necessarily severe. Eur Heart J 1988; 9:1317-1323

11 Ambrose JA, Tannenbaum MA, Alexopoulos D, et al. Angiographic progression of coronary artery disease and the development of myocardial infarction. J Am Coll Cardiol 1988; 12:56-62

12 Giroud D, Li JM, Urban P, et al. Relation of the site of acute myocardial infarction to the most severe coronary arterial stenosis at prior angiography. Am J Cardiol 1992; 69:729-732

13 Brown BG, Zhao XQ, Sacco DE, et al. Lipid lowering and plaque regression. New insights into prevention of plaque disruption and clinical events in coronary disease. Circulation 1993; 87:1781-1791

14 Davies MJ, Thomas AC. Plaque fissuring--the cause of acute myocardial infarction, sudden ischaemic death, and crescendo angina. Br Heart J 1985; 53:363-373

15 Davies MJ. A macro and micro view of coronary vascular insult in ischemic heart disease. Circulation 1990; 82:II38-46

16 Davies MJ. Anatomic features in victims of sudden coronary death. Coronary artery pathology. Circulation 1992; 85:I19-24

17 Boden WE, O'Rourke RA, Teo KK, et al. Optimal medical therapy with or without PCI for stable coronary disease. N Engl J Med 2007; 356:1503-1516
18 Manning WJ, Li W, Edelman RR. A preliminary report comparing magnetic resonance coronary angiography with conventional angiography. N Engl J Med 1993; 328:828-832
19 Moshage WE, Achenbach S, Seese B, et al. Coronary artery stenoses: three-dimensional imaging with electrocardiographically triggered, contrast agent-enhanced, electron-beam CT. Radiology 1995; 196:707-714
20 Rensing BJ, Bongaerts A, van Geuns RJ, et al. Intravenous coronary angiography by electron beam computed tomography: a clinical evaluation. Circulation 1998; 98:2509-2512
21 Bluemke DA, Achenbach S, Budoff M, et al. Noninvasive coronary artery imaging: magnetic resonance angiography and multidetector computed tomography angiography: a scientific statement from the american heart association committee on cardiovascular imaging and intervention of the council on cardiovascular radiology and intervention, and the councils on clinical cardiology and cardiovascular disease in the young. Circulation 2008; 118:586-606
22 Topol EJ, Nissen SE. Our preoccupation with coronary luminology. The dissociation between clinical and angiographic findings in ischemic heart disease. Circulation 1995; 92:2333-2342
23 Min JK, Shaw LJ, Devereux RB, et al. Prognostic value of multidetector coronary computed tomographic angiography for prediction of all-cause mortality. J Am Coll Cardiol 2007; 50:1161-1170

2

Critical Appraisal of the Role of Noninvasive Cardiac Computed Tomography from an Interventional Cardiology Perspective

Carlos A.G. Van Mieghem, MD[1,2]; Steve Ramcharitar, DPhil, BMBCH[1]; Patrick W. Serruys, MD, PhD[1]; Pim J. de Feyter, MD, PhD[1,2]

From the departments of Cardiology[1] and Radiology [2], Erasmus MC, Rotterdam, The Netherlands

Submitted

ABSTRACT

Computed tomography coronary angiography is considered an appropriate diagnostic test for evaluation of symptomatic patients with a low-to-intermediate pre-test likelihood of coronary artery disease. A negative CT scan reliably rules out the presence of coronary artery disease, has a favourable prognostic value and might therefore significantly impact on the need for invasive coronary angiography. Those patients with significant atherosclerotic disease on CT benefit from further functional assessment to decide upon the appropriate therapeutic approach. Beyond this gatekeeper function, computed tomography coronary angiography overcomes the inherent 2-dimensional limitations of the catheter-based approach and might be valuable as a complementary technique in patients with complex coronary artery disease.

INTRODUCTION

Although in-vivo assessment of the coronary arteries only became feasible towards the end of the 1950s, its introduction revolutionized the practice of cardiology.[1] Less than half a century later a noninvasive alternative, computed tomography coronary angiography (CTCA), became available.[2,3] The high diagnostic accuracy of CTCA both for the detection and the exclusion of hemodynamically significant (> 50% stenosis) coronary artery stenosis is now well established. Ongoing advances in scan technology have resulted in the current generation of 64-slice CT scanners that allow accurate assessment of clinically relevant segments of the coronary tree (vessels with a diameter of 1.5 mm or more) within 10 seconds, a breath hold that is comfortable for the vast majority of patients. The technique still has limitations, notably the challenges posed by extensive calcification or irregular cardiac rhythms, and does not yet provide the same spatial and temporal resolution as its invasive counterpart. However, its 3-dimensional (3-D) nature offers insights into both lesion and vessel characteristics that cannot be obtained with conventional 2-D angiography, and that may prove valuable in planning and guiding interventional procedures.

In current practice, invasive coronary angiography (ICA) is the initial imaging procedure performed to confirm or exclude obstructive coronary disease as a cause of chest pain and to triage patients towards percutaneous or surgical revascularization. These procedures are often performed by cardiologists who are not trained in percutaneous coronary intervention (PCI). Not infrequently, when these studies are reviewed by an interventional cardiologist and a cardiac surgeon with a view to planning the best revascularization strategy, they are deemed

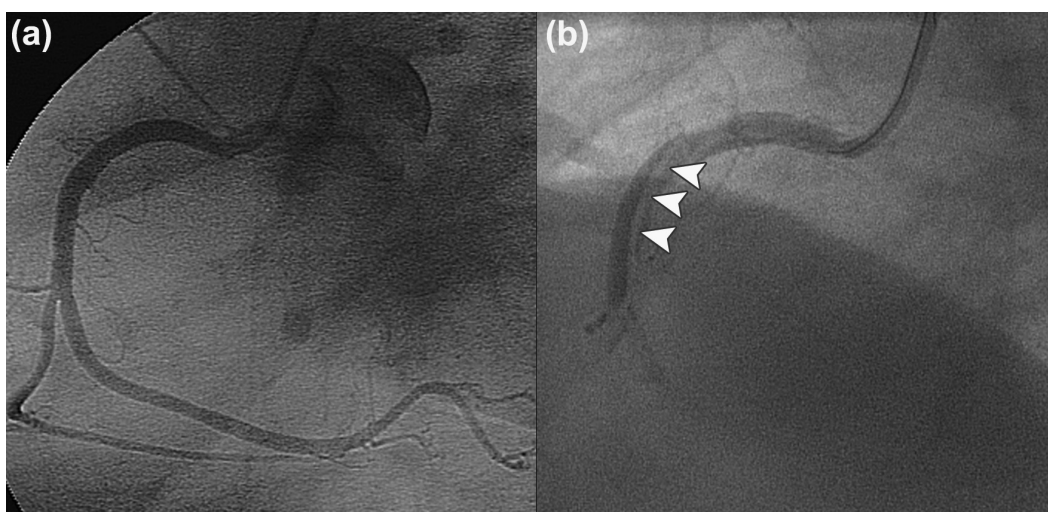

Figure 1. Invasive coronary angiogram of the right coronary artery. (a) Normal appearance of the vessel at initial catheterization. (b) A repeat coronary angiogram was scheduled 2 weeks later in order to perform an intravascular ultrasound. This resulted in a proximal dissection of the vessel (arrowheads).

to be suboptimal. Additional projections to assess overlapped lesions, to determine the exact anatomy of bifurcating or ostial lesions, or to clarify the hemodynamic significance of lesions are deemed to be necessary to determine if revascularization is indicated or to determine the best revascularization strategy. CTCA has the potential to replace ICA in a significant proportion of patients especially those with a low or intermediate probability of coronary disease at initial presentation.[4,5] Higher risk patients could be referred directly to centers where ad hoc PCI could be performed where indicated. This approach should theoretically reduce the inherent risks of peripheral and coronary arterial injury that can occur during ICA. (Figure 1)

This article aims to critically evaluate the potential of CTCA to alter the management of patients with suspected coronary disease, to illustrate the potential of CTCA to overcome the inherent limitations of ICA, and to highlight how the information provided by CTCA can aid in planning or performing coronary and non-coronary interventions.

CT CORONARY ANGIOGRAPHY: CURRENT STATUS

As a new diagnostic imaging tool CTCA has been systematically validated against ICA, the gold standard technique, to assess for the presence or absence of obstructive CAD. By default,

Table 1. Patient-based diagnostic performance of 64-slice CT coronary angiography to detect significant coronary artery disease (≥ 50% lumen diameter stenosis). PPV, positive predictive value; NPV, negative predictive value.

Reference	No. of patients	Excluded segments, % (n)	Sensitivity, %	Specificity, %	PPV, %	NPV, %
Ehara68	67	8 (82/966)	98	86	98	86
Ghostine69	66	0 (0/990)	97	95	93	97
Leber70	45	0 (0/798)	88	85	88	85
Leschka71	67	0 (0/1005)	100	100	100	100
Meijboom72	70	0 (0/1003)	100	92	82	100
Meijboom73	104	0 (0/1525)	100	75	96	100
Mollet74	51	0 (0/725)	100	92	97	100
Muhlenbruch75	51	5 (39/765)	98	50	94	75
Nikolaou76	68	10 (97/1020)	97	79	86	96
Oncel77	80	0 (0/1200)	100	100	100	100
Pugliese78	35	0 (0/494)	100	90	96	100
Raff79	70	12 (130/1065)	95	90	93	93
Ropers80	81	4 (45/1128)	96	91	83	98
Schuijf81	60	1 (12/854)	94	97	97	93
Mean		3 (405/13538)				
Weighted mean			98	87	93	95

the patients that have been included in these validation studies almost invariably had a high pretest-probability of significant CAD as all of them had an indication for ICA based on clinical grounds. Although coronary artery imaging is feasible with 4-slice and 16-slice technology a substantial proportion of the coronary tree cannot be fully evaluated due to insufficient spatial and temporal resolution. However, current 64-slice and dual-source CT technology has substantial improvement in image quality so as to reduce the percentage of otherwise non-diagnostic coronary segments to less than 5%. The diagnostic performance of 64-slice CT scanners in patients with native vessel disease is presented in Table 1. The diagnostic performance obtained with dual-source CT is summarized in Table 2.

Table 2. Patient-based diagnostic performance of dual-source CT coronary angiography to detect significant coronary artery disease (≥ 50% lumen diameter stenosis). PPV, positive predictive value; NPV, negative predictive value.

Reference	No. of patients	Non-diagnostic segments, % (n)	Sensitivity, %	Specificity, %	PPV, %	NPV, %
Scheffel82	30	1.4 (6/420)	96	97	86	99
Weustink83	100	6 (89/1489)	99	87	96	95
Leber84	88	0 (0/1216)	95	90	74	99
Ropers85	100	3.7 (51/1394)	98	81	79	98
Alkadhi86	150	1.9 (39/2059)	97	87	83	97
Scheffel87	120	1.7 (30/1803)	100	93	94	100
Mean		2.6				
Weighted mean			98	88	86	98

DIAGNOSTIC WORK-UP OF PATIENTS WITH SUSPECTED CORONARY ARTERY DISEASE: CURRENT STATUS AND FUTURE PERSPECTIVE

Due to its invasive nature, ICA should ideally be reserved for patients in whom the likelihood of proceeding to coronary revascularization is high. Current guidelines recommend the use of noninvasive stress testing as a first-line test before proceeding to a catheter-based assessment of the coronary anatomy.[6,7] However, in daily practice, the approach to patients with suspected or proven stable coronary artery disease is different. The majority of patients undergoing coronary revascularization do not have objectively demonstrated ischemia.[8] Recent surveys demonstrate that up to 20% of all coronary angiograms are reported as being normal.[9] Furthermore, only around a third of patients undergoing ICA are referred for revascularization.[10] Mason Sones suggested, at the dawn of coronary angiography, that its major role would be to exclude significant coronary disease as a cause of chest pain and it is therefore not surprising that today ICA is still widely used for this purpose.[11] The frequent

recourse to ICA in patients with a low-to-intermediate pretest probability of disease reflects the diagnostic uncertainty related to inconclusive noninvasive stress testing in patients with unexplained chest pain.[12] A normal nuclear scan or dobutamine stress echocardiogram has a well documented favorable prognostic value.[13-16] However, it does not definitively exclude the presence of significant coronary artery disease as a cause of unexplained chest pain. Standard single photon emission computed tomography (SPECT) and positron emission tomography imaging rely on normalization of acquired data to the region of the myocardium with maximal perfusion, although this area of perfusion may not, in fact, be normal and may provide false negative results particularly in patients with significant three-vessel or left main disease.[17,18] Stress echocardiography has limited sensitivity for the detection of single-vessel disease. This makes it a useful tool for clarifying prognosis but less useful for excluding coronary disease as a cause of symptoms.[19]

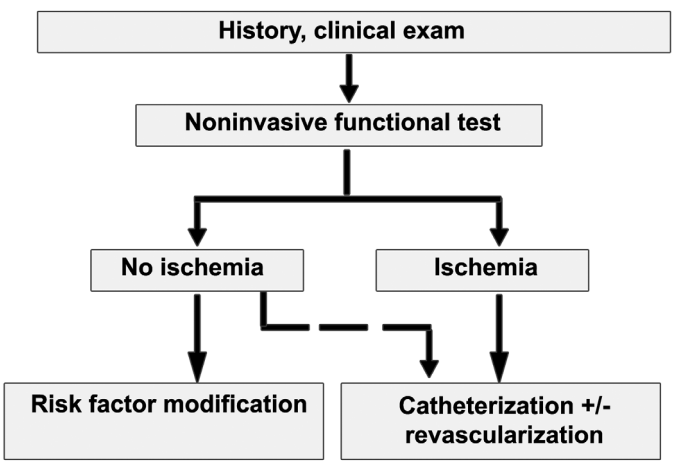

Figure 2. Flow chart showing current diagnostic work-up of patients with suspected stable coronary artery disease. Multiple non-invasive functional tests are available, such as exercise stress testing, nuclear scintigraphy, stress echocardiography and magnetic resonance imaging. When exercise is well tolerated and the rest ECG is normal, exercise electrocardiography is the first choice test. Low tolerability for physical stress and/or electrocardiographic abnormalities at rest are good reasons to choose an imaging technique combined with pharmacological stress instead. Documentation of myocardial ischemia is the preferred situation to proceed with invasive coronary angiography (ICA). However, an inconclusive stress test or findings that are discordant with clinical presentation are often sufficient reason to perform an ICA to reduce level of uncertainty.

Current 64-slice CT scanners have been shown, in numerous studies, to have high sensitivity and specificity for the exclusion of significant coronary artery disease. In this regard it is important to note that the prognosis of a patient with a normal scan result appears to be very favorable.[20-22] As a result, a CT-based approach seems most useful in patients with a low to intermediate pre-test likelihood of CAD, in whom it is deemed necessary to evaluate the coronary anatomy.[23] Most clinicians would advocate ICA, in an interventional center, as the preferred strategy in patients with a high pre-test likelihood of CAD, because of the additional

option, in patients with suitable anatomy and who have been appropriately pretreated, to perform an ad hoc therapeutic intervention.

Figure 2 summarizes the current work-up of patients presenting with chest discomfort in whom stable angina is suspected. A careful history and clinical examination remains the cornerstone of the diagnostic assessment.[7] Stress testing whether or not combined with an imaging modality, using echocardiography, SPECT, or magnetic resonance imaging, is usually recommended as the next step in order to document the presence and severity of myocardial ischemia. The

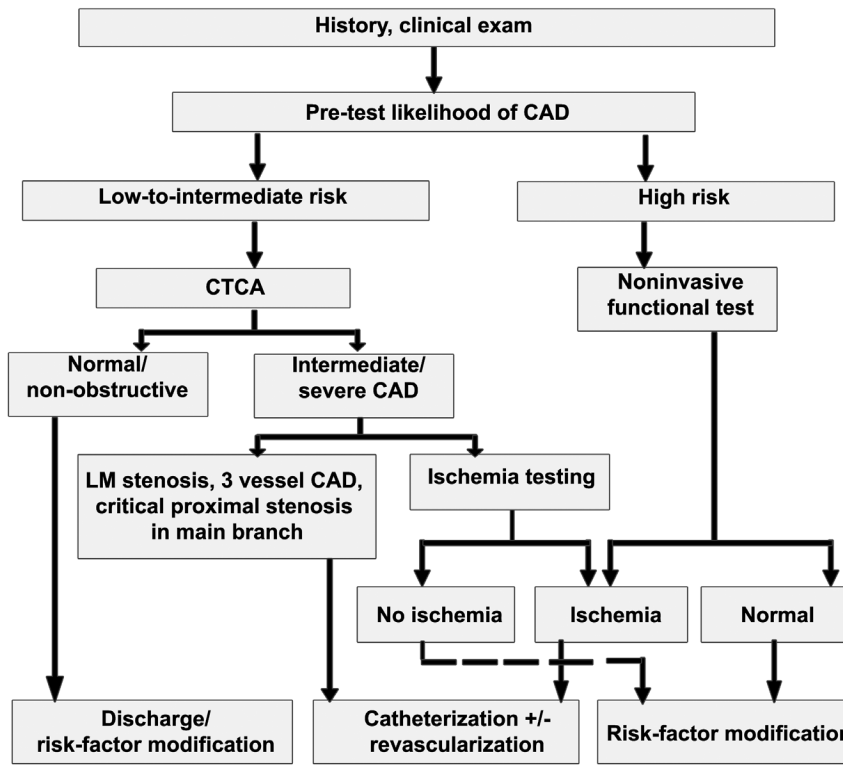

Figure 3. Potential algorithm incorporating CT coronary angiography (CTCA) into the existing diagnostic armamentarium of noninvasive functional tests. Patients are triaged for further testing based on the pre-test likelihood of coronary artery disease. Patients with a low-to-intermediate likelihood are ideal candidates for noninvasive anatomical imaging. Patients with high pretest likelihood preferably undergo a functional test before referral for invasive coronary angiography. CAD, coronary artery disease; LM, left main.

demonstration of ischemia is an important consideration for further management as its presence impacts on the prognosis of a given patient.[24] Recent guidelines and trial data endorse this strategy before proceeding to an invasive assessment of coronary anatomy and eventual revascularization.[25-27] The exact place of CTCA within the current diagnostic work-up of CAD

has not yet been fully defined. Its high negative predictive value makes it most useful as a rule-out-test for the presence of clinically relevant CAD. For the purpose of exclusion of CAD, CTCA is most effective when used for the symptomatic patient with a low or intermediate pre-test likelihood of significant CAD.[4] A negative CTCA would preclude the need for further diagnostic testing and therefore represents a strong addition to the diagnostic armamentarium. A possible diagnostic algorithm incorporating the advantages of CTCA is presented in Figure 3. As a morphological test, CTCA has limited value for predicting the hemodynamic impact of overt CAD. Head-to-head comparisons with nuclear perfusion data and invasive measurements of coronary flow performed in the catheterization laboratory show that about half of coronary lesions graded as ≥50% diameter stenosis by CTCA do not induce ischemia under stress.[28,29] Patients with a high pre-test likelihood of CAD therefore continue to benefit most from an approach providing functional information, using stress imaging tests. Patients in the low-to-intermediate range, who exhibit significant anatomical disease on CTCA, preferably undergo a combined approach with a subsequent functional test to reveal the physiological relevance of the coronary narrowing. Referral to the catheterization laboratory for further invasive assessment and definitive exclusion of the functional severity of a specific epicardial stenosis, using fractional flow reserve (FFR), might be the preferred approach for patients with significant left main- or multivessel CAD on CTCA, due to underestimation of the extent of ischemia by non-invasive functional tests.[18,30]

LIMITATIONS OF INVASIVE CORONARY ANGIOGRAPHY

ICA is only a reliable technique when it provides optimal images, which include appropriate, non-standard projections, to clarify ambiguities and images after the intracoronary injection of nitrate, where necessary.[31] In the hands of less experienced operators, or of operators who do not perform PCI, this is often not achieved.[32,33] Furthermore, contrary to the general belief, ICA does not always prove to be the gold standard technique for the visualization of the coronary anatomy even in the hands of an expert angiographer.[34] Indeed, the intrinsic limitations of an imaging technique that is inherently 2-dimensional make it sometimes impossible to accurately assess the presence or severity of a coronary narrowing especially where the anatomy is complex.[35] (Figures 4 and 5)

Complex Anatomy

Failure to visualize or to understand the anatomical course of a coronary artery has become a frequent reason to refer a patient for an alternative imaging technique. Coronary anomalies are the prototype example where the cardiac catheterization findings often are inconclusive or result in a prolonged procedure with excessive use of contrast material. (Figure 6) In this regard, cardiac CT is becoming the investigation of choice to depict the complex 3-D course

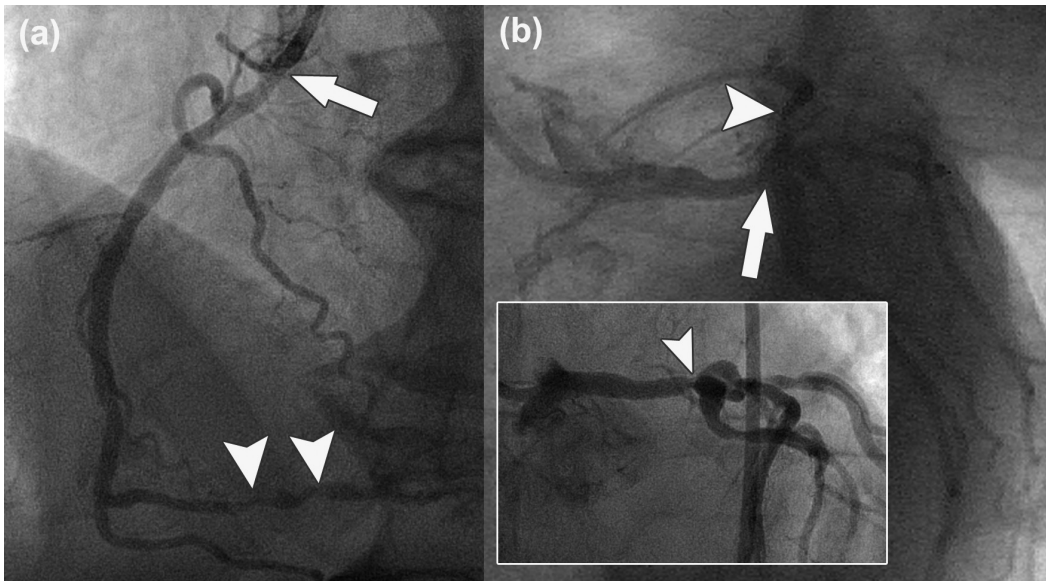

Figure 4. (a) Invasive coronary angiogram (ICA) of the right coronary artery (RCA). The diagnostic catheter (arrow) is obscuring the ostium of the vessel. The distal segment has significant stenoses (arrowheads). (b) ICA of the left coronary artery, showing a significant narrowing in the proximal left anterior descending coronary artery (arrowhead). The distal part of the left main coronary artery (arrow) was judged to have atheroma without significant narrowing. A straight anteroposterior view (inset), which was performed when the patient was scheduled for a percutaneous coronary intervention, clearly shows a severe stenosis at this level (arrowhead).

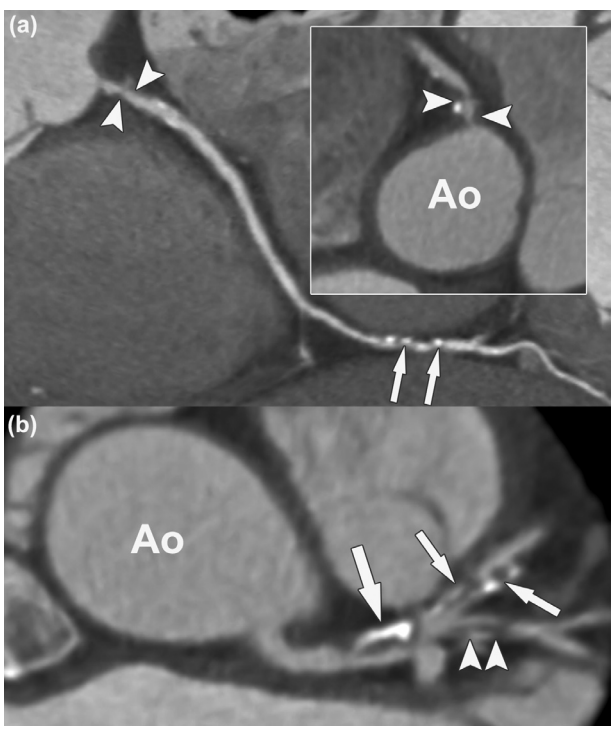

Figure 5. Corresponding CT coronary angiogram. (a) Curved multiplanar reconstruction of the right coronary artery confirming the stenoses in the distal segment (arrows). The ostium (inset) also shows a high-grade stenosis (arrowheads), which was not visualized on the invasive coronary angiogram. (b) Multiplanar reconstruction of the proximal segments of the left coronary artery, clearly showing significant stenoses in the distal part of the left main coronary artery (large arrow), the proximal left anterior descending coronary artery (small arrows) and the large intermediate branch (arrowheads). Ao, indicates ascending aorta.

of coronary arteries and their relation to surrounding structures.[36,37] In experienced centers, coronary magnetic resonance angiography presents an excellent alternative and offers the additional advantages of not using ionizing radiation and contrast material.[38]

Moreover, CTCA can provide accurate information to facilitate the subsequent therapeutic approach in other difficult anatomical settings, such as ostial lesions, lesions at bifurcations or in the left main artery, and chronic total occlusions

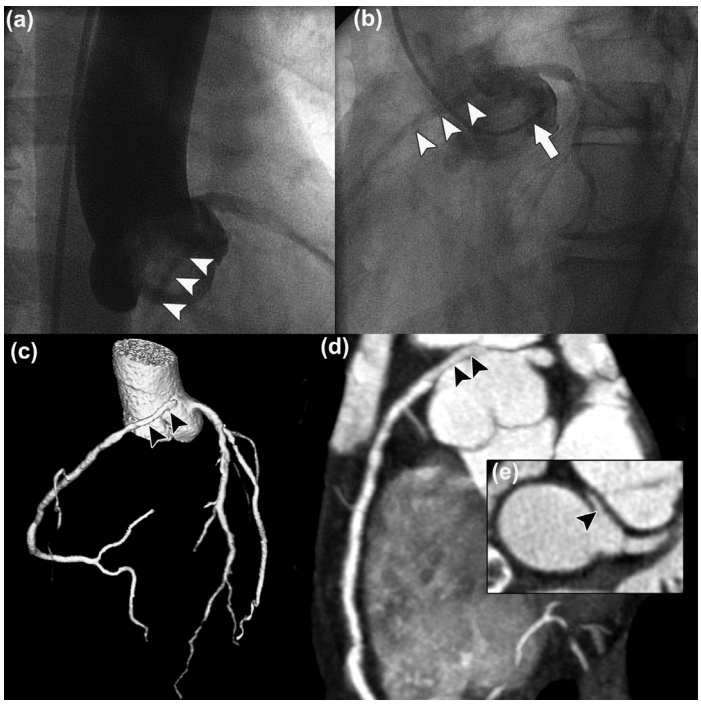

Figure 6. Anomalous origin of the right coronary artery (RCA). (a) An aortogram was performed to localize the origin of the RCA, whose contours are faintly visible (arrowheads). (b) Non-selective injection confirms its origin (arrowheads) in the left coronary cusp. (c, d, e) CT coronary angiogram clearly showing the anomalous origin (arrowheads) and course of the RCA.

Ostial Lesions

Catheter-based imaging of coronary ostial disease can be technically challenging because of difficulties in obtaining adequate contrast opacification while keeping the catheter outside the ostium. More often, the ostium is not properly assessed due to deep catheter intubation. (Figure 7) Failure to recognize catheter-induced spasm, a condition that typically affects the right coronary artery may lead to inappropriate intervention. (Figure 8) These caveats are not an issue in cardiac CT. Indeed, in our experience CTCA has become the preferred imaging tool for re-assessment of suspected ostial pathology in patients whose initial ICA has been inconclusive.

Bifurcations

Coronary atherosclerosis exhibits a predilection for areas of low shear stress, typically at bifurcation sites. Plaque build-up usually is already extensive in these areas before it is detected on ICA. Currently, PCI for bifurcation pathology involves up to 20% of attempted lesion subsets.[39] PCI of bifurcation lesions remains quite challenging and the most effective treatment strategy remains as yet undefined. Important determinants of the chosen approach are the distribution of plaque in main vessel and side branch, as well as the degree of angulation between both branches. Coronary bifurcations are notoriously difficult to examine completely by ICA despite multiple angiographic projections, due to factors such as vessel overlap and foreshortening.[40] Cardiac CT offers accurate 3-D information and is not subject to the limitations of ICA.

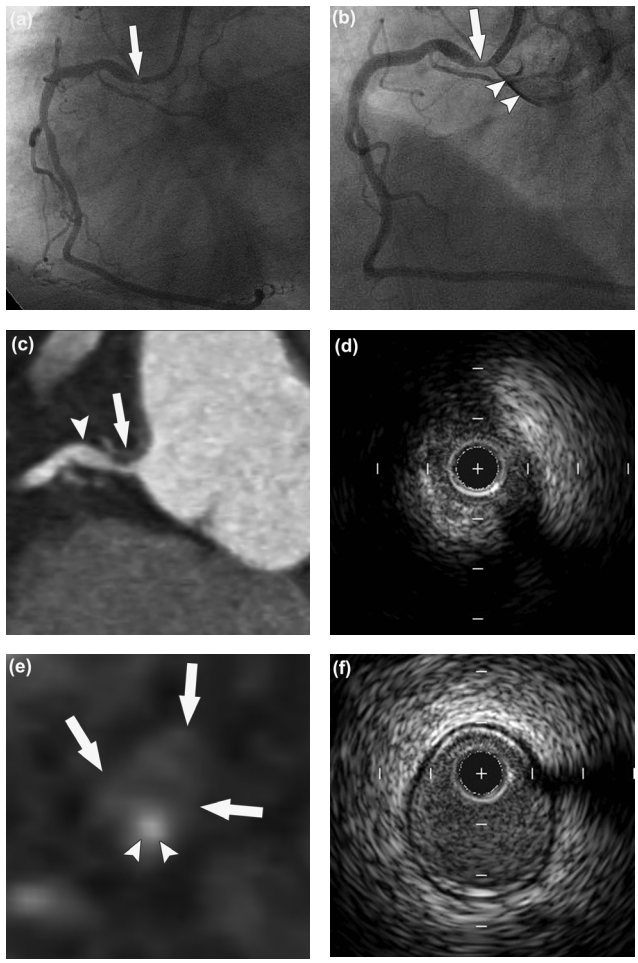

Figure 7. Patient with a true ostial stenosis of the right coronary artery. (a) Initial invasive coronary angiogram showing the stenosis (arrow). (b) These findings are confirmed (arrow) when the patient was rescheduled to undergo a percutaneous coronary intervention. The contrast injection this time was nonselective, as is obvious from the appearance of contrast in the right coronary cusp (arrowheads), to minimize the chances of catheter-induced spasm. (c) A significant ostial lesion (arrow) is seen on the corresponding CT coronary angiogram. (d, e, f, g) Cross-sectional intravascular ultrasound (d and f) and CT (e and g) images, clearly showing the significant narrowing of the lumen (d and e). The extent of disease (e, arrows) in the vessel wall is quite obvious on CT and the residual lumen area (arrowheads) is very small. (f, g) Corresponding cross-sections at the reference site (panel c, arrowhead), distal to the stenosis.

(Figure 9) CTCA reliably assesses the plaque distribution across the bifurcation and in contrast to ICA allows a more precise assessment of coronary bifurcation angles.[41,42] These advantages are of potential benefit for deciding on an adequate treatment strategy.

Left Main Coronary Artery

Evaluation of the left main (LM) coronary artery on ICA combines the difficulties that arise when assessing both ostial and bifurcation disease. Indeed, ostial lesions of the left anterior descending or circumflex arteries frequently involve the distal LM bifurcation. Despite its clinical significance, LM disease may not be accurately evaluated by ICA alone.[43,44] CTCA overcomes the limitations of ICA and can be a clinically useful, adjunctive method to evaluate ostial and distal bifurcation LM coronary artery disease where the results of ICA are ambiguous. (Figure 10)

Chronic Total Occlusions

Coronary chronic total occlusions (CTOs) are found in up to 50% of patients with significant coronary artery disease, but PCI is attempted in only a fraction of these lesions.[45] The relatively low procedural success rate compared to PCI of non-occluded coronary arteries and the higher risk of procedural-related complications in

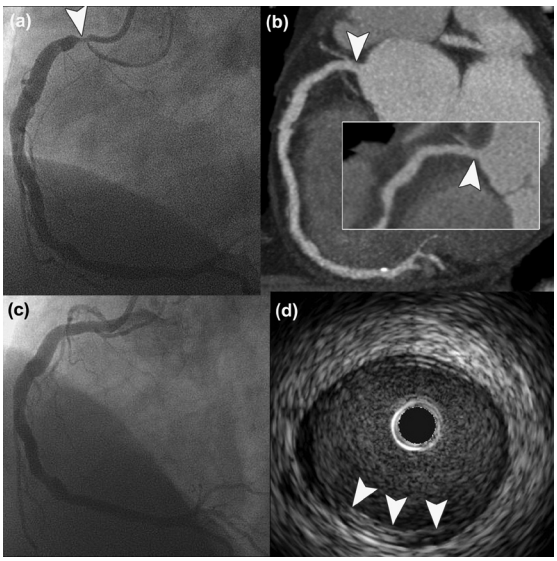

Figure 8. Patient who was referred to undergo a percutaneous coronary intervention for an ostial stenosis of the right coronary artery. (a) Initial angiographic image showing the coronary narrowing (arrowhead). (b, with inset) On cardiac CT the vessel had a normal appearance. (c) A repeat coronary angiogram confirmed the CT findings. (d) On intravascular ultrasound the ostium was indeed widely patent with only minimal intimal thickening (arrowheads).

case of failed recanalization account for the rather low rate of attempted PCI.[46] Several angiographic features have been identified as predictors for successful recanalization, and the presence or absence of these can influence the decision regarding whether PCI is attempted or the patient is referred for bypass surgery.[47] CTCA not only assesses the luminal impact of atherosclerosis, but also visualizes the disease process in the coronary artery wall and by consequence in occluded parts of the coronary arteries. (Figure 11) Independent predictors of PCI failure for CTOs, are the length of the occlusion and the presence of heavy calcifications within the occluded segment: both variables are more precisely defined by CTCA as compared to CCA.[48] Preprocedural evaluation of CTOs by means of CTCA is becoming routine in several institutions as it provides the interventional cardiologist a roadmap that appears to be helpful in the selection of the guidewire for crossing the occlusion.[49,50] This is important as differentiating the nature of the occluding plaque whether it is soft (lipid-rich) or hard (fibrocalcific), will have an impact on device selection and clini-

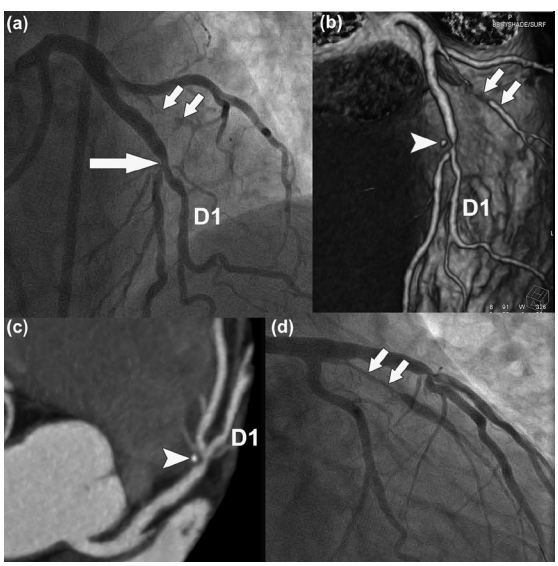

Figure 9. (a) Invasive coronary angiogram showing a significant bifurcation lesion (large arrow) of the left anterior descending coronary artery with the first diagonal branch (D1). Also note the limited contrast enhancement (small arrows) in what looks like a small side branch. (b) Three-dimensional reconstruction of the heart with CT showing the bifurcation lesion. The dense spot within the lesion (arrowhead) corresponds to calcification. The branch that was faintly visible angiographically, can now clearly be recognized without interference of overlapping vessels as the intermediate branch (arrows). (c) 3-mm thick maximum intensity projection clearly showing the calcified (arrowhead) and non-calcified plaque components causing the lumen narrowing. (d) After wiring the intermediate branch its true dimension can be well appreciated (arrows).(A full color version of this illustration can be found in the color section)

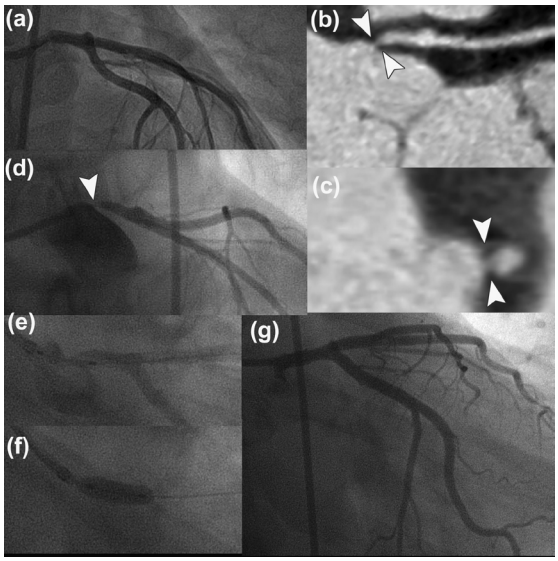

Figure 10. (a) Invasive coronary angiogram (ICA) of the left coronary artery in a female patient with atypical chest pain who presented with ventricular fibrillation during a bicycle stress test. Although not visible there was a suspicion of ostial left main disease because of the absence of contrast back flow in the coronary sinus. (b and c) The CT coronary angiogram clearly shows a severe ostial narrowing (arrowheads). (d) A non-selective repeat ICA confirms the CT findings (arrowhead). (e and f) A percutaneous coronary intervention was performed: shown are the positioning and deployment of the stent. (g) Postprocedural coronary angiogram.

cal outcome.[51] Also the 3-D visualization of the course of the occluded vessel part enables the interventional cardiologist to steer the guidewire towards the direction of the distal vessel beyond the occlusion. (Figure 12)

Plaque imaging

CTCA has provided non-invasive confirmation of the fact, often reiterated by surgeons and pathologists, that ICA greatly underestimates the extent of coronary atherosclerotic disease. The fundamental difference between ICA and CTCA is the basic image format. While ICA provides high-resolution imaging, it only provides a 2-D representation of the coronary artery lumen. CTCA overcomes the limitations of silhouette imaging and reveals details of the distribution and composition of atherosclerosis within the vessel wall. (Figure 13)

It is not yet clear whether a targeted interventional approach, a systemic pharmacological approach, or a hybrid

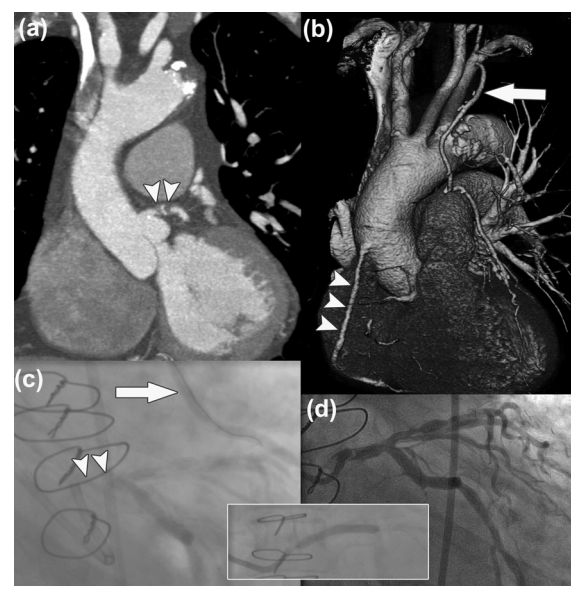

Figure 11. Patient with recurrent angina after previous coronary bypass graft surgery, including a venous graft to the right coronary artery (RCA) and left internal mammary artery (LIMA) to the left anterior descending coronary artery. At initial invasive coronary angiography the origin of the left coronary artery appeared occluded. (a) Cardiac CT scan, coronal view, indeed showing a short occlusion (arrowheads) of the left main stem. (b) Three-dimensional reconstruction of the heart showing the patent LIMA (arrow) and venous graft to the RCA (arrowheads). (c) Contrast injection after wiring of the LIMA (arrow) results in opacification of the native coronary artery up to the distal part of the left main stem. (d) Six-month angiographic result after successful PCI (inset) of the left main stem. (A full color version of this illustration can be found in the color section).

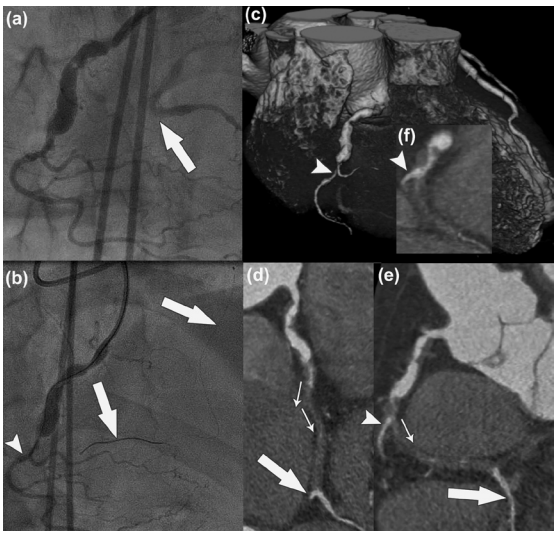

Figure 12. (a) Invasive coronary angiogram, showing a chronic total occlusion of the right coronary artery. Simultaneous contrast injection in the left coronary artery shows filling of the distal part of the RCA (arrow) through collaterals. (b) Antegrade attempt at recanalising the RCA shows movement of the wire into smaller branches supplying the right ventricle (arrowhead). To facilitate the direction of the antegrade wire, a second wire (arrows) was positioned retrograde through the collateral system. (c, d, e and f) The CT images provide a roadmap to show which direction the wire should go. Clearly shown are the small right ventricular branches (c, e and f, arrowhead), the path of the occluded vessel in the sagittal plane (d, small arrows) and frontal plane (e, small arrow). The distal part of the RCA (d and e, large arrow) is filled with contrast through collaterals. (A full color version of this illustration can be found in the color section).

approach to the treatment of plaques, identified as being at high-risk of causing future adverse events, will prevail. However, visualization and characterization of coronary plaques with CTCA is feasible and may provide us a novel way of assessing the coronary atherosclerotic disease process. A role for CTCA in identifying high-risk plaque or in natural history studies that use novel compounds to alter plaque burden or characteristics may emerge in the future. Currently, no data is available that show a patient benefit from using CTCA as a tool for risk stratification in asymptomatic individuals.

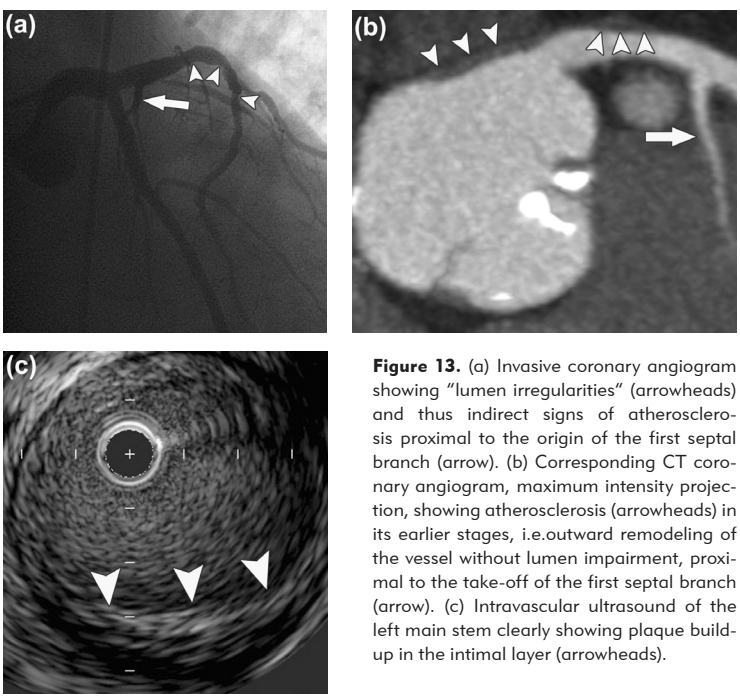

Figure 13. (a) Invasive coronary angiogram showing "lumen irregularities" (arrowheads) and thus indirect signs of atherosclerosis proximal to the origin of the first septal branch (arrow). (b) Corresponding CT coronary angiogram, maximum intensity projection, showing atherosclerosis (arrowheads) in its earlier stages, i.e.outward remodeling of the vessel without lumen impairment, proximal to the take-off of the first septal branch (arrow). (c) Intravascular ultrasound of the left main stem clearly showing plaque build-up in the intimal layer (arrowheads).

THERAPEUTIC USE OF CARDIAC CT IMAGING

Guidance During Complex Percutaneous Coronary Interventions

In addition to its diagnostic value, cardiac CT images may also facilitate the performance of PCI. This is currently being investigated by integration of CTCA datasets into magnetic navigation systems.[52] Precise control of the direction of a guidewire or a device in three-dimensional space offers a means to access difficult lesions and tortuous vessels that are often challenging to approach with conventional methods.[53,54] (Figure 14)

Percutaneous Treatment of Valvular Heart Disease

In addition to the investigation of the coronary arteries, cardiac CT systems can be used to assess the dimensions of the aortic root, left ventricular function, and disease of the large extra-cardiac arteries. Percutaneous aortic valve replacement (PAVR) is an emerging technology in the management of patients with severe aortic stenosis who are felt to be unsuitable for surgical management.[55,56] These percutaneous heart valves are routinely implanted via a transfemoral arterial access using large diameter sheaths (18 to 24 French). There is limited experience with this technology to date; however, in the few centers that offer this therapeutic option, CT scans are routinely used to evaluate the size of the aortic annulus and iliac arteries to ensure appropriate sizing of the prosthesis as to ensure that the 18-to-24 French system can safely negotiate the peripheral arterial system. (Figure 15)

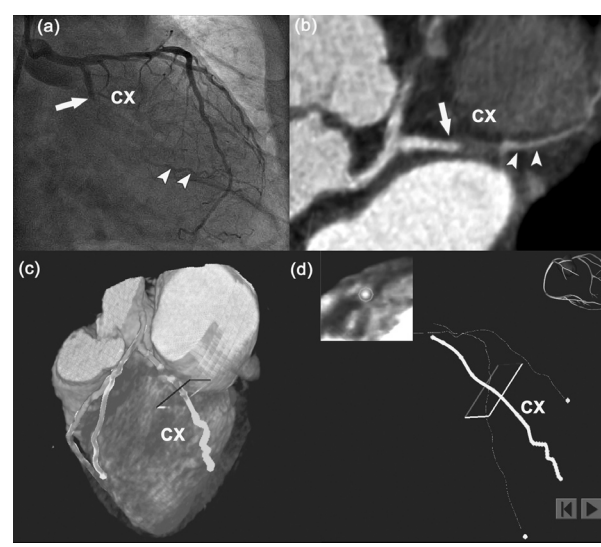

Figure 14. (a) Invasive coronary angiogram, showing a chronic total occlusion (arrow) of the circumflex artery (CX). Only the very distal part of the vessel is visible through collaterals (arrowheads) (b) Corresponding CT image (curved multiplanar reconstruction): compared to the angiographic information the occlusion appears much shorter and consists of non calcified tissue. (c) The CT dataset has been uploaded in the navigation software; the course of the CX, including the path of the occlusion, is marked by a green line overlay. (d) The course of the CX has been marked as a yellow line. The rectangular that is present in panel c and d marks the location of the wire tip in the vessel. The inset in panel d represents the perpendicular cross-sectional view of the vessel allowing the operator to steer the guidewire in the desired direction. (A full color version of this illustration can be found in the color section).

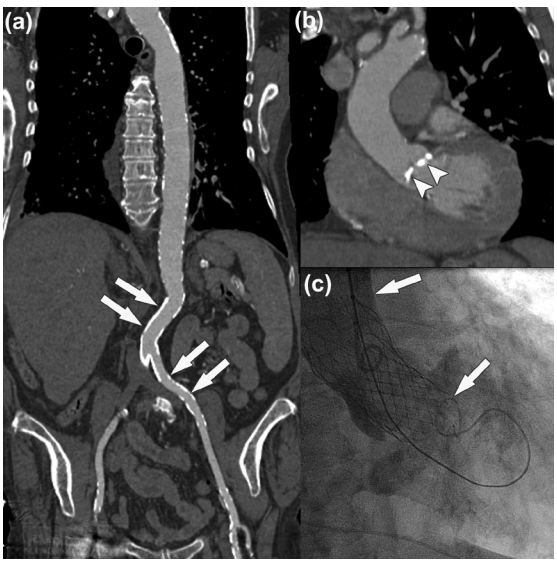

Figure 15. Eighty-three year-old woman with symptomatic severe aortic valve stenosis who was considered a candidate for percutaneous aortic valve replacement. (a) The thoraco-abdominal CT scan revealed severe calcifications (arrows) of the abdominal aorta and iliac arteries. (b) CT image, coronal view, showing the severe calcifications of the aortic valve (arrowheads). (c) Because of the expected difficult femoral access, the valve replacement was successfully performed through the left subclavian artery. The arrows are showing the borders of the freshly implanted aortic valve, which consists of an equine pericardial valve mounted on a stainless steel bioprosthesis.

LIMITATIONS OF CTCA: A NOTE OF CAUTION

Ongoing refinements in CT scan technology have brought this cardiac imaging tool to a point where accurate noninvasive assessment of coronary anatomy is feasible. As for any new technology being considered for clinical use, an important consideration is the incremental information provided by a new modality in comparison to existing standard assessments. Continuing increases in the cost of health care and the increasing use of cardiac imaging tests in particular, underscore the need for a test to be cost-effective before changing existing diagnostic pathways.[57,58] While acknowledging the need for further scientific evidence, several societies have issued guidelines describing the optimal use of cardiac CT in an appropriate clinical context.[23,59] In general, CTCA proves most valuable for clinical situations where one seeks to confidently establish the absence of coronary artery disease. Initial studies have highlighted the potential of CTCA to be cost-effective in this regard.[60] Determination of the target patient population is just one of the determinants of a successful cardiac CT program. Other factors, such as adequate heart rate control, the body mass index of the patient, and the extent of coronary artery calcification, are equally important and contribute to the " readability" of a scan.[61,62] A cardiac CT scan is not entirely limited to the heart, but also includes the adjacent thoracic structures. Non-cardiac findings requiring clinical or radiological follow-up are reported in up to 25% of patients undergoing cardiac CT and emphasize the need for a multidisciplinary approach.[63] The potential increase in cancer risk due to CT-related ionizing radiation is an important limiting factor and is providing impetus for the development of dose-saving algorithms and new scanning protocols that will reduce the effective radiation dose to the level

of ICA.[64-66] Finally, state-of-the-art cardiac CT imaging and interpretation requires adequate training both in cardiovascular disease and radiology imaging; ideally, at least 6 months active participation in a joint cardiology and radiology program in a dedicated teaching hospital.[5,67]

CONCLUSION

CTCA is a promising technique that has the potential to radically alter the diagnostic pathways we currently employ in patients with suspected coronary disease. Based on current knowledge, the use of CTCA as a diagnostic test is considered appropriate for clinical scenarios where one seeks to confidently exclude the presence of CAD. The more widespread use of CTCA, replacing more costly diagnostic imaging modalities, in particular ICA and nuclear imaging studies, could result in substantial cost savings for the health care system. The cost-effectiveness of CTCA is currently being evaluated in large clinical trials.

ICA remains the preferred option for the patient with typical angina as it provides the option of ad hoc intervention. As illustrated in this review, complementary coronary imaging using CTCA might be of value in certain circumstances to clarify whether surgery or PCI is a better option or to provide specific information that might aid in planning PCI. This complementary role of cardiac CT imaging already results in so-called "reverse referrals", i.e. patients initially referred for ICA are subsequently referred for CTCA.

Finally, although CTCA is finding its place as a diagnostic tool in clinical cardiology, it is critical to ensure that those performing it have adequate training in the technique and adhere to guidelines issued by professional societies.

REFERENCES

1 Sones FM, Shirey EK, Proudfit WL, et al. Cine coronary arteriography. Circulation 1959; 20:773-775

2 Moshage WE, Achenbach S, Seese B, et al. Coronary artery stenoses: three-dimensional imaging with electrocardiographically triggered, contrast agent-enhanced, electron-beam CT. Radiology 1995; 196:707-714

3 Rensing BJ, Bongaerts A, van Geuns RJ, et al. Intravenous coronary angiography by electron beam computed tomography: a clinical evaluation. Circulation 1998; 98:2509-2512

4 Meijboom WB, van Mieghem CA, Mollet NR, et al. 64-slice computed tomography coronary angiography in patients with high, intermediate, or low pretest probability of significant coronary artery disease. J Am Coll Cardiol 2007; 50:1469-1475

5 Schroeder S, Achenbach S, Bengel F, et al. Cardiac computed tomography: indications, applications, limitations, and training requirements: report of a Writing Group deployed by the Working Group Nuclear Cardiology and Cardiac CT of the European Society of Cardiology and the European Council of Nuclear Cardiology. Eur Heart J 2008; 29:531-556
6 Scanlon PJ, Faxon DP, Audet AM, et al. ACC/AHA guidelines for coronary angiography. A report of the American College of Cardiology/American Heart Association Task Force on practice guidelines (Committee on Coronary Angiography). Developed in collaboration with the Society for Cardiac Angiography and Interventions. J Am Coll Cardiol 1999; 33:1756-1824
7 Fox K, Garcia MA, Ardissino D, et al. Guidelines on the management of stable angina pectoris: executive summary: the Task Force on the Management of Stable Angina Pectoris of the European Society of Cardiology. Eur Heart J 2006; 27:1341-1381
8 Topol EJ, Ellis SG, Cosgrove DM, et al. Analysis of coronary angioplasty practice in the United States with an insurance-claims data base. Circulation 1993; 87:1489-1497
9 Uretsky BF, Wang FW. Implementation and application of a continuous quality improvement (CQI) program for the cardiac catheterization laboratory: one institution's 10-year experience. Catheter Cardiovasc Interv 2006; 68:586-595
10 Togni M, Balmer F, Pfiffner D, et al. Percutaneous coronary interventions in Europe 1992-2001. Eur Heart J 2004; 25:1208-1213
11 Sones FM, Jr. Indications and value of coronary arteriography. Circulation 1972; 46:1155-1160
12 Fleischmann KE, Hunink MG, Kuntz KM, et al. Exercise echocardiography or exercise SPECT imaging? A meta-analysis of diagnostic test performance. Jama 1998; 280:913-920
13 Hachamovitch R, Hayes SW, Friedman JD, et al. Stress myocardial perfusion single-photon emission computed tomography is clinically effective and cost effective in risk stratification of patients with a high likelihood of coronary artery disease (CAD) but no known CAD. J Am Coll Cardiol 2004; 43:200-208
14 Marwick TH, Case C, Sawada S, et al. Prediction of mortality using dobutamine echocardiography. J Am Coll Cardiol 2001; 37:754-760
15 Steinberg EH, Madmon L, Patel CP, et al. Long-term prognostic significance of dobutamine echocardiography in patients with suspected coronary artery disease: results of a 5-year follow-up study. J Am Coll Cardiol 1997; 29:969-973
16 Tsutsui JM, Elhendy A, Anderson JR, et al. Prognostic value of dobutamine stress myocardial contrast perfusion echocardiography. Circulation 2005; 112:1444-1450
17 Lima RS, Watson DD, Goode AR, et al. Incremental value of combined perfusion and function over perfusion alone by gated SPECT myocardial perfusion imaging for detection of severe three-vessel coronary artery disease. J Am Coll Cardiol 2003; 42:64-70

18 Ragosta M, Bishop AH, Lipson LC, et al. Comparison between angiography and fractional flow reserve versus single-photon emission computed tomographic myocardial perfusion imaging for determining lesion significance in patients with multivessel coronary disease. Am J Cardiol 2007; 99:896-902
19 Elhendy A, van Domburg RT, Bax JJ, et al. Accuracy of dobutamine technetium 99m sestamibi SPECT imaging for the diagnosis of single-vessel coronary artery disease: comparison with echocardiography. Am Heart J 2000; 139:224-230
20 Pundziute G, Schuijf JD, Jukema JW, et al. Prognostic value of multislice computed tomography coronary angiography in patients with known or suspected coronary artery disease. J Am Coll Cardiol 2007; 49:62-70
21 Min JK, Shaw LJ, Devereux RB, et al. Prognostic value of multidetector coronary computed tomographic angiography for prediction of all-cause mortality. J Am Coll Cardiol 2007; 50:1161-1170
22 Gilard M, Le Gal G, Cornily JC, et al. Midterm prognosis of patients with suspected coronary artery disease and normal multislice computed tomographic findings: a prospective management outcome study. Arch Intern Med 2007; 167:1686-1689
23 Budoff MJ, Achenbach S, Blumenthal RS, et al. Assessment of coronary artery disease by cardiac computed tomography: a scientific statement from the American Heart Association Committee on Cardiovascular Imaging and Intervention, Council on Cardiovascular Radiology and Intervention, and Committee on Cardiac Imaging, Council on Clinical Cardiology. Circulation 2006; 114:1761-1791
24 Hachamovitch R, Berman DS, Shaw LJ, et al. Incremental prognostic value of myocardial perfusion single photon emission computed tomography for the prediction of cardiac death: differential stratification for risk of cardiac death and myocardial infarction. Circulation 1998; 97:535-543
25 Silber S, Albertsson P, Aviles FF, et al. Guidelines for percutaneous coronary interventions. The Task Force for Percutaneous Coronary Interventions of the European Society of Cardiology. Eur Heart J 2005; 26:804-847
26 Eagle KA, Guyton RA, Davidoff R, et al. ACC/AHA 2004 guideline update for coronary artery bypass graft surgery: a report of the American College of Cardiology/American Heart Association Task Force on Practice Guidelines (Committee to Update the 1999 Guidelines for Coronary Artery Bypass Graft Surgery). Circulation 2004; 110:e340-437
27 Shaw LJ, Berman DS, Maron DJ, et al. Optimal medical therapy with or without percutaneous coronary intervention to reduce ischemic burden: results from the Clinical Outcomes Utilizing Revascularization and Aggressive Drug Evaluation (COURAGE) trial nuclear substudy. Circulation 2008; 117:1283-1291
28 Schuijf JD, Wijns W, Jukema JW, et al. Relationship between noninvasive coronary angiography with multi-slice computed tomography and myocardial perfusion imaging. J Am Coll Cardiol 2006; 48:2508-2514

29 Meijboom WB, Van Mieghem CA, van Pelt N, et al. Comprehensive assessment of coronary artery stenoses: computed tomography coronary angiography versus conventional coronary angiography and correlation with fractional flow reserve in patients with stable angina. J Am Coll Cardiol 2008; 52:636-643
30 Berman DS, Kang X, Slomka PJ, et al. Underestimation of extent of ischemia by gated SPECT myocardial perfusion imaging in patients with left main coronary artery disease. J Nucl Cardiol 2007; 14:521-528
31 Di Mario C, Sutaria N. Coronary angiography in the angioplasty era: projections with a meaning. Heart 2005; 91:968-976
32 White CJ, Ramee SR, Collins TJ, et al. Ambiguous coronary angiography: clinical utility of intravascular ultrasound. Cathet Cardiovasc Diagn 1992; 26:200-203
33 Lee DY, Eigler N, Luo H, et al. Effect of intracoronary ultrasound imaging on clinical decision making. Am Heart J 1995; 129:1084-1093
34 Yamashita T, Colombo A, Tobis JM. Limitations of coronary angiography compared with intravascular ultrasound: implications for coronary interventions. Prog Cardiovasc Dis 1999; 42:91-138
35 Topol EJ, Nissen SE. Our preoccupation with coronary luminology. The dissociation between clinical and angiographic findings in ischemic heart disease. Circulation 1995; 92:2333-2342
36 Berbarie RF, Dockery WD, Johnson KB, et al. Use of multislice computed tomographic coronary angiography for the diagnosis of anomalous coronary arteries. Am J Cardiol 2006; 98:402-406
37 Datta J, White CS, Gilkeson RC, et al. Anomalous coronary arteries in adults: depiction at multi-detector row CT angiography. Radiology 2005; 235:812-818
38 Bunce NH, Lorenz CH, Keegan J, et al. Coronary artery anomalies: assessment with free-breathing three-dimensional coronary MR angiography. Radiology 2003; 227:201-208
39 Lemos PA, Serruys PW, van Domburg RT, et al. Unrestricted utilization of sirolimus-eluting stents compared with conventional bare stent implantation in the "real world": the Rapamycin-Eluting Stent Evaluated At Rotterdam Cardiology Hospital (RESEARCH) registry. Circulation 2004; 109:190-195
40 Green NE, Chen SY, Hansgen AR, et al. Angiographic views used for percutaneous coronary interventions: a three-dimensional analysis of physician-determined vs. computer-generated views. Catheter Cardiovasc Interv 2005; 64:451-459
41 Pflederer T, Ludwig J, Ropers D, et al. Measurement of coronary artery bifurcation angles by multidetector computed tomography. Invest Radiol 2006; 41:793-798
42 Van Mieghem CA, Thury A, Meijboom WB, et al. Detection and characterization of coronary bifurcation lesions with 64-slice computed tomography coronary angiography. Eur Heart J 2007; 28:1968-1976

43 Fisher LD, Judkins MP, Lesperance J, et al. Reproducibility of coronary arteriographic reading in the coronary artery surgery study (CASS). Cathet Cardiovasc Diagn 1982; 8:565-575

44 Johnston PW, Fort S, Cohen EA. Noncritical disease of the left main coronary artery: limitations of angiography and the role of intravascular ultrasound. Can J Cardiol 1999; 15:297-302

45 Christofferson RD, Lehmann KG, Martin GV, et al. Effect of chronic total coronary occlusion on treatment strategy. Am J Cardiol 2005; 95:1088-1091

46 Hoye A, van Domburg RT, Sonnenschein K, et al. Percutaneous coronary intervention for chronic total occlusions: the Thoraxcenter experience 1992-2002. Eur Heart J 2005; 26:2630-2636

47 Puma JA, Sketch MH, Jr., Tcheng JE, et al. Percutaneous revascularization of chronic coronary occlusions: an overview. J Am Coll Cardiol 1995; 26:1-11

48 Mollet NR, Hoye A, Lemos PA, et al. Value of preprocedure multislice computed tomographic coronary angiography to predict the outcome of percutaneous recanalization of chronic total occlusions. Am J Cardiol 2005; 95:240-243

49 Soon KH, Selvanayagam JB, Cox N, et al. Percutaneous revascularization of chronic total occlusions: review of the role of invasive and non-invasive imaging modalities. Int J Cardiol 2007; 116:1-6

50 Van Mieghem CA, van der Ent M, de Feyter PJ. Percutaneous coronary intervention for chronic total occlusions: value of preprocedural multislice CT guidance. Heart 2007; 93:1492

51 Garcia-Garcia HM, Van Mieghem CA, Gonzalo N, et al. Computed Tomography in Totally Occluded lesions (CTTO Registry): Focus on radiation exposure and predictors of successful percutaneous intervention. Euro Interv. 2008; in press.

52 Ramcharitar S, Patterson MS, van Geuns RJ, et al. Technology Insight: magnetic navigation in coronary interventions. Nat Clin Pract Cardiovasc Med 2008; 5:148-156

53 Patterson MS, Schotten J, van Mieghem C, et al. Magnetic navigation in percutaneous coronary intervention. J Interv Cardiol 2006; 19:558-565

54 Atmakuri SR, Lev EI, Alviar C, et al. Initial experience with a magnetic navigation system for percutaneous coronary intervention in complex coronary artery lesions. J Am Coll Cardiol 2006; 47:515-521

55 Webb JG, Pasupati S, Humphries K, et al. Percutaneous transarterial aortic valve replacement in selected high-risk patients with aortic stenosis. Circulation 2007; 116:755-763

56 Grube E, Schuler G, Buellesfeld L, et al. Percutaneous aortic valve replacement for severe aortic stenosis in high-risk patients using the second- and current third-generation self-expanding CoreValve prosthesis: device success and 30-day clinical outcome. J Am Coll Cardiol 2007; 50:69-76

57 Lucas FL, DeLorenzo MA, Siewers AE, et al. Temporal trends in the utilization of diagnostic testing and treatments for cardiovascular disease in the United States, 1993-2001. Circulation 2006; 113:374-379
58 Redberg RF. Computed tomographic angiography: more than just a pretty picture? J Am Coll Cardiol 2007; 49:1827-1829
59 Hendel RC, Patel MR, Kramer CM, et al. ACCF/ACR/SCCT/SCMR/ASNC/NASCI/SCAI/SIR 2006 appropriateness criteria for cardiac computed tomography and cardiac magnetic resonance imaging: a report of the American College of Cardiology Foundation Quality Strategic Directions Committee Appropriateness Criteria Working Group, American College of Radiology, Society of Cardiovascular Computed Tomography, Society for Cardiovascular Magnetic Resonance, American Society of Nuclear Cardiology, North American Society for Cardiac Imaging, Society for Cardiovascular Angiography and Interventions, and Society of Interventional Radiology. J Am Coll Cardiol 2006; 48:1475-1497
60 Goldstein JA, Gallagher MJ, O'Neill WW, et al. A randomized controlled trial of multi-slice coronary computed tomography for evaluation of acute chest pain. J Am Coll Cardiol 2007; 49:863-871
61 Leschka S, Wildermuth S, Boehm T, et al. Noninvasive coronary angiography with 64-section CT: effect of average heart rate and heart rate variability on image quality. Radiology 2006; 241:378-385
62 Brodoefel H, Reimann A, Burgstahler C, et al. Noninvasive coronary angiography using 64-slice spiral computed tomography in an unselected patient collective: Effect of heart rate, heart rate variability and coronary calcifications on image quality and diagnostic accuracy. Eur J Radiol 2007
63 Onuma Y, Tanabe K, Nakazawa G, et al. Noncardiac findings in cardiac imaging with multidetector computed tomography. J Am Coll Cardiol 2006; 48:402-406
64 Einstein AJ, Henzlova MJ, Rajagopalan S. Estimating risk of cancer associated with radiation exposure from 64-slice computed tomography coronary angiography. Jama 2007; 298:317-323
65 Hausleiter J, Meyer T, Hadamitzky M, et al. Radiation dose estimates from cardiac multislice computed tomography in daily practice: impact of different scanning protocols on effective dose estimates. Circulation 2006; 113:1305-1310
66 Husmann L, Valenta I, Gaemperli O, et al. Feasibility of low-dose coronary CT angiography: first experience with prospective ECG-gating. Eur Heart J 2008; 29:191-197
67 Budoff MJ, Achenbach S, Berman DS, et al. Task force 13: training in advanced cardiovascular imaging (computed tomography) endorsed by the American Society of Nuclear Cardiology, Society of Atherosclerosis Imaging and Prevention, Society for Cardiovascular Angiography and Interventions, and Society of Cardiovascular Computed Tomography. J Am Coll Cardiol 2008; 51:409-414

68 Ehara M, Surmely JF, Kawai M, et al. Diagnostic accuracy of 64-slice computed tomography for detecting angiographically significant coronary artery stenosis in an unselected consecutive patient population: comparison with conventional invasive angiography. Circ J 2006; 70:564-571

69 Ghostine S, Caussin C, Daoud B, et al. Non-invasive detection of coronary artery disease in patients with left bundle branch block using 64-slice computed tomography. J Am Coll Cardiol 2006; 48:1929-1934

70 Leber AW, Knez A, von Ziegler F, et al. Quantification of obstructive and nonobstructive coronary lesions by 64-slice computed tomography: a comparative study with quantitative coronary angiography and intravascular ultrasound. J Am Coll Cardiol 2005; 46:147-154

71 Leschka S, Alkadhi H, Plass A, et al. Accuracy of MSCT coronary angiography with 64-slice technology: first experience. Eur Heart J 2005; 26:1482-1487

72 Meijboom WB, Mollet NR, Van Mieghem CA, et al. Pre-operative computed tomography coronary angiography to detect significant coronary artery disease in patients referred for cardiac valve surgery. J Am Coll Cardiol 2006; 48:1658-1665

73 Meijboom WB, Mollet NR, van Mieghem CA, et al. 64-slice Computed Tomography Coronary Angiography in Patients with Non-ST Elevation Acute Coronary Syndrome. Heart 2007

74 Mollet NR, Cademartiri F, van Mieghem CA, et al. High-resolution spiral computed tomography coronary angiography in patients referred for diagnostic conventional coronary angiography. Circulation 2005; 112:2318-2323

75 Muhlenbruch G, Seyfarth T, Soo CS, et al. Diagnostic value of 64-slice multi-detector row cardiac CTA in symptomatic patients. Eur Radiol 2007; 17:603-609

76 Nikolaou K, Knez A, Rist C, et al. Accuracy of 64-MDCT in the diagnosis of ischemic heart disease. AJR Am J Roentgenol 2006; 187:111-117

77 Oncel D, Oncel G, Tastan A, et al. Detection of significant coronary artery stenosis with 64-section MDCT angiography. Eur J Radiol 2007; 62:394-405

78 Pugliese F, Mollet NR, Runza G, et al. Diagnostic accuracy of non-invasive 64-slice CT coronary angiography in patients with stable angina pectoris. Eur Radiol 2006; 16:575-582

79 Raff GL, Gallagher MJ, O'Neill WW, et al. Diagnostic accuracy of noninvasive coronary angiography using 64-slice spiral computed tomography. J Am Coll Cardiol 2005; 46:552-557

80 Ropers D, Rixe J, Anders K, et al. Usefulness of multidetector row spiral computed tomography with 64- x 0.6-mm collimation and 330-ms rotation for the noninvasive detection of significant coronary artery stenoses. Am J Cardiol 2006; 97:343-348

81 Schuijf JD, Pundziute G, Jukema JW, et al. Diagnostic accuracy of 64-slice multislice computed tomography in the noninvasive evaluation of significant coronary artery disease. Am J Cardiol 2006; 98:145-148
82 Scheffel H, Alkadhi H, Plass A, et al. Accuracy of dual-source CT coronary angiography: First experience in a high pre-test probability population without heart rate control. Eur Radiol 2006; 16:2739-2747
83 Weustink AC, Meijboom WB, Mollet NR, et al. Reliable high-speed coronary computed tomography in symptomatic patients. J Am Coll Cardiol 2007; 50:786-794
84 Leber AW, Johnson T, Becker A, et al. Diagnostic accuracy of dual-source multi-slice CT-coronary angiography in patients with an intermediate pretest likelihood for coronary artery disease. Eur Heart J 2007; 28:2354-2360
85 Ropers U, Ropers D, Pflederer T, et al. Influence of heart rate on the diagnostic accuracy of dual-source computed tomography coronary angiography. J Am Coll Cardiol 2007; 50:2393-2398
86 Alkadhi H, Scheffel H, Desbiolles L, et al. Dual-source computed tomography coronary angiography: influence of obesity, calcium load, and heart rate on diagnostic accuracy. Eur Heart J 2008; 29:766-776
87 Scheffel H, Alkadhi H, Leschka S, et al. Low-dose CT coronary angiography in the step-and-shoot mode: diagnostic performance. Heart 2008; 94:1132-1137

PART II

VALIDATION OF THE TECHNIQUE

3

Rationale and Methods of the Integrated Biomarker and Imaging Study (IBIS): Combining Invasive and Non-Invasive Imaging with Biomarkers to Detect Subclinical Atherosclerosis and Assess Coronary Lesion Biology

Carlos A.G. Van Mieghem[1], Nico Bruining[1], Johannes A. Schaar[2], Eugene McFadden[1], Nico R. Mollet[1], Filippo Cademartiri[1], Frits Mastik[2], Jurgen M.R. Ligthart[1], Gaston A. Rodriguez Granillo[1], Marco Valgimigli[1], Georgios Sianos[1], Willem J. van der Giessen[1], Bianca Backx[4], Marie-Angele M. Morel[4], Gerrit-Anne van Es[4], Jonathon D. Sawyer[3], June Kaplow[3], Andrew Zalewski[3], Anton F.W. van der Steen[2], Pim J. de Feyter[1], Patrick W. Serruys[1]

[1]Erasmus Medical Center, Thoraxcenter, Rotterdam, the Netherlands; [2]Interuniversity Cardiology Institute of the Netherlands, Utrecht; [3]GlaxoSmithKline, Philadelphia, PA, USA; [4]Cardialysis, Rottterdam, The Netherlands.

Int J Cardiovasc Imaging. 2005; 21: 425-441

ABSTRACT

Death or myocardial infarction, the most serious clinical consequences of atherosclerosis, often result from plaque rupture at non-flow limiting lesions. Current diagnostic imaging with coronary angiography only detects large plaques that already impinge on the lumen and cannot accurately identify those that have a propensity to cause unheralded events. Accurate evaluation of the composition or of the biomechanical characteristics of plaques with invasive or non-invasive methods, alone or in conjunction with assessment of circulating biomarkers, could help identify high-risk patients, thus providing the rationale for aggressive treatments in order to reduce future clinical events. The IBIS (Integrated Biomarker and Imaging Study) study is a prospective, single-center, non-randomized, observational study conducted in Rotterdam. The aim of the IBIS study is to evaluate both invasive (quantitative coronary angiography, intravascular ultrasound (IVUS) and palpography) and non-invasive (multislice spiral computed tomography) imaging techniques to characterize non-flow limiting coronary lesions. In addition, multiple classical and novel biomarkers will be measured and their levels correlated with the results of the different imaging techniques. A minimum of 85 patients up to a maximum of 120 patients will be included. This paper describes the study protocol and methodological solutions that have been devised for the purpose of comparisons among several imaging modalities. It outlines the analyses that will be performed to compare invasive and non-invasive imaging techniques in conjunction with multiple biomarkers to characterize non-flow limiting subclinical coronary lesions.

BACKGROUND

Although coronary atherosclerosis is common, clinical events are relatively rare and not linearly related to either the extent or severity of atherosclerosis. The majority of acute coronary events arise from non-flow limiting lesions and are often the first clinical manifestation of previously subclinical atherosclerosis [1-5]. These observations, among others, led to the concept of the vulnerable atherosclerotic plaque, a plaque that has a high probability of causing a clinical event [6-8]. The most common post-mortem histological features in such plaques are the presence of a thin fibrous cap, a lipid-rich core, and infiltration by inflammatory cells [9-14]. Less common pathological substrates for fatal clinical events are plaque erosion, nodular calcification and intraplaque hemorrhage [9,15].

Coronary angiography is the standard technique to define the presence and to assess the extent of coronary atherosclerosis; however, it can only detect plaques that impinge on the lumen. Given the diffuse nature of coronary atherosclerosis and the phenomenon of arterial remodeling, an extensive amount of plaque can be present yet go undetected on angiography [16,17]. To detect potentially vulnerable plaque before it impinges on the lumen, other diagnostic modalities are needed [18-20]. Furthermore, accurate evaluation of the composition or biomechanical characteristics of such plaques could aid in the detection of high-risk lesions.

Several circulating plasma biomarkers related to increased inflammatory burden, platelet activation or endothelial activation correlate with the risk of cardiovascular events both in patients who have previously had an acute coronary event and in apparently healthy individuals [21-28] . Despite these epidemiological results, little data exist on the relation between circulating biomarkers and local biomechanical or other structural characteristics of coronary plaques.

The aim of the IBIS study is to characterize non-flow limiting subclinical coronary lesions by invasive and non-invasive imaging techniques in conjunction with multiple biomarkers.

METHODS

Patients and Study Protocol

From March to November 2003 we enrolled 90 patients in IBIS a prospective, single center, non-randomized, observational study. No formal sample size calculations have been performed. Follow-up will be completed in summer 2004. Patients 18 years of age or older were eligible for inclusion if (1) they presented with stable angina pectoris, documented silent

ischaemia or an acute coronary syndrome (unstable angina pectoris, non ST segment elevation or ST segment elevation myocardial infarction) and (2) they underwent successful percutaneous coronary intervention (PCI) of one or more lesions in the native coronary circulation. Successful PCI was defined as attainment of residual diameter stenosis <20% (visual assessment), TIMI 3 flow and no residual dissection. Exclusion criteria are listed in table 1. Patients who met all the inclusion criteria and none of the exclusion criteria were enrolled. The study was performed in accordance with the principles set out in the Declaration of Helsinki and was approved by the Medical Ethics Committee of the Erasmus MC. All patients gave written informed consent.

A coronary artery, other than the vessel that was the target for percutaneous coronary intervention (PCI), was designated as "the study vessel". In order of preference, the left anterior descending artery (LAD), right coronary artery (RCA) or circumflex artery (CX, including large intermediate branches) were selected. In addition, interrogation of the PCI vessel could be undertaken at the discretion of the investigator. All invasive imaging procedures (coronary angiography, IVUS and palpography) were performed immediately after the PCI procedure or the morning following the PCI (where PCI was performed for STEMI). MSCT was preferably performed prior to invasive imaging; otherwise it was done within 21 days after PCI. Blood samples were obtained, whenever possible, prior to PCI from the arterial sheath before administration of unfractionated heparin. In order to correlate the different imaging techniques, a region of interest (ROI) in the study vessel was defined. This was based on the MSCT scan;

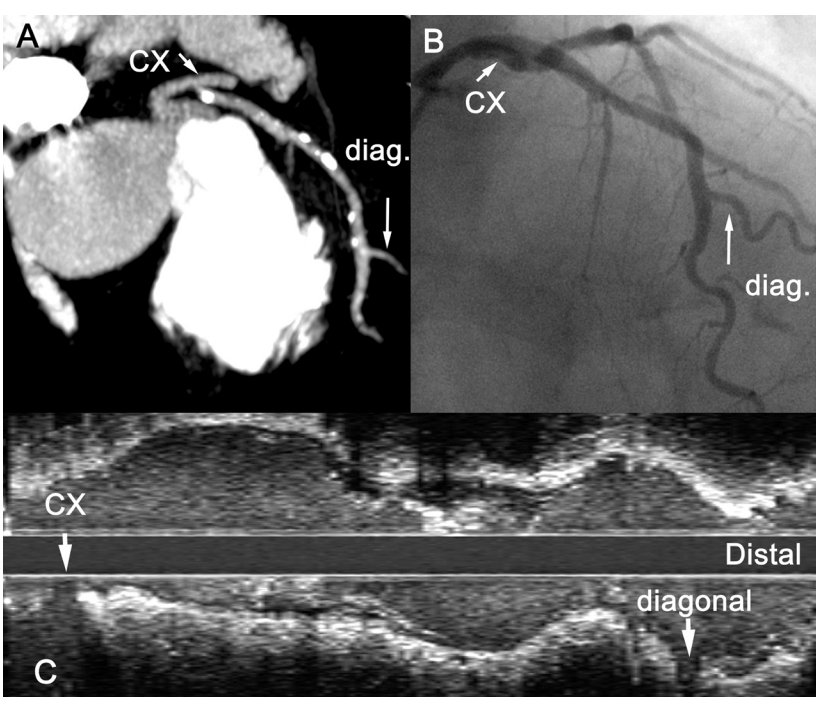

Figure 1. The region of interest (ROI) within the study vessel, in this example the LAD, as determined by MSCT (A) is appropriately matched with the angiographic (B) and IVUS (C) image. This ROI is demarcated by clear distal (in this example the first diagonal branch) and proximal (in this example the ostium of the Cx) anatomical landmarks. LAD = left anterior descending artery; Cx = circumflex artery; diag = diagonal branch.

Table 1. Exclusion criteria

General and clinical criteria
a. Braunwald class IA, IIA, IIIA (unstable angina caused by non¬cardiac illness)
b. Pregnant women or women of childbearing potential who do not use adequate contraception
c. Known allergies to aspirin, clopidogrel bisulfate (Plavix ®), Ticlopidine (Ticlid ®), heparin, stainless steel, copper or a sensitivity to contrast media, which cannot be adequately premedicated
d. Life expectancy of less than one year or factors making clinical and/or angiographic follow-up difficult
e. Planned coronary bypass surgery or major non-cardiac surgery
f. Impaired renal function (creatinine >2 mg/dl or ≥ 150 mmol/L)
g. A history of bleeding diathesis or coagulopathy
h. Previous disabling stroke within the past year
Criteria related to invasive imaging
a. Severe 3-vessel coronary artery and/or left main disease with ≥ 50% stenosis
b. Minimal lumen diameter <2mm in the segments to be analyzed within the study vessel
c. Diameter stenosis >70% or total occlusion of the study vessel
d. In case the study-vessel has been stented previously more than 1/3 (outside the length of the stent plus 5mm proximal and distal to the stent) of the study vessel should be available for examination
e. Ejection fraction ≤ 30%
f. Moderate to severe tortuosity (moderate: 2 bends >75° or one bend > 90°) of the proximal vessel in the segment(s) to be analyzed
g. Known tendency to coronary vasospasm
Criteria related to non-invasive imaging
a. Heart rate>70 beats/minute 1 hour after administration of an oral beta-blocker
b. Contra-indication to iodinated contrast material (e.g. known allergy, serum creatinine ≥150 mmol/L, thyroid disorders)
c. Inability to hold breath for 20 seconds
d. Irregular heart rate (e.g. atrial fibrillation or very frequent PVCs)

a side branch was chosen as the distal boundary of the region of interest and a second side branch, or the ostium of the vessel, as the proximal boundary. An example is provided in Figure 1.

Clinical follow-up visits were scheduled at 3 and 6 months. At each visit, an ECG and blood samples for biomarker analysis were obtained and data collected on clinical events. At 6 months, repeat MSCT was performed, followed by repeat invasive imaging procedures on the study vessel. Whenever clinically-driven angiography was performed before the 3-month follow-up, patients were asked to return for the previously scheduled angiogram at 6 months. When angiography was performed after 3 months follow-up, this angiogram was considered as the final follow-up angiogram. All different invasive imaging techniques (angiography, IVUS, palpography) were repeated at follow-up; when PCI of the "study vessel" was indicated at follow-up, the imaging procedures were performed before intervention. Patients who failed to attend the follow-up visits were contacted by phone or by letter or information was obtained

through the general practitioner, the patient's next of kin or referring cardiologist. The patient was considered lost to follow-up if all these avenues were unsuccessful.

Coronary Angiography

Conventional selective coronary angiography was performed with standard techniques. In order to obtain accurate and reproducible quantitative coronary angiographic (QCA) measurements, each angiogram was preceded by the intra-coronary injection of nitrates (1-3 mg isosorbide dinitrate) and the catheter tip was cleared of contrast. QCA analysis was performed by the core laboratory using the Cardiovascular Angiography Analysis System II algorithm (CAAS II), as previously described in detail [29].

QCA: Definitions

The mean and minimal lumen diameters of the ROI were measured in all individual suitable projections. The average of these values for all available projections was calculated to provide an overall mean and minimal luminal diameter for the ROI diameter. A plaque was defined as luminal narrowing that resulted in ≥20% diameter stenosis within the ROI with respect to the interpolated reference diameter. The reproducibility for QCA has previously been reported [30]. An additional qualitative analysis will be performed on the pre-intervention angiogram(s) to assess the presence and severity of atherosclerosis, based on angiography, in the study population in order to allow comparison of the "total plaque burden" on angiography with that on MSCT. All segments of the coronary tree were analyzed by an independent experienced cardiologist. Each segment was classified as normal (smooth or tapering borders), as atheromatous without an identifiable plaque (<20% diameter stenosis visually), as atheromatous with a distinct but <50% stenosis, as atheromatous with a >50% stenosis but without occlusion or as occluded.

IVUS Imaging

The IVUS catheter used was a commercially available mechanical sector scanner with a 30- or 40-MHz transducer (Ultracross™ 2.9F 30 MHz catheter or CVIS Atlantis™ SR Pro 2.5F 40 MHz catheter, Boston Scientific Corporation, Santa Clara, USA), connected to the Galaxy™ ultrasound console from Boston Scientific. Using an automated pullback device, the transducer was withdrawn at a continuous speed of 0.5 mm/s. Cine runs before and during contrast injection were performed to define the position of the IVUS catheter before the pullback was started. IVUS data were acquired after the intracoronary administration of isosorbide dinitrate and the data were stored on S- VHS videotape. The videotapes were digitized on a computer system, transformed into the DICOM medical image standard and stored on an IVUS Picture Archiving and Communications System (PACS).

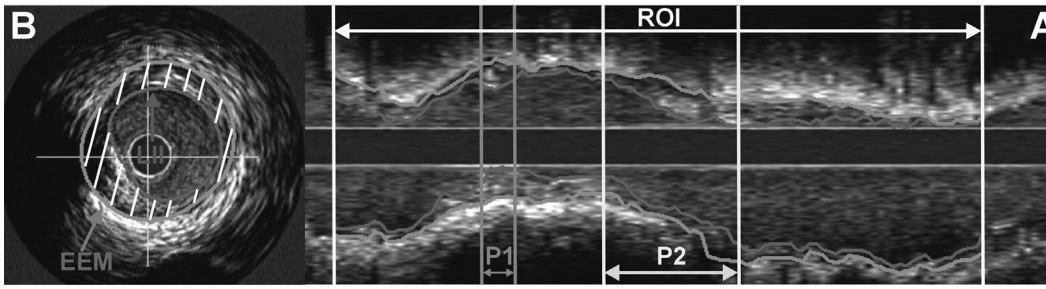

Figure 2. Longitudinal view (A) of the ROI on IVUS, as obtained by the IntelligateTM method [33]. The tissue between the external elastic membrane (EEM), depicted in green, and the lumen-intima interface, depicted in red, is defined as the coronary plaque plus media volume. For the purpose of this study, significant coronary plaque was defined as a plaque that occupied >50% of the area within the EEM. This is indicated in the longitudinal view by P1 (plaque 1) and P2 (plaque 2) and shown in a cross-sectional image of P2 (B). LII = lumen-intima interface. (A full color version of this illustration can be found in the color section).

Quantitative Coronary Ultrasound (QCU) Analysis

QCU analysis was performed by the core laboratory using validated software (Curad, version 3.1, Wijk bij Duurstede, the Netherlands), which allows semi-automated detection of luminal and external elastic membrane boundaries in reconstructed longitudinal planes (L-mode views) [31]. Due to catheter motion during the cardiac cycle, non-gated IVUS pullbacks result in a sawtooth-appearance of the coronary segment on the longitudinal views and thus interfere with the contour detection algorithms used in most QCU software packages. This phenomenon can also lead to inaccurate measurements. In order to obtain a smooth appearance of the vessel wall structures in the longitudinal views, the Intelligate™ image-based gating method was applied [32, 33]. This validated technique eliminates catheter-induced image artefacts, by retrospectively selecting end-diastolic frames, thus resulting in more reliable volumetric measurements. Assuming a heart rate of 60 beats per minute and given a pullback speed of 0.5 mm/sec, the Intelligate™ method selects 2 IVUS frames per mm for data analysis. After performing QCU, the borders of the external elastic membrane (EEM) and the lumen-intima interface enclose a volume that was defined as the coronary plaque plus media volume (Figure 2). The intra- and interobserver variability in our institution for measurements of lumen, EEM and plaque+media cross-sectional area has been reported in a previous study [34]. Because of recent adjustments and improvements in the whole IVUS imaging chain, from catheter until final analysis, the observer-related variability data will again be determined for a subset of patients included in the IBIS study [33, 35].

IVUS plaque characterization: Computer-aided grey-scale analysis

In addition to plaque volume, IVUS also provides information on plaque echogenicity, a potential source of information on plaque composition. The acoustic characterization of a coronary plaque has been investigated by in vitro and in vivo studies that support a role for echogenicity as a predictor of histological plaque composition [18, 36-39]. In the present study, we used a computer-aided grey scale value analysis program for plaque characterization [40]. Using the

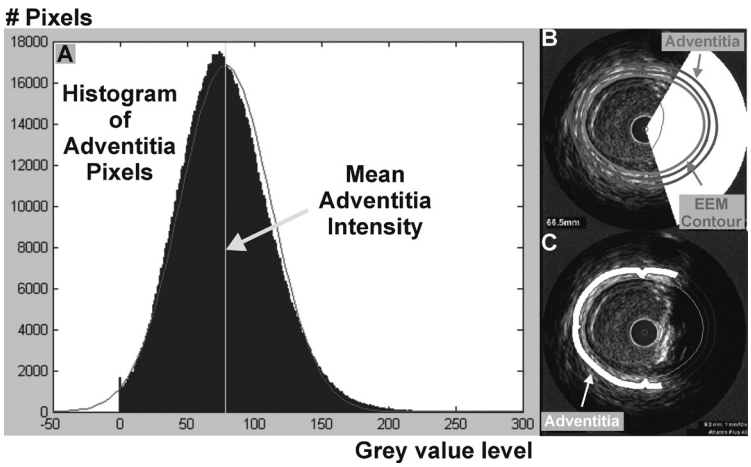

Figure 3. Panel A shows a histogram of the distribution of the grey level intensities of the pixels in the adventitia, which is located outside the EEM contour, in all the cross-sections of the ROI. In order to obtain a reliable reference value, parts of the adventitia with reduced intensity, due to acoustic shadowing, are excluded. When the distribution of the grey values in the histogram follows a normal distribution, shown here as a red line, the ultrasound images can be reliably used for image based tissue characterization. An example of a calcified plaque with acoustic shadowing of the adventitia is provided in panel B and C. The non-shadowed part of the adventitia is colored white (panel C). (A full color version of this illustration can be found in the color section).

mean grey level of the adventitia as a threshold, 5 main tissue types can be characterized (Figure 3): (1) hypoechogenic tissue has a mean grey level lower than that of the adventitia, (2) hyperechogenic tissue, defined as tissue with a mean grey value higher than that of the adventitia, (3) calcified tissue, defined as a tissue with a mean grey value higher than that of the adventitia with associated acoustic shadowing, (4) unknown tissue, defined as tissue shadowed by calcification and (5) "upper" tissue, defined as tissue that has a mean grey value higher than the mean adventitial intensity plus two times its standard deviation but is not typical calcified tissue with acoustic shadowing. An example of a recording illustrating some of the types of tissue described is presented in Figure 4.

Plaque Size and Composition by IVUS: Definitions

For the purpose of the IBIS protocol, significant plaque was defined as the presence of echolucent media and echogenic plaque area that resulted in a ≥50% reduction in the cross-sectional area circumscribed by the external elastic membrane (EEM). Plaque composition was classified, as defined previously, based on tissue echogenicity. Plaque within the ROI was considered calcified if it contained calcium in at least 2 consecutive cross-sections (0.5mm < calcified plaque <1mm) and was scored in a binary fashion.

Palpography

Intravascular palpography is a new parametric imaging technique based on IVUS that assesses the local mechanical properties of the vessel wall and plaque. The underlying principle is that soft material will deform more compared with hard material when force is applied to the tissue. The naturally occurring pulsatile arterial pressure provides the force. The relative deformability of coronary plaque components can be estimated by measuring the relative displacements of radiofrequency (RF) signals, recorded during IVUS acquisition, at 2 differ-

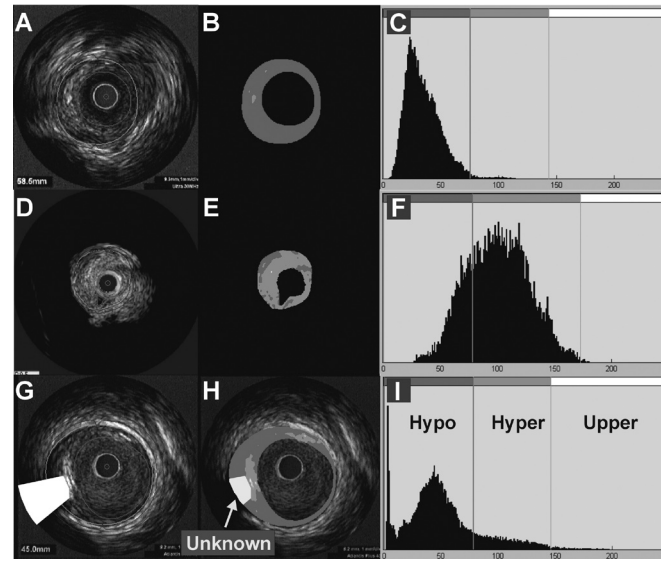

Figure 4. Examples of tissue types as defined by the computer-aided grey scale analysis program. Panels a, d and g show the delineation of the lumen-intima (red), EEM (green) and adventitia (blue). Panels b, e and h are the corresponding cross sections and depict the different tissue types in different colors: red structures are hypoechogenic; green spots are hyperechogenic. Panel h also explains the principle of unknown tissue, colored yellow: tissue that cannot be characterized due to acoustic shadowing from calcium.
The histograms (c, f, i panels) are divided in three portions, each portion showing the main tissue type of the plaque. Panel c, the majority of the plaque is located in the left portion of the histogram and is therefore hypoechogenic. Panel f, example of a hyperechogenic plaque. Panel i, example of a mainly hypoechogenic plaque, with a rim of calcium. (A full color version of this illustration can be found in the color section).

ent pressure levels [41]. Post-processing of RF signals derives data regarding deformation of the tissue and allows the construction of a "strain" image in which "harder" (low strain) and "softer" regions (high strain) can be identified. The local strain is displayed color-coded from blue for 0% strain via red to yellow for 2% strain as a complementary image to the IVUS echogram (Figure 5) [42]. The resolution of the strain measurement in the radial direction is 200 μm. In vitro and in vivo studies have validated the technique and found higher strain values in fatty as compared to fibrous plaques [19, 41, 43]. A recent in vitro study demonstrated the diagnostic potential of palpography to identify thin cap fibroatheromas [42].

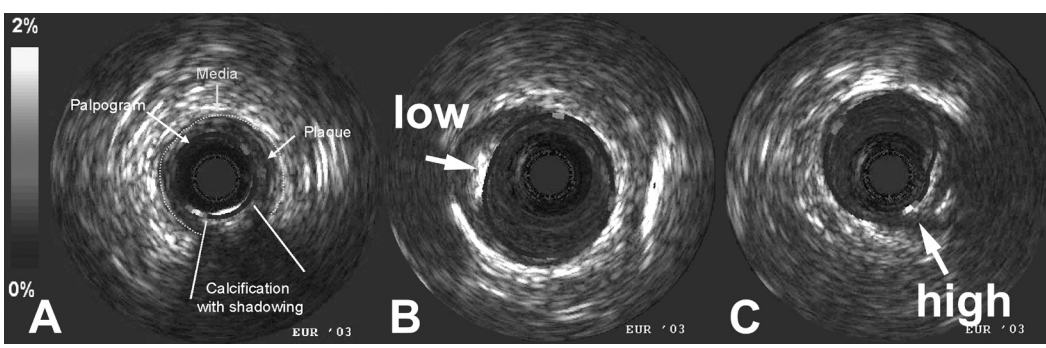

Figure 5. A, the intravascular palpogram is superimposed on the IVUS image. This technique measures the deformation of the underlying vessel wall and plaque in the radial direction. The resulting strain values are plotted as a color-coded contour at the lumen vessel boundary.
B is an example of a plaque with a low strain on the surface. C shows a plaque with high strain. (A full color version of this illustration can be found in the color section).

All data in IBIS were acquired using a 20 MHz Jovus Avanar F/X IVUS catheter (Volcano, Rancho Cordova, CA, USA), which was connected to an InVision Gold IVUS console. Recordings were obtained at a pullback speed of 1 mm/sec using a mechanical pullback device (Trackback II, Volcano, Rancho Cordova, CA, USA). Simultaneously, the ECG and intraluminal pressure signals were recorded. Acquisition was done with a custom made dedicated workstation connected to the digital interface of the IVUS machine. Each acquisition was stored on a separate DVD. Processing and analysis of the data was done independently by observers unaware of the results of the other techniques. The reproducibility of three-dimensional palpography at our institution has been recently reported [44].

Palpography: Definitions

The strain value that best discriminates a plaque at risk of rupture has a threshold of 1.26% [42]. Strain values were classified according to the ROC classification (ROtterdam Classification) as low strain spots (ROC I: 0.0 - <0.6%), moderate strain spots (ROC II: 0.6 - <0.9%), medium strain spots (ROC III: 0.9 - <1.2%), or high strain spots (ROC IV: >1.2%).

Multislice Spiral Computed Tomography (MSCT)

Intravenous contrast injection with multislice coronary tomography allows non-invasive visualization of coronary arteries including visualization and evaluation of non-calcified and calcified plaques [45, 46]. Patients with resting heart rates >65 beats/minute received a single oral dose of 100 mg metoprolol (SelokeenÒ, AstraZeneca Pharmaceuticals, UK), one hour prior to the MSCT scan. All scans were performed using a true 16-row detector MSCT scanner (Sensation 16, Straton) with a gantry rotation time of 375 ms. Other scan parameters were: 16 x 0.75 detector collimation, table feed 3.0 mm/rotation, tube voltage 120 kV, tube current 500-600 mAs. A bolus of 140 ml Iodixanol with an Iodine content of 320 mgI/ml (Visipaque 320, Amersham Health, UK) was intravenously injected in an antecubital vein at 4 ml/s. A bolus tracking technique was used to synchronize the arrival of contrast material inside the coronary arteries and the start of the scan: a ROI was positioned inside the ascending aorta and the mean density within the ROI was monitored at intervals of 1.25 ms after the start of the injection. The patient was instructed, via an automated prerecorded message, to perform a breath hold when the mean density reached a predefined threshold (+100 HU), and the scan started 4 s later. All data were acquired during a single breath hold of 20 seconds, and images were reconstructed using retrospective ECG gating. An image reconstruction algorithm was used, which uses data obtained in half gantry rotation time resulting in a temporal resolution of up to 188 ms. To obtain motion-free images, standard reconstruction windows were selected during the mid-to-end diastolic phase (350, 400, and 450 ms prior to the next R-wave), but additional image reconstruction windows were explored when deemed necessary. The dataset with least motion-artefacts was selected and loaded into an off-line workstation (Leonardo, Siemens, Forchheim, Germany). Then, a ROI in the study vessel was selected on multiplanar

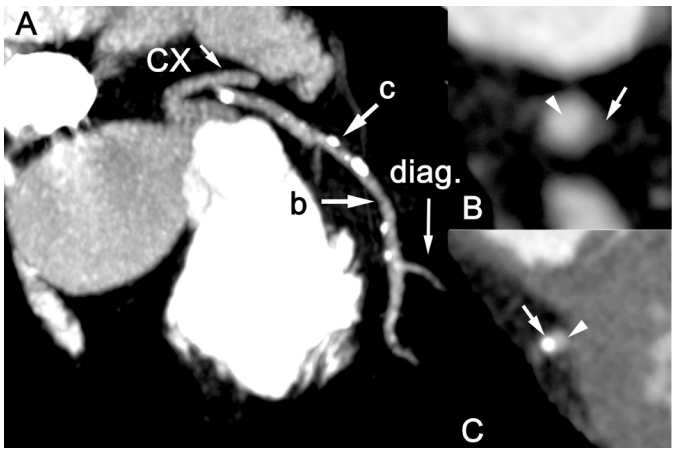

Figure 6. (A), using the same region of interest as in Figure 1, different plaque types can be identified on MSCT. (B), cross-section at location 1, showing noncalcified plaque (23 HU). (C), cross-section at location 2, showing calcified plaque (579 HU).

reconstructed (MPR) images, using easily identified anatomic landmarks (sidebranches or the ostium). Thereafter, the dataset was loaded into a semi-automated vessel-tracking software program and a central lumen line was created throughout the ROI. Ten, twenty, or thirty cross-sectional MPR images (depending on the length of the ROI) were reconstructed orthogonal to this central lumen line, and used for image analysis. A cardiologist and a radiologist, unaware of the results of other imaging modalities, independently evaluated the cross-sectional images. Disagreements were resolved by consensus. The image quality of all cross-sectional images was classified as reliable, adequate, or unreliable. Images with unreliable image quality were excluded from further analysis.

MSCT: Definitions

Reliable cross-sectional MSCT images were visually evaluated for the presence of plaque; plaque was further classified based on size - as small, medium, or large- and composition - non-calcified, calcified, or mixed. A plaque was defined as a visually apparent abnormal space-occupying lesion, within the wall of the coronary artery that was clearly distinguishable both from the adjacent epicardial fat and from the coronary lumen. The mean Hounsfield unit (HU) of a plaque was defined as the average HU of the individual cross-sections with plaque.

Plaque size was further classified, based on their measured maximal thickness, as small (<1 mm), medium (1-2 mm), or large (>2 mm). Plaque was defined as calcified if it contained high-density (>130 HU) components (Figure 6). Plaque tissue with both calcified and non-calcified components was classified as mixed. HU of non-calcified and calcified tissue components were measured in all cross-sections with medium and large plaques by positioning a ROI as far as possible from the lumen and adjacent epicardial fat. The k-values in our institution for inter- and intra-observer agreement regarding plaque size, using the 16-row detector MSCT scanner, have been determined in a group of 78 patients and are 72% and 74% respectively.

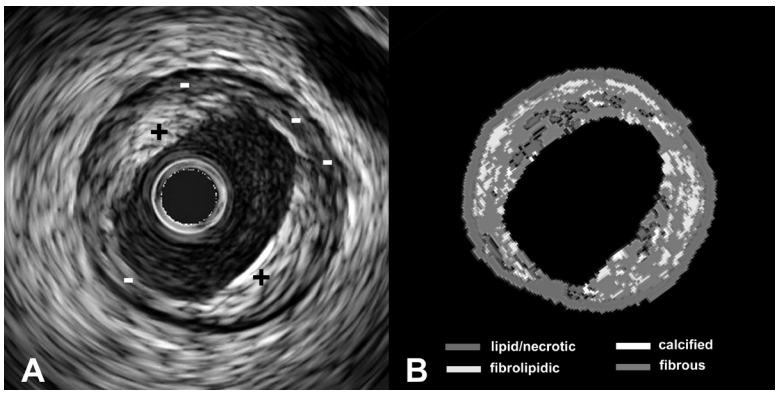

Figure 7. Atheroma morphology by IVUS (A) and IVUS virtual histology (VH) (B).
A, Concentric plaque with soft (-) and fibrous (+) components. B, The same cross-section in IVUS VH shows that this plaque has a more heterogeneous composition: fibrous (green), fibrolipidic (light green), lipid core (red) and calcified (white) components can be identified. (A full color version of this illustration can be found in the color section).

Finally, the total plaque burden of the entire coronary tree was assessed on MSCT. All coronary segments were assessed. Where not possible (vessel <2mm, vessel segment distal to an apparent total occlusion, motion or other artefact rendering interpretation unreliable), this was noted. Plaque was defined as mentioned above and was further classified as non-calcified, mixed, or calcified. Where MSCT was performed after the intervention, evaluation of plaque burden in the stented segments was obviously not possible. In these patients, an independent observer assessed the preintervention coronary angiogram as follows: the segments that had been stented were scored, by imputation. The segment(s) that were the site of the culprit lesion were classified as having a large plaque. In some patients, segments that were stented had no significant stenosis on angiography. This mainly reflected our practice of stenting from "normal" to "normal" with drug-eluting-stents; in other situations, multiple stents were implanted to cover a dissection or to protect a compromised side branch. These segments were considered as non-assessable for the presence of plaque. Qualitative assessment for calcium was performed, as described above, in all stented segments.

IVUS Virtual Histology (IVUS-VH): an IBIS Substudy

IVUS VH is an intravascular ultrasound derived technique that analyses the radiofrequency component of the reflected ultrasound signal. As compared with standard IVUS, this imaging modality has the potential for more detailed assessment of different plaque components. In preliminary in vitro studies, four plaque types (fibrous, fibrolipidic, lipid core and calcium) as defined by histology could be correlated with a specific spectrum of the radiofrequency signal [47, 48]. The different plaque components are assigned colour codes: fibrous, fibrolipidic, lipid core and calcified regions are labelled green, light green, red and white, respectively (Figure 7). This technique, given its ability to identify lipid-rich plaques, could be of great value in identifying potentially vulnerable plaque.

IVUS VH derives its data from the RF output of a conventional IVUS console and is ECG-gated for accurate data analysis. Since validation of the technique so far only exists for a 30 MHz system, the same 30 MHz IVUS catheter, used for the acquisition of the IVUS data, was utilized. The RF and ECG signal were transferred from the Boston Scientific console to a dedicated IVUS VH (Volcano) platform. The IVUS VH data were stored on a CD-ROM and sent to the Imaging Core Lab at Cardialysis for offline analysis by one independent observer.

IVUS Virtual Histology: Definitions and Endpoints

In analogy with QCU, the tissue in between the EEM and lumen-intima interface was defined as the coronary plaque plus media. Classification of the coronary plaque into its 4 components within the ROI was assessed independently from the media. Since IVUS VH was not incorporated at the start of the IBIS protocol, the results of this technique will only be reported as a substudy. The primary endpoints of this substudy are: (1) the volumetric correlation with QCU, (2) the correlation of the different plaque components with clinical presentation and biomarkers, (3) the correlation between plaque composition and strain pattern observed on palpography. Furthermore, the design of the IBIS study provides the means to address changes in plaque composition.

Biomarker and Blood Analysis

Cardiac enzymes (including troponin), hemoglobin, hematocrit, red blood cell (RBC) count, white blood cell (WBC) count, platelet count, urea, creatinine, total cholesterol, HDL cholesterol (HDL-C) and triglycerides were analyzed by the local laboratory. Plasma concentration of LDL cholesterol (LDL-C) was calculated by the use of the Friedewald formula [LDL-C= total cholesterol minus HDL-C minus (triglycerides/5)].

Plasma and sera used for biomarker analysis was centrifugally separated within 30 minutes of draw and stored at -70C. Analytes were measured using commercial ELISA kits from R&D Systems except where noted. Plasma high sensitivity interleukin 6 (hs IL-6), tumor necrosis factor alpha (TNFa), serum high sensitivity C-reactive protein (hsCRP- Diagnostic Systems Laboratories), lipoprotein phospholipase A2 ($LpPLA_2$- GSK), ultrasensitive pregnancy associated plasma protein A (PAPP-A-Diagnostic Systems Laboratory), matrix metalloproteinase 9 (MMP-9), soluble CD40L (sCD40L- Bender MedSystems) and monocyte chemoattratact protein (MCP-1), were measured in the Human Biomarker Centre, GlaxoSmithKline, using protocols provided by the manufacturer. Results from the standardized ELISA assays were measured on a MRX Revelation microplate reader with 4.2 software. Plasma LpPLA2 activity assay measures the proportional release of aqueous ^3H acetate resulting from the enzymatic cleavage of the ^3H acetyl-platelet activating factor substrate using methodology developed at GlaxoSmithKline. All simple analyses were done in batches representing the three time points (baseline, 3 and 6 months follow-up). Internally developed matrix matched or kit provided

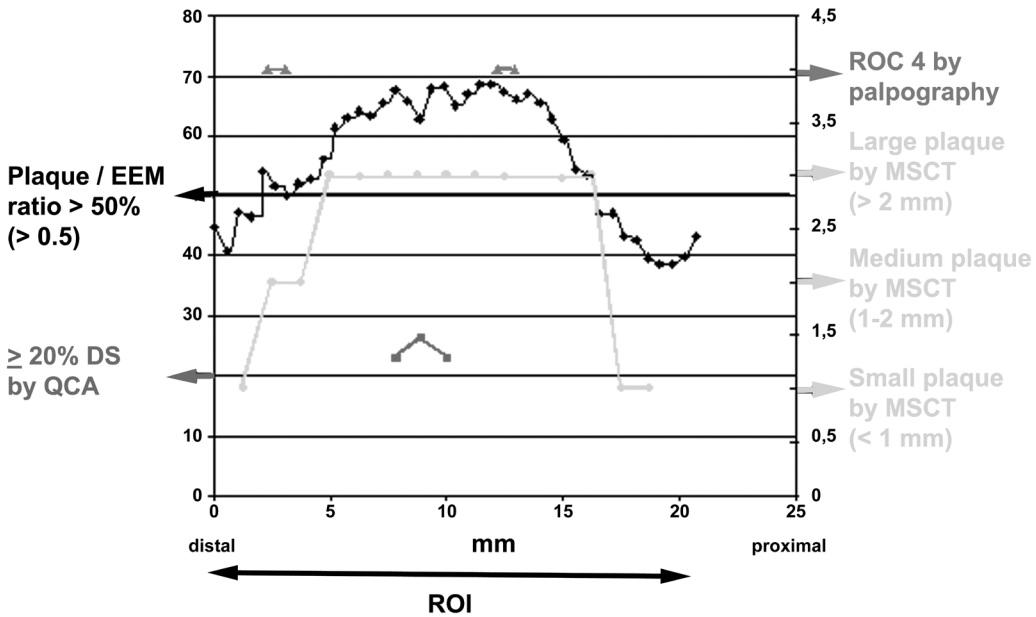

Figure 8. Integration of the different imaging modalities, used in IBIS, into one graph provides a more comprehensive view on coronary atherosclerosis. Visualizing the same coronary artery segment, it becomes clear that the coronary angiogram grossly underestimates the coronary plaque burden: a significant amount of plaque on IVUS (plaque/ EEM ratio > 50%) and MSCT (plaque thickness > 2mm) produces only a mild lumen reduction on angiography. The palpogram provides additional information on the plaque surface: in this patient two high strain areas (ROC 4) were identified. The ROI is shown in the x-axis (in this patient 22 mm). The percent EEM-area reduction (on IVUS) and diameter reduction (on angiography) is depicted on the left y-axis. The right y-axis visualizes the plaque thickness in mm (MSCT) and the ROC score (palpography). Distal and proximal indicate the distal and proximal reference point in the coronary artery, with respect to the coronary ostium. (A full color version of this illustration can be found in the color section).

controls were incorporated to ensure consistency in the assay performance. NT pro BNP was measured in EDTA plasma by Quest Diagnostics using a two-site electrochemiluminescent assay. The lipoprotein subclass distribution was analyzed by Liposciences Inc. using NMR based technology. The analysis provided to us for the IBIS trial used the newest NMR LipoProfile II methodology.

In addition, serum batched by patient sets from all baseline and follow-up visits, were measured using an analyte defined (closed format) protein chip. Protein chips provide capability for the analysis of between 10 to 157 different chemokines, cytokines and growth factors depending on the platform. Our analyses to date include the Zyomyx™ protein chip. The limits of quantification for the above analytes are as follows: 2.5 uIU/mL for PAPP-A, 0.18 ng/mL for MMP-9, 0.0048 mg/L for CRP, 6.31 pg/mL for MCP-1, 0.78 ng/mL for sCD40L, 0.057 pg/mL for IL-6, 0.88 pg/mL for TNF-α, and 3.92 nmols/min/mL for $LpPLA_2$ activity.

Off-line Analysis of Imaging Techniques: Principles and Resolution of Problems

No previous study has attempted to identify and characterize either coronary atherosclerosis or potentially vulnerable coronary plaques with such a wide range of invasive and non-invasive imaging techniques (Figure 8) in conjunction with multiple analyses of classic and novel biomarkers.

In the present study all imaging techniques were analyzed independently. The QCA and QCU were performed by an independent Core Lab (Cardialysis) using standard operating procedures and validated methodology. The IVUS based tissue echogenicity, palpography, and MSCT analyses were performed independently by the research groups that developed or refined the techniques in our institution.

Ideally, we aimed to study a common ROI ≥30 mm long for all techniques. This was possible for the majority of patients but specific difficulties related to each technique required either a redefinition of the original ROI, before database lock, or the use of a shorter ROI within the initially defined region, in some patients. For all patients, the initial ROI was to be determined on MSCT. However, in some cases the landmarks on MSCT were not identifiable on IVUS. This primarily occurred in the RCA when the ostium was chosen as a landmark on MSCT but was not reliably identified on IVUS because the distal tip of the guiding catheter was within the coronary artery. In a few cases, the ROI could not be determined on MSCT. This was mainly related to uninterpretable images due to artefact related to high heart rates, irregular heart rates, or cardiac motion (exclusively in the RCA). Finally, in some cases, MSCT was not performed.

Imaging Techniques: Parameters Measured at Baseline

IVUS

Mean plaque area in the ROI as defined by QCU was used for comparisons among imaging techniques and for exploratory analyses on the relation between clinical and biological variables and the extent of subclinical atheroma in the ROI. To this end, mean plaque area (MPA) was calculated as the difference between mean total vessel area (A_{TV}) and mean total lumen area (A_{TL}). Total plaque volume (TPV) was calculated as the sum of the differences between external elastic membrane (EEM) and lumen areas across all frames in the region of interest [49] .The plaque variables we measured and their definitions are presented in Table 2. Calcified plaque was measured in the ROI based on the presence or absence of calcium in each 5 mm segment.

Table 2. IVUS coronary plaque measurements

Volumetric variables (mm^3)

Absolute plaque volume (mm^3)

Total plaque volume (TPV) = $\sum$ (EEMCSA – LUMENCSA)

Relative (percent) plaque volume (%)

Relative plaque volume (RPV) = $\frac{\sum (EEM_{CSA} - LUMEN_{CSA})}{EEM_{CS}} \times 100$

Area variables (mm^2)

Mean plaque area (MPA) = Mean total vessel area (ATV) – mean total lumen area (ATL)

MSCT

The ROI was subdivided into 5 mm segments. Each 5 mm segment was classified as plaque free or as containing a small, medium, or large plaque. Each plaque was classified as non-calcified, calcified, or mixed. Finally the longitudinal extent of calcium was expressed as an integer score based on the presence or absence of calcium in each 5 mm segment.

Comparison of QCU with MSCT

Based on QCUderived measurements of coronary atheroma (i.e. plaque and media), the ability of MSCT to detect coronary plaques resulting in ≥50% EEM area reduction and to detect calcification was assessed. To ensure that the same plaques were assessed by the different techniques and to allow correlations, the ROI within the study vessel was subdivided into 5 mm segments as outlined above. The QCU and MSCT data were compared in corresponding 5 mm segments in the ROI.

Using these definitions, the ability of MSCT to detect plaque (binary classification; plaque present or absent) was compared with that of IVUS (binary classification, coronary plaque area ≥50% of the area enclosed by the EEM, yes/no). The effect of the presence or absence of calcium detected on IVUS on the specificity and sensitivity of MSCT plaque detection was also assessed, using a binary classification: calcium present/absent on MSCT or IVUS within the 5 mm segments.

QCA

The overall mean and minimal lumen diameters of the ROI were measured. The number of plaques, defined as luminal narrowing that resulted in ≥20% diameter stenosis within the ROI, was also assessed.

Tissue Echogenicity

The major variables measured using the tissue echogenicity program were absolute hypo-echogenic and hyper-echogenic plaque volume (mm^3). Other variables measured, defined in the methods section, were upper volume and unknown volume (mm^3). These variables were also assessed for contiguous 5 mm segments within the ROI.

Palpography

The number of ROC III and IV scores was measured in the ROI and in individual 10 mm segments of the ROI (ROC 3/4 density).

Safety

The occurrence of Major Adverse Cardiac and Cerebral Events (MACCE) was assessed after the procedure, at discharge, and at 3 and 6 months, as were the individual components: death, MI, revascularization by PCI or CABG, hospitalization for ischaemia and/or anginal symptoms, and stroke. They were classified, where possible, as related to the "study vessel", the PCI vessel, or a non-PCI/non-study-vessel. The definition of myocardial infarction was identical to that defined in the ACC/ESC joint document on the redefinition of myocardial infarction [50]. Major bleeding and vascular complications were also prospectively recorded using standard definitions [51].

Statistics

For the comparison between and within techniques for each patient, for each analysis technique, and each time point, the same ROI, selected by the Core Lab, will be studied. Comparisons between techniques and within techniques (baseline versus follow-up) will be performed with use of either two-by-two tables (sensitivity, specificity) for qualitative outcomes or linear regression analysis (regression coefficient, scatter plots) for quantitative outcomes. For the analysis on a per patient level, including biomarkers, clinical parameters, and imaging technique results, the data will be summarized by vessel (ROI) and for 5 mm increments of the ROI. For each 5mm increment in each technique it was judged whether or not plaque could be detected. On the vessel level, plaque was defined as plaque in any of the 5 mm increments of the ROI. Circulating biomarkers will be correlated with imaging endpoints using the univariate Pearson correlation coefficients. We will also use Box and Whisker plots to compare biomarker distributions in predefined subgroups of the study population (diabetic status, anginal status, etc). Statistical analyses will be performed with use of SAS Version 8.

Discussion

Coronary atherosclerosis remains one of the major causes of mortality and morbidity in the Western Hemisphere. Advances in medical research have resulted in the introduction of new pharmacological agents that have significantly contributed to our ability to decrease the risk

of clinical events related to atherosclerosis. Furthermore, the discipline of interventional cardiology has evolved from an experimental technology that was an option in highly selected patients to a discipline that complements and may soon largely replace coronary artery bypass surgery.

In parallel, advances in our understanding of the mechanisms underlying atherosclerosis have clearly demonstrated that clinical events are not necessarily related to the severity of luminal narrowing in large epicardial coronary arteries. The potential contribution of a low-grade inflammation, infectious agents, genetic factors, and other putative mechanisms to the occurrence of atherosclerosis-related clinical events is the subject of intense investigation.

Finally, the recognition that death or myocardial infarction is often related to plaque rupture at the site of non-flow limiting subclinical atherosclerosis has evolved into the concept of the vulnerable atherosclerotic plaque. Post-mortem studies have shown that plaque rupture at the site of thin-cap fibroatheromas is the most common mechanism that leads to death from atherosclerosis. However, it has also been clearly shown that such ruptures often remain clinically silent and contribute to lesion progression. As atherosclerosis is a diffuse process that involves many vascular beds and several sites within the coronary vasculature, better identification of plaque compositional characteristics is needed. The quest to identify reliable technique(s) to detect plaques that are at high risk of causing future clinical events is currently the subject of intense research activity. Ideally, biomarkers in peripheral blood, singly or in combination, could be used to identify patients at risk for new or recurrent clinical events such as sudden death or acute myocardial infarction. Appropriate non-invasive or invasive techniques could then be used to further refine risk stratification.

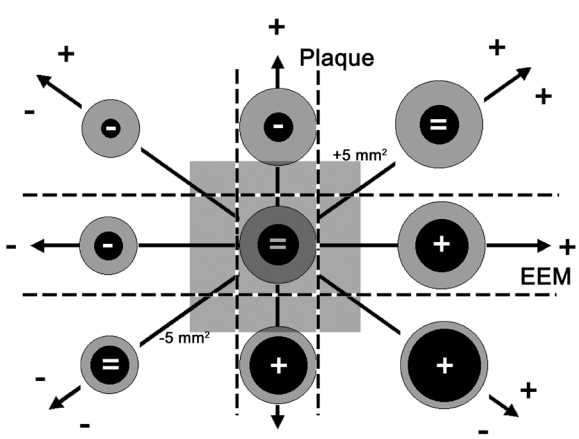

Figure 9. Schematic outline of the remodeling process in coronary atherosclerosis, as assessed by IVUS. In theory nine remodeling patterns can be defined, as depicted. Determinants of the coronary artery lumen diameter are the change in plaque size and the process of vascular remodeling, which is the change in the size of an artery over time. The change in the vascular lumen is indicated in the figure by the + (increase), - (decrease) or = (unchanged) signs.
By taking into account the, still to be determined, observer related variability of the IVUS data in this study, as indicated by the (hypothetical) dotted lines, the natural history of the remodeling process can be defined for the IBIS population. The shaded box in grey indicates a change of 5 mm² along the x- and y-axis.

The aim of the IBIS study is to evaluate the feasibility and safety of both invasive (quantitative coronary angiography, intravascular ultrasound with tissue echogenicity and palpography) and non-invasive (multislice spiral computed tomography) imaging techniques to characterize non-flow limiting coronary lesions. The performance of MSCT to identify and characterize coronary plaque will be directly compared with that of IVUS, the current gold standard. Multiple classical and novel biomarkers will be measured and their levels will be correlated with the results of the different imaging techniques. In addition, the potential utility of novel techniques such as tissue echogenicity and palpography will be evaluated.

Beyond these specific goals, the longitudinal character of the IBIS study will be utilized to assess the natural history of arterial remodeling (Figure 9). Serial studies, like IBIS, that measure changes in vessel area at the same site over time are the ideal way to assess the remodeling process since they are not subjected to the limitations of using a reference site [52, 53]. A few IVUS studies with serial long-term (≥ 12 months) follow-up in patients with atherosclerotic coronary artery disease have recently been reported [54, 55].They substantiate the earlier knowledge that changes in the arterial lumen correlate more closely with the direction and magnitude of the remodeling process than with plaque size.

Study Limitations

We used 2 different IVUS catheters in the present study. During the first 3 months of patient inclusion IVUS imaging was done using a 40-MHz catheter; all subsequent baseline and all follow-up analyses were done using the 30-MHz system. This approach was driven by the decision to include IVUS VH as an additional imaging technique 3 months after the start of the IBIS study. Ideally, the same IVUS catheter used at baseline should again be selected for the follow-up procedure. However, since both IVUS catheters were operated on the same display system (Galaxy™console, Boston Scientific), this should not affect IVUS measurements [35].

Plaque assessment by MSCT was based on visual evaluation. While automated programs with the possibility of manual contour correction, such as used for QCA and IVUS, are under development for MSCT imaging, none are currently available for use.

IVUS examinations performed with a 40-MHz IVUS catheter will not be used for evaluation by IVUS VH since validation only exists for the 30-MHz system.

Where the initial ROI on MSCT could not be used for correlation with the other imaging techniques due to a problem with the identification of the landmarks, a new ROI was defined on MCST by the Core Lab in conjunction with an independent cardiologist, familiar with but not involved in the analysis of the various techniques. Where MSCT was not performed or

could not be interpreted, a ROI was defined on IVUS using proximal and distal anatomic landmarks.

Acknowledgement
This study was supported by an unrestricted educational grant from GlaxoSmithKline.

REFERENCES

1. Ambrose JA, Tannenbaum MA, Alexopoulos D, Hjemdahl-Monsen CE, Leavy J, Weiss M, et al. Angiographic progression of coronary artery disease and the development of myocardial infarction. J Am Coll Cardiol 1988; 12(1): 56-62.
2. Haft JI, Haik BJ, Goldstein JE, Brodyn NE. Development of significant coronary artery lesions in areas of minimal disease. A common mechanism for coronary disease progression. Chest 1988; 94(4): 731-6.
3. Little WC, Constantinescu M, Applegate RJ, Kutcher MA, Burrows MT, Kahl FR, et al. Can coronary angiography predict the site of a subsequent myocardial infarction in patients with mild-to-moderate coronary artery disease? Circulation 1988; 78(5 Pt 1): 1157-66.
4. Falk E, Shah PK, Fuster V. Coronary plaque disruption. Circulation 1995; 92(3): 657-71.
5. Kullo IJ, Edwards WD, Schwartz RS. Vulnerable plaque: pathobiology and clinical implications. Ann Intern Med 1998; 129(12): 1050-60.
6. Naghavi M, Libby P, Falk E, Casscells SW, Litovsky S, Rumberger J, et al. From vulnerable plaque to vulnerable patient: a call for new definitions and risk assessment strategies: Part II. Circulation 2003; 108(15): 1772-8.
7. Naghavi M, Libby P, Falk E, Casscells SW, Litovsky S, Rumberger J, et al. From vulnerable plaque to vulnerable patient: a call for new definitions and risk assessment strategies: Part I. Circulation 2003; 108(14): 1664-72.
8. Schaar JA, Muller JE, Falk E, Virmani R, Fuster V, Serruys PW, et al. Terminology for high-risk and vulnerable coronary artery plaques. Eur Heart J 2004; 25(12): 1077-82.
9. Virmani R, Kolodgie FD, Burke AP, Farb A, Schwartz SM. Lessons from sudden coronary death: a comprehensive morphological classification scheme for atherosclerotic lesions. Arterioscler Thromb Vasc Biol 2000; 20(5): 1262-75.
10. Ross R. Atherosclerosis is an inflammatory disease. Am Heart J 1999; 138(5 Pt 2): S419-20.
11. Kolodgie FD, Burke AP, Farb A, Gold HK, Yuan J, Narula J, et al. The thin-cap fibroatheroma: a type of vulnerable plaque: the major precursor lesion to acute coronary syndromes. Curr Opin Cardiol 2001; 16(5): 285-92.
12. Libby P. Inflammation in atherosclerosis. Nature 2002; 420(6917): 868-74.

13. Libby P, Ridker PM, Maseri A. Inflammation and atherosclerosis. Circulation 2002; 105(9): 1135-43.
14. Davies MJ. Stability and instability: two faces of coronary atherosclerosis. The Paul Dudley White Lecture 1995. Circulation 1996; 94(8): 2013-20.
15. Kolodgie FD, Gold HK, Burke AP, Fowler DR, Kruth HS, Weber DK, et al. Intraplaque hemorrhage and progression of coronary atheroma. N Engl J Med 2003; 349(24): 2316-25.
16. Glagov S, Weisenberg E, Zarins CK, Stankunavicius R, Kolettis GJ. Compensatory enlargement of human atherosclerotic coronary arteries. N Engl J Med 1987; 316(22): 1371-5.
17. Schoenhagen P, Ziada KM, Vince DG, Nissen SE, Tuzcu EM. Arterial remodeling and coronary artery disease: the concept of "dilated" versus "obstructive" coronary atherosclerosis. J Am Coll Cardiol 2001; 38(2): 297-306.
18. Nissen SE, Yock P. Intravascular ultrasound: novel pathophysiological insights and current clinical applications. Circulation 2001; 103(4): 604-16.
19. de Korte CL, Pasterkamp G, van der Steen AF, Woutman HA, Bom N. Characterization of plaque components with intravascular ultrasound elastography in human femoral and coronary arteries in vitro. Circulation 2000; 102(6): 617-23.
20. de Feyter PJ, Nieman K, van Ooijen P, Oudkerk M. Non-invasive coronary artery imaging with electron beam computed tomography and magnetic resonance imaging. Heart 2000; 84(4): 442-8.
21. Ross R. Atherosclerosis--an inflammatory disease. N Engl J Med 1999; 340(2): 115-26.
22. Pearson TA, Mensah GA, Alexander RW, Anderson JL, Cannon RO, 3rd, Criqui M, et al. Markers of inflammation and cardiovascular disease: application to clinical and public health practice: A statement for healthcare professionals from the Centers for Disease Control and Prevention and the American Heart Association. Circulation 2003; 107(3): 499-511.
23. Ridker PM, Rifai N, Rose L, Buring JE, Cook NR. Comparison of C-reactive protein and low-density lipoprotein cholesterol levels in the prediction of first cardiovascular events. N Engl J Med 2002; 347(20): 1557-65.
24. Ridker PM. Clinical application of C-reactive protein for cardiovascular disease detection and prevention. Circulation 2003; 107(3): 363-9.
25. Ridker PM, Hennekens CH, Roitman-Johnson B, Stampfer MJ, Allen J. Plasma concentration of soluble intercellular adhesion molecule 1 and risks of future myocardial infarction in apparently healthy men. Lancet 1998; 351(9096): 88-92.
26. Biasucci LM, Vitelli A, Liuzzo G, Altamura S, Caligiuri G, Monaco C, et al. Elevated levels of interleukin-6 in unstable angina. Circulation 1996; 94(5): 874-7.

27. Cesari M, Penninx BW, Newman AB, Kritchevsky SB, Nicklas BJ, Sutton-Tyrrell K, et al. Inflammatory markers and onset of cardiovascular events: results from the Health ABC study. Circulation 2003; 108(19): 2317-22.
28. Bayes-Genis A, Conover CA, Overgaard MT, Bailey KR, Christiansen M, Holmes DR, Jr., et al. Pregnancy-associated plasma protein A as a marker of acute coronary syndromes. N Engl J Med 2001; 345(14): 1022-9.
29. de Feyter PJ, Serruys PW, Davies MJ, Richardson P, Lubsen J, Oliver MF. Quantitative coronary angiography to measure progression and regression of coronary atherosclerosis. Value, limitations, and implications for clinical trials. Circulation 1991; 84(1): 412-23.
30. Reiber JHC, Van Der Zwet PM, Koning GH, Von Land CD, Van Meurs B, Gerbrands JJ, et al. Accuracy and precision of quantitative digital coronary arteriography; observer-, as well as short- and medium-term variabilities. In: Serruys PW, Foley DP and de Feyter PJ, editors. Quantitative coronary angiography in clinical practice. Dordrecht: Kluwer Academic Publishers; 1994:7-26.
31. Hamers R, Bruining N, Knook M, Sabate M, Roelandt JRTC. A novel approach to quantitative analysis of Intravascular Ultrasound Images. In: Computers in Cardiology; 2001; 28: 589-592.
32. Bruining N, von Birgelen C, de Feyter PJ, Ligthart J, Li W, Serruys PW, et al. ECG-gated versus nongated three-dimensional intracoronary ultrasound analysis: implications for volumetric measurements. Cathet Cardiovasc Diagn 1998; 43(3): 254-60.
33. De Winter SA, Hamers R, Degertekin M, Tanabe K, Lemos PA, Serruys PW, et al. Retrospective image-based gating of intracoronary ultrasound images for improved quantitative analysis: the intelligate method. Catheter Cardiovasc Interv 2004; 61(1): 84-94.
34. von Birgelen C, de Vrey EA, Mintz GS, Nicosia A, Bruining N, Li W, et al. ECG-gated three-dimensional intravascular ultrasound: feasibility and reproducibility of the automated analysis of coronary lumen and atherosclerotic plaque dimensions in humans. Circulation 1997; 96(9): 2944-52.
35. Bruining N, Hamers R, Teo TJ, de Feijter PJ, Serruys PW, Roelandt JR. Adjustment method for mechanical Boston scientific corporation 30 MHz intravascular ultrasound catheters connected to a Clearview console. Mechanical 30 MHz IVUS catheter adjustment. Int J Cardiovasc Imaging 2004; 20(2): 83-91.
36. Nishimura RA, Edwards WD, Warnes CA, Reeder GS, Holmes DR, Jr., Tajik AJ, et al. Intravascular ultrasound imaging: in vitro validation and pathologic correlation. J Am Coll Cardiol 1990; 16(1): 145-54.
37. Prati F, Arbustini E, Labellarte A, Dal Bello B, Sommariva L, Mallus MT, et al. Correlation between high frequency intravascular ultrasound and histomorphology in human coronary arteries. Heart 2001; 85(5): 567-70.

38. Okimoto T, Imazu M, Hayashi Y, Fujiwara H, Ueda H, Kohno N. Atherosclerotic plaque characterization by quantitative analysis using intravascular ultrasound: correlation with histological and immunohistochemical findings. Circ J 2002; 66(2): 173-7.
39. Schartl M, Bocksch W, Koschyk DH, Voelker W, Karsch KR, Kreuzer J, et al. Use of intravascular ultrasound to compare effects of different strategies of lipid-lowering therapy on plaque volume and composition in patients with coronary artery disease. Circulation 2001; 104(4): 387-92.
40. de Winter SA, Heller I, Hamers R, de Feyter PJ, Serruys PWC, Roelandt JRTC, et al. Computer assisted three-dimensional plaque characterization in ultracoronary ultrasound studies. Computers in Cardiology 2003; 30: 73-76.
41. de Korte CL, Sierevogel MJ, Mastik F, Strijder C, Schaar JA, Velema E, et al. Identification of atherosclerotic plaque components with intravascular ultrasound elastography in vivo: a Yucatan pig study. Circulation 2002; 105(14): 1627-30.
42. Schaar JA, De Korte CL, Mastik F, Strijder C, Pasterkamp G, Boersma E, et al. Characterizing vulnerable plaque features with intravascular elastography. Circulation 2003; 108(21): 2636-41.
43. de Korte CL, Carlier SG, Mastik F, Doyley MM, van der Steen AF, Serruys PW, et al. Morphological and mechanical information of coronary arteries obtained with intravascular elastography; feasibility study in vivo. Eur Heart J 2002; 23(5): 405-13.
44. Schaar JA, Mastik F, Regar E, de Korte CL, van der Steen AFW, Serruys PW. Reproducibility of three-dimensional palpography. Eur Heart J 2003; suppl. p2203.
45. Schroeder S, Kopp AF, Baumbach A, Meisner C, Kuettner A, Georg C, et al. Noninvasive detection and evaluation of atherosclerotic coronary plaques with multislice computed tomography. J Am Coll Cardiol 2001; 37(5): 1430-5.
46. Nieman K, Cademartiri F, Lemos PA, Raaijmakers R, Pattynama PM, de Feyter PJ. Reliable noninvasive coronary angiography with fast submillimeter multislice spiral computed tomography. Circulation 2002; 106(16): 2051-4.
47. Nair A, Kuban BD, Tuzcu EM, Schoenhagen P, Nissen SE, Vince DG. Coronary plaque classification with intravascular ultrasound radiofrequency data analysis. Circulation 2002; 106(17): 2200-6.
48. Moore MP, Spencer T, Salter DM, Kearney PP, Shaw TR, Starkey IR, et al. Characterisation of coronary atherosclerotic morphology by spectral analysis of radiofrequency signal: in vitro intravascular ultrasound study with histological and radiological validation. Heart 1998; 79(5): 459-67.
49. Nissen SE, Tuzcu EM, Schoenhagen P, Brown BG, Ganz P, Vogel RA, et al. Effect of intensive compared with moderate lipid-lowering therapy on progression of coronary atherosclerosis: a randomized controlled trial. JAMA 2004; 291(9): 1071-80.

50. Alpert JS, Thygesen K, Antman E, Bassand JP. Myocardial infarction redefined--a consensus document of The Joint European Society of Cardiology/American College of Cardiology Committee for the redefinition of myocardial infarction. J Am Coll Cardiol 2000; 36(3): 959-69.
51. Serruys PW, Emanuelsson H, van der Giessen W, Lunn AC, Kiemeney F, Macaya C, et al. Heparin-coated Palmaz-Schatz stents in human coronary arteries. Early outcome of the Benestent-II Pilot Study. Circulation 1996; 93(3): 412-22.
52. Mintz GS, Nissen SE, Anderson WD, Bailey SR, Erbel R, Fitzgerald PJ, et al. American College of Cardiology Clinical Expert Consensus Document on Standards for Acquisition, Measurement and Reporting of Intravascular Ultrasound Studies (IVUS). A report of the American College of Cardiology Task Force on Clinical Expert Consensus Documents. J Am Coll Cardiol 2001; 37(5): 1478-92.
53. Ward MR, Pasterkamp G, Yeung AC, Borst C. Arterial remodeling. Mechanisms and clinical implications. Circulation 2000; 102(10): 1186-91.
54. von Birgelen C, Hartmann M, Mintz GS, Baumgart D, Schmermund A, Erbel R. Relation between progression and regression of atherosclerotic left main coronary artery disease and serum cholesterol levels as assessed with serial long-term (> or =12 months) follow-up intravascular ultrasound. Circulation 2003; 108(22): 2757-62.
55. von Birgelen C, Hartmann M, Mintz GS, Bose D, Eggebrecht H, Gossl M, et al. Spectrum of remodeling behavior observed with serial long-term (>/=12 months) follow-up intravascular ultrasound studies in left main coronary arteries. Am J Cardiol 2004; 93(9): 1107-13.

4

Noninvasive Detection of Subclinical Coronary Atherosclerosis Coupled with Assessment of Changes in Plaque Characteristics Using Novel Invasive Imaging Modalities. The Integrated Biomarker and Imaging Study (IBIS)

Carlos A.G. Van Mieghem[1], Eugène P. McFadden[1], Pim J. de Feyter[1], Nico Bruining[1], Johannes A. Schaar[1], Nico R. Mollet[1], Filippo Cademartiri[1], Dick Goedhart[2], Sebastiaan de Winter[1], Gaston A. Rodriguez Granillo[1], Marco Valgimigli[1], Frits Mastik[1], Anton F.W. van der Steen[1], Willem J. van der Giessen[1], Georgios Sianos[1], Bianca Backx[2], Marie-Angèle M. Morel[2], Gerrit-Anne van Es[2], Andrew Zalewski[3,4], Patrick W. Serruys[1]

[1]Erasmus Medical Center, Thoraxcenter, Rotterdam, the Netherlands; [2]Cardialysis, Rottterdam, The Netherlands; [3]GlaxoSmithKline, Philadelphia, Pennsylvania; and [4]Thomas Jefferson University, Philadelphia, Pennsylvania.

J Am Coll Cardiol. 2006; 47:1134-42

ABSTRACT

Objectives

Our purpose was to assess non-invasive imaging in detection of subclinical atherosclerosis and to examine novel invasive modalities to describe prevalence and temporal changes in putative characteristics of "high-risk" plaques.

Background

Conventional coronary imaging cannot identify "high-risk" lesions.

Methods

Conventional (quantitative angiography and intravascular ultrasound [IVUS]) and novel imaging (IVUS-based palpography and gray scale echogenicity) were performed at baseline and 6 months later in 67 patients with diverse clinical presentations. Different imaging techniques were compared within a common segment defined by multislice computed tomography (MSCT).

Results

Compared with IVUS, the sensitivity, specificity, and positive and negative predictive value of MSCT for detecting significant plaque was 86%, 69%, 90%, and 61% respectively. In coronary arteries with <50% stenosis, there were no temporal changes in luminal and plaque dimensions measured by quantitative coronary angiography or IVUS; however, a significant reduction in abnormal strain pattern was detected on palpography (density high strain spots/cm: 1.6 $\pm$ 1.5 vs. 1.2 $\pm$ 1.4, $p = 0.0123$). These changes were mainly related to significant changes in patients who presented with ST-segment elevation myocardial infarction. The assessment of plaque echogenicity showed no temporal changes. There were no correlations between circulating biomarkers and quantifiable imaging parameters.

Conclusions

Mild angiographic disease is associated with large atherosclerotic plaques on MSCT. Conventional invasive coronary imaging reveals static luminal and plaque dimensions on standard medical therapy with plaque hypoechogenicity remaining unchanged over the 6-month period. By contrast, palpography measurements of strain correlate with clinical presentation and significantly decrease on standard medical therapy. Novel imaging modalities, such as palpography, may provide insights into plaque biology and might eventually serve as intermediate end points in interventional trials.

INTRODUCTION

Atherosclerosis is a systemic disease in which the clinical sequelae only weakly correlate with its extent or severity. Furthermore, sudden death or acute coronary syndromes are frequently the first manifestation of previously subclinical atherosclerosis, and the majority of such events (i.e. 60-70%) occur as a result of plaque rupture at sites with noncritical luminal narrowing (1-5). Pathologic studies have correlated specific coronary plaque characteristics with fatal ischemic events, but conventional imaging techniques, such as quantitative angiography and quantitative intravascular ultrasound (IVUS) cannot reliably identify high-risk, rupture-prone, plaques prospectively (6). Thus, development of novel coronary imaging modalities to detect structural and compositional plaque characteristics has been the subject of intensive preclinical and clinical research (7,8). In parallel with the advances in novel invasive imaging, noninvasive multislice computed tomographic angiography (MSCTA) has matured to the extent that it can reliably identify flow-limiting coronary lesions in relatively unselected patients.

The aim of this study was four-fold: 1/ to determine the potential of MSCTA in the detection of subclinical, non-flow limiting coronary atherosclerosis; 2/ to assess the prevalence of high-risk characteristics in such plaques with two novel IVUS-based imaging modalities (palpography and echogenicity plaque characterization); 3/ to assess temporal changes in IVUS-based plaque characteristics of high-risk lesions; and 4/ we attempted to relate changes in imaging parameters to changes in systemic biomarker levels.

METHODS

Study Design and Patient Selection

This was a prospective, observational, single-center pilot study. The study design has been described in detail elsewhere (9). Briefly, patients with stable angina, unstable angina, non-ST-segment elevation or ST-segment elevation myocardial infarction (STEMI), referred for percutaneous coronary intervention (PCI), were eligible for inclusion. Major clinical exclusion criteria included significant renal dysfunction (creatinine $>$ 2 mg/dl), prior coronary intervention in the region of interest (ROI), life expectancy $<$ 1 year, or factors that made follow-up difficult. Major imaging-related exclusion criteria included coronary anatomy that precluded safe IVUS examination of a suitable ROI or criteria that precluded acquisition of diagnostic noninvasive angiographic images (irregular heart rhythm or inability to hold breath for 20 s). Between March 2003 and November 2003, 90 consecutive patients were enrolled and follow-up was completed in summer 2004. The study vessel was preferably a non-intervened artery. At the discretion of the operator, a second artery could be studied. The ROI was defined on the basis of MSCTA, using landmarks, such as branches or the vessel origin. At six months

follow-up, patients underwent repeat invasive imaging. The medical ethics committee of the Erasmus Medical Center Rotterdam approved the study protocol, and all patients provided written informed consent.

Quantitative Coronary Angiography and IVUS

Quantitative angiographic analyses were performed by a core laboratory (Cardialysis, Rotterdam, the Netherlands) with the use of edge-detection techniques (CAAS II, Pie Medical, Maastricht, the Netherlands). Mean and minimum luminal diameters and diameter stenosis were measured in at least two, preferentially orthogonal, projections, and averaged.

The IVUS was performed with commercially available catheters (30 MHz, Ultracross, or 40 MHz, Atlantis SR Pro, Boston Scientific, Santa Clara, California) using standard procedures with an automated pullback device (0.5 mm/s) (10). Data were stored on videotape, transformed into the Digital Imaging and Communication in Medicine (DICOM) image standard, and archived. Quantitative analysis was performed by the core laboratory with validated software (Curad, version 3.1, Wijk bij Duurstede, the Netherlands) and retrospective image-based gating (11). The borders of the external elastic membrane (EEM) and of the lumen were traced. The enclosed area was defined as the coronary plaque plus media area (subsequently referred to as plaque area). Significant plaque was defined as a plaque that occupied 50% or more of the cross-sectional vessel area circumscribed by the EEM. Other IVUS measurements included length of the ROI, lumen volume, and vessel volume. Plaque volume (PV) was calculated as vessel volume minus lumen volume. The interobserver variability was determined by re-analyzing the baseline and follow-up IVUS recordings of 16 patients by a different core lab analyst. Sixteen patients (32 recordings) were randomly selected among recordings that fulfilled the following two criteria: 1) ROI $\geq$30 mm long, and 2) both pullbacks were performed with the same type of IVUS catheter (30 MHz catheter).

Novel IVUS-Based Plaque Imaging: Echogenicity

We used a computer-aided, gray-scale value analysis program for plaque characterization(12). Based on the mean gray level (brightness) of the adventitia, plaque was classified as brighter (hyperechogenic) or less bright (hypoechogenic) than the adventitia. Calcified plaque was defined as plaque brighter than the adventitia with associated acoustic shadowing. The variables measured in the previously defined ROI included hypoechogenic PV and hyperechogenic PV (mm^3) and relative plaque echogenicity, calculated as (hypoechogenic plaque volume/ sum of hypoechogenic and hyperechogenic plaque volume) x 100. For the comparison with MSCT, plaque within the ROI was considered calcified if it contained calcium in at least 2 consecutive cross-sections corresponding to an IVUS segment with a length of at least 0.5mm.

Novel IVUS-Based Plaque Imaging: Palpography

Palpography is an IVUS-based technique that assesses the local mechanical properties of the coronary plaque. The technique measures the relative displacements of backscattered radiofrequency signals, recorded during IVUS acquisition, at two different blood pressure levels to detect differences in deformability or strain of various plaque components. As such, lipid-rich plaques will deform more and thus show a higher strain value compared with calcified or fibrous plaques (13). Palpography data were acquired during an IVUS pullback (1 mm/s) with a commercially available catheter (20 MHz Jovus Avanar, Volcano, Rancho Cordova, California). With previously described and validated methodology, plaque strain values were assigned a ROtterdam Classification (ROC) score ranging from 1 to 4 (ROC 1: 0% to 0.6%; ROC 2: 0.6% to <0.9%; ROC 3: 0.9% to <1.2%; ROC 4: >1.2%) (13-16). The parameters measured included the number of ROC 3 or 4 spots in the ROI and the density of ROC 3/4 spots, defined as the total number of ROC 3 and 4 scores that were counted in all cross sections that were acquired at 1-mm intervals in the whole ROI. This number was divided by the length of the ROI and multiplied by 10 to normalize to the pullback length.

MSCTA

All scans were performed on a 16-row detector scanner (Sensation 16, Straton, Siemens, Forchheim, Germany). The scan protocol and image reconstruction parameters were recently published (17). The dataset with least motion artifacts was loaded on an off-line workstation (Leonardo, Siemens) and the ROI identified on multiplanar reconstructions, on the basis of anatomic landmarks. Datasets were loaded on a semi-automated vessel-tracking software program and a central lumen line created throughout the ROI. Ten through 30 cross sections were reconstructed orthogonal to the center of the lumen and analyzed independently by two observers. Disagreements were resolved by consensus. Plaque was defined as an abnormal mass within the artery wall, clearly distinguishable from epicardial fat and the coronary lumen. On the basis of manually measured maximal thickness, plaques were classified as small (<1 mm), medium (1 to 2 mm), or large (>2 mm). Calcification was defined by the presence of high-density components (>130 Hounsfield units).

Lipoprotein Levels and Biomarkers

Plasma concentrations of total cholesterol, high-density lipoprotein cholesterol (HDL-C), and triglycerides were measured in the local laboratory. The Friedewald formula was used to derive low-density lipoprotein cholesterol (LDL-C) levels (18). Blood samples for additional biomarker analysis were stored at –70°C. Serum C-reactive protein (Diagnostic Systems Laboratories, Webster, Texas), plasma interleukin 6, and tumor necrosis factor-alpha (R&D Systems, Minneapolis, Minnesota) were measured in the Human Biomarker Center (GlaxoSmithKline, Philadelphia, Pennsylvania) on the basis of protocols provided by the manufacturer. Lipoprotein associated phospholipase A2 activity assay was measured by the proportional release of

aqueous 3H acetate resulting from the enzymatic cleavage of the 3H acetyl-platelet activating factor substrate (100 μmol/l). N-terminal pro brain natriuretic peptide was measured with use of a two-site electrochemiluminescent assay.

Definition of Events and Follow-Up for Major Adverse Cardiac Events

The occurrence of major adverse cardiovascular events was assessed after the procedure, at discharge, and at three and six months, as were the individual components: death, myocardial infarction (MI), revascularization by PCI or coronary artery bypass graft surgery, hospital stay for ischaemia and/or anginal symptoms, and stroke. The diagnosis of MI was consistent with the American College od Cardiology/European Society of Cardiology definition (19).

Statistical Analysis

Discrete variables are presented as counts and percentages. Continuous variables are presented as means ± SD, unless otherwise indicated. Comparisons between quantitative outcomes were performed with use of scatter plots and linear regression analysis (regression coefficient). When appropriate, biomarker analyses were performed after natural logarithmic transformation. Correlations between imaging end points and circulating biomarkers were assessed, and univariate Pearson correlation coefficients were calculated. Comparisons among patient subgroups, grouped by clinical presentation, with findings on palpography and on echogenicity, were performed at both vessel and patient level. In the latter case, the imaging findings from two ROIs in the same patient were averaged. Differences in means among groups were analyzed by a two-sample t-test. A value $p < 0.05$ (two-sided) was indicative of statistical significance. No formal hypotheses were

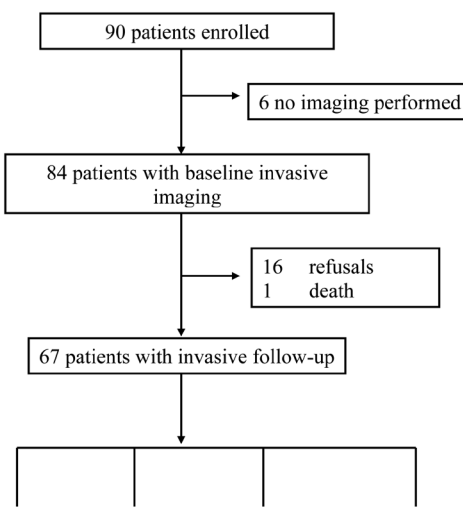

	QCA	IVUS	Echogenicity	Palpography
Baseline	67 (74)	63 (69)	63 (67)	53 (58)
Follow-up	67 (74)	62 (64)	55 (60)	57 (60)
Matched results	67 (74)	58 (63)	55 (60)	49 (52)

Figure 1. Flow chart detailing number of patients at baseline and follow-up. Values in parentheses reflect number of vessels examined with different imaging modalities. IVUS = intravascular ultrasound; QCA = quantitative coronary angiography.

Table 1. Baseline characteristics of patients with invasive follow-up evaluation

Demographics and Clinical History	Patients (n =67)
Male	57 (85)
Age (yrs)	58 + 11
Previous myocardial infarction	27 (40)
Previous coronary bypass surgery	1 (1)
Previous percutaneous coronary intervention	11 (16)
History of diabetes	6 (9)
History of stroke	1 (1)
Family history of coronary disease	36 (54)
Hypertension*	29 (43)
Hypercholesterolemia†	57 (85)
Previous smoker	23 (34)
Current smoker	26 (39)
Medication at inclusion	
Aspirin	59 (88)
Clopidogrel	38 (57)
ACE-I/AT2	20 (30)
Beta-blocker	44 (66)
Statin therapy	48 (72)
Medication at 6 months follow-up	
Aspirin	61 (91)
Clopidogrel	63 (94)
ACE-I/AT2	34 (51)
Beta-blocker	50 (75)
Statin therapy	66 (99)
Clinical Status at enrolment	
Stable angina	32 (48)
Unstable angina or non-STEMI	21 (31)
STEMI	14 (21)
Extent of Disease‡	
Non significant disease	4 (6)
Single-vessel disease	36 (53.7)
Two-vessel disease	21 (31.3)
Three-vessel disease	3 (4.5)
Left main stem (plus two-vessel) disease	3 (4.5)

Categorical data are presented as n (%) and continuous data as mean values ± SD. *Blood pressure >160/95 mmHg or treatment for hypertension, †Total cholesterol >215 mg/dL or treatment for hypercholesterolemia. ‡Significant disease was defined as >50% (visual estimate) stenosis in a major epicardial vessel or in branches > 2.5 mm diameter.
ACE-I = angiotensin-converting enzyme inhibitor; AT2 = angiotensin-II receptor antagonist; STEMI = ST-segment elevation myocardial infarction.

tested in this exploratory study; therefore p-values are given as such, without any correction for multiplicity of testing. Statistical analyses were performed using the Statistical Analysis System software version 8.2 (SAS Institute, Cary, North Carolina).

RESULTS

Patient Population

A flow diagram detailing the number of patients undergoing multimodality coronary imaging is presented in Figure 1. Sixty-seven patients underwent serial invasive imaging of non-culprit segments of coronary artery at baseline and 196 ± 19 days later. Nine patients had one or both IVUS recordings that were not further analyzable, owing to artifact or use of an incorrect scale. An additional three patients could not be analyzed for IVUS echogenicity, owing to extensive calcification overshadowing a large part of the adventitia, which is used as a reference for the interpretation of gray-scale values of surrounding tissue. Reasons for inaccurate palpogram readings (n = 18) were related to extensive catheter motion during data acquisition. Baseline characteristics of patients who completed the study are shown in Table 1.

Table 2. Changes in lipid parameters

	Total cholesterol, mg/dL	LDL cholesterol, mg/dL	HDL cholesterol, mg/dL	Triglycerides, mg/dL
Entire cohort (n=64)				
Baseline	176.8±48	113±44.7	39.7±13.7	143.1±83.9
Follow-up	171.1±31.8	104.5±29.6	44.1±14.4	165.9±82.3
Change	-5.9±51	-10.6±44.6	4.3±9	21.1±79.9
P value	NS	NS	0.001	0.008
STEMI (n=13)				
Baseline	210±37.5	145±32.8	43.5±12	143.4±68.6
Follow-up	166.7±34.6	102.6±30.9	39.9±10.3	162.5±67.6
Change	-40.9±39.2	-36.1±41.1	-3.3±6.1	27.2±58.5
P value	0.003	0.006	NS	NS
UA or NSTEMI (n=21)				
Baseline	167.1±45.2	107.8±36.4	36.8±11.6	144.5±81
Follow-up	169.9±26.6	100.2±25.1	47.2±15.7	152.7±87.1
Change	7.5±54	-4.6±39.6	9.6±6.5	5.9±80.7
P value	NS	NS	<0.001	NS
Stable angina (n=30)				
Baseline	169.2±49	102.7±49	40±15.7	142±94
Follow-up	174.2±34.4	108.2±32.4	44.1±15.3	176.1±87.4
Change	3.6±47.8	-2.3±46.3	4.5±9.2	28.1±89.5
P value	NS	NS	0.026	0.014

HDL = high-density lipoprotein; LDL = low-density lipoprotein; STEMI = ST-segment elevation myocardial infarction; UA = unstable angina.

They were comparable to those of the entire cohort of 84 patients enrolled at baseline (not shown). Almost all patients (99%) received treatment with a statin within the 6-month study period, mainly as a result of starting treatment in the group who presented initially with STEMI (treatment started in 13 of 14 STEMI patients). Mean total cholesterol, LDL-C, HDL-C, and triglyceride values for patients who completed the study are presented in Table 2.

Table 3. Accuracy of multislice computed tomography for the detection of significant coronary plaque*: comparison with IVUS for the entire region of interest and for its 5 mm subsegments

	Entire region of interest	5-mm subsegments
Sensitivity	44/51 (86, 74-93)	136/185 (74, 67-79)
Specificity	11/16 (69, 44-86)	140/192 (73, 66-79)
Positive predictive value	44/49 (90, 78-96)	136/188 (72, 66-78)
Negative predictive value	11/18 (61, 39-80)	140/189 (74, 67-80)

Values are n (%, 95% confidence interval). *Significant plaque on intravascular ultrasound (IVUS) was defined as mean plaque area obstruction {(Vesselarea - Lumenarea / Vesselarea) x 100} > 50%, or the presence of calcium on 2 consecutive slices on IVUS.

MSCTA Versus IVUS at Baseline

MSCTA and IVUS were compared, at baseline, in 61 patients (67 vessels). The sensitivity and specificity of MSCTA to detect significant plaque identified on IVUS (> 50% EEM area obstruction or the presence of calcification on two consecutive slices) was calculated for the entire ROI and for 5-mm sub-segments (Table 3). The sensitivity, specificity, positive and negative predictive values of MSCTA for detection of any significant plaque was 86%, 69%, 90%, and 61%, respectively. The sensitivity of MSCTA to detect plaque was 60% (30/50) for small (<1mm), 76% (80/105) for medium (1 to 2 mm), and 79% (26/33) for large (>2 mm) plaques.

Reproducibility of IVUS Measurements

Interobserver variability for IVUS analysis (n= 32 pullbacks) showed no systematic error and good reproducibility. Mean differences in area (mm^2) measurements were: 0.04 ± 0.56 for EEM, 0.02 ± 0.50 for lumen, and –0.06 ± 0.59 for plaque. The mean difference in PV (mm^3) was –2.43 ± 22.

Conventional Imaging: Quantitative Coronary Angiography and IVUS

There were no statistically significant changes in the angiographic variables measured in the ROI (Table 4). Likewise, IVUS-derived measurements remained unchanged in matched segments (Table 5). Figure 2 illustrates the spread of the individual data points for PV. When

Table 4. Quantitative angiographic parameters (n=67)

	Length (mm)	Mean Diameter (mm)	Minimal Diameter (mm)	Diameter Stenosis (%)
Entire cohort (n=67)				
Baseline	27.2±13.1	2.78±0.6	2.31±0.6	25±11
Follow-up	27.2±13.1	2.84±0.8	2.38±0.7	25±11
Change	0.0±2.5	0.06±0.4	0.06±0.4	0.0±8
p value	NS	NS	NS	NS

Values are mean ± SD.

Table 5. Quantitative IVUS (n = 58) and echogenicity (n = 55) parameters

Variable	Length (mm)	Lumen volume (mm^3)	Vessel volume (mm^3)*	Total Plaque Volume (mm^3)†	Hypo Volume (mm^3)‡	Hyper Volume (mm^3)§
Baseline	29.3±14.4	285±161	481±250	195±117	171±104	15±11
Follow-up	29.2±14.2	279±161	469±243	190±107	177±98	12±14
Change	-0.1±1.6	-7±52	-12±61	-5.2±33	6±53	-3±13
p-value	NS	NS	NS	NS	NS	NS

Values are mean ± SD. *Vessel volume denotes the volume circumscribed by the external elastic membrane. †Total plaque volume denotes Vesselvolume-Lumenvolume including echolucent media. ‡Hypo volume = hypoechogenic plaque volume. §Hyper volume = hyperechogenic plaque volume.

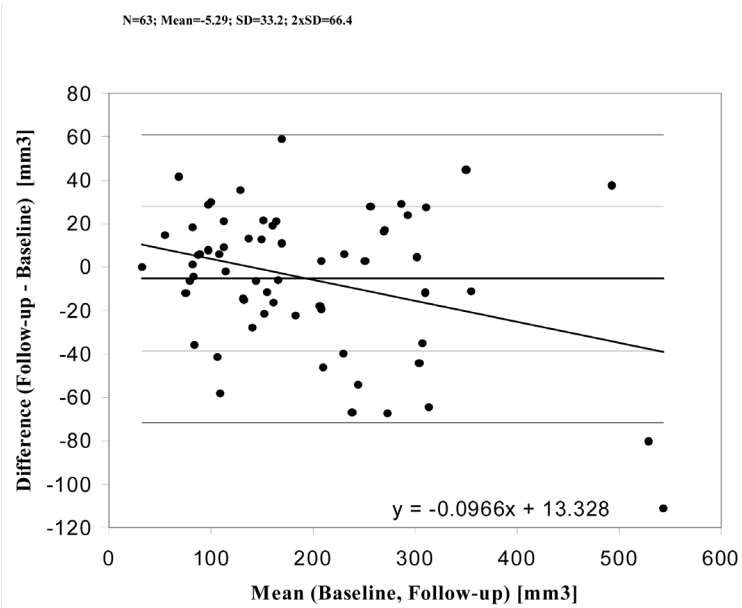

Figure 2. Bland-Altman plot of the intravascular ultrasound data on plaque volume. The green (top) and blue (bottom) line indicate the borders of 2 x SD.

patients were grouped according to initial diagnosis (i.e., STEMI, unstable angina, stable angina), there were no significant changes in either angiographic or IVUS measurements between baseline and follow-up (data not shown).

Novel IVUS-Based Imaging

Temporal changes in plaque characteristics on the basis of IVUS-based palpography and echogenicity are shown in Tables 5 and 6. At baseline, the predominant plaque component was hypoechogenic tissue (91.6% of PV). There was no significant change in the absolute volume of hypoechogenic or hyperechogenic plaque over the course of the study. On palpography, both the absolute number of high-strain spots (grade 3/4) in the ROI ($p = 0.009$) and their density per cm ($p = 0.012$) decreased significantly between baseline and follow-up. This decrease in the overall population was largely driven by changes in the subgroup of patients with STEMI; this group had both the highest number of high-strain spots at baseline and the most marked relative decrease during follow-up, compared with patients with other clinical presentations. At 6-month follow-up, the density of high-strain spots (1.2 ± 1.4/cm) was comparable among clinical subgroups. Representative imaging findings are presented in Figure 3.

Correlation of Biomarkers with Imaging Techniques

Not surprisingly, several inflammatory mediators (C-reactive protein, interleukin-6, IL-6, lipoprotein-associated phospholipase A2 and a marker of hemodynamic stress (NT-proBNP) decreased over time, particularly in patients presenting with acute coronary syndromes. There were no significant correlations noted between circulating biomarkers and imaging parameters (data not shown). Among lipid parameters (total cholesterol, LDL-C, HDL-C, and triglycerides), a correlation with the change in IVUS-derived plaque area was only noted for the change in HDL-C (Pearson correlation coefficient -0.37, $p < 0.05$, data not shown).

Table 6. Plaque characterization with palpography (n= 49 patients/ 52 vessels).

	Palpography	
	Number of high strain spots	**Density of high strain spots**
Total population (n=52)		
Baseline	4.8±4.5	1.6±1.5
Follow-up	3.6±4.4	1.2±1.4
p value	0.009	0.0123
STEMI (n=12)		
Baseline	7.2 ± 5.8	2.3 ± 1.8
Follow-up	3.8±4.6	1.1±1.4
p value	0.003	0.0003
UA or non-STEMI (n=16)		
Baseline	4.1±3.9	1.8±1.8
Follow-up	3.1±3.5	1.4±1.7
p value	0.17	0.29
Stable Angina (n=24)		
Baseline	4.0±4.0	1.2±1.1
Follow-up	3.8±4.9	1.2±1.1
p value	0.69	0.56

Values are expressed using the total number and density of high strain spots, given as mean ± SD. Density refers to the number of Rotterdam Classification 3/4 spots per 10 mm of vessel. STEMI = ST-segment elevation myocardial infarction; UA = unstable angina.

Adverse Events

One patient died 2 weeks after inclusion, because of a second MI. All imaging procedures were performed without complications.

DISCUSSION

The major findings of the study were four-fold. First, using IVUS as a gold standard, non-invasive MCSTA can identify atherosclerotic plaque, in vessels with only minimal angiographic disease, with high sensitivity and moderate specificity. Second, further investigation of such plaque with novel IVUS-based imaging techniques (palpography and echogenicity) showed that features potentially indicative of vulnerable plaques are both widespread and highly prevalent. Third, although conventional imaging with quantitative coronary angiography and IVUS demonstrates no significant changes in lumen or plaque dimensions, the biomechanical properties of the plaques, assessed by palpography, showed significant changes over a relatively

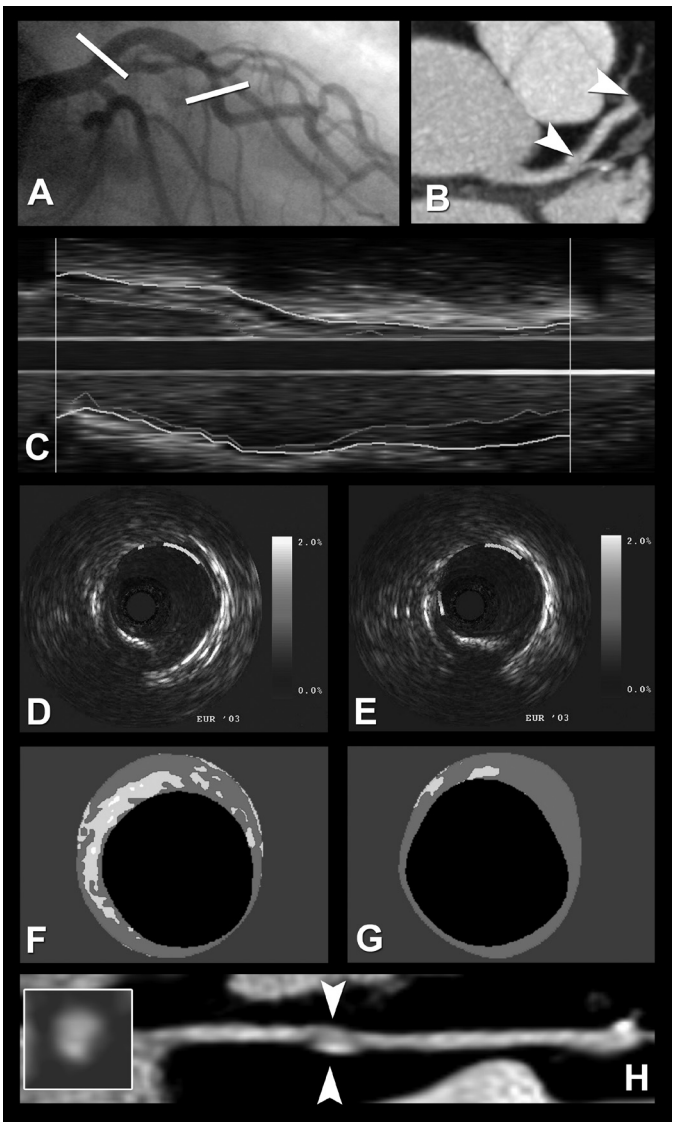

Figure 3. Example of multimodality coronary imaging of the proximal left anterior descending coronary artery. (A, B) Region of interest (ROI) is defined by the ostium of the left anterior descending and a large septal branch, as marked by white lines on the conventional angiogram (A) and arrowheads on multislice computed tomography maximum intensity projection reconstruction (B). (C) Gated longitudinal intravascular ultrasound (IVUS) reconstruction. The vertical lines mark the boundaries of the ROI. The red line indicates the lumen-intima interface and the green line the external border of the plaque plus echolucent media. (D, E) Representative color-coded cross-sectional palpograms that are superimposed on the IVUS image. Strain values are color-coded from 0% (blue) to 2% (yellow), as shown on the vertical scale. (D) Shows non-deformable eccentric plaque with calcification and acoustic shadowing. The blue line around the lumen indicates a non-deformable plaque with 0% strain. In the regions without plaque, the gray color indicates that no strain value can be measured. (E) Shows eccentric partly calcified plaque with a high strain (yellow) spot on one shoulder of the plaque (nine o'clock). On the other shoulder (four o'clock) the blue color (0% strain) indicates that the plaque is not deformable in this region. (F, G) Representative color-coded echogenicity cross-sections. Hypoechogenic tissue is represented in red and hyperechogenic tissue in green. (F) Shows a cross section with a relatively large hyperechogenic area. The white spots visible most likely represent thick fibrous tissue and not calcification, as there was no acoustic shadowing on the corresponding IVUS images (not shown). (G) Shows a cross section, which predominantly contains hypoechogenic tissue. (H) Multislice computed tomography reconstruction and (inset) a cross section in an area with calcified plaque (arrows). (A full color version of this illustration can be found in the color section).

short period. Finally, circulating levels of measured biomarkers showed no significant correlations with focal imaging end points identified by conventional and novel imaging modalities.

Subclinical Atherosclerosis: Role of Noninvasive Imaging

The development of noninvasive angiography with MSCTA can be used to reliably identify significant epicardial coronary atherosclerosis (20). Recent studies have shown its potential for detecting non-obstructive coronary plaques in highly selected patients (21,22). Our results

extend these findings by showing that non-obstructive coronary plaque can be detected, in an arbitrarily selected ROI, with moderately high sensitivity and specificity in a broader patient population; however, when examined in more detail, with novel invasive techniques, we found that putative "high-risk" characteristics (i.e. hypoechogenic plaques with a high-strain pattern) were very common. This observation provides additional arguments to support recommendations discouraging the indiscriminate use of noninvasive coronary imaging to detect subclinical atherosclerosis at the present time (23).

Subclinical Atherosclerosis: Insights from Novel Invasive Techniques

We have previously validated the potential of palpography to identify thin-capped fibroatheromas in vitro (13,14,24,25). Subsequently, we showed that the number of high-strain spots in culprit epicardial vessels was correlated with clinical presentation (16). The present study extends these findings by demonstrating that, within arbitrarily selected segments of non-culprit vessels, high-strain areas were quite common, despite only mild angiographic disease. The most marked changes occurred in patients with an acute MI, most of who were statin-naïve (93%) at the time of the initial presentation. Although acute MI patients had a higher extent of high-strain spots, all subgroups were comparable six months later, regardless of the initial presentation. Interestingly, the persistence of abnormal strain patterns might reflect the inadequacy of standard medical care. This hypothesis would be consistent with recent data that indicate the need for intensive intervention for LDL-C (<70 mg/dl) and inflammation (C-reactive protein <2 mg/l) to achieve the best clinical outcomes in the course of therapy with statins in post-ACS patients (26,27).

Prior studies suggest that gray-scale echogenicity is related to the histological components of carotid and coronary plaques (28-30). Although carotid plaque echogenicity can be assessed noninvasively, assessment of coronary plaque echogenicity requires invasive techniques and has been restricted to research settings. In the present study, we used a quantitative computer-assisted index of echogenicity, on the basis of gray-scale values of adventitia, and demonstrated that hypoechogenic tissue was the predominant plaque component. We found no significant change in absolute hypoechogenic or hyperechogenic PV over the average six months. Our findings differ from the observations of Schartl et al. (31), who found a small but significant increase in the hyperechogenic plaque component; however, their study had a longer follow-up period and patients had intensive, carefully monitored, statin therapy. A recent study conducted at our institution suggested that the changes in plaque echogenicity require a much longer period to occur (more than 2 years) (32). Accordingly, the high preponderance of hypoechogenic plaque (>90% of the PV) coupled with the lack of significant change during the short-term follow-up suggests that plaque echogenicity lacks the discrimination necessary either for risk stratification or as a surrogate measure of plaque composition on serial studies.

Study Limitations

This observational study has limitations. First, our patient population was intentionally heterogeneous and the study was underpowered to correlate compositional imaging end points with clinical outcomes. Although follow-up was incomplete (67/84, 80%), it compares favorably with recent serial IVUS studies (33,34). Moreover, baseline characteristics of the 67 patients with completed follow-up were the same as in the overall study population. Second, the present study did not demonstrate changes in plaque size. By contrast, recently published studies demonstrated regression of coronary atherosclerosis in patients with acute coronary syndromes treated with aggressive statin regimen (34). In contrast, in those with stable coronary artery disease maximal dose of atorvastatin given for 18 months only halted plaque growth (33). Potential explanation for these disparate results may be due to different duration of follow-up (6 vs. 18 months), underlying index event (stable vs. acute coronary syndrome), or suboptimal intensity of statin treatment noted in many IBIS patients that reflects slow adoption of current guidelines into clinical practice settings. With these caveats, however, data from recent trials, such as Reversing Atherosclerosis with Aggressive Lipid Lowering (REVERSAL) and Pravastatin or Atorvastatin Evaluation and Infection Therapy (PROVE-IT), indicate that intensive treatment with statins affects plaque size and event rates, respectively (33,35). Third, although our results underscore the heterogeneity of coronary atheroma, much larger studies are needed to ultimately define the role of novel plaque imaging techniques in clinical practice. Fourth, our attempt to relate circulating biomarkers to coronary plaque imaging in an arbitrarily selected ROI can only be regarded as exploratory. We did not further discuss this possible interaction because the correlations we found were weak. Fifth, the suboptimal spatial and temporal resolution of the 16-slice MSCT scanner precludes accurate assessment of coronary artery segments <2 mm. Although the ROI as selected by MSCT was chosen randomly, distal coronary segments are inevitably underrepresented. The same argument holds true, however, for IVUS examination of the coronary tree, where for safety reasons only the larger coronary segments are targeted for interrogation.

CONCLUSIONS

Mild angiographic disease is associated with large atherosclerotic plaques identified with noninvasive MSCTA. This study also confirms that conventional invasive imaging modalities frequently reveal static luminal and plaque dimensions, whereas novel IVUS-based plaque palpography can detect significant alterations in coronary plaque characteristics over a relatively short time interval. Our results highlight the dynamic changes in the strain of coronary plaques that are remote from the culprit lesions, particularly in patients with MI. Whether the persistence of a high-strain pattern is a harbinger of cardiovascular events remains to be determined in future much larger studies. The novel imaging modalities used in this study provide insights

into plaque biology, whereas temporal changes detected with these modalities might eventually serve as intermediate end points in interventional trials.

Acknowledgement
Supported by a research grant from GlaxoSmithKline, Philadelphia, PA, USA.

REFERENCES

1. Kullo IJ, Edwards WD, Schwartz RS. Vulnerable plaque: pathobiology and clinical implications. Ann Intern Med 1998;129:1050-60.
2. Falk E, Shah PK, Fuster V. Coronary plaque disruption. Circulation 1995;92:657-71.
3. Libby P. Molecular bases of the acute coronary syndromes. Circulation 1995;91:2844-50.
4. Willerson JT, Ridker PM. Inflammation as a cardiovascular risk factor. Circulation 2004;109:II2-10.
5. Virmani R, Kolodgie FD, Burke AP, Farb A, Schwartz SM. Lessons from sudden coronary death: a comprehensive morphological classification scheme for atherosclerotic lesions. Arterioscler Thromb Vasc Biol 2000;20:1262-75.
6. Schoenhagen P, Tuzcu EM, Ellis SG. Plaque vulnerability, plaque rupture, and acute coronary syndromes: (multi)-focal manifestation of a systemic disease process. Circulation 2002;106:760-2.
7. Madjid M, Zarrabi A, Litovsky S, Willerson JT, Casscells W. Finding vulnerable atherosclerotic plaques: is it worth the effort? Arterioscler Thromb Vasc Biol 2004;24:1775-82.
8. Fayad ZA, Fuster V. Clinical imaging of the high-risk or vulnerable atherosclerotic plaque. Circ Res 2001;89:305-16.
9. Van Mieghem CAG, Bruining N, Schaar JA, et al. Rationale and methods of the integrated biomarkers and imaging study (IBIS): combining invasive and non-invasive imaging with biomarkers to detect subclinical atherosclerosis and assess coronary lesion biology. Int J Cardiovasc Imaging 2005;21: 425-441.
10. Mintz GS, Nissen SE, Anderson WD, et al. American College of Cardiology Clinical Expert Consensus Document on Standards for Acquisition, Measurement and Reporting of Intravascular Ultrasound Studies (IVUS). A report of the American College of Cardiology Task Force on Clinical Expert Consensus Documents. J Am Coll Cardiol 2001;37:1478-92.
11. De Winter SA, Hamers R, Degertekin M, et al. Retrospective image-based gating of intracoronary ultrasound images for improved quantitative analysis: the intelligate method. Catheter Cardiovasc Interv 2004;61:84-94.

12. de Winter SA, Heller I, Hamers R, et al. Computer assisted three-dimensional plaque characterization in ultracoronary ultrasound studies. Computers in Cardiology 2003;30:73-76.
13. de Korte CL, Sierevogel MJ, Mastik F, et al. Identification of atherosclerotic plaque components with intravascular ultrasound elastography in vivo: a Yucatan pig study. Circulation 2002;105:1627-30.
14. de Korte CL, Carlier SG, Mastik F, et al. Morphological and mechanical information of coronary arteries obtained with intravascular elastography; feasibility study in vivo. Eur Heart J 2002;23:405-13.
15. Schaar JA MF, Regar E, de Korte CL, van der Steen AFW, Serruys PW. Reproducibility of three-dimensional palpography. Eur Heart J 2003;suppl.:2203.
16. Schaar JA, Regar E, Mastik F, et al. Incidence of high-strain patterns in human coronary arteries: assessment with three-dimensional intravascular palpography and correlation with clinical presentation. Circulation 2004;109:2716-9.
17. Mollet NR, Cademartiri F, Nieman K, et al. Multislice spiral computed tomography coronary angiography in patients with stable angina pectoris. J Am Coll Cardiol 2004;43:2265-70.
18. Friedewald WT, Levy RI, Fredrickson DS. Estimation of the concentration of low-density lipoprotein cholesterol in plasma, without use of the preparative ultracentrifuge. Clin Chem 1972;18:499-502.
19. Alpert JS, Thygesen K, Antman E, Bassand JP. Myocardial infarction redefined--a consensus document of The Joint European Society of Cardiology/American College of Cardiology Committee for the redefinition of myocardial infarction. J Am Coll Cardiol 2000;36:959-69.
20. Nieman K, Cademartiri F, Lemos PA, Raaijmakers R, Pattynama PM, de Feyter PJ. Reliable noninvasive coronary angiography with fast submillimeter multislice spiral computed tomography. Circulation 2002;106:2051-4.
21. Achenbach S, Ropers D, Hoffmann U, et al. Assessment of coronary remodeling in stenotic and nonstenotic coronary atherosclerotic lesions by multidetector spiral computed tomography. J Am Coll Cardiol 2004;43:842-7.
22. Schoenhagen P, Tuzcu EM, Stillman AE, et al. Non-invasive assessment of plaque morphology and remodeling in mildly stenotic coronary segments: comparison of 16-slice computed tomography and intravascular ultrasound. Coron Artery Dis 2003;14:459-62.
23. O'Rourke RA, Brundage BH, Froelicher VF, et al. American College of Cardiology/American Heart Association Expert Consensus document on electron-beam computed tomography for the diagnosis and prognosis of coronary artery disease. Circulation 2000;102:126-40.
24. Schaar JA, De Korte CL, Mastik F, et al. Characterizing vulnerable plaque features with intravascular elastography. Circulation 2003;108:2636-41.

25. Schaar JA, de Korte CL, Mastik F, et al. Three-Dimensional Palpography of Human Coronary Arteries. Ex-vivo validation and In-Patient Evaluation. Herz 2005;30:125-33.
26. Nissen SE, Tuzcu EM, Schoenhagen P, et al. Statin therapy, LDL cholesterol, C-reactive protein, and coronary artery disease. N Engl J Med 2005;352:29-38.
27. Ridker PM, Cannon CP, Morrow D, et al. C-reactive protein levels and outcomes after statin therapy. N Engl J Med 2005;352:20-8.
28. El-Barghouty NM, Levine T, Ladva S, Flanagan A, Nicolaides A. Histological verification of computerised carotid plaque characterisation. Eur J Vasc Endovasc Surg 1996;11:414-6.
29. Gronholdt ML, Nordestgaard BG, Wiebe BM, Wilhjelm JE, Sillesen H. Echo-lucency of computerized ultrasound images of carotid atherosclerotic plaques are associated with increased levels of triglyceride-rich lipoproteins as well as increased plaque lipid content. Circulation 1998;97:34-40.
30. Rasheed Q, Dhawale PJ, Anderson J, Hodgson JM. Intracoronary ultrasound-defined plaque composition: computer-aided plaque characterization and correlation with histologic samples obtained during directional coronary atherectomy. Am Heart J 1995;129:631-7.
31. Schartl M, Bocksch W, Koschyk DH, et al. Use of intravascular ultrasound to compare effects of different strategies of lipid-lowering therapy on plaque volume and composition in patients with coronary artery disease. Circulation 2001;104:387-92.
32. Aoki J, Abizaid AC, Serruys PW, et al. Evaluation of four-year coronary artery response after sirolimus-eluting stent implantation by using serial quantitative IVUS and computer assisted grey-scale value analysis for plaque composition. J Am Coll Cardiol 2005;In press.
33. Nissen SE, Tuzcu EM, Schoenhagen P, et al. Effect of intensive compared with moderate lipid-lowering therapy on progression of coronary atherosclerosis: a randomized controlled trial. Jama 2004;291:1071-80.
34. Okazaki S, Yokoyama T, Miyauchi K, et al. Early statin treatment in patients with acute coronary syndrome: demonstration of the beneficial effect on atherosclerotic lesions by serial volumetric intravascular ultrasound analysis during half a year after coronary event: the ESTABLISH Study. Circulation 2004;110:1061-8.
35. Cannon CP, Braunwald E, McCabe CH, et al. Intensive versus moderate lipid lowering with statins after acute coronary syndromes. N Engl J Med 2004;350:1495-504.

5

OCT Plaque Characterization: Comparison to Multislice Computed Tomography

Carlos A.G. Van Mieghem[1,2], Nico R. Mollet[1,2], Pim J. de Feyter[1,2]

From the departments of Cardiology[1] and Radiology[2],
Erasmus MC, Rotterdam, the Netherlands

Chapter in: Optical Coherence Tomography in Cardiovascular Reasearch. Informa Healthcare, 2007. Editors: Evelyn Regar, Ton G. van Leeuwen, Patrick W. Serruys

INTRODUCTION

Invasive coronary angiography remains the standard of reference for the assessment of advanced coronary artery disease, which is typically characterized by significant narrowing of the coronary lumen and provides the necessary road map for defining the type and extent of coronary revascularization (percutaneous coronary intervention or coronary artery bypass graft surgery). Unfortunately, "luminographic" involvement is a late manifestation of coronary artery disease since a large amount of atherosclerotic plaque accumulates in the vessel wall before affecting the coronary artery lumen[1,2]. Identification of the earlier stages of coronary artery disease is critically important, as it has been shown that the majority of acute coronary events, manifesting as acute myocardial infarction or sudden cardiac death, are initiated by sudden rupture and subsequent thrombosis of atherosclerotic plaques that are not causing significant stenosis[3]. In vivo visualization of the extent of the angiographically invisible coronary atherosclerotic process was initially demonstrated by intravascular ultrasound (IVUS), another invasive imaging technique[4]. Non-invasive alternatives for imaging of the coronary arteries became available one decade ago. Coronary imaging by magnetic resonance imaging as first demonstrated in the early 1990s looked very promising[5]. However, long acquisition times and insufficient spatial resolution limit its clinical usefulness for the assessment of coronary artery disease[6]. By contrast, rapid developments in computed tomography (CT) techniques have provided the necessary spatial and temporal resolution for coronary imaging. As a result, cardiac CT is emerging as the preferred non-invasive imaging tool that has the ability to visualize both the coronary artery lumen and vessel wall. In this chapter we describe the potential of cardiac CT for coronary plaque imaging and relate this feature to the current possibilities of optical coherence tomography (OCT).

CT Technology

A CT scanner consists of an x-ray tube that rotates around the patient, with images collected by a row of detectors on the opposite side (Figure 1). The patient is continuously moved through the X-ray field while data are digitally recorded from the detectors. The resulting X-ray projection data form a helix or spiral, hence the description 'spiral-CT'. While CT has been available for clinical use since the early 1970s, it has been poorly suited to cardiac imaging until a few years ago. Indeed, accurate non-invasive assessment of the coronary arteries poses several

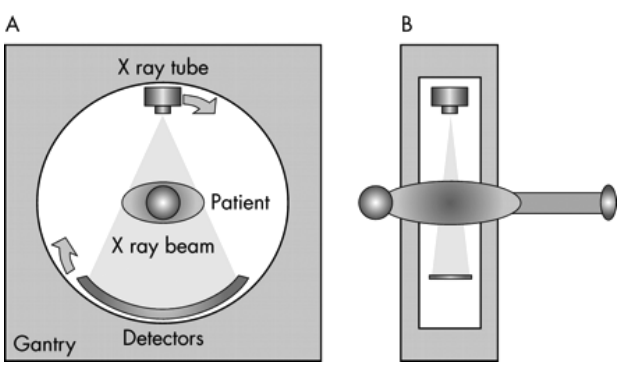

Figure 1. Frontal (A) and side (B) view of a CT scanner.

difficulties. First, high spatial resolution is required for accurate visualization of their small size and tortuous three-dimensional anatomy. Second, sufficient temporal resolution is needed to minimize artifacts related to rapid coronary motion. Third, the scan must be performed within a single short breath hold to avoid respiratory motion artifacts. To obtain motion-free images data are typically obtained during the diastolic phase of the cardiac cycle. Image acquisition must therefore be synchronized to the cardiac cycle using electrocardiogram (ECG) gating. In most instances retrospective ECG gating is used. This means that data are acquired during the whole cardiac cycle. After data acquisition, different reconstruction windows during the diastolic phase of the heart can be explored to obtain images with the lowest number of motion artifacts. Heart-rate-lowering drugs are generally recommended for patients with a resting heart rate above 70 beats/minute[7].

Two types of CT scanners, electron-beam CT (EBCT) and multislice CT (MSCT), exist for non-invasive cardiac imaging. EBCT offers better temporal resolution, but MSCT scanners provide higher spatial resolution, shorter scan time and higher signal-to-noise ratio and are currently the preferred CT imaging modality. MSCT scanners enable the simultaneous acquisition of multiple sections per rotation of the X-ray tube, hence the terminology 'multislice' spiral CT. Current 64-slice CT scanners allow data acquisition by up to 64 detector rows in one rotation. They feature a temporal resolution of 165 ms and isotropic (i.e., equal voxel dimensions in x, y, and z axes) through plane spatial resolution of 0.4 mm[8].

Plaque Evaluation and Characterization

Based on clinical grounds the presence of coronary artery disease in a patient is usually noted if there is a history of angina pectoris, myocardial infarction or coronary revascularization. Current diagnostic work-up of patients with suspicion of coronary artery disease targets the detection of myocardial ischemia due to flow-limiting coronary stenoses. However, this approach identifies coronary atherosclerosis only in an advanced development stage and falls short in identifying a large group of patients who present with acute coronary syndromes, such as unstable angina, myocardial infarction or sudden cardiac death, that are often the first clinical manifestation of coronary artery disease. Rupture or erosion with concomitant thrombosis of non-obstructive coronary plaques is the most frequent cause of these acute cardiac events (Figure 2)[9]. Pathological studies have identified several characteristics of plaques at increased risk for thrombosis, the so-called vulnerable plaque: they typically present eccentric remodeling, contain a large lipid core and are covered by a very thin fibrous cap showing an abundance of macrophages in the shoulder regions of the plaque[10]. Once vulnerable plaques have ruptured and resulted in an acute coronary syndrome, survival is diminished. Early identification and prophylactic stabilization of vulnerable plaque(s) may therefore play an important role in future strategies to prevent acute coronary syndromes. Coronary angiography, the reference standard for the identification of obstructive coronary artery disease, provides little or no infor-

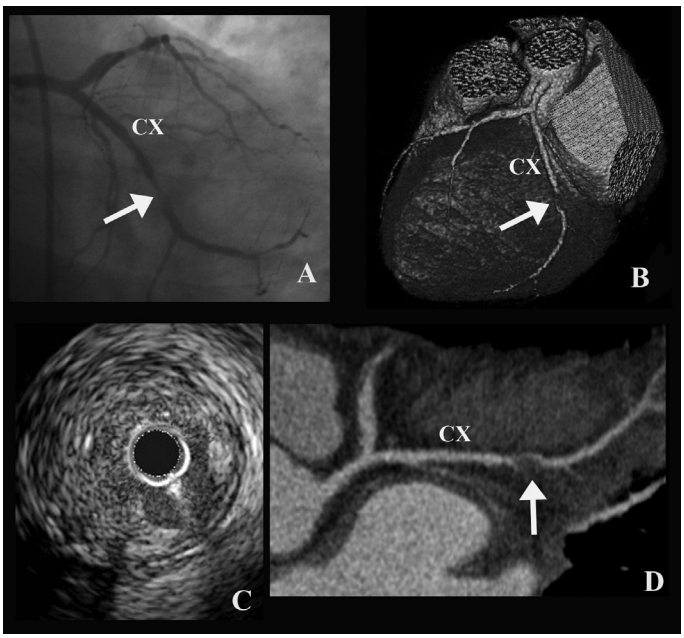

Figure 2. Patient with acute coronary syndrome showing a thrombotic subocclusive lesion of the circumflex coronary artery (CX) on conventional coronary angiography (A, arrow). Volume-rendered (B) and multiplanar reformatted (D) CT image confirm the presence of a subocclusive non-calcified plaque (arrows). On intravascular ultrasound (C) this lesion is hypechogenic in composition. The speckled appearance within the lumen is compatible with thrombus. (A full color version of this illustration can be found in the color section).

mation on the actual extent of the atherosclerotic process or on the composition of the atherosclerotic plaque[11]. As a result, coronary angiography cannot be used for the detection of vulnerable plaque(s). Unlike conventional angiography, coronary CT has the ability to depict the vessel wall and coronary plaque irrespective of the amount of lumen involvement, thus allowing assessment of both non-flow limiting and flow-limiting plaques[12].

CT Stenosis Detection

MSCT and to a lesser extent EBCT provide the necessary spatial and temporal resolution for accurate detection of significant obstructive coronary artery disease. Early reports using four-slice MSCT showed promising results. However, this technique was not robust enough, owing to its relatively long scan time and limited resolution, resulting in a number of non-evaluable coronary segments as high as 43%[13]. The diagnostic accuracy of CT coronary angiography significantly improved with 16-slice and the latest 64-slice MSCT, allowing reliable evaluation of coronary artery segments up to 1.5 mm in diameter[8,14-16]. The reported results depend largely on patient selection and several factors including elevated heart rates or severe coronary calcification cause suboptimal image quality, making it sometimes difficult to correctly assess the coronary arteries. Consequently, patients with arrhythmias are generally excluded and heart-rate-lowering medication is routinely administered for heart rates above 65-70 bpm.

CT Plaque Imaging

EBCT and non-enhanced MSCT can accurately detect coronary calcium[17,18]. Because arterial calcification almost always represents atherosclerosis, detection of coronary artery calcium by means of CT is a reliable, non-invasive tool for determining the presence of coronary

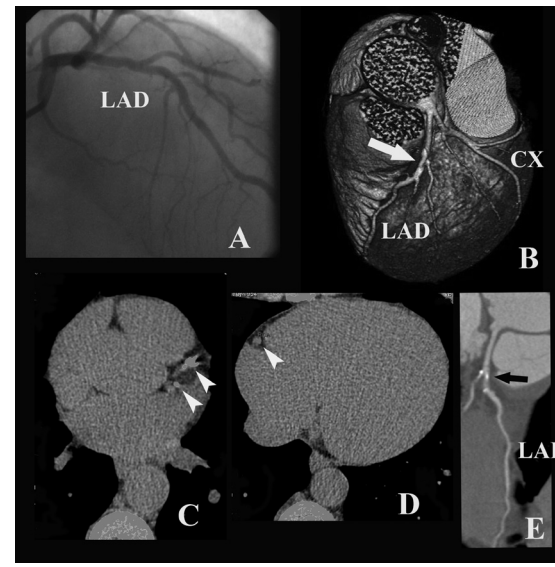

Figure 3. A 51-year-old man presented with an acute coronary syndrome with transient ST-segment depression in the anterior ECG leads. On conventional coronary angiography mild wall irregularities in the proximal left anterior descending coronary artery (LAD) were noted (A). Coronary artery calcifications in the proximal part of the left coronary artery (C) and right coronary artery (D) were detected on non-enhanced MSCT confirming the presence of coronary atherosclerosis. Total Agatston calcification score was 292. The calcified plaque in the LAD was non-obstructive as illustrated on MSCT coronary angiography (white arrow,E). Volume-rendered CT image (white arrow,B) confirms the presence of a calcified plaque in the proximal LAD. CX, circumflex coronary artery. (A full color version of this illustration can be found in the color section).

atherosclerosis. The amount of coronary calcium is closely correlated with the total atherosclerotic plaque burden and strongly predicts future cardiac events (Figure 3)[19]. Higher amounts of calcium are associated with a higher likelihood of adverse coronary events. At a population level, the coronary calcium score provides incremental value compared with traditional risk factors such as the Framingham Risk Score for predicting future cardiac events, and is therefore suggested as an adjunctive risk-stratification tool in intermediate-risk patients[20, 21]. However, up to 20% of patients presenting an acute coronary event may have mildly calcified or non-calcified culprit lesions and thus are not identified by coronary calcium scoring (Figure 4)[22].

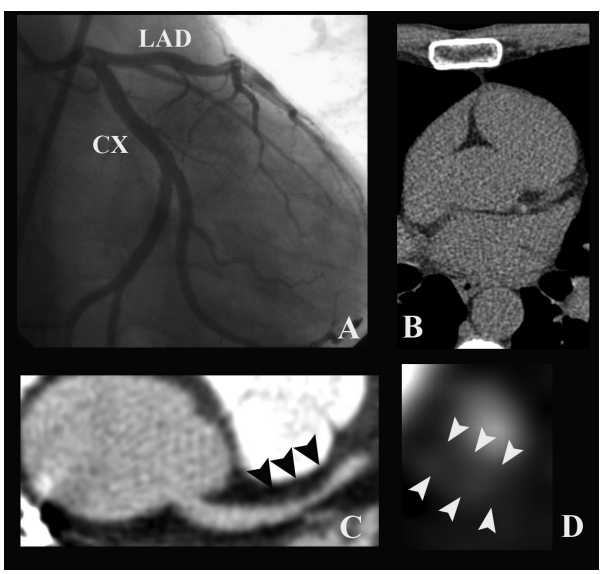

Contrast-enhanced MSCT is able to detect calcified and non-calcified coronary plaques. Based on the tissue-specific X-ray attenuation characteristics, it is possible to differentiate between fibrous tissue, lipid and calcium[23-27]. CT also has the abil-

Figure 4. 40-year-old patient presenting with two episodes of non-ST-segment elevation myocardial infarction in a 1-month time interval. Conventional coronary angiography (A) and non-enhanced MSCT (B) were normal. However, MSCT coronary angiography revealed a large non-calcified plaque without lumen obstruction in the proximal left anterior descending coronary artery (LAD) (C, black arrowheads). (D)Cross-sectional CT image with arrowheads indicating the non-calcified plaque occupying the vessel wall. CX, circumflex coronary artery.

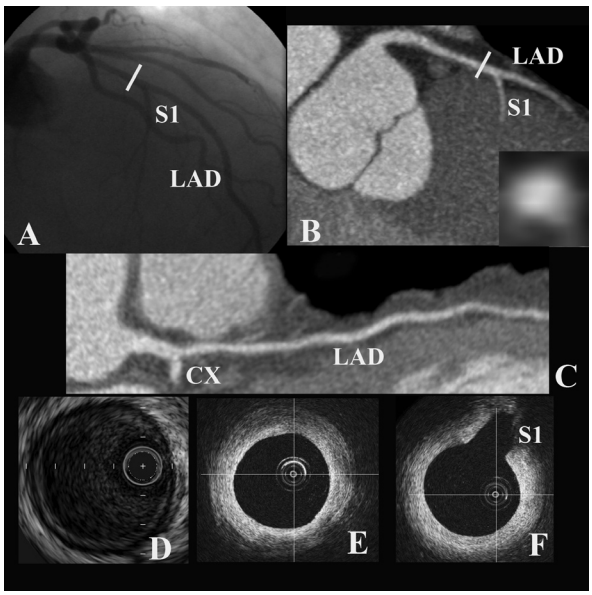

Figure 5. Comparison of intravascular OCT with findings on conventional coronary angiography, MSCT and intravascular ultrasound (IVUS). OCT was performed on the left anterior descending coronary artery (LAD) proximal to the first septal branch (S1). Angiographically (A) and on multislice computed tomography coronary angiography (B with inset, C) this part of the vessel has a normal appearance. The cross-sectional IVUS (D) and OCT images (E, F) show a normal appearance of the vessel wall except for some minimal thickening of the intima. CX, circumflex coronary artery.

ity to detect coronary segments with positive remodeling that can harbor substantial amounts of plaque without significant luminal stenosis[12]. The clinical relevance of this information is unclear and is the subject of ongoing studies. In addition, several limitations have to be taken into account: reported data were exclusively obtained in patients with high CT-image quality and are restricted to larger advanced plaques in sufficiently large coronary artery segments (at least 2 mm in diameter). Furthermore, lipid-rich and fibrous plaque shows overlapping CT attenuation characteristics and makes accurate subclassification of non-calcified plaques difficult.

OCT Plaque Characterization

OCT is an invasive imaging modality that can visualize the structure of normal and atherosclerotic coronary arteries with ultrahigh resolution (Figure 5)[28]. Compared to MSCT, OCT

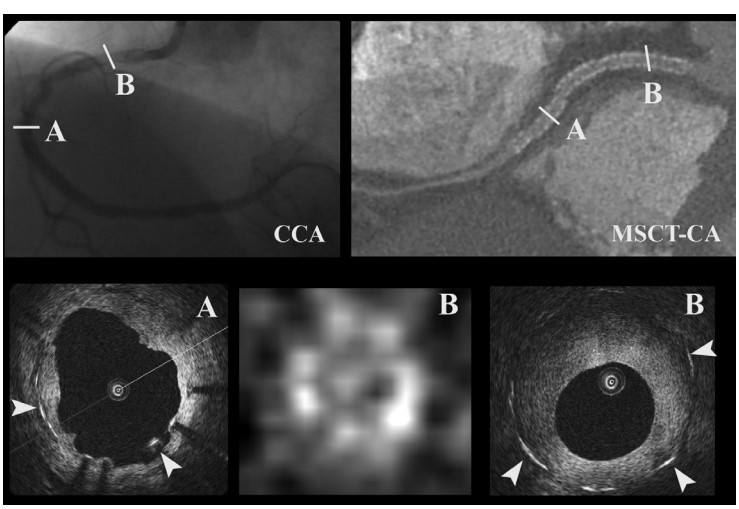

Figure 6. Normal appearance of the right coronary artery (RCA) on conventional coronary angiography (CCA) 6 months after implantation of three overlapping stents. Hypoattenuating circular tissue is clearly present on the cross-sectional computed tomography image of the proximal part of the RCA (cross-section B). Neointimal tissue growth within the stent is much better appreciated on intravascular OCT, also in the more distal part of the RCA (A and B). Arrowheads indicate the stent struts. Some minor stent malapposition can be appreciated at 5 o'clock (OCT cross-sectional image, A, arrowheads). (A full color version of this illustration can be found in the color section).

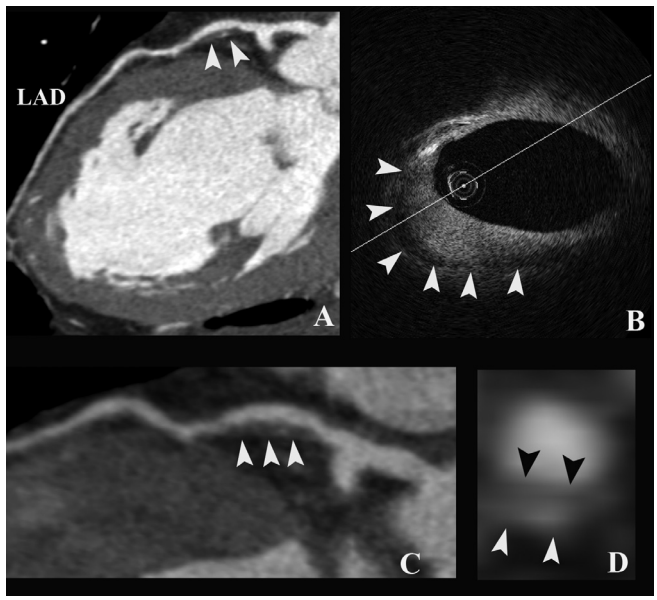

Figure 7. Non-calcified plaque as visualized with MSCT in the proximal part of the left anterior descending coronary artery (LAD) (A and C, arrowheads). The optical coherence tomography (OCT) cross-sectional image (B, arrowheads) with uniform highly reflective tissue is compatible with fibrous plaque. By contrast, lipid-rich plaques are visualized as low reflective structures within the arterial wall. This distinction in plaque appearance cannot be appreciated on MSCT, which uniformly depicts a non-calcified plaque as a structure within the range of 10-100 Hounsfield units. Also, the appearance of the plaque has much less image resolution as compared with OCT (see cross-sectional CT image in D, arrowheads). (A full color version of this illustration can be found in the color section).

allows much more detailed analysis of different coronary structures such as presence of in-stent intimal hyperplasia or advanced plaque characterization (Figure 6)[29]. Indeed, lipid-rich plaques have some unique differing OCT features compared to fibrous plaques (Figure 7). The high-resolution capacity of OCT offers the potential to detect some of the key features of the vulnerable plaque in vivo: a large lipid pool, a thin fibrous cap, and the accumulation of macrophages near the fibrous cap[30].

CONCLUSIONS

MSCT of the heart is a rapidly developing technology. In a selected patient population, current 64-slice CT scanners allow comprehensive non-invasive coronary imaging, including assessment of luminal stenosis and detection of non-obstructive atherosclerotic plaque. The high negative predictive value makes MSCT most suitable for exclusion of obstructive coronary plaques in patients with a low or intermediate likelihood of coronary artery disease. Beyond the detection of stenosis, MSCT may prove useful to identify high-risk coronary plaque characteristics. The possibility that MSCT can be used as an initial non-invasive technique to establish, in a high-risk individual, the presence and location of a possible high-risk lesion is currently investigated in a prospective study that will correlate MSCT coronary plaque characteristics with the propensity for future adverse coronary events. Ultimately, non-invasive imaging techniques such as MSCT might help targeting the use of invasive imaging modalities such as OCT in the search of patients at risk for acute coronary syndromes and sudden cardiac death[31, 32].

REFERENCES

1. Topol EJ, Nissen SE. Our preoccupation with coronary luminology. The dissociation between clinical and angiographic findings in ischemic heart disease. Circulation 1995;92(8):2333-42.
2. Glagov S, Weisenberg E, Zarins CK, Stankunavicius R, Kolettis GJ. Compensatory enlargement of human atherosclerotic coronary arteries. N Engl J Med 1987;316(22):1371-5.
3. Falk E, Shah PK, Fuster V. Coronary plaque disruption. Circulation 1995;92(3):657-71.
4. Nissen SE, Gurley JC, Grines CL, et al. Intravascular ultrasound assessment of lumen size and wall morphology in normal subjects and patients with coronary artery disease. Circulation 1991;84(3):1087-99.
5. Manning WJ, Li W, Edelman RR. A preliminary report comparing magnetic resonance coronary angiography with conventional angiography. N Engl J Med 1993;328(12):828-32.
6. Achenbach S, Daniel WG. Noninvasive coronary angiography--an acceptable alternative? N Engl J Med 2001;345(26):1909-10.
7. Mollet NR, Cademartiri F, de Feyter PJ. Non-invasive multislice CT coronary imaging. Heart 2005;91(3):401-7.
8. Mollet NR, Cademartiri F, van Mieghem CA, et al. High-resolution spiral computed tomography coronary angiography in patients referred for diagnostic conventional coronary angiography. Circulation 2005;112(15):2318-23.
9. Libby P. Current concepts of the pathogenesis of the acute coronary syndromes. Circulation 2001;104(3):365-72.
10. Virmani R, Kolodgie FD, Burke AP, Farb A, Schwartz SM. Lessons from sudden coronary death: a comprehensive morphological classification scheme for atherosclerotic lesions. Arterioscler Thromb Vasc Biol 2000;20(5):1262-75.
11. Monroe VS, Parilak LD, Kerensky RA. Angiographic patterns and the natural history of the vulnerable plaque. Prog Cardiovasc Dis 2002;44(5):339-47.
12. Achenbach S, Ropers D, Hoffmann U, et al. Assessment of coronary remodeling in stenotic and nonstenotic coronary atherosclerotic lesions by multidetector spiral computed tomography. J Am Coll Cardiol 2004;43(5):842-7.
13. Kuettner A, Kopp AF, Schroeder S, et al. Diagnostic accuracy of multidetector computed tomography coronary angiography in patients with angiographically proven coronary artery disease. J Am Coll Cardiol 2004;43(5):831-9.
14. Leschka S, Alkadhi H, Plass A, et al. Accuracy of MSCT coronary angiography with 64-slice technology: first experience. Eur Heart J 2005;26(15):1482-7.

15. Leber AW, Knez A, von Ziegler F, et al. Quantification of obstructive and nonobstructive coronary lesions by 64-slice computed tomography: a comparative study with quantitative coronary angiography and intravascular ultrasound. J Am Coll Cardiol 2005;46(1):147-54.
16. Raff GL, Gallagher MJ, O'Neill WW, Goldstein JA. Diagnostic accuracy of noninvasive coronary angiography using 64-slice spiral computed tomography. J Am Coll Cardiol 2005;46(3):552-7.
17. Agatston AS, Janowitz WR, Hildner FJ, Zusmer NR, Viamonte M, Jr., Detrano R. Quantification of coronary artery calcium using ultrafast computed tomography. J Am Coll Cardiol 1990;15(4):827-32.
18. O'Rourke RA, Brundage BH, Froelicher VF, et al. American College of Cardiology/American Heart Association Expert Consensus Document on electron-beam computed tomography for the diagnosis and prognosis of coronary artery disease. J Am Coll Cardiol 2000;36(1):326-40.
19. Rumberger JA, Simons DB, Fitzpatrick LA, Sheedy PF, Schwartz RS. Coronary artery calcium area by electron-beam computed tomography and coronary atherosclerotic plaque area. A histopathologic correlative study. Circulation 1995;92(8):2157-62.
20. Arad Y, Goodman KJ, Roth M, Newstein D, Guerci AD. Coronary calcification, coronary disease risk factors, C-reactive protein, and atherosclerotic cardiovascular disease events: the St. Francis Heart Study. J Am Coll Cardiol 2005;46(1):158-65.
21. Taylor AJ, Bindeman J, Feuerstein I, Cao F, Brazaitis M, O'Malley PG. Coronary calcium independently predicts incident premature coronary heart disease over measured cardiovascular risk factors: mean three-year outcomes in the Prospective Army Coronary Calcium (PACC) project. J Am Coll Cardiol 2005;46(5):807-14.
22. Shemesh J, Stroh CI, Tenenbaum A, et al. Comparison of coronary calcium in stable angina pectoris and in first acute myocardial infarction utilizing double helical computerized tomography. Am J Cardiol 1998;81(3):271-5.
23. Schroeder S, Kopp AF, Baumbach A, et al. Noninvasive detection and evaluation of atherosclerotic coronary plaques with multislice computed tomography. J Am Coll Cardiol 2001;37(5):1430-5.
24. Leber AW, Knez A, Becker A, et al. Accuracy of multidetector spiral computed tomography in identifying and differentiating the composition of coronary atherosclerotic plaques: a comparative study with intracoronary ultrasound. J Am Coll Cardiol 2004;43(7):1241-7.
25. Achenbach S, Moselewski F, Ropers D, et al. Detection of calcified and noncalcified coronary atherosclerotic plaque by contrast-enhanced, submillimeter multidetector spiral computed tomography: a segment-based comparison with intravascular ultrasound. Circulation 2004;109(1):14-7.

26. Schroeder S, Kuettner A, Leitritz M, et al. Reliability of differentiating human coronary plaque morphology using contrast-enhanced multislice spiral computed tomography: a comparison with histology. J Comput Assist Tomogr 2004;28(4):449-54.
27. Becker CR, Nikolaou K, Muders M, et al. Ex vivo coronary atherosclerotic plaque characterization with multi-detector-row CT. Eur Radiol 2003;13(9):2094-8.
28. Jang IK, Tearney GJ, MacNeill B, et al. In vivo characterization of coronary atherosclerotic plaque by use of optical coherence tomography. Circulation 2005;111(12):1551-5.
29. Yabushita H, Bouma BE, Houser SL, et al. Characterization of human atherosclerosis by optical coherence tomography. Circulation 2002;106(13):1640-5.
30. Tearney GJ, Yabushita H, Houser SL, et al. Quantification of macrophage content in atherosclerotic plaques by optical coherence tomography. Circulation 2003;107(1):113-9.
31. Naghavi M, Libby P, Falk E, et al. From vulnerable plaque to vulnerable patient: a call for new definitions and risk assessment strategies: Part I. Circulation 2003;108(14):1664-72.
32. Naghavi M, Libby P, Falk E, et al. From vulnerable plaque to vulnerable patient: a call for new definitions and risk assessment strategies: Part II. Circulation 2003;108(15):1772-8.

INTERLUDE 1

Myocardial Infarction in a Patient with Sickle Cell Trait. Treatment Dilemmas and Imaging Findings at Follow-Up.

Carlos A.G. Van Mieghem[1], Steve Ramcharitar[1], Peter Barlis[1], Wolter Oosterhuis[2], Charles Kik[3], Pim J. de Feyter[1], Patrick W. Serruys[1]

From the departments of Interventional Cardiology1, Anatomopathology[2], and Cardiac Surgery[3], Erasmus MC, Rotterdam, the Netherlands

EuroInterv. 2008; 3: 627-634

SUMMARY

Background
A 43-year-old woman with a 2-hour history of chest pain presented with an anterior infaction and was referred for primary percutaneous coronary intervention.

Investigations
Physical examination, electrocardiography, laboratory tests, coronary angiography, abdominal angiography, cardiac CT, histology, immunohistochemistry, intravascular ultrasound.

Diagnosis
ST-segment elevation anterior myocardial infarction

Management
Coronary angiography, antithrombotic therapy, statin, angiotensin-converting enzyme inhibitor, thrombectomy, coronary artery bypass graft surgery

HOW SHOULD I TREAT?

Presentation of the case
A 43-year-old woman with no previous cardiac history presented with a 2 hour history of central chest pain with radiation to the left arm unresponsive to sublingual nitroglycerin. A pre-hospital electrocardiogram (ECG) showed ST-segment elevation in the precordial anterior leads consist with an evolving anterior infarction and was referred to our hospital for primary percutaneous coronary intervention (PCI). On admission to the coronary care unit (CCU), the pain had almost completely resolved. A 12-lead ECG showed persistent, but to a lesser degree, ST-segment elevation in all precordial leads (V1 to V6), including the inferior leads (II, III and aVF).

The woman was from African origin and had a history of sickle cell disease. She had arterial hypertension, which was treated with a thiazide diuretic, and a positive family history of premature coronary artery disease. She reported no history of diabetes or dyslipidemia, and was a non-smoker. Her blood pressure on admission was 135/ 65 mm Hg, and on physical examination there were no signs of heart failure.

Aspirin (300 mg), unfractionated heparin (5000 IU), and nitroglycerine as a continuous intravenous infusion had been administered in the ambulance. Clopidogrel bisulfate (600 mg bolus) was added in the CCU. Coronary angiography showed a significant stenosis with fresh

thrombotic material in the left main coronary artery (LMCA) that extended towards the ostium of the left anterior descending artery (LAD) (Figure 1). The angiographic appearance of left circumflex artery (LCX), large intermediate branch (IB) and dominant right coronary artery (RCA) was unremarkable with normal epicardial flow, but the flow in the LAD was mildly impaired (TIMI flow, grade 2) .

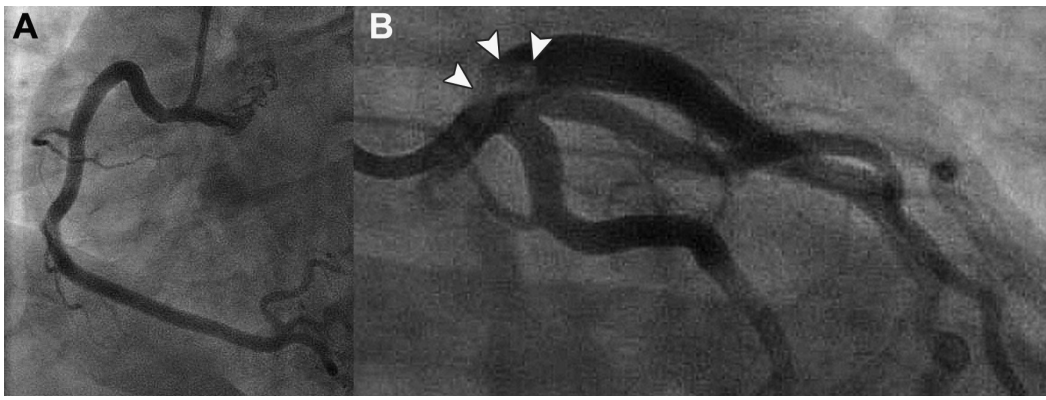

Figure 1. (A) Normal appearance of the right coronary artery. (B) Large filling defect (arrows) in the left main extending into the proximal left anterior descending artery.

At this stage, it was unclear what would be the optimal treatment strategy. It was deemed too high risk to performing a PCI due to the location of the thrombus and the complexity of the 3 major epicardial vessels. Any attempt of thrombotic aspiration had the risk of possible embolization towards the 3 distal run-off vessels. An early consultation with our surgical colleagues suggested that ideally, coronary artery bypass graft surgery (CABG) would carry the least risk, but preferably not in the acute phase of a MI.

Since the patient was now completely pain free following catheterisation and there was spontaneous reperfusion of the infarct-related-vessel(s), it was decided for aggressive anticoagulant and anti-platelet therapy. On a regime of aspirin, clopidogrel, unfractionated heparin, and IV eptifibatide, a glycoprotein IIb/ IIIa receptor antagonist, the patient's clinical condition stabilised. The CK values peaked at 454 U/l (CKMB mass of 47.6 U/l) 16 hours after admission. But one day after admission she developed a spontaneous bleeding of the right iliopsoas muscle accompanied by fall in haemoglobin level from 6 to 4.3 mmol/l. The treatment with eptifibatide was stopped and she was transfused 2 units of packed red blood cells. On selective abdominal angiography there was no obvious bleeding focus. The patient underwent a CT coronary angiography (CTCA) 3 days later to re-evaluate the left main stem and other coronary arteries. The CT scan showed a persistent severe narrowing of the LMCA with normal appearance of the other coronary vessels (Figure 2). Assessment of the total coronary calcium burden did not reveal any calcium. The invasive coronary angio-

gram that was repeated the same day confirmed these findings. By this stage, the CK level had normalised (134 U/l).

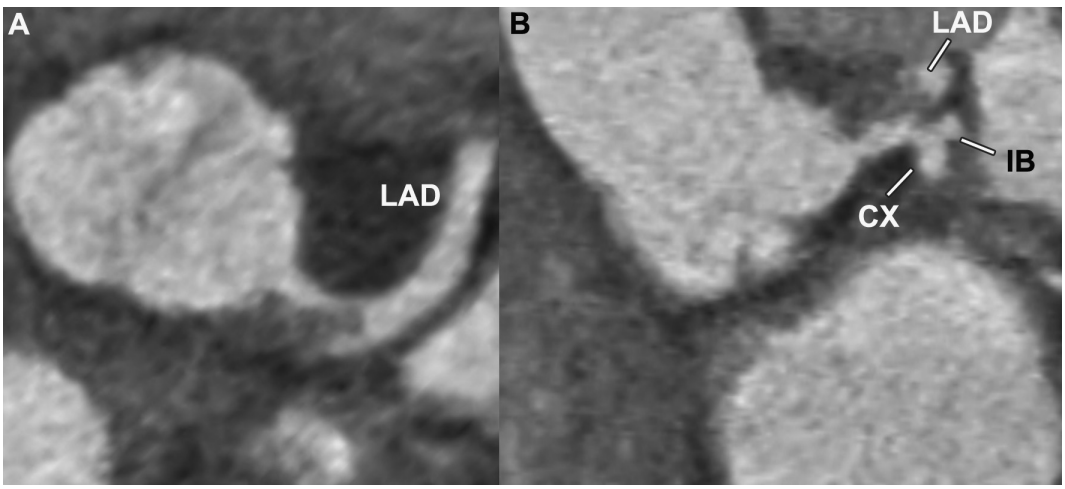

Figure 2. Axial (A) and coronal (B) CT image showing the thrombus in the LMCA. The thrombus extends towards the LAD. The IB and CX are not affected. CX, circumflex artery; IB, intermediate branch; LAD, left anterior descending artery; LMCA, left main coronary artery.

HOW COULD I TREAT?

The invited experts opinion

The Interventionalist point of view
David Antoniucci, MD
Division of Cardiology, Careggi Hospital, Florence, Italy

Despite the lack of the typical signs of fat embolism syndrome, the hypothesis of fat embolism in a young woman with sickle cell disease as the cause of an acute myocardial infarction with persistent nonocclusive thrombosis of the left main should be considered. Again, there is no angiographic evidence of atherosclerosis or spontaneous coronary dissection as the cause of thrombosis. It could be useful to see the distal bed of the left anterior descending artery, since ST segment elevation in both precordial and inferior leads associated with a subsequent small infarct suggest a persistent occlusive embolism of the distal left anterior descending artery. It has been hypothesised that fat emboli may reach the systemic arterial circulation via a patent foramen ovale or other intracardiac or pulmonary arteriovenous shunts (1) and appropriate investigations to identify these pathologies should be performed (ECHO, CT scan). The lack of any visible effect after three days of aggressive antiplatelet and anticoagulant treatment makes stronger the suspicion that the mass in the left main cannot be a thrombus. Another possible role of sickle cell disease in this case is that the thrombosis may be the result of endothelial

damage attributable to shear injury by sickle cells and resulting prothrombotic state. At this stage, my strategy would be to perform an IVUS examination in order to exclude the possibility of coronary atherosclerotic disease or spontaneous dissection complicated by thrombosis. Again, there is the possibility that IVUS virtual histology could define the characteristics of the mass going into the left main. In the case of a fat embolism diagnosis, I think that the best strategy is the surgical removal of the material, since all endoluminal techniques (thrombectomy devices, atherectomy devices, aspiration devices also with large catheters such as the Proxis used as an aspiration catheter without proximal occlusion of the vessel) seem likely to be unsuccessful in removal the entire material, while the risk of distal occlusive embolisation is high. Conversely, if the mass is a thrombus, the treatment should be endoluminal and should include rheolytic thrombectomy before stenting, or thrombectomy alone if IVUS doesn't show any disrupted plaque or dissection. Whatever the nature of the mass going into the left main and the chosen treatment (endoluminal or surgical treatment), in my opinion there is the indication for acute exchange transfusion before treatment in order to decrease the haemoglobin S level to less than 30%. It has been shown that hyper-transfusion may prevent sickling and decrease the pro-coagulant state of sickle cell disease (2).

REFERENCES

1. Martin CR, Johnson CS, Cobb C, Tatter D, Haywood JL. Myocardial infarction in sickle cell disease. J Natl Med Assoc 1996; 88: 428-432.
2. The Optimizing Primary Stroke Prevention in Sickle Cell Anemia (STOP 2) Trial Investigators. Discontinuing prophylactic transfusions used to prevent stroke in sickle cell disease. N Engl J Med 2005: 353: 2768-2778.

The Surgeon's point of view

David P. Taggart, MD(Hons), PhD, FRCS
University of Oxford, Oxford, United Kingdom

This is a particularly interesting and unusual case of left main stem (LMS) stenosis. The optimal method of revascularisation (between surgery and stents) will be influenced by how general recommendations for LMS stenosis are influenced by key features specific to this patient including:

- Young woman (43 years old)
- Presentation with established acute infarct with ST elevation and enzyme rise
- Complex left main stem stenosis involving ostium, shaft and extending to proximal LAD and containing thrombus (may require IVUS confirmation)
- Normal intermediate, obtuse marginal and right coronary artery
- Significant bleed on anti-platelet medication

Additional information required to determine optimal treatment decision:

- Precise extent and complexity of LMS stenosis can be delineated by IVUS
- Assessment of left ventricular function (good, moderate, poor) to guide risk of surgery
- Any other contraindication to surgery such as significantly impaired renal function

The case for and against stents:

In general outcomes with stents in LMS stenosis are critically dependent on

- the precise anatomic location and complexity (including calcification) of the lesion
- the simultaneous presence of multivessel coronary artery disease (in up to 80% of patients).

Up to 90% of LMS stenosis involve the distal segment of the artery and extend into the proximal coronary arteries (1) and such bifurcation or trifurcation lesions are at notoriously high risk of restenosis with both bare metal stents and drug eluting stents (2). The angiographic appearance in this patient suggests diffuse involvement of the left main including extension to the LAD (if there is uncertainty this can be confirmed with IVUS). Furthermore -and ominously- restenosis in this critical location, even with drug eluting stents, is frequently asymptomatic and therefore mandates intensive and possibly serial angiographic follow up (3).

In contrast, a recent multicentre retrospective registry of 147 patients with non-bifurcation LMS appears to be safe and effective with restenosis of <1% at 6-month angiographic follow-up, major adverse clinical event rates of 7%, and a cumulative cardiac mortality of 2.7% at a median follow-up of around two and a half years (4). However even in this series the authors pointed out that there were four late unexplained deaths (4) raising the spectre of late stent thrombosis. If stenting is advocated then the relative merits of drug eluting (DES) and bare metal stents (BMS) need to be considered. While DES reduce the rate of restenosis it is increasingly likely that they will require lifelong dual anti platelet medication. In view of a previous significant bleed in this patient DES may be contraindicated.

The case for and against CABG

Both randomised trials and Registry data show that CABG offers the most durable and proven treatment for LMS stenosis (1). In contrast to the location of stents, placing the bypass grafts to the mid coronary vasculature has two important beneficial prognostic implications (1):

- the complexity and location of LMS stenosis (as well as its frequently associated proximal multivessel coronary artery disease) are irrelevant
- the grafts offer prophylaxis against the development of new disease in the proximal coronary vasculature

And the current results of CABG in LMS stenosis are reassuring. The Society of Cardiothoracic Surgery in the UK reported a mortality of 3% for all 5,003 patients undergoing CABG for LMS

stenosis including high risk and urgent cases (5) and two recent British studies reported excellent two year survival rates of 94% and 95% (6,7). As for all cardiac surgical procedures the mortality is strongly influenced by co-morbidities; for example Ellis et al reported that three year mortality for CABG in LMS stenosis varied from 4% in low risk patients to 40% in those with significant and multiple co-morbidities (8). The fact that this patient has had a recent infarct would significantly increase the immediate risk of surgery with the risk decreasing rapidly after two weeks and towards normal elective risk within six weeks assuming that the ventricle is not significantly impaired. The survival benefit of CABG is increased by the use of an IMA graft to the left anterior descending coronary artery and may be further magnified by the use of a second IMA graft. The angiographic patency of both IMA placed to left sided coronary vessels is over 95% at one week and at seven years and may translate into a significant survival benefit (9). In a systematic review of over 15,000 CABG patients matched for age, gender, diabetes and left ventricular function, the HR for death was 0.82 with bilateral vs single IMA grafts (NNT of 13-16) (9). And the use of bilateral IMA grafts appears safe; the ART trial of bilateral versus single IMA (10) grafts reported an overall 30-day mortality of 1% in over 3,100 patients [Taggart DP; unpublished observations].

Recommendation

If the patient remains stable, she should be kept in hospital to undergo CABG in 10-14 days (assuming LV function is at least moderate) as this offers the best prospect of a good long-term outcome and particularly in view of her young age. An initial strategy of stenting, to defer surgery, carries risk because of an increased risk of death before crossover to CABG occurs. CABG should be performed with three bypass grafts because of the diffuse nature of LMS disease and ideally should be done with both IMA grafts to the two best left sided vessels. If the patient is unstable or has sustained significant myocardial damage (when risks of CABG would be high) then an initial strategy of stenting is reasonable but mandates intensive – including angiographic – follow-up. In view of previous significant bleed then a bare metal stent might be favoured to avoid the need for dual antiplatelet medication.

REFERENCES

1. Taggart DP, Kaul S, Boden WE et al Revascularisation for Unprotected Left Main Stem, Coronary Artery Stenosis: Stenting or Surgery. J Am Coll Cardiol 2008 (in press)
2. Valgimigli M, Malagutti P, Rodriguez-Granillo GA, et al. Distal left main coronary disease is a major predictor of outcome in patients undergoing percutaneous intervention in the drug-eluting stent era: an integrated clinical and angiographic analysis based on the RESEARCH and T-SEARCH registries. J Am Coll Cardiol 2006;47:1530-7.

3. Price MJ, Cristea E, Sawhney N, et al. Serial angiographic follow-up of sirolimus-eluting stents for unprotected left main coronary artery revascularization. J Am Coll Cardiol 2006;47:871-7.
4. Chieffo A, Park SJ, Valgimigli M, et al. Favorable Long-Term Outcome After Drug-Eluting Stent Implantation in Nonbifurcation Lesions That Involve Unprotected Left Main Coronary Artery. A Multicenter Registry. Circulation. 2007; 116: 158-62.
5. Keogh BE, Kinsman R. Fifth national adult cardiac surgical database report 2003. Dendrite Clinical Systems (Henley-on Thames, Oxfordshire, UK) 2004.
6. Yeatman M, Caputo M, Ascione R, Ciulli F, Angelini GD. Off-pump coronary artery bypass surgery for critical left main stem disease: safety, efficacy and outcome. Eur J Cardiothorac Surg 2001;19:239-44.
7. Lu JC, Grayson AD, Pullan DM. On-pump versus off-pump surgical revascularization for left main stem stenosis: risk adjusted outcomes. Ann Thorac Surg 2005;80:136-42.
8. Ellis SG, Hill CM, Lytle BW. Spectrum of surgical risk for left main coronary stenoses: benchmark for potentially competing percutaneous therapies. Am Heart J 1998;135:335-8.
9. Taggart DP, D'Amico R, Altman DG. Effect of arterial revascularisation on survival: a systematic review of studies comparing bilateral and single internal mammary arteries. Lancet 2001; 358:870-5.
10. Taggart DP, Lees B, Gray A et al; ART Investigators. Protocol for the Arterial Revascularisation Trial (ART). A randomised trial to compare survival following bilateral versus single internal mammary grafting in coronary revascularisation [ISRCTN46552265]. Trials. 2006 Mar 30;7:7.

HOW DID I TREAT?

Actual treatment and management of the case

The patient was deemed eligible for enrollment in the SYNTAX study, a multicenter, prospective study, randomising patients with de novo 3-vessel disease and/or left main disease to undergo either PCI or CABG. She was randomized to the CABG-arm of the study and eight days after admission she underwent uneventful revascularization of the LAD using the left internal mammary artery graft, and of the intermediate branch using the right internal mammary artery graft. A small aortotomy was performed to remove the focal lesion in the LMCA, which was sent for pathologic evaluation (Figure 3). She made an uneventful recovery and was discharged 8 days later on 100 mg aspirin, 100 mg metoprolol, 40 mg atorvastatin, 4 mg perindopril once daily, and oral iron supplements. To re-assess the surgical result, a repeat cardiac CT scan was performed 6 months later, which showed a patent LMCA without residual stenosis and occlusion of both bypass grafts (Figure 4a). A repeat invasive angiogram

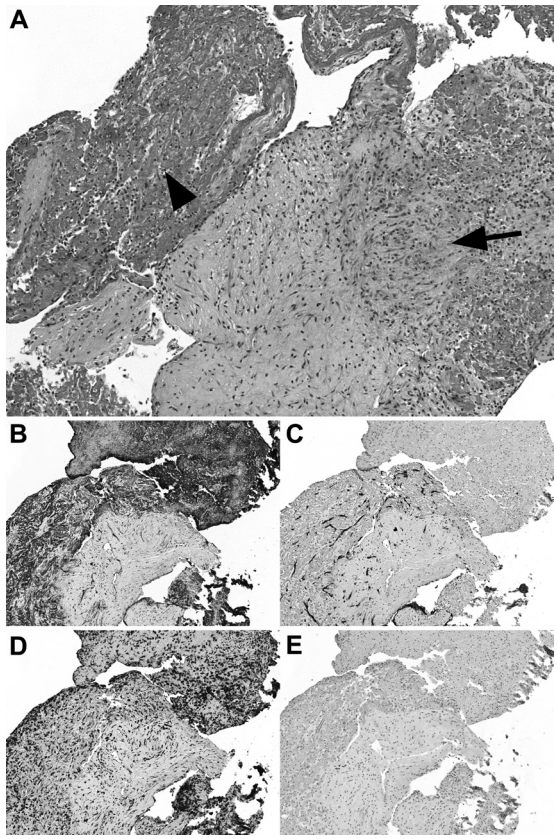

Figure 3. (A) Tangential cut of fibrotic initima with attached thrombus that is being organized in view of the ingrowth of fibroblasts (arrow) and capillaries (arrowhead) (hematoxylin and eosine, original magnification 50 x). (B) Same area stained for CD31 shows diffuse staining of thrombotic material including platelets and capillaries. (C) Same area stained for CD34, highlighting the growth of capillaries into the thrombus. (D) Same area stained for CD68, showing numerous histiocytic cells/macrophages scattered throughout the intima and the thrombus. (E) Same area stained for desmin showing the absence of smooth muscle cells in the intima. (A full color version of this illustration can be found in the color section).

showed the LIMA to be hypoplastic with competitive filling from the native coronary circulation (Figure 4b); the RIMA graft was occluded early on in its course (Figure 4c).

Intravascular ultrasound (IVUS) showed the persistence of a large noncalcified plaque in the LMCA, that was clearly present on CT but not visible angiographically (Figures 5a and b). IVUS radiofrequency data analysis (RDA) and optical coherence tomography (OCT) showed this plaque to have a fibrous composition (Figures 5c and d). Serology revealed that the patient was heterozygous for the hemoglobin S gene without any other pro-thrombophilic condition.

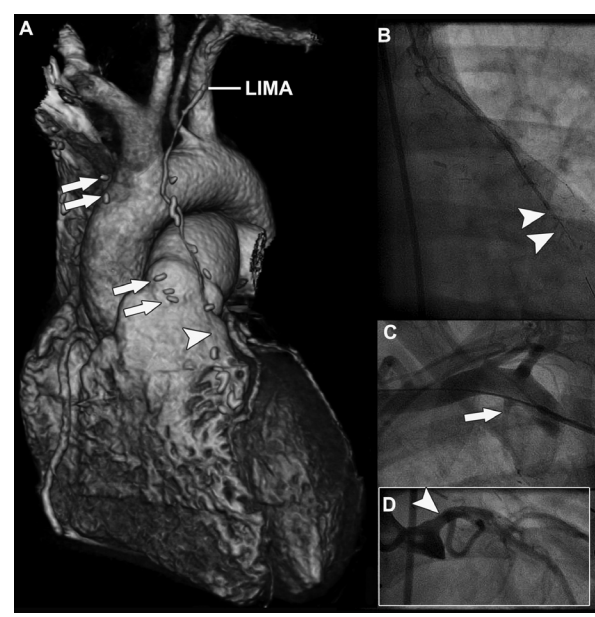

Figure 4. (A) Three-dimensional volume-rendered CT image showing the occlusion of the LIMA (left internal mammary artery graft) [arrowhead] at the level of the right ventricular outflow tract. The RIMA (right internal mammary artery graft) is also occluded: its previous course is still marked by vascular clips (arrows). (B, C) Corresponding invasive angiogram showing the LIMA graft to be hypoplastic with only minimal contrast filling distally (arrowheads) and an occlusion of the RIMA in its proximal part (arrow). (D) Invasive coronary angiogram showing a normal appearance of the left main coronary artery (arrowheads). (A full color version of this illustration can be found in the color section).

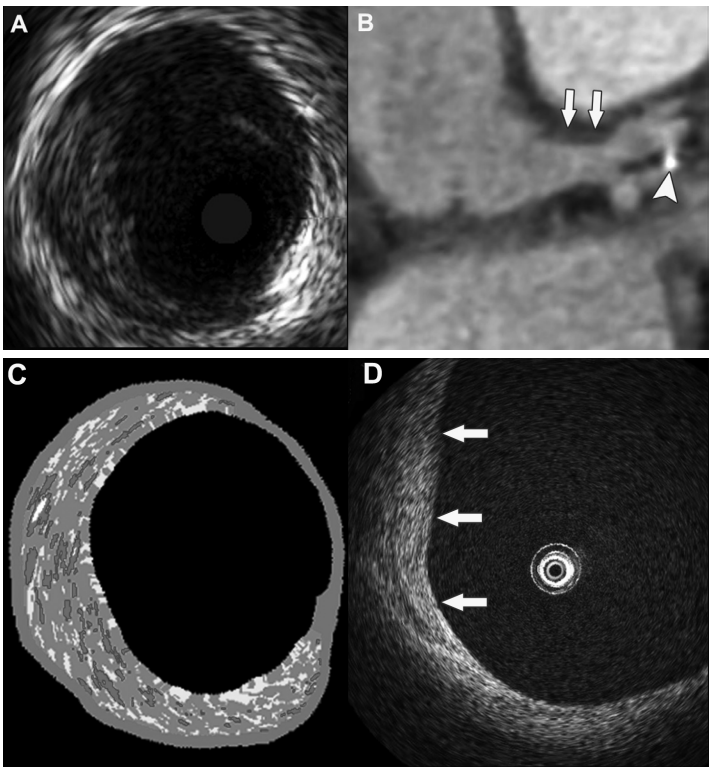

Figure 5. (A) Intravascular ultrasound of the distal left main coronary artery showing a large noncalcified plaque, extending from the 6 to 12 o'clock position. (B) This plaque is also visible on the corresponding CT image (arrows). The previous connection of the right internal mammary artery graft to the intermediate branch is indicated by the vascular clip (arrowhead). (C) Radiofrequency data analysis (RDA) showed that the plaque was predominantly fibrous in nature. (D) Optical coherence tomography (OCT) also showed features consistent with a fibrous plaque with a high reflectivity, homogenous and finely textured appearance (arrows). (A full color version of this illustration can be found in the color section).

An overview of the relevant laboratory tests performed since hospital admission is provided in Table 1. Since she remains asymptomatic, her medical therapy was continued.

Table 1. Results of laboratory tests.

Variable	Normal range	First admission	6 months follow-up
Total cholesterol (mmol/la)	<4.1	4.0	2.2
HDL cholesterol (mmol/la)	>1.0	1.5	1.2
LDL cholesterol (mmol/la)	<3.4	2.3	0.9
Triglycerides (mmol/lb)	<1.7	0.3	0.6
Antitrombine III (IU/ml)	0.8-1.2		0.84
Factor II (E/ml)	0.8-1.25		0.93
Factor V Leiden	Absent		Absent
Protein C activity (IU/ml)	0.7-1.4		0.48
Protein S activity (IU/ml)	0.7-1.4		0.38
Antiphospholipid antibodiesc	Absent		absent

a For conversion to mg/dl divide by 0.0259. b For conversion to mg/dl divide by 0.0113.
c Antiphospholipid antibodies: consisting of anticardiolipin, anti-beta2-glycoprotein I and lupus anticoagulant antibodies.

Discussion of diagnosis

The occurrence of an acute MI in a female patient of relatively young age, i.e., less than 45 years, is quite unusual and represents only ~ 2% of the women diagnosed with a heart attack each year.[1] Except for arterial hypertension and a positive family history of premature coronary artery disease our patient did not have other risk factors that would put her at risk for developing an acute MI. Using the Framingham-risk score her 10-year risk for developing a major coronary event was calculated as less than 1%.[2] Illicit drug uses, which our patient denied, is a well recognized precipitating factor in this age group and should be scrutinized. Coronary calcium, as measured and quantified by cardiac CT, documents the presence of coronary atherosclerosis and adds precision to the risk estimate of cardiac events based on traditional risk factors.[3] The risk of cardiac events in patients without coronary calcification is very low, i.e. 0.1% per year.[4,5] However, the absence of coronary calcium does not exclude the presence of atherosclerotic disease. In fact, it is not unusual to find a calcium score of zero in relatively young patients (i.e. below the age of 60) who present with an acute coronary event.[6] Plaque rupture and ensuing thrombosis most often occurs in non-calcified coronary lesions. CTCA allows the identification of these so-called soft plaques provided they are sufficiently large. This case illustrates this concept and is a nice in-vivo illustration of plaque erosion with thrombosis occurring in an atherosclerotic lesion with non-calcified morphology. Coronary plaque erosion is a less frequent cause of coronary thrombosis and typically occurs in relatively young and female patients.[7] As compared to the classical rupture-prone plaques, this type of vulnerable plaque typically lacks a large lipid core but instead is composed of smooth muscle cells and proteoglycan-rich extracellular matrix.

Patients with sickle cell disease, who are homozygous for the abnormal hemoglobin S, can present with cardiac problems, including the occurrence of acute MI.[8] In contrast to atherosclerotic disease, coronary thrombosis with obstruction usually affects the small arteries and it is rare to find abnormalities of the large epicardial vessels. Furthermore, heterozygosity for the sickle cell gene (sickle cell trait) usually does not result in clinical manifestations. Although the pathogenesis of the acute cardiac event in this case is related to atherosclerotic disease, the abundance of endothelial cells within the removed thrombus-like material in the left main stem, fits with the histopathologic findings of patients with sickle cell disease.[9] Factors such as endothelial dysfunction and increased platelet activation, which are well described in patients with sickle cell disease, might have contributed to the sequence of events in this patient.[10]

Current 64-slice and dual-source 64-slice CT scanners offer sufficient resolution to provide reliable non-invasive access to the different cardiac anatomical structures. Of particular value is the direct way of looking at coronary artery disease by revealing the presence of disease in the vessel wall and lumen and the robustness in visualizing larger vessel structures such as bypass

grafts, which sometimes are difficult to depict by invasive coronary angiography. The cardiac CT scan in this case accurately reflected the course of the disease by showing the presence and subsequent disappearance of the large plaque with luminal narrowing in the LMCA and the occlusion of the bypass grafts at six months follow-up.

Treatment and management

Primary PCI using stents performed within 90 minutes of first medical contact is the preferred treatment strategy for patients with STEMI who present within 12 hours of symptom onset.[11]

However, up to 5% of patients with STEMI who undergo emergency cardiac catheterization are not deemed suitable for PCI but undergo CABG instead.[12] The main reason to select CABG as the preferred reperfusion strategy in patients with acute MI is the presence of left main disease or other unfavourable anatomy for PCI. In selected patients, in particular acute MI patients with an occlusion of the left main stem and/or hemodynamic instability, the percutaneous approach is often pursued. In the current case, spontaneous reperfusion of the infarct-related artery had occurred, which gave the opportunity to reconsider the different therapeutic options. The presence of unprotected left main disease is considered a surgical indication, thus surgery would have been the preferred therapeutic approach.[13]

However, several advancements in the field of interventional cardiology, such as the advent of drug-eluting stents (DES), have improved the outcome of patients with more complex coronary disease and are challenging the results of CABG. Large randomised trials currently underway comparing PCI using DES with CABG for LMCA disease such as the SYNergy between percutaneous coronary intervention with TAXus and cardiac surgery (SYNTAX) study and the COMparison of Bypass surgery and AngioplasTy using SES in patients with LMCA disease (COMBAT) study, will better define the role of PCI in this particular group of patients.[14]

When CABG is deemed necessary in a patient with STEMI, the timing of surgery becomes important. Recent studies have demonstrated that, as for PCI, CABG is preferably performed within 6 hours of symptom onset or alternatively to delay surgery for at least 24 hours and preferentially 7 days. In-hospital mortality becomes excessively high within the 6 to 24 hour time interval and there is general consensus to avoid this critical period whenever possible.[15]

The third option would have been to perform an isolated percutaneous or surgical resection of the thrombotic material. Percutaneous thrombectomy has not been shown to be effective in randomized studies, although there might be a niche application for this practice in lesions with a large thrombus load.[16] In this case, the thrombotic lesion was removed surgically in combination with the implantation of 2 bypass grafts. As documented by the CT scan and confirmed angiographically, both grafts became functionally and/or anatomically occluded.

This is not an unexpected finding since it is well documented that bypass grafts often occlude when they are attached to native coronary arteries with only mild or moderate stenoses.[17]

CONCLUSION

Primary PCI is advocated as the preferred therapy for patients with STEMI. However, a patient-specific approach is necessary and cardiac surgery remains an appropriate choice in patients with unfavourable coronary lesion anatomy. In the latter situation, bypass grafts are not always needed and become unnecessary in the case of non-flow limiting coronary lesions.
This case furthermore demonstrates the possibilities of cardiac CT as a non-invasive imaging tool to visualize disease-related issues of native coronary arteries and bypass grafts.

REFERENCES

1. Rosamond W, Flegal K, Friday G, Furie K, Go A, Greenlund K, Haase N, Ho M, Howard V, Kissela B, Kittner S, Lloyd-Jones D, McDermott M, Meigs J, Moy C, Nichol G, O'Donnell CJ, Roger V, Rumsfeld J, Sorlie P, Steinberger J, Thom T, Wasserthiel-Smoller S, Hong Y. Heart disease and stroke statistics--2007 update: a report from the American Heart Association Statistics Committee and Stroke Statistics Subcommittee. Circulation. 2007;115:e69-171.
2. Greenland P, Gaziano JM. Clinical practice. Selecting asymptomatic patients for coronary computed tomography or electrocardiographic exercise testing. N Engl J Med. 2003;349:465-73.
3. Budoff MJ, Achenbach S, Blumenthal RS, Carr JJ, Goldin JG, Greenland P, Guerci AD, Lima JA, Rader DJ, Rubin GD, Shaw LJ, Wiegers SE. Assessment of coronary artery disease by cardiac computed tomography: a scientific statement from the American Heart Association Committee on Cardiovascular Imaging and Intervention, Council on Cardiovascular Radiology and Intervention, and Committee on Cardiac Imaging, Council on Clinical Cardiology. Circulation. 2006;114:1761-91.
4. Arad Y, Goodman KJ, Roth M, Newstein D, Guerci AD. Coronary calcification, coronary disease risk factors, C-reactive protein, and atherosclerotic cardiovascular disease events: the St. Francis Heart Study. J Am Coll Cardiol. 2005;46:158-65.
5. Taylor AJ, Bindeman J, Feuerstein I, Cao F, Brazaitis M, O'Malley PG. Coronary calcium independently predicts incident premature coronary heart disease over measured cardiovascular risk factors: mean three-year outcomes in the Prospective Army Coronary Calcium (PACC) project. J Am Coll Cardiol. 2005;46:807-14.

6. Pohle K, Ropers D, Maffert R, Geitner P, Moshage W, Regenfus M, Kusus M, Daniel WG, Achenbach S. Coronary calcifications in young patients with first, unheralded myocardial infarction: a risk factor matched analysis by electron beam tomography. Heart. 2003;89:625-8.
7. Farb A, Burke AP, Tang AL, Liang TY, Mannan P, Smialek J, Virmani R. Coronary plaque erosion without rupture into a lipid core. A frequent cause of coronary thrombosis in sudden coronary death. Circulation. 1996;93:1354-63.
8. Pavlu J, Ahmed RE, O'Regan DP, Partridge J, Lefroy DC, Layton DM. Myocardial infarction in sickle-cell disease. Lancet. 2007;369:246.
9. James TN. Homage to James B. Herrick: a contemporary look at myocardial infarction and at sickle-cell heart disease: the 32nd Annual Herrick Lecture of the Council on Clinical Cardiology of the American Heart Association. Circulation. 2000;101:1874-87.
10. Ataga KI, Key NS. Hypercoagulability in sickle cell disease: new approaches to an old problem. Hematology Am Soc Hematol Educ Program. 2007;2007:91-6.
11. Keeley EC, Boura JA, Grines CL. Primary angioplasty versus intravenous thrombolytic therapy for acute myocardial infarction: a quantitative review of 23 randomised trials. Lancet. 2003;361:13-20.
12. Stone GW, Brodie BR, Griffin JJ, Grines L, Boura J, O'Neill WW, Grines CL. Role of cardiac surgery in the hospital phase management of patients treated with primary angioplasty for acute myocardial infarction. Am J Cardiol. 2000;85:1292-6.
13. Smith SC, Jr., Feldman TE, Hirshfeld JW, Jr., Jacobs AK, Kern MJ, King SB, 3rd, Morrison DA, O'Neil WW, Schaff HV, Whitlow PL, Williams DO, Antman EM, Adams CD, Anderson JL, Faxon DP, Fuster V, Halperin JL, Hiratzka LF, Hunt SA, Nishimura R, Ornato JP, Page RL, Riegel B. ACC/AHA/SCAI 2005 guideline update for percutaneous coronary intervention: a report of the American College of Cardiology/American Heart Association Task Force on Practice Guidelines (ACC/AHA/SCAI Writing Committee to Update 2001 Guidelines for Percutaneous Coronary Intervention). Circulation. 2006;113:e166-286.
14. Chieffo A, Colombo A. Treatment of unprotected left main coronary artery disease with drug-eluting stents: is it time for a randomized trial? Nat Clin Pract Cardiovasc Med. 2005;2:396-400.
15. Voisine P, Mathieu P, Doyle D, Perron J, Baillot R, Raymond G, Metras J, Dagenais F. Influence of time elapsed between myocardial infarction and coronary artery bypass grafting surgery on operative mortality. Eur J Cardiothorac Surg. 2006;29:319-23.
16. Sianos G, Papafaklis MI, Daemen J, Vaina S, van Mieghem CA, van Domburg RT, Michalis LK, Serruys PW. Angiographic stent thrombosis after routine use of drug-eluting stents in ST-segment elevation myocardial infarction: the importance of thrombus burden. J Am Coll Cardiol. 2007;50:573-83.

17. Berger A, MacCarthy PA, Siebert U, Carlier S, Wijns W, Heyndrickx G, Bartunek J, Vanermen H, De Bruyne B. Long-term patency of internal mammary artery bypass grafts: relationship with preoperative severity of the native coronary artery stenosis. Circulation. 2004;110:II36-40.

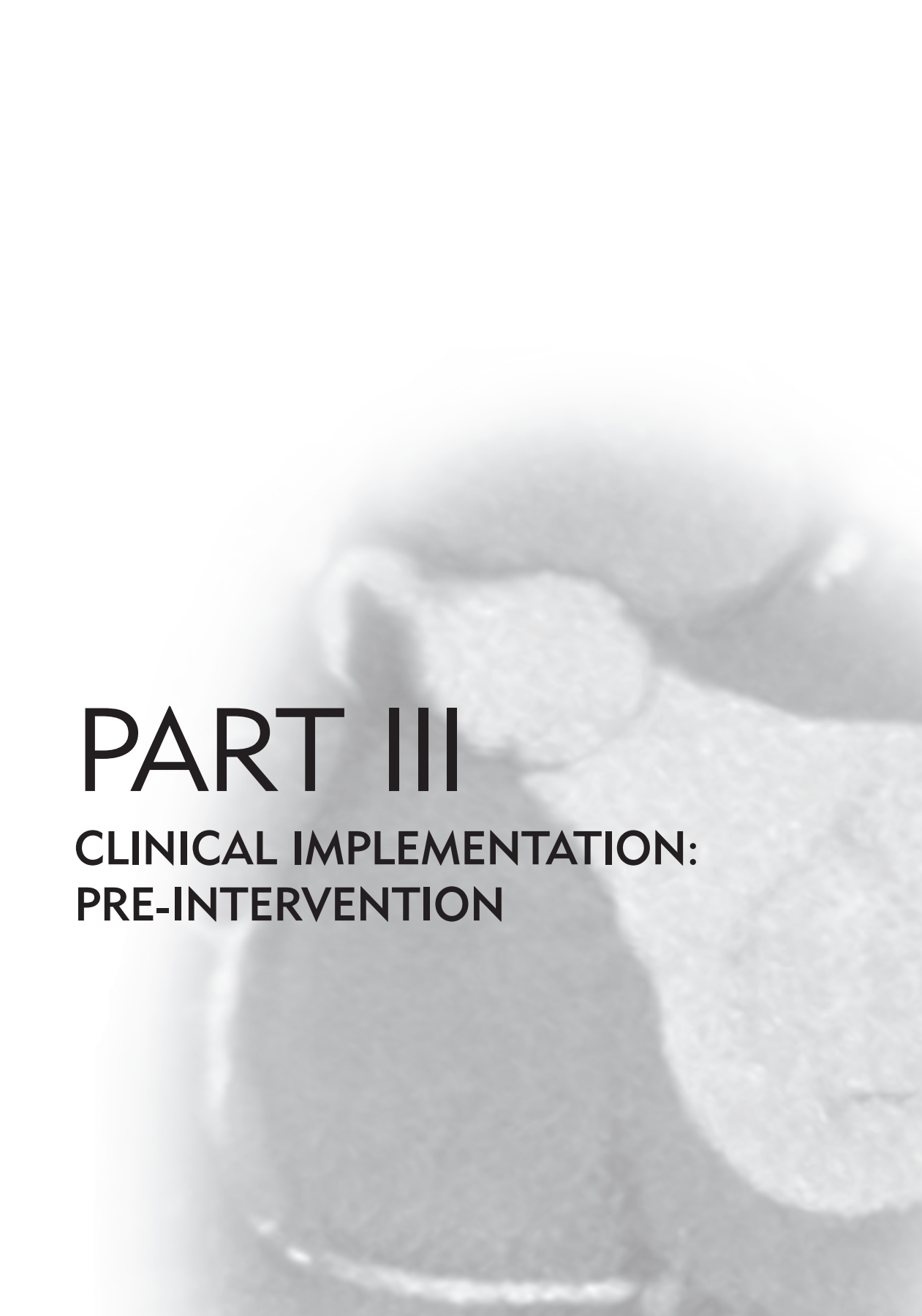

PART III

CLINICAL IMPLEMENTATION: PRE-INTERVENTION

6

High-Resolution Spiral CT Coronary Angiography in Patients Referred for Diagnostic Conventional Coronary Angiography

Nico R. Mollet[1,2], Filippo Cademartiri[1,2], Carlos A.G. Van Mieghem[1,2], Giuseppe Runza[2], Eugène P. Mc Fadden[1], Timo Baks[1,2], Patrick W. Serruys[1], Gabriel P. Krestin[2], Pim J. de Feyter[1, 2]

From the departments of Cardiology[1] and Radiology [2], Erasmus MC, Rotterdam, The Netherlands

Circulation. 2005; 112:2318-23

ABSTRACT

Background

The diagnostic performance of the latest 64-slice CT scanner, with increased temporal (165 ms) and spatial (0.4 mm^3) resolution, to detect significant stenoses in the clinically relevant coronary tree is unknown.

Methods and Results

We studied 52 patients (34 men, mean age 59.6±12.1 years) with atypical chest pain, stable or unstable angina pectoris, or non-ST-segment elevation myocardial infarction scheduled for diagnostic conventional coronary angiography. All patients had stable sinus rhythm. Patients with initial heart rates ≥70 bpm received ß-blockers. Mean scan-time was 13.3±0.9 seconds. The CT scans were analysed by 2 observers unaware of the results of invasive coronary angiography, which was used as the standard of reference. All available coronary segments, regardless of size, were included in the evaluation. Lesions with ≥50 % luminal narrowing were considered significant stenoses.

Invasive coronary angiography demonstrated the absence of significant disease in 25% (13/52), single-vessel disease in 31% (16/52), and multi-vessel disease in 45% (23/52) of patients. One unsuccessful CT-scan was classified as inconclusive. Ninety-four significant stenoses were present in the remaining 51 patients. Sensitivity, specificity, and positive and negative predictive value of CT for the detection of significant stenoses on a segment-by-segment analysis were 99% (93 of 94, 95% CI: 94 to 99), 95% (601 of 631, 95% CI: 93 to 96), 76% (93 of 123, 95% CI: 67 to 89), and 99% (601 of /602, 95% CI: 99 to100), respectively.

Conclusions

Noninvasive 64-slice CT coronary angiography accurately detects coronary stenoses in patients in sinus rhythm and presenting with atypical chest pain, stable or unstable angina, or non-ST-segment elevation myocardial infarction.

INTRODUCTION

Spiral Computed Tomography (CT) coronary angiography has emerged rapidly, thanks to technical improvements as a sensitive diagnostic modality[1-12]. The newest generation spiral CT scanners are significantly improved. They feature 64 slices and thinner detectors, and the X-ray tube permits higher X-ray output and faster tube rotation. These improvements result in high-quality, nearly motion-free, isotropic image quality. Data are acquired during a single breathhold of ≈13 seconds. We report the diagnostic performance of 64-slice CT coronary angiography in 52 patients with atypical chest pain, stable or unstable angina, or non-ST-segment elevation myocardial infarction referred for diagnostic invasive coronary angiography to assess the extent and severity of coronary stenoses in the clinically relevant coronary tree.

METHODS

Study Population

During a period of 6 weeks, we studied 70 consecutive patients scheduled for diagnostic conventional coronary angiography who fulfilled the following criteria: sinus heart rhythm, able to breath hold for 15 seconds, and no previous percutaneous coronary intervention or coronary bypass surgery. Eighteen patients were excluded because of the logistical inability to perform a CT-scan before the conventional angiogram (n=9), presence of arrhythmia (n=4), impaired renal function (serum creatinine >120 mmol/L) (n=4), and known contrast allergy (n=1). Thus, the study population comprised 52 patients (34 male, mean age 59.6±12.1 years). Our institutional review board approved the study protocol and all patients gave informed consent.

Patient Preparation

Patients with heart rates above 70 bpm received, unless they had known overt heart failure or ECG AV conduction abnormalities, a single oral dose of 100 mg metoprolol 45 minutes before the scan. Patients with heart rates above 80 bpm received an additional single oral dose of 1 mg lorazepam.

Scan Protocol and Image Reconstruction

All patients were scanned with a 64-slice CT scanner (Sensation 64, Siemens) equipped with a new feature in multislice CT technology, so-called z-axis flying focus technology[13]. The central 32 detector rows acquire 0.6-mm slices, and the flying focus spot switches back and forth between 2 z-positions between each reading. Two slices per detector row are acquired, which results in a higher oversampling rate in the z axis, thereby reducing artifacts related to the spiral acquisition and improving spatial resolution down to 0.4 mm^3 [13]. Angiographic scan

parameters included the following: number of slices per rotation, 32 x 2; individual detector width, 0.6 mm; rotation time, 330 ms; table feed, 3.8 mm per rotation; tube voltage, 120 kV; tube current, 900 mA; and no prospective X-ray tube modulation. Calcium scoring parameters (similar unless indicated) were a tube current 150 mA and prospective X-ray tube modulation. The radiation exposure for CT coronary angiography with this scan protocol was calculated as 15.2 to 21.4 mSv (for men and women, respectively)using dedicated software (WinDose, Institute of Medical Physics). The radiation exposure of calcium scoring using a comparable scan protocol (including prospective x-ray tube modulation) on a 16-slice scanner was calculated as 1.3 to -1.7 mSv (for men and women, respectively)[15].

A bolus of 100 mL contrast material (iomeprol, Iomeron 400) was injected through an arm vein at a flow rate of 5 mL/s. A bolus-tracking technique was used to synchronize the arrival of contrast in the coronary arteries with the initiation of the scan. To monitor the arrival of contrast material, axial scans were obtained at the level of the ascending aorta with a delay of 10 seconds after the start of the contrast injection. The scan was automatically started when a threshold of 100 Hounsfield units was reached in a region of interest positioned in the ascending aorta.

Images were reconstructed using ECG gating to obtain optimal, motion-free image quality. Data sets were reconstructed immediately after the scan following a stepwise pattern. Initially, a single data set was reconstructed during the mid- to end-diastolic phase (350 ms before the next R wave). Image quality was assessed on a per-segment level. In case of insufficient image quality of ≥1 coronary segments, additional data sets were reconstructed (300, 400, and 450 ms before the next R wave). In case of persistent artifacts related to coronary motion, a second reconstruction approach was carried out, including reconstruction of data sets both during the mid- to end-diastolic phase (between 60% and 70% of the R-R interval) and the end-systolic phase (between 25% and 35% of the R-R interval). If necessary, multiple data sets of a single patient were used separately to obtain optimal image quality of all available coronary segments. The reconstruction algorithm uses data from a single heartbeat, obtained during half-x-ray tube rotation, resulting in a temporal resolution of 165 ms.

Quantitative Coronary Angiography

All scans were performed within 2 weeks of the conventional diagnostic angiogram. A single observer unaware of the multislice CT results identified coronary segments using a 17-segment modified AHA classification[14] (right coronary artery: 1, proximal; 2, mid; 3, distal; 4a, posterior descending; 4b postero-lateral; left main coronary artery: 5; left anterior descending coronary artery: 6, proximal; 7, mid; 8, distal; 9, first diagonal; 10, second diagonal; circumflex coronary artery: 11, proximal; 12, first marginal; 13, mid; 14, second marginal; 15, distal; 16, intermediate branch). All segments, regardless of size, were included for comparison with

CT coronary angiography. Segments were classified as normal (smooth parallel or tapering borders), as having nonsignificant disease (luminal irregularities or <50% stenosis), or as having significant stenoses. Stenoses were evaluated in 2 orthogonal views and classified as significant if the mean lumen diameter reduction was ≥50% using a validated quantitative coronary angiography (QCA) algorithm (CAAS, Pie Medical).

CT Image Evaluation

All scans were analysed independently by a radiologist and a cardiologist who were unaware of the results of conventional coronary angiography and used an offline workstation (Leonardo, Siemens). Total calcium scores of all patients were calculated using dedicated software and expressed as Agatston scores. The Agatston score is a commonly used scoring method that calculates the total amount of calcium based on the basis of the number, areas, and peak Hounsfield units of the detected calcified lesions[16].

All available coronary segments were visually scored for the presence of significant stenosis. Maximum-intensity projections were used to identify coronary lesions and (curved) multi-planar reconstructions to classify lesions as significant or nonsignificant. Disagreement between observers was resolved by consensus.

Image quality was evaluated on a per-segment basis and classified as good (defined as absence of any image-degrading artifacts related to motion, calcification, or noise), adequate (presence of image-degrading artifacts but evaluation possible with moderate confidence), or poor (presence of image-degrading artifacts and evaluation possible only with low confidence).

Statistical Analysis

The diagnostic performance of CT coronary angiography for the detection of significant lesions in coronary arteries with QCA as the standard of reference is presented as sensitivity, specificity, positive and negative predictive value and positive and negative likelihood ratios with the corresponding exact 95% CIs. Comparison between CT coronary angiography and QCA was performed on 3 levels: segment by segment, vessel by vessel (no or any disease per vessel), and patient by patient (no or any disease per patient). We performed an additional sensitivity analysis after random selection of a single segment per patient to explore the effect of nesting; repeated assessments (segment by segment and vessel by vessel) within the same patient were made that were not independent observations. Intraobserver and interobserver variability for the detection of significant coronary stenosis was determined by k statistics.

RESULTS

Patient characteristics are shown in Table 1. Seventy-three percent of the patients (38 of 52) received a ß-blocker and, 31% (16 of 52) also received lorazepam. The mean heart rate in these patients dropped within 45 minutes from 68.2±10.2 to 57.8±6.8 bpm. The mean scan time was 13.3±0.6 seconds. One unsuccessful CT scan was classified as inconclusive because the development of ventricular bigeminy during the angiography scan.

Table 1. Patient characteristics (n=52)

Symptoms	
Atypical chest pain	6 (12)
Stable angina pectoris	32 (63)
Unstable angina pectoris	3 (6)
Non-ST-elevation myocardial infarction	11 (22)
Risk factors	
Hypertension	17 (33)
Hypercholesterolemia	36 (71)
Diabetes Mellitus	7 (14)
Smoking	15 (29)
Family history of acute coronary syndrome	13 (26)
Obese (body mass index ≥30 kg/m^2)	14 (28)
Calcium score, median (interquartile range)*	231 (15-736)
Conventional angiography	
Absence of coronary artery disease	7 (13)
Nonsignificant disease	6 (12)
Single-vessel disease	16 (31)
Multivessel disease	23 (45)

N=52. Value are n (%) unless otherwise indicated.
* Agatston-score

A single data set for the assessment of significant stenoses was used in 69%, 2 data sets in 27%, and 3 data sets in 4% of patients to obtain optimal image quality of on a per-segment level. Data sets reconstructed during the end-systolic phase were used in 27% of patients (14/51). Image quality was classified as good in 90%, moderate in 7%, and poor in 3% of coronary segments. Reasons for poor image quality were motion artifacts (60%, 12 of 20), severe calcifications (20%, 4 of 20), or low contrast-to-noise ratio (20%, 4 of 20).

Diagnostic Performance of 64-Slice CT Coronary Angiography: Segment-by-Segment Analysis

A total of 725 segments were included for comparison with QCA. Potentially, 17 segments per patient can be present for analysis. However, 142 segments were not visualized on the conventional angiogram because of variations in coronary anatomy (absence of an intermediate branch or hypoplastic, nondominant coronary arteries in which not all segments could be identified; 102 segments), and the presence of a proximal occlusion and poorly filled distal segments by collaterals (40 segments).

Interobserver and intraobserver variability for detection of significant lesions had k values of 0.73 and 0.79, respectively. The diagnostic performance of CT coronary angiography for detecting significant lesions on a segment-based analysis is detailed in Table 2. One significant

Table 2. Diagnostic Performance and Predictive Value of 64-slice CT Coronary Angiography for the Detection of ≥50% Stenoses on QCA

	N	Sensitivity, %	Specificity, %	PPV, %	NPV, %	+LR	-LR
Segment-based analysis							
All segments	725	99 (94-98)	95 (93-96)	76 (67-89)	100 (99-100)	20.81	0.01
Proximal segments	204	100 (89-100)	97 (93-98)	83 (67-97)	100 (97-100)	29.00	0.00
Mid segments	142	97 (83-99)	94 (88-97)	81 (63-96)	99 (94-99)	15.47	0.04
Distal segments	121	100 (68-100)	97 (92-99)	73 (39-98)	100 (96-100)	37.67	0.00
Side branches	258	100 (87-100)	94 (90-96)	65 (48-85)	100 (98-100)	16.57	0.00
LM	51	100 (21-100)	100 (93-100)	100 (92-100)	100 (2-100)	∞	0.00
LAD	230	97 (85-100)	92 (88-95)	69 (53-86)	99 (96-99)	12.68	0.03
LCx	235	100 (88-100)	97 (94-99)	83 (66-97)	100 (98-100)	34.33	0.00
RCA	209	100 (89-100)	95 (91-97)	77 (60-95)	100 (97-100)	19.89	0.00
Patient-based analysis							
All segments	51	100 (91-100)	92 (67-99)	97 (86-99)	100 (73-100)	13.00	0.00

PPV indicates positive predictive value, NPV, negative predictive value; +LR, positive likelihood ratio; -LR, negative likelihood ratio; LM, left main coronary artery; LCx, circumflex coronary artery; and RCA: right coronary artery. For segment-based analysis, analysis of 725 segments visualized on the conventional angiogram and classified according to a 17-segment modified AHA classification was performed. Segments were further classified on the basis of their location within the coronary tree (proximal, mid, or distal segments of the main coronary artery arteries or side branches) and their location within a single vessel (LM, LAD, LCx, or RCA). For patient-based analysis, analysis of 51 patients was performed. Values in parentheses represent 95% CIs.

stenosis (lumen diameter reduction: 52%) located at the mid part of the LAD was detected with CT, but the severity of the stenosis was underestimated and classified as nonsignificant. Thirty nonsignificant lesions were detected with CT, but the severity of these stenoses was overestimated, resulting in incorrect classification as significant stenoses on the CT scan. Conventional angiography revealed only wall irregularities in 8 and nonsignificant stenoses in the remaining 22 lesions (mean lumen reduction: 34.7±7.9%; range, 23 to 49%). The vast majority (83%, 25 of 30) of these segments were calcified. The presence of coronary calcium

Table 3. Influence of Coronary Calcification on Diagnostic Accuracy of 64-slice CT Coronary Angiography on a Segment-Based Analysis.

Calcium Score	n	Mean (±SD) Agatston Score	TP	TN	FP	FN	Sensitivity, %	Specificity, %	Positive PV,%	Negative PV, %
0-10	12	0 ± 0	8	171	2	0	100 (63-100)	99 (95-99)	80 (44-98)	100 (97-100)
11-400	21	174 ± 122	36	240	13	0	100 (90-100)	95 (91-97)	73 (58-88)	100 (98-100)
401-1000	12	718 ± 166	31	129	10	1	97 (83-98)	93 (87-96)	76 (59-89)	99 (95-99)
>1000	6	1731 ± 621	18	61	5	0	100 (81-100)	92 (83-97)	78 (56-96)	100 (94-100)

TP indicates true positive; TN, true negative; FP, false positive; FN, false negative; PV, predictive value; Values in parentheses represent 95% CIs.

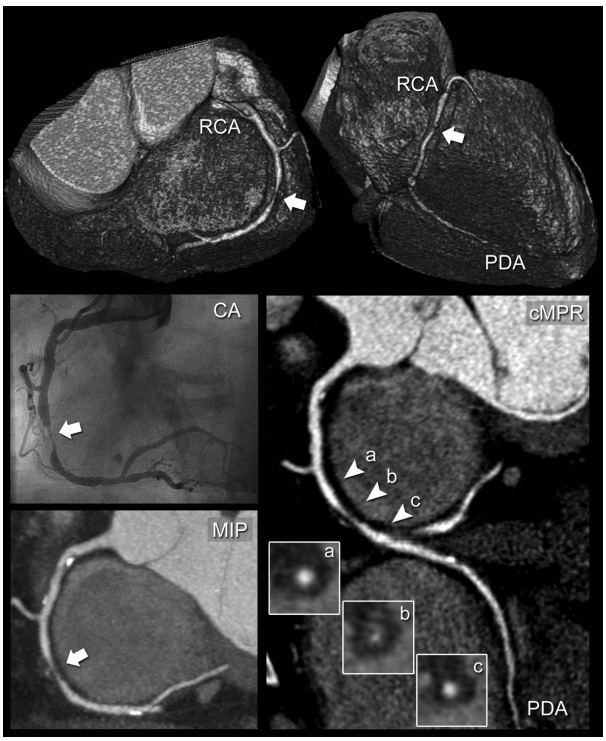

Figure 1a, CT coronary angiogram and corresponding conventional angiogram of the right coronary artery (RCA) in a patient presenting with stable angina pectoris and a calcium (Agatston) score of 79. The arrow indicates a significant lesion located at the mid RCA. Cross-sectional CT images show a large noncalcific plaque (b) and a normal coronary lumen proximal and distal of the lesion (a, c). Note that the volume-rendered images (colored images) provide an excellent anatomical overview of the coronary arteries but should not be used to score the presence and degree of coronary stenoses.

induced overestimation of the severity of these lesions on the CT scan (Table 3). Agreement between CT coronary angiography and QCA on a per-segment level was very good (k value, 0.83).

After random selection of a single segment per patient, the sensitivity for detecting significantly diseased vessels was 100% (13 of 13, 95% CI, 75 to 100), specificity was 95% (36 of 38; 95% CI, 82 to 99), positive predictive value was 87% (13 of 15; 95% CI, 59 to 99), and negative predictive value was 100% (36 of 36; 95% CI, 90 to 100).

Diagnostic Performance of 64-slice CT Coronary Angiography: Vessel-by-Vessel Analysis

The diagnostic performance of CT coronary angiography for detectng significant lesions on a vessel-based analysis is detailed in Table 2. One significantly diseased LAD was incorrectly classified as nonsignificantly diseased on the CT scan. Sensitivity for the detection of significantly diseased LAD was 96% and 100% in all other main coronary arteries. Agreement between CT coronary angiography and QCA on a per-vessel level was very good (k value: 0.85).

Diagnostic Performance of 64-Slice CT Coronary Angiography: Patient-by-Patient Analysis

The diagnostic performance of CT coronary angiography for detecting significant lesions on a patient-based analysis is detailed in Table 2. Twelve patients with either an angiographically normal coronary angiogram (n=7) or with non-significant disease (n=5) were correctly identified with CT. However, 1 patient with only wall irregularities on the conventional angiogram

was incorrectly classified as having single-vessel disease on the CT scan. All 38 patients with significant coronary artery disease on conventional angiography were correctly identified on the CT scan (Figure 1 and, 2).

However, in 7 patients with single-vessel disease also, another lesion was detected and its severity was overestimated which resulted in incorrect classification as having multivessel disease on CT coronary angiography. Agreement between CT coronary angiography and QCA on a per-patient (no or any disease) level was very good (k value, 0.95); agreement between both techniques to classify patients as having no, single-vessel, or multivessel disease was good (k value, 0.72).

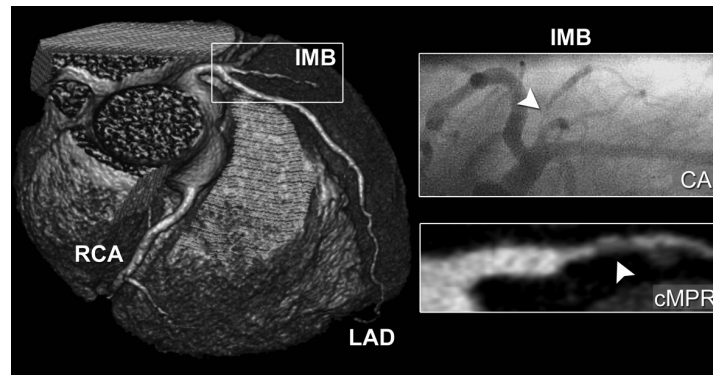

Figure 1b, Volume-rendered CT image (colored image) providing an overview of the coronary anatomy and showing a small (lumen diameter, 1.5 mm) intermediate branch (IMB). A detailed curved multiplanar reconstructed (cMPR) CT image reveals the presence of a significant stenosis (arrowhead) located at the proximal IMB, which was confirmed on the conventional angiogram (CA). The patient was correctly classified as having 2-vessel disease on the CT scan. MIP indicates maximum-intensity projection; PDA, posterior descending coronary artery; RCA, right coronary artery.

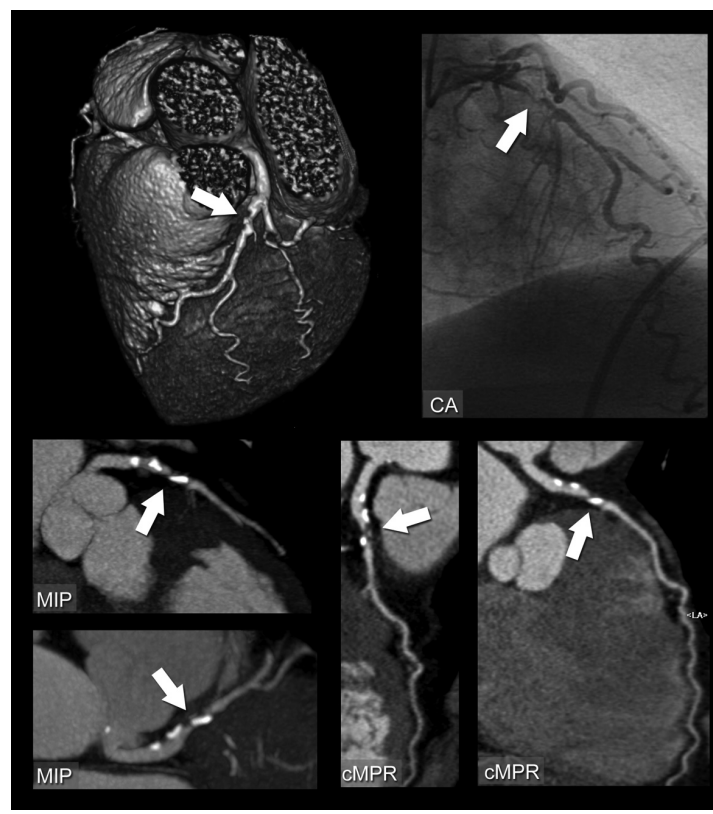

Figure 2. Volume-rendered CT image (colored image) providing an overview of the coronary anatomy and suggesting a significant stenosis of the proximal LAD (indicated by the arrow). More detailed analysis using different CT postprocessing techniques (maximum-intensity projections [MIP] and curved multiplanar reconstructions [cMPR]) confirms the presence of a significant stenosis, which corresponds with the conventional angiogram (CA).

DISCUSSION

Recent reports demonstrated that earlier-generation multislice CT scanners showed promise for noninvasive detection of coronary stenoses.[1-12] The reported diagnostic values were high but one should bear in mind that the calculated sensitivity and specificity were based on analyzable coronary segments rather than on those of all examined coronary segments. In fact, the most recent reports of 16-slice CT coronary angiography excluded 6% to 17% of the available coronary segments, and only a few included all available segments. In addition, only the larger parts of the coronary tree were examined; smaller parts with a diameter of <1.5 mm or 2 mm were excluded from analysis. Most recently, Leschka et al[17] presented the first study exploring the diagnostic performance of 64-slice CT coronary angiography. They evaluated all available coronary segments ≥ 1.5 mm and reported a high sensitivity and specificity for detecting significant lesions using a 64-slice CT scanner with a rotation time of 375 ms.

The newest 64-slice CT scanners have a shorter rotation time (330 ms) and offer not only a shorter scan time and a higher spatial resolution but also a higher temporal resolution compared with previous scanner generations. Multislice CT coronary angiography of the clinically relevant coronary segments, as designated by the AHA classification, is now possible. We found that significant coronary stenoses were detected using the latest 64-slice CT scanner with a sensitivity of 99% and a specificity of 95% compared with conventional invasive diagnostic coronary angiography. All but 1 patients with angiographically normal coronary angiograms were correctly identified, rendering the CT-technique highly reliable to identify patients with no significant coronary obstruction. Furthermore, all patients with significant coronary artery disease were correctly diagnosed, and only a single coronary lesion was missed on the CT scan. In addition, we found good agreement between CT coronary angiography and QCA in the classification of patients with no, single-vessel, or multivessel disease. Our results were obtained in patients with a wide spectrum of clinical settings, including atypical chest pain, stable or unstable angina, or non-ST-segment elevation, who had varying degrees of coronary artery disease, ranging from normal coronary angiograms to obstructive disease of 1, 2 or 3 vessels.

We did not include patients with ST-segment elevation myocardial infarction; these patients should undergo immediate percutaneous intervention without delay, and the role of CT in these patients is highly questionable. In our study the specificity was somewhat lower because we tended to overestimate the severity of a lesion on the CT scan, resulting in a number of false-positive outcomes, rather than underestimating the lesion severity and thereby "missing" lesions, which may have serious consequences in a symptomatic patient population.

Study Limitations

The estimated radiation dose during CT coronary angiography (15.2 to 21.4 mSv for men and women, respectively) is a cause of concern and higher than the radiation dose associated with conventional coronary angiography. The radiation exposure can be reduced by technical adjustments such as prospective x-ray tube current modulation. This technique reduces the radiation exposure by ≈ 50% in patients with low heart rates[15] but is sensitive to arrhythmia and limits the possibility to reconstruct datasets during the end-systolic phase. This proved useful in 27% of our patients. Persistent irregular heart rhythm such as atrial fibrillation and frequent extrasystoles preclude multislice coronary angiography. Motion artifacts caused by mild arrhythmia (e.g. a single ventricular extrasystole) can be diminished by manual repositioning the reconstruction windows. Severe coronary calcification obscures the coronary lumen and can lead to overestimation of severity of lesions due to blooming artifacts, resulting in a lower specificity in patients with high calcium scores. The presence of coronary calcifications also severely limits the applicability of QCA algorithms. In fact, no software able to detect and quantify coronary stenoses has been adequately validated yet.

When evaluating the diagnostic performance of CT coronary angiography on 3 levels (segment by segment, vessel by vessel, and patient by patient), we made repeated assessments within the same patient. However, we performed a sensitivityanalysis after random selection of a single segment per patient and found values that are in line with the values obtained after clustering all available segments. This finding suggests that the nesting of observations within a single patient did not have an important impact on the estimates of the diagnostic performance of CT for detecting significant stenoses in present study.

Patients with initial heart rates >70 bpm received prescan medication, reducing the mean heart rate to 57 bpm. Future improvements in temporal resolution should diminish motion artifacts related to high heart rates, which could make the administration of prescan ß-blockers unnecessary.

CONCLUSIONS

Our results show that noninvasive 64-slice CT coronary angiography is a reliable technique to detect coronary stenoses in patients with sinus rhythm presenting with atypical chest pain, stable or unstable angina pectoris, or non-ST-segment elevation myocardial infarction and suggest that this noninvasive technique can now be considered as an alternative to invasive diagnostic coronary angiography in selected patients.

REFERENCES

1. Nieman K, Oudkerk M, Rensing BJ, van Ooijen P, Munne A, van Geuns RJ, de Feyter PJ. Coronary angiography with multi-slice computed tomography. Lancet. 2001;357:599-603.
2. Achenbach S, Giesler T, Ropers D, Ulzheimer S, Derlien H, Schulte C, Wenkel E, Moshage W, Bautz W, Daniel WG, Kalender WA, Baum U. Detection of coronary artery stenoses by contrast-enhanced, retrospectively electrocardiographically-gated, multislice spiral computed tomography. Circulation. 2001;103:2535-8.
3. Knez A, Becker CR, Leber A, Ohnesorge B, Becker A, White C, Haberl R, Reiser MF, Steinbeck G. Usefulness of multislice spiral computed tomography angiography for determination of coronary artery stenoses. Am J Cardiol. 2001;88:1191-4.
4. Vogl TJ, Abolmaali ND, Diebold T, Engelmann K, Ay M, Dogan S, Wimmer-Greinecker G, Moritz A, Herzog C. Techniques for the detection of coronary atherosclerosis: multi-detector row CT coronary angiography. Radiology. 2002;223:212-20.
5. Kopp AF, Schroeder S, Kuettner A, Baumbach A, Georg C, Kuzo R, Heuschmid M, Ohnesorge B, Karsch KR, Claussen CD. Non-invasive coronary angiography with high resolution multidetector-row computed tomography. Results in 102 patients. Eur Heart J. 2002;23:1714-25.
6. Nieman K, Cademartiri F, Lemos PA, Raaijmakers R, Pattynama PM, de Feyter PJ. Reliable noninvasive coronary angiography with fast submillimeter multislice spiral computed tomography. Circulation. 2002;106:2051-4.
7. Ropers D, Baum U, Pohle K, Anders K, Ulzheimer S, Ohnesorge B, Schlundt C, Bautz W, Daniel WG, Achenbach S. Detection of coronary artery stenoses with thin-slice multi-detector row spiral computed tomography and multiplanar reconstruction. Circulation. 2003;107:664-6.
8. Kuettner A, Trabold T, Schroeder S, Feyer A, Beck T, Brueckner A, Heuschmid M, Burgstahler C, Kopp AF, Claussen CD. Noninvasive detection of coronary lesions using 16-detector multislice spiral computed tomography technology: initial clinical results. J Am Coll Cardiol. 2004;44:1230-7.
9. Mollet NR, Cademartiri F, Nieman K, Saia F, Lemos PA, McFadden EP, Pattynama PMT, Serruys PW, Krestin GP, De Feyter PJ. Multislice Spiral CT Coronary Angiography in Patients With Stable Angina Pectoris. J Am Coll Cardiol. 2004;43:2265-70.
10. Martuscelli E, Romagnoli A, D'Eliseo A, Razzini C, Tomassini M, Sperandio M, Simonetti G, Romeo F. Accuracy of thin-slice computed tomography in the detection of coronary stenoses. Eur Heart J. 2004;25:1043-8.

11. Kuettner A, Kopp AF, Schroeder S, Rieger T, Brunn J, Meisner C, Heuschmid M, Trabold T, Burgstahler C, Martensen J, Schoebel W, Selbmann HK, Claussen CD. Diagnostic accuracy of multidetector computed tomography coronary angiography in patients with angiographically proven coronary artery disease. J Am Coll Cardiol. 2004;43:831-9.
12. Mollet NR, Cademartiri F, Krestin GP, McFadden EP, Arampatzis CA, Serruys PW, De Feyter PJ. Improved Diagnostic Accuracy With 16-row Multislice CT Coronary Angiography. J Am Coll Cardiol. 2005;45:128-32.
13. Flohr T, Bruder H, Stierstorfer K, Schaller S. Evaluation of approaches to reduce spiral artifacts in multi-slice spiral CT. 89th Scientific Assembly of the Radiological Society of North America (abstract). 2004.
14. Austen WG, Edwards JE, Frye RL, Gensini GG, Gott VL, Griffith LS, McGoon DC, Murphy ML, Roe BB. A reporting system on patients evaluated for coronary artery disease. Report of the Ad Hoc Committee for Grading of Coronary Artery Disease, Council on Cardiovascular Surgery, American Heart Association. Circulation. 1975;51:5-40.
15. Trabold T, Buchgeister M, Kuttner A, Heuschmid M, Kopp AF, Schroder S, Claussen CD. Estimation of Radiation Exposure in 16-Detector Row Computed Tomography of the Heart with Retrospective ECG-gating. Rofo Fortschr Geb Rontgenstr Neuen Bildgeb Verfahr. 2003;175:1051-5.
16. Agatston AS, Janowitz WR, Hildner FJ, Zusmer NR, Viamonte M, Jr., Detrano R. Quantification of coronary artery calcium using ultrafast computed tomography. J Am Coll Cardiol. 1990;15:827-32.
17. Leschka S, Alkadhi H, Plass A, Desbiolles L, Grünenfelder J, Marincek B, Wildermuth S. Accuracy of MSCT coronary angiography with 64-slice technology: first experience. Eur Heart J. 2005;0:2611.

7

64-slice CT Coronary Angiography in Patients with Non-ST Elevation Acute Coronary Syndrome

Willem B. Meijboom[1,2], Nico R. Mollet[1,2], Carlos A.G. Van Mieghem[1,2], Annick C. Weustink[1,2], Francesca Pugliese[1,2], Niels van Pelt[1,2], Filippo Cademartiri[2], Eleni Vourvouri[1,2], Peter de Jaegere[1], Gabriel P. Krestin[2], Pim J. de Feyter[1,2]

From the departments of Cardiology[1] and Radiology [2], Erasmus MC, Rotterdam, The Netherlands

Heart. 2007; 93:1386-92

ABSTRACT

Background

A high diagnostic accuracy of 64-slice CT coronary angiography (CTCA) has been reported in selected patients with stable angina pectoris, but only scant information is available in patients with non-ST elevation acute coronary syndrome (ACS).

Objectives

To study the diagnostic performance of 64-slice CTCA in patients with non-ST elevation ACS.

Patients and methods

64-slice CTCA was performed in 104 patients (mean (SD) age 59 (9) years) with non-ST elevation ACS. Two independent, blinded observers assessed all coronary arteries for stenosis, using conventional quantitative angiography as a reference. Coronary lesions with ≥50 % luminal narrowing were classified as significant.

Results

Conventional coronary angiography demonstrated the absence of significant disease in 15% (16/104) of patients, and the presence of single-vessel disease in 40% (42/104) and multivessel disease in 44% (46/104) of patients. Sensitivity for detecting significant coronary stenoses on a patient-by-patients analysis was 100% (88/88; 95% CI 95 to 100), specificity 75% (12/16; 95% CI 47 to 92), and positive and negative predictive values were 96% (88/92; 95% CI 89 to 99) and 100% (12/12; 95% CI 70 to 100), respectively.

Conclusion

64-slice CTCA has a high sensitivity to detect significant coronary stenoses, and is reliable to exclude the presence of significant coronary artery disease in patients who present with a non-ST elevation ACS.

INTRODUCTION

Patients with a non-ST elevation acute coronary syndrome (ACS) are usually stratified into high and low risk for progression to myocardial infarction or death on the basis of their clinical presentation, ECG changes, biomarkers, electrical or hemodynamical instability, and presence of diabetis mellitus.[1] An invasive management strategy, including conventional coronary angiography (CCA) and revascularization, is recommended in high-risk patients, whereas a conservative strategy with ischemia-guided revascularization is recommended in low-risk patients.[1-3] We investigated the feasibility and diagnostic accuracy of 64-slice CT coronary angiography (CTCA) in 104 patients with non-ST elevation ACS as a first step to evaluate the potential decision-making role of CT in this patient cohort.

METHODS

Study Population

Over a 12-month period we included 104 patients presenting with unstable angina pectoris or non-ST-segment elevation myocardial infarction. They were stratified as either high or low risk group according to the current European guidelines, on the basis of baseline characteristics, troponin rise or ECG changes.[1] High-risk patients and low-risk patients with a positive or inconclusive exercise ECG test or high suspicion for obstructive coronary artery disease (CAD underwent both CTCA and CCA. Furthermore, patients presenting with a ST-segment elevation myocardial infarction were not included, but were immediately referred for direct percutaneous coronary intervention (PCI). No patients with previous history of PCI or coronary artery bypass graft (CABG), impaired renal function (serum creatinine>120 μmol/l), known intolerance to iodinated contrast material and atrial fibrillation were included. All patients underwent CCA, which was the standard of reference. The institutional review board of Erasmus MC Rotterdam approved the study and all subjects gave informed consent.

Patient Preparation

Patients with a heart rate >65 bpm before the examination received additional beta-blockers (50/100mg Metoprolol), and all were given thorough breath-hold instructions.

Scan Protocol

All scans were made with a 64-slice CT scanner, which had a gantry rotation time of 330 ms, a temporal resolution of 165 ms, and a spatial resolution of 0.4 mm^3 (Sensation 64, Siemens, Forchheim, Germany). Initially, a calcium scan was performed using standardized scan parameters 64×0.6 mm collimation, 330 ms rotation time, 3.8 mm/rotation table feed, 120 kV tube voltage, 150 mA tube current and prospective x ray tube modulation. Then the CTCA

was completed, which had similar parameters except for a higher tube current of 900 mA and absence of x-ray tube modulation. The radiation exposure for CTCA using this scan protocol was calculated as 15.2-21.4 (male/female) mSv using dedicated software (WinDose®, Institute of Medical Physics, Erlangen, Germany). The radiation exposure for calcium scoring using a comparable scan protocol (including prospective x ray tube modulation) on a 16-slice scanner was calculated as 1.3-1.7 (male/female) mSv.[4]

A bolus of 80-100 ml of contrast material (400 mgI/mL; Iomeron, Bracco, Milan, Italy) was injected intravenously in an antecubital vein at a flow rate of 5 ml/s. A bolus-tracking technique was used to synchronise the arrival of contrast in the coronary arteries, and the scan was started once the contrast attenuation in a preselected region of interest in the ascending aorta had reached a predefined threshold of +100 HU.

Image Reconstruction

Images were obtained during a half x ray tube rotation, resulting in an effective temporal resolution of 165 ms. Datasets were reconstructed immediately after the scan. To obtain optimal image quality, datasets were reconstructed in the mid-to-end diastolic phase using retrospective ECG gating with an absolute reverse or percentage technique as described previously by Mollet.[5] In case of impaired image quality due to motions artefacts or breathing artefacts additional reconstructions were made in the end-systolic phase.

Quantitative Coronary Angiography

All CT scans were carried out within 1-2 days of performing CCA. One experienced cardiologist, blinded to the results of CTCA, identified and analyzed all coronary segments, using a 17-segment modified American Heart Association classification.[6]

All segments, regardless of size, were included for comparison with CTCA. Segments were classified as normal (smooth parallel or tapering borders), as having non-significant disease (wall irregularities or <50% stenosis) or having significant disease (stenosis ≥50%). Stenoses were evaluated in the worst view, and were classified as significant if the reduction in lumen diameter exceeded 50 % of that measured by the validated quantitative coronary angiographic (QCA) algorithm (CAAS, Pie Medical, Maastricht, the Netherlands).

CT Image Evaluation

One observer analyzed total calcium scores of all patients using the appropriate software (Syngo, Calcium Scoring, Siemens Fonchheim, Germany), expressing results as an Agatston score.[7] Two experienced observers, a radiologist and a cardiologist, all unaware of the results of CCA, evaluated the CTCA datasets on an offline workstation (Leonardo, Siemens, Forchheim, Germany). The axial slices were initially evaluated for the presence of significant seg-

mental disease and, additionally, multiplanar and curved multiplanar reconstructed images were used. Segments located distally to a chronic total occlusion were excluded because of poor distal filling by collaterals. Interobserver disagreements were resolved by a third reader.

Statistical Analysis

The diagnostic performance of CTCA for detecting significant stenoses in the coronary arteries using QCA as the standard of reference is presented in terms of sensitivity, specificity, positive predictive value and negative predictive values with the corresponding 95% CIs. Positive (sensitivity/ [1-specificity]) and negative ([1-sensitivity]/specificity) likelihood ratios are given. The likelihood ratio incorporates both the sensitivity and specificity of a test and provides a direct estimate of how much a test result will change the odds of having a disease. Post-test odds can be calculated by multiplying the pre-test odds by the likelihood ratios. Comparison between CTCA and QCA was performed on three levels of analysis: patient by patient, vessel by vessel and segment by segment. To investigate the effect of nesting, an additional sensitivity analysis was done; repeated assessments (segment by segment and vessel by vessel) within the same patient were made, which were not independent observations. Interobserver and intraobserver variabilities for the detection of significant coronary stenosis and agreement between techniques to classify patients as having no, single or multi-vessel disease were determined using k statistics.

RESULTS

Table 1 shows the patient demographics. In all, 86% (89/104) the patients received oral ß-blockers as treatment for ACS. Additional ß-blockers were administered in 63% (65/104) of patients, and the mean (SD) heart rate dropped within 60 min from 66 (9) to 60 (8) bpm in these patients. The mean (SD) scan time was 12.3 (1.2) s. As a first step, all datasets were reconstructed in the mid-to-end diastolic phase. In 34% (35/104) of cases, additional higher quality end-systolic reconstructions were used.

Diagnostic performance of 64-slice CT coronary angiography: patient-by-patient analysis

The prevalence of significant CAD, defined as having at least one ≥ 50% stenosis per patient was 85%. Tabel 2 details the diagnostic performance of CTCA for detecting significant stenoses on a patient-based analysis. The diagnostic accuracy of patients in the low- and high-risk groups were similar.

Twelve patients with either an angiographically normal CCA (n=4) or with non-significant disease (n=8) were correctly identified with CT. However, two patients with only wall irregularities on the CCA were incorrectly classified as having single-vessel disease on the CT scan

Table 1. Patient demographics (n=104)

	Low risk	High risk
n	33	71
Mean (SD) age, range (years)	58 ± 7 (38-75)	59 ± 10 (30-84)
Males	23 (70)	52 (73)
Mean (AD) calcium score*	473.9 ± 738.2	440.0 ± 513.6
Mean (SD) BMI†	25.8 ± 3.6	26.5 ± 3.7
Recurrent ischemia ‡	-	49 (71)
Early postinfarct unstable angina	-	9 (13)
Elevated troponin levels	-	55 (78)
Diabetes Mellitus	-	9 (13)
Normal ECG	21 (64)	-
ECG with negative or flat T-waves	12 (36)	-
Positive exercise ECG test	23 (70)	-
Inconclusive exercise ECG test	3 (9)	
Highly suspicious for obstructive CAD	7 (21)	
Traditional risk factors		
Hypertension	17 (52)	37 (52)
Hypercholesterolemia	22 (67)	40 (56)
Diabetes mellitus	0 (0)	9 (13)
Smoker	14 (42)	35 (49)
Ex-smoker	2 (6)	2 (3)
Family history of CAD	24 (73)	32 (45)
Obese †	8 (24)	15 (21)
Previous myocardial infarction	1 (3)	17 (24)
Conventional angiography		
Absence of coronary disease	2 (6)	2 (3)
Nonsignificant disease	3 (9)	9 (13)
Single-vessel disease	15 (45)	27 (38)
Two-vessel disease	10 (30)	26 (37)
Three-vessel disease	3 (9)	7 (10)

BMI, body mass index; CAD coronary artery disease.
Values are n (%) unless otherwise indicated
According to European Society for Cardiology guidelines, patients were stratified into high and low-risk groups, which give a risk estimate for progression to myocardial infarction or death. which give a risk estimate for progression to myocardial infarction or death.
* Agatston score
† BMI≥ 30 kg/m^2
‡ Recurrent ischemia defined as either recurrent chest pain or dynamic ST-segment changes (in particular ST-segment depression, or transient ST-segment elevation)

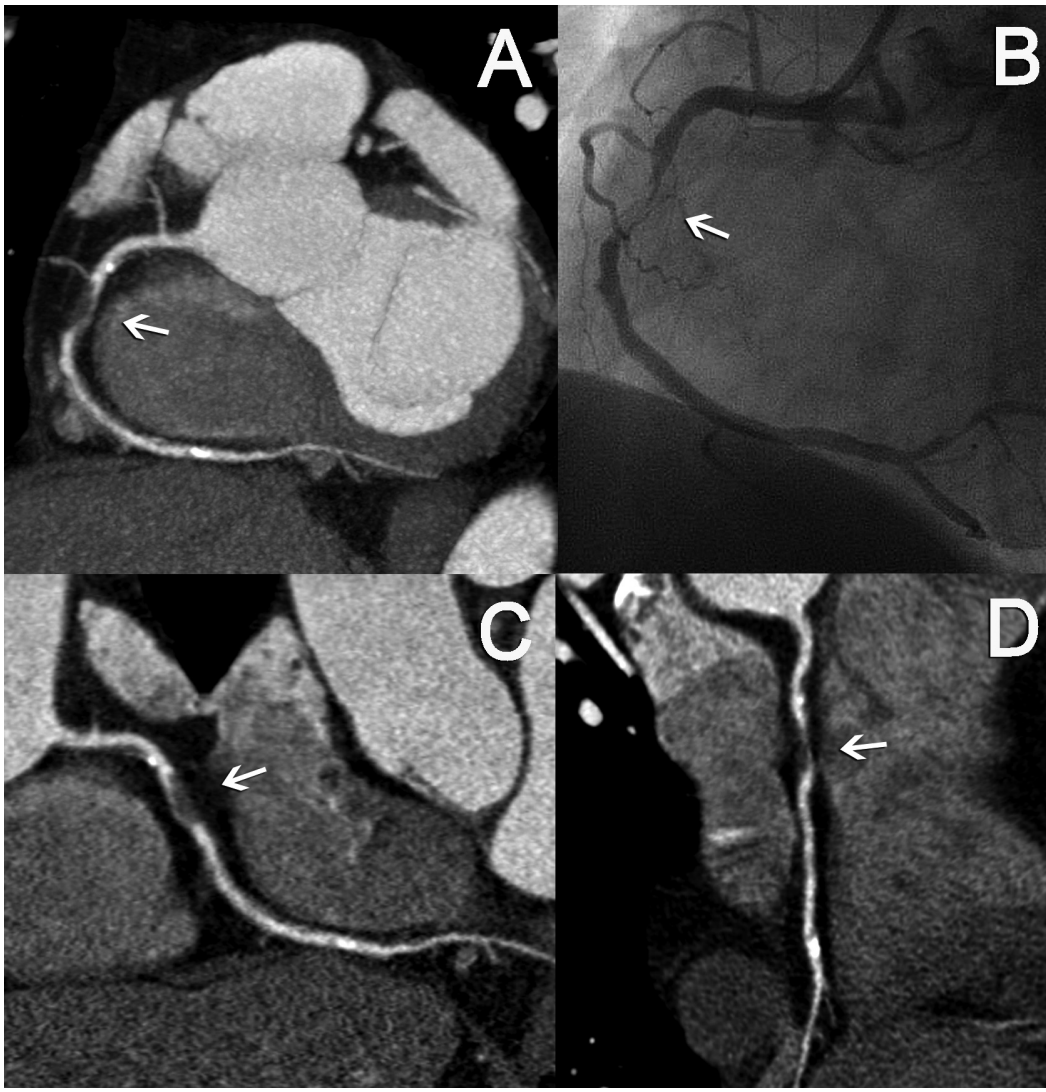

Figure 1. This patient with prior history of a mitral valve plasty for endocarditis was admitted with a non-ST segment elevation myocardial infarction. A volume-rendered CT coronary angiography image (A) reveals the anatomy of the right coronary artery. Two curved multiplanar reconstructed images (C, D) disclose a significant stenosis (arrow) in the proximal right coronary artery, which was corroborated by conventional coronary angiography (B).

and two patients as having multi-vessel disease. All 88 patients with significant CAD on CCA were correctly identified on the CT-scan (figs 1 and 2). However, in 23 patients with single-vessel disease on CCA, CTCA overestimated the severity of additional lesions, which resulted in incorrect classification as having multi-vessel disease on CTCA. In all, 27 patients in the low-risk group underwent PCI, 1 underwent CABG and 5 were treated medically. In the high-risk group, 55 underwent PCI, 5 underwent CABG and 11 were treated medically. Agreement

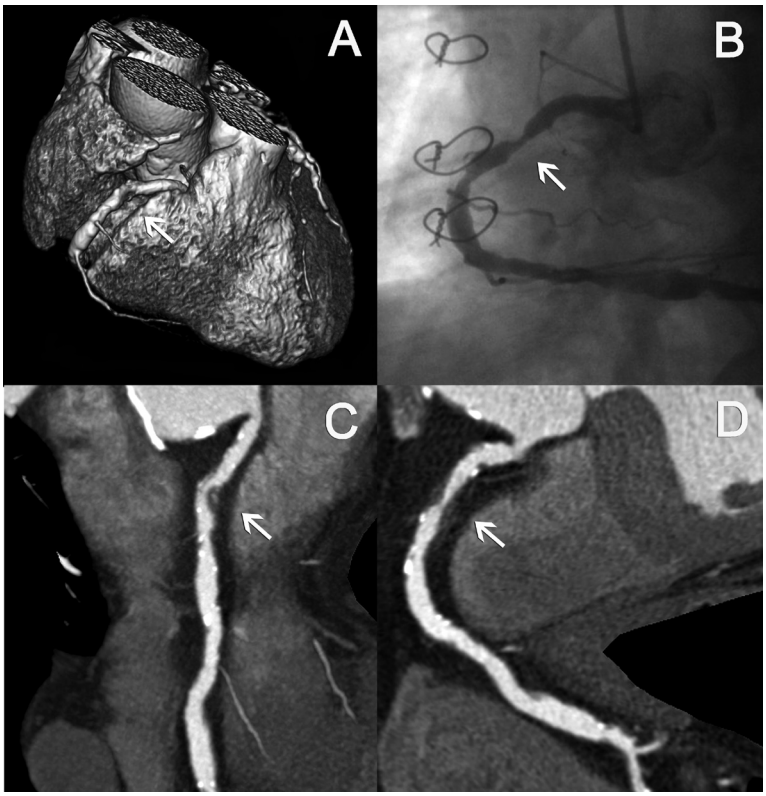

Figure 2. A maximum intensity projected CT coronary angiography image shows a large non-calcified plaque in the proximal segment of the right coronary artery (A). Two curved multi-planar reconstructed images (C, D) disclose the high-grade stenosis, confirmed by conventional coronary angiography (B).

between CTCA and QCA on a per-patient (no or any disease) level was very good (k value 0.84), whereas agreement between techniques to classify patients as having no, single-, and multi-vessel disease was moderate (k value 0.55).

Diagnostic Performance of 64-Slice CT Coronary Angiography: Vessel-By-Vessel Analysis

Table 2 details the diagnostic performance of CTCA for the detection of significant lesions in a vessel-based analysis. Two significantly diseased right coronary arteries and one diseased circumflex coronary artery were incorrectly classified as non-significantly diseased on the CT-scan. Of a total of 416 vessels, 59 non-obstructive vessels were overestimated and scored as false positives. Agreement between CTCA and QCA on a per-vessel level was good (k value: 0.70).

Diagnostic Performance of 64-slice CT Coronary Angiography: Segment-By-Segment Analysis

A total of 1525 segments were included for comparison with QCA. Potentially, 17 segments per patient can be present for analysis. A total of 243 segments were not visualized on the

Table 2. Diagnostic performance and predictive value of 64-Slice CTCA for the detection of ≥ 50% stenosis on quantitative coronary angiography

	Prevalence of disease, %	n	TP	TN	FP	FN	k	Sensitivity, % (95% CI)	Specificity, % (95% CI)	PPV, % (95% CI)	NPV, % (95% CI)	+LR	- LR
All patients	85	104	88	12	4	0	0.84	100 (95-100)	75 (47-92)	96 (89-99)	100 (70-100)	4.00	0.00
High risk	85	71	60	8	3	0	0.82	100 (93-100)	73 (39-93)	95 (86-99)	100 (60-100)	3.67	0.00
Low risk	85	33	28	4	1	0	0.87	100 (85-100)	80 (30-99)	93 (80-100)	100 (40-100)	5.00	0.00
Vessel based analysis													
All vessels	35	416	141	214	58	3	0.70	98 (94-99)	79 (73-83)	71 (64-77)	99 (96-100)	4.59	0.03
RCA	48	104	48	39	15	2	0.68	96 (85-99)	72 (58-83)	76 (64-86)	95 (82-99)	3.46	0.06
LM	3	104	3	98	3	0	0.65	100 (31-100)	97 (91-99)	50 (14-86)	100 (95-100)	33.67	0.00
LAD	47	104	49	32	23	0	0.57	100 (91-100)	58 (44-71)	68 (56-78)	100 (87-100)	2.39	0.00
CX	39	104	40	46	17	1	0.66	98 (86-100)	73 (60-83)	70 (56-81)	98 (87-100)	3.62	0.03
Segment based analysis													
All segments	13	1525	183	1205	122	15	0.68	92 (88-96)	91 (89-92)	60 (54-65)	99 (98-99)	10.05	0.08
Proximal	14	416	58	312	44	2	0.65	97 (87-99)	88 (84-91)	57 (47-67)	99 (97-100)	7.82	0.04
Mid	23	302	67	199	34	2	0.71	97 (89-99)	85 (80-90)	66 (56-75)	99 (96-100)	6.65	0.03
Distal	9	327	24	286	11	6	0.71	80 (61-92)	96 (93-98)	69 (51-83)	98 (95-99)	21.60	0.21
Side branch	8	480	34	408	33	5	0.60	87 (72-95)	92 (90-95)	51 (38-63)	99 (97-100)	11.65	0.14

CTCA, CT coronary angiography; FN, false negative; FP, false positive; LAD, left anterior descending coronary artery; LCx, circumflex coronary artery; LM, left main coronary artery; +LR, positive likelihood ratio; -LR, negative likelihood ratio; NPV, negative predictive value; PPV, positive predictive value; RCA, right coronary artery; TP, true positive; TN, true negative.

According to the 17-segment modified American Heart Association (AHA) classification, 1525 segments and 416 vessels visualised with conventional coronary angiography were included for segment and vessel analysis.

Table 3. Influence of coronary calcifications on the diagnostic accuracy of 64-slice CT coronary angiography on a segment-based analysis

Calcium score	Patients, n	Segments, n	Mean (SD), (range) Agatston Score	TP	TN	FP	FN	k	Sensitivity, % (95% CI)	Specificity, % (95% CI)	PPV, % (95% CI)	NPV, % (95% CI)	+ LR	-LR
First tertile	35	530	30 (34) (0-105)	42	465	20	3	0.76	93 (81-98)	96 (94-97)	68 (55-79)	99 (98-100)	22.63	0.07
Second tertile	35	505	266 (81) (107-375)	57	394	47	7	0.62	89 (79-95)	89 (86-92)	55 (45-64)	98 (96-99)	8.36	0.12
Third tertile	34	490	1073 (665) (400-2870)	84	346	55	5	0.66	94 (87-98)	86 (82-89)	60 (52-69)	99 (97-99)	6.88	0.07

FN, false negative; FP, false positive; LAD, left anterior descending coronary artery; +LR, positive likelihood ratio; -LR, negative likelihood ratio; NPV, negative predictive value; PPV, positive predictive value;TP, true positive; TN, true negative.

CCA. A total of 181 segments were excluded owing to variations in coronary anatomy, and 62 segments owing to the presence of a proximal occlusion and poorly filled distal segments by collaterals. All segments were included, irrespective of the presence of calcifications or poor image quality. Interobserver and intraobserver variabilities for detection of a significant stenosis per segment had a k value of 0.69 and 0.73, respectively. Tabel 2 details the performance of CTCA for detecting significant stenoses. Agreement between CTCA and QCA on a per-segment level was good (k value 0.68).

Fifteen significant coronary stenoses were underestimated or missed and classified as non-significant. Most of these significant lesions (11/15) were located in distal segments or in side branches. In all, 123 non-significant lesions were detected with CTCA, but the severity of these stenoses was overestimated. This overestimation, in 67% (83/123) owing to heavy calcification, resulted in incorrect classification as significant stenoses on the CT scan. Patients were divided into tertiles based on the mean calcium score. The presence of calcium decreased the diagnostic accuracy (low calcium score 0.95, mid 0.89 and high 0.88; table 3).

To exclude the possible confounding effect of nesting, random selection of a single segment per patient was performed. The diagnostic accuracy for detecting significant CAD was a sensitivity 93% (13/14; 95% CI 64 to 100), a specificity 93 % (84/90; 95% CI 93 to 97), a positive predictive value of 68% (13/19; 95% CI 43 to 86) and a negative predictive value 99% (84/85; 95% CI 93 to 100).

DISCUSSION

Several recent reports about the diagnostic performance of 64-slice CTCA have shown a high sensitivity and neg-

ative predictive value to detect or exclude the presence of significant coronary stenosis in patients scheduled for CCA.[5,8-14] However, only scant information is available about the diagnostic performance of CTCA in a limited number of patients with ACS.[5,8,15,16]

In our study, the prevalence of obstructive CAD was 85% which was in keeping with previous reports evaluating ACS angina syndromes.[2,3,17-19] In this high pre-test risk population we demonstrated a high diagnostic accuracy in patients with non-ST elevation ACS. In segments where interpretation was difficult owing to heavy calcification, there was a tendency for observers to score these as positive for significant stenosis in order to reduce the chance of missing an important lesion. This "defensive scoring" approach is also likely to be used in clinical practice when evaluating symptomatic patients. The high negative predictive value of the CT scan despite significant coronary calcification and the high prevalence of CAD demonstrates that significant CAD can be ruled out in this patients group.

Patients with non-segment elevation ACS classified as at high risk on the basis of baseline characteristics, troponin or ECG changes are best managed with an invasive strategy.[1-3] These patients should generally have a CCA followed by revascularisation, if appropriate, in the first few days after admission to hospital. The role of CTCA in these patients is not just for the detection of significant disease, the detailed delineation of coronary anatomy may also be useful to guide subsequent management. In this study, the agreement between CTCA and QCA in the classification of patients as having no, single or multivessel disease was moderate. This is due to the relatively high number of false positive segments scored predominantly because of calcification. In 41 out of the 104 patients, at least one vessel was overestimated as having a significant stenosis. Given this current limitation, CTCA may need to evolve further before it can more accurately guide future management, in particular either percutaneous or surgical revascularisation in these high-risk patients. At the moment, even though the results are promising, a clinical role of CTCA in these high-risk patients is not defined.

Currently, CTCA may be more suited in the low-risk non-segment-elevation ACS group. These patients, without recurrent chest pain or evidence of myocardial necrosis, are recommended to undergo a stress test after an observation period. CCA is recommended in these patients only if significant ischemia is demonstrated during stress testing.[1] However, stress testing, particularly treadmill or bicycle stress testing may be inconclusive. The role of CTCA may be to replace the stress test as the first investigation in this population group. Given the excellent negative predictive value as demonstrated in this study, a negative CTCA would allow patients to be discharged and other non-cardiac causes of the presenting chest pain to be considered. Patients with non-obstructive CAD on CTCA would continue to be managed medically, including appropriate secondary prevention, and the need for future stress testing or CCA would depend on further symptoms.

Patients with significant disease on CTCA in this patient group could be referred directly for CCA, particularly if there was left main disease, three-vessel or proximal segment disease of a main coronary artery. Patients with small-vessel disease (ie, distal disease < 2mm), equivocal lesions or uninterpretable scans could undergo a stress test to further guide the need for CCA. However, the use of sequential testing is controversial, as no data is available showing better test results than a stress test alone.

Limitations of the study

We did not include patients with severe ongoing ischemia, or hemodynamic or electrical instability, to prevent further delays of revascularization treatment. Furthermore, inclusion comprised a non-consecutive group of patients. Owing to logistic reasons, it was not feasible to scan and include every patient presenting with a non-ST elevation ACS. Moreover, patients in the low-risk group with a negative exercise ECG test were not included, since these patients did not receive a CCA.

Heart rate reduction with ß-blockers is standard practice in patients presenting with a non-ST elevation ACS. Additional ß-blockers were given to reduce the heart rate even more in order to achieve optimal heart rate control. With the next generation dual-source CT scanners, scanning at higher heart rates will be possible owing to the improved temporal resolution of 83 ms[20,21].

The rather high radiation exposure of CTCA as compared to CCA is of concern.[22,23] The radiation exposure can be reduced by 40% using prospective x ray tube current modulation. However, this limits the possibility to reconstruct valuable datasets during the end-systolic phase.

The presence of atrial fibrillation precludes the use of CTCA and was one of the exclusion criteria.

CONCLUSIONS

The 64-slice CT angiography has a high sensitivity to detect significant coronary stenoses and is reliable to exclude the presence of significant CAD in patients who present with a non-ST elevation ACS. The role of CTCA in these patients, particularly in the low-risk group, needs to be further evaluated.

REFERENCES

1. Bertrand ME, Simoons ML, Fox KA, et al. Management of acute coronary syndromes in patients presenting without persistent ST-segment elevation. Eur Heart J 2002;23:1809-40.
2. Invasive compared with non-invasive treatment in unstable coronary-artery disease: FRISC II prospective randomised multicentre study. FRagmin and Fast Revascularisation during InStability in Coronary artery disease Investigators. Lancet 1999;354:708-15.
3. Cannon CP, Weintraub WS, Demopoulos LA, et al. Comparison of early invasive and conservative strategies in patients with unstable coronary syndromes treated with the glycoprotein IIb/IIIa inhibitor tirofiban. N Engl J Med 2001;344:1879-87.
4. Trabold T, Buchgeister M, Kuttner A, et al. Estimation of radiation exposure in 16-detector row computed tomography of the heart with retrospective ECG-gating. Rofo 2003;175:1051-5.
5. Mollet NR, Cademartiri F, van Mieghem CA, et al. High-resolution spiral computed tomography coronary angiography in patients referred for diagnostic conventional coronary angiography. Circulation 2005;112:2318-23.
6. Austen WG, Edwards JE, Frye RL, et al. A reporting system on patients evaluated for coronary artery disease. Report of the Ad Hoc Committee for Grading of Coronary Artery Disease, Council on Cardiovascular Surgery, American Heart Association. Circulation 1975;51:5-40.
7. Agatston AS, Janowitz WR, Hildner FJ, et al. Quantification of coronary artery calcium using ultrafast computed tomography. J Am Coll Cardiol 1990;15:827-32.
8. Leschka S, Alkadhi H, Plass A, et al. Accuracy of MSCT coronary angiography with 64-slice technology: first experience. Eur Heart J 2005;26:1482-7
9. Raff GL, Gallagher MJ, O'Neill WW, et al. Diagnostic accuracy of noninvasive coronary angiography using 64-slice spiral computed tomography. J Am Coll Cardiol 2005;46:552-7.
10. Leber AW, Knez A, von Ziegler F, et al. Quantification of obstructive and nonobstructive coronary lesions by 64-slice computed tomography: a comparative study with quantitative coronary angiography and intravascular ultrasound. J Am Coll Cardiol 2005;46:147-54.
11. Ropers D, Rixe J, Anders K, et al. Usefulness of multidetector row spiral computed tomography with 64- x 0.6-mm collimation and 330-ms rotation for the noninvasive detection of significant coronary artery stenoses. Am J Cardiol 2006;97:343-8.
12. Schuijf JD, Pundziute G, Jukema JW, et al. Diagnostic accuracy of 64-slice multislice computed tomography in the noninvasive evaluation of significant coronary artery disease. Am J Cardiol 2006;98:145-8.

13. Ehara M, Surmely JF, Kawai M, et al. Diagnostic accuracy of 64-slice computed tomography for detecting angiographically significant coronary artery stenosis in an unselected consecutive patient population: comparison with conventional invasive angiography. Circ J 2006;70:564-71.
14. Nikolaou K, Knez A, Rist C, et al. Accuracy of 64-MDCT in the diagnosis of ischemic heart disease. AJR Am J Roentgenol 2006;187:111-7.
15. Dirksen MS, Jukema JW, Bax JJ, et al. Cardiac multidetector-row computed tomography in patients with unstable angina. Am J Cardiol 2005;95:457-61.
16. Dorgelo J, Willems TP, Geluk CA, et al. Multidetector computed tomography-guided treatment strategy in patients with non-ST elevation acute coronary syndromes: a pilot study. Eur Radiol 2005;15:708-13.
17. Diver DJ, Bier JD, Ferreira PE, et al. Clinical and arteriographic characterization of patients with unstable angina without critical coronary arterial narrowing (from the TIMI-IIIA Trial). Am J Cardiol 1994;74:531-7.
18. Roe MT, Harrington RA, Prosper DM, et al. Clinical and therapeutic profile of patients presenting with acute coronary syndromes who do not have significant coronary artery disease.The Platelet Glycoprotein IIb/IIIa in Unstable Angina: Receptor Suppression Using Integrilin Therapy (PURSUIT) Trial Investigators. Circulation 2000;102:1101-6.
19. Glaser R, Herrmann HC, Murphy SA, et al. Benefit of an early invasive management strategy in women with acute coronary syndromes. Jama 2002;288:3124-9.
20. Flohr TG, McCollough CH, Bruder H, et al. First performance evaluation of a dual-source CT (DSCT) system. Eur Radiol 2006;16:256-68.
21. Achenbach S, Ropers D, Kuettner A, et al. Contrast-enhanced coronary artery visualization by dual-source computed tomography--initial experience. Eur J Radiol 2006;57:331-5.
22. Hausleiter J, Meyer T, Hadamitzky M, et al. Radiation dose estimates from cardiac multislice computed tomography in daily practice: impact of different scanning protocols on effective dose estimates. Circulation 2006;113:1305-10.
23. Coles DR, Smail MA, Negus IS, et al. Comparison of radiation doses from multislice computed tomography coronary angiography and conventional diagnostic angiography. J Am Coll Cardiol 2006;47:1840-5.

INTERLUDE 2

Spontaneous Dissection of the Left Main Coronary Artery in a Patient with Osler-Weber-Rendu Disease

Carlos A.G. Van Mieghem[1,2], Jurgen M.R. Ligthart[1], Filippo Cademartiri[2]

From the departments of Cardiology[1] and Radiology[2],
Erasmus MC, Rotterdam, the Netherlands

Heart. 2005; 92: 394

A 33 year old woman, with hereditary haemorrhagic telangiectasia (Osler-Weber-Rendu disease), presented to the hospital 48 hours after a prolonged episode of chest pain. The ECG, showing pathological Q waves in leads V1-V3, and inverted T waves in leads V1-V6, and cardiac enzymes confirmed the diagnosis of a semi-recent anterior myocardial infarction. Cardiac 64 row multislice computed tomography (panels A and B) revealed a dissection originating from the left main (LM) with antegrade extension along the course of the left anterior descending coronary artery (LAD) and re-entry distal to the first diagonal branch (D1). These findings were subsequently confirmed by coronary angiography and intravascular ultrasound (IVUS) (panels C and D). Both the LM and mid-LAD were successfully treated with a bare metal stent.

Spontaneous coronary artery dissection is a rare condition, the aetiology of which in general remains unclear. In this case it might be related to the fragility of the vessel wall, which characterizes Osler-Weber-Rendu disease.

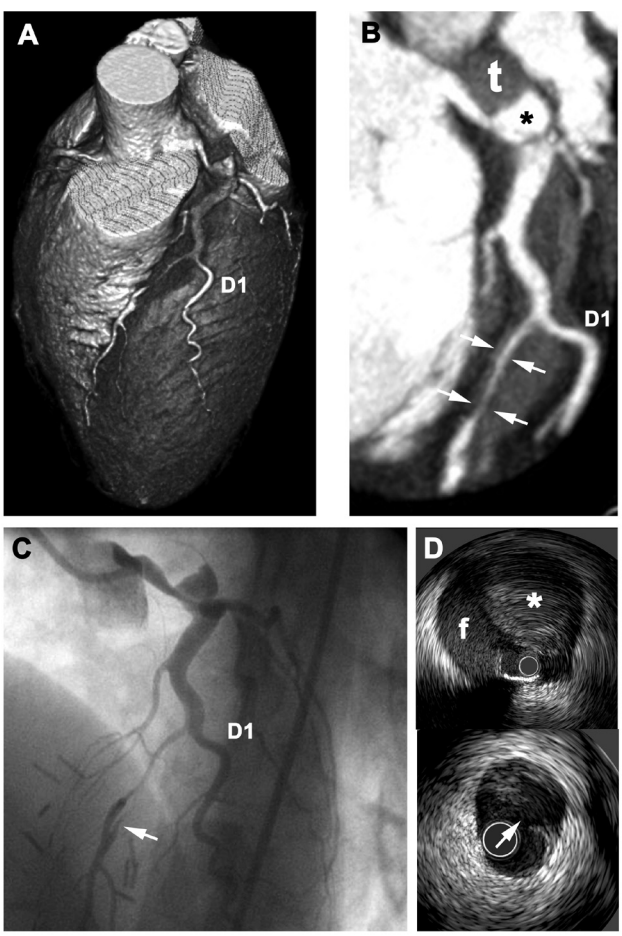

Figure Three dimensional (A) and multiplanar reconstructed (B) multislice computed tomography image showing the false lumen (asterisk) with thrombus (t) within the LM artery. The dissection is accompanied by a large haematoma along the course of the LAD that compresses the lumen (arrows) distal to the origin of D1. (C) Coronary angiography confirms the LM dissection and critical narrowing of the mid LAD. (D) IVUS shows the false lumen (f) with thrombus (asterisk) and an intimal tear (arrow) corresponding to the distal re-entry point of the dissection. Angiographically the tear is visible as a "flap" within the lumen. (A full color version of this illustration can be found in the color section).

8

64-slice Computed Tomography Coronary Angiography in Patients with High, Intermediate, or Low Pretest Probability of Significant Coronary Artery Disease

W. Bob Meijboom[1,2], Carlos A.G. Van Mieghem, Nico R. Mollet[1,2], Francesca Pugliese[1,2], Annick C. Weustink[1,2], Niels van Pelt[1,2], Filippo Cademartiri[2], Koen Nieman[1], Eric Boersma[1], Peter de Jaegere[1], Gabriel P. Krestin[2], Pim J. de Feyter[1,2]

From the departments of Cardiology[1] and Radiology[2], Erasmus MC, Rotterdam, the Netherlands

J Am Coll Cardiol. 2007; 50:1469-75

ABSTRACT

Objectives

We assessed the usefulness of 64-slice computed tomography coronary angiography (CTCA) to detect or rule out coronary artery disease (CAD) in patients with various estimated pretest probabilities of CAD.

Background

The pretest probability of the presence of CAD may impact on the diagnostic performance of CTCA.

Methods

Sixty-four-slice CTCA (Sensation 64, Siemens, Forchheim, Germany) was performed in 254 symptomatic patients. Patients with heart rates ≥65 beats/min received beta-blockers before CTCA. The pretest probability for significant CAD was estimated by type of chest discomfort, age, gender, traditional risk factors and defined as high (≥71%), intermediate (31% to 70%), and low (≤30%). Significant CAD was defined as the presence of at least 1 ≥50% coronary stenosis on quantitative coronary angiography, which was the standard of reference. No coronary segments were excluded from analysis.

Results

The estimated pretest probability of CAD in the high (n = 105), intermediate (n = 83), and low (n = 66) group was 87%, 53% and 13%, respectively. The diagnostic performance of the CT scan was different in the 3 subgroups. The estimated post-test probability of the presence of significant CAD after a negative CT scan was 17%, 0%, and 0%, and after a positive CT scan 96%, 88% and 68%, respectively.

Conclusions

Computed tomography coronary angiopraphy is useful in symptomatic patients with a low or intermediate estimated pretest probability of having significant CAD, and a negative CT scan reliably rules out the presence of significant CAD. Computed tomography coronary angiopraphy does not provide additional relevant diagnostic information in symptomatic patients with a high estimated pretest probability of CAD.

INTRODUCTION

The estimated pretest probability of having significant coronary artery disease (CAD) in a study population should be taken into account in the evaluation of the diagnostic accuracy of computed tomography coronary angiography (CTCA) to detect or rule out the presence of coronary stenosis. The estimated pretest probability of having obstructive CAD in patients who present with chest pain is related to age, gender, type of chest discomfort, and traditional risk factors. The estimated pretest probability is lowest in younger female patients with nonanginal chest pain and highest in older male patients with typical angina (1).

The diagnostic performance of CTCA has mostly been tested in symptomatic patient populations with a high estimated pretest probability of having significant CAD, and a few studies have reported on the impact of different estimated pretest probabilities on the performance of CTCA (2).

The purpose of this study was to evaluate the diagnostic performance and clinical usefulness of 64-slice CTCA in 254 patients with high, intermediate or low estimated pretest probability of having significant coronary stenosis.

METHODS

Study population

During a 24-month period, 254 patients presenting with typical angina pectoris, atypical angina pectoris and nonanginal chest pain who were referred for conventional coronary angiography (CCA) were included into the study. Typical angina was defined as having 3 characteristics: 1) substernal discomfort, 2) that is precipitated by physical exertion or emotion and 3) relieved with rest or nitroglycerine within 10 min. Atypical angina pectoris was defined as having 2 out of 3 of the definition characteristics. Nonanginal chest pain was characterized as 1 or absence of the described chest pain features. The estimated pretest probability for obstructive CAD was estimated using the Duke Clinical Score, which includes type of chest discomfort, age, gender, and traditional risk factors (3, 4). Patients were categorized into a low (1% to 30%), intermediate (31% to 70%), or high (71% to -99%) estimated pretest probability group of having significant CAD. No patients with previous history of percutaneous coronary intervention, coronary artery bypass surgery, prior myocardial infarction, impaired renal function (serum creatinine $>120\ \mu$mol/l), persistent arrhythmias or known allergy to iodinated contrast material, were included. Conventional coronary angiogram was performed before or after the CTCA and served as the standard of reference. The institutional review board of the Erasmus Medical Center Rotterdam approved the study, and all subjects gave informed consent.

Patient preparation

Patients with a heart rate exceeding 65 beats/min received additional beta-blockers (50/100mg Metoprolol) 1 h before the computed tomography (CT) examination.

Scan protocol

All scans were performed with a 64-slice CT scanner that features a gantry rotation time of 330 ms, a temporal resolution of 165 ms and a spatial resolution of 0.4 mm3 (Sensation 64, Siemens, Forchheim, Germany). A calcium scoring scan was performed with following parameters; 64 × 0.6 mm collimation, 330 ms rotation time, 120 kV tube voltage, 150 mAs tube current, 3.8 mm/rotation table feed, prospective electrocardiogram (ECG) X-ray tube modulation. Afterwards, the CTCA was performed using identical parameters aside from a higher tube current between 850 and 960 mAs and without the use of prospective ECG X-ray tube modulation. The radiation exposure was estimated using dedicated software (ImPACT ®, version 0.99x, St. George's Hospital, Tooting, London, United Kingdom).

A bolus of 95 ml of contrast material (400 mgI/ml; Iomeron, Bracco, Milan, Italy) was injected intravenously in an antecubital vein at 5 ml/s, and a bolus-tracking technique was used to synchronize the arrival of contrast in the coronary arteries and the initiation of the scan.

Image reconstruction

Datasets were reconstructed immediately after the scan after a stepwise approach as previously described (5, 6). If necessary, multiple datasets of a single patient were used separately in order to obtain optimal image quality for all available coronary segments.

Quantitative coronary angiography (QCA)

All scans were carried out within 1 week before or after CCA. One experienced cardiologist, unaware of the results of CTCA, identified and analyzed all coronary segments, using a 17-segment modified American Heart Assiciation classification. All segments, regardless of size, were included for comparison with CTCA. Segments were classified as normal (smooth parallel or tapering borders), as having non-significant disease (wall irregularities or <50% stenosis) or having significant disease (stenosis ≥50%). Stenoses were evaluated in the worst view, and classified as significant if the lumen diameter reduction exceeded ≥50% measured by validated QCA algorithm (CAAS, Pie Medical, Maastricht, the Netherlands).

CT image evaluation

One observer analyzed total calcium scores of all patients using dedicated software. Two experienced observers, a radiologist and a cardiologist, unaware of the results of CCA, evaluated the CTCA data sets on an offline workstation (Leonardo, Siemens) using (curved) multiplanar reconstruction. Segments were scored positive for significant CAD if there was ≥ 50% diam-

eter reduction of the lumen by visual assessment. Segments distal to a chronic total occlusion were excluded. Interobserver disagreements were resolved by a third reader.

Statistical analysis

The diagnostic performance of CTCA for the detection of significant coronary artery stenoses as defined by QCA is presented as sensitivity, specificity, positive and negative predictive values with the corresponding 95% (CIs), and positive and negative likelihood ratios (LRs) were calculated. Comparison between CTCA and QCA was performed on 3 levels: patient-by-patient, vessel-by-vessel and segment-by-segment analysis. A Mantel-Haenszel test was performed to evaluate the trend in sensitivity and specificity relative to the estimated pre-test probability for obstructive CAD.

Categorical characteristics are expressed as numbers and percentages, and compared between the 3 groups using the chi square test. Continuous variables are expressed as means (standard deviation) and compared with one-way analysis of variance followed by post-hoc Bonferroni correction to adjust for multiple comparisons. If not normally distributed, continuous variables are expressed as medians (25th to 75th percentile range) and compared with Kruskal-Wallis test.

An additional analysis was done to investigate the effect of nesting since repeated assessments within the same patient were made that were not independent observations. A random selection of a single segment per patient was done, and the diagnostic accuracy for detecting significant artery disease was calculated. Interobserver and intraobserver variability for the detection of significant coronary stenosis and agreement between techniques to classify patients as having no, single-, or multivessel disease was determined by κ-statistics.

RESULTS

Patient demographics are shown in Table 1. Additional beta-blockers prior to CT scanning were administered in 74 % (188 of 254) of patients decreasing the mean heart rate from 71 ± 11 beats/min to 59 ± 8 beats/min. The mean scan time was 12.7 ± 1.6 s. Initially, all datasets were reconstructed in the mid- to end diastolic phase. In 34% of the cases (86 of 254), additional higher quality reconstructions obtained during end systole were used for evaluation.
The estimated radiation exposure using prospective X-ray tube modulation for the calcium score in women and men was 1.8 and 1.4 mSv, respectively. The estimated radiation exposure for the contrast-enhanced scan without prospective X-ray tube modulation was 17.0 mSv in women and 13.4 mSv in men, which is in line with previous reports (7).

Table 1 : Patient demographics (n=254)

	Pretest Probability of Significant CAD			
	> 70% High (n = 105)	30-70% Intermediate (n = 83)	< 30% Low (n = 66)	p Value
Typical angina	89 (85)	31 (37)	3 (4)	< 0.0001
Atypical angina	16 (15)	29 (35)	21 (32)	
Nonanginal chest pain	0 (0)	23 (28)	42 (64)	
Men	97 (92)	47 (57)	27 (41)	< 0.0001
Age (yrs)*	63 ± 9	61 ± 8	50 ± 12	< 0.0001
BMI (kg/m^2)*	27.5 ± 4.2	27.1 ± 4.8	26.7 ± 4.2	ns
Heart rate (beats/min)*	57 ± 8	60 ± 7	61 ± 7	< 0.01
Risk factors				
Hypertension†	68 (65)	43 (52)	30 (45)	< 0.05
Hypercholesterolemia‡	71 (68)	52 (63)	14 (21)	< 0.0001
Diabetes mellitus§	16 (15)	11 (13)	4 (6)	ns
Current smoker	32 (30)	16 (19)	16 (24)	ns
Previous smoker	14 (13)	6 (7)	4 (6)	ns
Family history of CAD||	57 (54)	39 (47)	29 (44)	ns
Obesity¶	32 (30)	21 (25)	13 (20)	ns
Calcium score (Agatston score)#	354 (103-814)	134 (1-296)	0 (0-56)	< 0.0001
Conventional coronary angiography				
Prevalence of obstructive CAD	82 (78)	32 (39)	12 (18)	< 0.0001
Absence of CAD	6 (6)	21 (25)	36 (55)	< 0.0001
Nonsignificant disease	17 (16)	30 (36)	18 (27)	
Single-vessel disease	42 (40)	22 (27)	9 (14)	
Multivessel disease	40 (38)	10 (12)	3 (5)	

* Mean and standard deviation. ‡ Blood pressure ≥ 140/90 mm Hg or treatment for hypertension. ‡Total cholesterol > 180 mg/dl or treatment for hypercholesterolemia. §Treatment with oral anti-diabetic medication or insulin. ||Family history of coronary artery disease (CAD), having first- or second-degree relatives with premature CAD (age <55 years). ¶Body mass index (BMI) ≥ 30 kg/m2. #Median and quartiles. Values are n (%) unless otherwise indicated. Categorical variables were tested with chi-square test. Continuous variables were tested with 1-way analysis of variance . If not normally distributed, continuous variables were compared with Kruskal-Wallis test. The p-values < 0.05 were considered statistically significant.

Diagnostic performance of 64-slice CTCA: all patients with chest pain

The observed pretest probability of significant CAD, defined as having at least 1 ≥50% coronary stenosis per patient was 50%. The diagnostic performance of CTCA for detecting significant stenoses on a patient level is detailed in Table 2. Eighteen patients with angiographic

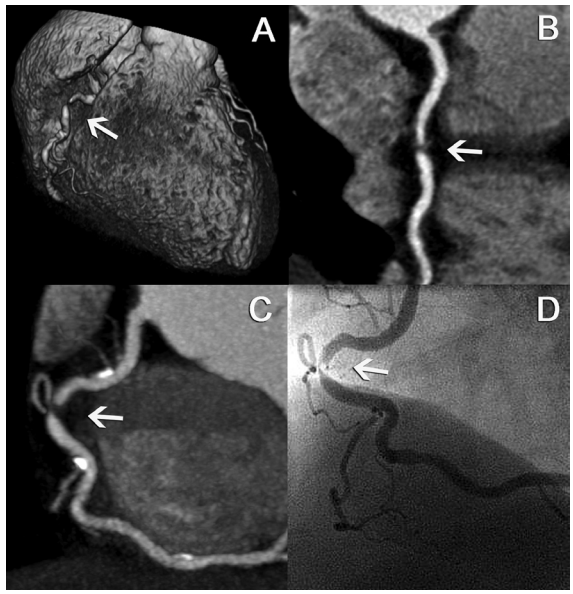

Figure 1. CTCA image of the right coronary artery. Volume-rendered computed tomography coronary angiography (CTCA) image (A) of the right coronary artery. A curved multiplanar reconstructed image (B) and a thick maximum-intensity projected image (C) disclose a significant coronary stenosis (arrow) in the mid right coronary artery, which was corroborated by conventional coronary angiogram (D). Proximally and distally of the significant obstructed lesion, nonsignificant calcified plaques can be seen (C)

nonsignificant disease were incorrectly classified as having significant CAD by CT: 17 patients were scored as having single-vessel disease, and 1 patient was misinterpreted as having multivessel disease. Ninety-eight percent (124 of 126) of patients with significant CAD on CCA were correctly identified by CTCA (Fig. 1). The 2 patients in whom the severity of disease was underestimated both showed significant lumen narrowing in the circumflex coronary artery (both 53% diameter reduction, one in the proximal and one in the midsegment). Forty patients with single-vessel disease were evaluated as having multivessel disease by CTCA due to overestimation of disease severity in other vessels. Agreement between CTCA and QCA on a per-patient (no or any disease) level was very good (κ-value: 0.84), whereas agreement between techniques to classify patients as having no, single-, and multivessel disease was good (κ-value: 0.61).

Diagnostic performance of 64-slice CT coronary angiography: patient-by-patient analysis

The analysis comprised 105 (43%) patients with a high estimated pretest probability for CAD, 83 (33%) patients with an intermediate, and 66 (26%) patients with a low estimated pretest probability for CAD. The mean age between patients with high estimated probability and intermediate estimated probability group was significantly different from the mean age in the low probability group, and the median calcium score was significantly different in all 3 groups. The mean heart rate was significantly lower in the high estimated probability group compared with those seen in the intermediate and low estimated probability group (Table 1).

The diagnostic performance of CTCA was different in the patient groups with various estimated pretest probabilities. The specificity showed a trend with a lower specificity in the high estimated pretest probability ($p: < 0.05$, sensitivity, $p = NS$). The diagnostic impact of CTCA on the estimated pretest probability of having significant CAD is shown in Figure 2 and 3.

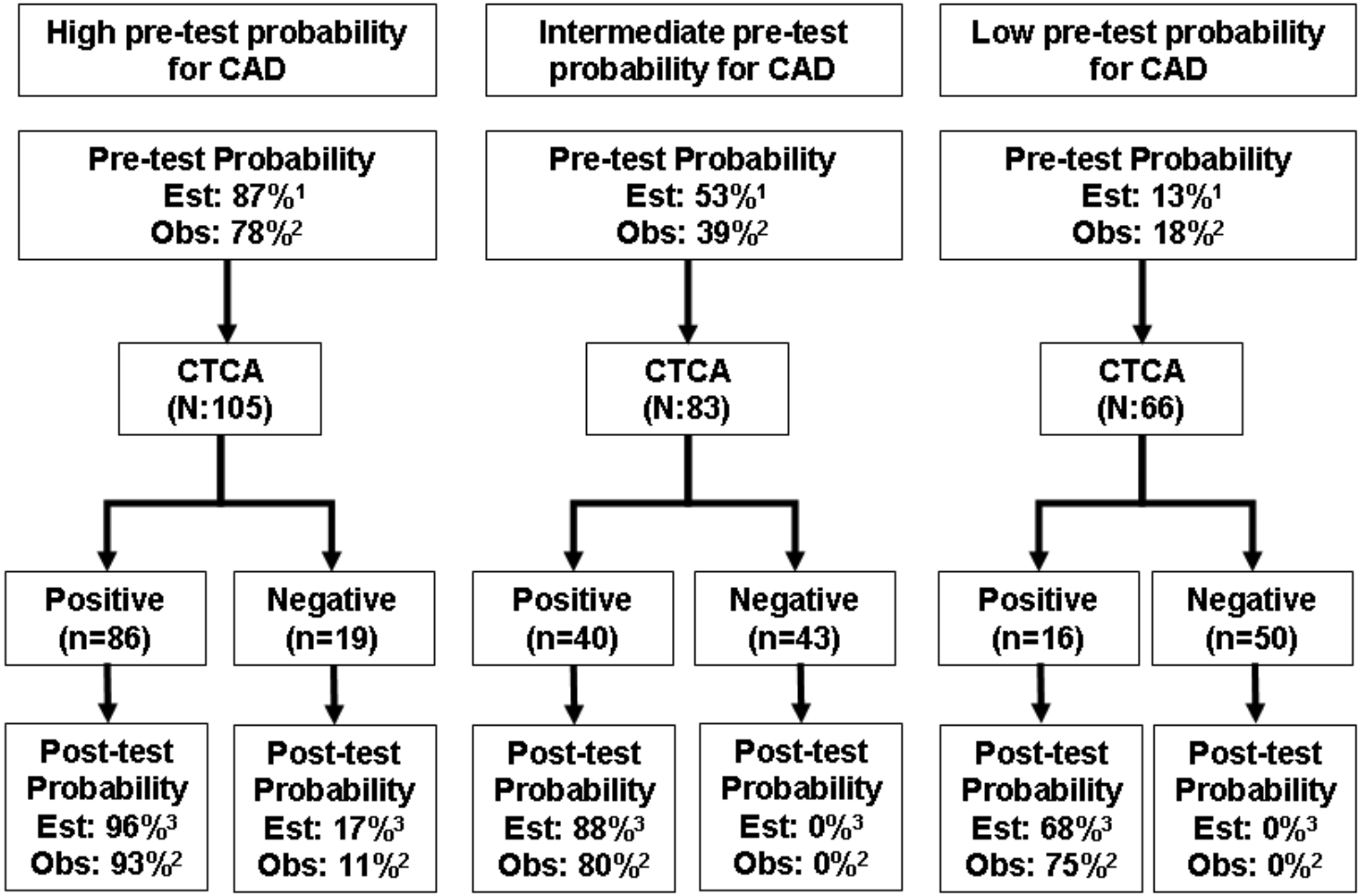

Figure 2. Impact of CTCA on various estimated pretest probabilities of significant CAD.

[1] Estimated using Duke Clinical Score (including Diamond-Forrester criteria and prognostic clinical variables); [2]based on conventional coronary angiography (≥1 significant coronary stenosis as determined by quantitative coronary angiography); [3]calculated using Bayesian statistics (post-test odds= pre-test odds × likelihood ratio). CAD = coronary artery disease; CTCA = computed tomography coronary angiography; Est = Estimated; Obs = Observed.

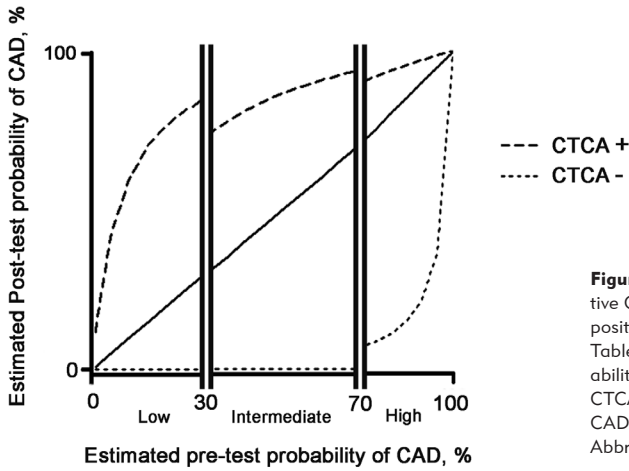

Figure 3. Influence of CTCA on probability of obstructive CAD as a function of pretest probability. Using the positive and negative likelihood ratios obtained from Table 2, we calculated the estimated post-test probabilities of CAD after positive and negative findings on CTCA from various estimated pre-test probabilities of CAD. Dashed lines = CTCA+; dotted lines = CTCA-. Abbreviations as in Figure 2.

Diagnostic performance of 64-slice CT coronary angiography: vessel-by-vessel analysis

The diagnostic performance of CTCA for the detection of significant lesions on a vessel-based analysis is detailed in Table 2. Two significantly diseased right coronary arteries, 1 left anterior descending artery, and 5 diseased circumflex coronary arteries were incorrectly classified as non-significantly diseased by CTCA. Of a total of 1016 vessels, the severity of a lesion was overestimated in 97 nonobstructive vessels (false positives). The diagnostic performance of the CT scan was different in the 3 subgroups. The specificity showed a trend towards lower specificity in the high estimated pretest probability ($p < 0.0001$, sensitivity, p = NS). Agreement between CTCA and QCA on a per-vessel level was good (κ-value: 0.71).

Diagnostic performance of 64-slice CT coronary angiography: segment-by-segment analysis

Overall, 3647 (of 4318 potentially available segments) were included for comparison with QCA. Unavailable segments included 547 anatomically absent segments on CCA and 124 segments distal to an occluded coronary segment. Segments were not excluded for reasons such as severe calcifications or poor image quality. The κ-value for interobserver - and intraobserver variability was 0.70 and 0.72, respectively. The diagnostic performance of CTCA for detecting significant stenoses is detailed in Table 2. Agreement between CTCA and QCA on a per-segment level was good (κ-value, 0.64).

The severity of 32 significant coronary stenoses was underestimated or missed and classified as nonsignificant by CTCA. Most of these significant lesions (24 of 32) were located in distal segments or in side branches. The severity of 193 nonsignificant lesions was overestimated

by CTCA. The diagnostic performance of the CT scan was different in the 3 subgroups with a lower sensitivity ($p < 0.05$) and a higher specificity ($p < 0.0001$) in the low pretest probability group.

Analysis on the randomly selected segments resulted in a sensitivity 92% (24 of 26; 95% CI 73% to 99%), specificity 93% (212 of 228; 95% CI, 89% to 96%), positive predictive value 60% (16 of 40; 95% CI, 43% to 75%), negative predictive value 99% (212 of 214; 95% CI, 96% to 100%). The effect of nesting is probably minimal as the result of this analysis is very similar to the results shown in the per-segment analysis (Table 2).

DISCUSSION

The diagnostic performance of 64-slice CTCA to detect or rule out the presence of significant coronary stenosis has mainly been reported for patients with stable angina pectoris scheduled for invasive CCA, and these studies have shown that CTCA can reliably rule out significant CAD (5, 8-10). The majority of these patients presented with a high estimated pretest probability of having significant CAD, and only scant information is available on the diagnostic performance of 64-slice CTCA in patients with a low or intermediate estimated pretest probability of having significant CAD.

In this study, we used the Duke Clinical Score, which incorporates clinical presentation of chest pain, age, gender and traditional risk factors, to estimate the pre-test probability of having significant CAD. Using the LRs of the tests, which were obtained in this study, post-test probabilities were calculated.

The pretest probability of CAD may impact of the diagnostic performance of the CT scan. Indeed, the diagnostic performance of CTCA in the 3 groups was different. The specificity was lower in the high pretest probability group compared with the low pretest probability group, whereas sensitivity was lower in the per-segment analysis in the low pretest probability group. This observation can probably be explained by the higher calcium scores in the higher probability groups, which tend to overestimate the severity of stenosis.
A negative CT-scan was present in 75% of the patients with a low estimated pretest probability and in approximately 50% of the patients with an intermediate estimated pretest probability. The negative predictive value of CTCA to exclude significant CAD was excellent in these patients, reducing the estimated post-test probability to zero. Thus, these patients would not need further downstream diagnostic tests. They may be candidates for secondary prevention measures, such as statin therapy in the presence of nonobstructive plaques or could be discharged from further cardiac follow-up in the absence of any visible plaque.

Table 2: Diagnostic performance and predictive value of 64-Slice CT coronary angiography for the detection of ≥ 50% stenosis on QCA; analysis for high, intermediate, and low pretest likelihood for obstructive CAD.

	Observed * pretest probability %	Estimated † Pretest Probability %	n	TP	TN	FP	FN	Kappa	Sensitivity ‡ %	Specificity § %	PPV%	NPV%	+LR	- LR
Patient based	50	-	254	124	110	18	2	0.84	98 (94-100)	86 (78-91)	87 (80-92)	98 (93-100)	7.00	0.02
analysis: all														
High	78	87	105	80	17	6	2	0.76	98 (91-100)	74 (51-89)	93 (85-97)	89 (65-98)	3.74	0.03
Intermediate	39	53	83	32	43	8	0	0.81	100 (87-100)	84 (71-93)	80 (64-90)	100 (90-100)	6.38	0.00
Low	18	13	66	12	50	4	0	0.82	100 (70-100)	93 (81-98)	75 (47-92)	100 (91-100)	13.50	0.00
Vessel based	19	-	1016	181	730	97	8	0.71	96 (92-98)	88 (86-90)	65 (59-71)	99 (98-99)	8.16	0.05
analysis : all														
High	31	-	420	126	229	60	5	0.68	96 (91-99)	79 (74-84)	68 (60-74)	98 (95-99)	4.63	0.05
Intermediate	13	-	332	40	261	28	3	0.67	93 (80-98)	90 (86-93)	59 (46-70)	99 (96-100)	9.60	0.08
Low	6	-	264	15	240	9	0	0.75	100 (75-100)	96 (93-98)	63 (41-80)	100 (98-100)	27.67	0.00
Segment based	7	-	3647	228	3194	193	32	0.64	88 (83-91)	94 (93-95)	54 (49-59)	99 (99-99)	15.39	0.13
analysis: all														
High	12	-	1468	163	1161	126	18	0.64	90 (85-94)	90 (88-92)	56 (50-62)	98 (98-99)	9.20	0.11
Intermediate	4	-	1219	46	1112	54	7	0.58	87 (74-94)	95 (94-96)	46 (36-56)	99 (99-100)	18.74	0.14
Low	3	-	960	19	921	13	7	0.65	73 (52-88)	99 (98-99)	59 (41-76)	99 (98-100)	52.50	0.27

* Observed pre-test probability: based on conventional coronary angiography (≥1 significant coronary stenosis as determined by quantative coronary angiography |QCA|). † Estimated pretest probability: estimated using Duke Clinical Score. ‡ The sensitivity showed a trend with a lower sensitivity in the low estimated pretest probability in the per-segment analysis ($p < 0.05$). § the specificity showed a trend with a lower specificity in the high estimated pretest probability in the per-patient, per-vessel and per-segment analysis. ($p < 0.05$, p: < 0.0001, $p < 0.0001$, respectively). Values in parentheses represent 95 % confidence intervals.

CAD = coronary artery disease; FN = false negative; FP = false positive; NPV = negative predictive value; PPV = positive predictive value; TN = true negative; TP = true positive;;+LR = positive likelihood ratio; -LR = negative likelihood ratio.

A positive CT-scan occurred in approximately 25% and 50% of the patients with a low or intermediate estimated pretest probability, respectively. The number of false positive outcomes was rather high in these patients, which renders a positive CT scan rather unreliable for clinical decision making. In these patients it may be reasonable to proceed to invasive CCA in the case of left main disease, 3-vessel disease and in the presence of a critical stenosis in the proximal part of a major coronary artery. In case of vessel disease in distal vessels or side branches, equivocal lesions or uninterpretable scans, one may consider a non-invasive stress test to determine the functional significance of a doubtful coronary stenosis. A negative functional test may overrule the clinical significance of a (false)-positive CT-scan and reduce the need for invasive coronary angiography. A positive functional test may further increase the probability of having significant CAD and should be followed by invasive coronary angiography and coronary revascularisation if symptoms are not alleviated by the antianginal mediation. However, further studies are necessary to evaluate the diagnostic value of the combination of functional data from a stress test with the anatomical data provided by CTCA.

In the high estimated pretest probability group a negative CTCA reduced the estimated post-test probability to 17%, whereas a positive CTCA increased the estimated post-test probability to as high as 96%. Given the high estimated pretest probability of significant CAD in this group, the majority of these symptomatic patients are likely to proceed to invasive CCA even if CTCA is negative, since the post-test probability of significant CAD was still >10%. Computed tomography coronary angiography, therefore, appears to be of limited clinical value in the evaluation of the high estimated pretest probability group. Assessment for the presence of myocardial ischemia with a functional test may be more appropriate in this situation.

Study limitations

The studied patients were not a prospective, consecutive group of patients. However, selection was not based on particular patient demographics, but rather on the availability of the 64 slice CT scanner for the examination of cardiac patients. The rather high estimated radiation exposure of 64-slice CTCA (17 to –13.4 mSv) as compared to CCA (3 to 6 mSv) is of concern (7). In this study we did not use prospective ECG X-ray tube modulation, which can significantly reduce radiation exposure, but requires a regular heart rhythm and limits the possibility of reconstructing images in the end-systolic phase. In our study end-systolic data sets provided optimal image quality in 34% of patients.

Currently, there is no validated software available able to quantify the degree of stenoses. So far, the severity of coronary stenosis as assessed by CT is rather crudely visually estimated as more or less than 50% luminal diameter stenosis.

REFERENCES

1. Diamond GA, Forrester JS. Analysis of probability as an aid in the clinical diagnosis of coronary-artery disease. N Engl J Med 1979;300:1350-8.
2. Hendel RC, Patel MR, Kramer CM, et al. CCF/ACR/SCCT/SCMR/ASNC/NASCI/SCAI/SIR 2006 appropriateness criteria for cardiac computed tomography and cardiac magnetic resonance imaging. J Am Coll Cardiol 2006;48:1475-97.
3. Gibbons RJ, Balady GJ, Bricker JT, et al. ACC/AHA 2002 guideline update for exercise testing: summary article. A report of the American College of Cardiology/American Heart Association Task Force on Practice Guidelines (Committee to Update the 1997 Exercise Testing Guidelines). J Am Coll Cardiol 2002;40:1531-40.
4. Pryor DB, Shaw L, McCants CB, et al. Value of the history and physical in identifying patients at increased risk for coronary artery disease. Ann Intern Med 1993;118:81-90.
5. Mollet NR, Cademartiri F, van Mieghem CA, et al. High-resolution spiral computed tomography coronary angiography in patients referred for diagnostic conventional coronary angiography. Circulation 2005;112:2318-23.
6. Meijboom WB, Mollet NR, Van Mieghem CA, et al. Pre-operative computed tomography coronary angiography to detect significant coronary artery disease in patients referred for cardiac valve surgery. J Am Coll Cardiol 2006;48:1658-65.
7. Hausleiter J, Meyer T, Hadamitzky M, et al. Radiation dose estimates from cardiac multislice computed tomography in daily practice: impact of different scanning protocols on effective dose estimates. Circulation 2006;113:1305-10.
8. Leschka S, Alkadhi H, Plass A, et al. Accuracy of MSCT coronary angiography with 64-slice technology: first experience. Eur Heart J 2005.
9. Raff GL, Gallagher MJ, O'Neill WW, Goldstein JA. Diagnostic accuracy of noninvasive coronary angiography using 64-slice spiral computed tomography. J Am Coll Cardiol 2005;46:552-7.
10. Leber AW, Knez A, von Ziegler F, et al. Quantification of obstructive and nonobstructive coronary lesions by 64-slice computed tomography: a comparative study with quantitative coronary angiography and intravascular ultrasound. J Am Coll Cardiol 2005;46:147-54.

9

Pre-operative Computed Tomography Coronary Angiography to Detect Significant Coronary Artery Disease in Patients Referred for Cardiac Valve Surgery

Willem B. Meijboom[1,2], Nico R. Mollet[1,2], Carlos A.G. Van Mieghem[1,2], Jolanda Kluin[3], Annick C. Weustink[1,2], Francesca Pugliese[1,2], Eleni Vourvouri[1,2], Filippo Cademartiri[1,2], Ad J.J.C. Bogers[3], Gabriel P. Krestin[2], Pim J. de Feyter[1,2]

From the departments of Cardiology[1], Radiology[2], and Cardiothoracic surgery[3], Erasmus MC, Rotterdam, the Netherlands

J Am Coll Cardiol. 2006; 48:1658–65

ABSTRACT

Objectives

We studied the diagnostic performance of 64-slice CT coronary angiography (CTCA) to rule out or detect significant coronary stenosis in patients referred for valve surgery.

Background

Invasive conventional coronary angiography (CCA) is recommended in most of patients scheduled for valve surgery.

Methods

During a 6-month period, 145 patients were prospectively identified from a consecutive patient population scheduled for valve surgery. Thirty-five patients were excluded because of CTCA criteria: irregular heart rhythm (n = 26), impaired renal function (n = 5), and known contrast allergy (n = 4). General exclusion criteria were: hospitalization in community hospital (n = 4), no need for CCA (n = 4), previous coronary artery bypass surgery (n = 1), or percutaneous coronary intervention (n = 4). Of the remaining 97 patients, 27 denied written informed consent. Thus, the study population comprised 70 patients (49 male, 21 female; mean age 63 ± 11years).

Results

Prevalence of significant coronary artery disease, defined as having at least 1 ≥50% stenosis per patient, was 25.7%. Beta-blockers were administered in 71% and 64% received lorazepam. The mean heart rate dropped from 72.5 ± 12.4 to 59.5 ± 7.5 beats/min. The mean scan time was 12.8 ± 1.3 s. On a per-patient analysis, the sensitivity, specificity, and positive and negative predictive value were: 100% (18 of 18; 95% confidence interval [CI] 78 to 100), 92% (48 of 52; 95% CI 81 to 98), 82% (18 of 22; 95% CI 59 to 94), 100% (48 of 48; 95% CI 91 to 100), respectively.

Conclusions

The diagnostic accuracy of 64 slice CTCA for ruling out the presence of significant coronary stenoses in patients undergoing valve surgery is excellent and allows CTCA implementation as a gatekeeper for invasive CCA in these patients.

INTRODUCTION

Pre-operative detection of obstructive coronary artery disease (CAD) with conventional coronary angiography (CCA) is recommended in most of patients scheduled for valve surgery (1). Although CCA is considered a safe procedure, it still carries a small but relevant risk for major (death, stroke, or vascular dissection) and minor (inguinal haematoma) complications (2). Furthermore, the catheterization procedure is rather expensive, as its invasive nature involves admission to a hospital or day-care facility and requires surveillance of an experienced team. A non-invasive, patient-friendly pre-operative work-up for these patients would be desirable.
The newest–generation 64 slice computed tomography (CT) scanner with improved spatial and temporal resolution shows excellent diagnostic accuracy to detect significant coronary artery lesions (3-6). In this study, we evaluated the clinical value of computed tomography coronary angiography (CTCA) in patients scheduled for elective valve surgery.

METHODS

Study population

During a 6-month period, we screened 145 consecutive patients scheduled for valve surgery. Patients were contacted before their final pre-operative appointment requesting them to conduct an additional CTCA. Thirty-five patients were excluded because of CTCA criteria and 13 patients because of general criteria (Table 1). Of the remaining 97 patients, 27 denied written informed consent. Thus, the study population comprised 70 patients (49 male, 21 female;

Table 1. Patient inclusion

Screened patient population	145
Atrial fibrillation/ severe arrhythmia	26
Impaired renal function (serum creatinine > 120 mmol/l)	5
Known contrast allergy	4
Patient population after CTCA exclusion criteria	110
Hospitalisation in community hospital	4
Percutaneous coronary intervention	4
Coronary artery bypass graft	1
No conventional angiogram	4
Patient population after general exclusion criteria	97
Refusal of informed consent	27
Final patient population	70

CTCA = computed tomography coronary angiogram.

mean age 63 ± 11 years). The institutional review board of the Erasmus Medical Center Rotterdam approved the study, and all 70 subjects gave written informed consent.

Patient preparation

Patients with an aortic stenosis and a good left ventricular function (LVF) with a heart rate exceeding 65 beats/min were given 50 mg metoprolol and 1 mg lorazepam 60 min before the CT scan. If the LVF was impaired, beta-blockers were withheld and only lorazepam was administered. Patients with other valve pathology and a heart rate above 65 and 70 beats/min were given 1 mg of lorazepam and 50 and 100 mg metoprolol, respectively. If the LVF was impaired in these patients, the doses of beta-blockers were reduced or not given.

Scan protocol

All scans were performed with a 64-slice CT scanner having a temporal resolution of 330 ms and a spatial resolution of 0.4 mm3 (Sensation 64, Siemens, Forchheim, Germany). Angiographic scan parameters were: number of slices per rotation, 32×2; individual detector width, 0.6 mm; table feed, 3.8 mm per rotation, tube voltage, 120 kV; tube current, 900 mAs. Prospective X-ray tube modulation was not used. Calcium scoring parameters (similar unless indicated) were a tube current of 150 mAs, and prospective X-ray tube modulation was used. The radiation exposure for CTCA with this scan protocol was calculated as 15.2 to 21.4 mSv (for men and women, respectively) using dedicated software (WinDose, Institute of Medical Physics, Erlangen, Germany), which is in line with previously reported X-ray radiation exposure (7,8). The radiation exposure of calcium scoring (including prospective X-ray tube modulation) was calculated as 1.3 to 1.7 mSv (for men and women, respectively) (9).

A bolus of 100 ml of contrast material (400 mgI/ml; Iomeron, Bracco, Milan, Italy) was injected intravenously in an antecubital vein at 5 ml/s. A bolus-tracking technique was used to synchronize the arrival of contrast in the coronary arteries, and the scan was started once the contrast material in the ascending aorta reached a pre-defined threshold of +100 Hounsfield units.

Image reconstruction

The post-processing technique to acquire the best possible image quality is previously described by Mollet et al. (6). In short, images are obtained during a half X-ray tube rotation, resulting in an effective temporal resolution of 165 ms. Images were reconstructed with electrocardiographic (ECG) gating to obtain nearly motion-free image quality. Optimal data sets were reconstructed in the mid- to end-diastolic phase. If non-diagnostic image quality was obtained, additional datasets were reconstructed in the end-systolic phase.

Quantitative coronary angiography (QCA)

All scans were carried out within 2 months after CCA. One experienced cardiologist, unaware of the results of CTCA, identified and analyzed all coronary segments, using a 17-segment modified American Heart Association (AHA) classification (10).
All segments, regardless of size, were included for comparison with CTCA. Segments were classified as normal (smooth parallel or tapering borders), as having non-significant disease (wall irregularities or <50% stenosis), or as having significant stenosis (stenosis ≥50%). Stenoses were evaluated in 2 orthogonal views, and were classified as significant if the mean lumen diameter reduction exceeded 50 % as measured by validated QCA algorithm (CAAS, Pie Medical, Maastricht, The Netherlands).

CT image evaluation

One observer analyzed total calcium scores of all patients with dedicated software, and results were expressed as Agatston score (11). Two experienced observers, a radiologist and a cardiologist, unaware of the results of CCA, evaluated the CTCA datasets on an offline workstation (Leonardo, Siemens, Forchheim, Germany). The axial slices were initially evaluated for the presence of significant segmental disease, and additionally (curved) multiplanar reformatted reconstructions were used. Segments distal to a chronic total occlusion were excluded because of poor distal filling by collaterals. Inter-observer disagreements were resolved by consensus in a joint session.

Statistical analysis

The diagnostic performance of CTCA for the detection of significant stenoses in the coronary arteries with QCA as the standard of reference is presented as sensitivity, specificity, positive and negative predictive values with the corresponding 95% confidence intervals (CIs). Positive (Sensitivity/[1-Specificity]) and negative ([1-Sensitivity]/Specificity) likelihood ratios are given. The likelihood ratio incorporates both the sensitivity and specificity of a test and provides a direct estimate of how much a test result will change the odds of having a disease. Post-test odds can be calculated by multiplying the pre-test odds by the likelihood ratios.

Comparison between CTCA and QCA was performed on 3 levels: patient-by-patient, vessel-by-vessel and, segment-by-segment analysis. Furthermore, the relation of angina pectoris to angiographically significant CAD was analyzed.

A subanalysis was performed for patients with aortic stenosis compared to other valve pathology and patients with or without angina pectoris. An unpaired 2-sided Student t test was performed to reveal possible differences in age, calcium score and heart rate during the CTCA between both groups. A p value <0.05 was considered statistically significant.

Table 2. Patient demographics (n=70)

Age (yrs)§	63 ± 11 (35-80)
Aortic stenosis (yrs)§	68 ± 8 (44-80)
Other valve pathology (yrs)§	59 ± 11 (35-80)
Males	49/70 (70)
Symptoms	
Angina pectoris	21 (30)
No angina pectoris	49 (70)
Previous MI	5 (7)
Risk factors	
Hypertension	33 (47)
Hypercholesterolemia	29 (41)
Diabetes mellitus	2 (3)
Smoker	15 (21)
Ex-smoker	4 (6)
Family history of CAD	26 (37)
Obese (body mass index ≥ 30 kg/m^2)	11 (16)
Calcium score, median*	214,4
Aortic stenosis, median*	391.9
Other valve pathology, median*	116.6
Valve operation	
Aortic valve stenosis	31 (44)
Mitral valve insufficiency	24 (34)
Aortic valve insufficiency	9 (13)
Mitral valve stenosis	2 (3)
Pulmonary valve insufficiency	2 (3)
Congenital aortic stenosis	2 (3)
Tricuspid valve insufficiency	1 (1)
Tricuspid valve stenosis	1 (1)
Reoperation	6 (9)
Conventional angiography	
Absence of coronary disease	17 (24)
Non-significant disease	35 (50)
Single-vessel disease	11 (16)
Multivessel disease	7 (10

Values are n (%) unless otherwise indicated. §Age ranges. *Agatston score.
CAD = coronary artery disease; MI = myocardial infarction.

An additional sensitivity analysis was done to investigate the effect of nesting; repeated assessments (segment by segment and vessel by vessel) within the same patient were made that were not independent observations. Interobserver and intraobserver variability for the detection of significant coronary stenosis was determined by κ-statistics.

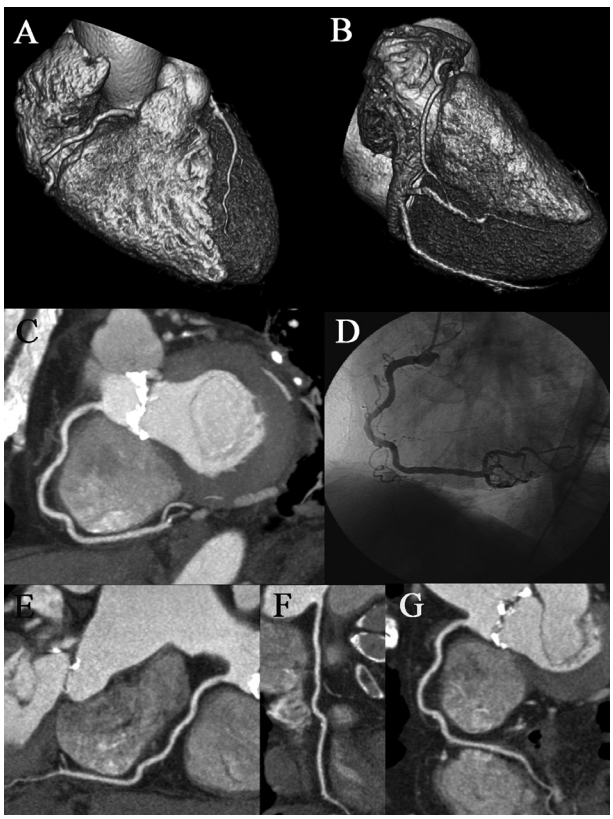

Figure 1. Three different types of post-processing techniques are shown: volume-rendered computed tomography coronary angiogram (CTCA) images (A and B), a maximum-intensity projected image (C), and 3 curved multiplanar reconstructed images (E, F, and G), which show a patent right coronary artery, which is confirmed by conventional coronary angiogram (CCA) (D). The bright white spots (C, E, and G) represent calcifications of the stenotic aortic valve.

RESULTS

Patient demographics are shown in Table 2. One patient had combined valve pathology: aortic stenosis and mitral regurgitation. Beta-blockers were administered in 71% of patients, and 64% received lorazepam. The mean heart rate in these patients dropped within 60 min from 73 ± 12 to 60 ± 8 beats/min. The mean scan time was 12.8 ± 1.3 s. Initially all datasets were reconstructed in the mid- to end diastolic phase. In 30% of the cases (21 of /70), additional higher quality reconstructions from data of the end-systolic phase were used.

Diagnostic performance of 64-slice CT coronary angiography: patient-by-patient analysis

The diagnostic performance of CTCA for detecting significant stenoses on a patient-based analysis is detailed in Table 3. Computed tomography coronary angiography documented absence of significant disease in 48 patients, for an overall specificity per patient of 92 % (Fig. 1). The severity of a stenosis was overestimated in 4 patients who were misclassified as having significant CAD. The CTCA correctly identified significant disease in all patients (18 of 70, prevalence 25.7%) with at least 1 significant stenosis, resulting in a sensitivity per patient of

100% (Fig. 2). An accurate determination of the presence or absence of significant CAD was made in 66 of 70 patients (94%). In 3 out of 11 patients with single-vessel disease, another stenosis was detected with CTCA.

The severity of these stenoses was overestimated, which resulted in incorrect classification as multivessel disease. Agreement between CTCA and QCA on a per-patient level was very good (κ value, 0.86); agreement between both techniques for classifying patients as having no, single-vessel or multivessel disease was good (κ value, 0.78)

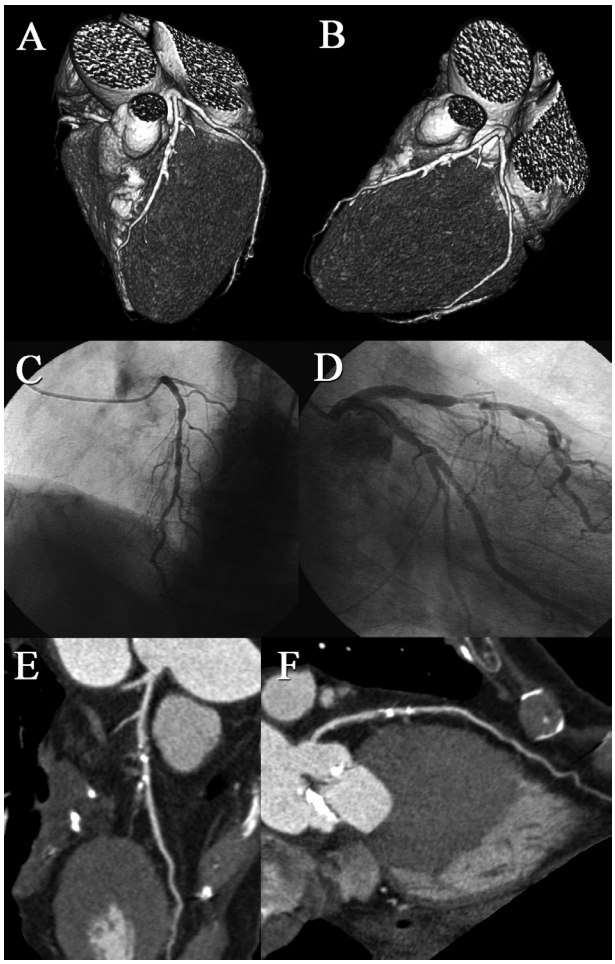

Figure 2. Volume-rendered CTCA image (A and B) reveal the anatomy of the left coronary artery. Two curved multiplanar reconstructed images (E and F) disclose a significant stenosis in the left anterior descending coronary artery, which was corroborated by CCA (C and D). Although the volume-rendered images provide an excellent overview of the coronary anatomy, they should not be used for the diagnostic assessment of presence of coronary stenoses. Abbreviations as in Figure 1.

Diagnostic performance of 64-slice CT coronary angiography: vessel-by-vessel analysis

The mean total per vessel calcium score for the left anterior descending coronary artery (LAD), right coronary artery (RCA) and circumflex coronary artery (CX) were 96.72, 47.89 and 40.22, respectively. The diagnostic performance of CTCA for detecting significant stenoses is detailed in Table 3. All vessels with significantly disease, as classified by QCA, were detected with CTCA. Of a total of 280 vessels, the severity of the stenoses in these 8 vessels, 6 in the LAD and 2 in the RCA, were overestimated and scored as false positives. Agreement between CTCA and QCA on a per-vessel level was very good (κ value, 0.85).

Table 3. Diagnostic performance and predictive value of 64-Slice CTCA for the detection of ≥ 50% stenosis on QCA

	Prevalence of disease, %	n	TP	TN	FP	FN	Kappa	Sensitivity, %	Specificity, %	PPV, %	NPV, %	+LR	- LR
Patient-based analysis	25.7	70	18	48	4	0	0.86	100 (78-100)	92 (81-98)	82 (59-94)	100 (91-100)	13,00	0,00
Vessel-based analysis	9.3	280	26	246	8	0	0.85	100 (84-100)	97 (94-99)	76 (58-89)	100 (98-100)	31,75	0,00
RCA	14.3	70	10	58	2	0	0.89	100 (66-100)	97 (84-99)	83 (51-97)	100 (92-100)	30,00	0,00
LM	0.0	70	0	70	0	0	-	-	100 (94-100)	-	100 (94-100)	-	-
LAD	14.3	70	10	54	6	0	0.72	100 (66-100)	90 (79-96)	63 (36-84)	100 (92-100)	10,00	0,00
Cx	8.6	70	6	64	0	0	1.00	100 (52-100)	100 (93-100)	100 (52-100)	100 (93-100)	∞	0,00
Segment-based analysis	3.6	1003	34	949	18	2	0.76	94 (80-99)	98 (97-99)	65 (51-78)	100 (99-100)	50.74	0.06
Patient-based sub-analysis													
AP	38.1	21	8	12	1	0	0.90	100 (60-100)	92 (62-100)	89 (51-99)	100 (70-100)	13,00	0,00
No AP	20.4	49	10	36	3	0	0.83	100 (66-100)	92 (78-98)	77 (46-98)	100 (88-100)	13,00	0,00
AS	29.0	31	9	19	3	0	0.79	100 (63-100)	86 (64-96)	75 (43-93)	100 (79-100)	7.33	0,00
No AS	23.1	39	9	29	1	0	0.93	100 (63-100)	97(81-100)	90 (54-99)	100 (85-100)	30.00	0.00

According to the 17-segment modified American Heart Association classification, 1003 segments and 280 vessels visualized with conventional angiogram were included for segment and vessel analysis, respectively. For patient-based analysis 70 patients were included, which were divided according to symptoms of AP. Sub-analysis for AS (n = 31) and other valve pathology is described. Values in parentheses represent 95% CIs.

AP = angina pectoris; AS = aortic stenosis; CI = confidence interval; Cx = circumflex coronary artery; FN = false negative; FP = false positive; LAD = left anterior descending coronary artery; LM = left main coronary artery; MR = mitral regurgitation; NPV = negative predictive value; PPV = positive predictive value; QCA = quantitative coronary angiography; RCA = right coronary artery; TN = true negative; TP = true positive; +LR = positive likelihood ratio; -LR = negative likelihood ratio; other abbreviations as in Table 1.

Diagnostic performance of 64-slice CT coronary angiography: segment-by-segment analysis

A total of 1003 segments were included for comparison with QCA. Inter- and intraobserver variability for detection of a significant stenosis per segment had a κ value of 0.71 and 0.74, respectively. The diagnostic performance of CTCA for detecting significant stenoses is detailed in Table 3. Two significant stenoses were detected by CTCA, but the severity of the stenosis was underestimated. Both lesions were adjacent to a correctly detected stenosis. Eighteen non-significant stenoses were detected with CT, and the severity of the stenoses was overesti-

Table 4. Influence of coronary calcifications on diagnostic accuracy of 64-slice CTCA on a segment-based analysis

Calcium score	n (patients)	n (Segments)	Agatston-Score, Mean (±SD)	TP	TN	FP	FN	Kappa	Sensitivity, %	Specificity, %	PPV, %	NPV, %
0-10	23	338	0,3 ± 0,9	0	338	0	0	-	-	100 (99-100)	-	100 (99-100)
11-400	33	465	184 ± 131	15	443	7	0	0.80	100 (75-100)	98 (97-99)	68 (45-85)	100 (99-100)
401-1000	10	146	675 ± 23	16	124	5	1	0.82	94 (69-100)	96 (91-99)	76 (52-91)	99 (95-100)
>1000	4	54	1394 ± 273	3	44	6	1	0.40	75 (22-99)	88 (75-95)	33 (9-69)	98 (87-100)

Values in parentheses represent 95% CIs. Abbreviations as in Table 1 and 3.

mated, resulting in false positive scores. Conventional coronary angiography revealed 5 wall irregularities and 13 non-significant stenoses, whereas the majority (83.3%, 15 of 18) of these segments was calcified.

The presence of coronary calcium induced overestimation of the severity of these stenoses with the CT scan (Table 4). Agreement between CTCA and QCA on a per-segment level was good (κ value, 0.76).

To exclude the possible confounding effect of nesting, random selection of a single segment per patient was done, and the diagnostic accuracy for detecting significant artery disease resulted in a sensitivity of 100 % (5 of 5; 95% CI 46 to 100), a specificity of 98 % (63 of 64; 95% CI 90 to 100), a positive predictive value 83 % (5 of 6; 95% CI 36 to 99), and a negative predictive value 100 % (63 of 63; 95% CI 93 to 100).

Sub-analysis for patients with aortic stenosis versus other valve pathology

The sub-analysis comprised 31 patients with aortic stenosis and 39 with other valve pathology. The diagnostic performance of CTCA for detecting significant stenoses on a patient-based analysis in patients with and without aortic stenosis is detailed in Table 3. The average age (68 vs. 59 yrs.; p = 0.0004) and calcium score (391.9 vs.116.6; p = 0.02) of patients with aortic stenosis were significantly higher than in patients not having aortic stenosis (Table 2). The heart rate during CTCA for both groups was the same (both 60 beats/min).

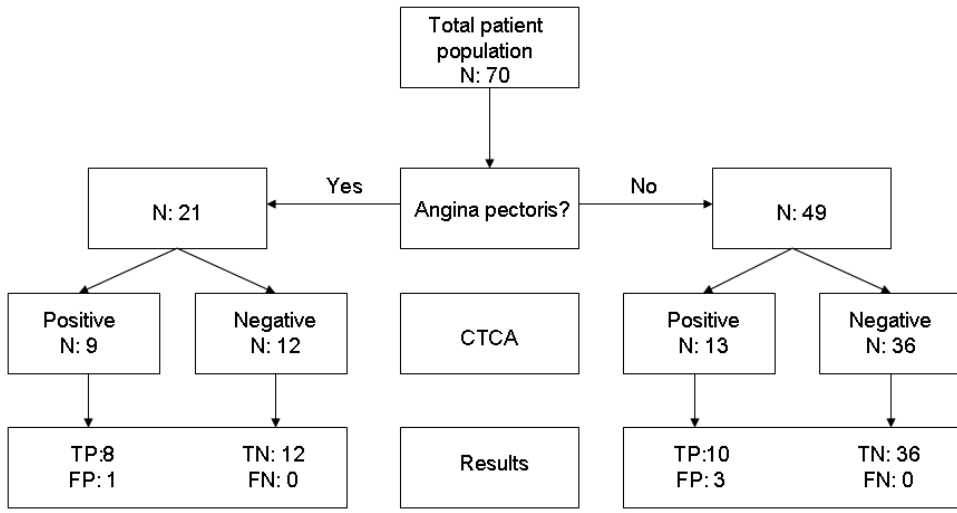

Figure 3. Discordance between angina pectoris and the presence of significant coronary artery disease. FN = false negative; FP = false positive; TN = true negative; TP = true positive; other abbreviations as in Figure 1.

The relation of angina pectoris to significant CAD

The discordance between angina pectoris and the presence of significant CAD is displayed in Figure 3. Twenty-one patients had angina pectoris; 8 of these had significant obstructive disease. Moreover, 10 patients of 49 without angina pectoris did have significant stenoses. The diagnostic accuracy of angina pectoris was calculated, and the sensitivity, specificity, and positive and negative predictive values were 44% (8 of 18; 95% CI 22 to 67), 75% (39 of 52; 95% CI 61 to 86), 38% (8 of 21; 95% CI 19 to 61) and 80%, (39 of 49; 95% CI 65 to 89), respectively.

DISCUSSION

The presence of concomitant obstructive CAD in patients undergoing cardiac valvular surgery worsens prognosis (12-14). Various studies have shown that combined valve and bypass surgery of significant CAD reduced early and late mortality (13,15). Because aortic stenosis and CAD share common risk factors and occur with advancing age, and because mitral regurgitation is often the consequence of CAD, concomitant, significant CAD is found in approximately one-third of these patients (16-19). Angina pectoris is present in 25% to 35% of patients with valvular heart disease. Angina pectoris is a poor predictor of obstructive CAD in patients with valvular disease because angina pectoris can have multiple causes, such as left ventricular enlargement, increased wall stress, or wall thickening with subendocardial ischemia (17,20). This was also shown in our study, and the low sensitivity of 44% and specificity of 75% is in keeping with the results observed in earlier reports. The value of non-invasive ECG stress test-

ing to detect concomitant CAD is limited due to the presence of left ventricular hypertrophy and left bundle branch block in patients with valvular disease. Resting or exercise induced wall motion abnormalities and myocardial perfusion abnormalities, as seen with stress echo and nuclear tests, lack sufficient accuracy for reliable detection of concomitant CAD (21-24).

Because of the poor predictive value of angina pectoris and the lack of accuracy of non-invasive tests, the following guideline is recommended by the American College of Cardiology/ AHA committee; pre operative CCA is indicated in symptomatic patients and/or those with left ventricular dysfunction in men ≥35 years, pre-menopausal women ≥35 years with risk factors for CAD, and post-menopausal women (1).

Non-invasive coronary angiography using 4- and 16-slice CT is a relatively recent development. The early results were promising but lacked sufficient robustness to be useful in clinical practice, but the diagnostic performance of 64-slice CT scanners to detect coronary stenoses is very good in patients who have a high prevalence (more than 70%) of CAD. In these patients the negative predictive value of 64-slice CT -scanners is very high, allowing one to exclude the presence of significant CAD (3-6). However, there is little information about the diagnostic performance of CTCA in patients with a low or intermediate prevalence of CAD.

In our study, the prevalence of concomitant CAD was 25.7%. We found that significant coronary stenoses were detected using a 64-slice CT scanner with a sensitivity of 100% and a specificity of 92% compared with CCA. A negative CT scan was correct in 92% (48 of 52) patients in ruling out significant disease, and all patients (18 of 18) with significant CAD were correctly diagnosed. The stenosis severity was overestimated in 4 patients using CTCA. Given the high reliability of CTCA, this would mean that CCA could have been avoided in 69% (48 of 70) of patients, in 26% (18 of 70) a CCA was performed to confirm the CTCA diagnosis, and in 6% (4 of 70) an unnecessary CCA would have been performed on the basis of CTCA outcome.

Coronary calcium

The presence of calcium causes problems in the correct interpretation of the CTCA. Calcium creates blooming artifacts, which obscure the visualization of the underlying non-calcified plaque or lumen. Calcium tends to overestimate the severity of adjacent lesions, either because of the blooming effect itself or because, in the case of doubt or fear of "missing" a significant stenosis a "defensive" scoring is exercised. This has led to an ongoing debate whether a CTCA should be aborted when the calcium score exceeds a certain threshold. A generally accepted cutoff value is lacking, and proposed thresholds are arbitrarily chosen. Usually a chosen cutoff level is derived from the total calcium score. The total calcium score is somewhat misleading, because calcium distributed along the entire coronary tree would make the

interpretation of a CTCA examination relatively easy, whereas a single heavily calcified plaque would make interpretation doubtful.

Recently, Gilard et al. (25) reported good accuracy of a 16-slice scanner in 55 patients referred for elective aortic valve surgery who had a mean calcium score of 609 ± 860. They used the Agatston score of ≥1000 as a cutoff point by showing that patients with this score had a higher frequency of non-interpretable segments. In our subgroup of patients with aortic stenosis we found, not unexpectedly, a higher calcium score. In this subgroup, the diagnostic accuracy of CTCA was lower because the extensive calcifications negatively influenced grading of stenoses and resulted in overestimation of the stenosis severity.

What would be the role of CTCA in patients referred for CCA before cardiac valve surgery? We do recommend to first obtaining a calcium score in all patients without atrial fibrillation, persistent irregular heart rhythm, or renal dysfunction. If the calcium score exceeds ≥ 1000, we would advice not to proceed with CTCA. If lower, patients may be advised to undergo CTCA. Patients with a scan negative for significant CAD can directly be referred for cardiac valve surgery. In case of doubt, and in the presence of significant CAD, a confirmative CCA is required to either confirm or refute the presence of significant CAD.

Heart rate reduction in patients in patients with heart rates > 65 beats/min is part of the protocol used with current 64-slice CT scanners to increase image quality. Next-generation dual-source CT scanners will allow scanning at higher heart rates because of the improved temporal resolution of 83 ms, thereby avoiding the use of heart-rate reduction with beta-blockers (26,27). Especially, patients with severe aortic stenosis would benefit, since the administration of beta-blockers is limited. The radiation exposure can be decreased with the ultrafast dual-source CT scanner during higher heart rates and use of X-ray tube modulation compared to 64-slice CT scanning.

Study limitations

The presence of atrial fibrillation, which occurs frequently with mitral valve disease, precludes the use of CTCA and was indeed a significant reason for exclusion in our study. Only patients scheduled for elective valve surgery were screened, and patients in acute settings with hemodynamic comprise were not studied. Since most patients were referred from community hospitals for valve surgery, the pre-operative diagnostic work-up, including the CCA, was performed in many study patients. This may have created a bias, although the CT scoring was done blinded to the coronary angiogram. The rather high radiation exposure of CTCA as compared to CCA is of concern (7,8). The radiation exposure can be reduced by 50% with use of prospective X-ray tube current modulation (28). However, this limits the possibility to reconstructing valuable datasets during the end-systolic phase (29). In our study, we found

that in 30% of the patients, end-systolic phase reconstructions were useful and were of higher image quality than the mid- t o-end diastolic phase reconstructed images.

Conclusions

The diagnostic accuracy of 64-slice CTCA for ruling out the presence of significant coronary lesions in patients undergoing elective valve surgery is excellent and allows CTCA implementation as a gatekeeper in these patients.

REFERENCES

1. Bonow RO, Carabello B, de Leon AC, Jr., et al. Guidelines for the management of patients with valvular heart disease: executive summary. A report of the American College of Cardiology/American Heart Association Task Force on Practice Guidelines (Committee on Management of Patients with Valvular Heart Disease). Circulation 1998;98:1949-84.
2. Scanlon PJ, Faxon DP, Audet AM, et al. ACC/AHA guidelines for coronary angiography. A report of the American College of Cardiology/American Heart Association Task Force on practice guidelines (Committee on Coronary Angiography). Developed in collaboration with the Society for Cardiac Angiography and Interventions. J Am Coll Cardiol 1999;33:1756-824.
3. Leschka S, Alkadhi H, Plass A, et al. Accuracy of MSCT coronary angiography with 64-slice technology: first experience. Eur Heart J 2005.
4. Raff GL, Gallagher MJ, O'Neill WW, Goldstein JA. Diagnostic accuracy of noninvasive coronary angiography using 64-slice spiral computed tomography. J Am Coll Cardiol 2005;46:552-7.
5. Leber AW, Knez A, von Ziegler F, et al. Quantification of obstructive and nonobstructive coronary lesions by 64-slice computed tomography: a comparative study with quantitative coronary angiography and intravascular ultrasound. J Am Coll Cardiol 2005;46:147-54.
6. Mollet NR, Cademartiri F, van Mieghem CA, et al. High-resolution spiral computed tomography coronary angiography in patients referred for diagnostic conventional coronary angiography. Circulation 2005;112:2318-23.
7. Hausleiter J, Meyer T, Hadamitzky M, et al. Radiation dose estimates from cardiac multislice computed tomography in daily practice: impact of different scanning protocols on effective dose estimates. Circulation 2006;113:1305-10.
8. Coles DR, Smail MA, Negus IS, et al. Comparison of radiation doses from multislice computed tomography coronary angiography and conventional diagnostic angiography. J Am Coll Cardiol 2006;47:1840-5.

9. Trabold T, Buchgeister M, Kuttner A, et al. Estimation of radiation exposure in 16-detector row computed tomography of the heart with retrospective ECG-gating. Rofo 2003;175:1051-5.
10. Austen WG, Edwards JE, Frye RL, et al. A reporting system on patients evaluated for coronary artery disease. Report of the Ad Hoc Committee for Grading of Coronary Artery Disease, Council on Cardiovascular Surgery, American Heart Association. Circulation 1975;51:5-40.
11. Agatston AS, Janowitz WR, Hildner FJ, Zusmer NR, Viamonte M, Jr., Detrano R. Quantification of coronary artery calcium using ultrafast computed tomography. J Am Coll Cardiol 1990;15:827-32.
12. Lytle BW. Impact of coronary artery disease on valvular heart surgery. Cardiol Clin 1991;9:301-14.
13. Mullany CJ, Elveback LR, Frye RL, et al. Coronary artery disease and its management: influence on survival in patients undergoing aortic valve replacement. J Am Coll Cardiol 1987;10:66-72.
14. Iung B, Drissi MF, Michel PL, et al. Prognosis of valve replacement for aortic stenosis with or without coexisting coronary heart disease: a comparative study. J Heart Valve Dis 1993;2:430-9.
15. Lund O, Nielsen TT, Pilegaard HK, Magnussen K, Knudsen MA. The influence of coronary artery disease and bypass grafting on early and late survival after valve replacement for aortic stenosis. J Thorac Cardiovasc Surg 1990;100:327-37.
16. Vandeplas A, Willems JL, Piessens J, De Geest H. Frequency of angina pectoris and coronary artery disease in severe isolated valvular aortic stenosis. Am J Cardiol 1988;62:117-20.
17. Alexopoulos D, Kolovou G, Kyriakidis M, et al. Angina and coronary artery disease in patients with aortic valve disease. Angiology 1993;44:707-11.
18. Olofsson BO, Bjerle P, Aberg T, Osterman G, Jacobsson KA. Prevalence of coronary artery disease in patients with valvular heart disease. Acta Med Scand 1985;218:365-71.
19. Ramsdale DR, Bennett DH, Bray CL, Ward C, Beton DC, Faragher EB. Angina, coronary risk factors and coronary artery disease in patients with valvular disease. A prospective study. Eur Heart J 1984;5:716-26.
20. Green SJ, Pizzarello RA, Padmanabhan VT, Ong LY, Hall MH, Tortolani AJ. Relation of angina pectoris to coronary artery disease in aortic valve stenosis. Am J Cardiol 1985;55:1063-5.
21. Rask P, Karp K, Edlund B, Eriksson P, Mooe T, Wiklund U. Computer-assisted evaluation of dipyridamole thallium-201 SPECT in patients with aortic stenosis. J Nucl Med 1994;35:983-8.

22. Samuels B, Kiat H, Friedman JD, Berman DS. Adenosine pharmacologic stress myocardial perfusion tomographic imaging in patients with significant aortic stenosis. Diagnostic efficacy and comparison of clinical, hemodynamic and electrocardiographic variables with 100 age-matched control subjects. J Am Coll Cardiol 1995;25:99-106.
23. Kettunen R, Huikuri HV, Heikkila J, Takkunen JT. Preoperative diagnosis of coronary artery disease in patients with valvular heart disease using technetium-99m isonitrile tomographic imaging together with high-dose dipyridamole and handgrip exercise. Am J Cardiol 1992;69:1442-5.
24. Kupari M, Virtanen KS, Turto H, et al. Exclusion of coronary artery disease by exercise thallium-201 tomography in patients with aortic valve stenosis. Am J Cardiol 1992;70:635-40.
25. Gilard M, Cornily JC, Pennec PY, et al. Accuracy of multislice computed tomography in the preoperative assessment of coronary disease in patients with aortic valve stenosis. J Am Coll Cardiol 2006;47:2020-4.
26. Flohr TG, McCollough CH, Bruder H, et al. First performance evaluation of a dual-source CT (DSCT) system. Eur Radiol 2006;16:256-68.
27. Achenbach S, Ropers D, Kuettner A, et al. Contrast-enhanced coronary artery visualization by dual-source computed tomography--initial experience. Eur J Radiol 2006;57:331-5.
28. Jakobs TF, Becker CR, Ohnesorge B, et al. Multislice helical CT of the heart with retrospective ECG gating: reduction of radiation exposure by ECG-controlled tube current modulation. Eur Radiol 2002;12:1081-6.
29. Vogl TJ, Abolmaali ND, Diebold T, et al. Techniques for the detection of coronary atherosclerosis: multi-detector row CT coronary angiography. Radiology 2002;223:212-20.

10

Adjunctive Value of CT Coronary Angiography in the Diagnostic Work-up of Patients with Typical Angina Pectoris

Nico R. Mollet[1,2], Filippo Cademartiri[2], Carlos A.G. Van Mieghem[1,2], W. Bob Meijboom[1,2], Francesca Pugliese[1,2], Giuseppe Runza[2], Timo Baks[1,2], Jolmer Dikkeboer[2], Eugène P. McFadden[1], Michel P. Freericks[3], Jacques P. Kerker[3], Stieneke K. Zoet[3], Eric Boersma[1], Gabriel P. Krestin[2], Pim.J. de Feyter[1,2]

From the departments of Cardiology[1] and Radiology[2], Erasmus MC, Rotterdam, the Netherlands; and Ikazia hospital[3], department of cardiology, Rotterdam, the Netherlands

Eur Heart J. 2007; 28:1872-8

ABSTRACT

Aims

To determine the adjunctive value of CT coronary angiography (CTCA) in the diagnostic work-up of patients with typical angina pectoris.

Methods and results

CTCA was performed in 62 consecutive patients (45 male, mean age 58.8 ± 7.7 years) with typical angina undergoing diagnostic work-up including exercise-ECG and conventional coronary angiography. Only patients with sinus heart rhythm and ability to breath hold for 20 s were included. Patients with initial heart rates ≥70 beats/min received β-blockers. We determined the post-test-likelihood ratios, to detect or exclude patients with significant (≥50% lumen diameter reduction) stenoses, of exercise-ECG and CTCA separately, and of CT performed after exercise-ECG testing.

The prevalence of patients with significant coronary artery disease (CAD) was 74%. Positive and negative likelihood ratios for exercise-ECG were 2.3 [95% confidence interval (CI): 1.0-5.3] and 0.3 (95%CI: 0.2-0.7) and for CTCA 7.5 (95%CI: 2.1-27.1) and 0.0 (95%CI: 0.0-8), respectively. CTCA increased the post-test probability of significant CAD after a negative exercise-ECG from 58 to 91%, and after a positive exercise-ECG from 89 to 99%, while CT correctly identified patients without CAD (probability 0%).

Conclusion

Non-invasive CTCA is a potentially useful tool, in the diagnostic work-up of patients with typical angina pectoris, both to detect and to exclude significant CAD.

INTRODUCTION

Stress-testing is useful in selecting patients for coronary angiography and can help guide subsequent revascularization strategies. Current guidelines recommend stress-testing in the work-up of patients with stable angina and a treadmill exercise-ECG is the first-choice stress-test in the majority of patients1-4. CT coronary angiography (CTCA) is a non-invasive technique that can reliably detect significant coronary stenoses in selected patient populations5-14. However, the value of CTCA in addition to exercise-ECG in the diagnostic work-up of patients with typical angina pectoris in the clinical setting is yet unknown.
We sought to establish the diagnostic value, to detect or exclude significant coronary artery disease (CAD), of exercise-ECG and CTCA, alone and in combination, in a consecutive cohort of patients with typical angina pectoris.

METHODS

Study population

During a 1-year-period, we studied 62 (45 male, mean age 58.8 ± 7.7 years) consecutive patients who fulfilled all of the following criteria: first history of typical angina pectoris, and two specific CT criteria: sinus heart rhythm and ability to breath hold for ≥20 s. Of 103 patients eligible for inclusion, 41 patients were excluded with contra-indications (known allergy, serum creatinine >120 μmol/L, or thyroid disorders) to iodinated contrast (n = 4), baseline ECG abnormalities precluding reliable exercise-ECG interpretation (≥1 mm rest ST-depression, complete left bundle-branch block, n = 6), and inability to perform CTCA before conventional angiography for logistic reasons (n = 23); eight patients refused to participate in the study. Patients were recruited in a community hospital where the diagnostic work-up including exercise-ECG and conventional coronary angiography (CCA) was performed. CTCA was performed in a university hospital on an outpatient basis. The study complies with the Declaration of Helsinki. The institutional review boards of both hospitals approved the study protocol and all patients gave informed consent.

Patient preparation

Patients with a heart rate above 70 beats/min received a single oral dose of 100mg metoprolol ≥45min before the scan, unless contraindicated (e.g. overt heart failure or chronic obstructive pulmonary disease).

Scan protocol, image reconstruction, and evaluation

All patients were scanned using a second generation 16-slice CT-scanner (Sensation16 Straton®, Siemens, Forchheim, Germany). Scan parameters were: 16x0.75mm collimation,

rotation time 375ms, temporal resolution 188ms, table feed 3.0 mm/rotation, tube voltage 120kV, 600mAs; tube modulation was not applied. Radiation exposure was estimated as 11.8-16.3 mSv (WinDose®, Institute of Medical Physics, Erlangen, Germany). A bolus of 100ml contrast material (Iomeron®400, Bracco, Milan, Italy) was injected through an arm vein (4 ml/s) using a bolus-tracking technique to initiate the CT-scan (mean scan time: 18.2 ± 1.0s). Datasets were reconstructed using ECG gating and high image quality was generally obtained when datasets were reconstructed during the mid-to-end diastolic phase. All available ≥2mm coronary branches were independently analysed by two observers, unaware of the results of CCA, using conventional post-processing techniques. Patients with at least 1 ≥50% stenosis were considered as having significant CAD on the CT-scan.

Quantitative coronary angiography (QCA)

All CT-scans were performed within 4 weeks of CCA. A single observer, unaware of the results of CTCA, determined the diameter of all coronary branches using a quantitative algorithm (CAAS, Pie Medical, Maastricht, The Netherlands). All ≥2mm branches were included for comparison with CT. Stenoses were evaluated in two orthogonal views, and classified as significant if the mean lumen diameter reduction was ≥50%, which was considered as the standard of reference. Patients were labelled as having significant CAD if they had at least one significant coronary stenosis.

Exercise-ECG

All exercise tests were performed prior to CT coronary angiography to avoid the influence of β-blockers on the diagnostic accuracy of exercise-ECG. Exercise-ECG was performed using a cycle ergometer and a protocol starting with an initial workload of 25W, followed by increments of 25W every 2 min. Heart rate and blood pressure were recorded at rest and at the end of each stage of exercise. A 12-channel electrocardiogram was obtained each minute and 3-channel monitoring of cardiac rhythm was performed continuously.

Exercise-ECG examinations were classified as positive where there was horizontal or downsloping ST-segment depression of ≥1mm at 80 ms after the J-point occurring during or after exercise15.

An exercise-ECG tests in patients who did not reach the reference exercise capacity normalized for age, gender, and weight and which did not show a significant ST-segments depression were classified as inconclusive.

Statistical analysis

Descriptive statistics were used to evaluate the diagnostic performance of exercise-ECG and CTCA to detect patients with significant CAD, including sensitivity, specificity, positive and negative predictive value, and positive and negative likelihood ratios. These diagnostic parameters were expressed with a 95% confidence interval (CI) calculated with binomial expansion.

The pre-test likelihood was estimated using the Duke Clinical Score, which includes Diamond-Forrester criteria and clinical variables that are known to have prognostic value 3,16,17. Post-test likelihoods after exercise-ECG and CTCA were calculated using Bayes' theorem (post-test odds = pre-test odds x likelihood ratio). Patient characteristics between included and excluded patients were compared using unpaired, two-sided T-test (continuous variables) or Pearson Chi-Square test (dichotomous variables).

Prevalence of significant CAD was based on the presence of greater than or equal to one significant stenosis as determined by QCA, which was considered as the gold standard. Agreement between CCA and CTCA was calculated using κ-statistics.

RESULTS

Patient characteristics of those included and excluded from the study are shown in Table 1. There were no significant differences between the two groups. Fifty percent (31/62) of the patients received a pre-scan β-blocker; mean heart rate during scanning was 59.3 ± 8.3 beats/min. No contra-indications to β-blockers were present in patients presenting with high (≥70 beats/min) heart rates. One CT-examination was classified as inconclusive due to the presence of extensive motion artifacts (mean heart rate: 84 beats/min). CCA revealed absence of significant stenoses in 26% (16/62), single vessel disease in 32% (20/62), and multi-vessel disease in 42% (26/62) of patients. Thus, the prevalence of significant CAD was 74%. The pre-test likelihood was estimated as 81 ± 17% (see the statistical analysis section).

Diagnostic performance of exercise-ECG and CTCA

Nine exercise-ECG tests were classified as inconclusive. Sensitivity of exercise-ECG to detect significant CAD in the remaining 53 patients was 78% (95%CI: 62-89), specificity was 67% (95%CI: 34-90), and positive and negative predictive value was 89% (95%CI: 73-96) and 47% (95%CI: 22-72), respectively. Sensitivity of CTCA to detect significant CAD in 61 patients (one patient was classified as inconclusive) was 100% (95%CI: 92-100), specificity was 87% (95%CI: 59-98), and positive and negative predictive value was 96% (95%CI: 85-99) and 100% (95%CI: 75-100), respectively. Agreement between CCA and CTCA on a per-patient level was high (κ -value: 0.91).

Positive and negative likelihood ratios to detect or exclude significant CAD were; 2.3 (95%CI: 1.0-5.3) and 0.3 (95%CI: 0.2-0.7) for exercise-ECG; 7.5 (95%CI: 2.1-27.1) and 0.0 (95%CI: 0.0-∞) for CTCA, respectively. Figure 1 shows the diagnostic impact on the probability of significant coronary artery disease of exercise-ECG. Figure 2 shows the diagnostic impact on the probability of significant coronary artery disease after CTCA.

Table 1. Patient characteristics

	Included patients (n = 62)	Excluded patients (n = 41)	P-value
Mean age (± SD)[1]	60,4±9.3	59,5±9.2	0.643
Risk factors, n (%)			
Hypercholesterolemia[2]	43 (69)	27 (66)	0.589
Systemic hypertension[2]	42 (68)	24 (59)	0.271
Smoking[2]	25 (40)	18 (44)	0.797
Family history of premature CAD[2]	23 (37)	17 (41)	0.728
Obese (BMI ≥30)[2]	16 (26)	11 (27)	0.965
Diabetes Mellitus[2]	8 (13)	4 (10)	0.597
Medication, n (%)			
Aspirin[2]	59 (95)	37 (90)	0.185
β-blocker[2]	51 (82)	34 (84)	0.866
ACE inhibitors / AT-II antagonist[2]	20 (32)	10 (24)	0.351
Calcium-antagonist[2]	20 (32)	14 (34)	0.909
Nitrates (systemic)[2]	18 (29)	9 (22)	0.385
Statins[2]	43 (69)	28 (68)	0.773
Prevalence of significant CAD, n (%)[2, 3]	46 (74)	30 (75)	0.755

BMI, body mass index.
P-values < 0.05 were considered significant.
[1]Calculated using unpaired T-test.
[2]Calculated using the Pearson Chi-Square test.
[3]Based on the presence of a significant (≥50% lumen reduction) stenosis as determined by QCA

Diagnostic performance of CTCA in addition to exercise-ECG to detect significant stenoses

The prevalence of significant CAD after a positive exercise-ECG test of 89% (with an estimated post-test likelihood of 91%) was refined by CTCA to respectively 100% after a positive CT-scan [with an estimated post-test likelihood of 99%) and 0% after a negative CT-scan (with an estimated post-test likelihood of 0%, (Figure 3)].

The prevalence of significant CAD after a negative exercise-ECG test of 53% (with an estimated post-test likelihood of 58%) was refined by CTCA to respectively 90% after a positive CT-scan [with an estimated post-test likelihood of 91%, (Figure 4)] and 0% after a negative CT-scan (with an estimated post-test likelihood of 0%). The prevalence of significant CAD after CTCA in patients with an inconclusive exercise-ECG test was respectively 83% after a positive CT-scan [with an estimated post-test likelihood of 96%, (Figure 5)] and 0% after a negative CT-scan (with an estimated post-test likelihood of 0%).

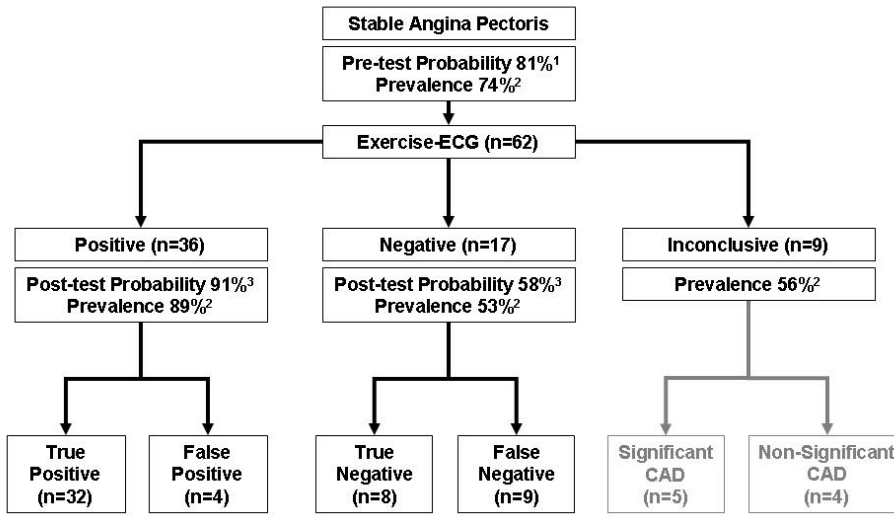

[1] Estimated using Duke Clincal Score (including Diamond-Forrester criteria and prognostic clinical variables)
[2] Based on conventional coronary angiography (≥1 significant coronary stenosis as determined by QCA)
[3] Calculated using Bayes' Theorem (pre-test odds = post-test odds x likelihood ratio)

Figure 1. The diagnostic impact on the probability of significant CAD of exercise-ECG.

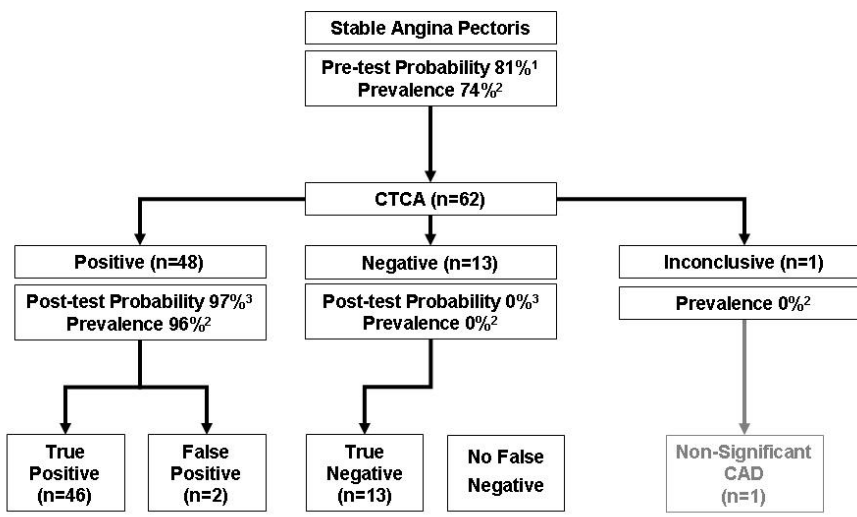

[1] Estimated using Duke Clincal Score (including Diamond-Forrester criteria and prognostic clinical variables)
[2] Based on conventional coronary angiography (≥1 significant coronary stenosis as determined by QCA)
[3] Calculated using Bayes' Theorem (pre-test odds = post-test odds x likelihood ratio)

Figure 2. The diagnostic impact on the probability of significant CAD of CTCA

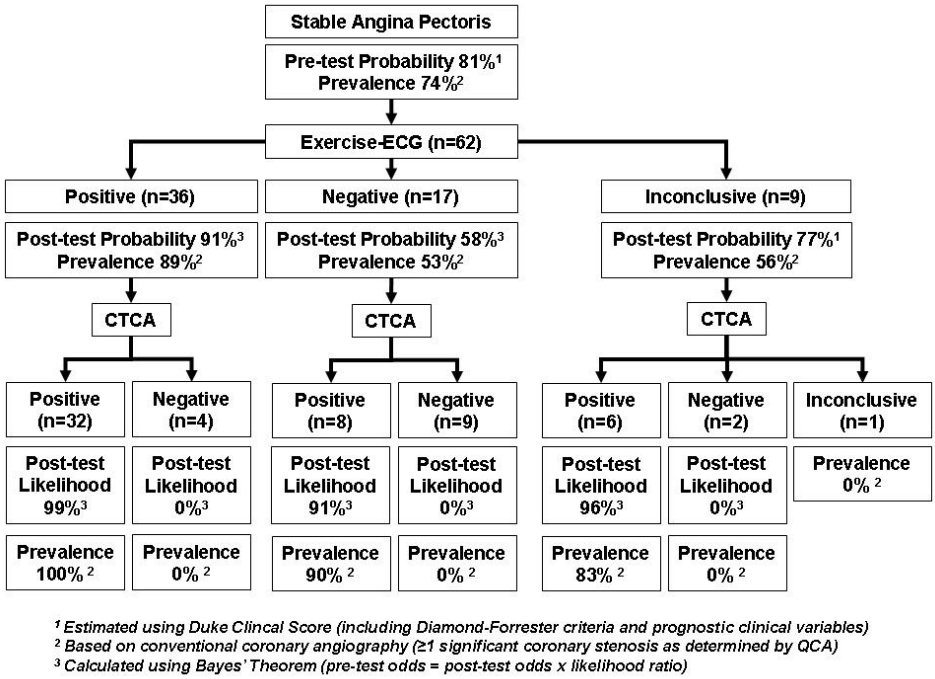

Figure 3. The diagnostic impact on the probability of significant CAD of CTCA as an adjunct to exercise-ECG

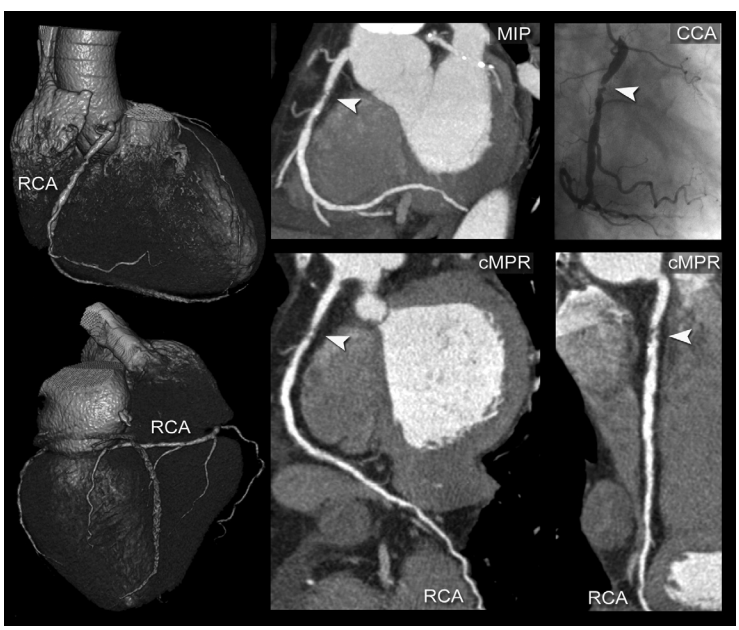

Figure 4. Example of CT vs. CCA in a patient with single vessel disease and a negative exercise-ECG test. Volume-rendered CT images (coloured images) provide a nice anatomical overview of a dominant right coronary artery (RCA). Maximum intensity projected (MIP) and two orthogonally curved multiplanar reconstructed (cMPR) CT images indicate the presence of a significant stenosis at the proximal RCA (arrowhead), which was confirmed on the conventional coronary angiogram (CCA).

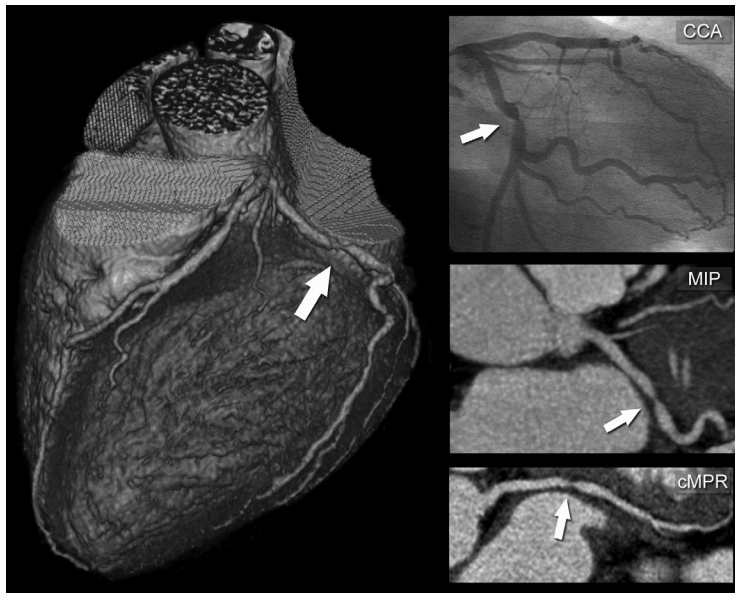

Figure 5. Example of CT vs. CCA in a patient with single vessel disease and an inconclusive exercise-ECG test. A volume rendered CT image (coloured image) suggests the presence of a significant stenosis of the proximal circumflex coronary artery. More detailed analyses using maximum intensity projected (MIP) curved multiplanar reconstructed (cMPR) post-processing techniques confirm these findings, which was also found on the conventional angiogram (CCA).

DISCUSSION

Exercise-ECG testing is safe, inexpensive, and widely available. Current guidelines recommend documentation of exercise- or stress-induced ischemia in patients with stable angina who are evaluated for revascularization[1,2]. Patients with a positive exercise-ECG test will be further evaluated by diagnostic CCA to determine further management with percutaneous intervention, bypass surgery, or pharmacological treatment. Patients with a negative exercise-ECG require (depending on the level of clinical suspicion of the presence of CAD based upon history, physical examination, and rest-ECG), either further non-invasive diagnostic work-up, or referral for CCA, or a regular clinical follow-up on an outpatient basis.

In our study, we evaluated the diagnostic value of exercise-ECG alone, of CTCA alone, and in particular the additional value of CTCA after exercise-ECG in 62 consecutive patients with typical angina and an intermediate-to-high pre-test probability of significant CAD. We only included patients with typical symptoms of stable angina pectoris. The prevalence of significant CAD in our patient cohort was 74%, which is in line with the estimated pre-test likelihood of 81 ± 17% using clinical variables such as age, gender, symptoms, and cardiovascular risk factors3,16,17. Our results show that exercise-ECG was able to correctly predict the presence or absence of significant CAD in 65% (40/62) of patients, whereas CTCA correctly classified all patients with significant CAD (n = 46), but misclassified 19% (3/16) of patients without significant CAD.

The post-test probability of significant CAD after a negative exercise-ECG test was 58%, which represents such a high diagnostic uncertainty level that further diagnostic work-up is required. In this context, CTCA proved particularly useful; a positive CTCA increased the probability of significant CAD to 91% whereas a negative CTCA decreased it to 0%. Thus, the additional diagnostic information provided by CTCA is of particular use in patients with an intermediate likelihood of having significant CAD (e.g. patients with typical angina and a negative stress-test).

The estimated post-test probability of significant CAD after a positive exercise-ECG test was 91%. The subsequent step in such patients, where indicated, is conventional diagnostic angiography, as the high probability of significant CAD in patients with typical angina pectoris and a positive stress test makes further non-invasive diagnostic work-up unhelpful. However, despite this high probability of disease, CTCA was able to even further perfect this to a prevalence of 100% in case of a positive CT-scan and to 0% in case of a negative CT-scan.

The question remains what would be the role of CTCA in the diagnostic work-up of patients with a (very) high pre-test likelihood of significant CAD. According to the guidelines, the majority of patients with a high pre-test likelihood should undergo non-invasive testing, followed by diagnostic CCA to refer these patients for appropriate therapy. Some investigators suggest that these patients should immediately be referred for a diagnostic coronary angiogram, followed in the same session by percutaneous intervention, thereby obviating the need for further non-invasive diagnostic tests including CTCA. In keeping with current guidelines, such an ad-hoc approach has important disadvantages when compared to a staged approach, which allows time to inform the patient about risks, benefits, and alternatives of the selected therapy as well as optimal hydration and pre-treatment with oral anti-platelet agents before coronary intervention[4]. This immediate approach does not allow general discussion between the general cardiologist, interventional cardiologist, and cardiac surgeon to reach consensus about the most optimal treatment strategy. In addition, a single session approach may result in a considerable kidney contrast burden and associated contrast induced nephrotoxicity[4]. Moreover, such approach may result in a high diagnostic workload with a significant burden on the availability of percutaneous interventional laboratories. In fact, the majority of patients who undergo elective percutaneous revascularization procedures in the Netherlands -as in many other European countries- are being sent to referral hospitals after a complete diagnostic work-up including CCA in a community hospital without percutaneous intervention facilitations. The findings of our pilot study suggest that CTCA may be used as an “intermediate“ step to guide referral for diagnostic angiography followed by percutaneous intervention in the same session (patients with one- or two-vessel disease) or bypass surgery (left main or three-vessel disease). Our results also indicate that CTCA may even function as a “gatekeeper" for diagnostic coronary angiography in patients with an intermediate-to-high likelihood of

significant CAD. For these reasons, CTCA may still be of use in patients with a high pre-test likelihood of significant CAD.

We have studied a relatively small number of patients who are at high risk of having significant CAD and excluded a significant number of patients because of logistic inability to perform CTCA before the conventional angiogram. The main reason was the short interval between exercise-ECG and conventional angiography (3-7 days) which in some cases did not allow timely CT examination (e.g. no available time slots, CT maintenance, or not able to contact the patient). It is of note that these patients could have been examined by CT in a clinical setting because of the elective nature of diagnostic angiography in stable patients. Moreover, we did not find significant differences in patient characteristics between included and excluded patients (Table 1). Larger prospective studies are needed evaluating the diagnostic value of CTCA in addition to stress testing in patients with a low or intermediate pre-test likelihood of significant CAD (e.g. patients with atypical angina or non-anginal chest pain). These patients may potentially benefit more from CTCA whereas the impact of CT as "gatekeeper" for diagnostic coronary angiography may be higher. If such studies would confirm our initial results, CTCA may become a routinely used technique in the diagnostic work-up of patients suspected of having CAD.

Limitations

We have classified stenoses with a mean lumen diameter reduction of ≥50% as determined by QCA as "significant". It is known that this threshold is the best-chosen anatomical threshold that correlates with myocardial ischemia18. However, it is of note that some ≥50% stenoses on the conventional angiogram may have been haemodynamically non-significant, and that a negative stress-test in these patients incorrectly was classified as false negative, thereby stressing that the cut-off values of anatomy and function do not always result in concordant outcomes.

CTCA has specific limitations; it is only reliable in selected patients with a slow (<70 beats/min, spontaneous or β-blocker induced) and regular heart rhythm, who are able to breath hold for at least 20 s. Furthermore, the high radiation exposure associated with CTCA [11.8-16.3 (male/female) mSv] is a matter of concern and significantly higher when compared to diagnostic conventional angiography (3-6 mSv).

CONCLUSIONS

While exercise-ECG testing provides important information that aids in the management of patients with typical angina, it is of limited diagnostic value for the detection of significant

coronary disease. A combined diagnostic work-up of exercise-ECG testing and CTCA markedly improved the post-test probability of the presence or absence of significant CAD.

REFERENCES

1. Management of stable angina pectoris. Recommendations of the Task Force of the European Society of Cardiology. Eur Heart J. 1997;18:394-413.
2. Gibbons RJ, Abrams J, Chatterjee K, Daley J, Deedwania PC, Douglas JS, Ferguson TB, Jr., Fihn SD, Fraker TD, Jr., Gardin JM, O'Rourke RA, Pasternak RC, Williams SV. ACC/AHA 2002 guideline update for the management of patients with chronic stable angina--summary article: a report of the American College of Cardiology/American Heart Association Task Force on practice guidelines (Committee on the Management of Patients With Chronic Stable Angina). J Am Coll Cardiol. 2003;41:159-68.
3. Gibbons RJ, Balady GJ, Bricker JT, Chaitman BR, Fletcher GF, Froelicher VF, Mark DB, McCallister BD, Mooss AN, O'Reilly MG, Winters WL, Antman EM, Alpert JS, Faxon DP, Fuster V, Gregoratos G, Hiratzka LF, Jacobs AK, Russell RO, Smith SC. ACC/AHA 2002 guideline update for exercise testing: summary article. A report of the American College of Cardiology/American Heart Association Task Force on Practice Guidelines (Committee to Update the 1997 Exercise Testing Guidelines). J Am Coll Cardiol. 2002;40:1531-40.
4. Smith SC, Jr., Dove JT, Jacobs AK, Kennedy JW, Kereiakes D, Kern MJ, Kuntz RE, Popma JJ, Schaff HV, Williams DO, Gibbons RJ, Alpert JP, Eagle KA, Faxon DP, Fuster V, Gardner TJ, Gregoratos G, Russell RO. ACC/AHA guidelines for percutaneous coronary intervention (revision of the 1993 PTCA guidelines)-executive summary: a report of the American College of Cardiology/American Heart Association task force on practice guidelines (Committee to revise the 1993 guidelines for percutaneous transluminal coronary angioplasty) endorsed by the Society for Cardiac Angiography and Interventions. Circulation. 2001;103:3019-41.
5. Nieman K, Cademartiri F, Lemos PA, Raaijmakers R, Pattynama PM, de Feyter PJ. Reliable noninvasive coronary angiography with fast submillimeter multislice spiral computed tomography. Circulation. 2002;106:2051-4.
6. Ropers D, Baum U, Pohle K, Anders K, Ulzheimer S, Ohnesorge B, Schlundt C, Bautz W, Daniel WG, Achenbach S. Detection of coronary artery stenoses with thin-slice multi-detector row spiral computed tomography and multiplanar reconstruction. Circulation. 2003;107:664-6.
7. Mollet NR, Cademartiri F, Krestin GP, McFadden EP, Arampatzis CA, Serruys PW, de Feyter PJ. Improved diagnostic accuracy with 16-row multi-slice computed tomography coronary angiography. J Am Coll Cardiol. 2005;45:128-32.

8. Mollet NR, Cademartiri F, Nieman K, Saia F, Lemos PA, McFadden EP, Pattynama PMT, Serruys PW, Krestin GP, De Feyter PJ. Multislice Spiral CT Coronary Angiography in Patients With Stable Angina Pectoris. J Am Coll Cardiol. 2004;43:2265-70.
9. Martuscelli E, Romagnoli A, D'Eliseo A, Razzini C, Tomassini M, Sperandio M, Simonetti G, Romeo F. Accuracy of thin-slice computed tomography in the detection of coronary stenoses. Eur Heart J. 2004;25:1043-8.
10. Kuettner A, Trabold T, Schroeder S, Feyer A, Beck T, Brueckner A, Heuschmid M, Burgstahler C, Kopp AF, Claussen CD. Noninvasive detection of coronary lesions using 16-detector multislice spiral computed tomography technology: initial clinical results. J Am Coll Cardiol. 2004;44:1230-7.
11. Hoffmann U, Moselewski F, Cury RC, Ferencik M, Jang IK, Diaz LJ, Abbara S, Brady TJ, Achenbach S. Predictive value of 16-slice multidetector spiral computed tomography to detect significant obstructive coronary artery disease in patients at high risk for coronary artery disease: patient-versus segment-based analysis. Circulation. 2004;110:2638-43.
12. Hoffmann MH, Shi H, Schmitz BL, Schmid FT, Lieberknecht M, Schulze R, Ludwig B, Kroschel U, Jahnke N, Haerer W, Brambs HJ, Aschoff AJ. Noninvasive coronary angiography with multislice computed tomography. Jama. 2005;293:2471-8.
13. Kuettner A, Beck T, Drosch T, Kettering K, Heuschmid M, Burgstahler C, Claussen CD, Kopp AF, Schroeder S. Diagnostic accuracy of noninvasive coronary imaging using 16-detector slice spiral computed tomography with 188 ms temporal resolution. J Am Coll Cardiol. 2005;45:123-7.
14. Achenbach S, Ropers D, Pohle FK, Raaz D, von Erffa J, Yilmaz A, Muschiol G, Daniel WG. Detection of coronary artery stenoses using multi-detector CT with 16 x 0.75 collimation and 375 ms rotation. Eur Heart J. 2005.
15. Abrams J. Clinical practice. Chronic stable angina. N Engl J Med. 2005;352:2524-33.
16. Pryor DB, Harrell FE, Jr., Lee KL, Califf RM, Rosati RA. Estimating the likelihood of significant coronary artery disease. Am J Med. 1983;75:771-80.
17. Pryor DB, Shaw L, McCants CB, Lee KL, Mark DB, Harrell FE, Jr., Muhlbaier LH, Califf RM. Value of the history and physical in identifying patients at increased risk for coronary artery disease. Ann Intern Med. 1993;118:81-90.
18. Arnese M, Salustri A, Fioretti PM, Cornel JH, Boersma E, Reijs AE, de Feyter PJ, Roelandt JR. Quantitative angiographic measurements of isolated left anterior descending coronary artery stenosis. Correlation with exercise echocardiography and technetium-99m 2-methoxy isobutyl isonitrile single-photon emission computed tomography. J Am Coll Cardiol. 1995;25:1486-91.

11

Comprehensive Assessment of Coronary Artery Stenoses: Computed Tomography Coronary Angiography versus Conventional Coronary Angiography and Correlation with Fractional Flow Reserve in Patients with Stable Angina

W. Bob Meijboom[1,2], Carlos A.G. Van Mieghem[1,2], Niels van Pelt[1,2], Annick Weustink[1,2], Francesca Pugliese[1,2], Nico R. Mollet[1,2], Eric Boersma[1], Eveline Regar[1], Robert J. van Geuns[1,2], Peter J. de Jaegere[1], Patrick W. Serruys[1], Gabriel P. Krestin[2], Pim J. de Feyter[1,2]

From the departments of Cardiology[1] and Radiology[2], Erasmus MC, Rotterdam, the Netherlands

J Am Coll Cardiol. 2008; 52: 636-43

ABSTRACT

Objectives

We sought to determine the diagnostic accuracy of noninvasive visual computed tomography coronary angiography (CTCA) and quantitative computed tomography coronary angiography (QCT) to predict the hemodynamic significance of a coronary stenosis, using intracoronary fractional flow reserve (FFR) as the reference standard.

Background

It has been demonstrated that CTCA provides excellent diagnostic sensitivity for identifying coronary stenoses, but may lack accurate delineation of the hemodynamic significance

Methods

We investigated 79 patients with stable angina pectoris who underwent both 64-slice or dual-source CTCA and FFR measurement of discrete coronary stenoses. CTCA and conventional coronary angiography (CCA), and QCT and quantitative coronary angiography (QCA), were performed to determine the severity of a stenosis that was compared with FFR measurements. A significant anatomical or functional stenosis was defined as $\geq$ 50% diameter stenosis or an FFR $<$ 0.75. Stented segments and bypass grafts were not included in the analysis.

Results

A total of 89 stenoses were evaluated of which 18% (16 of 89) had an FFR $<$ 0.75. The diagnostic accuracy of CTCA, QCT, CCA and QCA to detect a hemodynamic significant coronary lesion was 49%, 71%, 61% and 67%, respectively. Correlation between QCT and QCA with FFR measurement was weak (R values of -0.32 and -0.30, respectively). Correlation between QCT and QCA was significant, but only moderate ($R = 0.53$; $p < 0.0001$).

Conclusions

The anatomical assessment of the hemodynamic significance of coronary stenoses determined by visual CTCA, CCA or QCT or QCA does not correlate well with the functional assessment of FFR. Determining the hemodynamic significance of an angiographically intermediate stenosis remains relevant before referral for revascularization treatment.

INTRODUCTION

Currently available 64-slice cardiac computed tomography (CT) scanners and recently introduced dual-source scanners have the ability to completely assess the entire coronary tree and have been demonstrated to have good diagnostic accuracy for the identification of anatomically important coronary artery disease (CAD), generally defined as coronary artery stenoses with a lumen diameter reduction of at least 50 % (1-11). However, the anatomical significant appearance of a coronary stenosis does not always equate with functional significance, and this is particularly true for intermediate type coronary lesions (12-16). According to the guidelines (European Society of Cardiology, American College of Cardiology/American Heart Association), the decision to perform angioplasty or bypass surgery should integrate anatomical information with a test that provides objective proof of ischemia (17,18).

Only few reports have studied the relationship between the significance of a stenosis in a coronary vessel as defined by computed tomography coronary angiography (CTCA) and the functional importance of this stenosis in that particular coronary vessel territory (19-22). This study evaluates the relationship between the anatomy and functional significance of a coronary stenosis in patients who both underwent CTCA and conventional coronary angiogram (CCA) using the lesion-specific intracoronary fractional flow reserve (FFR) measurement.

METHODS

Study population

We retrospectively analyzed all patients who in the period between July 2004 and March 2007 underwent both a cardiac CT scan and invasive CCA and a subsequent measurement of the FFR. The decision to measure FFR was based entirely on the appearance of a coronary narrowing on CCA and was performed at the interventional cardiologist's discretion. All patients were assessed by either a 64-slice CT scanner (period July 2004 to March 2006) or dual-source CT scanner (period April 2006 to March 2007). Contra-indications for a CT scan included impaired renal function (creatinine clearance < 60 ml/min as defined with the Cockroft formula), irregular heart rhythm and known contrast allergy. Patients with previous percutaneous coronary intervention using stents or coronary artery bypass surgery were excluded from further analysis. Due to the hemodynamic interaction between 2 or more stenoses in series (23,24), we only included patients in whom FFR of a single discrete lesion had been performed. In total, 89 segments in 79 patients were included in the study. Sixteen segments were excluded due to CTCA-related artefacts and 1 because of inability to obtain a good angiographic view to perform quantitative coronary angiography (QCA).

For this retrospective analysis, all patients gave their informed consent to undergo CTCA as part of research protocols approved by the institutional review board. FFR was carried out as part of routine clinical management.

CCA.

All patients underwent CCA through the femoral approach, using a 6- or 7-F guiding catheter. After intracoronary injection of 2 mg isosorbide dinitrate, an angiogram of the right and left coronary artery was performed in multiple projections using standard techniques. All angiograms were analyzed off-line by 2 cardiologists who were not involved in the patient's medical care. They independently analyzed the selected coronary artery stenosis where FFR had been informed using visual estimation and quantitative assessment, the latter using an automated edge contour detection system (Cardiovascular Angiographic Analysis System, Pie Medical Equipment, Maastricht, the Netherlands)(25). Qualitative and quantitative analysis was based on the angiographic projection showing the most severe narrowing. A coronary stenosis was defined as significant based on visual inspection or when the degree of stenosis as measured with QCA was ≥ 50%.

FFR measurement.

Fractional flow reserve was measured with a sensor-tipped 0.014-inch guide wire (Pressure Wire, Radi Medical Systems, Uppsala, Sweden). After positioning of the pressure sensor just distal to the stenosis, maximal myocardial hyperemia was induced by a continuous intravenous infusion of adenosine in a femoral vein at an infusion rate of 140 μg/kg body-weight per minute for minimum of 2 min. During maximum hyperemia, FFR was calculated as the ratio of mean distal pressure measured by the pressure wire divided by the mean proximal pressure measured by the guiding catheter (26). A coronary stenosis with an FFR value <0.75 was considered functionally significant (27-29).

CTCA. Patient preparation.

Patients scanned with the 64-slice scanner who had a heart rate exceeding 65 beats/min received additional oral and/or intravenous beta-blockers (metoprolol) before the CT scan in order to obtain a heart rate below 65 beats/min. Patients scanned with dual-source CT did not receive pre-medication irrespective of the heart rate.

Scan protocol.

Thirty-eight patients were scanned with a 64-slice CT scanner (Sensation 64, Siemens, Forchheim, Germany). Angiographic scan parameters were: 32 x 2 x 0.6 mm collimation with z-flying focal spot, 330 ms rotation time, temporal resolution 165ms, 120 kV tube voltage, 900 mAs tube current, 3.8 mm/rotation table feed. Prospective X-ray tube modulation was not applied.

Forty patients were scanned using a dual-source CT scanner (Somatom Definition, Siemens, Forcheim, Germany). Dual-source CT angiographic scan parameters were: 120 kV, 330 ms rotation time, temporal resolution 83ms and 32x 2 X 0.6 mm collimation with z-flying focal spot for both detectors. Pitch values were adapted to heart rate based on the average of the last 10 heartbeats preceding the scan. Each tube provided 412 mAs/rot. Prospective tube modulation was applied with full dose radiation only given during 25% to 70% of the RR-interval.

With the 64-slice scanner, a bolus of 100 ml of contrast material (400 mgI/mL; Iomeron, Bracco, Milan, Italy) was injected intravenously in an antecubital vein at 5 ml/s. With dual- source CT, the volume of iodinated contrast material (Ultravist 370 mgI/ml, Schering AG, Germany) was adapted to the scan time, which varied between 5 and 13 s. A bolus of contrast material (60 to 90 ml) was injected in an antecubital vein at a flow rate of 5 ml/s followed by a saline chaser of 40 ml at 5 ml/s. In both scanners a bolus-tracking technique was used to synchronize the arrival of contrast in the coronary arteries, and the scan was started once the contrast material in the ascending aorta reached a predefined threshold of +100 Hounsfield units.

Image reconstruction

Images were reconstructed with electrocardiogram gating to obtain near motion-free image quality. Optimal datasets were reconstructed in the mid- to end-diastolic phase and in the end- systolic phase.

Qualitative evaluation of the CTCA.

Two experienced observers unaware of the results of CCA evaluated the CTCA data sets on an offline workstation (Leonardo, Siemens, Forchheim, Germany). Initially the specific lesion was evaluated with axial slices for the presence of significant disease, and additionally (curved) multiplanar reformatted reconstructions were used.

Quantitative evaluation of the CTCA.

Two experienced observers performed the quantification manually. After positioning the planes orthogonal to the course of the coronaries , cross-sectional images were obtained in the most severe narrowing and in the proximal and distal reference site. In these 3 images, the minimal lumen diameter was measured. The reference diameter was calculated by averaging the proximal and distal minimal lumen diameters. The percent diameter stenosis was calculated by subtracting the reference diameter from the minimal lumen diameter, which was divided by the reference diameter. The average of both measurements by the 2 observers was reported. A 50% diameter stenosis measured with quantitative computed tomography coronary angiography (QCT) was described as significant.

Statistical analysis

The diagnostic performance of qualitative and quantitative CCA and CTCA for the detection of significant stenoses in the coronary arteries with FFR as the standard of reference is presented as sensitivity, specificity and diagnostic accuracy (true positives + true negatives/ true positives + true negatives + false positives + false negatives), with the corresponding 95% confidence intervals. The relation between anatomical (QCA and QCT) and functional parameters (FFR) were analyzed with correlation statistics. The Pearson correlation-coefficient was used because QCA, QCT, and FFR were normally distributed. Bland-Altman analysis was performed by plotting the difference of QCA and QCT versus QCA (30). Interobserver variability for the detection of significant coronary stenosis and agreement between techniques to classify segments as having a functional significant lesion was determined by κ-statistics.

Table 1. Patient and lesion characteristics

Patients (n=79)	
Segments, n	89
Gender, male/ female	64/15
Mean age, yrs	60 ± 9
Body mass index, mean (kg/m²)	26.6 ± 3.9
Prior myocardial infarction	10
Angiographic data	
Affected artery	
Left main coronary artery	5
Left anterior descending coronary artery	41
Circumflex coronary artery	19
Right coronary artery	24
Reference diameter (mm)	2.82 ± 0.67
Percent diameter stenosis (%)	44 ± 11
Minimal luminal diameter (mm)	1.57 ± 0.50

Table 2. Patient management

Therapeutic decision, n	
Medical therapy	57
Percutaneous coronary intervention	29
Coronary artery bypass grafting	3
Revascularized segments, n	
FFR < 0.75	16
0.75 < FFR < 0.80	11
FFR > 0.80, IVUS obstructive plaque	5

FFR = fractional flow reserve; IVUS = intravascular ultrasound

RESULTS

Patients' characteristics and angiographic data are shown in Table 1. A total of 17 segments were excluded due to the presence of heavy calcifications (11 segments), motion artifacts (2 segments), breathing artifacts (2 segments), low contrast opacification (1 segment) and absence of a good angiographic view to perform QCA (1 segment). Average heart rate during CT data acquisition was 60 ± 9 beats/min for 64-slice CT and 68 ±11 beats/min for dual-source CT.

Overall, 89 discrete stenoses in 79 patients were included for comparison with FFR. Seventy-one percent (63 of 89) of these stenoses were of angiographic intermediate severity (between 40 and 70% diameter stenosis as determined by QCA), 29 stenoses were less than 40%, and 1 stenosis was measured as more than 70%. Of these 89 coronary stenoses, 35

had a diameter stenosis of more than 50% by QCA, but only 16 lesions were hemodynamically significant (FFR <0.75). Patient management is shown in Table 2.

Diagnostic performance of CTCA and CCA versus FFR: visual assessment

The diagnostic performance of CTCA and CCA for the assessment of a functionally important coronary stenosis (FFR < 0.75) is detailed in Table 3 and Figure 1. Agreement between visual CT and FFR assessment was present in 49% (44 of 89) of the evaluated segments; 15 of the 16 hemodynamically significant stenoses were identified correctly. One functionally important lesion in the mid left anterior descending coronary artery was underestimated and classified as nonsignificant by CTCA (44% diameter stenosis by QCA) (Fig. 2). Overestimation of hemodynamic severity occurred in 44 cases (Fig. 3). Corresponding sensitivity and specificity were, respectively, 94% and 40%. Interobserver variability for detection of a functionally important coronary stenosis was good (kappa value of 0.76). Agreement between CTCA and FFR was poor (kappa value of 0.16).

By comparison, visual lesion assessment by CCA showed an agreement with FFR in 61% (54 of 89) of the segments. Visual scoring identified 10 of the 16 functionally important lesions and 44 of the 73 functionally insignificant lesions. Six functionally important lesions were underestimated (Fig. 2). In 29 lesions, the hemodynamic severity was overestimated (Fig. 3). Consequently, the sensitivity was 63% and the specificity 60% for CCA to detect a functionally signifi-

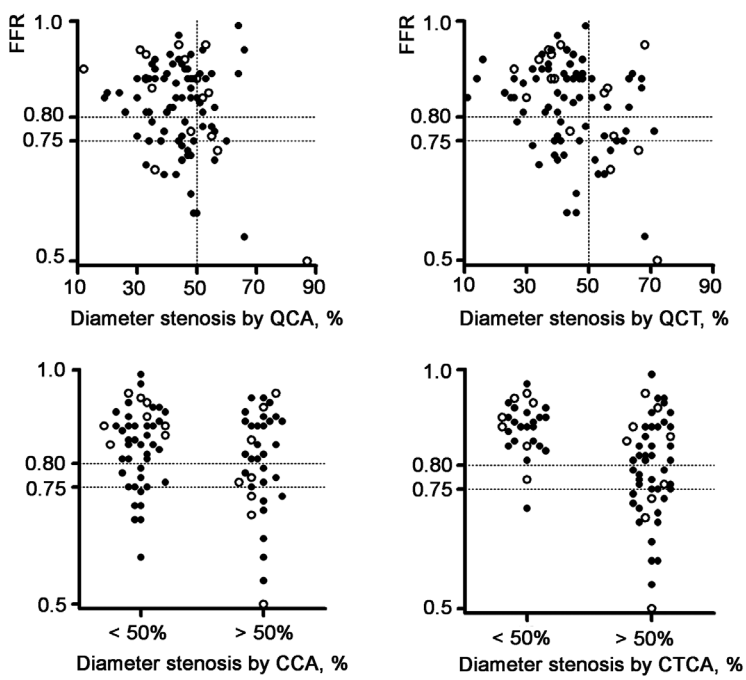

Figure 1. Scatter plots of FFR versus QCA, QCT, CCA, and CTCA
Quantitative coronary angiography (QCA), quantitative computed tomography coronary angiography (QCT), CCA, and CTCA are plotted versus FFR. There was a weak, but significant, negative correlation between QCA and FFR (r = -0.30) and between QCT and FFR (r = -0.32). Coronary arteries smaller than 3.5 mm are depicted as solid circles, coronary arteries larger than 3.5 mm as open circles.

Table 3. Diagnostic performance of CCA and CTCA to detect a functionally significant coronary stenosis (FFR < 0.75, FFR < 0.80).

	TP	TN	FP	FN	kappa	Sensitivity %	Specificity %	Diagnostic accuracy, %
FFR <0.75 (n = 16)								
CT coronary angiography, visual score	15	29	44	1	0.16	94 (82-100)	40 (29-51)	49 (39-60)
Quantitative CT coronary angiography	8	55	18	8	0.20	50 (26-75)	75 (65-85)	71 (61-80)
Conventional coronary angiography, visual score	10	44	29	6	0.15	63 (39-86)	60 (49-72)	61 (51-71)
Quantitative coronary angiography	11	49	24	5	0.25	69 (46-91)	67 (56-78)	67 (58-77)
FFR <0.80 (n = 31)								
CT coronary angiography, visual score	29	28	30	2	0.35	94 (58-100)	48 (35-61)	64 (54-74)
Quantitative CT coronary angiography	14	46	12	17	0.25	45 (28-63)	79 (69-90)	67 (58-77)
Conventional coronary angiography, visual score	17	36	22	14	0.16	55 (37-72)	62 (50-75)	60 (49-70)
Quantitative coronary angiography	17	41	18	13	0.25	57 (39-74)	69 (58-81)	65 (55-75)

CCA = conventional coronary angiogram; CT = computed tomography; CTCA = computed tomography coronary angiogram; FFR = fractional flow reserve; FN = false negative; FP = false positive; TN = true negative; TP = true positive.

cant lesion. Interobserver variability for the detection of a functionally important coronary stenosis was moderate (kappa value of 0.61). Agreement between CCA and FFR was poor (kappa value of 0.15). Furthermore, the diagnostic performance of CTCA and CCA for the assessment of a functionally important coronary stenosis, defined as a FFR <0.80, is detailed in Table 3 and Figure 1.

Diagnostic performance of QCT and QCA versus FFR: quantitative assessment

The diagnostic accuracy of QCT and QCA for detecting functionally relevant coronary stenoses is described in Table 3 and Figure 1. Overall, the diagnostic accuracy for both quantitative measures was slightly better than when performed with visual estimation.

Agreement between QCA and FFR as well as between QCT and FFR (Table 3) was only fair (kappa value of 0.25 and 0.20, respectively). The interobserver variability for QCA (kappa value of 0.58) and QCT (kappa value of 0.69) was moderate.

The correlation between QCT and FFR was R= -0.32 and between QCA and FFR was R= -0.30. Correlation of the percent diameter stenosis as determined by QCT and QCA was significant, but only mod-

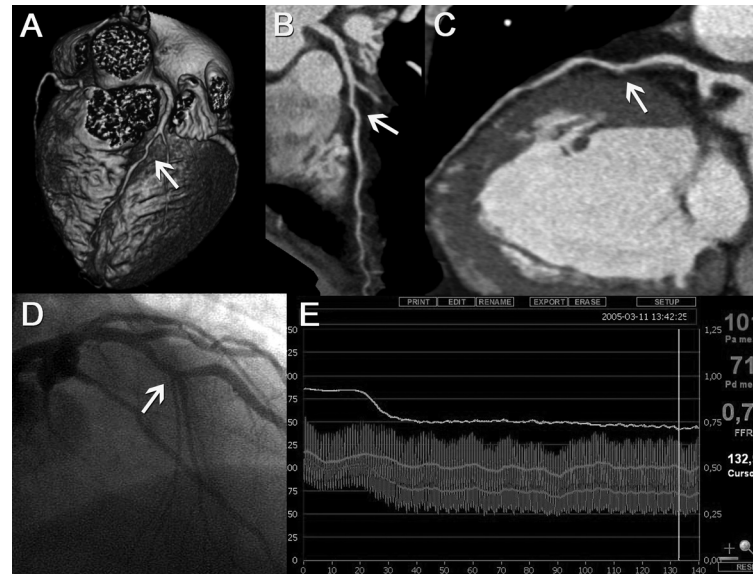

Figure 2. CTCA and CCA with FFR measurement of intermediate coronary lesion
Patient showing a coronary artery stenosis (arrow) in the left anterior descending coronary artery, as visualized with computed tomography coronary angiography (CTCA) (A, volume-rendered image; B and C, 2 orthogonal curved multiplanar reconstructions) and conventional coronary angiography (CCA) (D). By visual assessment, the coronary lesion was estimated as less than 50% diameter stenosis, both by CTCA and CCA. By quantitative analysis, the diameter stenosis was measured as 44% by quantitative coronary angiography and 40% by quantitative CTCA. The fractional flow reserve (FFR) was 0.71 (E). Based on the functional assessment, the patient underwent a successful percutaneous coronary intervention for this anatomically intermediate stenosis. (A full color version of this illustration can be found in the color section).

erate (R = 0.53; p< 0.0001) (Fig. 4). The Bland-Altman analysis plot revealed important variability: the mean difference between QCA and QCT was +2% with 95% limits of agreement ranging from – 21% to + 25% (Fig. 4).

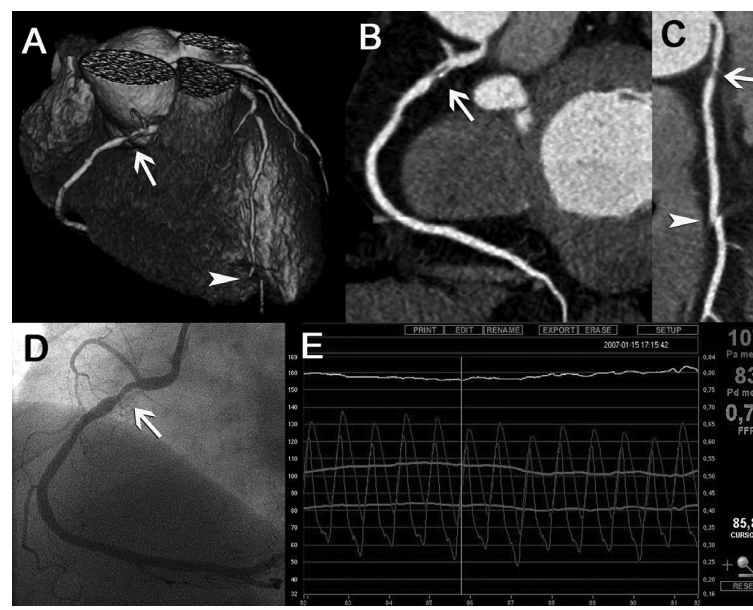

Figure 3. CTCA and CCA with FFR measurement of intermediate coronary lesion
Patient with a coronary artery stenosis (arrow) in the proximal part of the right coronary artery, as visualized with CTCA (A, volume-rendered image; B and C, 2 orthogonal curved multiplanar reconstructions) and CCA (D). Visually, the diameter stenosis was estimated as more than 50%, both by CTCA and CCA. Also, after quantification (56% diameter stenosis by quantitative coronary angiography, 70% diameter stenosis by quantitative CTCA), the lesion appeared to be anatomically significant. The FFR was 0.78 (E). In the distal segments, a step artefact can be seen (A and C, arrowhead). (A full color version of this illustration can be found in the color section).

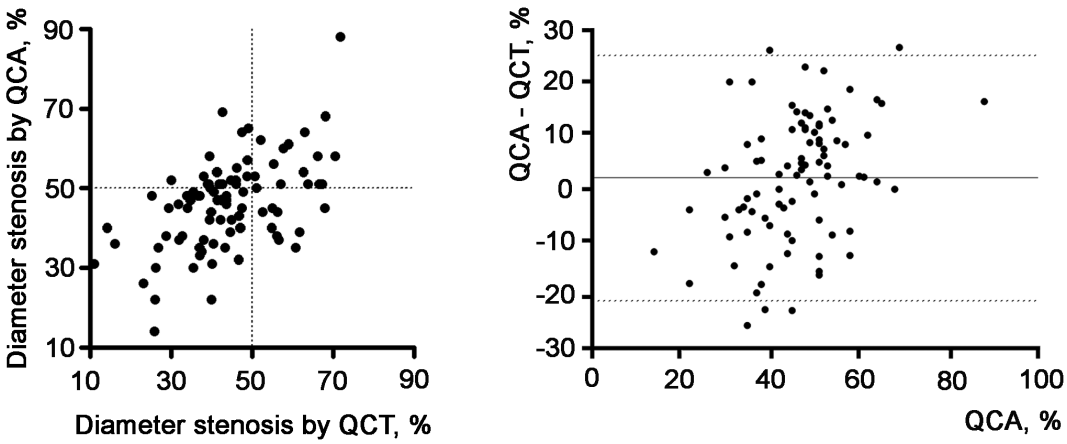

Figure 4. Scatter plot and Bland-Altman analysis of QCT versus QCA
In the left panel, QCT is plotted versus QCA. A significant correlation is seen between both anatomical techniques (r = 0.53). In the right panel, Bland-Altman analysis showed a bias of +2% with 95% limit of agreement ranging from -21% to 25%.

DISCUSSION

Fractional flow reserve is a lesion-specific technique to determine the functional importance of a coronary stenosis and is correlated with non-invasive tests that demonstrate ischemia (27,31-34). It has been shown to be a useful guide for decision making regarding the revascularisation of a specific lesion. In lesions where the FFR is ≥ 0.75, revascularization can be safely deferred (35-37).

Limitations of anatomical imaging. Previous reports have demonstrated that the anatomical assessment of a coronary stenosis as determined by CCA correlates poorly with the hemodynamic significance of the stenosis in particular in intermediate severity lesions (12-16). Although QCA is accurate and reproducible, it does not reflect the hemodynamic impairment of coronary flow. The QCA does not account for the effects of factors such as collateral circulation, mass of viable myocardium, shape and length of stenosis, inflow and outflow configuration, and transient vasoconstriction with resulting dynamic changes in the diameter of a stenosis (38). The diffuseness of the atherosclerotic process often results in disease in the reference segments proximal and distal to the site of maximal diameter reduction and as a result leads to underestimation of extent and severity of coronary atherosclerosis (39).

Integrating anatomy with functional information. These findings were also demonstrated in this study, not only for CTCA, but also when assessing the severity of a coronary artery stenosis with CCA. Using visual assessment, CTCA had high sensitivity to detect lesions with functional significance (FFR < 0.75). However, it had poor specificity due to frequent false positives;

CTCA overestimated the functional severity of a coronary stenosis, even when excluding segments with extensive calcifications or coronary motion. Quantification of stenosis severity by QCT and QCA improved the prediction of a functional relevant coronary stenosis slightly.

Previous studies have compared the anatomical findings of CTCA with functional imaging using nuclear stress testing (19,20,22). These studies also showed a poor correlation between anatomy and function with only ~ 50% of patients with significant coronary stenosis as demonstrated by CTCA having ischemia demonstrated by nuclear stress testing. Besides methodological limitations, these noninvasive tests measure the effect of impaired coronary perfusion at the level of the myocardium and thus do not discriminate between epicardial flow impairment and microvascular perfusion abnormalities. Intracoronary measurement of the FFR has the disadvantage of being invasive, but has the benefit of determining the ischemic potential of a specific epicardial coronary stenosis.

Clinical implementation. Given the previously discussed findings, and the consistently high negative predictive value of CTCA in different population groups, CTCA appears best suited as an effective rule out test for significant CAD. Those patients with suspected CAD and no or minimal coronary atherosclerosis on CTCA would not need further investigation (40,41). However patients with obstructive CAD on CTCA may best be investigated using a combined approach with a subsequent functional test such as nuclear stress testing, stress echocardiography or magnetic resonance perfusion imaging.

Anatomical evaluation of CAD has limitations and makes functional assessment necessary. Comprehensive non invasive anatomical and functional imaging may best identify patients who are likely to benefit most from secondary preventive measures and medical therapy (coronary atherosclerosis without ischemia) or who may be candidates for coronary revascularization (coronary atherosclerosis with ischemia). All-in-one approaches, such as single-photon emission CT-CTCA or positron-emission tomography-CTCA, that provide integrated evaluation of anatomy and physiology in a noninvasive way might theoretically solve these diagnostic problems.

Now that we are able to noninvasively access coronary anatomy, we should be remindful of the limitations of noninvasive functional tests, especially in patients with multivessel disease or significant left main stenosis on CTCA, without evidence of ischemia of a noninvasive functional test (42,43). In case of doubt, it seems prudent to refer such a patient to the catheterization laboratory for further invasive assessment and definitive exclusion of the functional severity of a specific epicardial stenosis using FFR.

Study limitations.

Patient inclusion was not performed in a prospectively designed study, but as a retrospective analysis. Consecutive patients were enrolled based on the access to the 64-slice or dual-source CT scanner. Seventeen segments in 15 patients had to be excluded due to the presence of heavy calcifications, motion artifacts, breathing artifacts, low contrast opacification and absence of a good angiographic view which made it, both visually as well as quantitatively, impossible to reliably estimate stenoses severity.

Quantification of coronary artery stenoses with CTCA continues to be a challenge due to the difficulty in ascertaining the normal reference segment of the coronary artery because of atherosclerotic involvement of the vessel wall proximal and distal to the stenosis (2,3,44). Especially in the presence of extensive calcifications of the artery it becomes impossible to accurately define the reference vessel diameters. Further improvement in spatial resolution will enhance the ability to accurately grade stenosis severity. However, particularly in coronary stenoses of intermediate severity, this may not improve the ability to predict functional significance, as is also observed with invasive CCA.

CONCLUSION

The correlation between stenosis severity as determined by CTCA or CCA and ischemia measured by FFR in coronary lesions of intermediate severity is poor. Functional information, whether provided by FFR or a noninvasive stress test, is essential in these circumstances for appropriate clinical decision making.

REFERENCES

1. Leschka S, Alkadhi H, Plass A, et al. Accuracy of MSCT coronary angiography with 64-slice technology: first experience. Eur Heart J 2005; 26(15):1482-7.
2. Raff GL, Gallagher MJ, O'Neill WW, Goldstein JA. Diagnostic accuracy of noninvasive coronary angiography using 64-slice spiral computed tomography. J Am Coll Cardiol 2005;46:552-7.
3. Leber AW, Knez A, von Ziegler F, et al. Quantification of obstructive and nonobstructive coronary lesions by 64-slice computed tomography: a comparative study with quantitative coronary angiography and intravascular ultrasound. J Am Coll Cardiol 2005;46:147-54.
4. Mollet NR, Cademartiri F, van Mieghem CA, et al. High-resolution spiral computed tomography coronary angiography in patients referred for diagnostic conventional coronary angiography. Circulation 2005;112:2318-23.

5. Ropers D, Rixe J, Anders K, et al. Usefulness of multidetector row spiral computed tomography with 64- x 0.6-mm collimation and 330-ms rotation for the noninvasive detection of significant coronary artery stenoses. Am J Cardiol 2006;97:343-8.
6. Schuijf JD, Pundziute G, Jukema JW, et al. Diagnostic accuracy of 64-slice multislice computed tomography in the noninvasive evaluation of significant coronary artery disease. Am J Cardiol 2006;98:145-8.
7. Nikolaou K, Knez A, Rist C, et al. Accuracy of 64-MDCT in the diagnosis of ischemic heart disease. AJR Am J Roentgenol 2006;187:111-7.
8. Fine JJ, Hopkins CB, Ruff N, Newton FC. Comparison of accuracy of 64-slice cardiovascular computed tomography with coronary angiography in patients with suspected coronary artery disease. Am J Cardiol 2006;97:173-4.
9. Ehara M, Surmely JF, Kawai M, et al. Diagnostic accuracy of 64-slice computed tomography for detecting angiographically significant coronary artery stenosis in an unselected consecutive patient population: comparison with conventional invasive angiography. Circ J 2006;70:564-71.
10. Leber AW, Johnson T, Becker A, et al. Diagnostic accuracy of dual-source multi-slice CT-coronary angiography in patients with an intermediate pretest likelihood for coronary artery disease. Eur Heart J 2007;28:2354-2360.
11. Weustink AC, Meijboom WB, Mollet NR, et al. Reliable high-speed coronary computed tomography in symptomatic patients. J Am Coll Cardiol 2007;50:786-94.
12. White CW, Wright CB, Doty DB, et al. Does visual interpretation of the coronary arteriogram predict the physiologic importance of a coronary stenosis? N Engl J Med 1984;310:819-24.
13. Kern MJ, Lerman A, Bech JW, et al. Physiological assessment of coronary artery disease in the cardiac catheterization laboratory: a scientific statement from the American Heart Association Committee on Diagnostic and Interventional Cardiac Catheterization, Council on Clinical Cardiology. Circulation 2006;114:1321-41.
14. Tobis J, Azarbal B, Slavin L. Assessment of intermediate severity coronary lesions in the catheterization laboratory. J Am Coll Cardiol 2007;49:839-48.
15. Christou MA, Siontis GC, Katritsis DG, Ioannidis JP. Meta-analysis of fractional flow reserve versus quantitative coronary angiography and noninvasive imaging for evaluation of myocardial ischemia. Am J Cardiol 2007;99:450-6.
16. Uren NG, Melin JA, De Bruyne B, Wijns W, Baudhuin T, Camici PG. Relation between myocardial blood flow and the severity of coronary-artery stenosis. N Engl J Med 1994;330:1782-8.
17. Silber S, Albertsson P, Aviles FF, et al. Guidelines for percutaneous coronary interventions. The Task Force for Percutaneous Coronary Interventions of the European Society of Cardiology. Eur Heart J 2005;26:804-47.

18. Smith SC, Jr., Feldman TE, Hirshfeld JW, Jr., et al. ACC/AHA/SCAI 2005 guideline update for percutaneous coronary intervention: a report of the American College of Cardiology/American Heart Association Task Force on Practice Guidelines (ACC/AHA/SCAI Writing Committee to Update 2001 Guidelines for Percutaneous Coronary Intervention). Circulation 2006;113:e166-286.
19. Schuijf JD, Wijns W, Jukema JW, et al. Relationship between noninvasive coronary angiography with multi-slice computed tomography and myocardial perfusion imaging. J Am Coll Cardiol 2006;48:2508-14.
20. Hacker M, Jakobs T, Hack N, et al. Sixty-four slice spiral CT angiography does not predict the functional relevance of coronary artery stenoses in patients with stable angina. Eur J Nucl Med Mol Imaging 2007;34:4-10.
21. Rispler S, Keidar Z, Ghersin E, et al. Integrated single-photon emission computed tomography and computed tomography coronary angiography for the assessment of hemodynamically significant coronary artery lesions. J Am Coll Cardiol 2007;49:1059-67.
22. Hacker M, Jakobs T, Matthiesen F, et al. Comparison of spiral multidetector CT angiography and myocardial perfusion imaging in the noninvasive detection of functionally relevant coronary artery lesions: first clinical experiences. J Nucl Med 2005;46:1294-300.
23. De Bruyne B, Pijls NH, Heyndrickx GR, Hodeige D, Kirkeeide R, Gould KL. Pressure-derived fractional flow reserve to assess serial epicardial stenoses: theoretical basis and animal validation. Circulation 2000;101:1840-7.
24. Pijls NH, De Bruyne B, Bech GJ, et al. Coronary pressure measurement to assess the hemodynamic significance of serial stenoses within one coronary artery: validation in humans. Circulation 2000;102:2371-7.
25. Reiber JH, Serruys PW, Kooijman CJ, et al. Assessment of short-, medium-, and long-term variations in arterial dimensions from computer-assisted quantitation of coronary cineangiograms. Circulation 1985;71:280-8.
26. Pijls NH, Van Gelder B, Van der Voort P, et al. Fractional flow reserve. A useful index to evaluate the influence of an epicardial coronary stenosis on myocardial blood flow. Circulation 1995;92:3183-93.
27. De Bruyne B, Bartunek J, Sys SU, Heyndrickx GR. Relation between myocardial fractional flow reserve calculated from coronary pressure measurements and exercise-induced myocardial ischemia. Circulation 1995;92:39-46.
28. Pijls NH, De Bruyne B, Peels K, et al. Measurement of fractional flow reserve to assess the functional severity of coronary-artery stenoses. N Engl J Med 1996;334:1703-8.
29. Kern MJ. Coronary physiology revisited : practical insights from the cardiac catheterization laboratory. Circulation 2000;101:1344-51.
30. Bland JM, Altman DG. Statistical methods for assessing agreement between two methods of clinical measurement. Lancet 1986;1:307-10.

31. De Bruyne B, Baudhuin T, Melin JA, et al. Coronary flow reserve calculated from pressure measurements in humans. Validation with positron emission tomography. Circulation 1994;89:1013-22.
32. Bartunek J, Marwick TH, Rodrigues AC, et al. Dobutamine-induced wall motion abnormalities: correlations with myocardial fractional flow reserve and quantitative coronary angiography. J Am Coll Cardiol 1996;27:1429-36.
33. Costa MA, Shoemaker S, Futamatsu H, et al. Quantitative magnetic resonance perfusion imaging detects anatomic and physiologic coronary artery disease as measured by coronary angiography and fractional flow reserve. J Am Coll Cardiol 2007;50:514-22.
34. Rieber J, Huber A, Erhard I, et al. Cardiac magnetic resonance perfusion imaging for the functional assessment of coronary artery disease: a comparison with coronary angiography and fractional flow reserve. Eur Heart J 2006;27:1465-71.
35. Pijls NH, van Schaardenburgh P, Manoharan G, et al. Percutaneous coronary intervention of functionally nonsignificant stenosis: 5-year follow-up of the DEFER Study. J Am Coll Cardiol 2007;49:2105-11.
36. Legalery P, Schiele F, Seronde MF, et al. One-year outcome of patients submitted to routine fractional flow reserve assessment to determine the need for angioplasty. Eur Heart J 2005;26:2623-9.
37. Wongpraparut N, Yalamanchili V, Pasnoori V, et al. Thirty-month outcome after fractional flow reserve-guided versus conventional multivessel percutaneous coronary intervention. Am J Cardiol 2005;96:877-84.
38. Gould KL, Kelley KO, Bolson EL. Experimental validation of quantitative coronary arteriography for determining pressure-flow characteristics of coronary stenosis. Circulation 1982;66:930-7.
39. de Feyter PJ, Serruys PW, Davies MJ, Richardson P, Lubsen J, Oliver MF. Quantitative coronary angiography to measure progression and regression of coronary atherosclerosis. Value, limitations, and implications for clinical trials. Circulation 1991;84:412-23.
40. Gilard M, Le Gal G, Cornily JC, et al. Midterm prognosis of patients with suspected coronary artery disease and normal multislice computed tomographic findings: a prospective management outcome study. Arch Intern Med 2007;167:1686-9.
41. Min JK, Shaw LJ, Devereux RB, et al. Prognostic value of multidetector coronary computed tomographic angiography for prediction of all-cause mortality. J Am Coll Cardiol 2007;50:1161-70.
42. Ragosta M, Bishop AH, Lipson LC, et al. Comparison between angiography and fractional flow reserve versus single-photon emission computed tomographic myocardial perfusion imaging for determining lesion significance in patients with multivessel coronary disease. Am J Cardiol 2007;99:896-902.

43. Lima RS, Watson DD, Goode AR, et al. Incremental value of combined perfusion and function over perfusion alone by gated SPECT myocardial perfusion imaging for detection of severe three-vessel coronary artery disease. J Am Coll Cardiol 2003;42:64-70.
44. Hoffmann MH, Shi H, Schmitz BL, et al. Noninvasive coronary angiography with multislice computed tomography. Jama 2005;293:2471-8.

INTERLUDE 3

Combining Non-Invasive Coronary Anatomical Imaging with Invasive Functional Information. An Unconventional but Appropriate Hybrid Approach.

Carlos A.G. Van Mieghem[1,2] and Pim J. de Feyter[1,2]

From the departments of Cardiology[1] and Radiology[2],
Erasmus MC, Rotterdam, the Netherlands

Submitted

ABSTRACT

CT coronary angiography (CTCA) allows accurate non-invasive imaging of the coronary arteries. As illustrated by this case report, the 3-dimensional information provided by this technique might be of value to resolve complex coronary anatomy encountered in the cathlab. However, the limitations inherent to an anatomical test also apply for CTCA, and bring in the need for functional information to ensure adequate patient management.

INTRODUCTION

Catheter-based coronary angiography (CCA) is considered the gold-standard technique to assess the presence of coronary artery disease. It has become the essential diagnostic tool for the interventional cardiologist and cardiac surgeon to decide upon the most optimal revascularization strategy. The catheter-based approach allows an ad-hoc percutaneous coronary intervention or the acquirement of additional morphologic or functional information, using intravascular ultrasound or measurement of the fractional flow reserve, in case of intermediate coronary stenosis.

The last decade, computed tomography coronary angiography (CTCA) has developed into a robust non-invasive alternative providing detailed anatomical information of the coronary arteries. Difficult coronary anatomy can easily be resolved due to the 3-dimensional nature of the technique. However, for clinical decision making, functional information remains essential and complementary in addition to accurate anatomical data.

This report describes a case highlighting the limitations of CCA and documents the advantages of CTCA. Invasively obtained functional information was necessary to reach a correct therapeutic decision.

CASE REPORT

A 56-year-old man was referred to undergo aortic valve replacement because of severe symptomatic aortic valve stenosis. Before final acceptance for surgery, all cases are preoperatively discussed in our daily heart team conference, which is attended by a cardiac surgeon, interventional cardiologist and a staff member of general cardiology. The patient received medical treatment for hypercholesterolemia and arterial hypertension. Otherwise he had no significant medical history. He recently underwent further investigation in the cardiology service of a community hospital because of anginal symptoms. On transthoracic echocardiography a se-

vere aortic valve stenosis was diagnosed based on severe calcifications of the valve with a mean gradient of 60 mmHg. Left ventricular systolic function was normal. Invasive coronary angiography revealed a left dominant coronary system. The right and left coronary artery were considered normal by the referring cardiologist (Figure.1). However, due to poor contrast opacification the left coronary artery was difficult to assess. Although the angiographic report did not mention the presence of pressure dampening when the left coronary system was cannulated, the absence of backward contrast filling into the left sinus of Valsalva, suggested the presence of an ostial left main abnormality. To clarify this issue, we performed a dual-source cardiac CT scan with a specific emphasis on evaluating the left main coronary artery. The cardiac CT scan revealed a large noncalcified plaque at the origin of the left main stem causing a narrowing of the vessel lumen of at least 50% (Figure. 2). Because of these findings the patient was scheduled again for a repeat invasive coronary angiogram in combination with measurement of the fractional flow reserve across the stenosis. Using a 0.014" pressure sensor wire and intravenous adenosine (140 mcg/kg/min during 2 minutes) the obtained fractional flow reserve was 0.68, confirming the functional severity of the coronary narrowing. Instead of isolated cardiac valve surgery with implantation of a St.Jude mechanical valve prosthesis, the patient also received a venous jumpgraft to the intermediate branch and obtuse marginal branch of the circumflex artery and

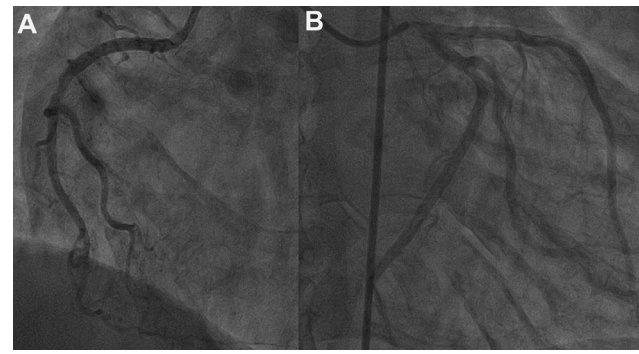

Figure 1. Conventional coronary angiogram of the right (A) and left coronary artery (B). The left coronary system is difficult to evaluate due to poor contrast opacification.

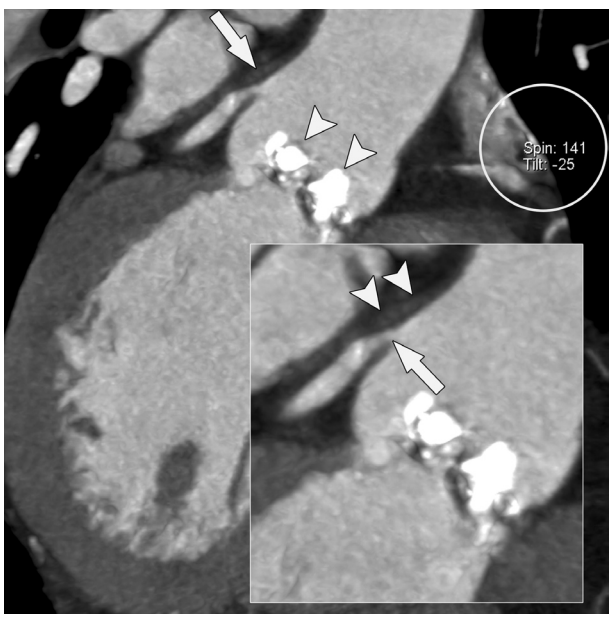

Figure 2. Cardiac CT scan showing a large non-calcified plaque (arrow) with accompanying significant lumen narrowing of the left main coronary ostium (inset, arrow). The aortic valve is severely calcified (arrowheads). The CT image provides the physician the coordinates of the projection (encircled) in which the coronary narrowing is clearly visible, in this case an RAO 141 projection with 25 degrees of caudal inclination.

a left internal mammary graft anastomosis to the left anterior descending artery. He made an uneventful recovery and remains symptom-free at one year follow-up.

DISCUSSION

Currently, CTCA is preferably used as a rule-out-test for the presence of clinically relevant coronary artery disease (CAD), generally defined as a coronary stenosis with more than 50% diameter obstruction. For the purpose of exclusion of CAD, CTCA is most effective when used for symptomatic patients who are at low or intermediate pre-test risk of CAD.[1] By contrast, patients with typical angina in general are not referred to diagnose CAD, but rather undergo the test with the aim to provide information who best to treat medically or by revascularization. These patients usually present with an advanced stage of atherosclerosis that is hallmarked by calcifications. Severe vessel wall calcifications are the main obstacle for the use of CTCA today as it prevents assessment of the integrity of the underlying coronary lumen or leads to overestimation of coronary stenosis severity. A major role in the assessment of patients with a high pre-test likelihood of CAD is therefore not to be expected. However, CCA has limitations that sometimes result in an incomplete assessment of the coronary anatomy. As illustrated by this case, CTCA offers a useful alternative especially in patients with complex coronary anatomy.[2,3] The accurate three-dimensional visualization of cardiac structures with CTCA explains the phenomenon of so-called "reverse referrals", i.e. patients who initially underwent a CCA are sometimes referred for a CTCA to complement the catheter-based angiographic findings.

Both CCA and CTCA are anatomical imaging techniques that provide detailed information of the location and severity of possible coronary artery stenoses. Quantification of lesion severity using quantitative coronary angiography has limited value for predicting the hemodynamic impact of a coronary stenosis, especially for an intermediately severe luminal narrowing (approximately 40% to 70% diameter narrowing).[4] Recently, this disconcordance between anatomical based assessment of lesion severity and its functional importance has been reported in patients who undergo CTCA.[5] The documentation of myocardial ischemia is essential information to guide the therapeutic management of patients with anatomically important CAD.[6] It is therefore advisable to clarify the physiological relevance of obstructive CAD on a cardiac CT scan by using a combined approach with a functional test. For the patient who is referred to the cathlab, invasive measurement of the FFR is the recommended test as it provides functional information about an angiographic stenosis.

REFERENCES

1. Schroeder S, Achenbach S, Bengel F, Burgstahler C, Cademartiri F, de Feyter P, George R, Kaufmann P, Kopp AF, Knuuti J, Ropers D, Schuijf J, Tops LF, Bax JJ. Cardiac computed tomography: indications, applications, limitations, and training requirements: report of a Writing Group deployed by the Working Group Nuclear Cardiology and Cardiac CT of the European Society of Cardiology and the European Council of Nuclear Cardiology. Eur Heart J 2008;29:531-56.
2. Mollet NR, Hoye A, Lemos PA, Cademartiri F, Sianos G, McFadden EP, Krestin GP, Serruys PW, de Feyter PJ. Value of preprocedure multislice computed tomographic coronary angiography to predict the outcome of percutaneous recanalization of chronic total occlusions. Am J Cardiol 2005;95:240-3.
3. Van Mieghem CA, Thury A, Meijboom WB, Cademartiri F, Mollet NR, Weustink AC, Sianos G, de Jaegere PP, Serruys PW, de Feyter P. Detection and characterization of coronary bifurcation lesions with 64-slice computed tomography coronary angiography. Eur Heart J 2007;28:1968-76.
4. Bartunek J, Sys SU, Heyndrickx GR, Pijls NH, De Bruyne B. Quantitative coronary angiography in predicting functional significance of stenoses in an unselected patient cohort. J Am Coll Cardiol 1995;26:328-34.
5. Schuijf JD, Wijns W, Jukema JW, Atsma DE, de Roos A, Lamb HJ, Stokkel MP, Dibbets-Schneider P, Decramer I, De Bondt P, van der Wall EE, Vanhoenacker PK, Bax JJ. Relationship between noninvasive coronary angiography with multi-slice computed tomography and myocardial perfusion imaging. J Am Coll Cardiol 2006;48:2508-14.
6. Shaw LJ, Berman DS, Maron DJ, Mancini GB, Hayes SW, Hartigan PM, Weintraub WS, O'Rourke RA, Dada M, Spertus JA, Chaitman BR, Friedman J, Slomka P, Heller GV, Germano G, Gosselin G, Berger P, Kostuk WJ, Schwartz RG, Knudtson M, Veledar E, Bates ER, McCallister B, Teo KK, Boden WE. Optimal medical therapy with or without percutaneous coronary intervention to reduce ischemic burden: results from the Clinical Outcomes Utilizing Revascularization and Aggressive Drug Evaluation (COURAGE) trial nuclear substudy. Circulation 2008;117:1283-91.

12

Detection and Characterization of Coronary Bifurcation Lesions with 64-slice Computed Tomography Coronary Angiography

Carlos A.G. Van Mieghem[1,2], Attila Thury[1], Willem B. Meijboom[1,2], Filippo Cademartiri[1,2], Nico R. Mollet[1,2], Annick C. Weustink[1,2], Georgios Sianos[1], Peter P.T. de Jaegere[1], Patrick W. Serruys[1], Pim J. de Feyter[1,2]

From the departments of Cardiology[1] and Radiology[2],
Erasmus MC, Rotterdam, the Netherlands

Eur Heart J. 2007; 28:1968-76

ABSTRACT

Aims

To compare the performance of 64-slice computed tomography coronary angiography (CTCA) and invasive coronary angiography (ICA) in the detection and classification (according to the Medina system) of bifurcation lesions (BL).

Methods and results

We studied 323 consecutive patients undergoing 64-slice CTCA prior to ICA. All coronary segments ≥ 2 mm in diameter were evaluated for the presence of a significant (≥50% diameter reduction on quantitative coronary angiography) BL. Evaluation of BL by CTCA included the assessment of significant lumen obstruction in both main and side branch vessels. Forty-one out of 43 patients (46/48 lesions) with significant BL were identified by CTCA. Excluding coronary segments with non-diagnostic image quality (5%), the sensitivity, specificity, positive and negative predictive values of CTCA for detecting significant BL was 96, 99, 85 and 99% respectively. In 39 of these 41 patients, CTCA assessment was concordant with the Medina lesion classification on ICA.

Conclusion

64-slice CTCA allows accurate assessment of complex BL.

INTRODUCTION

Invasive coronary angiography is regarded as the reference standard for the diagnosis of significant coronary artery disease and to plan and guide percutaneous coronary intervention (PCI). However, coronary angiography has major limitations. Factors such as vessel overlap and foreshortening may make it difficult to accurately assess the severity and extent of coronary artery lesions.[1] Furthermore, as angiography only visualizes the lumen, it cannot identify plaque accumulation related to positive remodeling, a ubiquitous phenomenon at bifurcation sites.[2]

The high diagnostic accuracy of computed tomography coronary angiography (CTCA) in the non-invasive detection of significant coronary artery disease (CAD) is well established.[3,4] However, the potential role of CTCA in the detection and characterisation of coronary bifurcations is unclear. CTCA allows 3-dimensional evaluation of both the lumen and the wall of the vessel; thus, it has potential to provide a more comprehensive assessment of the complex geometry of bifurcation lesions (BLs). The purpose of the present study is to evaluate the diagnostic accuracy of CTCA in patients with bifurcation pathology. Furthermore, we provide a detailed comparison with conventional angiographic data by categorizing each BL according to a simplified classification system (Medina).[5]

METHODS

Patient selection

The study population comprised 323 consecutive patients who underwent 64-slice CTCA, within a 2-week period prior to invasive coronary angiography (ICA) between March and December 2005. In patients with prior PCI or coronary artery bypass graft surgery (CABG), only the nonintervened coronary artery segments were included in the analysis. Contra-indications for CTCA were: an irregular heart rhythm, inability to breath hold for 15 seconds, renal dysfunction (creatinine clearance < 60 ml/min), and known contrast allergy. The institutional ethical review board approved the study protocol, which complied with the declaration of Helsinki. All patients gave written informed consent.

MSCT protocol, radiation dose calculation and image reconstruction

Patients with a resting heart rate above 65 beats per minute (bpm) received oral beta-blockers (metoprolol 50-100 mg) or a non-dihydropyridine calcium-antagonist (diltiazem 60-120 mg) together with 0.5-1 mg lorazepam 1 hour before the scan. An additional IV bolus of metoprolol (5-10 mg) was occasionally administered where the heart rate remained above 65 bpm. The examination was performed using previously reported methodology.[4] In brief, CTCA data were

acquired using a 64-slice CT scanner (Sensation 64, Siemens, Germany). A non-enhanced calcium-scoring scan was only obtained in patients without previous PCI or CABG using the following parameters: collimation 64 x 0.6 mm, tube rotation time 330 ms, table feed 3.8 mm per rotation, tube current 150 mAs at 120 kV, and prospective x-ray tube modulation. Angiographic scan parameters were identical aside from a tube current that ranged between 850 and 960 mAs without the use of dose pulsing. The effective radiation dose was calculated separately for patients with and without previous CABG using dedicated software (ImPACT CT Patient Dosimetry Calculator, version 0.99x), as described in the European Guidelines on Quality Criteria for Computed Tomography (Available at: http://www.drs.dk/guidelines/ct/quality/index.htm).[6]

A bolus of 100 ml of contrast (iomeprol, 400 mg iodine/ml, Iomeron®, Bracco, Milan, Italy) was administered in all patients. The standard injection rate was 5 ml/sec, but was decreased to 4 ml/sec in patients who had previous CABG. We did not use a saline chaser after contrast administration. A bolus tracking technique was used to monitor the appearance of contrast material in the aortic root cranial to the origin of the left coronary artery. Once the signal in the ascending aorta reached a predefined threshold of 100 Hounsfield units, CT data were acquired during an inspiratory breath-hold.

All scans were analyzed off-line using a Leonardo workstation (Siemens Medical Solutions) by 2 independent observers who were blinded to the results of ICA. Images were reconstructed using ECG-gating to obtain optimal, motion free image quality. Datasets were routinely obtained during the mid-to-end diastolic phase (–300, -350, -400, –450 ms before the next R-wave or at 60 to 70% of the R-R interval). Additional reconstruction windows in systole (in general at 25% to 35% of the R-R interval) were explored when image quality was suboptimal on the standard reconstructions. In 31% of the cases the end-systolic dataset was used for image analysis.

Image quality was evaluated on a per segment basis and classified as good (defined as absence of any image-degrading artefacts related to motion, calcification, or insufficient contrast enhancement), adequate (presence of image-degrading artefacts, but evaluations possible with moderate confidence), or poor (presence of image-degrading artefacts and evaluation only possible with low confidence). Coronary artery segments with poor image quality were judged to be "unevaluable".

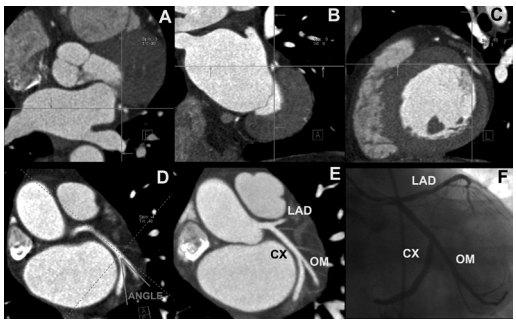

Figure 1a. Visualization of the circumflex obtuse marginal bifurcation by invasive coronary angiography (a) and volume-rendered computed tomography coronary angiography (b). The three-dimensional representation of the heart, as shown in (b), can be obtained by summation of the 'raw' axial computed tomography images that have a defined x-y-z dimension. The conventional planes that are used for visualization of this volume data set are the axial plane (axial), the coronal plane (coronal) and the sagittal plane (sagittal). CX, circumflex coronary artery; LAD, left anterior descending coronary artery; OM, obtuse marginal branch. (A full color version of this illustration can be found in the color section).

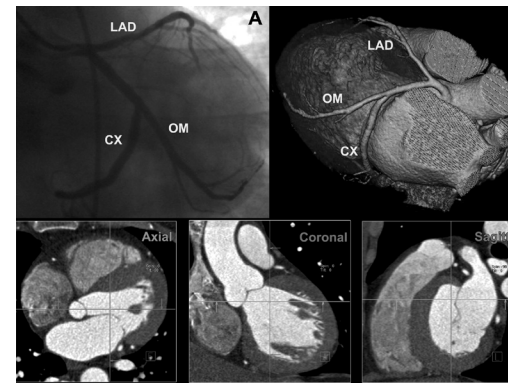

Figure 1b. Scrolling of axial images provides a quick view of the data set to assess crudely the main features of the coronary anatomy. To obtain a precise view of the structure of interest, in this example the circumflex-obtuse marginal bifurcation, the planes of visualization need to be orientated to the geometrical orientation of the coronary structures. As a first step, the three conventional image planes are centered at the level of the branching point (a-c). The three-dimensional nature of the CT data allows to subsequently tilt these image planes in any orientation. The resulting multiplanar reconstruction (d) precisely shows the relationship of the main vessel with the side branch and is used to assess the angle between the initial course of distal portion of the main vessel and side branch (in this example, 31°). Also shown is a maximum intensity projection computed tomography image (e) to demonstrate the anatomical correlation with the angiographic view. We did not use this maximum intensity projection reconstruction to determine bifurcation angles. CX, circumflex coronary artery; LAD, left anterior descending coronary artery; OM, obtuse marginal branch. (A full color version of this illustration can be found in the color section).

CTCA analysis

All evaluable coronary segments were visually scored for the presence of significant BLs (diameter reduction of ≥50%) by careful axial scrolling and using (curved) multiplanar reconstructions. A bifurcation lesion was defined as a stenosis that involved the origin of a side branch, equal to or more than 2.0 mm in diameter.[7] The presence or absence of side branch pathology was determined by evaluating the first 10 mm of the side branch for the presence of significant lumen narrowing. Disagreement between observers was resolved by a third observer, and the consensus reading was subsequently compared with the ICA.

High-resolution thin slab multiplanar reconstructions (reconstructed slice thickness of 0.75 mm) were used for assessment of bifurcation angles. The 3 orthogonal planes as provided when opening a CT dataset were carefully orientated according to the geometrical orientation of the main vessel and side branch at the bifurcation point (Figure 1A). To determine the angle of bifurcation, we depicted 2 lines (in the centre of each vessel lumen) along the initial course of the distal part of the main branch (MBd) and side branch (SB) using the MPR view in which the angulation between the proximal parts of these 2 vessels was maximal (Figure 1B). We only used diastolic datasets to measure bifurcation angles. Subsequently, BL with significant

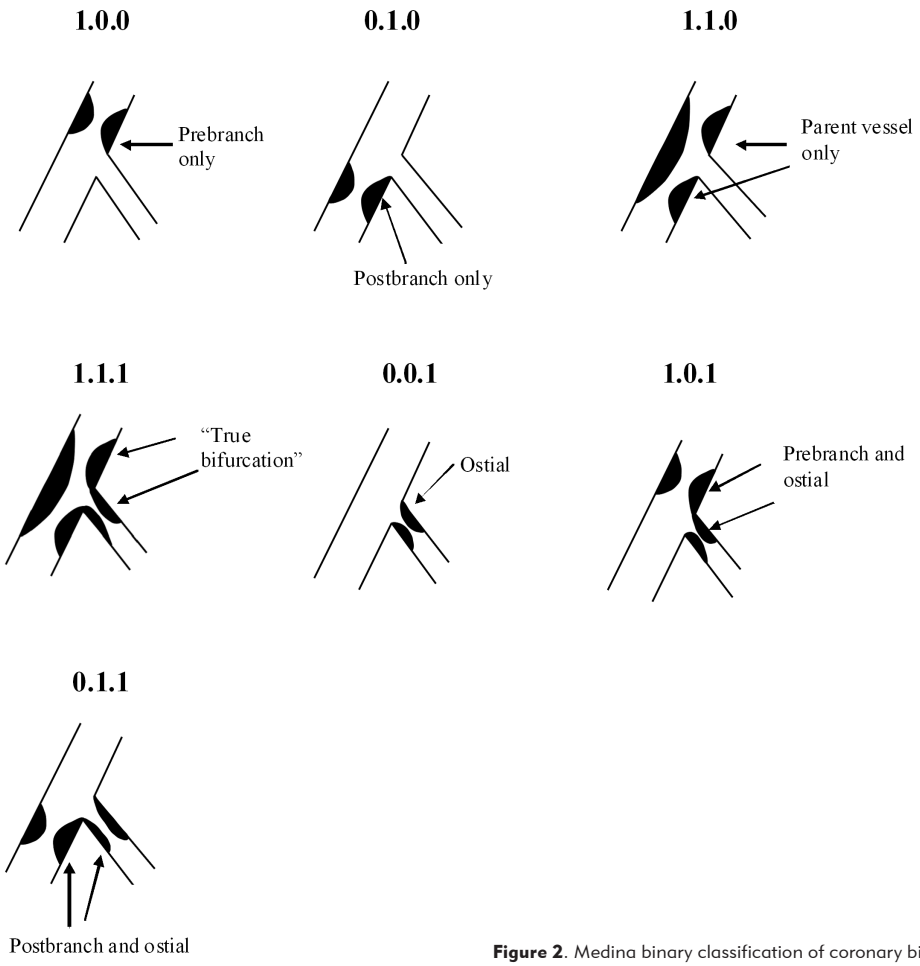

Figure 2. Medina binary classification of coronary bifurcation lesions.

lumen narrowing were categorized using a recently introduced classification scheme, known as the MEDINA bifurcation classification (Figure 2).[5] The Medina classification is a simple binary system whereby significant lumen narrowing is classified as present (1) or absent (0) in the proximal MB, distal MB, and SB. Modification and scrolling of MPR images originating from the bifurcation site was used to confirm the exact spatial relation of the lumen obstruction in relation to the branching point.

Quantitative coronary angiography

Coronary angiograms were obtained in multiple projections after intracoronary nitrate administration with standard techniques. Two experienced cardiologists blinded to CTCA results identified all available coronary segments using a 17-segment modified American Heart As-

sociation (AHA) classification and classified all coronary segments as < 2 and ≥ 2 mm in diameter using validated, automated, edgedetection software (CAAS II, Pie Medical, Maastricht, The Netherlands).[8] Only segments classified as ≥ 2 mm in reference diameter were considered for comparison with CTCA. In the presence of an occluded coronary artery, we only assessed the segments that were located proximal to the occlusion. Standard measurements were made for the MB analysis; the proximal border of the SB was depicted manually by extending the reference point into the main vessel, as previously reported.[9] Significant lumen narrowing was defined as a lumen diameter reduction of ≥50% in the MB and/ or SB. Identified BLs were subsequently classified according to the Medina classification system.[5] All measurements, including bifurcation angles, were determined using end-diastolic frames.

Statistical analysis

Continuous variables are presented as mean ± standard deviation and compared by Student's t-test. A two-sided p-value of <0.05 was considered to be significant. Categorical variables are presented as counts and percentages. The diagnostic performance of CTCA for the detection of significant BL, when compared with quantitative coronary angiography (QCA), is presented as sensitivity, specificity, positive and negative predictive value and reported with associated 95% confidence intervals based on binomial probabilities. Diagnostic performance indices are presented separately for all "evaluable" segments and for the overall population, including coronary segments with poor image quality. These "unevaluable" segments were classified as having a stenosis on CTCA. Because of potentially interdependent observations, i.e. multiple bifurcations in the same patient, an additional measurement of diagnostic accuracy was performed for a random selection of single observations per patient. Statistical analysis was performed with SPSS, version 11.5 (SPSS Inc., Chicago, USA).

RESULTS

All 323 patients tolerated the CTCA procedure well and no complications occurred. The average time required for the cardiac CT examination, including patient preparation for scanning, image acquisition and reconstruction of the appropriate datasets was 20 to 25 min. Evaluation of the CT coronary angiogram took on average about 5-10 min; the extra time needed to specifically assess the bifurcations was about 5 min.

Patient characteristics are summarized in Table 1. Mean periscan heart rate was 58 ± 7.2 bpm. Of the theoretically available 5491 segments, 582 were excluded because the diameter was <2 mm and 161 because they were distal to an occluded segment. In addition, 470 segments were absent on CCA. After exclusion of 189 stented segments and 74 grafted vessels (267 segments), 3822 segments (1218 bifurcations) were available for further analysis. Poor image quality was present in 5% (211/ 3822; 88 bifurcations) of coronary segments and

Table 1. Patient characteristics (n= 323).

Characteristic	Value
Age	61.3 ± 10.4
Male (%)	72
Body mass index (kg/m^2)	27.2 ± 4.3
Clinical presentation	
Stable angina (%)	60
ACS (%)	14
Other (%)	26
Current smoker (%)	27
Hypertension (%)	53
Dyslipidemia (%)	81
Diabetes mellitus (%)	16
Creatinin (mg/dl)	0.97 ±0.2
Prior MI (%)	33
Prior PCI (%)	32
Prior CABG (%)	10
Vessel disease (%)	
Non-significant disease	28
1-vessel disease	38
2-vessel disease	18
3-vessel disease	8
Left main disease	5
Graft disease	3
Basal heart rate	68.5 ± 10.2
Heart rate during CTCA	58 ± 7.2
CTDIvol no previous CABG (Gy)	70.5
CTDIvol previous CABG (Gy)	61
Dose estimate (no previous CABG) (mSv)[a]	19
Dose estimate (previous CABG) (mSv)[a]	22

Categorical data are presented as numbers (%) and continuous data as mean values ±SD.
ACS, acute coronary syndrome; CABG, coronary artery bypass graft surgery; CAD, coronary artery disease; CTCA, computed tomography coronary angiography; CTDIvol , volume computed tomography dose index; MI, myocardial infarction; PCI, percutaneous coronary intervention.
a The estimated radiation dose is higher in bypass patients because of the longer scan length.

was related to a technically inadequate scan (breathing artifacts or fast or irregular heart rate, n=53), severe calcification (n=62), cardiac motion artifacts (n=58), or insufficient contrast enhancement (n=38). The effective radiation dose was calculated as 19 mSv (1.6 mSv for the calcium score scan and 17.4 mSv for the contrast-enhanced scan) in patients without previous CABG and 22 mSv in patients with previous CABG.

Table 2 summarizes the diagnostic accuracy of 64-slice CT compared with QCA for the evaluation of coronary bifurcations. A total of 1130 evaluable bifurcations were available for analysis. Fifty-four BL in 49 patients were identified on CTCA. QCA identified 48 BL in 43 patients. Thus, CTCA incorrectly classified the severity of BL in 10 patients. In 8 patients, a significant BL on CTCA was not confirmed on ICA; in 6 of these 8 patients this misclassification was related to the presence of calcification. In two patients the severity of the lesion was underestimated: one patient had a calcified lesion of the left main/ left anterior descending bifurcation; the second had a short lesion of the distal right coronary artery-posterolateral branch bifurcation. When the 88 bifurcations with poor image quality were arbitrarily scored as having significant lumen narrowing on CTCA, the sensitivity and specificity for detection of significant BL was 95% (41/43; 95% CI: 85-99)

Table 2. Diagnostic accuracy of 64-slice CTCA for the detection of significant coronary bifurcation lesions (≥ 50% lumen diameter stenosis as defined by quantitative coronary angiography) in evaluable segments.

	Evaluable	Sensitivity	Specificity	PPV	NPV
Patients (n	317/323	41/43	266/274	41/49	266/268
= 317)	98%	(95%, CI: 85-99)	(97%, CI: 94-98)	(84%, CI: 71-91)	(99%, CI: 97-100)
Bifurcations	1149/1218	46/48	1074/110	46/73	1074/1076
(n = 1149)	94%	(96%, CI: 86-99)	(97%, CI: 96-98)	(63%, CI: 52-73)	(99%, CI: 99-100)

Values are n (%, with 95 percent confidence interval). CI, confidence interval; CTCA, computed tomography coronary angiography; NPV, negative predictive value; PPV, positive predictive value.

Table 3. Angiographic and computed tomography characteristics of patients (n= 41) with bifurcation lesions (n= 46)

Variables	
Bifurcation lesions (n)	46
Location of bifurcation lesion	
Left main, n (%)	17 (37)
LAD/ diagonal, n (%)	22 (48)
CX/ OM, n (%)	6 (13)
RCA-PD/ RCA-PL, n (%)	1 (2)
Angiographic variables, main branch	
Lesion length (mm)	11.8 ± 6.6
Reference diameter (mm)	2.82 ± 0.53
MLD (mm)	1.14 ± 0.49
% diameter stenosis	59 ± 19
Angiographic variables, side branch	
Lesion length	6.54 ± 4.2
Reference diameter (mm)	2.34 ± 0.5
MLD (mm)	1.38 ± 0.64
% diameter stenosis	41 ± 24
Previous heart rate lowering medication (%)	82
Additional heart rate lowering drugs (%)	58
Angulation by CTCA (degrees)	60 ± 19
Angulation by ICA (degrees)	51 ± 18
Calcium score (mean ± SD)[a]	704 ± 955

CABG, coronary artery bypass graft surgery; CTCA, computed tomography coronary angiography; CX, circumflex coronary artery; ICA, invasive coronary angiography; MLD, minimal lumen diameter; OM, obtuse marginal branch; PCI, percutaneous coronary intervention; PD, posterior descendens coronary artery; PL, posterolateral branch; RCA, right coronary artery; SB, side branch.
[a]Agatston-score.

and 95% (266/280; 95% CI: 92-97) on a "patient-level" and 96% (46/48; 95% CI: 86-99) and 92% (1074/1170; 95% CI: 90-93) on a lesion level (1218 bifurcations).

The angiographic and CTCA characteristics of the patients with identified BL are shown in Table 3. Lesions were predominantly located in the left main or at the left anterior descending / first or second diagonal bifurcation. The angle between MV and SB differed significantly when assessed by CTCAwhen compared with ICA (60 ± 19 versus 51 ± 18° respectively, P<0.0001).

Table 4 describes in detail the lesion distribution in coronary bifurcations, as assessed by CTCA and ICA. In all but 2 patients, the bifurcation classification on CTCA was concordant with that on ICA (agreement between CTCA and ICA in 44/46 BLs). In one patient, ICA underestimated the severity of stenosis in the left main bifurcation and the patient was referred

Table 4. Medina bifurcation classification: comparison of invasive coronary angiography with computed tomography coronary angiography.

Medina classification	Conventional angiography	CTCA
Medina: 1.0.0 	n=10	n=10
Medina: 0.1.0 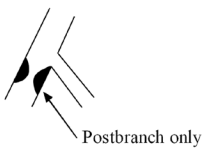	n=8	n=7 Medina 1.1.0: n=1
Medina: 1.1.0 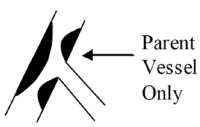	n=8	n=8
Medina: 1.1.1 	n=5	n=4 Medina 1.1.0: n=1
Medina: 0.0.1 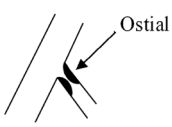	n=5	n=5
Medina: 1.0.1 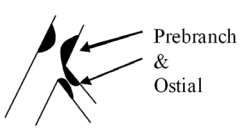	n=8	n=8
Medina: 0.1.1 	n=2	n=2

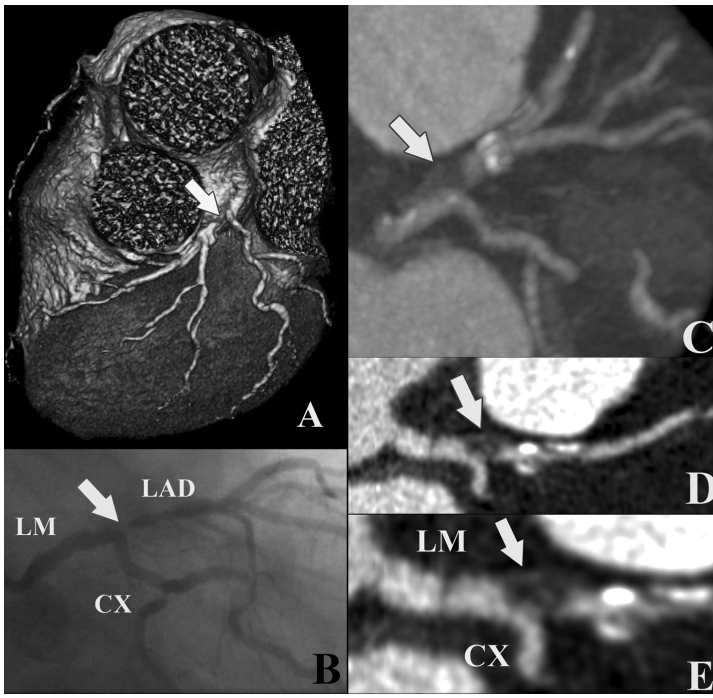

Figure 3. CT coronary angiogram and corresponding conventional angiogram in a patient presenting with unstable angina. The volume-rendered CT image (A) suggests the presence of a significant ostial narrowing (arrow) of the LAD. On ICA (B) the stenosis (arrow) was classified as Medina type 0.1.0. Maximal intensity projected (C) and multiplanar reconstructed (D and E) CT images however showed additional significant involvement of the distal LM (arrow) and thus reclassified the lesion as Medina type 1.1.0.
CX: circumflex coronary artery, LAD: left anterior descending coronary artery, LM: left main coronary artery. (A full color version of this illustration can be found in the color section).

for CABG, based on the CTCA assessment (Figure 3). In the second patient, significant involvement of the ostium of the first diagonal branch was not detected on CTCA and the lesion was classified as Medina type 1.1.0 instead of type 1.1.1.

DISCUSSION

Bifurcation lesions provide a challenge in terms of both assessment and management. Vessel overlap, foreshortening, beam attenuation (particularly in obese patients), and underopacification may hinder accurate assessment of the anatomy, particularly with respect to the assessment of ostial side branch involvement. Errors in diagnosis may have significant consequences for patient management.[10] When CABG is the treatment strategy, underestimation of a side branch lesion may inadvertently result in the side branch not being grafted. Where PCI is the preferred option, accurate anatomic information is crucial in planning the treatment strategy, to anticipate plaque shift with resulting lumen compromise.[11,12] In this study we demonstrated that in selected patients the use of 64 slice-CTCA accurately detected angiographically significant BL when compared to ICA, which is in keeping with the diagnostic accuracy of 64-CTCA to detect significant non-bifurcation coronary lesions with reported sensitivity values in the 90 to 95% range.[4,13-16]

For the purpose of percutaneous treatment of BL, several BL classifications have been used, with the aim to better define treatment strategies.[17,18] Such classifications may lead to initial treatment involving stenting of both the main and side branches (e.g. crush or culotte technique) rather than main branch stenting first, followed by provisional balloon angioplasty with or without stenting of the side branch. We have demonstrated that 64-slice CTCA accurately classified BLs when compared to ICA. Furthermore, the 3-dimensional nature of the data provided by CTCA has the potential to allow for evaluation of lesion anatomy without vessel overlap or foreshortening and hence allows detailed evaluation of BLs. Calcified BLs remain problematic due to blooming artefacts that may lead to overestimation of stenosis severity and subsequent misclassification.

The general consensus with regard to the treatment of BLs is that, ideally, the MV only should be stented, with provisional stenting of the SB where the ostium is severely compromised.[19] In situations where both branches need to be stented, the interventional approach (i.e. selection of stenting technique) is determined by the angle between the MV and SB. In our study, assessment of the bifurcation angle on CTCA was relatively straightforward. The angle determined by the 3-dimensional assessment on CTCA differed significantly from that measured on ICA. These findings are consistent with the results of a recent study demonstrating that bifurcation angles measured by CTCA were more accurate when compared with invasive angiography.[16]

Current 64-slice CT scanners are sufficiently reliable to exclude the presence of significant coronary artery stenoses. CTCA therefore seems most useful for the assessment of symptomatic patients who have a low-to-intermediate probability of significant coronary artery stenosis. A recent meta-analysis of all major published studies on 16- and 64-slice CT technology, showed that in patients with high prevalence of coronary artery disease the specificity of CT is still insufficient to allow its implementation as an alternative to ICA.[20] ICA should continue to be the preferred option in patients with typical angina and/or previously known CAD because it allows ad hoc PCI to be performed, where appropriate, and because the high prevalence of calcification in this population would hamper accurate assessment by CTCA. In the current study, the prevalence of pre-existing CAD was relatively high (50%) and severe calcifications were the main reason for uninterpretable coronary artery segments (39%, 62/158 segments) after exclusion of the 6 patients (53 segments) who had a technically inadequate CT scan. Our preliminary study provides proof of concept for the potential of CTCA to accurately detect coronary artery lesions, even in the presence of complex anatomy such as BLs.

Limitations

Although our report concerns a large consecutive series of patients who were scanned prior to ICA during a 9-month period, the retrospective nature of the study is a limitation. However,

even with a prospectively conducted study it would be difficult to prove the clinical benefit of a 'pre-interventional' CT evaluation since the optimal approach to PCI for a BL is currently unknown.

General limitations of CTCA are the additional contrast load and the considerably higher radiation exposure compared with ICA. However, these drawbacks should be balanced against the additional costs and risks of a prolonged angiographic procedure with, in general, the use of more contrast, catheters and additional invasive tools such as IVUS for assessment of difficult lesion subsets such as bifurcations.

In this study we demonstrated the feasibility of CTCA to accurately assess coronary bifurcations for the presence or absence of significant disease and we found CTCA to be more accurate than ICA for the measurement of bifurcation angles. Whether the information provided by a CT exam would influence the therapeutic strategy when attempting PCI for a BL remains unproven and needs further study.

The results of this study are only applicable to a selected patient population (patients in sinus rhythm, who are relatively young, with coronary arteries that do not contain severe calcifications) and were obtained in a center with experienced investigators.

Observations (bifurcations) within the same patient are not statistically independent. We recalculated the diagnostic accuracy parameters after random selection of a single bifurcation per patient. Sensitivity and specificity for detection of significant BLs was respectively 100% (10/10; 95% CI, 72 to 100) and 95% (296/313; 95% CI, 91 to 97). Fewer observations resulted in wider confidence intervals.

Finally, current studies reporting on the diagnostic accuracy of 64-slice CTCA in general included vessels with a reference size up to 1,5 mm. This is a reasonable threshold since smaller sized vessels usually do not constitute targets for revascularization. In this study, we limited the assessment of BL to branches with a reference diameter $\geq$ 2mm for two reasons: (i) this cut-off value is a generally accepted criterion to define clinically relevant side branches, and (ii) current spatial resolution is not sufficient for accurate plaque imaging in vessels with a reference size $<$2 mm. [17,21-24]

CONCLUSIONS

Sixty four-slice CTCA provides an accurate and comprehensive assessment of coronary bifurcation pathology in a selected patient population. These preliminary data support the poten-

tial of CTCA to replace coronary angiography as the preferred diagnostic tool for coronary imaging in this setting.

Acknowledgements
We would like to thank Eugene Mc Fadden, MD, FRCPI and Niels van Pelt, MBChB, FRACP for careful revision of the manuscript. We wish to acknowledge the contributions of Alina G. van der Giessen, MSc, Jolanda J. Kluin, MD, PhD and Jolanda J Wentzel, MD, PhD to the study.

REFERENCES

1. Topol EJ, Nissen SE. Our preoccupation with coronary luminology. The dissociation between clinical and angiographic findings in ischemic heart disease. Circulation. 1995;92:2333-42.
2. Badak O, Schoenhagen P, Tsunoda T, Magyar WA, Coughlin J, Kapadia S, Nissen SE, Tuzcu EM. Characteristics of atherosclerotic plaque distribution in coronary artery bifurcations: an intravascular ultrasound analysis. Coron Artery Dis. 2003;14:309-16.
3. Nieman K, Cademartiri F, Lemos PA, Raaijmakers R, Pattynama PM, de Feyter PJ. Reliable noninvasive coronary angiography with fast submillimeter multislice spiral computed tomography. Circulation. 2002;106:2051-4.
4. Mollet NR, Cademartiri F, van Mieghem CA, Runza G, McFadden EP, Baks T, Serruys PW, Krestin GP, de Feyter PJ. High-resolution spiral computed tomography coronary angiography in patients referred for diagnostic conventional coronary angiography. Circulation. 2005;112:2318-23.
5. Medina A, Suarez de Lezo J, Pan M. A New Classification of Coronary Bifurcation Lesions. Rev Esp Cardiol. 2006;59:183.
6. Morin RL, Gerber TC, McCollough CH. Radiation dose in computed tomography of the heart. Circulation. 2003;107:917-22.
7. Ellis SG, Vandormael MG, Cowley MJ, DiSciascio G, Deligonul U, Topol EJ, Bulle TM. Coronary morphologic and clinical determinants of procedural outcome with angioplasty for multivessel coronary disease. Implications for patient selection. Multivessel Angioplasty Prognosis Study Group. Circulation. 1990;82:1193-202.
8. Austen WG, Edwards JE, Frye RL, Gensini GG, Gott VL, Griffith LS, McGoon DC, Murphy ML, Roe BB. A reporting system on patients evaluated for coronary artery disease. Report of the Ad Hoc Committee for Grading of Coronary Artery Disease, Council on Cardiovascular Surgery, American Heart Association. Circulation. 1975;51:5-40.

9. Costa RA, Mintz GS, Carlier SG, Lansky AJ, Moussa I, Fujii K, Takebayashi H, Yasuda T, Costa JR, Jr., Tsuchiya Y, Jensen LO, Cristea E, Mehran R, Dangas GD, Iyer S, Collins M, Kreps EM, Colombo A, Stone GW, Leon MB, Moses JW. Bifurcation coronary lesions treated with the "crush" technique: an intravascular ultrasound analysis. J Am Coll Cardiol. 2005;46:599-605.
10. Green NE, Chen SY, Hansgen AR, Messenger JC, Groves BM, Carroll JD. Angiographic views used for percutaneous coronary interventions: a three-dimensional analysis of physician-determined vs. computer-generated views. Catheter Cardiovasc Interv. 2005;64:451-9.
11. Meier B, Gruentzig AR, King SB, 3rd, Douglas JS, Jr., Hollman J, Ischinger T, Aueron F, Galan K. Risk of side branch occlusion during coronary angioplasty. Am J Cardiol. 1984;53:10-4.
12. Fischman DL, Savage MP, Leon MB, Schatz RA, Ellis S, Cleman MW, Hirshfeld JW, Teirstein P, Bailey S, Walker CM, et al. Fate of lesion-related side branches after coronary artery stenting. J Am Coll Cardiol. 1993;22:1641-6.
13. Leschka S, Alkadhi H, Plass A, Desbiolles L, Grunenfelder J, Marincek B, Wildermuth S. Accuracy of MSCT coronary angiography with 64-slice technology: first experience. Eur Heart J. 2005;26:1482-7.
14. Leber AW, Knez A, von Ziegler F, Becker A, Nikolaou K, Paul S, Wintersperger B, Reiser M, Becker CR, Steinbeck G, Boekstegers P. Quantification of obstructive and nonobstructive coronary lesions by 64-slice computed tomography: a comparative study with quantitative coronary angiography and intravascular ultrasound. J Am Coll Cardiol. 2005;46:147-54.
15. Raff GL, Gallagher MJ, O'Neill WW, Goldstein JA. Diagnostic accuracy of noninvasive coronary angiography using 64-slice spiral computed tomography. J Am Coll Cardiol. 2005;46:552-7.
16. Pflederer T, Ludwig J, Ropers D, Daniel WG, Achenbach S. Measurement of coronary artery bifurcation angles by multidetector computed tomography. Invest Radiol. 2006;41:793-8.
17. Lefevre T, Louvard Y, Morice MC, Dumas P, Loubeyre C, Benslimane A, Premchand RK, Guillard N, Piechaud JF. Stenting of bifurcation lesions: classification, treatments, and results. Catheter Cardiovasc Interv. 2000;49:274-83.
18. Popma J, Bashore T. Qualitative and quantitative angiography- Bifurcation lesions. In: Topol E, ed. Textbook of interventional cardiology. 1994;Philadelphia: W.B. Sounders; 1994.: p. 1055-8.
19. Steigen TK, Maeng M, Wiseth R, Erglis A, Kumsars I, Narbute I, Gunnes P, Mannsverk J, Meyerdierks O, Rotevatn S, Niemela M, Kervinen K, Jensen JS, Galloe A, Nikus K, Vikman S, Ravkilde J, James S, Aaroe J, Ylitalo A, Helqvist S, Sjogren I, Thayssen P, Virtanen K, Puhakka M, Airaksinen J, Lassen JF, Thuesen L. Randomized study on simple versus complex stenting of coronary artery bifurcation lesions: the Nordic bifurcation study. Circulation. 2006;114:1955-61.

20. Hamon M, Biondi-Zoccai GG, Malagutti P, Agostoni P, Morello R, Valgimigli M. Diagnostic performance of multislice spiral computed tomography of coronary arteries as compared with conventional invasive coronary angiography: a meta-analysis. J Am Coll Cardiol. 2006;48:1896-910.
21. Williams DO, Abbott JD. Bifurcation intervention: is it crush time yet? J Am Coll Cardiol. 2005;46:621-4.
22. Pan M, Suarez de Lezo J, Medina A, Romero M, Segura J, Ramirez A, Pavlovic D, Hernandez E, Ojeda S, Adamuz C. A stepwise strategy for the stent treatment of bifurcated coronary lesions. Catheter Cardiovasc Interv. 2002;55:50-7.
23. Al Suwaidi J, Berger PB, Rihal CS, Garratt KN, Bell MR, Ting HH, Bresnahan JF, Grill DE, Holmes DR, Jr. Immediate and long-term outcome of intracoronary stent implantation for true bifurcation lesions. J Am Coll Cardiol. 2000;35:929-36.
24. Iakovou I, Ge L, Colombo A. Contemporary stent treatment of coronary bifurcations. J Am Coll Cardiol. 2005;46:1446-55.

13

Computed Tomography in Total Coronary Occlusions (CTTO Registry): Radiation Exposure and Predictors of Successful Percutaneous Intervention

Héctor M. García-García[1], Carlos A.G. Van Mieghem[1], Nieves Gonzalo[1], Willem B. Meijboom[1], Annick C. Weustink[1], Yoshinobu Onuma[1], Nico R. Mollet[1], Carl Johann Schultz[1], Emanuele Meliga[1], Martin van der Ent[1], Georgios Sianos[1], Dick Goedhart[2], Ad den Boer[1], Pim J. de Feyter[1], Patrick W. Serruys[1]

[1]Thoraxcenter, Erasmus Medical Center, Rotterdam, the Netherlands. [2]Cardialysis BV, Rotterdam, the Netherlands

Eurointerv. 2008, in press

ABSTRACT

Objectives

We investigated angiographic and computed tomography coronary angiography (CTCA) predictors of success and measured the amount of the radiation exposure in patients with chronic total occlusion (CTO), treated by percutaneous coronary intervention (PCI).

Background

There is no mention -in current appropriateness criteria for CTCA- of the need of CTCA investigation prior to an attempt at recanalization of a CTO.

Methods

Symptomatic patients due to a CTO, suitable for percutaneous treatment were included.

Results

One hundred and thirty nine (142 CTOs) patients were studied. Overall success rate was 62.7%. By CTCA, the occlusion length was 24.9±18.3 vs. 30.7±20.7mm in successful and failure cases (p=0.1), but the frequency of patients with an occlusion length >15 mm was different, ie, 63.2% vs. 82.7%, respectively (p=0.02). Severe calcification, (> 50% of the vessel cross sectioneal area) was more prevalent in failure cases (54.7% vs. 35.9%, p=0.03). Calcification at the entry of the occlusion was present in 58.5% of the failure cases vs. 41.6% of the successful cases (p=0.04), while calcium at the exit was not different.

The length of calcification was 8.5±8.4 vs. 5.5±6.6mm in the failure and successful cases respectively (p=0.027). By multivariable analysis, the only independent predictor of procedural success was the absence of severe calcification as defined by CTCA.

The mean effective radiation dose of the PCI was 39.3±30.1mSv. The mean effective radiation dose of the CT scan was 22.4 mSv: 19.2 ± 6.5 mSv for CTCA, 3.2 ± 1.7 mSv for the calcium scoring scan.

Conclusion

More severe calcified patterns, as assessed by CTCA, are seen in failure cases. The radiation exposure during a CT scan prior to PCI for a CTO is considerable, and further studies are required to determine whether this extra diagnostic study is warranted.

INTRODUCTION

Since success rate has remained unchanged over the last few years, there has been a decrease in the number of attempted percutaneous coronary interventions (PCI) in patients with chronic total occlusions (CTO)(1). In the search for new therapeutic approaches to reopen the occluded vessel many new CTO-dedicated guidewires and devices have become available(2). Until recently, innovative imaging tools to provide the operator guidance during the most exacting phase of the procedure, i.e. crossing the lesion, have been lacking. Commonly, in angiography these lesions appear as missing segments within two vessel ends. In addition, the angiogram does not provide reliable information with regard to the trajectory of the occluded segment, its length and tissue composition, variables that have been correlated with low procedural success rate(3). Computed tomography coronary angiography (CTCA) has developed into a reliable noninvasive technique to evaluate a patient for the presence of obstructive coronary artery disease(4). Although, preliminary data suggest that CTCA might be of beneficial guidance in attempting revascularization of a CTO (5), there is no mention -in current appropriateness criteria for CTCA, of the need of a CTCA investigation prior to an attempt at recanalization of a CTO.

To better define the role of CTCA in the treatment of patients with CTOs, we performed CTCA in a consecutive cohort of eligible patients who were scheduled for percutaneous recanalization of a CTO. We investigated angiographic and computed tomographic predictors of success and measured the amount of contrast material used during PCI and CTCA as well as the radiation exposure for both techniques.

MATERIAL AND METHODS

Study population

Between April 2002 and March 2007, those eligible for this study included all consecutive patients presenting with symptomatic coronary artery disease due to a CTO. Specifically, patients without contra-indications for CTCA, suitable for percutaneous treatment who had provided written informed consent, were included. CTCA was considered contra-indicated in following situations: irregular heart rhythm, inability to sustain a sufficiently long breath hold (20 seconds with the 16-slice CT scanner, 15 seconds with the 64-slice or dual-source CT scanner), renal dysfunction (creatinine clearance < 60 ml/min as defined with the Cockroft formula)(6), hearing disability, and known contrast allergy.

A CTO was defined as either an occlusion on angiography with no antegrade filling of the distal vessel other than via collaterals or minimal antegrade flow (TIMI flow 0 or 1)(7,8). All in-

cluded patients had a native vessel occlusion estimated to be at least of three months duration based on either a history of sudden chest pain, a previous acute myocardial infarction in the same target vessel territory, or the time between the diagnosis made on coronary angiography and PCI. The type of CTO was either de novo or due to in-stent restenosis.

The protocol was approved by the local ethics committee and is in accordance with the principles of Good Clinical Practice for Trials of Medicinal Products in the European Community and the Declaration of Helsinki. All patients signed a written informed consent.

All the CT scans were discussed between the operator of CTO procedure and someone trained to interpreting CTCA prior to the interventional procedure.

All interventional procedures were performed by operators who were highly experienced in the treatment of CTOs, with the interventional strategy left to the discretion of the operator. Wires were used in a stepwise progression, starting with a wire that had a relatively less traumatic tip (Graphix Intermediate, Boston Scientific Corporation, Miami, Florida) or a hydrophilic wire (Choice PT Plus, Boston Scientific Corporation, or Crosswire NT, Terumo Corporation, Tokyo, Japan) and progressing to stiffer wires (Miracle, Asahi Intec, Nagoya, Japan) and specialized technologies (Safe-Cross, Intraluminal Therapeutics, Carlsbad, New Mexico; The CROSSERTM CTO Recanalization System (FlowCardia Inc, CA; Laser Guidewire, Spectranetics, Colorado Springs, CO, USA). Detailed description of these devices and explanation of our approach to treat CTO patients has been previously reported(2).

Procedural failure was defined as the inability to cross the occlusion with a guidewire.
All patients were pretreated with 300mg of clopidogrel, which was continued at a dose of 75 mg/day for 6 months. All patients were advised to maintain aspirin (≥ 80 mg/day) lifelong.

Definitions

Procedural success: defined as successful opening of the chronic occlusion and restoration of flow (<50% residual stenosis and TIMI 2-3 flow).

Type of CTO: defined according to two characteristics, location (native vessel vs. graft) and quality (de novo or in-stent restenosis).

Occluded length: defined as the non-contrast enhanced segment of the vessel from the proximal to the distal end of the occlusion in the least foreshortened view on angiography or the 3-dimensional measurement of the occlusion using a dedicated software program (Circulation®, Siemens, Germany) of the CT workstation (Leonardo).

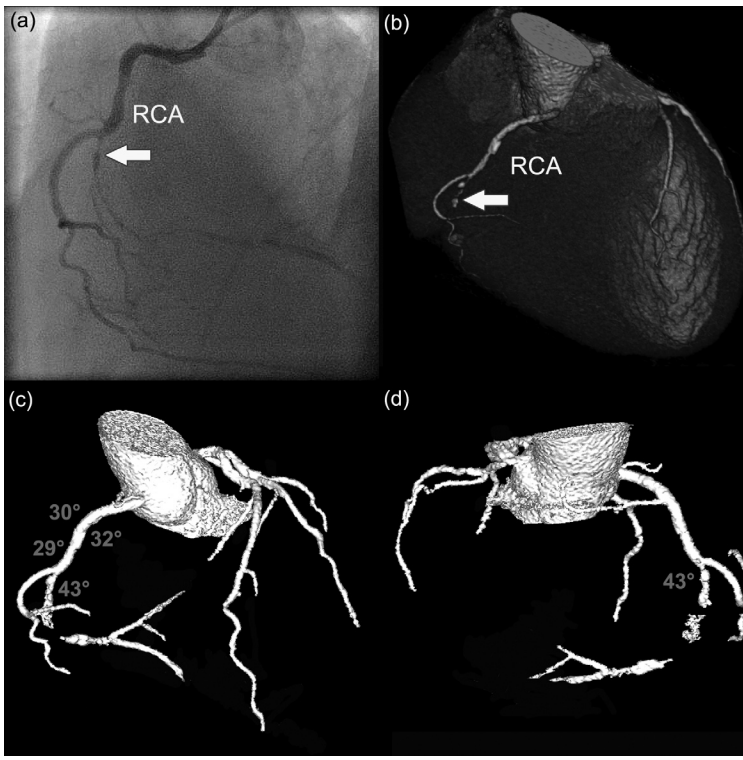

Figure 1. Assessment of tortuosity by computed tomography coronary angiography. (a) Angiographic image showing an occlusion (arrow) of the right coronary artery (RCA). (b) Volume-rendered CT image of the RCA, showing the occlusion (arrow) distal to the origin of the margo acutis. (c) 3-dimensional CT angiographic view of the coronary vasculature, illustrating the tortuosity of the vessel before the occlusion, with 4 consecutive bends. (d) same image as panel c but looking at the vessel from posterior; the final bend before the start of the occlusion is marked (43 degrees). (A full color version of this illustration can be found in the color section).

Stump morphology: defined as the entry site of the occlusion that has either a tapered- (central or eccentric) or a blunt appearance.

Side branch at the entry site: defined as the presence of any side branch, irrespective of the size, within 3 mm proximal to the entry of the occlusion.

Bridging collaterals: presence of multiple small collaterals connecting the proximal and distal lumens of the vessel by spanning through or around the occluded segment. This characteristic can only be measured by conventional angiography (CA).

Occlusion ends in bifurcation: the presence of a side branch larger than 1.5 mm within 3 mm distally to the distal end of the occlusion.

Rentrop classification(9): grading of collateral filling was as follows: 0 = none, 1 = filling of side branches only, 2 = partial filling of the epicardial segment, 3 = complete filling of the epicardial segment. This classification only applies for conventional angiography since in CTCA the distal part of the vessel is almost always filled with contrast and thus can be regarded as Rentrop class 2 or 3.

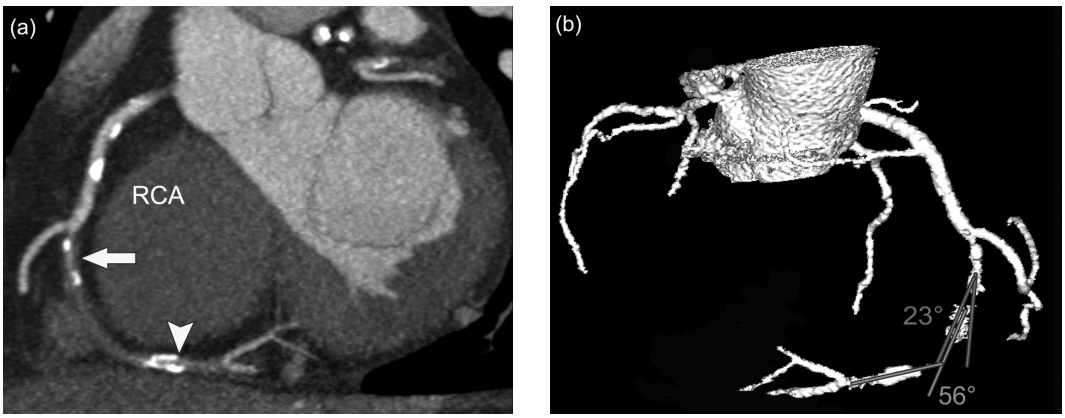

Figure 2. (a) Assessment of angulation by computed tomography coronary angiography.
Maximal intensity projection of the right coronary artery (RCA) showing the vessel with the entry (arrow) and exit side (arrowhead) of the occlusion in one plane. (b) 3-dimensional CT angiographic view, illustrating the angulation within the occlusion; in this case 2 bends are visible.

Calcification: was defined as follows:

- By conventional angiography, defined as mild, moderate or severe.
- By CTCA, the number of separate calcium spots was counted and their length measured. The presence of calcium at the entry and exit side of the occlusion was annotated. All the spots were evaluated in a cross-sectional view to assess whether the calcification occupied more than 50% of the cross-sectional vessel area at any location within the occluded vessel segment. Finally, the amount of calcium in the occluded segment was quantified, using dedicated software.

Tortuosity: was defined as the presence of bends proximal to the lesion. By angiography, this feature was only scored in a binary fashion (yes/no), i.e. < or > than 45 degrees, while by CT, the angle of all the separate vessel bends was measured. (Figure 1).

Angulation: was defined as the presence of bends within the occluded segment. By angiography, only a binary scoring system was used (yes/no), while by CT, the angle was measured in subsequent bends within the occlusion. (Figure 2).

Conventional coronary angiography (CCA)

Two experienced observers who were unaware of the results of the CT scans analyzed each film; consensus was needed for each assessed parameter. Quantitative angiographic analysis (CAAS II, Pie Medical, Maastricht, The Netherlands) was performed to measure the vessel diameter prior to the occlusion side. The length of the occluded vessel segment was also quantified. The other variables, i.e. location of the occlusion, morphology of the stump, the

presence of a side branch in the vicinity of the entry (<3 mm), collaterals and calcification were reported qualitatively.

Conventional coronary angiography: calculation of effective dose(10).

The Axiom study reports for each PCI procedure the used projections, the geometrical gantry settings and the generator settings for each digital cinematography (DCM), the used fluoroscopy time and the total dose-area product (DAP). The DAP is measured by an integral device in the x-ray tube, placed after the filters and the collimator and takes into account the quality, quantity, size and duration of the used x-ray beam.

A PC-based X-ray Monte Carlo program, from the Radiation and Nuclear Safety Agency – Helsinki – Finland, PCXMC, (reference Tapiovaara M, Lakkisto M, Servomaa A. A PC-Based Monte Carlo Program for calculating Patient Doses in Medical X-Ray Examinations. STUK-A139. Radiation and Nuclear Safety Agency, Helsinki, 1997) was used to estimate effective doses from conventional angiography. We did not correct for each gantry setting. We assumed all radiation was given in the Left Anterior Oblique 30 (LAO 30) projection, while the effective dose with careful simulation of all used gantry settings during DCM and fluoroscopy differed <2%. The focus-skin distance was 65 cm and the estimated entrance field size was 95 cm2 with a quality of 70 kV.

CT patient selection, scan protocol and image reconstruction

A cardiac CT scan was performed in the fortnight before PCI. During the described study period 3 successive scan generations were used in our center. Up to July 2004, CT data were acquired using a 16-slice CT scanner (Sensation 16, Siemens, Germany). From August 2004 to March 2006, CT data were acquired using a 64-slice CT scanner (Sensation 64, Siemens, Germany) and from April 2006 on the latest dual-source CT scanner (Somatom Definition, Siemens, Germany) was used. In the period until March 2006 we systematically slowed down the heart rate in patients with a heart rate above 65 bpm, using 100 mg metoprolol or a non-dihydropyridine calcium-antagonist (diltiazem 60-120 mg) orally 1 hour before the scan. An additional IV bolus of metoprolol (5-10 mg) was occasionally administered where the heart rate remained above 65 bpm. After that period we did not use extra medication to slow down the heart rate. Instead, nitrates were systematically given as a sublingual spray (0.4 mg) to all patients 5 minutes before initiation of the scan provided the systolic blood pressure was above 100 mmHg.

Scan parameters for each of the 3 scanner types were the following:

- 16-slice CT scanner: collimation 16 x 0.75 mm, tube rotation time 375 ms, tube voltage of 120 kV, table feed 3 mm per rotation. For the non-enhanced scan we used a tube current of 150 mAs and applied prospective x-ray tube modulation. For the angiographic

scan we used a tube current that ranged between 500 and 600 mAs without the use of dose pulsing.
- 64-slice CT scanner: collimation 64 x 0.6 mm, tube rotation time 330 ms, tube voltage of 120 kV, table feed 3.8 mm per rotation. For the non-enhanced scan we used a tube current of 150 mAs and applied prospective x-ray tube modulation. For the angiographic scan we used a tube current that ranged between 850 and 960 mAs without the use of dose pulsing.
- dual-source CT scanner: collimation 64 x 0.6 mm, tube rotation time 330 ms, tube voltage of 120 kV. For the non-enhanced scan we used a tube current of 84 mAs per tube and full X-ray tube current was given during 50-70% of the RR interval. For the angiographic scan we used a tube current of 412 mAs per tube and limited this amount of tube current to 25-70% of the RR-interval. Pitch values were adapted to heart rate (minimal pitch value of 0.2 for slow heart rates, up to a maximal pitch value of 0.45 with higher heart rates).

The contrast-enhanced scan was obtained after the intravenous injection of 70-100 ml of contrast material (iomeprol, 400 mg iodine/ml, Iomeron® with the 16- and 64-slice CT scanner or iopromide, 370 mg iodine/ml, Ultravist® with the dual source CT scanner) through a large antecubital vein at a flow rate of 4-5 ml/sec, followed by 40ml of saline flush at 4 ml/s. A bolus tracking technique was used to monitor the appearance of contrast material in the ascending aorta. Once the signal in the ascending aorta reached a predetermined density level of 100 Hounsfield units, CT acquisition was automatically started during an inspiratory breath hold. Images were reconstructed using ECG-gating to obtain optimal, motion free image quality.

The scan data were reconstructed at various phases of the cardiac cycle using medium-to-smooth (B26f) and sharp (B46f) convolution kernel. Image reconstruction was retrospectively gated to the ECG. The position of the reconstructed window within the cardiac cycle was individually optimized to minimize motion artifacts. Datasets containing no or minimal motion artifacts were transferred to a remote workstation (Leonardo workstation, Siemens). for further evaluation.

CT coronary angiography: calculation of effective dose.

The effective radiation dose was calculated from the scan parameters using dedicated software (ImPACT CT Patient Dosimetry Calculator, version 0.99x), as described in the European Guidelines on Quality Criteria for Computed Tomography (Available at: http://www.drs.dk/guidelines/ct/ quality/index.htm).

CT data analysis

Two experienced observers independently evaluated the CT data sets on both the original axial images and on multiplanar reformatted reconstructions for the presence of an occluded

vessel. This initial assessment was performed blinded to the angiographic data. Subsequently, the observer was provided with the angiographic information, i.e. the occluded vessel in which PCI was performed, without having access to the angiographic images. After confirmation of the right vessel, the further CT analysis was performed without knowledge of the angiographic characteristics of the occluded vessel. In a few occasions, especially in case of heavy calcifications of the vessel, angiographic information on the start and end of the occlusion was provided to allow calculation of the occlusion length. To measure the length of the occlusion on CT we used a dedicated software program (Circulation®, Siemens, Germany), which allows creating a central lumen line through the vessel. By rotating the vessel around this line the exact entry- and exit point of the occlusion can be visualized, thus allowing to measure the length of the occlussion along the 3-dimensional vessel path without foreshortening. (Figure 3).

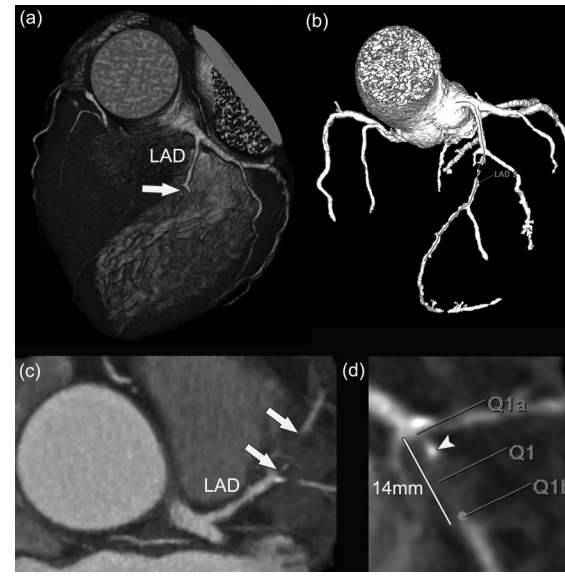

Figure 3. Measurement of the length of the occlusion by computed tomography coronary angiography. CT images showing an occlusion of the left anterior descending coronary artery (LAD). (a) Volume-rendered image showing the proximal part of the occlusion (arrow). (b) Using the Circulation® software the entire coronary tree can be extracted from the dataset. The start and end points for the vessel to be examined, in this example the LAD, are marked and a centerline through the middle of the vessel is displayed and labeled between these 2 points. (c) Maximal intensity projection showing the approximate length and composition, in this case non-calcified, of the occlusion. (d) After defining the centerline of the vessel, features of the occlusion such as length and composition can be evaluated. The markers Q1a and Q1b set the boundary marker at the beginning and end of the occlusion, which in this case measures 14mm. The proximal part of the occlusion shows a small amount of calcium (arrowhead).(A full color version of this illustration can be found in the color section).

Statistical analysis

Assumptions for normality were checked by Kolmogorov-Smirnov test and by visual assessment of Q-Q plots of residuals. Accordingly, log transformation was performed on the variables with skewed distribution. Continuous variables are presented as mean ± 1SD and differences were compared using Student t test or Mann Whitney test. Categorical variables are presented as counts and percentages and differences were assessed by Fisher exact test or chi-square test, as appropriate. A two-sided p value of less than 0.05 indicated statistical significance.

The following variables were included in the multivariable analysis dataset: baseline characteristics (gender, age, diabetes mellitus, previous myocardial infarction, family history of coronary artery disease, smoking, hypertension, hypercholesterolemia, previous PCI and

Table 1. Baseline characteristics, n=139

Age, yrs (mean+1SD)	60.7±10.8
Male (%)	87.3
Diabetes mellitus (%)	13.4
Hypertension (%)	40.1
Family history of CHD (%)	33.8
Current smoking (%)	23.9
Hypercholesterolemia (%)	50.0
Previous ACS (%)	40.8
Previous PCI (%)	20.4
Previous CABG (%)	7.7
Vessel disease (%)	
One vessel disease	51.4
Two vessel disease	31.7
Three vessel disease	16.9
Attempts to reopen the CTO (%)	
First	95.1
Second	4.9

SD, standard deviation; CHD, cardiovascular heart disease; ACS, acute coronary syndrome; PCI, percutaneous coronary intervention; CABG, coronary artery bypass graft.

previous coronary artery bypass surgery, vessel disease and target vessel), conventional angiographic characteristics (ostial location, stump morphology, presence of bridging collaterals, presence of sidebranch at the entry of the occlusion, degree of calcification and tortuosity (yes/no); and CTCA characteristics (ostial location, stump morphology, presence of sidebranch at the entry of the occlusion, calcification - at entry, at exit, >50% CSA, length of the calcification –, angulation – as continuous variable -, tortuosity – as continuous variable- and length of the occlusion – as continuous variable). Due to collinearity problems some variables were removed from the model. On the remainder of the variables we ran a backward selection procedure.
Statistical analyses were performed with use of SAS V8.02.

RESULTS

One hundred and thirty nine (142 CTOs) consecutive patients were enrolled in this prospective registry of patients treated for a chronic total occlusion.

The mean age was 60.7±10.8 years, most of the patients being male (87.3%) (Table 1). For the majority of the patients (95.1%) this was the first attempt to open the CTO. Most of the occlusions were de novo lesions and the most frequently treated coronary artery was the left anterior descending (Table 2). Overall success rate was 62.7%.

CTO characteristics by conventional coronary angiography and CTCA

By conventional coronary angiography, the mean vessel diameter was larger in successful procedures (2.9±0.4 vs 2.1±0.7, p=0.02) as compared to procedural failures. Overall the length of the occlusion was 16.6±12.8mm and there was no difference in successful vs. unsuccessful cases (16.0±12.7 and 18.0±13.4, p=0.5). The presence of a sidebranch at the entry was more frequently seen in failure cases (84.9 vs. 69.7%, p=0.03). Conversely, the presence of bridging collaterals was more frequently seen in successful cases (59.5 vs. 43.4%,

Table 2. Morphologic CTO characteristics, n=142 leasions

	Total	Failure, n=53	Success, n=89	p value
Conventional Angiography characteristics				
Type of CTO (%)				
De novo	94.4	92.5	95.5	0.6
Target vessel (%)				0.5
Left anterior descending	42.3	50.9	37.1	
Left circumflex	13.4	11.3	15.7	
Right coronary artery	42.3	35.9	46.1	
Occluded length (mean±1SD)	16.6±12.8	18.0+13.4	16.0+12.7	0.5
Ostial location (Y/N) (%)	17.8	20.8	15.7	0.4
Stump morphology (%)				0.8
Central	28.2	28.3	28.1	
Eccentric	26.1	24.5	34.8	
Blunt	37.3	41.5	34.8	
Side branch at entry (Y/N) (%)	75.4	84.9	69.7	0.03
Bridging collaterals (Y/N) (%)	53.5	43.4	59.5	0.04
Collateral filling [Rentrop Classification (%)]				0.45
0/1	21.5	22.7	13.5	
2	31.0	30.1	31.5	
3	42.3	37.7	44.9	
Angiographic calcification (%)				0.05
None/mild	40.1	39.6	40.4	
Moderate	32.4	22.6	38.5	
Severe	19.7	28.3	14.6	
Tortuosity (>45), (%)	45.8	43.4	47.2	0.58
Occlusion ends in bifurcation (Y/N)	23.2	17.0	27.0	0.18
Computed tomography angiographic characteristics				
Occluded length (mean±1SD)	27.1±19.4	30.7+20.7	24.9+18.3	0.1
Ostial location (Y/N) (%)	14.8	15.0	14.6	0.9
Stump morphology (%)				0.28
Central	16.4	17.0	15.7	
Eccentric	22.1	15.1	25.8	
Blunt	61.4	67.9	56.2	
Side branch at entry (Y/N)	42.3	43.4	41.6	0.8
Collateral filling [Rentrop Classification (%)]				
0/1				
2				

3	100	100	100	1
Number of spots of calcium (%)				0.69
No	27.5	22.6	30.3	
One spot	43.0	46.2	40.4	
Two spot	19.0	18.9	19.1	
Three o more	10.5	11.3	10.1	
Calcium at the entry (%)	52.1	58.5	41.6	0.04
Calcium at the exit (%)	35.9	39.6	33.7	0.6
Calcium >50% CSA (Y/N) (%)	43.0	54.7	35.9	0.03
Calcium score of the occluded segment				
Volume (mm3)	123.6±323.8	142.5±224.4	112.0±373.7	0.7
Equivalent mass (g)	25.0±81.0	24.5±33.4	25.4±100.1	0.9
Score (Agatston)	139.0±411.5	142.6±258.1	136.9±484.9	0.9
Tortuosity (%)				0.8
No	8.5	11.3	6.7	
One bend	43.3	41.5	43.8	
Two bends	31.2	26.4	33.7	
Three o more bends	12.8	15	11.2	
Angulation (%)				0.04
No	65.2	53.8	72.1	
One bend	29.7	40.4	23.3	
Two bends	1.4	0	2.3	
Three o more bends	3.6	5.7	2.3	

CTO, chronic total occlusion; CSA, cross-sectional area.

p=0.04). Severe calcification, as defined qualitatively, was more prevalent in failure cases (28.3 vs. 14.6%, p=0.05). (Table 2)

By CTCA, the occlusion length was widely dispersed, mean 27.1±19.4mm (range 2.6 to 93.4 mm) and longer as compared with CA. Although the occlusion length did not differ in successful as compared to failure cases (24.9±18.3 and 30.7±20.7, p=0.1), the frequency of patients with an occlusion length >15 mm was significantly different, i.e. 63.2% in those with procedural success vs. 82.7% in those with procedural failure (p=0.02).

CTOs without calcification were present in 27.5% of the treated lesions. The presence of severe calcification, defined as calcium that occupies more than 50% of the vessel cross-sectional area, was more prevalent in failure cases (54.7%) as compared to patients with a successful PCI procedure (35.9%) (p=0.03). The length of the calcified segments was longer in failure cases as compared to success cases (8.5±8.4 vs. 5.5±6.6mm, p=0.027).

Table 3. Comparison between CT calcium score and angiographic calcification score

CTCA calcium scoring	Angiographic scoring	Mean	SD	Min	Max
Volume (mm3)	None or mild	69.7	±103.1	1.9	462
	moderate	207.7	±546.0	3.3	2712.5
	Severe	122.9	±123.5	7.5	578
	p value	0.3			
Equivalent mass (g)	None or mild	12.6	±16.6	0	60.16
	moderate	39.5	±138.1	0	726.95
	Severe	31.7	±40.2	1.64	179.5
	p value	0.4			
Agatston score	None or mild	70.3	±97.5	0.8	371.2
	moderate	263.1	±707.7	1.1	3515.8
	Severe	111.2	±63.9	8.5	223.4
	p value	0.2			

CTCA, computed tomography coronary angiography; SD, standard deviation; Min, minimum; Max, maximum

When calcifications were present in the CTO, it was especially located at the entry side of the occlusion. Interestingly, calcification at the entry of the occlusion was present in 58.5% of the failure cases as compared to 41.6% of the successful cases (p=0.04), while the frequency of calcium at the exit was not different between the two patient groups. The absence of angulation in the occlusion was also a predictor of favourable outcome: procedural success was 72.1% in CTOs without angulation as compared to 53.8% in angulated CTOs (p=0.04) (Table 2).

Of note, the calcification patterns are affected by age but similar between genders (data not shown). Patients with severe calcification (>50% VCSA) were older than their counterparts (63.9±9.0 vs. 58.3±11.4, p=0.002). Patients with longer calcification segments (cut-off set on >4.3mm – median of the length of calcified segments in this population) were also older (63.4±9.7 vs. 55.8±11.2, p=0.005). Patients with calcification at the entry of the occlusion segment were 61.4±10.2 vs. 55.4±10.6 year old, p=0.0007, and also patients with calcification at the exit were older 62.6±9.5 vs. 55.9±10.7 year old, p<0.0001.

In table 3, a comparison between CCA and CTCA for the detection of calcium in the occlusion is shown. Conventional CA appears to be imprecise when assessing the presence and amount of calcium within the occlusion since the qualitative angiographic score did not correlate with the different CT calcium score indices (i.e. volumetric score, equivalent mass or Agatston calcium score).

Table 4. Angiographic and tomographic predictors of success: multivariate analysis

	Coefficient	OR	95% CIs		p value
Previous PCI	-1.6	0.2	0.034	1.215	0.08
Side branch at the entry (CCA)	-1.9	0.15	0.02	1.184	0.07
Tortuosity (CTCA)	-0.01	0.99	0.969	1.002	0.09
Calcification >50% VCSA (CTCA)	-1.8	0.17	0.036	0.747	0.02

CCA, conventional coronary angiography; CI, confidence interval; CTCA, computed tomography coronary angiography; OR, odds ratio; PCI, percutaneous coronary intervention; VCSA, vessel cross sectional area.

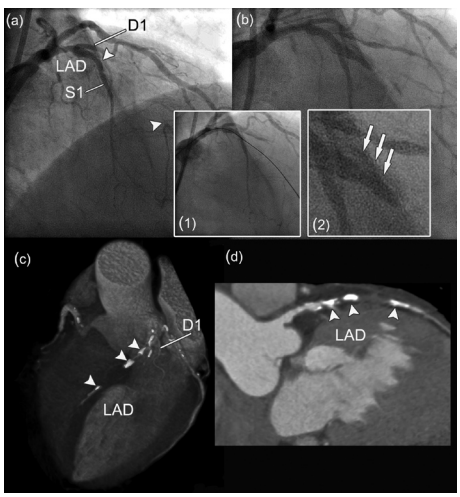

Figure 4. Assessment of calfication by computed tomography coronary angiography. Failed percutaneous coronary intervention in a patient with a chronic total occlusion of the left anterior descending coronary artery (LAD). (a) The angiographic borders of the occlusion are marked by arrows. (b) Final angiographic image showing persistent occlusion of the LAD. Insets show the wiring through the occlusion (inset 1) that appears to be in the false lumen as illustrated by the presence of contrast extravasation (arrows) once the wire is removed. (c) The volume-rendered CT image clearly shows heavy calcifications within the occluded segment (arrowheads). (d) Curved multiplanar reconstruction again highlighting the large calcifications (arrowheads) within the occlusion. D1, first diagonal branch. S1, septal branch. (A full color version of this illustration can be found in the color section).

In the multivariable analysis the only variable that remained a significant predictor of procedural success, was the absence of severe calcification, i.e. calcium occupying >50% of the vessel CSA, as defined by CTCA (table 4 and figure 4).

Procedure related characteristics and effective radiation dose (Table 5)

Overall, the mean amount of contrast used was 455.4 ± 202 ml and was not different between the patient treatment groups. The fluoroscopic time was higher in the failure cases as compared to the successful cases, 72.5 versus 53.1 minutes respectively, p=0.007. The mean effective radiation dose of the PCI procedure was 39.3±30.1mSv. The mean effective radiation dose of the preprocedural CT scan was 22.4 mSv: 19.2±6.5 mSv for the contrast-enhanced scan, 3.2±1.7 mSv for the calcium scoring scan. The mean effective radiation dose per scanner type was: 14.4±5.7mSv for 16-slice CTCA (n= 34 patients), 20.1±1.6 mSv for 64-slice CTCA (n=42 patients) and 21.8±6.5 mSv for dual-source CTCA (n= 63 patients).

Table 5. Procedure related characteristics and radiation parameters, n=142 lesions

	Total	Failure, n=53	Success, n=89	p value
Number of stents in the target vessel	1.8±1.4	0.7±0.9	2.9±1.3	<0.001
Average target vessel stent length (mm)	23.2±5.2	19.9±6.1	24.4±4.6	0.002
Average target vessel stent diameter (mm)	3.0±0.5	3.3±0.6	3.1±0.7	0.46
Biplane use (%)	70.8	76.6	68.8	0.4
Contrast used (ml)	455.4±201.9	457.8±214.7	454.2±195.8	0.93
Procedure time (min)	132.2±57.3	143.9±60.3	125.3±54.7	0.06
Fluoroscopic time (min)	60.3±40.1	72.5±41.9	53.1±37.5	0.007
Dose area product PCI (cGy*cm2)	16171.6±11539.0	17598±13765	15240±9814	0.3
Effective dose PCI (mSv)	39.26±30.1	42.5±36.5	37.1±25.1	0.34
Calcium scoring ctdi	10.5±5.1	10.1±5.8	10.7±4.8	0.6
Calcium scoring dlp	159.6±80.3	153.9±88.1	162.7±76.2	0.6
Effective dose calcium scoring (mSv)	3.2±1.7	3.1±1.8	3.3±1.6	0.5
CT ctdi	62.9±18.6	64.1±20.7	62.4±17.4	0.6
CT dlp	938.0±316.6	977.7±335.9	917.6±305.3	0.3
Effective dose CT (mSv)	19.2±6.5	20±7.1	18.8±6.2	0.3

CT, computed tomography; ctdi, computed tomography dose index; dlp, dose length index; mSv, milliesievert;

DISCUSSION

In this registry of 139 patients we evaluated the possible role of CTCA when attempting PCI of CTOs. We found that the distribution rather than the amount of calcium impacts on the procedural outcome of this particular group of patients. Not unexpectedly, CTCA was more accurate than CCA for defining the morphological features of CTOs. In particular, we found that the assessment of calcification by CTCA was more predictive of success than CCA in the multivariate model. It is difficult to prove the added value of a preprocedural CT scan in terms of procedural outcome. However, it is fair to say that a better understanding of the anatomical features of an occluded vessel can modify our intentional treatment strategy (11). Dedicated CTO wires and new treatment strategies have been developed recently and appear to be useful in selected cases (12). However, these new tools need to be used judiciously and in our view in the right anatomical context. A promising new strategy to treat CTOs, is the retrograde approach which has been introduced as an alternative route for recanalization of otherwise difficult or impossible lesions and is gaining acceptance among interventionalists due to its high success rate (13). A possible explanation is the fact that calcium is more prevalent at the entry of the occlusion, so a higher chance to cross/break the distal cap and make progress retrograde would encourage the operator to continue until success is achieved (figures 5a and 5b). Our data corroborate what intuitively was written in the consensus document from the EuroCTO club (14): "the distal fibrous cap is often less resistant than the proximal cap". Another

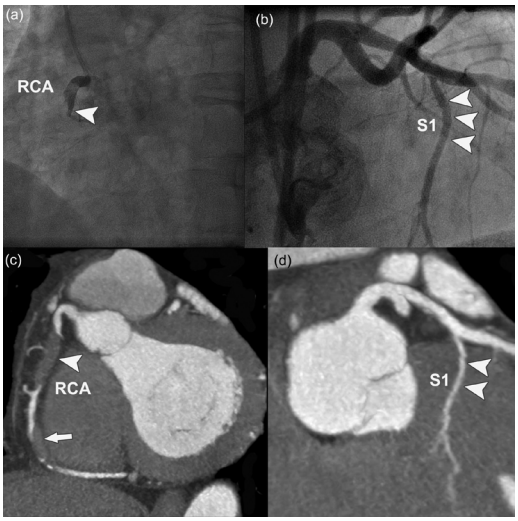

Figure 5a. (a) Retrograde approach. Angiographic image, showing proximal occlusion (arrowhead) of the right coronary artery (RCA). (b) Angiographic image of the left coronary artery, showing a large septal branch (arrowheads). (c) Corresponding CT image of the RCA showing 2 consecutive non-calcified occlusions of the vessel. (d) Corresponding CT image of the left coronary artery, also showing the large septal branch.

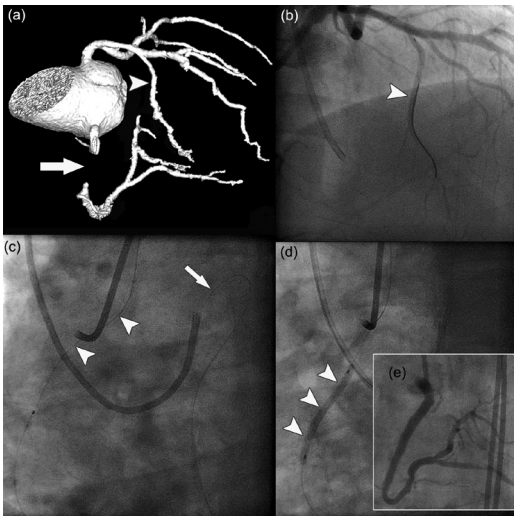

Figure 5b. Retrograde approach. Same patient as in 5a. Illustration of the percuteneous retrograde technique. (a) 3-dimensional CT angiographic view, showing he occlusion of the RCA (arrow) and the large septal branch (arrowhead). (b) Wiring of the septal branch (arrowhead). (c) The wire is introduced through the guiding catheter that is engaged in the left coronary artery (arrow) and was successfully advanced through the septal branch and finally retrograde through the RCA ending into the ascending aorta (arrowheads). (d) Balloon

anatomical factor that favors the retrograde approach is the presence of a sidebranch at the entry side of the occlusion that in our series was related to failure cases (figures 5a and 5b).

The location of calcification is not only a strong determinant for crossing the lesion with the guidewire, but also influences the balloon selection. In severely calcified lesions small diameter balloons, ie, 1.0, 1.1 and 1.25 mm, with a lubricious coating and acceptable shaft pushability are usually required (14). Calcification of the coronary arteries has been related to age in several publications (15,16). In our study, CTOs with longer and more severe calcified patterns were present in older patients. Also the mean age of patients with calcifications at the entry and exit sides of the occlusion was significantly higher.

Undoubtedly, this is a high-risk subset of patients in different aspects and the decision to choose for a percutaneous intervention should envisage a maximal chance of success at a minimal patient risk. The amount of contrast used and the radiation dose a patient receives are important variables that have an impact on patient's safety. The contrast load during a CTO recanalization attempt is higher as compared to non-CTO procedures (17,18). In this study, the average amount of contrast used was 455.4 ml. In addition, a PCI of a CTO is

often characterized by a long procedural time and a high radiation dose. Usually during the procedure one view is maintained, or two orthogonal views in case of biplane use, which leads to an intense exposition of the same skin areas (10) and body segments (14). The average radiation dose of a PCI procedure in this study was 39.26 mSv. This is 8 times higher than the dose received during a CCA(20). In addition, patients received a mean radiation dose during the preprocedural cardiac CT scan of 22.4 mSv.

Clinical implications

In experienced centres the success rate of a percutaneous CTO recanalization attempt is on average 70% (8,14). Knowing beforehand in which patients the chances of success are reasonably high appears to be worthwhile, as it has been shown that a failed recanalization is associated with a worse outcome and a higher rate of major cardiac events (21). The current study shows that CTCA is more precise than CCA for assessing the anatomical features of a CTO. At the cost of a significant additional amount of contrast and radiation, it would not be reasonable to propose a cardiac CT scan before each PCI attempt of a CTO. Instead, a cardiac CT scan seems most useful in patients in whom the angiographic features look unfavourable or in patients in whom a second PCI attempt is contemplated. The decision whether or not to perform a contrast-enhanced scan after the calcium scoring scan depends on the information one wants to obtain: if the question is to have an idea of the amount of calcium in the occluded segment, a calcium scoring scan might be sufficient considering the fact that most of the radiation exposure derives from the contrast-enhanced scan. Pursuing a "complete scan", including the administration of contrast, might be preferred in case of a suspected long occlusion where one aims to obtain information on the 3-dimensional course of the occlusion, including the distribution of calcium. In addition, the contrast- and radiation exposure of the patient should become less of an issue in the near future: new scanning protocols are dramatically reducing the radiation dose of a contrast-enhanced scan to less than 3mSv (22) and scheduling the cardiac CT scan at least a few days before the PCI would not increase the risk of contrast nephropathy.

The radiation from a PCI is considerable, but necessary to do the procedure. Good arguments are needed before embarking on a percutaneous recanalization attempt and this decision process in general should incorporate the symptomatic status of the patient, documentation of myocardial ischemia and if possible data with regard to the pre-procedural chances of success. The latter argument would be in favour of performing a cardiac CT scan in selected cases: patients in whom the CT characteristics of a CTO are unfavourable for PCI might be considered for an alternative therapeutic modality, i.e. medical treatment or bypass surgery.

Limitations of the study

Despite the fact that we failed to provide with accurate data for occlusion duration, which is an important marker of procedure failure (5), we performed a detailed and selective quantification of the calcium present in the occluded segment, for which occlusion duration is a surrogate marker as shown in a pathological study where fibrocalcific plaque increased with CTO age ($p = 0.008$) (23).

Although all the CTCA scans were discussed between the operator and someone trained to interpreting CTCA prior to the interventional procedure, there was no formal documentation of the changes in approach for treating the CTO in light of the CTCA findings. Thus, it was difficult to measure to what extent this knowledge on the CTO characteristics by CTCA impacts on the success rate. In order words, a severely calcified and long lesion might have discouraged the operator from a longer attempt.

In case of severe calcifications of the vessel, we relied on angiographic data to determine the length of the occlusion by CTCA. Although a limitation in this study, the repercussion in clinical practice would be minor as the angiographic data are an essential component of the therapeutic decision process for a given patient. As mentioned in the discussion part, we would only recommend a cardiac CT scan in selected cases to complement the angiographic information.

CONCLUSION

Evaluation of CTOs by means of CTCA offers a better description of its anatomical features as compared to conventional angiography and predicts procedural success in patients referred for PCI. More specifically, the presence of severe calcification, ie, calcium occupying >50% of the VCSA, as determined by CTCA is an independent predictor of procedural failure. The radiation exposure and amount of contrast used during a PCI attempt is considerable. The judicious use of a preprocedural cardiac CT scan makes sense and might modify the approach in case PCI is attempted or could drive the physician's preference to an alternative therapeutic modality, ie, medical treatment or bypass surgery.

REFERENCES

1. Abbott JD, Kip KE, Vlachos HA, et al. Recent trends in the percutaneous treatment of chronic total coronary occlusions. Am J Cardiol 2006;97:1691-6.
2. García-García HM KN, Daemen J, Tanimoto S, van Mieghem C, Gonzalo N, van der Ent M, Sianos G, de Feyter P, Serruys PW. Contemporary Treatment of Patients with Chronic Total Occlusion: Critical Appraisal of Different State-of-the-art Techniques and Devices. EuroInternvention 2007.
3. Puma JA, Sketch MH, Jr., Tcheng JE, et al. Percutaneous revascularization of chronic coronary occlusions: an overview. J Am Coll Cardiol 1995;26:1-11.
4. Achenbach S. Computed tomography coronary angiography. J Am Coll Cardiol 2006;48:1919-28.
5. Mollet NR, Hoye A, Lemos PA, et al. Value of preprocedure multislice computed tomographic coronary angiography to predict the outcome of percutaneous recanalization of chronic total occlusions. Am J Cardiol 2005;95:240-3.
6. Cockcroft DW, Gault MH. Prediction of creatinine clearance from serum creatinine. Nephron 1976;16:31-41.
7. Hoye A, Tanabe K, Lemos PA, et al. Significant reduction in restenosis after the use of sirolimus-eluting stents in the treatment of chronic total occlusions. J Am Coll Cardiol 2004;43:1954-8.
8. Stone GW, Kandzari DE, Mehran R, et al. Percutaneous recanalization of chronically occluded coronary arteries: a consensus document: part I. Circulation 2005;112:2364-72.
9. Rentrop KP, Cohen M, Blanke H, Phillips RA. Changes in collateral channel filling immediately after controlled coronary artery occlusion by an angioplasty balloon in human subjects. J Am Coll Cardiol 1985;5:587-92.
10. den Boer A, de Feijter PJ, Serruys PW, Roelandt JR. Real-time quantification and display of skin radiation during coronary angiography and intervention. Circulation 2001;104:1779-84.
11. Van Mieghem CA, van der Ent M, de Feyter PJ. Percutaneous coronary intervention for chronic total occlusions: value of preprocedural multislice CT guidance. Heart 2007;93:1492.
12. Saito S, Tanaka S, Hiroe Y, et al. Angioplasty for chronic total occlusion by using tapered-tip guidewires. Catheter Cardiovasc Interv 2003;59:305-11.
13. Kukreja N, Serruys PW, Sianos G. Retrograde recanalization of chronically occluded coronary arteries: illustration and description of the technique. Catheter Cardiovasc Interv 2007;69:833-41.

14. Di Mario C WG, Sianos G, Galassi AR, Buttner J, Dudek D, Chevalier B, Lefevre T, Schofer J, Koolen J, Sievert H, Reimers B, Fajadet J, Colombo A, Gershlick A, Serruys PW, Reinfart N. European Perspective in the Recanalization of Chronic Total Occlusions (CTO): consensus document from the EuroCTO Club. EuroInternvention 2007;3:30-43.
15. Haberl R, Becker A, Leber A, et al. Correlation of coronary calcification and angiographically documented stenoses in patients with suspected coronary artery disease: results of 1,764 patients. J Am Coll Cardiol 2001;37:451-7.
16. Kronmal RA, McClelland RL, Detrano R, et al. Risk factors for the progression of coronary artery calcification in asymptomatic subjects: results from the Multi-Ethnic Study of Atherosclerosis (MESA). Circulation 2007;115:2722-30.
17. Marenzi G, Assanelli E, Marana I, et al. N-acetylcysteine and contrast-induced nephropathy in primary angioplasty. N Engl J Med 2006;354:2773-82.
18. Le Feuvre C, Batisse A, Collet JP, et al. Cardiac events after low osmolar ionic or isosmolar nonionic contrast media utilization in the current era of coronary angioplasty. Catheter Cardiovasc Interv 2006;67:852-8.
19. Mehran R, Aymong ED, Nikolsky E, et al. A simple risk score for prediction of contrast-induced nephropathy after percutaneous coronary intervention: development and initial validation. J Am Coll Cardiol 2004;44:1393-9.
20. Morin RL, Gerber TC, McCollough CH. Radiation dose in computed tomography of the heart. Circulation 2003;107:917-22.
21. Hoye A, van Domburg RT, Sonnenschein K, Serruys PW. Percutaneous coronary intervention for chronic total occlusions: the Thoraxcenter experience 1992-2002. Eur Heart J 2005.
22. Husmann L, Valenta I, Gaemperli O, et al. Feasibility of low-dose coronary CT angiography: first experience with prospective ECG-gating. Eur Heart J 2008; 29:191-7.
23. Srivatsa SS, Edwards WD, Boos CM, et al. Histologic correlates of angiographic chronic total coronary artery occlusions: influence of occlusion duration on neovascular channel patterns and intimal plaque composition. J Am Coll Cardiol 1997;29:955-63.

INTERLUDE 4

Percutaneous Coronary Intervention for Chronic Total Occlusions: Value of Preprocedural MSCT Guidance.

Carlos A.G. Van Mieghem[1,2], Martin van der Ent[1], and Pim J. de Feyter[1,2]

From the departments of Cardiology[1] and Radiology[2],
Erasmus MC, Rotterdam, the Netherlands

Heart. 2007; 93:1492

A 50-year-old man with increasing anginal complaints was referred for percutaneous coronary intervention (PCI) of an occluded right coronary artery (RCA) (panel A, white arrows show distal filling of the vessels through collaterals from the left coronary artery). He had had an inferior myocardial infarction in 1998 and two previous attempts to open the RCA percutaneously had been unsuccessful. To appreciate fully the length and composition of the occlusion a preprocedural 64-slice CT coronary angiogram was performed. This showed a long occlusion (panel E, 82.4mm) up to the crux of the RCA (panel C, arrow), which mainly consisted of non-calcified tissue, except for the entry point that disclosed a dense but relatively short rim of calcium (panels B and C, arrowhead). With this information, we used a different strategic approach: after ablation of the calcified initial part of the occlusion using a therapeutic ultrasound device, we were easily able to cross the remainder of the lesion with a conventional guidewire and revascularise the vessel using three overlapping drug-eluting stents. The angiographic result at 6 months' follow-up remained perfect (panel D).

Chronic total occlusions are a common reason for referral to bypass surgery because of the relatively high failure rates when attempting a PCI. Unlike conventional coronary angiography, cardiac multislice CT provides an accurate assessment of the length and composition of the occluded segment, which are important predictors of procedural success. Preprocedural multislice CT guidance therefore has potential to identify which patients are most likely to benefit from attempted PCI.

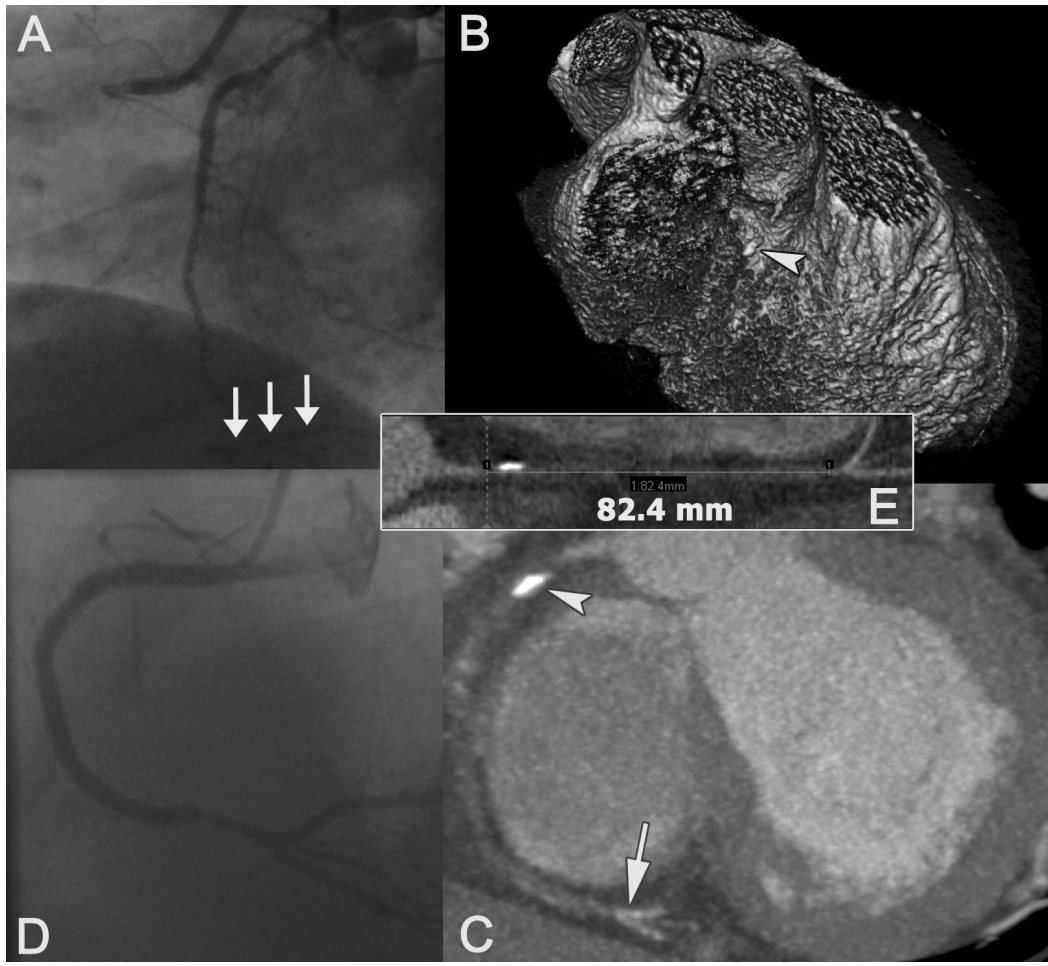

(A full color version of this illustration can be found in the color section).

14

Magnetic Navigation in Percutaneous Coronary Intervention

Mark S. Patterson, M.SC., M.R.C.P.,[1,2] Jeroen Schotten, M.D.,[1] Carlos van Mieghem, M.D.,[2] Ferdinand Kiemeneij, M.D., PH.D.,[1] and Patrick W. Serruys, M.D., PH.D.[2]

From the [1]Department of Cardiology, Onze Lieve Vrouwe Gasthuis, Amsterdam, The Netherlands; [2]Thoraxcenter, Erasmus Medical Center, Rotterdam, The Netherlands

J Interven Cardiol 2006;19:1–8

ABSTRACT

Magnetic navigation is the use of adjustable magnetic fields to precisely direct wires and equipment for clinical applications. It is a recently developed option that is now available for Interventional Cardiology. Procedures are based on the production of a three-dimensional reconstruction of the vessel lumen from standard angiographic images. Knowledge of the positions of the table and image intensifier during angiography allows calculation of the vessel coordinates in real space within the patient's chest. The applied magnetic field can be changed at any time to redirect the wire tip in order to improve navigation through complex and tortuous anatomy.

The digital information of the coronary reconstruction can be used in further novel ways. Firstly, the integration of multi-slice computerised tomography images adds information about the path of the previous lumen of chronic total occlusions. Secondly, the computed center-line of the reconstructed vessel can be superimposed onto the live fluoroscopy images as a three-dimensional guide. The combination of improved navigation together with the other available system features may improve time, contrast, and material usage in a range of coronary lesions. Future potential developments include improvements in equipment and software and potential therapeutic strategies under consideration include the use of equipment to perform remote control procedures, and the integration of the system to improve bone-marrow derived stem cell delivery.

INTRODUCTION

The field of interventional cardiology has been characterized by the rapid introduction and uptake of new treatments and devices such as stents,[1] clopidogrel,[2] drug eluting stents,[3] bivalirudin,[4] and new guidewire technology. These new technologies have driven the continuously increasing total number of percutaneous coronary interventions (PCI).[5]

A recent promising development is the use of a magnetic navigation system (MNS) to steer a guidewire through coronary arteries. This technology is already accepted for the performance of electrophysiological studies[6–9] and has tested favorably in neurosurgery both in animal models[10] and in humans.[11] Interventional coronary procedures present more of a moving target when compared with neurosurgery and requires smaller magnets when compared with electrophysiology. The combination of smaller wire tip magnets together with new software and imaging features has made the MNS available as a new platform for PCI.

Magnetic navigation allows a magnetically enabled wire tip to be pointed in any orientation. This allows the adjustment and readjustment of the direction of the wire tip in vivo whenever needed. In addition, the system produces three-dimensional images, integrates information with multislice computerized tomography (MSCT), and is able to use this three-dimensional information superimposed on live fluoroscopy. The potential areas where such a system provides new options include challenging and tortuous anatomy, chronic total occlusions (CTOs), reduction in time, contrast and materials, and remote control PCI. This article reviews a brief history of magnetic procedures, the current status, some future possibilities, and some limitations within the area of non-electrophysiological cardiac interventions.

THE SYSTEM

The magnetic navigation system (Niobe®, Stereotaxis, St Louis, Missouri) has been developed for use with digital coronary angiography. The system consists of two permanent magnets, mounted on mechanical positioners, on either side of the fluoroscopy table (see Fig. 1). These magnets produce an interacting magnetic field to produce an approximately spherical 15 cm uniform magnetic field of 0.8 T. The magnets move along three different coordinates and rotate about the z axis, move toward or away from the navigation volume along he z axis, and tilt about an axis located just behind the magnet. This allows the direction of the applied magnetic field vector to be orientated in 360° in all planes. The three-dimensional location of the X-ray image is known from the positions of the image intensifier, angiography system, and table. A three-dimensional reconstruction is created from the angiographic images using dedicated reconstruction software (CardiOp-B, Paieon Medical Inc., Rosh Ha'ayin, Israel). This

reconstruction is used by the MNS to give three-dimensional coordinates that are localized in real space (within the Figure 1. Magnetic navigation system is shown with the magnets in position on either side of the patient. chest in a patient during a procedure). This provides two new abilities. Firstly, the three-dimensional model allows the computation of the orientations of the magnetic field needed for alignment with the center-line at every point of the virtual coronary artery. Secondly, the three-dimensional coordinates are known in real space and this provides the data for the MNS to change the magnetic field vector, and therefore the resulting magnetic moment on the wire tip, at every location in the vessel.

The magnetic moment is equal to the product of the strength of the applied magnetic field, the crosssectional area of the tip magnet, and the sine of the angle of the magnet direction relative to the applied magnetic field. The result is control of the direction of the wire tip, in vivo, without the need for a preshaped wire tip angle.

There is a recently introduced and broadened range of dedicated, magnetically enabled wires (TitanTM series) for PCI available for use with the MNS.

Figure 1. Magnetic navigation system is shown with the magnets in position on either side of the patient.

HISTORY

The use of magnets to control an intravascular catheter was first reported in 1951[12] while the first human use was a neonatal heart catheterization in 1991 for the diagnosis of anomalous congenital cardiac drainage.[13] The current MNS has been developed over the past 15 years. Previous systems were only suitable for relatively large vessels because of the size of the catheter magnets required. The current system now has tiny magnets (≤0.014) and is the most widely used. This system received regulatory approval for human clinical use in cardiac electrophysiology and interventional neuroradiology in 2000, and for interventional cardiology in 2003. It has been shown to be feasible in neurosurgery[10,11] and is a well-accepted technique in electrophysiology.[6–9]

Figure 2. This shows the three-dimensional reconstruction in the left panel and the endoluminal view of the LAD/diagonal bifurcation in the right panel. Note that these are live, moving, real-time images during a procedure.

CURRENT STATUS

Navigation. The core feature of the system is the ability to alter the direction of the wire tip within a patient during a procedure to give improved wire tip control compared to conventional procedures. First, the ability to precisely direct the wire tip means that the wire can be redirected and readjusted throughout the procedure to configurations that exactly suit the angulations and direction of the vessel, or alternatively used in a precisely defined probing pattern to interrogate the vessel ahead. This ability is not affected by friction on the shaft of the wire that can impair manipulation in tortuous vessels. Second, it overcomes the problem of a conventional tip that can become damaged and misshapen during a procedure and so impair manipulation. Finally, the passage of the wire is guided by the magnetic vector rather then rotational manipulation and this may reduce wire entanglement. This problem sometimes occurs in bifurcation procedures where wires can become intertwined with manual manipulation and prevent passage of materials. These abilities mean that the lesion can be approached, and navigated through, with a straight tip. A straight tip may reduce the chance of the wire tip impacting against the vessel wall or unintentionally navigating into sidebranches.

Figure 3. The left panel shows 64 slice cardiac MSCT with vessels, a tissue attenuation line is seen in the RCA after the RV branch. The right panel shows a post-processed image of the vessel that more clearly shows the 30 mm occlusion.

A major goal in the development of this system has been to enable the successful passage of the wire through vessels that prove challenging to conventional guidewires. In this context, two situations are particularly relevant. Firstly tortuous and/or heavily calcified vessels where a conventional guidewire loses manipulability as described above. Secondly, CTOs where the path of the vessel is not visible and the required tip direction is unclear.

Difficult Anatomy. This technology has been examined in a number of different situations with regards to difficult lesions. Passage of a wire to distal segments of in vitro phantoms was not only successful but, in addition, fluoroscopy times were found to be significantly reduced.[14] This potentially reduces radiation exposure both to patients and personnel. The system has been shown to be feasible for PCI in vivo[15,16] and furthermore, both of these studies showed that the magnetically enabled wire was capable of crossing lesions where a conventional wire had failed. In addition to normal PCI, MNS can support other specialist specialist intracoronary procedures such as percutaneous alcohol septal ablation.[17] These navigational advantages are enhanced by a range of imaging possibilities including the three-dimensional lumenogram, the bullseye view, and the endoluminal view (see Figs. 2 and 5). In addition, the MNS has dedicated ranges of magnetically enabled guide wires (the Titan™ and Cronus R ranges) that vary in stiffness, magnet length, and tip angulation to tailor the system to each individual coronary artery. These 0.014 wires are entirely compatible with all current standard PCI equipment and standard access sites, both radial and femoral. The combination of precise navigation, together with the additional imaging options available, may reduce time, contrast, fluoroscopy, and material use.

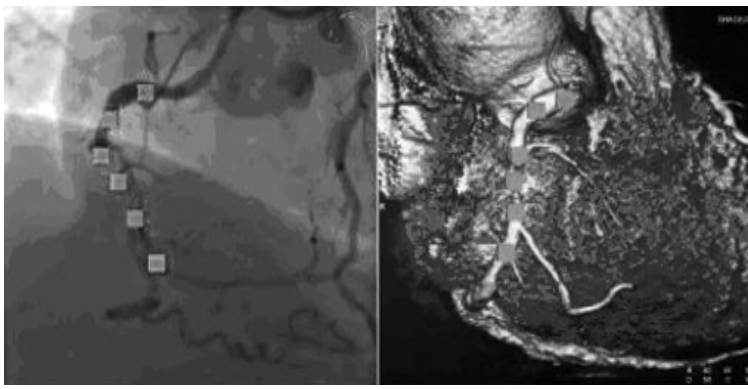

Figure 4. The fluoroscopy image is marked on the system with dots ready for three-dimensional integration in the left panel with the MSCT marked with dots for integration in the right panel. These give the specific three-dimensional coordinates that allow integration of the two modalities (see Fig. 5).

CTOs and MSCT Integration. A second lesion type that continues to be vexing is the CTO. Success rates for PCI of CTOs are around 65% to 80%, depending on the technique used and presence of other diseases such as diabetes.[18–21] A number of strategies have been suggested to facilitate the treatment of CTOs, e.g., in tracoronary thrombolytic infusion,[22] the use of tapered-tip guidewires,[20] imaging with (16 slice) MSCT,23 and the use of a laser guidewire.[24] The ability to precisely steer and change the orientation of the wire tip may be crucially important in avoiding wire exit, and may hold a major advantage in comparison with a conventional

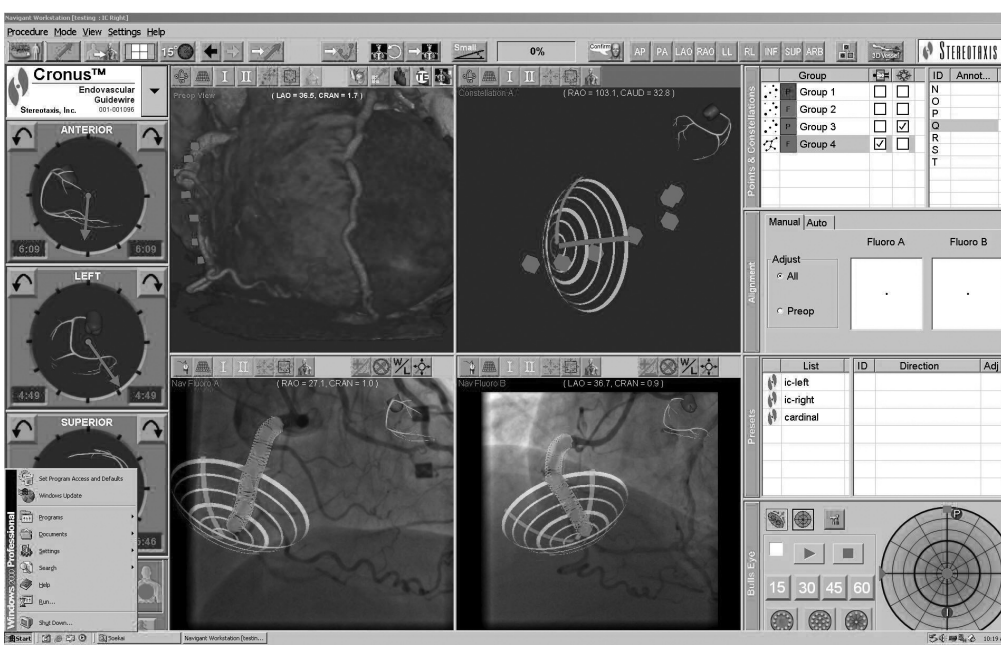

Figure 5. The Stereotaxis screen is shown with the integrated MSCT image and reconstruction made. In the upper panels the green dots indicate where attenuated tissue of previous vessel was seen on the MSCT, while the lower panels show fluoroscopy images with a superimposed three-dimensional reconstruction that follows the path identified by the MSCT.

wire that has afixed, unchangeable angulation. However, with regard to CTOs, the MNS has a further major advantage as it can also integrate 64 slice MSCT images (see Figs. 3–5). This imaging technique can identify both a distal vessel that is filled via collaterals and also show a tissue attenuation line (the scarred tissue of the original vessel lumen). This imaging allows a path to be visualized and then synchronized with the MNS (see Figs. 3–5) to direct the wire tip along the previous vessel lumen (or at least the scar tissue) to the distal vessel. These features have helped the success of the MNS in the initial experience of CTO procedures.[25]

FUTURE DEVELOPMENTS

The MNS is a flexible system and, as well as improvements in the areas described above, it can be expected that the current capabilities will be extended and further potential strategies will be discovered. This system is a platform that adds new abilities to conventional PCI. Some possibilities in both strategy and equipment currently under consideration are described below.

Newer and Improved Equipment. The newest system available offers tilting magnets for better imaging (the older system limits RAO and LAO projections to approximately 30° because of the magnets) and software upgrades. In addition, the current range of wires is being increased. A new intermediate grade wire will increase the range of stiffness of the wires and a new blended nitinol-stainless steel wire may offer improved flexibility with memory. Further potential wire developments include coil magnet and multi-magnet configurations of the wire tip that may offer increased flexibility within tortuous anatomy and better deformation in extremely tortuous segments.

Contrast Reduction. A further feature of the MNS is the ability to project a white line overlay onto the fluoroscopy screen. This can be used as a guide for wire passage and enables the op-

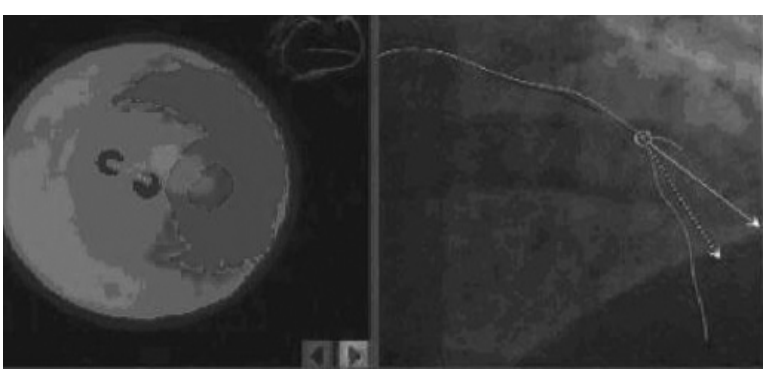

Figure 6. The left panel shows the endoluminal view that is synchronized with the position of the marker on the fluoroscopy screen. The right panel shows the fluoroscopy screen with the white line overlay, the dashed line is the desired vector, and the solid line is the applied vector (in this example the desired vector has just been moved and the applied vector is in the process of moving to that position). Note that these are live, moving, real-time images during a procedure.

erator to pass the wire with minimal or no use of contrast[26] (see Fig. 6). Contrast-induced renal dysfunction, and the dialysis needed in some cases, remains a cause of morbidity and mortality in procedures involving intravascular contrast.[27] While some medical maneuvers, such as fluid,[28] N-acetyl-cysteine,[29] and theophylline[30] administration, may confer some protection, evidence suggests that limiting intravascular contrast load to 100 mL may be a cut-off dose for the development of acute renal failure requiring dialysis.[27] The ability to pass the wire without contrast may allow such a goal to be reached in patients with preexisting renal problems.

Chronic Total Occlusions. In addition to the advantages described above for the treatment of CTOs, the ongoing development of a magnetically enabled radiofrequency ablating wire may be highly advantageous. This will combine the current advantages of highly adjustable steering, the identification of the missing section of the vessel (shown by MSCT integration), and the ability to ablate intervening scar tissue.

Remote Control. A further new concept in PCI is the ability to remotely control the delivery system. remote control equipment (see Fig. 7) in the form of the Remote Navigation System®

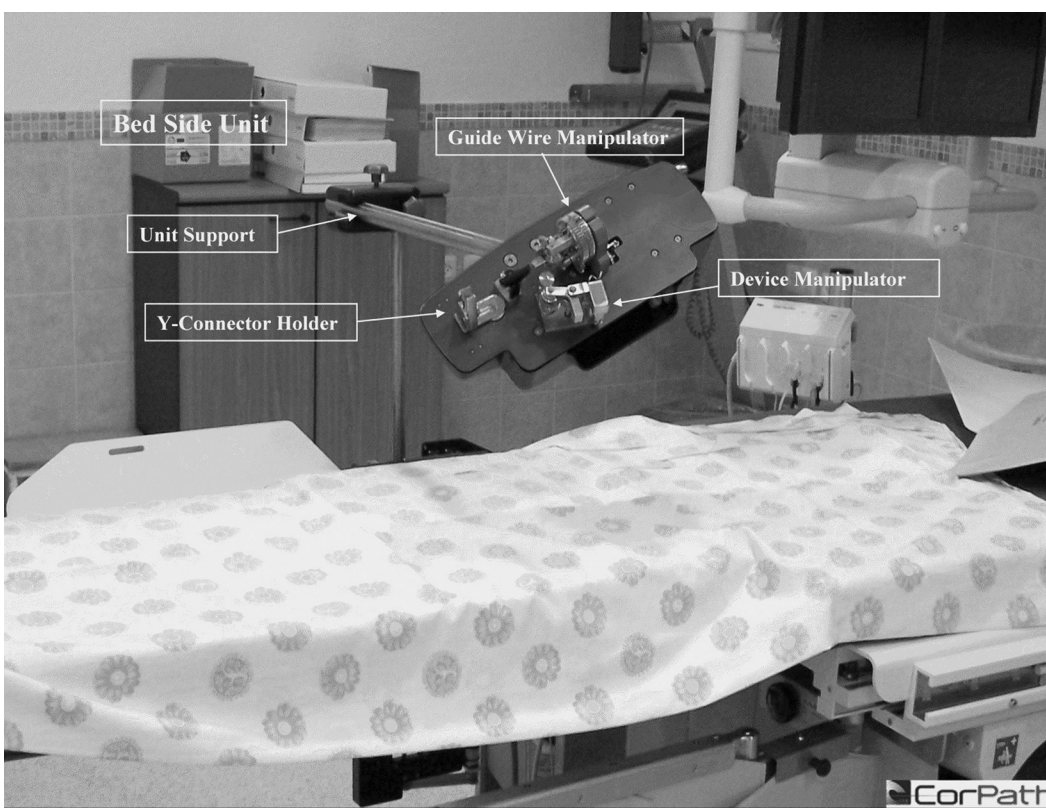

Figure 7. The Remote Navigation System® is shown in a catheterization suite. (courtesy of T. Wenderow, CEO, Navicath Ltd).

(Navicath Ltd, Haifa, Israel) has been successfully tested in both in vitro and in vivo models.[31] This successful testing in models was mirrored by the successful use in the majority of a series of clinical PCI cases.[32] Remote control procedures have already been shown to be possible in electrophysiology.[6] Such remote control procedures have the advantages of more exact movement of wires. Wire advancement by a remote system could potentially be integrated with the MNS to advance the wire and change the magnetic vector in tandem thereby enabling robotic procedures. Theoretically such movements could even be gated to the ECG to advance the tip and this might overcome some of the limitations of the static three-dimensional reconstruction. This combination would add the advantages of improved wire control to those of remote control procedures with reduction of irradiation of personnel and the reduction of collateral problems such as back pains from wearing lead coats.

Stem Cell Therapy. Stem cell therapy presents another possibility for MNS that may give both precisely directed delivery and also utilize integration with other forms of imaging. Intramyocardial injections of bonemarrow derived stem cells have been shown to have a potential for improving regional and global left ventricular function.[33] However, delivery of stem cells to the correct areas has remained inexact with relatively crude methods of identifying where the injections are to be placed on delivery and where they have been placed on restudy. The identification of infarcted areas onMSCT[34] mayadd a further tool that can be integrated into the MNS for such target localization. The MNS gives highly precise three-dimensional control and, with the possible development of a magnetically enabled injection catheter, the current MSCT integration may help localization of the infarct area to give a more tailored delivery. The combination of such localization techniques with the mapping abilities of systems like he recently developed NOGA® XP Cardiac Navigation System (BiosenseWebster Inc./Biologics Delivery Q1 System Group, Cordis Corporation) may give complementary information and result in more exact delivery. Integration of other digitized information from sources such as three-dimensional intracardiac echocardiography or magnetic resonance imaging could give functional data on improvements in wall segment motion.

LIMITATIONS

This new system has a number of weaknesses that may be considered in terms of software, hardware, strategy, and general limitations.

Software. The Navigant software has many useful features however, some aspects remain limited. Reconstructions are static images with no variation with respiration and heart motion, there is a restricted range of forward advancement along the virtual vessel to 1–5 mm per touch of the screen, and the alignment can be problematic. Vessel reconstructions are

restricted to two branches and are based on angiography films alone resulting in limited resolution. Reconstructions of the exact vessel borders and hazy lesions may have poor definition leading to underestimation of stenoses and difficulty with sharp, short lesions.

Hardware. The equipment has some physical limitations such as the length of the wire tip magnet that, with a standard of 3 mm, may hinder advancement in extremely tortuous and narrowed segments. In addition the integration of other imaging modalities directly into the system remains incompletely explored.

Strategy. Strategies for using this system in the performance of PCI are under development and these will depend on the indication for the procedure. The system remains relatively new with limited operator experience and current strategies utilize ad hoc reconstruction of the vessel that may be time consuming during a procedure. The timing of the reconstruction may have an impact on image quality and readiness for use in procedures. The usefulness of the center-line overlay for the minimization of the contrast load is not yet clarified.

General. As a whole, currently, the system functions well. However this system is still in further development and further refinements are expected. Furthermore, this system is an aid in the performance of PCI so should problems occur or, in the worst case scenario, the system fails then standard PCI can be performed.

CONCLUSION

The MNS is a new platform for PCI that gives the operator more precise control of wire tip direction as well as the broadening imaging and integration abilities. This system facilitates navigation for difficult vessels and CTOs, it gives useful control of direction derived from MSCT integration and it may lead to a reduction in irradiation and discomfort to operators, personnel, and patients. For the future, the versatility of the system indicates further possible avenues for investigation such as reductions in contrast and irradiation, and navigable ablation and injection capabilities. Further investigation and development is underway.

REFERENCES

1 Serruys PW, de Jaegere P, Kiemeneij F, et al. A comparison of balloon expandable stent implantation with balloon angioplasty in patients with coronary artery disease. N Engl J Med 1994; 331:489–495.

2 M¨uller C, B¨uttner HJ, Petersen J, et al. A randomized comparison of clopidogrel and aspirin versus ticlopidine and aspirin after the placement of coronary-artery stents. Circulation 2000;101:590–593.
3 Morice MC, Serruys PW, Sousa JE, et al. A randomized comparison of a sirolimus-eluting stent with a standard stent for coronary revascularization. N Engl J Med 2002;346:1773–1780.
4 Lincoff AM, Bittl JA, Harrington RA, et al. Bivalirudin and provisional glycoprotein IIb/IIIa blockade compared with heparin and planned glycoprotein IIb/IIIa blockade during percutaneous coronary intervention: REPLACE-2 randomized trial. JAMA 2003;289:853–863.
5. American Heart Association. 2001 Heart and Stroke Statistical Q2 Update. Dallas, TX, 2000.
6. Pappone C, Vicedomini G, Manguso F, et al. Robotic magnetic navigation for atrial fibrillation ablation. J Am Coll Cardiol 2006;47:1390–1400. Epub 2006 Mar 15.
7. Ernst S, Hachiya H, Chun JK, et al. Remote catheter ablation of parahisian accessory pathways using a novel magnetic navigation system—a report of two cases. J Cardiovasc Electrophysiol 2005;16:659–662.
8. Ernst S, Ouyang F, Linder C, et al. Initial experience with remote catheter ablation using a novel magnetic navigation system: Magnetic remote catheter ablation. Circulation 2004;109:1472–1475. Epub 2004 Mar 15.
9. Ernst S, Ouyang F, Linder C, et al. Modulation of the slow pathway in the presence of a persistent left superior caval vein using the novel magnetic navigation system Niobe. Europace 2004;6:10–14.
10. Grady MS, Howard MA 3rd, Dacey RG Jr, et al. Experimental study of the magnetic stereotaxis system for catheter manipulation within the brain. J Neurosurg 2000; 93:282–288.
11. Chu JC, Hsi WC, Hubbard L, et al. Performance of magnetic eld-guided navigation system for interventional neurosurgical and cardiac procedures. J App Clin Med Phys 2005;6:143–149.
12. Tilander H. Magnetic guidance of a catheter with articulated steel tip. Acta Radiol 1951;35:62–64.
13. Ram W, Meyer H. Heart catheterization in a neonate by interacting magnetic fields: A new and simple method of catheter guidance. Catheter Cardiovasc Diagn 1991; 22:317–319.
14. Garcia-Garcia HM, Tsuchida K, Meulenbrug H, et al. Magnetic navigation in coronary phantom: Experimental results. EuroInterv 2005;1:321–328.
15. Tsuchida K, Garcia-Garcia HM, Tanimoto S, et al. Feasibility and safety of guidewire navigation using a magnetic navigation system in coronary artery stenoses. EuroInterv 2005;1:329– 335.

16. Atmakuri SR, Lev EI, Alviar C, et al. Initial experience with a magnetic navigation system for percutaneous coronary intervention in complex coronary artery lesions. J Am Coll Cardiol 2006;47:515–521.
17. Bach RG, Leach C, Milov SA, et al. Use of magnetic navigation to facilitate transcatheter alcohol septal ablation for hypertrophic obstructive cardiomyopathy. J Invasive Cardiol 2006;18:E176–E178.
18. Safley DM, House JA, Rutherford BD, et al. Success rates of percutaneous coronary intervention of chronic total occlusions and long-term survival in patients with diabetes mellitus. Diab Vasc Dis Res 2006;3:45–51.
19. Abbott JD, Kip KE, Vlachos HA, et al. Recent trends in the percutaneous treatment of chronic total coronary occlusions. Am J Cardiol 2006;97:1691–1696.
20. Olivari Z, Rubartelli P, Piscione F, et al. Angioplasty for chronic total occlusion by using tapered-tip guidewires. Catheter Cardiovasc Interven 2003;59:305–311.
21. Hoye A, van Domburg RT, Sonnenschein K, et al. Percutaneous coronary intervention for chronic total occlusions: The Thoraxcenter experience 1992–2002. Eur Heart J 2005;26:2630– 2636.
22. Abbas AE, Brewington SD, Dixon SR, et al. Intracoronary fibrin-specific thrombolytic infusion facilitates percutaneous recanalization of chronic total occlusion. J Am Coll Cardiol 2005;46:793–798.
23. Yokoyama N, Yamamoto Y, Suzuki S, et al. Impact of 16slice computed tomography in percutaneous coronary intervention of chronic total occlusions. Catheter Cardiovasc Interven 2006;68:1–7.
24. Segev A, Strauss BH. Novel approaches for the treatment of chronic total coronary occlusions. J Interven Cardiol 2004;17:411–416.
25. Garcia-Garcia HM, Tsuchida K, van Mieghem C, et al. Multi-slice computed tomography and magnetic navigation-initial experience of cutting edge new technology in the treatment of chronic total occlusions. Eurointervention, in press. Q3
26. Patterson M, Tanimoto S, Tsuchida K, et al. Magnetic Navigation with the Endo-Luminal View and the X-ray overlay— Major advances in novel technology. Eurointervention, in press.
27. McCullough PA, Wolyn R, Rocher LL, et al. Acute renal failure after coronary intervention: Incidence, risk factors, and relationship to Mortality. Am J Med 1997;103:368–375.
28. Bader BD, Berger ED, Heede MB, et al. What is the best hydration regimen to prevent contrast-induced nephrotoxicity? Clin Nephrol 2004;62:1–7.
29 Tepel M, van der Giet M, Schwarzfeld C, et al. Prevention of radiographic-contrast-agent-induced reductions in renal function by acetylcysteine. N Eng J Med 2000;343:180–184.
30. Katholi RE, Taylor GJ, McCann WP, et al. Nephrotoxicity from contrast media: Attenuation with theophylline. Radiology 1995:195:17–22.

31. Beyar R, Wenderow T, Lindner D, et al. Concept, design and pre-clinical studies for remote control percutaneous coronary interventions. EuroInterv 2005;1:340–345.
33. Perin PC, Dohman HFR, Borojevic R, et al. Transendocardial, autologous bone marrow cell transplantation for severe, chronic ischaemic heart failure. Circ 2003;107:2294–2302.
34. Nieman K, Cury RC, Fecencik M, et al. Differentiation of recent and chronic myocardial infarction by cardiac computed tomography. AJC 2006; doi:10.1016/j.amjcard.2006.01.101.

PART IV

CLINICAL IMPLEMENTATION: POST-INTERVENTION

15

Multislice Computed Tomography for Visualization of Coronary Stents

Francesca Pugliese[1,2], Filippo Cademartiri[2], Carlos A. G. Van Mieghem[1,2], W. Bob Meijboom[1,2], Patrizia Malagutti[2], Nico R. Mollet[1,2], Carlo Martinoli[3], Pim J. de Feyter[1,2], Gabriel P. Krestin[2].

From the departments of Cardiology[1] and Radiology[2], Erasmus MC, Rotterdam, the Netherlands. From the department of Radiology[3], University of Genoa, Genoa, Italy.

RadioGraphics 2006; 26:887-904.

ABSTRACT

Whereas the clinical diagnosis of in-stent thrombosis is straightforward, that of in-stent restenosis remains a problem, because although many patients experience chest pain after coronary stent placement, that symptom is secondary to ischemia in only a few.

The use of a noninvasive technique to identify such patients for early invasive intervention versus more conservative management is thus highly desirable. Multidetector computed tomography (CT) performed with 16-section scanners recently emerged as such a technique and has overtaken modalities such as electron-beam CT and magnetic resonance imaging as an alternative to conventional angiography for the assessment of in-stent restenosis.

The improved hardware design of the current 64-section CT scanners allows even better delineation of stent struts and lumen. The more reliable criterion of direct lumen visualization thus may be substituted for the presence of distal runoff, which lacks specificity for a determination of in-stent patency because of the possibility of collateral pathways.

However, the capability to accurately visualize the in-stent lumen depends partly on knowledge of the causes of artifacts and how they can be compensated for with postprocessing and proper image display settings. In addition, an understanding of the major stent placement techniques used in the treatment of lesions at arterial bifurcations is helpful.

INTRODUCTION

Over the past 25 years, catheter-based intervention has become the dominant form of coronary revascularization. Percutaneous coronary interventions are increasingly performed instead of coronary artery bypass graft surgery, even in patients with three-vessel disease or left main coronary artery disease. The most important advance in the field of percutaneous coronary interventions was the introduction of coronary stent implantation in the 1990s, which led to reductions in both the risk of acute major complications and the incidence of restenosis, compared with the risks after balloon angioplasty (1,2). Although the use of recently introduced drug-eluting stents has resulted in even further reductions in the occurrence of restenosis, in-stent thrombosis and neointimal hyperplasia may still occur and cause partial or complete obstruction.

Whereas the clinical diagnosis of stent occlusion due to thrombosis is usually straightforward in patients with a recent stent implantation and with a subsequent onset of acute myocardial ischemia leading to acute myocardial infarction, the assessment of in-stent restenosis is more challenging. Restenosis occurs in approximately 10%–20% of patients with complex lesion characteristics (3).

Moreover, although several characteristics of high-risk populations have been described as clinical predictors, the likelihood of restenosis in a particular patient remains largely unpredictable (4 –7). For these reasons, conventional coronary angiography is still the technique of choice for the diagnosis of in-stent restenosis, although cardiac catheterization may involve major complications and is associated with moderate to high costs. Magnetic resonance (MR) angiography also can depict the coronary anatomy and help detect stenoses in the proximal segments of coronary arteries (8). However, metallic stents cause magnetic susceptibility artifacts that may prevent visualization of the lumen (9). Electron-beam computed tomography (CT) has been used more successfully to visualize coronary stents (10,11). Electron-beam CT is the modality with the shortest image acquisition times, namely 100 msec for a 3-mm-thick section suitable for morphologic interpretation and 50 msec for an 8-mm-thick section used for flow analysis without direct visualization of the in-stent lumen.
However, image noise is extremely high with the first technique, and only severe, flow-limiting stenoses can be detected by using the flow technique. Thus, the occurrence of nonobstructive neointimal hyperplasia remains unnoticed at electron-beam CT. In addition, patients who undergo percutaneous coronary intervention may experience a progression of atherosclerosis in native coronary vessels without a stent implant, but electron-beam CT is suboptimal for monitoring such progression, because it requires the sequential triggered acquisition of multiple 3-mm-thick sections.
\

Hence, the latest generation of multidetector (multisection) CT scanners, which offer a smaller voxel size, faster gantry rotation speed, and reconstruction of 64 sections per gantry rotation, provide an appealing alternative for noninvasive luminal assessment in patients with chest pain after coronary stent placement (12). The improved hardware configuration of 64-section CT scanners allows direct visualization of the stent struts and lumen for a more reliable assessment of in-stent patency than is allowed by the visualization of distal runoff. In symptomatic patients, multidetector CT may be used as a complement or a substitute for treadmill testing; because the latter lacks specificity, additional noninvasive investigations such as stress echocardiography and scintigraphy often are required before cardiac catheterization is undertaken. Multidetector CT also can be useful to assess the condition of the whole coronary tree, as it provides information about the number, severity, and location of coronary lesions. In the follow-up of asymptomatic patients after stent implantation, multidetector CT might help overcome the limited accuracy of treadmill testing to rule out restenosis and thus enable a reduction in the number of further examinations (ie, stress echocardiography, scintigraphy) needed because of a positive or inconclusive test result.

In this article, the capability of 64-section CT coronary angiography for the evaluation of in-stent patency is discussed. The authors provide explanatory illustrations of the major stent implantation techniques used to treat lesions at or near arterial branching points. They describe the CT features and artifacts that may be observed in or near stent implants on multiplanar reformatted images and volume-rendered images, the causes of those visual characteristics, and the postprocessing and image display methods that may be used to avoid or minimize artifacts.

PERCUTANEOUS CORONARY INTERVENTION AND STENT PLACEMENT

Indications and outcomes

The clinical indications for percutaneous coronary interventions cover the spectrum of ischemic heart disease, from unstable angina pectoris and acute myocardial infarction to silent ischemia, as summarized in the guidelines of the American College of Cardiologists and the American Heart Association (13). In patients with significant narrowing of a single coronary artery, the main benefit of revascularization is the relief of angina rather than an improvement of the already good prognosis with medical therapy. In contrast, in patients with significant left main coronary artery stenosis or multiple-vessel disease, revascularization may both relieve angina and improve long-term survival.

Epidemiology

An estimated 1,204,000 inpatients underwent percutaneous coronary interventions in the United States in 2002, and coronary stent placement accounted for 537,000 of such procedures (14–16). More than 80% of percutaneous interventions that were performed in 2004 involved the placement of a drug-eluting stent coated with sirolimus or paclitaxel (17). The procedural success rate of percutaneous revascularization is higher than 90%, and the risk of sudden arterial occlusion and subsequent myocardial infarction is low (13). Despite contradictory reports (18), there is evidence that the long-term survival of patients who have undergone percutaneous revascularization for two- or three-vessel disease is no worse than that achieved with bypass graft surgery (19). Thus, percutaneous coronary intervention has become the preferred coronary revascularization strategy in many countries.

Coronary Stents

Coronary stents are expandable devices that are delivered to the coronary artery via catheter and then expanded to preserve the luminal diameter. The currently available stents are pre-mounted on dedicated delivery systems. Occurrences that may limit the success of stent implantation include in-stent restenosis and thrombosis, which may obstruct the flow through the stent.

Thrombosis

The frequency of in-stent thrombosis is low, with a cumulative incidence of 1.3%–1.7% at 9-month follow-up (20). However, even this incidence is clinically important because in-stent thrombosis is associated with high mortality and morbidity due to acute myocardial infarction. In the era of uncoated metallic stents, in-stent thrombosis typically occurred acutely (less than 48 hours after stent implantation) or sub-acutely (2–30 days after implantation). One of the current concerns about drug-eluting stents is the occurrence of delayed in-stent thrombosis that is manifested more than 30 days after stent implantation. This late manifestation may be related to delayed endothelialization of the stent and typically occurs when antiplatelet therapy is discontinued (21,22). In patients with additional risk factors (eg, renal failure, diabetes mellitus, or low ejection fraction), stents implanted at the level of coronary artery bifurcations are considered to present a higher risk of thrombosis (23). The same applies when very long stents are used, with a reported 1.03 relative risk of thrombosis for each 1-mm increase in length (20).

Restenosis

Restenosis, the major limitation to the long-term outcome of percutaneous coronary intervention, is defined as vessel lumen narrowing of more than 50% after angioplasty, with the resultant recurrence of angina. Restenosis is an iatrogenic process caused by an excessive arterial healing response to vessel injury associated with dilation. It results from the combined effects

of elastic recoil (24), vascular remodeling (25), and neointimal hyperplasia (26). Coronary stents represent a mechanical approach to the prevention of restenosis by virtually eliminating elastic recoil and negative remodeling of the vessel after balloon dilation (26). The occurrence of neointimal hyperplasia is mainly responsible for the observed rates of restenosis, which range from less than 10% with a drug-eluting stent to 40% with an uncoated metallic stent (1,2,27,28). For both stent types, excess stent length is associated with an increased risk of in-stent restenosis (29); thus, the arbitrary use of stents much longer than the actual lesion length is not advisable (30).

Drug-eluting Stents

Drug-eluting stents were developed to help prevent in-stent restenosis. Coating of a conventional metallic stent with an antiproliferative agent helps preserve the mechanical scaffolding properties of the stent; the drug is released locally, at the site of the vascular injury (31). The most extensive accumulated clinical experience to date is that with polymer-coated sirolimus- and paclitaxel-eluting stents. Favorable safety profiles and decreased restenosis rates have resulted in the widespread use of percutaneous coronary interventions and drug-eluting stents since their release in early 2003 (32–34). Ongoing developments in stent design include the creation of biodegradable, nonmetallic, and MR-compatible devices. Theoretically, a biodegradable drug-eluting stent may be the ideal solution to prevent in-stent restenosis. The response to vessel wall damage can be suppressed by the drug, while elastic recoil and negative remodeling are prevented by the stent. Eventually, the stent degrades, and chronic vessel injury related to the metal or polymer is thereby prevented (35).

MULTIDETECTOR CT FOR VISUALIZATION OF CORONARY STENTS

Four– and 16–detector row CT scanners

The diagnostic accuracy of electron-beam CT and multidetector CT performed with different generations of scanners is summarized in the Table. Whereas in-stent lumen evaluation with CT was almost impossible with four–detector row scanners (36–38), the introduction of 16–detector row scanners (in combination with dedicated convolution filters) made CT a much more viable modality for the detection of significant in-stent restenosis, with reported sensitivity and specificity values in the ranges of 54%–100% and 88%–100%, respectively (12,39–44) (Table). It is worth noting that the observation of distal runoff cannot be considered an absolute indicator of patency, since the presence of vessel enhancement distal to a stent could also be secondary to retrograde filling. Indeed, whereas in conventional coronary angiography the contrast agent is selectively injected into the coronary artery, CT requires injection into a peripheral vein instead. This allows retrograde flow via collateral branches to the vessel seg-

Diagnostic accuracy of electron-beam CT and multi–detector row CT in the evaluation of coronary stents

CT Technique and Study	No. Patients	No. Stents	Stent Location	Stent Caliber (mm)	No. Assessable Stents	Criteria for Patency	Sens (%)	Spec (%)
Electron beam CT								
Pump et al (10)	202	321 (221 vessels)	LM, RCA, LAD, LCX, Bypass grafts		(216 vessels)	Dynamic study distal runoff	78	98
Knollman et al (11)	117	152		2.5–3.0	144	Dynamic study distal runoff	72	60
Four–detector CT								
Kruger et al (36)	20	32	RCA, LAD, LCX		32	Distal runoff		
Maintz et al (37)	29	47		3–5	38	Distal runoff	100	100
Ligabue et al (38)	48	72	RCA, LAD, LCX		53	Distal runoff	100	100
		15		≥3.5	14	Lumen visualization		
		45		3.0–3.4	35			
		12		<3	4			
16–detector CT								
Schuijf et al (12)	22	68		2.25–5	50	Distal runoff	78	100
Cademartiri et al (39)	51	76		>2	74	Lumen visualization	84	99
Gilard et al (40)	29	29	LM		27	Lumen visualization	100	92
Gilard et al (41)	143	232	LM, RCA, LAD, LCX		122	Lumen visualization		
		1		4.5	1		86	100
		42		4.0	28			
		61		3.5	41			
		86		3.0	40		56	100
		42		2.5	12			
Kitagawa et al (42)	42	61			42	Lumen visualization		
		15		4.0	14			
		22		3.5	17			
		19		3.0	11			
		5		2.5	0			
Hong et al (43)	19	26		2.25–5	26	Contrast enhancement measurement		
Ohnuki et al (44)	16	20		>3	19	Pixel count method	75	88

Sens = sensitivity, Spec = specificity, LAD = left anterior descending artery, LCX = left circumflex artery, LM = left main coronary artery, RCA = right coronary artery.

ment distal to an occluded or diseased stent. Attempts also have een made to assess coronary artery stent patency with 16–detector row CT scanners on the basis of contrast enhancement measurements (43) or pixel count methods (44). However, the detection of more subtle degrees of in-stent neointimal hyperplasia was beyond the capabilities of that generation of CT scanners.

Multidetector 64-section CT systems

Although the calibers of coronary stents are no smaller than those of the major native coronary arteries and their branches, the depiction of the in-stent coronary lumen at CT is a greater challenge than is that of the native coronary artery lumen because of high-attenuation artifacts secondary to the metallic stent struts. High in-plane and through-plane spatial resolution, optimal contrast resolution, and minimization of high attenuation artifacts are paramount in order to overcome the technical challenges. The superiority of 64-section CT systems over earlier generations of CT scanners with regard to the detection of coronary artery stenoses in native vessels has been demonstrated in recent investigations (45–47). Improvements in CT hardware technology, such as high x-ray output, isotropic voxel size of 0.4 x 0.4 x 0.4 mm (48), acquisition times of 6–14 seconds, and the capability of rendering 64 sections per rotation, can play a valuable role also in the evaluation of the intra–coronary artery stent lumen. Indeed, advances in multidetector CT technology mean that thinner sections can be obtained in a shorter time, with resultant increased spatial resolution along the z-axis and with almost motion-free data sets (49). Temporal resolution depends primarily on a gantry rotation speed faster than those available with earlier scanners. The reduced breath-holding time is better tolerated by patients and contributes to the minimization of motion-related artifacts. Coupled with these improvements in hardware design, electrocardiography (ECG)-based gating techniques and specialized methods of image reconstruction are used. Depending on the patient's heart rate, data acquired during one cardiac cycle (monosegmental) or multiple cardiac cycles (multisegmental) can be used for section reconstruction. With these combined advantages, current 64-section CT systems provide better spatial and temporal resolution than do earlier generations of multidetector CT scanners, and higher spatial resolution and a better signal-to-noise ratio than do electron-beam CT scanners (50). In the clinical evaluation of coronary stents, better delineation of the graft struts and of the presence of instent restenosis is possible with 64-section CT technology.

STENT IMAGING WITH MULTIDETECTOR CT

General issues

In addition to the specifications of scanner hardware, scanning technique, and dedicated postprocessing (ie, convolution filter), variables such as stent diameter, material, and design as

well as patient characteristics may heavily affect the visibility of the in-stent lumen. The earliest experiments to assess the feasibility of coronary stent imaging with multidetector CT were performed in vitro with varying collimations, contrast material concentrations, stent calibers, and stent positions within the gantry (51–53). When imaging is performed in vivo, stent-related beam hardening artifacts are a constant phenomenon, and assessment is further complicated by vessel wall calcifications, poor contrast-to-noise ratios in obese patients, and motion.

Beam hardening and blooming effect

Metallic struts cause a severe CT artifact known as blooming effect. Blooming effect results from beam hardening and causes the stent struts to appear thicker than they are (51) and, often, to overlap the vessel lumen. The result is an underestimation of the in-stent luminal diameter (Figure 1A). The energy spectrum of the x-ray beam as it passes through a hyperattenuating structure increases because lower-energy photons are absorbed more rapidly than are higher-energy photons, with the result that the beam is more intense when it reaches the detectors. Calcified spots of the vessel wall near or at the outer surface of an implanted stent also contribute to beam hardening, which further erodes the assessability of the stent lumen (Figure 1B, 1C). Depending on the type of metal and the design of the stent, the magnitude of the artifact varies (Figure 2) (53). As a rule, the depiction of stents with the slimmest profile is least affected by blooming artifacts. Beam hardening is counterbalanced mainly by increasing the spatial resolution (decreasing the voxel size) and performing dedicated data filtering.

Tube voltage is usually a constant parameter in cardiac protocols, but the contrast between structures on images also depends on the amount of x-ray energy. At lower-voltage settings, which correspond to lower energy of the x-ray beam, the CT number of metal increases substantially, and, hence, beam hardening artifacts are more likely to occur. Beam hardening artifacts also may be exacerbated by motion or by inappropriate selection of the reconstruction window (54). Conversely, they may be minimized by reducing the amount of motion inherent in the data set and optimizing the reconstruction window.

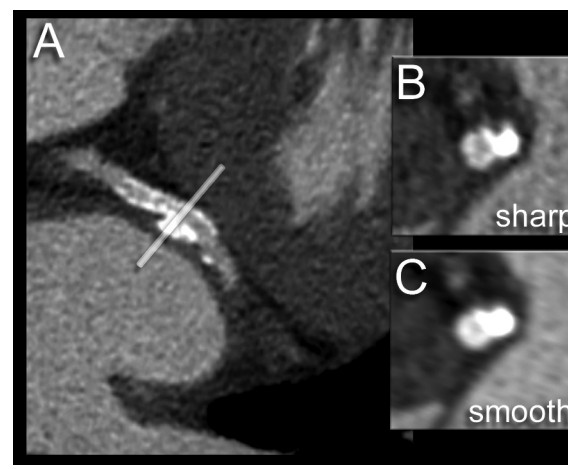

Figure 1. Blooming effect on follow-up images obtained with 64-section CT in a patient who underwent stent implantation in the left circumflex coronary artery. (A) Longitudinal multiplanar reformatted image shows, at the outer edge of the stent, a calcified spot that contributes to beam hardening and hampers visualization of the in-stent lumen. Note the insufficient dilation of the stent proximal to the bulky calcification. (B, C) Sharp-kernel-filtered cross-sectional image (B), obtained at the level indicated in A (line), is less affected by blooming than is the smooth-kernel-filtered cross-sectional image (C).

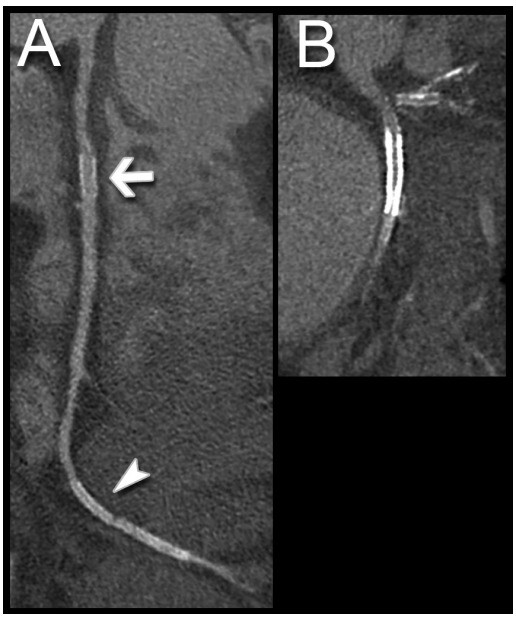

Figure 2. Variation in the severity of metal-related artifacts at 64-section CT with variations in metallic content, design, and luminal diameter of the stent. (A) Curved multiplanar reformatted image obtained in a patient with a 4-mm-caliber stent in the proximal right coronary artery (arrow) and 2.50-mm-caliber (arrowhead) and 2.25-mm-caliber stents in the posterolateral artery. Although all three stents consist of the same material, the in-stent lumen in the two stents in the posterolateral artery is not visible because of the small stent caliber.
Note the gap between the stents implanted in the posterolateral artery. (B) Image obtained in another patient, who underwent stent implantation (different stent type, 5-mm caliber) in the proximal circumflex artery, shows a more pronounced metal-related artifact than is visibel in A.

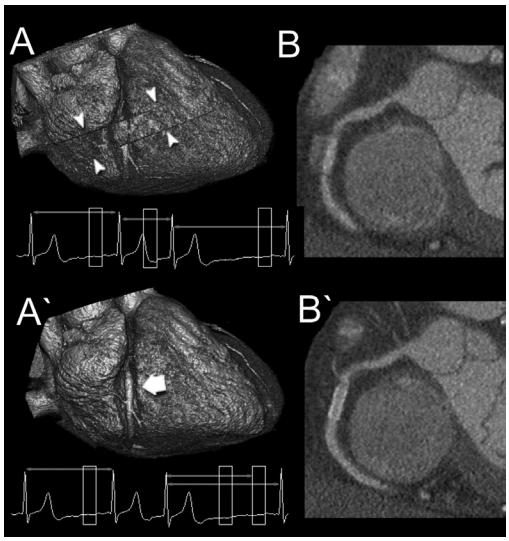

Figure 3. Residual cardiac motion exacerbates metal-related artifacts at 64-section CT in a patient with a stent in the midportion of the right coronary artery and with a premature heartbeat recorded at ECG during scanning. (A, B) Images obtained from data acquired during gating with the original ECG tracing. On the volume-rendered image (A), a stepladder artifact (arrowheads) is visible at the level of the midportion of the right coronary artery. On the multiplanar reformatted image (B), a blurring of contours is visible. (A', B') Images obtained with cardiac gating after editing of the ECG tracing. To avoid a gap in the image data, the reconstruction window during the premature heartbeat was deleted and another was added to the subsequent cardiac cycle. This step eliminated the abrupt heart rate change related to the premature beat and allowed a more coherent reconstruction of the data set. On the volume-rendered image (A'), the appearance of the stent (arrow) is unaffected by motion artifacts. Likewise, the in-stent lumen is well depicted on the multiplanar reformatted image (B').

Partial volume averaging and interpolation

Another obstacle to coronary stent imaging is related to partial volume averaging and interpolation. Inherent in all digital tomographic imaging techniques, partial volume averaging yields a CT number that represents the average attenuation of the materials within a voxel. At stent imaging in vessels with a large diameter, such as the aorta or iliac arteries, beam hardening and partial volume averaging effects are present but are limited to the proximity of the vessel wall. In coronary arteries with smaller diameters, the artifacts are of the same magnitude, but a reliable assessment of the lumen is much more problematic. The smaller the stent, the more detrimental the effect of partial volume averaging on the assessability of the in-stent lumen (Figure 2A).

The thinner detector width on 64-section CT scanners partly solves this problem by reducing the voxel size and thereby the general assessability of the stent lumen (48,55,56).

Optimization of contrast enhancement

Prominent contrast enhancement in the lumen is a prerequisite for robust coronary CT angiography (57). It is achieved not only by optimizing the contrast material injection parameters (ie, using a high-concentration contrast agent and a fast injection rate) but also by accurately synchronizing the CT data acquisition with the passage of the contrast agent by means of bolus tracking or a test bolus. Edge-enhancing convolution filters, which may be used for better delineation of stents, have the drawback of producing noisier data sets. If such a convolution filter is used, the assessability of the in-stent lumen particularly benefits from the presence of a high degree of intraluminal contrast enhancement, which somewhat compensates for the kernel-related noise. A high degree of intraluminal enhancement is recommended especially for the investigation of stent patency in vessels that have a small diameter and thus contain less blood.

Residual cardiac motion

Residual cardiac motion is of the utmost importance as a cause of vessel non assessability at multidetector CT coronary angiography. Residual cardiac motion also plays a role in exacerbating metal-related artifacts such as beam hardening and partial volume averaging effects (Figure 3).

The use of high gantry rotation speeds, multisegmental reconstruction techniques, and β-blockers to lower the heart rate consistently improves the interpretability of multidetector CT coronary angiograms. ECG-based editing techniques allow an improvement of image quality for patients with mild irregularities in sinus rhythm, such as premature beats, and for those with bundle-branch block.

CONVOLUTION FILTERS

Once the technical requirements and acquisition parameters for adequate coronary CT angiography have been fulfilled, additional dedicated postprocessing can be performed to optimize the visualization of the stent. The use of a dedicated edge-enhancing convolution kernel allows a significant decrease in the severity of blooming artifacts at the edges of high-attenuation structures. Indeed, the in-stent contrast-enhanced attenuation measured on sharp-kernel images is closer to that measured in the proximal or distal lumen than is the in-stent attenuation measured on smooth-kernel images (43).

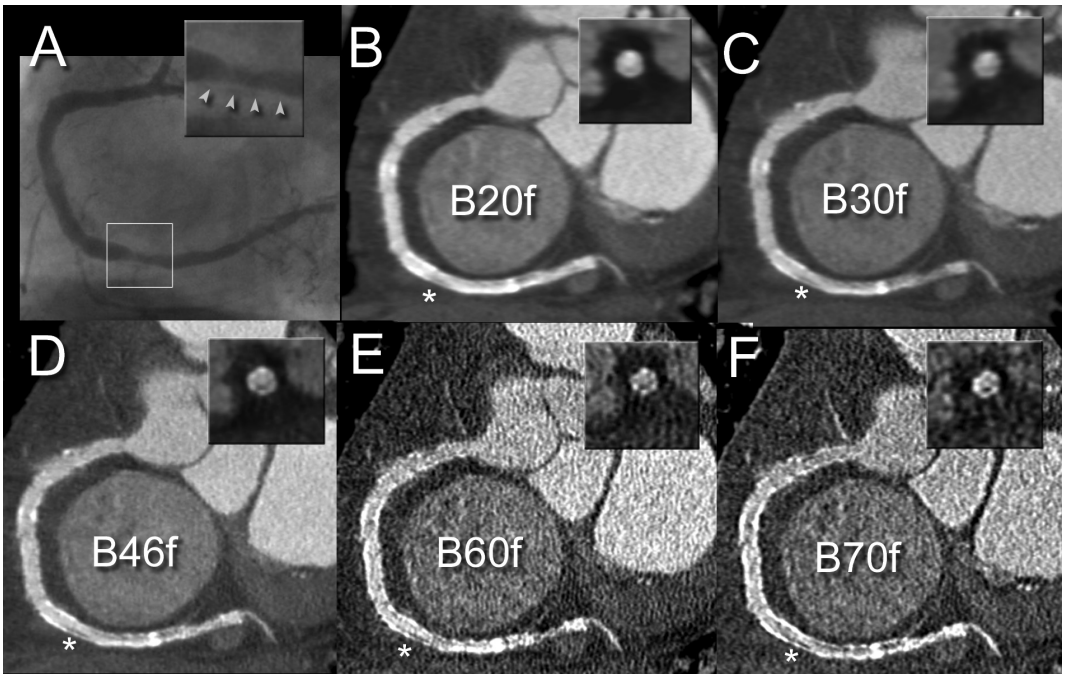

Figure 4. Visibility of low-contrast structures with different convolution filters. The most appropriate filter must be chosen so that an advantageous balance is achieved between the visibility of low-contrast structures and the quantity of image noise. (A) Conventional coronary angiogram shows nonsignificant neointimal hyperplasia in the distal portion
of the right coronary artery (arrowheads). (B–F) Multidetector 64-section CT angiograms obtained in a patient with multiple stents in the right coronary artery. On the image reconstructed with a smooth convolution filter (B20f) (B), the luminal defect (*) is hardly visible. On the image reconstructed with a medium-smooth convolution filter (B30f) (C), the defect (*) is visible but quite blurred. The image reconstructed with a dedicated edge-enhancing kernel (B46f) (D) allows visualization of in-stent neointimal hyperplasia (*), with good contrast between the defect and the surrounding structures (stent scaffold, enhanced lumen). On the images reconstructed with sharp (B60f) (E) and very sharp (B70f) (F) convolution filters, the edge enhancement does not provide clearer depiction of the defect (*) but, instead, greater amounts of image noise.

According to the authors of a recently published article about the effects of reconstruction kernels on the delineation of coronary stents (58), when a medium-smooth filter is applied, as a consequence of the blooming effect an average in-stent lumen narrowing of 37% is observed in comparison with the diameter of the untreated vessel segment, and the measured in-stent attenuation exceeds the aortic attenuation by more than 100 HU because of the partial volume averaging effect. In contrast, the in-stent lumen narrowing is 29% of the diameter of the normal vessel segment on sharp-filtered images, and the in-stent attenuation exceeds the attenuation in the aorta by only 60 HU.

The results of such studies support the superior depiction of the stent lumen with dedicated edge-enhancing convolution kernels in comparison with conventional medium-smooth kernels. While spatial resolution is increased and blooming artifact is reduced by the application of edge-enhancing filters, an increase in image noise has to be accepted as a trade-off. Thus, the most appropriate filter must be chosen so that an advantageous balance is achieved

between the visualization of low contrast structures and image noise (Figure 4). In these instances, high intraluminal contrast enhancement is also very helpful to counterbalance the increased image noise. Additional "intelligent" noise-reduction filters may prove beneficial for the depiction of low-contrast structures within the in-stent lumen and therefore may help detect in-stent restenosis (58).

INTERPRETATION OF MULTIDETECTOR CT DATA

Display techniques and windowing

The clinical evaluation of coronary arteries on CT angiograms is routinely performed by using multiplanar reformation of the data volume. Curved multiplanar reformation, maximum intensity projection, and volume rendering techniques also are often used. The same techniques are applied for the evaluation of coronary stents on CT angiograms. Multiplanar reformatted images and cross-sectional images of the stent are the most useful views on which to assess patency, restenosis, or a minor degree of neointimal hyperplasia. Advances in CT technology have provided 64-section CT scanners with submillimeter spatial resolution of 0.4 x 0.4 x 0.4 mm (43,48). With the very small isotropic voxel size, the assessability of the stent lumen on multiplanar reformatted images remains unaffected by angulation in relation to the z-axis.

CT window settings affect image contrast and noise. If the window is set too narrow, image noise may be significantly increased, and grayscale differentiation of fine structural details may be lost. Wide window settings are necessary for accurate evaluation of the in-stent lumen at CT angiography (window width, 1500 HU; window center, 300 HU) (Figure 5). Although they are not routinely used to assess CT scans in the clinical setting, other three-dimensional volume rendering techniques are available with current CT scanners.

After suitable threshold ranges or transparency settings are selected, an endoscopic view of the internal surface of the vessel can be simulated (Figure 6). This technique may allow visualization of different stent designs (eg, slotted tube and corrugated ring stents) (59). In stents with small diameters, though, the amount of image noise may be too great for such techniques to be reproducibly applied.

In-stent lumen evaluation

As mentioned earlier (39), the direct visualization of the in-stent lumen is important for assessing patency, because collateral vessels may be feeding the vessel segment distal to the occluded stent in a retrograde direction.

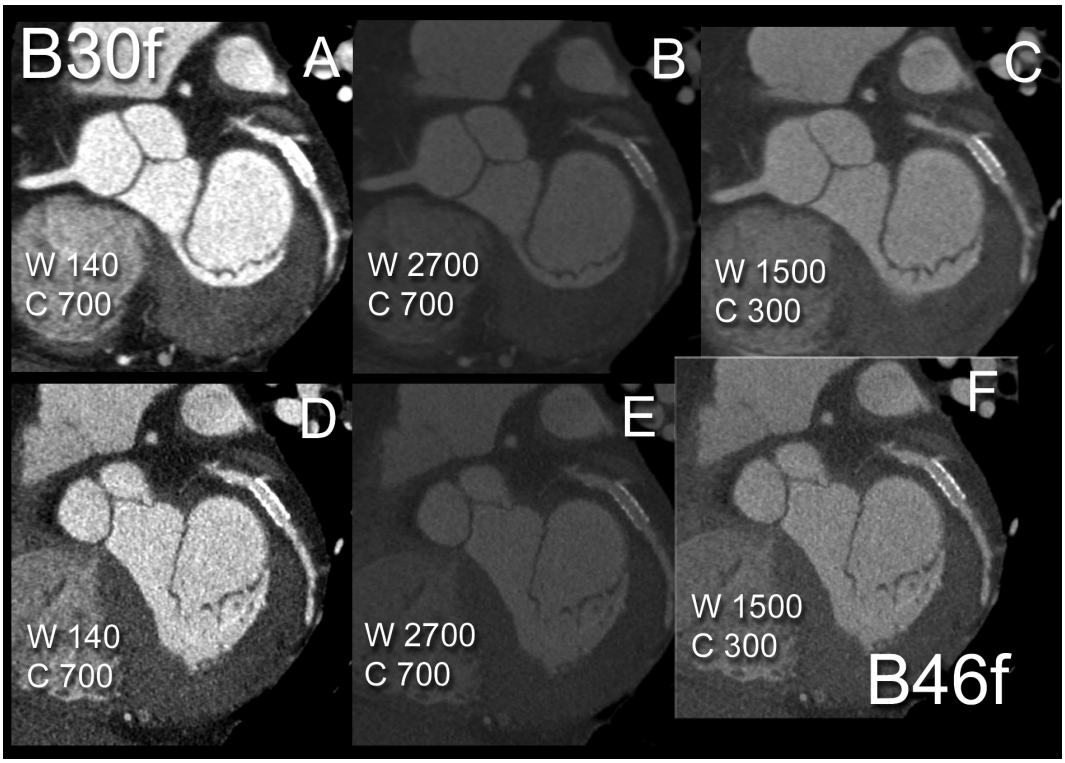

Figure 5. Combined effects of the selected filter and window settings on image contrast and noise at 64-section CT coronary angiography. (A–C) Images obtained with a medium-smooth convolution kernel (B30f). (D–F) Images obtained with a dedicated sharp convolution kernel (B46f). Note that D–F more clearly depict the in-stent lumen than do A–C. The standard soft-tissue window width (W) (A, D) is too narrow and accentuates blooming artifacts. On the
image filtered with a medium-smooth convolution kernel (A), the blooming effect totally obscures the in-stent lumen. With exaggerated widening of the window (B, E), the blooming effect is decreased, but this occurs at the expense of overall image contrast. Setting the window center (C) at approximately 300 HU and choosing a width (W) of approximately
1500 HU allows a more favorable balance between image contrast and noise (C, F). However, the window settings alone are not sufficient to ensure optimal depiction of the inner lumen (C). The combined use of a dedicated edge-enhancing convolution kernel, which increases image spatial resolution, and appropriate window settings to compensate for filter-related noise allows the most favorable in-stent lumen visualization (F).

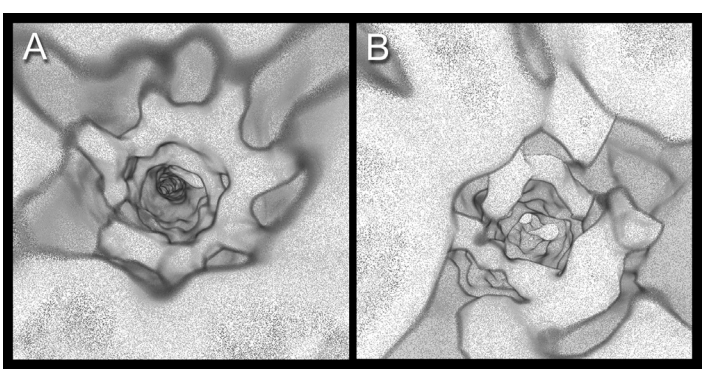

Figure 6. Selection of suitable threshold ranges and opacity settings allows simulation of an endoscopic view of the inner vessel surface and makes it possible to recognize different designs of the metal scaffold in stents. A slotted tubular stent (A) and a corrugated ring stent (B) are currently used for the treatment of most coronary lesions. Both stents have a diameter of 3 mm. The amount of image noise may prevent successful application of this technique for depiction of the lumen in stents with very small diameters.

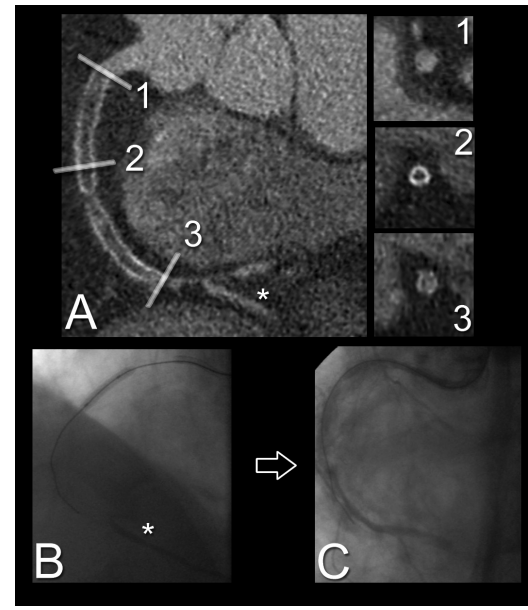

Figure 7. In-stent occlusion in a patient with recurrent angina pectoris 18 months after implantation of two stents in the right coronary artery. CT was performed after conventional angiography failed to depict the right coronary artery. (A) Multiplanar reformatted image shows lower attenuation inside the stent lumina than in the proximal untreated tract of the right coronary artery, a gap between the occluded stents, and collateral filling (*). (1–3) Cross-sectional images obtained at the proximal end of the stent (1), in the middle portion (2), and at the distal end (3) show the appearances of patency, occlusion, and patency, respectively. (B, C) Conventional angiograms provide information about the presence of collateral filling (* in B) and the length of the occlusion. This information enabled planning for percutaneous revascularization, which was successful, as evident from a comparison of the pre-treatment image (B) and the post-treatment image (C).

An accurate intraluminal evaluation can best be performed by means of multiplanar reformation of the CT data volume. The stent may be considered to be occluded if the lumen inside the device appears darker than the contrast-enhanced vessel lumen proximal to the stent.

Unless severe artifacts affect the CT data set, stent evaluation may proceed beyond a judgment of patency or occlusion. Nonocclusive in-stent neointimal hyperplasia is characterized by the presence of a darker rim between the stent and the contrast-enhanced vessel lumen (Figure 4) and is secondary to the healing response to procedure-related vessel injury. If neointimal hyperplasia exceeds a luminal diameter reduction of 50%, the process is consistent with hemodynamically significant in-stent restenosis (Figure 7) (39).

In-stent restenosis typically occurs as a localized nonenhancing lesion, often (but not invariably) associated with complex lesion anatomy (ie, ostial lesions) and discontinuity in lesion coverage. It occurs with higher frequency in patients with diabetes mellitus (26). Restenosis may occur either within or adjacent to the stent (within 5 mm of the stent extremities). Edge restenosis might occur because of a decrease in local drug availability, incomplete lesion coverage due to a gap between two stents, procedure-related trauma, or damage to the polymer coating of a stent from calcifications or an overlapping stent (33).

Bifurcation lesions

Arterial branching points are particularly vulnerable to the atherosclerotic process and its complications. The treatment of lesions located at coronary artery bifurcations, including the left main artery bifurcation, currently accounts for approximately 15% of all percutaneous

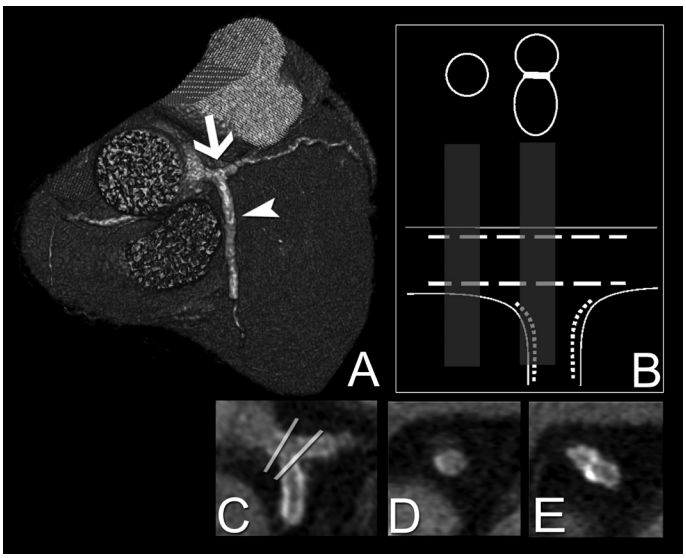

Figure 8. T stent implantation at the left main coronary artery bifurcation. (A) Volume-rendered image obtained with 64-section CT shows the left main coronary artery and circumflex artery (arrow), which constitute the main branch, and the anterior descending artery (arrowhead), the side branch for stent implantation. (B–E) T-stent cross-sectional diagram (B), curved multiplanar reformatted image (C), and cross-sectional images (D, E) obtained in the planes indicated in C show overlap of the metal struts only at the bifurcation point.

coronary artery interventions (20,60,61). Stent implantation at coronary artery bifurcations remains technically challenging and is associated with higher restenosis rates than is stent placement for simple lesions (62). An accurate and noninvasive coronary imaging tool thus is highly desirable for the follow-up of these patients.

Numerous techniques of stent deployment in bifurcation lesions have been described (63–72). The preferred stent implantation strategy depends on the bifurcation anatomy and takes into account the plaque location in relation to the side branch (63–65). In accordance with the strategy applied, different stent configurations may be observed on CT images.

If the lesion anatomy allows it, the provisional stent implantation technique is preferred. This technique consists of stent placement in the main branch first, with subsequent implantation of a second stent in the side branch only if residual stenosis or dissection is present (66). However, in many patients, both the main branch and the side branch are severely diseased. In such cases, the simultaneous implantation of a stent in both branches is favored.

The "T" stent technique (Fig 8) was developed for the treatment of vessels with a bifurcation angle close or equal to 90°. Side branches that originate with a narrower angle (less than 70°) are preferably treated by using one of many available "Y" stent techniques, since incomplete coverage of the side-branch ostium may lead to the recurrence of stenosis at that spot (67,68).

Another variant, the "V" stent technique, involves the implantation of two stents together: one stent is advanced into the side branch; the other, into the main branch. The two stents are in direct contact proximally and form a new bifurcation angle (69). If this angle extends a con-

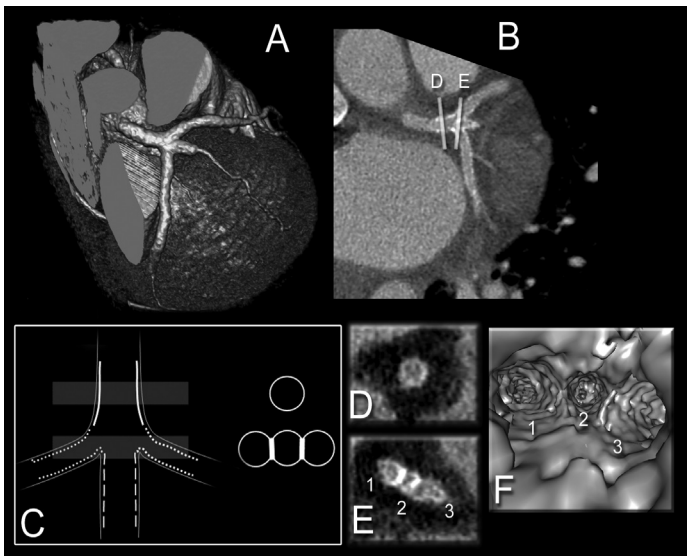

Figure 9. V stent implantation in the left coronary artery. (A, B) Volume-rendered image (A) and multiplanar reformatted image (B) show the left main artery and the anterior descending, intermediate, and circumflex branches, in which stents were placed to provide full coverage of the branching point. (C) Diagram of the V stent technique shows overlap of the metal struts only at the trifurcation. (D, E) Cross-sectional images, obtained in the planes shown in B, show the slim and symmetric profiles of the stents, both proximally (D) and at the level of the carina (E). (F) Volume-rendered image obtained for visualization of the vessel lumen provides a simulated endoscopic view of the origin of the three branches (1–3).

siderable distance (usually, 5 mm or more) into the proximal part of the main branch, the technique is referred to as "simultaneous kissing stents" (3,69). V stents and simultaneous kissing stents are suitable for proximal lesions, such as lesions located at the left main coronary artery bifurcation (Figure 9), provided that the part of the main branch that is proximal to the bifurcation is free of disease.

The "culottes" or "trousers" technique (Figure 10) is another well-known Y stent variant that ensures full coverage of the side-branch ostium. First, a stent is deployed across the branch that has the greatest angulation, usually the side branch. Next, a balloon catheter is passed through the struts of the stent, into the other branch, and dilated; a second stent is then delivered into that branch (usually the main branch). This technique is suitable for use at bifurcations of any angulation. The bifurcation itself is fully covered, albeit at the expense of an excess of metal at the proximal end (70,71).

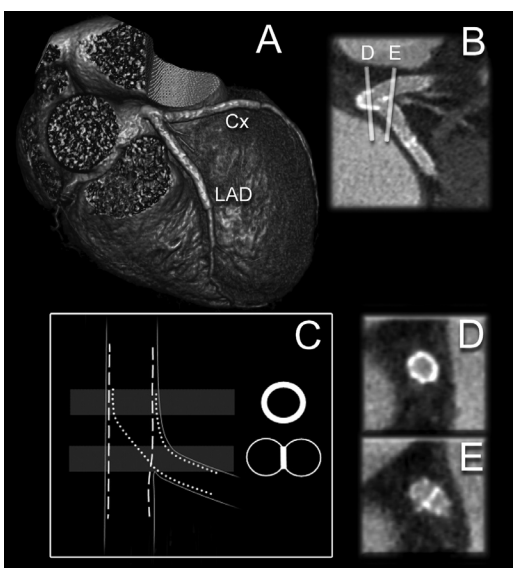

Figure 10. Y stent implantation at the bifurcation of the left main coronary artery. (A) Volume-rendered image shows the point of bifurcation, at which two stents were implanted in a configuration resembling a pair of trousers or culottes. Cx = left circumflex artery, LAD = left anterior descending artery. (B) Multiplanar reformatted image shows stent patency at the level of the bifurcation. (C) Diagram shows the concentrically deployed stents, which overlap near the point of bifurcation. (D, E) Cross-sectional images, obtained in the planes shown in B, depict a thicker stent profile in the parent vessel (D) at a level near the side-branch ostium (E).

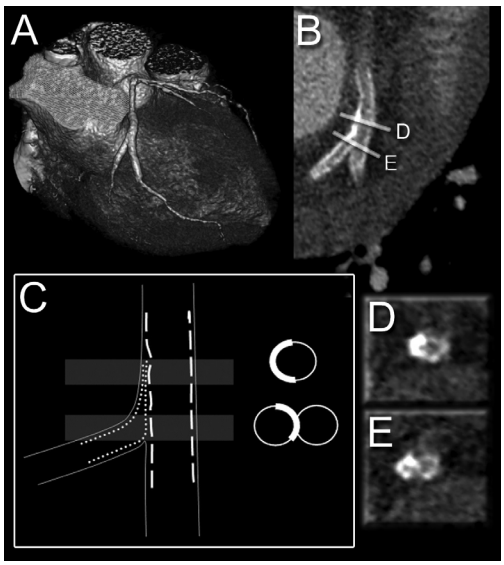

Figure 11. Crush stent placement at the circumflex-marginal artery bifurcation. (A, B) Volume rendered image (A) and curved multiplanar reformatted image (B) allow assessment of the stent configuration. (C) Diagram shows the multiple layers of metal that produce an asymmetric appearance of the cross-sectional stent profile. (D, E) Cross-sectional images, obtained in the planes shown in B, show asymmetric high attenuation where the layers of metal overlap, both proximal to the bifurcation (D) and across the ostium of the side-branch vessel (E).

This excess of metal produces marked hyperattenuation at the bifurcation on the CT image, an effect that may prevent visualization of the lumen. The "crush" technique, like the V technique, involves the simultaneous insertion of two stents (Figure 11) (72). he side-branch stent, which protrudes minimally into the main branch, is deployed at the bifurcation. Subsequently, the main-branch stent is deployed across the ostium of the side-branch vessel and causes the protruding side-branch stent to be flattened against the vessel wall (hence the term crush). As a result, three layers of metal are applied to the vessel wall of the main branch immediately upstream of the side-branch ostium, a stent configuration that results in an area of hyperattenuation on one side of the vessel on multidetector CT angiograms.

SUMMARY

Considering the high number of percutaneous coronary interventions that involve stent implantation, the development of relatively inexpensive and noninvasive methods for assessing stent patency is an issue of growing interest. Multidetector CT has recently emerged above competing modalities such as electron-beam CT and MR imaging as a practical alternative to invasive coronary angiography. Despite image-degrading effects caused by the metallic scaffold of the stent, recent experience with the current generation of 64-section scanners suggests improved assessability of the in-stent lumen with the capability to appreciate more subtle degrees of in-stent neointimal hyperplasia. Knowledge of the different types of artifacts and how they can be compensated for with dedicated postprocessing and appropriate image views and window settings is a prerequisite for reliable depiction of the in-stent lumen and leads to a more robust application of CT findings in the clinical context. In future, the development of biodegradable stents may create optimal conditions for noninvasive post-implantation follow-up with multidetector CT.

REFERENCES

1. Serruys PW, de Jaegere P, Kiemeneij F, et al. A comparison of balloon-expandable-stent implantation with balloon angioplasty in patients with coronary artery disease. Benestent Study Group. N Engl J Med 1994;331:489–495.
2. Fischman DL, Leon MB, Baim DS, et al. A randomized comparison of coronary-stent placement and balloon angioplasty in the treatment of coronary artery disease. Stent Restenosis Study Investigators. N Engl J Med 1994;331:496–501.
3. Sharma SK, Choudhury A, Lee J, et al. Simultaneous kissing stents (SKS) technique for treating bifurcation lesions in medium-to-large size coronary arteries. Am J Cardiol 2004;94:913–917.
4. de Feyter PJ, Kay P, Disco C, Serruys PW. Reference chart derived from post-stent-implantation intravascular ultrasound predictors of 6-month expected restenosis on quantitative coronary angiography. Circulation 1999;100:1777–1783.
5. Mercado N, Boersma E, Wijns W, et al. Clinical and quantitative coronary angiographic predictors of coronary restenosis: a comparative analysis from the balloon-to-stent era. J Am Coll Cardiol 2001;38:645–652.
6. Serruys PW, Kay IP, Disco C, Deshpande NV, de Feyter PJ. Periprocedural quantitative coronary angiography after Palmaz-Schatz stent implantation predicts the restenosis rate at 6 months: results of a meta-analysis of the Belgian Netherlands Stent study (BENESTENT) I, BENESTENT II Pilot, BENESTENT II and MUSIC trials. Multicenter Ultrasound Stent In Coronaries. J Am Coll Cardiol 1999;34:1067–1074.
7. Jeremias A, Kutscher S, Haude M, et al. Nonischemic chest pain induced by coronary interventions: a prospective study comparing coronary angioplasty and stent implantation. Circulation 1998;98:2656–2658.
8. Kim WY, Danias PG, Stuber M, et al. Coronary magnetic resonance angiography for the detection of coronary stenoses. N Engl J Med 2001;345:1863–1869.
9. Hug J, Nagel E, Bornstedt A, Schnackenburg B, Oswald H, Fleck E. Coronary arterial stents: safety and artifacts during MR imaging. Radiology 2000;216:781–787.
10. Pump H, Mohlenkamp S, Sehnert CA, et al. Coronary arterial stent patency: assessment with electronbeam CT. Radiology 2000;214:447–452.
11. Knollmann FD, Moller J, Gebert A, Bethge C, Felix R. Assessment of coronary artery stent patency by electron-beam CT. Eur Radiol 2004;14:1341–1347.
12. Schuijf JD, Bax JJ, Jukema JW, et al. Feasibility of assessment of coronary stent patency using 16-slice computed tomography. Am J Cardiol 2004;94:427–430.

13. Smith SC Jr, Dove JT, Jacobs AK, et al. ACC/AHA guidelines of percutaneous coronary interventions (revision of the 1993 PTCA guidelines)— executive summary. A report of the American College of Cardiology/American Heart Association Task Force on Practice Guidelines (committee to revise the 1993 guidelines for percutaneous transluminal coronary angioplasty). J Am Coll Cardiol 2001;37:2215–2239.
14. Coronary artery disease statistics—2005 edition [database online]. Oxford, England: British Heart Foundation, 2005. British Heart Foundation Statistics Website. http://www.heartstats.org. Accessed May 28, 2005. Updated June 9, 2005.
15. Health care in America: trends in utilization. Hyattsville, Md: NCHS/CDC, 2004. Centers for Disease Control, National Center for Health Statistics Web site. http://www.cdc.gov/nchs/pressroom/04facts/healthcare.htm. Published January 30, 2004. Accessed May 28, 2005.
16. Heart disease and stroke statistics—2005 update. Dallas, Tex: American Heart Association, 2005. American Heart Association Web site. http://www.americanheart.org. Accessed May 28, 2005. Updated January 11, 2006.
17. Abrams J. Clinical practice. Chronic stable angina. N Engl J Med 2005;352:2524–2533.
18. Hannan EL, Racz MJ, Walford G, et al. Long-term outcomes of coronary-artery bypass grafting versus stent implantation. N Engl J Med 2005;352:2174–2183.
19. de Feyter PJ, Serruys PW, Unger F, et al. Bypass surgery versus stenting for the treatment of multivessel disease in patients with unstable angina compared with stable angina. Circulation 2002;105:2367–2372.
20. Iakovou I, Schmidt T, Bonizzoni E, et al. Incidence, predictors, and outcome of thrombosis after successful implantation of drug-eluting stents. JAMA 2005; 293:2126–2130.
21. McFadden EP, Stabile E, Regar E, et al. Late thrombosis in drug-eluting coronary stents after discontinuation of antiplatelet therapy. Lancet 2004;364:1519–1521.
22. Ong AT, McFadden EP, Regar E, de Jaegere PP, van Domburg RT, Serruys PW. Late angiographic stent thrombosis (LAST) events with drug-eluting stents. J Am Coll Cardiol 2005;45:2088–2092.
23. Ong AT, Hoye A, Aoki J, et al. Thirty-day incidence and 6-month clinical outcome of thrombotic stent occlusion after bare-metal, sirolimus, or paclitaxel stent implantation. J Am Coll Cardiol 2005;45:947–953.
24. Rensing BJ, Hermans WR, Beatt KJ, et al. Quantitative angiographic assessment of elastic recoil after percutaneous transluminal coronary angioplasty. Am J Cardiol 1990;66:1039–1044.
25. Mintz GS, Popma JJ, Pichard AD, et al. Arterial remodeling after coronary angioplasty: a serial intravascular ultrasound study. Circulation 1996;94:35–43.
26. Hoffmann R, Mintz GS, Dussaillant GR, et al. Patterns and mechanisms of in-stent restenosis: a serial intravascular ultrasound study. Circulation 1996;94:1247–1254.

27. Kiemeneij F, Serruys PW, Macaya C, et al. Continued benefit of coronary stenting versus balloon angioplasty: 5-year clinical follow-up of Benestent-I trial. J Am Coll Cardiol 2001;37:1598–1603.
28. Morice MC, Serruys PW, Sousa JE, et al. A randomized comparison of a sirolimus-eluting stent with a standard stent for coronary revascularization. N Engl J Med 2002;346:1773–1780.
29. Mauri L, O'Malley AJ, Popma JJ, et al. Comparison of thrombosis and restenosis risk from stent length of sirolimus-eluting stents versus bare metal stents. Am J Cardiol 2005;95:1140–1145.
30. Wong SC, Hong MK, Ellis SG, et al. Influence of stent length to lesion length ratio on angiographic and clinical outcomes after implantation of bare metal and drug-eluting stents (the TAXUS-IV Study). Am J Cardiol 2005;95:1043–1048.
31. Lemos PA, Hofma SH, Regar E, Saia F, Serruys PW. Drug-eluting stents for the treatment of coronary disease: state-of-the-art. In: Marco J, Serruys P, Biamino G, et al, eds. EuroPCR textbook. Paris, France: Europa, 2004.
32. Moses JW, Leon MB, Popma JJ, et al. Sirolimus-eluting stents versus standard stents in patients with stenosis in a native coronary artery. N Engl J Med 2003; 349:1315–1323.
33. Lemos PA, Saia F, Ligthart JM, et al. Coronary restenosis after sirolimus-eluting stent implantation: morphological description and mechanistic analysis from a consecutive series of cases. Circulation 2003;108:257–260.
34. Ong AT, Serruys PW, Aoki J, et al. The unrestricted use of paclitaxel- versus sirolimus-eluting stents for coronary artery disease in an unselected population: 1-year results of the Taxus-Stent Evaluated at Rotterdam Cardiology Hospital (T-SEARCH) registry. J Am Coll Cardiol 2005;45:1135–1141.
35. van der Hoeven BL, Pires NM, Warda HM, et al. Drug-eluting stents: results, promises and problems. Int J Cardiol 2005;99:9–17.
36. Kruger S, Mahnken AH, Sinha AM, et al. Multislice spiral computed tomography for the detection of coronary stent restenosis and patency. Int J Cardiol 2003;89:167–172.
37. Maintz D, Grude M, Fallenberg EM, Heindel W, Fischbach R. Assessment of coronary arterial stents by multislice-CT angiography. Acta Radiol 2003;44:597–603.
38. Ligabue G, Rossi R, Ratti C, Favali M, Modena MG, Romagnoli R. Noninvasive evaluation of coronary artery stents patency after PTCA: role of multislice computed tomography. Radiol Med (Torino) 2004; 108:128–137.
39. Cademartiri F, Mollet N, Lemos PA, et al. Usefulness of multislice computed tomographic coronary angiography to assess in-stent restenosis. Am J Cardiol 2005;96:799–802.
40. Gilard M, Cornily JC, Rioufol G, et al. Noninvasive assessment of left main coronary stent patency with 16-slice computed tomography. Am J Cardiol 2005; 95:110–112.
41. Gilard M, Cornily JC, Pennec PY, et al. Assessment of coronary artery stents by 16-slice computed tomography. Heart 2006;92:58–61.

42. Kitagawa T, Fujii T, Tomohiro Y, et al. Noninvasive assessment of coronary stents in patients by 16-slice computed tomography. Int J Cardiol 2005. doi: 10.1061/j.ijcard.2005.06.012. Published July 14, 2005. Accessed September 15, 2005.
43. Hong C, Chrysant GS, Woodard PK, Bae KT. Coronary artery stent patency assessed with in-stent contrast enhancement measured at multi– detector row CT angiography: initial experience. Radiology 2004; 233:286–291.
44. Ohnuki K, Yoshida S, Ohta M, et al. New diagnostic technique in multi-slice computed tomography for in-stent restenosis: pixel count method. Int J Cardiol 2005. doi:10.1016/j.ijcard.2005.05.013. Published June 27, 2005. Accessed September 15, 2005.
45. Leschka S, Alkadhi H, Plass A, et al. Accuracy of MSCT coronary angiography with 64-slice technology: first experience. Eur Heart J 2005;26:1482–1487.
46. Leber AW, Knez A, von Ziegler F, et al. Quantification of obstructive and nonobstructive coronary lesions by 64-slice computed tomography: a comparative study with quantitative coronary angiography and intravascular ultrasound. J Am Coll Cardiol 2005;46:147–154.
47. Raff GL, Gallagher MJ, O'Neill WW, Goldstein JA. Diagnostic accuracy of noninvasive coronary angiography using 64-slice spiral computed tomography. J Am Coll Cardiol 2005;46:552–557.
48. Flohr T, Bruder H, Stierstorfer K, Simon J, Schaller S, Ohnesorge B. New technical developments in multislice CT. II. Sub-millimeter 16-slice scanning and increased gantry rotation speed for cardiac imaging. Rofo 2002;174:1022–1027.
49. Nakanishi T, Kayashima Y, Inoue R, Sumii K, Gomyo Y. Pitfalls in 16–detector row CT of the coronary arteries. RadioGraphics 2005;25:425–438.
50. Maintz D, Fischbach R, Juergens KU, Allkemper T, Wessling J, Heindel W. Multislice CT angiography of the iliac arteries in the presence of various stents: in vitro evaluation of artifacts and lumen visibility. Invest Radiol 2001;36:699–704.
51. Nieman K, Cademartiri F, Raaijmakers R, Pattynama P, de Feyter P. Noninvasive angiographic evaluation of coronary stents with multi-slice spiral computed tomography. Herz 2003;28:136–142.
52. Mahnken AH, Buecker A, Wildberger JE, et al. Coronary artery stents in multislice computed tomography: in vitro artifact evaluation. Invest Radiol 2004; 39:27–33.
53. Maintz D, Juergens KU, Wichter T, Grude M, Heindel W, Fischbach R. Imaging of coronary artery stents using multislice computed tomography: in vitro evaluation. Eur Radiol 2003;13:830–835.
54. Choi HS, Choi BW, Choe KO, et al. Pitfalls, artifacts, and remedies in multi– detector row CT coronary angiography. RadioGraphics 2004;24:787–800.
55. Mahnken AH, Seyfarth T, Flohr T, et al. Flat-panel detector computed tomography for the assessment of coronary artery stents: phantom study in comparison with 16-slice spiral computed tomography. Invest Radiol 2005;40:8–13.

56. Nieman K, Cademartiri F, Lemos PA, Raaijmakers R, Pattynama PM, de Feyter PJ. Reliable noninvasive coronary angiography with fast submillimeter multislice spiral computed tomography. Circulation 2002; 106:2051–2054.
57. Cademartiri F, Mollet NR, van der Lugt A, et al. Intravenous contrast material administration at helical 16–detector row CT coronary angiography: effect of iodine concentration on vascular attenuation. Radiology 2005;236:661–665.
58. Seifarth H, Raupach R, Schaller S, et al. Assessment of coronary artery stents using 16-slice MDCT angiography: evaluation of a dedicated reconstruction kernel and a noise reduction filter. Eur Radiol 2005; 15:721–726.
59. Colombo A, Stankovic G, Moses JW. Selection of coronary stents. J Am Coll Cardiol 2002;40:1021–1033.
60. Farb A, Burke AP, Kolodgie FD, Virmani R. Pathological mechanisms of fatal late coronary stent thrombosis in humans. Circulation 2003;108:1701–1706.
61. Koller P, Safian RD. Bifurcation stenosis. In: Freed E Sr, Grines C, eds. Manual of interventional cardiology. Birmingham, Mich: Physician Press, 1997; 229–241.
62. Hoye A, van der Giessen WJ. New approaches to ostial and bifurcation lesions. J Interv Cardiol 2004;17:397–403.
63. Lefevre T, Louvard Y, Morice MC, et al. Stenting of bifurcation lesions: classification, treatments, and results. Catheter Cardiovasc Interv 2000;49:274–283.
64. Gobeil F, Lefevre T, Guyon P, et al. Stenting of bifurcation lesions using the Bestent: a prospective dual-center study. Catheter Cardiovasc Interv 2002;55:427–433.
65. Colombo A, Moses JW, Morice MC, et al. Randomized study to evaluate sirolimus-eluting stents implanted at coronary bifurcation lesions. Circulation 2004;109:1244–1249.
66. Melikian N, Di Mario C. Treatment of bifurcation coronary lesions: a review of current techniques and outcome. J Interv Cardiol 2003;16:507–513.67. Al Suwaidi J, Berger PB, Rihal CS, et al. Immediate and long-term outcome of intracoronary stent implantation for true bifurcation lesions. J Am Coll Cardiol 2000;35:929–936.
68. Fort S, Lazzam C, Schwartz L. Coronary 'Y' stenting: a technique for angioplasty of bifurcation stenoses. Can J Cardiol 1996;12:678–682.
69. Schampaert E, Fort S, Adelman AG, Schwartz L. The V-stent: a novel technique for coronary bifurcation stenting. Cathet Cardiovasc Diagn 1996;39:320–326.
70. Khoja A, Ozbek C, Bay W, Heisel A. Trouser-like stenting: a new technique for bifurcation lesions. Cathet Cardiovasc Diagn 1997;41:192–196; discussion 197–199.
71. Chevalier B, Glatt B, Royer T. Kissing stenting in bifurcation lesions [abstract]. Eur Heart J 1996;17:218A.
72. Kobayashi Y, Colombo A, Akiyama T, Reimers B, Martini G, di Mario C. Modified "T" stenting: a technique for kissing stents in bifurcational coronary lesion. Cathet Cardiovasc Diagn 1998;43:323–326.

16

Multislice Spiral Computed Tomography for the Evaluation of Stent Patency after Left Main Coronary Artery Stenting: a Comparison with Conventional Coronary Angiography and Intravascular Ultrasound.

Carlos A.G. Van Mieghem[1,2], Filippo Cademartiri[1,2], Nico R. Mollet[1,2], Patrizia Malagutti[2], Marco Valgimigli[1], Willem B. Meijboom[1,2], Francesca Pugliese[2], Eugene P. McFadden[1], Jurgen Ligthart[1], Giuseppe Runza[2], Nico Bruining[1], Pieter C. Smits[3], Evelyn Regar[1], Willem J.van der Giessen[1], Georgios Sianos[1], Ron van Domburg[1], Peter de Jaegere[1], Gabriel P. Krestin[2], Patrick W. Serruys[1], Pim J. de Feyter[1,2]

From the departments of Cardiology[1] and Radiology[2], Erasmus MC, Rotterdam, the Netherlands. From the department of Cardiology[3], Medical Center Rijnmond Zuid, Rotterdam, the Netherlands.

Circulation. 2006; 114:645-53.

ABSTRACT

Background

Surveillance conventional coronary angiography (CCA) is recommended 2 to 6 months after stent-supported left main coronary artery (LMCA) percutaneous coronary intervention due to the unpredictable occurrence of in-stent restenosis (ISR), with its attendant risks. Multislice computed tomography (MSCT) is a promising technique for noninvasive coronary evaluation. We evaluated the diagnostic performance of high-resolution MSCT to detect ISR after stenting of the LMCA.

Methods and Results

Seventy-four patients were prospectively identified from a consecutive patient population scheduled for follow-up CCA after LMCA stenting and underwent MSCT before CCA. Until August 2004, a 16-slice scanner was used (n= 27), but we switched to the 64-slice scanner after that period (n=43). Patients with initial heart rates > 65 bpm received beta-blockers, resulting in a mean periscan heart rate of 57±7 beats/min. Among patients with technically adequate scans (n=70), MSCT correctly identified all patients with ISR (10/70), but misclassified 5 patients without ISR (false positives). Overall, the accuracy of MSCT for detection of angiographic ISR was 93%. The sensitivity, specificity, positive and negative predictive value were 100%, 91%, 67%, and 100%, respectively. When analysis was restricted to patients with stenting of the LMCA with or without extension into a single major side branch, accuracy was 98%. When both branches of the LMCA bifurcation were stented, accuracy was 83%. For the assessment of stent diameter and area, MSCT showed good correlation with IVUS (r = 0.78 and 0.73, respectively). An IVUS threshold value ≥1mm was identified to reliably detect in-stent neointima hyperplasia with MSCT.

Conclusions

Current MSCT technology, in combination with optimal heart rate control, allows reliable non-invasive evaluation of selected patients after LMCA stenting. CT is safe to exclude left main ISR and may therefore be an acceptable first-line alternative to CCA.

INTRODUCTION

Multislice computed tomography coronary angiography (MSCTA) is a promising non-invasive coronary imaging modality.[1,2] Although several reports have shown that it may be used to evaluate stent patency, more precise evaluation of the lumen within the stent is markedly hindered by artificial enlargement of the metallic stent struts caused by blooming artefact.[3] The impact of blooming artefact on the evaluation of structures inside stents is inversely related to stent diameter.[4] In large-diameter coronary stents, such as those implanted in the left main coronary artery (LMCA) or proximal left anterior descending artery (LAD), neointimal hyperplasia (NIH) within the stent can be visualized on multislice computed tomography (MSCT), demonstrating its potential for the detection of in-stent restenosis (ISR), in addition to stent patency, in specific lesion subsets.[5]

Although coronary artery bypass graft (CABG) surgery is still the recommended treatment for significant left main (LM) disease, the introduction of drug-eluting stents (DES) with much lower restenosis rates has increasingly resulted in the alternative use of percutaneous coronary intervention (PCI).[6,7] However, LM ISR still occurs with DES and may result in fatal myocardial infarction or sudden death.[8-10] Careful surveillance, including routine coronary angiography at 2 to 6 months after PCI, is therefore strongly recommended.[11] A noninvasive method to detect ISR and to potentially preempt its clinical consequences would be of evident clinical value. In the present study, we evaluated the potential of MSCT for detecting LM ISR.

METHODS

Patient selection

Between March 2004 and November 2005, we screened 91 consecutive patients scheduled for follow-up coronary angiography after LMCA stenting for inclusion in a protocol to compare MSCT with conventional angiography. In addition, most patients also underwent intravascular ultrasound (IVUS) evaluation of the LMCA. All patients in sinus rhythm who were able to hold their breath for 20 seconds were eligible for inclusion. We excluded patients with the following: previous allergic reaction to contrast, impaired renal function (serum creatinine >1.6 mg/dl), contra-indication to β-blockers (high-degree heart block, poor left ventricular function, asthma, or severe chronic obstructive pulmonary disease), obesity (body mass index >30 kg/m2 for patients scanned with the 16-row MSCT scanner), and those who had an acute coronary syndrome at the time of scheduled angiography. The institutional review board of Erasmus MC Rotterdam approved the study, and all subjects gave informed consent.

MSCT protocol and image acquisition

MSCT was performed in the fortnight before conventional angiography. Patients with a heart rate >65 bpm received 100 mg of metoprolol orally 1 hour before the scan. Up to July 2004, MSCT data were acquired with a 16-slice MSCT scanner (Sensation 16, Siemens, Germany). From August 2004 on, all scans were performed with a 64-slice MSCT scanner (Sensation 64, Siemens, Germany). A bolus of 100 ml of contrast (iodixanol, 320 mg of iodine per 1 ml [mgI/mL]; Visipaque, Nycomed, Inc, Princeton, NJ) was injected intravenously at 4 to 5 ml/sec. MSCT data were acquired during a single breath hold once the contrast material in the ascending aorta reached a predefined threshold of 100 Hounsfield units. The 16-slice MSCT scanner had the following scan parameters: detector collimation 16 x 0.75 mm, table feed 3.0 mm per rotation, gantry rotation time 420 ms, tube voltage 120 kV, and tube current 400 to 450 mA. The parameters for the 64-slice MSCT scanner were: detector collimation 64 x 0.6 mm, table feed 3.8 mm per rotation, gantry rotation time 330 ms, tube voltage 120 kV, and tube current of 900 mA. With dedicated software (WinDose, Institute of Medical Physics, Erlangen, Germany), the average radiation exposure was calculated as 11.8 to 16.3 mSv for the 16-slice MSCT scanner and 15.2 to 21.4 mSv for the 64-slice MSCT scanner. All data were reconstructed using a field of view of 50x50 mm, image matrix of 512x512 pixels, and a sharp heart view (B46f) convolution kernel. Image reconstruction was retrospectively gated to the ECG. The position of the reconstructed window within the cardiac cycle was individually optimized to minimize motion artifacts. Datasets containing no or minimal motion artifacts were transferred to a remote workstation for further evaluation.

MSCT data analysis

Two experienced observers, unaware of the results of convential angiography, evaluated the MSCT data sets on both the original axial images and on multiplanar reformatted reconstructions rendered orthogonal and perpendicular to the vessel course. In the case of LM bifurcation stenting, each of the three segments (LM, left anterior descending artery (LAD), and circumflex artery [CX]) was evaluated individually. To assess significant restenosis (≥50% decrease of lumen diameter as defined by angiography), we evaluated the stent in the LMCA and, where applicable, in related branches, including the 5-mm borders proximal and distal to the stent. The stent lumen was visually evaluated as (1) patent with no visible NIH, (2) patent with non-obstructive (<50% lumen diameter) NIH, (3) patent with obstructive (>50% lumen diameter) NIH, ie, restenosis, and (4) occluded. Disagreements were resolved by consensus. Where a single stent was placed across the LM bifurcation into the LAD or CX, with no intervention, or solely with balloon dilatation in the other branch, we also evaluated the proximal 5 mm of the untreated side branch unless a functional bypass graft was attached to the nonstented branch.

For comparison with IVUS, stent area and diameter at the proximal and distal stent edge and at the ostium of LAD and CX were measured in cross-sectional orthogonal image planes. The degree of luminal narrowing was quantified in the cross section with maximum stenosis as percent diameter and area stenosis by calculating the ratio of the minimal lumen diameter or area by the stent diameter or area.

Angiographic analysis

Conventional x-ray coronary angiography was performed with standard techniques after intracoronary injection of 2 mg of isosorbide dinitrate. Care was taken to ensure that the same views of the LM were obtained as at the time of intervention. An experienced cardiologist, unaware of the results of MSCT, analyzed all angiographic data quantitatively, using validated, automated, edgedetection software (CAAS II, Pie Medical, Maastricht, Netherlands). With the outer diameter of the catheter tip, not filled with contrast, as the calibration standard, we measured from multiple projections in diastole the minimal lumen diameter, the reference diameter, and the percentage diameter stenosis of the LMCA and, where indicated, the LAD and CX; the averaged results were recorded. Binary angiographic restenosis was defined as percentage diameter stenosis ≥50% anywhere within the stent or within the 5mm segments proximal or distal to the stent margins. This definition also applied to the proximal 5mm vessel segment of the untreated LAD or CX, where a stent was placed over the distal left main bifurcation.

IVUS imaging

IVUS was performed with a 2.9F, 40-MHz or a 3.2F, 30-MHz single-element mechanical transducer (Boston Scientific, Natick, Mass). After intracoronary injection of 2 mg of isosorbide dinitrate, the IVUS catheter was positioned at least 1 cm distal to the stent in the LMCA; for patients with bifurcation stenting a sufficiently distal starting point in the LAD or CX was chosen. IVUS images were recorded after initiation of automated pullback at 0.5 mm/s. In case of bifurcation stenting, only one of the 2 major branches, preferentially the LAD, was investigated. IVUS images of the entire pullback were recorded on both S-VHS videotape and CD-ROM for off-line analysis.

IVUS analysis

In our institution all IVUS pullbacks are retrospectively gated with a program that selects images recorded in the end-diastolic phase.[12] Two experienced observers, blinded to the angiography and MSCT results, analyzed and reviewed the IVUS image data sets using an off-line semi-automated software package (Curad, version 3.1, Wijk bij Duurstede, the Netherlands).[13] The stented portion of the LMCA, including the stented parts of the side branches, was evaluated for the presence of NIH. For each of the 3 coronary segments (ie, stented part of LM, LAD, and CX), the following IVUS parameters were measured: (1) minimal lumen crosssectional

area (CSA, mm^2), (2) mean stent CSA (mm^2), (3) minimal lumen diameter (mm), (4) mean stent diameter (mm), and (5) maximal NIH thickness (mm). Similar to the MSCT measurements, stent area and diameter at the proximal and distal stent edge and at the ostium of LAD or CX were determined. The percent diameter and area stenosis were comparably to MSCT determined in cross-sections with maximal in-stent lumen obstruction.

Statistical analysis

Continuous variables are presented as mean ± SD or median with 25% and 75% interquartile ranges. Categorical variables are presented as counts and percentages. Continuous variables were compared by Student t test for normally distributed values; otherwise the Mann-Whitney U test was used. All tests were 2-tailed, and a probability value of <0.05 was considered significant. Accuracy (percentage of patients correctly classified), sensitivity, specificity, and positive and negative predictive value of MSCT for the detection of ≥50% ISR, as determined by quantitative coronary angiography, was calculated on a per-patient basis. Diagnostic test results are reported with associated 95% CIs based on binomial probabilities.

Quantitative IVUS and MSCT data were correlated by means of Bland-Altman and linear regression analysis and by calculating the Pearson correlation coefficient.[14] Mean values were compared with the 2-tailed t-test. The degree of agreement between IVUS and MSCT was also measured by the κ-statistic and expressed as a function of NIH thickness, as determined by IVUS. The intraobserver and interobserver variability for the detection of ISR and NIH was determined with the κ-statistic. Statistical analysis was performed with SPSS, version 12.1 (SPSS Inc., Chicago, Ill).

The authors had full access to the data and take full responsibility for its integrity. All authors have read and agree to the manuscript as written.

RESULTS

Seventeen of the 91 potentially eligible patients (ie, those scheduled for conventional angiography during the inclusion period) had exclusion criteria as outlined in Table 1; 4 of the 74 patients included had a technically inadequate scan. One of those 4 patients had ISR on conventional angiography. The remaining 70 patients constitute the study population. The baseline clinical characteristics of these patients are summarized in Table 2. The median interval between stent placement and computed tomography (CT) imaging was 259 days (range 89 to 758 days), and the average interval between MSCT and conventional coronary angiography (CCA) was 14±16 days. Mean basal heart rate was 68±10 bpm; 49 patients (70%) received additional β-blockers, which resulted in a mean periscan heart rate of 57±7 beats/

Table 1. Reasons to exclude performance of MSCT (n=21 patients)

Reason for exclusion	No. of patients
Patients with exclusion criteria	17
Renal insufficiency	2
Respiratory insufficiency	1
Contra-indication to ¯-blocker (poor left ventricular function)	4
Obesity (BMI> 30 kg/m2)*	3
Atrial fibrillation	3
Acute coronary syndrome	1
Other†	3
Technically inadequate MSCT scan	4
Arrhythmia during the scan	1
Breathing artifact	1
Heart rate >70 bpm	1
Scan failure	1

* This exclusion criterion only applied to patients analyzed with the 16-slice MSCT scanner.
† Other reasons for exclusion were: patient refusal, hearing disability, and presence of an implantable cardioverter defibrillator.

Table 2. Clinical characteristics (n=70 patients)

Age, y, mean±SD	61.2±10.7
Male, %	83
Cardiac risk factors	
Hypertension, %*	44
Hypercholesterolemia, %†	90
Diabetes mellitus, %	19
Current smoking, %	29
Family history of coronary artery disease, %	54
Body mass index (kg/m2), median (IQR)	26.2 (24.2-28.6)
Previous PCI, %	29
Protected left main, %	17
Serum creatinine, mg/dl, mean±SD	1±0.23
Previous heart rate-lowering medication, %	87

IQR indicates interquartile range.
Protected left main indicates LM disease with at least 1 patent arterial or venous conduit to the LAD or CX.
*Blood pressure > 160/95 mmHg or treatment for hypertension. †Total cholesterol >200 mg/dl or treatment for hypercholesterolemia.

min. Mean scan time with the 64-row detector MSCT (n=43, 11.1±1.2 seconds) was significantly ($p < 0.001$) shorter than with the 16-row detector MSCT (n=27, 15.9±1.5 seconds).

Anatomic characteristics and procedural details of index interventions

Table 3 presents the anatomic characteristics of the lesions treated and the procedural details of the index interventions. The vast majority of patients (83%, 58/70) underwent PCI of unprotected LM stem lesions, and DES were used in all but 3 patients (96%). Two groups of patients were defined, according to the characteristics of the PCI procedure. The first group (n=46) was defined as a "simple stenting group" and comprised patients in whom single or

Table 3. Procedural Characteristics (n=70 patients)

No. and type of stents	n=162
Stents per patient, median (IQR)	2 (1-3)
Paclitaxel-eluting stent, n (%)*	123 (76%)
Sirolimus-eluting stent, n (%)†	31 (19%)
Bare metal stent, n (%)†	8 (5%)
Stent and balloon size	
Nominal stent diameter, mm, median (IQR)	3 (3-3.5)
Postdilatation with bigger balloon, %	63
Balloon size for postdilatation, mm, median (IQR)	4 (3.5-4)
Stenting technique	
Simple stenting, n (%)	46 (66%)
Stent only in LM, n	14
Stent from LM to LAD/ LCX, n‡	25/ 7
Complex Bifurcation Stenting, n (%)	24 (34%)
Culotte stenting, n§	13
Crush stenting, n§	2
T-stenting or V-stenting, n	9

IQR indicates interquartile range.
* Express stent (Boston Scientific).† Bx Velocity stent (Cordis).
‡ Additional balloon dilatation of the other branch vessel in 3 patients.
§ Kissing balloon postdilatation in 14 of the 15 patients.

overlapping stents were implanted in the LM stem alone (n=14) or in whom they extended from the LM stem into only the LAD or the CX (n=32). The second group was defined as a "complex bifurcation stenting group" and comprised patients in whom the LM stem and both the LAD and LCX were stented (n=24). Further details are presented in Table 3.

Overall MSCT results

The diagnostic accuracy of MSCT is summarized in Table 4. On the basis of conventional angiography, ISR occurred in 14% of the patients (10/70). In the overall population, MSCT identified all patients with restenosis and correctly classified 55 patients as having no ISR (Figures 1 and 2). In the group of pa-

Table 4. Diagnostic accuracy of MSCT to detect ISR as defined by CCA

	All patients	Simple stenting	Complex bifurcation stenting
Total No.	70	46	24
No. of true negatives	55	39	16
No. of true positives	10	6	4
No. of false negatives	0	0	0
No. of false positives	5	1	4
Sensitivity, %	100 (72-100)	100 (61-100)	100 (51-100)
Specificity, %	91 (82-96)	97 (87-99)	80 (58-92)
Accuracy, %	93 (84-97)	98 (89-99)	83 (64-93)
Positive predictive value, %	67 (42-85)	86 (49-97)	50 (22-78)
Negative predictive value, %	100 (93-100)	100 (91-100)	100 (81-100)

Simple stenting group includes patients who underwent stenting of the LM stem only or stenting of the distal LM extending into a single major side branch. The complex bifurcation stenting group comprises patients in whom the LM stem and both the LAD and CX were stented. Values in parentheses are 95% CIs.

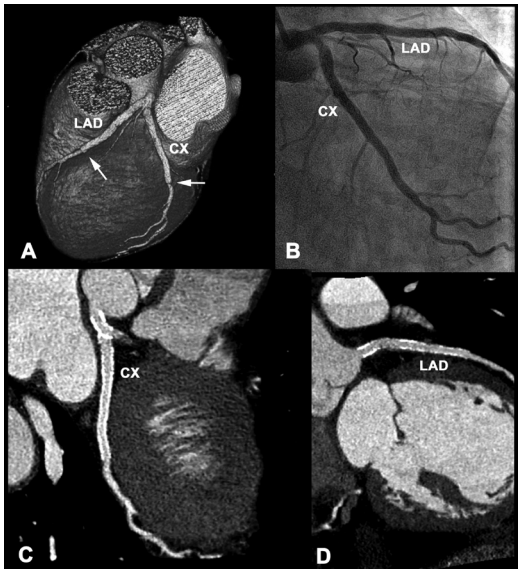

Figure 1. No evidence of ISR 5 months after culotte stenting (all DES) of the distal LM coronary artery: 3 overlapping stents toward the LAD (total stent length 60 mm, each stent with a diameter of 3.5mm) and 2 overlapping stents toward the CX (3.5x20 mm proximal and 3x32 mm distal). A, 64-slice MSCT coronary angiogram (volume-rendered 3D image), with stents in LM, LAD, and CX (arrows). B, Corresponding conventional coronary angiogram. C and D, The curved multiplanar reconstructions show stent patency of LM, LAD and CX and confirm the findings on CCA. C, Struts overlapping the ostium of the CX (arrowhead). (A full color version of this illustration can be found in the color section).

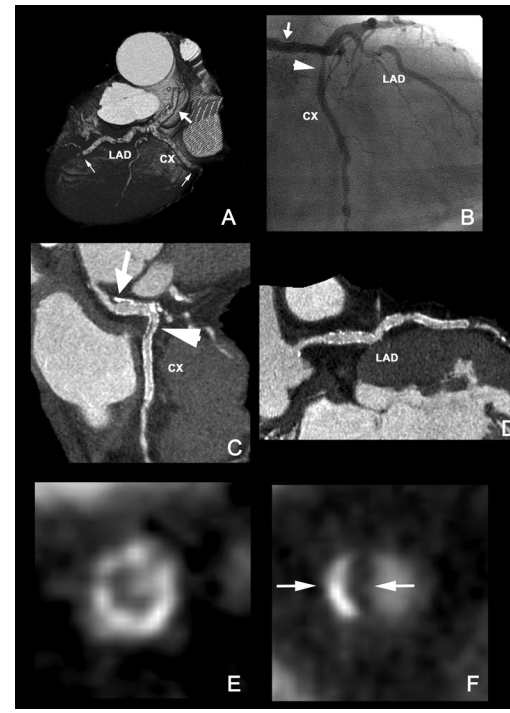

Figure 2. Restenosis of the ostium of the CX 6 months after stenting of the distal LM (crush technique): 3 overlapping stents had been placed from the LM to mid-LAD (3.5x24, 3.5x8 and 2.75x28 mm) and 2 overlapping stents toward the CX (each with a dimension of 3x20mm). A, 64-slice MSCT coronary angiogram (volume-rendered 3D image). The stents in LM, LAD and CX are clearly delineated (arrows). B, Corresponding CCA with restenosis in proximal CX (arrow). C and D, Curved multiplanar reconstructions of CX and LAD with ISR of the proximal CX. Cross-section 2, with inset, illustrates the ISR which appears as hypoattenuating tissue within the stent reducing the stent lumen diameter by >50%. The proximal stent edge in the LM shows non-obstructive plaque with <50% reduction of the normal contrast-enhanced lumen (C, cross section 1, with inset). The cross section discloses a large plaque (between the arrowheads) with a calcified (outer rim) and noncalcified (inner rim) component. The bright zone represents the lumen. This was confirmed by CCA (B, arrowhead). (A full color version of this illustration can be found in the color section).

tients (n=46) in whom simple stenting was performed, only 1 patient was incorrectly scored (false-positive) on MSCT. By contrast, in the complex bifurcation stenting group (n=24), 4 patients who did not have restenosis were scored as having ISR on MSCT. In 3 of the 5 false-positive scans, stent-related high density artifacts at the level of the CX ostium, due to the complex stenting strategy used, precluded correct assessment of the lumen within the stent. Three false-positives occurred among those evaluated with the 16-slice scanner; the other 2 occurred with the 64-slice scanner. Numbers were too small to support a statistical comparison among the 2 scanner types. The characteristics of the patients with restenosis and the 5 patients with a false-positive scan are reported in table 5. Seven of the 10 patients presented with restenosis in the ostium of the CX or intermediate branch. Three

Table 5. Characteristics of patients with restenosis or false positive scan.

Gender, age (ys)	Bifurcation stenting	Restenosis	Location	Symptomatic	Additional testing	Revascularization	CT-scanner
M, 50	No (stenting LM to LAD, kissing balloon postdilatation)	Yes	Ostium CX	Yes (CCS class 2)	No	No	16-slice
M, 73	No (stenting LM to IB)	Yes	Occlusion IB	Yes (CCS class 2)	No	Yes (PCI IB)	16-slice
M, 53	No (stenting LM to LAD)	Yes	LAD	Yes (CCS class 1)	No	No	16-slice
M, 59	Yes	Yes	Ostium CX	Yes (CCS class 3)	No	Yes (CABG)	64-slice
M, 58	Yes	Yes	Ostium CX	No	No	No	64-slice
F, 57	Yes	Yes	Ostium CX	No	No	No	64-slice
F, 72	Yes	Yes	LM	Yes (CCS class 3)	No	Yes (PCI LM)	64-slice
M, 48	No (stenting LM to LAD, kissing balloon postdilatation)	Yes	Ostium CX	Yes (CCS class 2)	No	No	64-slice
M, 58	No (stenting LM to LAD)	Yes	LM	No	Yes, FFR 0.82	No	64-slice
M, 61	No (stenting LM to LAD, kissing balloon postdilatation)	Yes	Ostium IB	No	No	No	64-slice
M, 70	Yes	No*	Ostium CX	No	No	No	16-slice
M, 63	No (stenting LM to LAD)	No*	LAD	No	No	No	16-slice
M, 67	Yes	No*	Ostium CX	No	No	No	16-slice
F, 70	Yes	No*	Ostium CX	No	No	No	64-slice
M, 59	Yes	No*	Distal stent edge IB	No	No	No	64-slice

M indicates male; CCS, Canadian Cardiovascular Society; F, female; FFR, fractional flow reserve; and IB, intermediate branch.
*Patients with false positive MSCT scan.

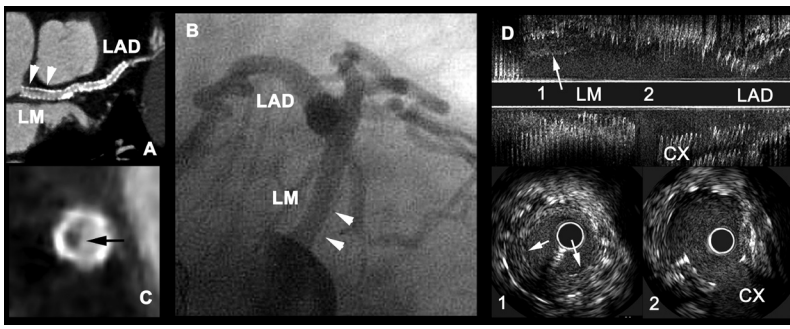

Figure 3. 63-year-old asymptomatic man underwent invasive and noninvasive coronary imaging 19 months after placement of 4 overlapping stents from LM toward LAD. A, CCA and C, corresponding 16-slice MSCT coronary angiogram (curved multiplanar reconstruction of LM and LAD). NIH presenting as a dark eccentric rim (C, arrow) was documented within the LM portion of the stent. D, Cross-sectional MSCT image confirms its nonobstructive nature (arrowhead). Although hardly visible with conventional angiography (A, arrowheads), NIH was clearly present on IVUS at the level of the proximal LM (arrowheads in B, longitudinal view, and in cross section 1). Cross section 2 is at the level of the origin of the CX and shows no signs of NIH.

patients were revascularized; 2 patients underwent re-PCI, and the third patient underwent CABG.

Ten patients presented with 11 de novo lesions in a previously untreated vessel segment, which required revascularization by PCI in 2 patients. All 11 lesions were correctly identified on MSCT; overestimation of lesion severity by MSCT occurred in 2 additional calcified lesions. In 12 patients, the presence of nonsignificant (<50% stenosis) NIH in the LM (n=5), LAD (n=5) and CX (n=2) on diagnostic coronary angiography was correctly classified as nonobstructive on MSCT (Figure 3).

Quantitative coronary angiography (QCA), IVUS, and MSCT

Quantitative coronary angiography (QCA) and IVUS data are shown in Table 6. The reference diameter and minimal lumen diameter of the patients who were wrongly classified did not differ from those who were correctly analyzed by MSCT (data not shown). Fifty-six nonconsecutive patients (90 segments) had technically adequate IVUS examinations. NIH was present in

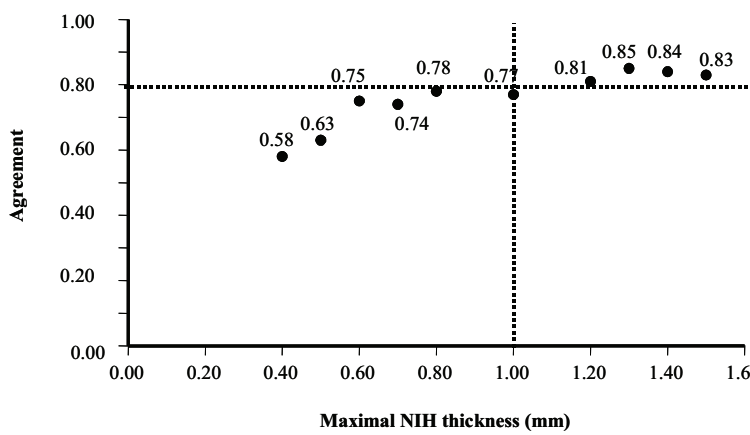

Figure 4. Maximal value of NIH thickness as measured by IVUS as a function of degree of agreement (expressed by the ·-value) between IVUS and MSCT. This analysis includes all patients with technically adequate IVUS examinations (n= 56). Values of NIH thickness <0.4 mm are not related to a ·-value, because values below this threshold are beyond the spatial resolution of currently available MSCT scanners.

Table 6. Quantitative angiographic and IVUS characteristics at follow-up

QCA, n	70
Reference diameter LAD, mm	2.57±0.51
Minimal lumen diameter LAD, mm	2.1±0.44
Reference diameter CX, mm	2.11±0.63
Minimal lumen diameter CX, mm	1.74±0.55
Reference diameter LM, mm	3.29±0.6
Minimal lumen diameter LM, mm	2.88±0.62
Quantitative IVUS	
Technically adequate IVUS pullback, n (%)	56 (80%)
LAD, n	31
Minimal lumen CSA, mm2	6.2 ± 2.54
Stent CSA, mm2	9.23 ± 2.53
Minimal lumen diameter, mm	2.76 ± 0.54
Stent diameter, mm	3.39 ± 0.47
CX, n	16
Minimal lumen CSA, mm2	5.24 ± 2.35
Stent CSA, mm2	7.67 ± 2.74
Minimal lumen diameter, mm	2.54 ± 0.47
Stent diameter, mm	3.1 ± 0.52
LM, n*	47
Minimal lumen CSA, mm2	9.40 ± 2.85
Stent CSA, mm2	12 ± 2.62
Minimal lumen diameter, mm	3.42 ± 0.52
Stent diameter, mm	3.89 ± 0.44

Values are mean±SD. CSA indicates cross-sectional area.
*In nine patients entire analysis of the LM was not possible due to a deeply intubated guiding catheter.

31 patients (38 segments). On the basis of a κ-value >0.8, which indicates very good agreement between the 2 imaging techniques, ie, MSCT and IVUS, a cutoff value of 1 mm was identified in which NIH could be identified with good confidence by MSCT (Figure 4). This corresponded to a 30% diameter obstruction as determined by QCA.

Quantitative IVUS and MSCT stent data were available for comparison in 50 patients (Figures 5 and 6). The mean stent diameter was 3.4 ± 0.70 mm with MSCT compared with 3.6 ± 0.6 mm with IVUS. The correlation coefficient was significant ($r = 0.78$, $p < 0.001$), but the Bland-Altman analysis showed a systematic overestimation of the stent diameter by MSCT (mean difference 0.22 ± 0.44 mm, $p<0.0001$). Mean stent area of MSCT compared to IVUS was 10 ± 3.3 mm2 versus 10.3 ± 3.5 mm2. Bland-Altman analysis for stent area demonstrated good correlation between both imaging techniques (mean difference 0.35 ± 2.53 mm2, $P=0.13$; $r = 0.73$, $P < 0.001$). Only 11 patients presented sufficient lumen narrowing to compare IVUS with MSCT. As shown in Figure 7, correlations were moderate for quantifying the degree of diameter and area stenosis ($r = 0.65$ and 0.55, respectively).

Observer variability

To assess internal validity, all MSCT datasets were analyzed twice by 2 observers. Interobserver agreement for the detection of ISR or NIH was good to moderate (κ- value of 0.74 and 0.6, respectively), whereas intraobserver agreement was very good in both situations (κ-value 0.82).

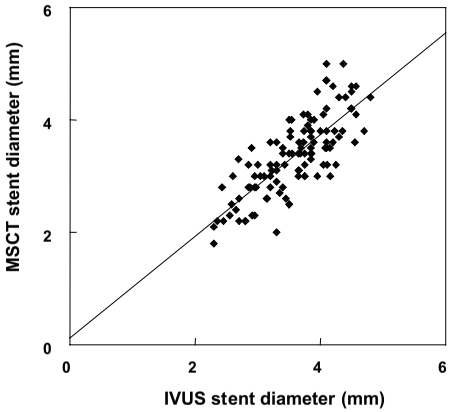

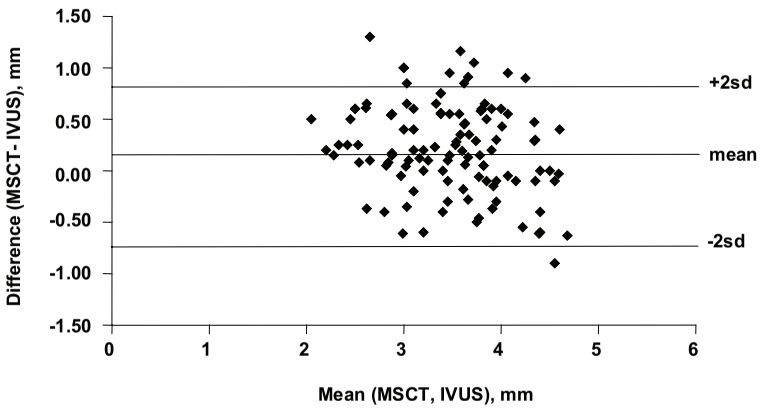

Figure 5. A, Correlation between MSCT and IVUS to quantify stent diameter (r = 0.78, P < 0.001). B, Bland-Altman analysis shows systematic overestimation of the stent diameter by MSCT (mean difference 0.22 ± 0.44 mm, P<0.0001). sd indicates standard deviation.

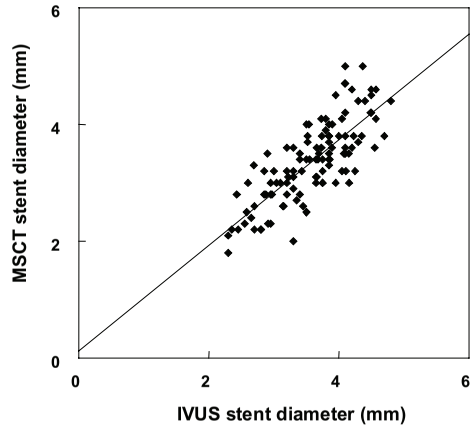

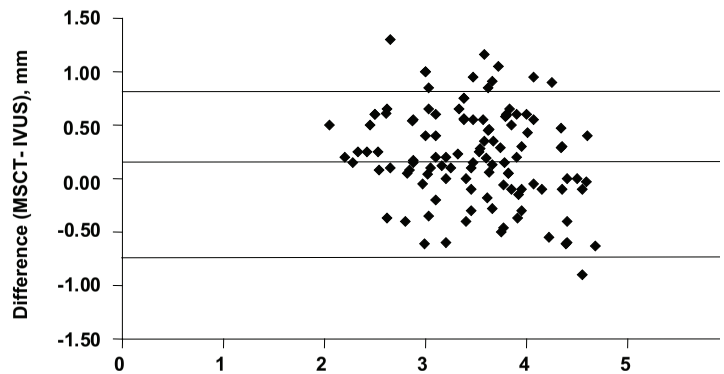

Figure 6. A, Correlation between MSCT and IVUS to quantify stent area (r = 0.73, P< 0.001). B, Bland-Altman analysis shows good correlation between both imaging techniques (mean difference 0.35 ± 2.53 mm2, P=0.13).

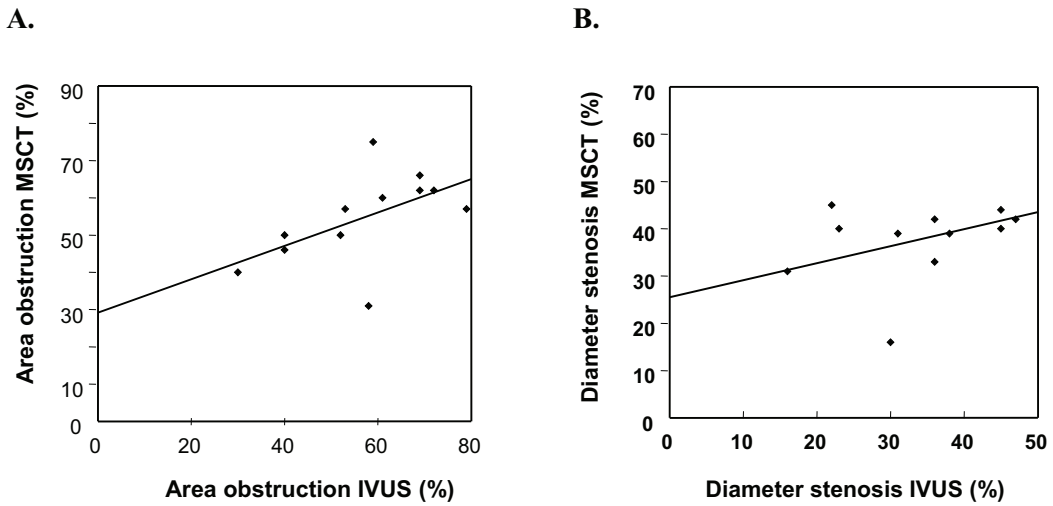

Figure 7. Correlation between MSCT and IVUS to quantify degree of in-stent area stenosis (A, Pearson correlation coefficient 0.55) and in-stent diameter stenosis (B, Pearson correlation coefficient 0.65).

DISCUSSION

Stent implantation in the LM and proximal LAD/CX provides the "best case scenario" for the use of MSCT in the detection of ISR for several reasons. First, stents implanted in the LM and proximal LAD/CX are relatively large; second, the LM and proximal LAD are usually running in an axial plane that corresponds to the scan direction, whereas the proximal CX generally runs in a slightly less favourable craniocaudal longitudinal plane; finally, this part of the coronary tree is relatively protected from motion artefact.

Recent technical improvements, including improved z-resolution, faster tube rotation, and the development of dedicated filters for image reconstruction in the presence of stents, have also significantly improved the potential of MSCT to assess coronary stent patency. Furthermore, preliminary experience with 16-detector row CT scanners showed promise for the evaluation of stents in the LMCA.[4,15]

The present study demonstrates that evaluation of stent patency in the LMCA is feasible with 16-slice and the latest 64-slice MSCT scanners. The technique is reliable (accuracy of 98%) for the evaluation of patients with stenting of the LM and for those patients with distal left main bifurcation lesions, in whom only 1 of the major branch vessels (ie, the LAD or the CX) is stented. However, in patients who required complex bifurcation stenting, ie, treatment of the LM and both major side branches, reliability was significantly less (accuracy of 83%). The most obvious explanation is the large quantity of metal, involving up to 3 layers of struts for

crush bifurcation stenting, at and around the ostium of the branch vessels, which is a major source of artifact on MCST.

A few studies reported reasonable accuracy of MSCT to quantify the degree of coronary artery stenosis in untreated coronary arteries.[16,17] This study reports on the quantification of stent dimensions and the amount of lumen narrowing within LMCA stents. Quantitative assessment by MSCT of stent diameter and area showed good correlation with IVUS. Not unexpectedly, metal-related artefacts, referred to as "blooming" effect, impair optimal visualization of the stent lumen and thus accurate quantification of lumen narrowing within the stent, especially for minor to moderate degrees of NIH. Nevertheless, NIH of > 1 mm thickness is recognized with sufficient sensitivity to allow the detection of clinically relevant restenosis in patients after LMCA stenting.

LMCA stent implantation traditionally represented a relatively small proportion of PCIs. Until recently, more widespread applicability of this revascularization modality had been hampered by the high occurrence of ISR.[9,18,19] The advent of DES has both significantly reduced restenosis rates and improved long-term clinical outcome; this has already resulted in an increasing proportion of patients with LM disease being treated percutaneously.[6,7] However, restenosis still occurs and when located in the LMCA may cause severe myocardial ischemia with potential fatal consequences.[19, 20] A noninvasive method for its detection, before clinical events occur, would be of major clinical value. The results of the present study indicate that current MSCT scanners may provide a reliable alternative to CCA. The low number of false-positive scans leading to "unnecessary" diagnostic coronary angiograms should in the light of potential serious consequences of LM ISR be acceptable.

Limitations of the study

The use of 2 different MSCT scanners in the present study might be criticized. However, the spatial resolution of the 16- and 64-slice scanner in the x- and y-axes has remained identical (0.4 mm) and only the resolution in the z-axis has improved with the 64-slice scanner. Because the LM and proximal LAD generally course in an axial plane, only the resolution in the x- and y-axes play a major role in the high-resolution visualization of these segments.

The rather high radiation dose of MSCT is a general limitation of the technique. However, new developments such as the recent introduction of dual-source CT scanners, systematically allow using ECG-pulsing, thereby significantly reducing patient dose. On the other hand, many physicians underestimate the radiation exposure of widely accepted imaging techniques such as CCA or technetium sestamibi scans that produce a dose as high as 5 to 20 mSv respectively.[21, 22]

The rather low positive predictive value (67%) is related to the low prevalence of ISR in patients treated with DES and reflects the limitations of current CT technology. New technical advances, such as the development of flat panel detectors and the general trend in interventional cardiology to use stents with thinner struts, will be beneficial for CT imaging of stents and reduce the number of false-positive scans.

The present study was limited by the relatively low number of patients with complex bifurcation stenting, because this group importantly affects the reported diagnostic accuracy data. Nonetheless, it is unlikely that this proportion will increase in the near future given the tendency to treat bifurcation lesions through a more simple approach and use a second stent towards the side branch only when strictly necessary.[23]

Finally, only 2 stent types with similar strut dimensions were used in this study. These results do not necessarily apply to different stent types since parameters such as strut thickness and stent design importantly influence the amount of blooming effect and thus assessability of the lumen inside.

CONCLUSIONS

In combination with optimal heart rate control, current MSCT technology allows reliable noninvasive evaluation of selected patients after LMCA stenting. A negative MSCT scan virtually rules out the presence of LM ISR and may therefore be an acceptable first-line alternative to CCA.

REFERENCES

1. Nieman K, Cademartiri F, Lemos PA, Raaijmakers R, Pattynama PM, de Feyter PJ. Reliable noninvasive coronary angiography with fast submillimeter multislice spiral computed tomography. Circulation. 2002;106:2051-4.
2. Ropers D, Baum U, Pohle K, Anders K, Ulzheimer S, Ohnesorge B, Schlundt C, Bautz W, Daniel WG, Achenbach S. Detection of coronary artery stenoses with thin-slice multidetector row spiral computed tomography and multiplanar reconstruction. Circulation. 2003;107:664-6.
3. Mahnken AH, Buecker A, Wildberger JE, Ruebben A, Stanzel S, Vogt F, Gunther RW, Blindt R. Coronary artery stents in multislice computed tomography: in vitro artifact evaluation. Invest Radiol. 2004;39:27-33.

4. Schuijf JD, Bax JJ, Jukema JW, Lamb HJ, Warda HM, Vliegen HW, de Roos A, van der Wall EE. Feasibility of assessment of coronary stent patency using 16-slice computed tomography. Am J Cardiol. 2004;94:427-30.
5. Mollet NR, Cademartiri F. Images in cardiovascular medicine. In-stent neointimal hyperplasia with 16-row multislice computed tomography coronary angiography. Circulation. 2004;110:e514.
6. Chieffo A, Stankovic G, Bonizzoni E, Tsagalou E, Iakovou I, Montorfano M, Airoldi F, Michev I, Sangiorgi MG, Carlino M, Vitrella G, Colombo A. Early and mid-term results of drug-eluting stent implantation in unprotected left main. Circulation. 2005;111:791-5.
7. Valgimigli M, van Mieghem CA, Ong AT, Aoki J, Granillo GA, McFadden EP, Kappetein AP, de Feyter PJ, Smits PC, Regar E, Van der Giessen WJ, Sianos G, de Jaegere P, Van Domburg RT, Serruys PW. Short- and long-term clinical outcome after drug-eluting stent implantation for the percutaneous treatment of left main coronary artery disease: insights from the Rapamycin-Eluting and Taxus Stent Evaluated At Rotterdam Cardiology Hospital registries (RESEARCH and T-SEARCH). Circulation. 2005;111:1383-9.
8. Baim DS. Is it time to offer elective percutaneous treatment of the unprotected left main coronary artery? J Am Coll Cardiol. 2000;35:1551-3.
9. Takagi T, Stankovic G, Finci L, Toutouzas K, Chieffo A, Spanos V, Liistro F, Briguori C, Corvaja N, Albero R, Sivieri G, Paloschi R, Di Mario C, Colombo A. Results and long-term predictors of adverse clinical events after elective percutaneous interventions on unprotected left main coronary artery. Circulation. 2002;106:698-702.
10. Price MJ, Cristea E, Sawhney N, Kao JA, Moses JW, Leon MB, Costa RA, Lansky AJ, Teirstein PS. Serial angiographic follow-up of sirolimus-eluting stents for unprotected left main coronary artery revascularization. J Am Coll Cardiol. 2006;47:871-7.
11. Smith SC, Jr., Feldman TE, Hirshfeld JW, Jr., Jacobs AK, Kern MJ, King SB, 3rd, Morrison DA, O'Neil WW, Schaff HV, Whitlow PL, Williams DO, Antman EM, Adams CD, Anderson JL, Faxon DP, Fuster V, Halperin JL, Hiratzka LF, Hunt SA, Nishimura R, Ornato JP, Page RL, Riegel B. ACC/AHA/SCAI 2005 guideline update for percutaneous coronary intervention: a report of the American College of Cardiology/American Heart Association Task Force on Practice Guidelines (ACC/AHA/SCAI Writing Committee to Update 2001 Guidelines for Percutaneous Coronary Intervention). Circulation. 2006;113:e166-286.
12. De Winter SA, Hamers R, Degertekin M, Tanabe K, Lemos PA, Serruys PW, Roelandt JR, Bruining N. Retrospective image-based gating of intracoronary ultrasound images for improved quantitative analysis: the intelligate method. Catheter Cardiovasc Interv. 2004;61:84-94.
13. Hamers R BN, Knook M, Sabate M, Roelandt JRTC. A novel approach to quantitative analysis of Intravascular Ultrasound Images. Computers Cardiol. 2001;28:589-592.
14. Bland JM, Altman DG. Statistical methods for assessing agreement between two methods of clinical measurement. Lancet. 1986;1:307-10.

15. Gilard M, Cornily JC, Rioufol G, Finet G, Pennec PY, Mansourati J, Blanc JJ, Boschat J. Noninvasive assessment of left main coronary stent patency with 16-slice computed tomography. Am J Cardiol. 2005;95:110-2.
16. Cury RC, Pomerantsev EV, Ferencik M, Hoffmann U, Nieman K, Moselewski F, Abbara S, Jang IK, Brady TJ, Achenbach S. Comparison of the degree of coronary stenoses by multidetector computed tomography versus by quantitative coronary angiography. Am J Cardiol. 2005;96:784-7.
17. Leber AW, Knez A, von Ziegler F, Becker A, Nikolaou K, Paul S, Wintersperger B, Reiser M, Becker CR, Steinbeck G, Boekstegers P. Quantification of obstructive and nonobstructive coronary lesions by 64-slice computed tomography: a comparative study with quantitative coronary angiography and intravascular ultrasound. J Am Coll Cardiol. 2005;46:147-54.
18. Kelley MP, Klugherz BD, Hashemi SM, Meneveau NF, Johnston JM, Matthai WH, Jr., Banka VS, Herrmann HC, Hirshfeld JW, Jr., Kimmel SE, Kolansky DM, Horwitz PA, Schiele F, Bassand JP, Wilensky RL. One-year clinical outcomes of protected and unprotected left main coronary artery stenting. Eur Heart J. 2003;24:1554-9.
19. Tan WA, Tamai H, Park SJ, Plokker HW, Nobuyoshi M, Suzuki T, Colombo A, Macaya C, Holmes DR, Jr., Cohen DJ, Whitlow PL, Ellis SG. Long-term clinical outcomes after unprotected left main trunk percutaneous revascularization in 279 patients. Circulation. 2001;104:1609-14.
20. Babapulle MN, Joseph L, Belisle P, Brophy JM, Eisenberg MJ. A hierarchical Bayesian meta-analysis of randomised clinical trials of drug-eluting stents. Lancet. 2004;364:583-91.
21. Morin RL, Gerber TC, McCollough CH. Radiation dose in computed tomography of the heart. Circulation. 2003;107:917-22.
22. Hoffmann U, Ferencik M, Cury RC, Pena AJ. Coronary CT angiography. J Nucl Med. 2006;47:797-806.
23. Williams DO, Abbott JD. Bifurcation intervention: is it crush time yet? J Am Coll Cardiol. 2005;46:621-4.

INTERLUDE 5

Reliable Angiographic Evaluation by 64-slice Computed Tomography after Trifurcation Stenting of the Left Main Coronary Artery.

Carlos A.G. Van Mieghem[1,2], Georgios Sianos[1], Bob Meijboom[1,2], Eleni Vourvouri[1,2], Patrick W. Serruys[1], Pim J. de Feyter[1,2]

From the departments of Cardiology[1] and Radiology[2], Erasmus MC, Rotterdam, the Netherlands

EuroInterv. 2006; 1: 482-483

A 39-year-old man underwent a complex percutaneous coronary intervention of the left main trifurcation due to unstable angina. Five paclitaxel-eluting stents were implanted successfully in the 3 major branches and left main trunk (Figure 1, panels A and B). Three months later follow-up 64-slice computed tomographic (MSCT) coronary angiography demonstrated excellent stent patency without signs of neointimal hyperplasia (Figure 2). Invasive coronary angiography and intravascular ultrasound (IVUS) confirmed these findings (Figure 1, panels C and D).

Current MSCT scanners provide a promising non-invasive alternative to conventional coronary angiography in the follow-up of patients after stenting of the left main coronary artery.

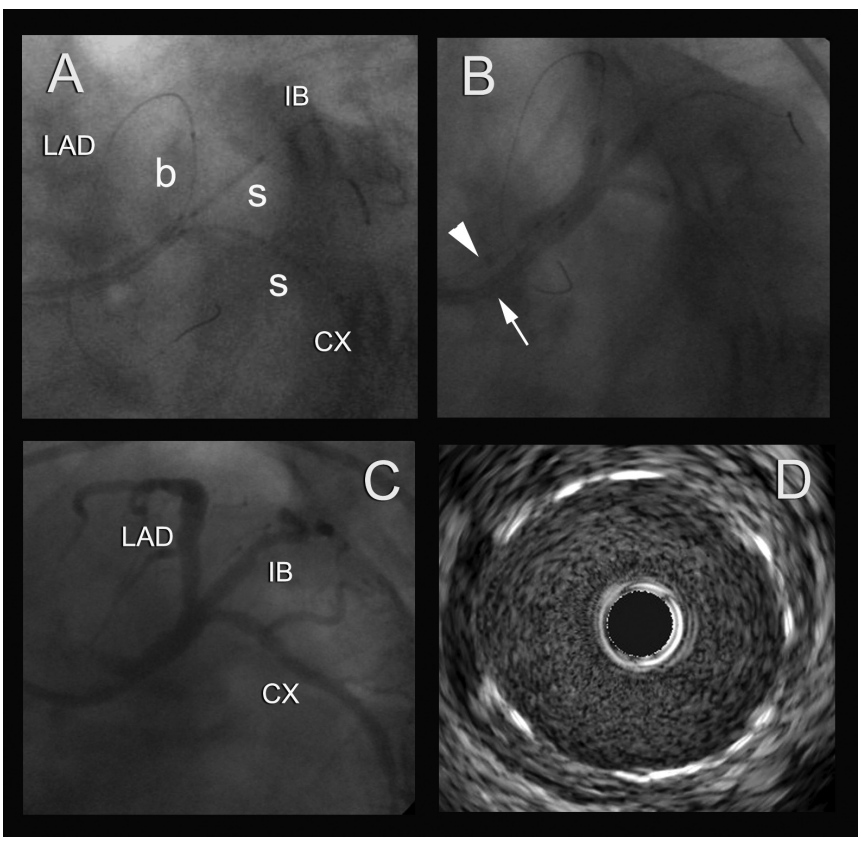

Figure 1. Two paclitaxel eluting stents (PES) were positioned simultaneously within the intermediate branch and circumflex artery (CX) together with balloon dilatation of the left anterior descending artery (LAD) to prevent plaque shift (panel A). The stent in the CX overlapped with a more distal stent in the same branch implanted at the start of the procedure. Due to dissection of the LAD ostium another PES was positioned in the proximal LAD and a fifth stent was deployed in the left main trunk (not shown). The procedure was completed with kissing balloon inflations of the 3 branches using 2 guiding catheters (one 5 and one 6 French guiding catheter), as indicated by the arrowhead and arrow (panel B). Invasive coronary angiography showed perfect patency of the 3 branches (panel C). Intravascular ultrasound confirmed the absence of neointimal hyperplasia, as shown by the IVUS cross-sectional image of the LMCA (panel D). b indicates balloon; CX, circumflex coronary artery; IB, intermediate branch; LAD, left anterior descending coronary artery; and s, stent.

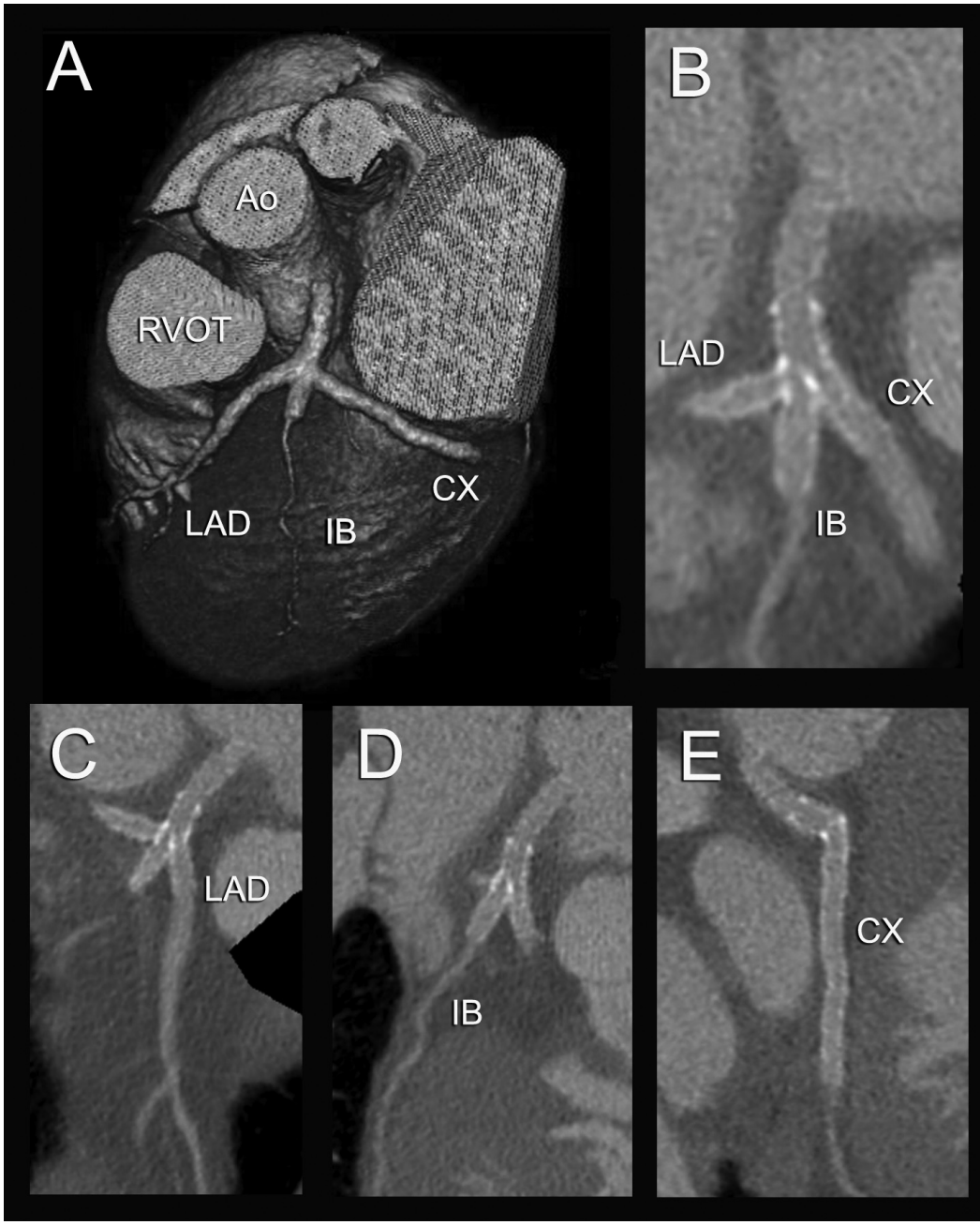

Figure 2. 64-slice CT coronary angiogram. Volume-rendered (panel A) and multiplanar reconstructed image (panel B) showing the stented left main trifurcation. The proximal stent edge in the left main trunk is well delineated (arrow). The lumen within the stents is clearly visible along the 3 branches of the trifurcation (panels C, D and E). It is obvious that the 4 stents, including the stent edges, are perfectly patent without signs of neointima hyperplasia.
Ao indicates ascending aorta; CX, circumflex coronary artery; IB, intermediate branch; LAD, left anterior descending coronary artery; RVOT, right ventricular outflow tract. (A full color version of this illustration can be found in the color section).

17

Dual Source Coronary Computed Tomography Angiography for Detecting In-Stent Restenosis.

Francesca Pugliese[1,2], Annick C. Weustink[1,2], Carlos A.G. Van Mieghem[1,2], Filippo Alberghina[2], Masato Otsuka[1], W. Bob Meijboom[1,2], Niels van Pelt1,2, Nico R. Mollet1,2, Filippo Cademartiri2, Gabriel P. Krestin[2], Myriam G. Hunink[2,3], Pim J. de Feyter[1,2]

From the departments of Cardiology[1], Radiology[2], Epidemiology and Biostatistics[3], Erasmus MC, Rotterdam, the Netherlands.

Heart 2008; 94:848-854.

ABSTRACT

Objective

To evaluate the performance of dual source CT coronary angiography (DSCT-CA) in the detection of in-stent restenosis (≥50% luminal narrowing) in symptomatic patients referred for conventional angiography (CA).

Design/patients

100 patients (78 males, age 62 (SD 10)) with chest pain were prospectively evaluated after coronary stenting. DSCT-CA was performed before CA.

Setting

Many patients undergo coronary artery stenting; availability of a non-invasive modality to detect in-stent restenosis would be desirable.

Results

Average heart rate (HR) was 67 (SD 12) (range 46-106) bpm. There were 178 stented lesions. The interval between stenting and inclusion in the study was 35 (SD 41) (range 3-140) months. 39/100 (39%) patients had angiographically proven restenosis. Sensitivity, specificity, positive predictive value (PPV) and negative predictive value (NPV) of DSCT-CA, calculated in all stents, were 94%, 92%, 77% and 98%, respectively.

Diagnostic performance at HR <70 bpm (n = 69; mean 58 bpm) was similar to that at HR ≥70 bpm (n = 31; mean 78 bpm); diagnostic performance in single stents (n = 95) was similar to that in overlapping stents and bifurcations (n = 83). In stents ≥3.5 mm (n = 78), sensitivity, specificity, PPV, NPV were 100%; in 3 mm stents (n = 59), sensitivity and NPV were 100%, specificity 97%, PPV 91%; in stents ≤2.75 mm (n = 41), sensitivity was 84%, specificity 64%, PPV 52%, NPV 90%.

Nine stents ≤2.75 mm were uninterpretable. Specificity of DSCT-CA in stents ≥3.5 mm was significantly higher than in stents ≤2.75 mm (OR = 6.14; 99%CI: 1.52 to 9.79).

Conclusion

DSCT-CA performs well in the detection of in-stent restenosis. Although DSCT-CA leads to frequent false positive findings in smaller stents (≤2.75 mm), it reliably rules out in-stent restenosis irrespective of stent size.

INTRODUCTION

Computed tomography angiography is a non-invasive diagnostic tool to visualize coronary arteries.[1] The evaluation of stents is, however, hampered by the occurrence of high-density artifacts ('blooming effect') caused by the stent struts. These artifacts cause an apparent enlargement of the stent and preclude appropriate assessment of the in-stent lumen.

In particular, the lumens of small stents, overlapping stents and bifurcation stents are difficult to assess.[2] Motion artifacts may further hinder the evaluation of stents.[3] Several investigations have evaluated the diagnostic performance of computed tomography in assessing stent patency or the presence of in-stent restenosis; [4-16] these studies have included patients with low heart rates and pre-scan preparation with β-blockers.

The introduction of dual source 64-slice computed tomography scanners, with an improved temporal resolution,[17] may be helpful to more accurately assess coronary stents.
In this study we evaluated the diagnostic performance of dual source computed tomography coronary angiography (DSCT-CA) for the detection of in-stent restenosis in patients with anginal symptoms after stent implantation.

METHODS

Population

From April 2006 to January 2007, 133 patients with chest pain and prior stent implantation were considered for inclusion in this prospective study. All patients were scheduled for diagnostic conventional angiography. Serum creatinine >120 μmol/l, irregular heart rhythm and known allergy to iodinated contrast agents were exclusion criteria. The recruitment procedure is described in figure 1. The institutional review board approved the study protocol and all the included patients gave informed consent.

DSCT-CA protocol

All patients were examined with a dual source CT scanner (Somatom Definition, Siemens, Forchheim, Germany). The scanner design consists of two x-ray tubes and two detector arrays mounted at an angle of 90°. Scan parameters were: 120 kV, 330 ms gantry rotation time, 2 x 32 x 0.6 mm collimation with z-flying focal spot for both detectors. Using this scan protocol, spatial resolution was 0.4x0.4x0.4 mm^3.[17] Pitch values were automatically adapted to the heart rate after an estimation based on the last 10 heartbeats preceding the scan, and varied between 0.20 and 0.43. Current x-ray tube modulation was used at full current for 25-70% of the R-R interval. Each tube provided a maximum of 412mAs/rotation. In patients with heart

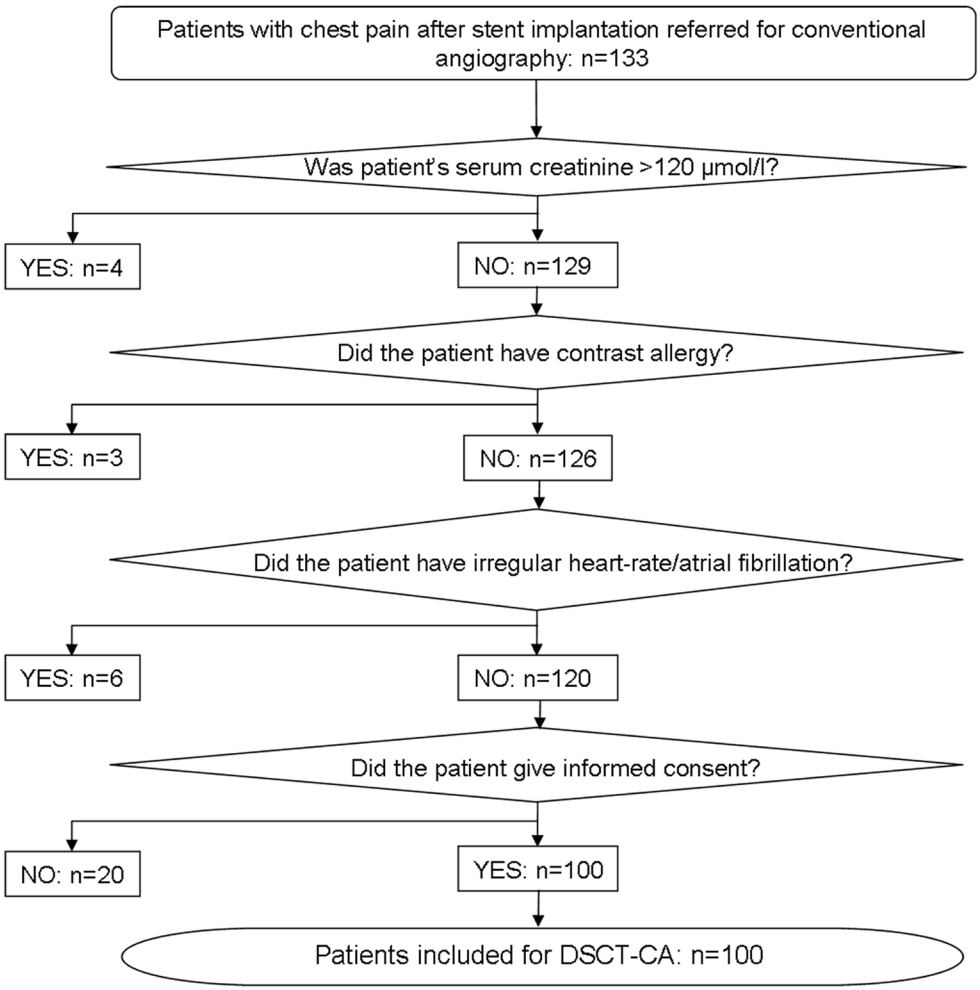

Figure 1. Inclusion procedure.
Inclusion procedure for the study (from April 2006 to January 2007).

rates <70bpm, x-ray exposure was (mean (SD)) 15.0 (4.1) mSv in men and 16.7 (5.0) mSv in women; in patients with heart rates ≥70bpm, x-ray exposure was 12.1 (2.6) mSv in men and 13.7 (4.7) in women (values calculated using ImPACT®, version 0.99x, St. George's Hospital, Tooting, London, UK).

All patients received sublingual nitroglycerin just before scanning. Contrast agent (Iomeron® 400 mgI/ml, Bracco, Italy) was injected into the antecubital vein at a flow rate of 5.0 ml/s, followed by a saline chaser (40 ml). We calculated the contrast volume with the following equa-

tion: estimated scan time + scan delay (7s). The contrast volume varied between 60 and 100 ml depending on the scan time, which in turn varied between 5 and 13 seconds. We used a bolus-tracking technique to synchronise the start of the scan with the arrival of contrast agent in the coronary arteries. A circular region-of-interest (ROI) was positioned in the ascending aorta and the scan was automatically started when a threshold of +100 Hounsfield Units was reached inside the ROI

Image reconstruction

Given the scanner geometry, a monosegmental algorithm using data from a single heartbeat obtained during a quarter gantry rotation was used for reconstruction. This translated into a temporal resolution equal to one-fourth of the gantry rotation time, that is, 330/4 = 83 ms.

First, 0.75 mm-thick images were retrospectively reconstructed during the mid-diastolic to end-diastolic phase. The position of the reconstruction window within the R-R interval varied according to the heart rate (from -400 ms before the R wave for low heart rates to -175 ms for high heart rates). Additional data sets were reconstructed during the end-systolic phase (from +400 ms after the R wave for low heart rates to +200 ms for high heart rates). The reconstruction increment was 0.4 mm. The data set with the fewest motion artifacts was chosen for analysis and reconstructed using a dedicated sharp convolution kernel (B46f, 'Heart View').

Quantitative coronary angiography (QCA)

A single observer unaware of the CT results examined the angiograms before contrast injection to identify the sites of stent implantation. The stents were then located within the coronary tree following a 17-segment modified AHA model, as previously described 18,19. Stents and stent edges, the latter defined as 5 mm-long coronary segments proximal and distal to the stents, were evaluated on multiple projections; luminal narrowing ≥50% was classified as significant (restenosis). A validated quantitative coronary angiography software (CAAS II®, Pie Medical, Maastricht, the Netherlands) was used to determine the minimal lumen diameter and derive the per cent diameter stenosis by means of the user-independent method of the interpolated reference diameter, using the angiographic catheter diameter as reference for calibration.[20]

DSCT-CA analysis

Two experienced readers evaluated the DSCT-CA studies independently; the readers were unaware of the findings of conventional angiography. In the event of diverging opinions, a consensus was reached and used in the final analysis.

Using axial images, multiplanar reconstructions (MPR) and curved MPR, the stents were visually screened for the presence of in-stent restenosis (≥50% lumen diameter reduction). When multiple stents were implanted contiguously to treat one lesion, they were considered as

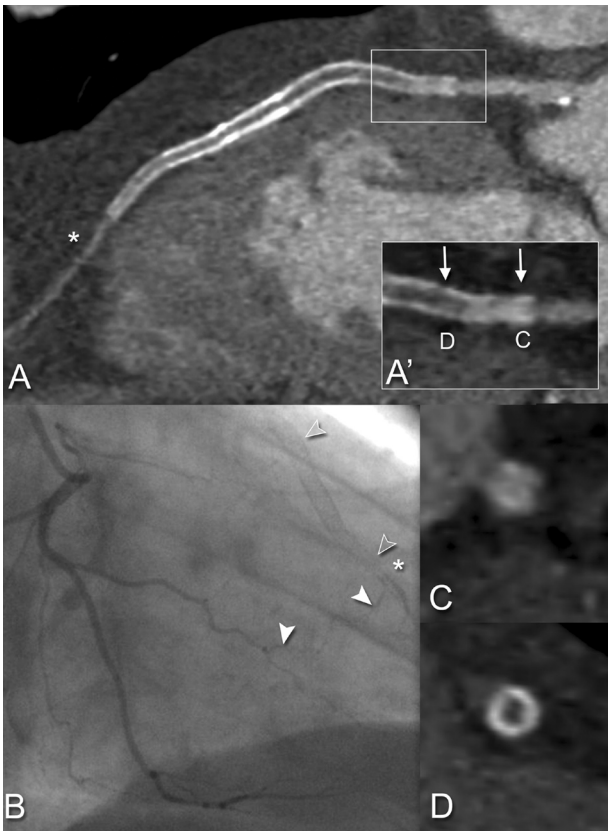

Figure 2. Distal run-off as a criterion of patency.
The presence of distal run-off is not always associated with stent patency. (A)A DSCT-CA curved multiplanar reconstruction shows a stented lesion consisting of 2 BX Velocity stents plus three Taxus stents (stent-in-stent) in the left anterior descending artery (LAD). In spite of the presence of distal run-off (asterisk), in-stent total occlusion is seen. (C-D) Stent cross-sections obtained as indicated in (A') (magnification of (A)) show the appearances of a patent stent (C) and of a totally occluded stent (D), respectively.(B) the corresponding conventional angiogram demonstrates that, distally to the stents (empty arrowheads), the LAD (asterisk) is fed by collateral flow (solid arrowheads). Direct visualisation of the stent lumen is therefore mandatory to rule-out in-stent restenosis with DSCT-CA. DSCT-CA, dual source coronary computed tomography angiography.

one single lesion. The assessment of restenosis was based exclusively on the visualisation of the in-stent lumen. The presence of distal run-off was not considered as an indicator of patency because retrograde or collateral filling in an occluded stent can also give distal contrast enhancement (figure 2). All stent edges, defined as 5 mm-long coronary segments proximal and distal to the stents, were also included in the evaluation. In the event of bifurcation stenting, each of the three branches was evaluated. When the stent lumen was uninterpretable (e.g., obscured by high-density artifacts), and in-stent restenosis could not be excluded by DSCT-CA, stents were considered to have restenosis (worst case scenario) [6,7] for the purpose of the analysis.

Statistics

The statistical analysis was performed with SPSS, version 12.1 (SPSS Inc., Chicago, Illinois, USA.). Results are reported in accordance with the STARD criteria.[21] Continuous variables are expressed as mean (standard deviation). Categorical variables are presented as counts and percentages.

Sensitivity, specificity, positive predictive value (PPV), and negative predictive value (NPV) of DSCT-CA for the detection of ≥50% in-stent restenosis, as determined by QCA as reference standard, were computed in two subgroups defined as low heart rate and high heart rate;

the definition of the two groups was based on a cut-off heart rate of 70 bpm as previously described by Leber et al[22] and Mollet et al[19]. The low heart rate subgroup comprised patients with heart rates <70 bpm, the high heart rate subgroup comprised patients with heart rates ≥70bpm.

Sensitivity, specificity, PPV and NPV were then computed in two subgroups defined as simple configuration and complex configuration: the simple configuration subgroup comprised lesions treated with the deployment of one single stent; the complex configuration subgroup comprised overlapping stents and bifurcation stenting.

We also computed sensitivity, specificity, PPV and NPV in three subgroups defined by stent diameters, that is, ≥3.5mm, 3mm and ≤2.75mm. When multiple stents were employed to treat one lesion, the diameter of the proximal stent determined the diameter subgroup. This criterion for subclassifying lesions with multiple stents was based on the expectation that small stents were more difficult to evaluate than large stents; we preferred to underestimate the diagnostic performance in the larger stent subgroups rather than overestimating the diagnostic performance in the smaller stent subgroup.

Sensitivity, specificity, PPV and NPV were also computed separately for the right coronary artery (RCA), left main (LM) stem, left anterior descending (LAD) and left circumflex (LCx) arteries. Because the accuracy of DSCT-CA to detect occluded stents might be greater than the accuracy to detect restenosis, we performed separate analyses after excluding totally occluded segments. Diagnostic test results are presented with corresponding 95% confidence intervals based on binomial probabilities. The χ^2 test was used to compare the frequency of occurrence of restenosis in the different subgroups. The Mann-Whitney U test was used to compare the mean stent diameters in the heart rate subgroups and in the configuration subgroups.

We determined the effect of heart rate, stent configuration and stent diameter on sensitivity, specificity, PPV, and NPV using logistic regression analysis including patient identification to correct for possible correlation within the individuals who had multiple stents.[23] To compensate for multiple testing, we used a significance level of 0.01 and computed 99% confidence intervals (CI).

Interobserver and intraobserver agreement for the detection of restenosis were determined by κ-statistics.

Table 1. Baseline characteristics, angiographic findings and stent types

Patient number	100
Age and gender	
Age (years) (mean (SD))	62 ± 10
Men/women	78/22
Cardiovascular risk factors: (number)	
Obesity (Body Mass Index ≥ 30 Kg/m2)	23
Smoking	25
Hypertension (≥160/95 mmHg or ongoing treatment)	45
Serum cholesterol >200 mg/dL (5.18 mmol/L)	51
Diabetes mellitus	21
Family history	29
Total number of stents used and types	247
Drug-eluting stents	157
Bare metal stents	90
Frequency of individual diameters and types (number (%))	
2.25	21/247 (9%)
2.5	31/247 (13%)
2.75	17/247 (7%)
3.0	82/247 (33%)
3.5	63/247 (25%)
4.0	20/247 (8%)
4.5	8/247 (3%)
5.0	5/247 (2%)
Taxus	136/247 (55%)
Cypher	21/247 (8%)
BX Velocity	32/247 (14%)
R Evolution	21/247 (8%)
NIR	7/247 (3%)
Multilink	4/247 (1.5%)
Palmaz-Schaz	4/247 (1.5%)
Other BMS*	22/247 (9%)
Number of lesions and stent types (number (%)) †	178
Drug-eluting stents	113 (63%)
Bare metal stents	65 (37%)
Vessel implanted: number (%)	
RCA	60 (34%)
LM stem	11 (6%)
LAD	58 (32%)
LCx	49 (28%)

Patients diagnosed with ≥50% restenosis (number)	39
Lesions with ≥50% restenosis (number (%))	39/178 (22%)
Restenosis	22/39 (56%)
Total occlusion	17/39 (44%)
Stent types with restenosis (number (%))	
Drug-eluting stents	12/113 (11%)
Bare metal stents	27/65 (42%)

*Type not available (implanted before 2003)
†One stent-in-stent implantation consisting of 2 BX Velocity plus 3 Taxus stents was classified as BMS; all other complex lesions consisted of stents of the same type.

RESULTS

Baseline characteristics and angiographic findings

Of the 133 patients screened for inclusion in our study, 33 were excluded because of serum creatinine level >120 μmol/l (n= 4), known contrast allergy (n = 3), irregular heart rate (n = 6) and refusal to undergo DSCT-CA (n = 20), so that 100 patients underwent DSCT-CA (figure 1).

DSCT-CA and conventional angiography were performed 35 (SD 41) months after stenting (range 3-140 months). Seventy patients were on treatment with β-blockers; none of the patients received additional β-blockers before the scan. The average heart rate during the scan was 67 (SD 12) (range 42-106) bpm. Sixty-nine patients had heart rates <70 bpm and were included in the low heart rate subgroup (the average heart rate in this subgroup was 58 (SD 6) (range 42-69) bpm); 31 patients had heart rates ≥70 bpm and were included in the high heart rate subgroup (the average heart rate in this subgroup was 78 (SD 9) (range 70-106) bpm).

We examined 178 stented lesions (247 stents used, 1.4 (SD 0.8) stents per lesion); 95 lesions consisted of single stents (simple configuration subgroup); the remaining 83 lesions consisted of overlapping stents (n = 62) and bifurcations (n = 21) (complex configuration subgroup). All but one complex lesions consisted of stents of the same type. One complex lesion was a stent-in-stent implantation consisting of two partially overlapped BX Velocity stents plus three Taxus stents implanted 1 year later (figure 2); this lesion was classified as a bare metal stent (BMS) lesion. BMS accounted for 37% (65/178) of the stented lesions, drug-eluting stents (DES) accounted for 63% (113/178) of the stented lesions. Restenosis was diagnosed angiographically in 39/178 (22%) stented lesions in 39/100 (39%) patients. Restenosis was found in

27/65 (42%) BMS and in 12/113 (11%) DES. Table 1 summarises patient baseline characteristics, main angiographic findings and stent types.

The frequency of in-stent restenosis was 23% (29/124) in the low heart rate subgroup and 19% (10/54) in the high heart rate subgroup. In the simple and complex configuration subgroups, frequencies were 18% (17/95) and 26% (22/83), respectively. In the ≥3.5 mm, 3 mm and ≤2.75 mm subgroups, frequencies of restenosis were 19% (15/78), 20% (12/59) and 31% (13/41), respectively. All p-values were not significant ($p > 0.05$).

The mean stent diameter in the entire sample was 3.15 (SD 0.58). The mean stent diameters in the simple and complex configuration subgroups were 3.16 (SD 0.60) mm and 3.15 (SD 0.61) mm, respectively. The mean stent diameters in the low and high heart rate subgroups were 3.17 (SD 0.61) mm and 3.15 (SD 0.66) mm, respectively. All p-values were not significant ($p > 0.05$).

Diagnostic performance of DSCT-CA

All 178 stented lesions were detected by DSCT-CA. The stent lumen was judged interpretable in 169/178 (95%) stents. In the remaining nine stents (5%), all of which were ≤2.75mm in diameter, the lumen was uninterpretable due to high-density artifacts obscuring the in-stent lumen; these stents were scored as having in-stent restenosis. However, these nine small stents were angiographically normal (no in-stent restenosis, DSCT-CA false positives).

Sensitivity, specificity, PPV and NPV in detecting ≥50% restenosis, calculated on all stents, were 94%, 92%, 77% and 98%, respectively. The diagnostic performance of DSCT-CA at heart rates <70bpm did not differ significantly from that obtained at heart rates ≥70bpm, as witnessed by widely overlapping confidence intervals. The diagnostic performances obtained in simple stents and overlapping stents/bifurcations were also similar. Likewise, no significant differences were seen between the four major coronary vessels. Table 2 gives sensitivity, specificity, PPV and NPV obtained in the heart rate subgroups, in simple and complex configuration subgroups and in the four major coronary vessels.

In the diameter-based subanalysis, we found that NPV was in the range 90-100% in all subgroups. Sensitivity was 100% in ≥3.5 mm stents and in 3 mm stents, but it dropped to 84% in ≤2.75 mm stents. Specificity and PPV were both 100% in the ≥3.5 mm subgroup; the values for specificity and PPV were 97% and 91%, respectively, in the 3 mm subgroup, and 64% and 52%, respectively, in the ≤2.75 mm subgroup. Table 2 gives the diagnostic performance of DSCT-CA in detecting ≥50% luminal narrowing in the different diameter subgroups.

Table 2. Diagnostic performance of DSCT-CA in detecting ≥50% luminal narrowing to all lesions and subgroup analysis

	All Lesions	HR<70 Mean=58 (SD 6)	HR≥70 Mean=78 (SD 9)	Simple	Complex	≥3.5mm	3.0mm	≤2.75mm	RCA	LM	LAD	LCx
Total	178	124	54	95	83	78	59	41	60	11	58	49
TP	37	28	9	16	21	15	11	11	8	0	15	14
TN	128	88	40	74	54	63	47	18	48	11	38	31
FP	11 (9)*	7	4	4	7	0	1	10 (9)*	4	0	4	3
FN	2	1	1	1	1	0	0	2	0	0	1	1
Sensitivity	37/39 **.94** (.81-.99)	28/29 **.96** (.80-.99)	9/10 **.90** (.54-.99)	16/17 **.94** (.69-.99)	21/22 **.95** (.75-.99)	15/15 **1** (.74-1)	11/11 **1** (.67-1)	11/13 **.84** (.53-.97)	8/8 **1** (.59 -1)	-	15/16 **.93** (.67-.99)	14/15 **.93** (.66-.99)
Specificity	128/139 **.92** (.85-.95)	88/95 **.92** (.84-.96)	40/44 **.90** (.77-.97)	74/78 **.94** (.86-.98)	54/61 **.88** (.77-.94)	63/63 **1** (.92-1)	47/48 **.97** (.79-.99)	18/28 **.64** (.44-.80)	48/52 **.92** (.80-.97)	11/11 **1** (.67-1)	38/42 **.90** (.76-.99)	31/34 **.91** (.75-.97)
PPV	37/48 **.77** (.62-.87)	28/35 **.80** (.62-.90)	9/13 **.69** (.38-.89)	16/20 **.80** (.55-.93)	21/28 **.75** (.54-.88)	15/15 **1** (.74-1)	11/12 **.91** (.59-.99)	11/21 **.52** (.30-.73)	8/12 **.66** (.35-.88)	-	15/19 **.78** (.53-.93)	14/17 **.82**(.55-.95)
NPV	128/130 **.98** (.93-.99)	88/89 **.98** .93-.99)	40/41 **.97** (.85-.99)	74/75 **.98** (.91-.99)	54/55 **.98** (.89-.99)	63/63 **1** (.92-1)	47/47 **1** (.90-1)	18/20 **.90** (.66-.98)	48/48 **1** (.90-1)	11/11 **1** (.67-1)	38/39 **.97** (.84-.99)	31/32 **.96** (.82-.99)
After exclusion of totally occluded stents												
Total	161	113	48	87	74	70	55	36	57	11	51	42
TP	20	17	3	8	12	7	7	6	5	0	8	7
TN	128	88	40	74	54	63	47	18	48	11	38	31
FP	11	7	4	4	7	0	1	10	4	0	4	3
FN	2	1	1	1	1	0	0	2	0	0	1	1
Sensitivity	20/22 **.90** (.69-.98)	17/18 **.94** (.70-.99)	3/4 **.75** (.21-.98)	8/9 **.88** (.50-.99)	12/13 **.92** (.62-.99)	7/7 **1** (.56-1)	7/7 **1** (.56-1)	6/8 **.75** (.35-.95)	5/5 **1** (.46-1)	-	8/9 **.88** (.50-.99)	7/8 **.87** (.46-.99)
Specificity	128/139 **.92** (.85-.95)	88/95 **.92** (.84-.96)	40/44 **.90** (.77-.97)	74/78 **.94** (.86-.98)	54/61 **.88** (.77-.94)	63/63 **1** (.92-1)	47/48 **.97** (.79-.99)	18/28 **.64** (.44-.80)	48/52 **.92** (.80-.97)	11/11 **1** (.67-1)	38/42 **.90** (.76-.96)	31/34. **91** (.75-.97)
PPV	20/31 **.64** (.45-.80)	17/24 **.70** (.48-.86)	3/7 **.42** (.11-.79)	8/12 **.66** (.35-.88)	12/19 **.63** (.38-.82)	7/7 **1** (.56-1)	7/8 **.87** (.46-.99)	6/16 **.37** (.16-.64)	5/9 **.55** (.22-.84)	-	8/12 **.66** (.35-.88)	7/10 **.70** (.31-.95)
NPV	128/130 **.98** (.93-.99)	88/89 **.98** (.93-.99)	40/41 **.97** (.85-.99)	74/75 **.98** (.91-.99)	54/55 **.98** (.89-.99)	63/63 **1** (.92-1)	47/47 **1** (.90-1)	18/20 **.90** (.66-.98)	48/48 **1** (.90-1)	11/11 **1** (.67-1)	38/39 **.97** (.84-.99)	31/32 **.96** (.82-.99)

*Nine stents had uninterpretable lumen; all these were ≤2.75 mm in diameter. These were considered positives for the purpose of the analysis. Values are expressed as means (95% confidence intervals). FN, false negative; FP, false positive; TN, true negative; TP, true positive.

In the logistic regression analysis predicting specificity, a stent diameter of ≥3.5 mm had an odds ratio of 6.14 (99%CI 1.52 to 9.79). In predicting the PPV, a stent diameter of ≥3.5 mm had an odds ratio of 3.70 (99%CI 0.98 to 8.90). All other variables were not significant.

The interobserver agreement in detecting restenosis was good (κ- value = 0.78). The intraobserver agreement was very good (κ- value = 0.87).

DISCUSSION

Cardiac catheterization is the technique of choice for the detection of in-stent restenosis. However, it may involve life-threatening complications and is relatively expensive. The diagnostic accuracy of non-invasive techniques such as exercise testing is known to be suboptimal;[24] therefore an alternative non-invasive 'gatekeeper' to invasive coronary angiography would be desirable. The reliability of such a technique would have to be demonstrated in various clinical situations (i.e., various stent sizes and configurations, higher heart rates) before it could be routinely used in patients with prior coronary artery stenting.

Feasibility of DSCT-CA at high heart rates

This study showed that DSCT-CA was accurate in detecting in-stent restenosis without the use of pre-scan β-blockers. Although the rate of false positives was slightly higher at high heart rates (PPV = 69%) than at low heart rates (PPV = 80%), the number of false negatives was low in both subgroups (NPV in the range 97-98%). In addition, the capability to perform DSCT-CA at higher heart rates without the use of β-blockers may be advantageous in terms of reducing radiation exposure. Table speed increases with increasing heart rates in DSCT-CA, which in turn translates into shorter scan times and reduced radiation exposure.

Stent configurations

To the best of our knowledge, the population evaluated in the present study is the largest available in the literature on coronary CT angiography including overlapping and bifurcation stenting (n = 83). Although the differences were not statistically significant, we found that specificity and PPV of DSCT-CA in bifurcation stenting and overlapping stents were slightly lower than those obtained in single stents, probably due to the large amount of metal at the ostium of side branches and at overlapping sites. This excess of metal is a major source of high-density artifacts in CT and may lead to lesion overestimation (figure 3).

It may be argued that restenosis occurs more frequently in patients with complex lesion characteristics than in patients with simple lesions.[25] This might have led to an overestimation of sensitivity in our complex configuration subgroup. However, the difference between the fre-

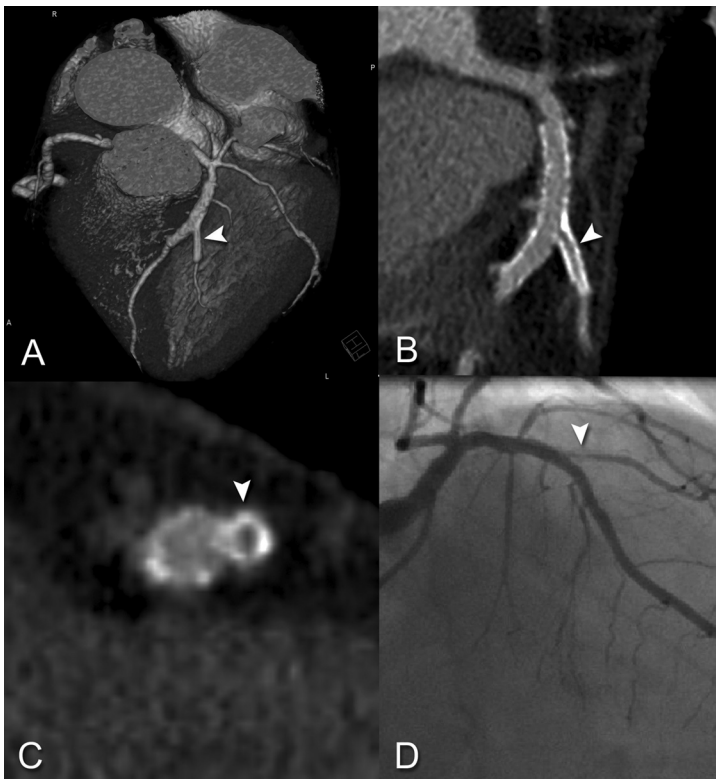

Figure 3. Bifurcations
Patient with in-stent restenosis 6 months after crush-stenting. (A) A volume-rendered DSCT-CA image shows bifurcation stenting of the left anterior descending artery (LAD) and second diagonal branch. The stent in the diagonal branch (side branch) has a diameter of 2.25 mm; the stent in the LAD (main branch) has a diameter of 4 mm. (B) MPR image (C) MPR cross-section obtained at the level of the carina, and (D) corresponding conventional angiogram demonstrate restenosis in the diagonal branch (arrowhead); the main branch is patent. In (B), note the typical CT appearance of the crush technique, characterized by three layers of metal crushed against the ostium of the side branch.
MPR, multiplanar reconstruction

quency of restenosis in our simple and complex configuration subgroups was not statistically significant.

Stent diameters

We found that stent diameter was the most important feature influencing the diagnostic performance of coronary CT angiography. This is in keeping with the findings of Gilard et al. [8] and of Rixe et al.[13], who performed 16-slice CT coronary angiography and 64-slice CT coronary angiography, respectively, in patients with low heart rates. In those studies though, up to 50% of the stents were judged unevaluable. With DSCT-CA, we judged unevaluable only 5% (n = 9) of the stents, and found a low rate of false negatives irrespective of stent diameter (NPV in all stents = 98%, NPV in stents ≤2.75mm = 90%). When stent diameter was ≤2.75mm, DSCT-CA had a high rate of false positives (specificity = 64%; PPV = 52%) and could not predict with certainty the presence of restenosis; in particular, the specificity of DSCT-CA in this subgroup was significantly lower than that obtained in stents ≥3.5mm (OR = 6.14; 99%CI: 1.52 to 9.79). Therefore our study confirms that DSCT-CA is not a suitable gatekeeper to conventional angiography in symptomatic patients with ≤2.75mm stents.

In a recent study, Cademartiri et al.[4] reported the relationship between diagnostic accuracy of 64-slice CT and stent size in terms of the rate of false diagnosis (false positives and false negatives). In contrast with our findings, the rate of false diagnosis reported in that study did not decrease with increasing stent diameters. In stents <3mm, the rate of false diagnosis was 6.1%; in 3mm stents, the rate of false diagnosis was 1.6% and surprisingly, in stents >3mm, the rate of false diagnosis was 12%. An explanation of these findings compared to our study is that only patients with stents larger than 2.5mm were included. Secondly, complex stent configurations such as overlapping stents and bifurcation stenting were not included in that study, which may have led to an overestimation of the diagnostic performance in smaller stents. Lastly, a 64-slice CT scanner was used, rather than the dual source CT scanner in this study.

It is conceivable that future developments in CT technology might further increase the diagnostic performance in patients with stents by improvements in spatial (eg, flat panel technology) and temporal resolution.

Totally occluded stents

Totally occluded stents might be easier to recognize on DSCT-CA. In our sample, 17 stents were totally occluded. Overall, the analysis after exclusion of totally occluded segments yielded similar sensitivity, specificity and NPV but lower PPV (Table 2).

Study limitations

We examined a selected symptomatic patient cohort; applicability to a wider population may therefore yield different results. This limitation was inevitable in order to compare DSCT-CA to the reference technique, i.e., conventional coronary angiography.

X-ray radiation exposure is a general limitation of multi-slice CT coronary angiography.[26,27] However, using x-ray tube modulation, full dose radiation may be given for a shorter duration of the cardiac cycle than used in this study. Radiation dose is further reduced by automated pitch adaptation with higher heart rates. Other widely accepted imaging techniques, such as technetium sestamibi scans, may deliver radiation doses as high as 20mSv.[26,27]

Conclusions

This study shows that, in patients with recurrent chest pain after stent implantation, DSCT-CA performs well in the detection of in-stent restenosis. Stent diameter is an important predictor of DSCT-CA diagnostic performance; when stent diameter is ≤2.75mm, the technique is associated with frequent false positives. However, due to the high NPV, DSCT-CA reliably rules-out in-stent restenosis irrespective of stent size.

REFERENCES

1. Hendel RC, Patel MR, Kramer CM, et al. ACCF/ACR/SCCT/SCMR/ASNC/NASCI/SCAI/SIR 2006 appropriateness criteria for cardiac computed tomography and cardiac magnetic resonance imaging: a report of the American College of Cardiology Foundation Quality Strategic Directions Committee Appropriateness Criteria Working Group, American College of Radiology, Society of Cardiovascular Computed Tomography, Society for Cardiovascular Magnetic Resonance, American Society of Nuclear Cardiology, North American Society for Cardiac Imaging, Society for Cardiovascular Angiography and Interventions, and Society of Interventional Radiology. J Am Coll Cardiol 2006;48(7):1475-97.
2. Pugliese F, Cademartiri F, van Mieghem C, et al. Multidetector CT for visualization of coronary stents. Radiographics 2006;26(3):887-904.
3. Ulzheimer S, Kalender WA. Assessment of calcium scoring performance in cardiac computed tomography. Eur Radiol 2003;13(3):484-97.
4. Cademartiri F, Schuijf JD, Pugliese F, et al. Usefulness of 64-slice multislice computed tomography coronary angiography to assess in-stent restenosis. J Am Coll Cardiol 2007;49(22):2204-10.
5. Cademartiri F, Mollet NR, Lemos PA, Pugliese F, Baks T, McFadden EP, Krestin GP, de Feyter PJ. Usefulness of Multislice Computed Tomographic Coronary Angiography to Assess In-Stent Restenosis. Am J Cardiol 2005;96:799-802.
6. Ehara M, Kawai M, Surmely JF, et al. Diagnostic accuracy of coronary in-stent restenosis using 64-slice computed tomography comparison with invasive coronary angiography. J Am Coll Cardiol 2007;49(9):951-9.
7. Gaspar T, Halon DA, Lewis BS, et al. Diagnosis of coronary in-stent restenosis with multidetector row spiral computed tomography. J Am Coll Cardiol 2005;46(8):1573-9.
8. Gilard M, Cornily JC, Pennec PY, et al. Assessment of coronary artery stents by 16 slice computed tomography. Heart 2006;92(1):58-61.
9. Hong C, Chrysant GS, Woodard PK, Bae KT. Coronary artery stent patency assessed with in-stent contrast enhancement measured at multi-detector row CT angiography: initial experience. Radiology 2004;233(1):286-91.
10. Kitagawa T, Fujii T, Tomohiro Y, et al. Noninvasive assessment of coronary stents in patients by 16-slice computed tomography. Int J Cardiol 2006;109(2):188-94.
11. Ohnuki K, Yoshida S, Ohta M, et al. New diagnostic technique in multi-slice computed tomography for in-stent restenosis: pixel count method. Int J Cardiol 2006;108(2):251-8.
12. Oncel D, Oncel G, Karaca M. Coronary Stent Patency and In-Stent Restenosis: Determination with 64-Section Multidetector CT Coronary Angiography--Initial Experience. Radiology 2007;242(2):403-9.
13. Rixe J, Achenbach S, Ropers D, et al. Assessment of coronary artery stent restenosis by 64-slice multi-detector computed tomography. Eur Heart J 2006;27(21):2567-72.

14. Schuijf JD, Bax JJ, Jukema JW, et al. Feasibility of assessment of coronary stent patency using 16-slice computed tomography. Am J Cardiol 2004;94(4):427-30.
15. Seifarth H, Raupach R, Schaller S, et al. Assessment of coronary artery stents using 16-slice MDCT angiography: evaluation of a dedicated reconstruction kernel and a noise reduction filter. Eur Radiol 2005;15(4):721-6.
16. Van Mieghem CA, Cademartiri F, Mollet NR, et al. Multislice spiral computed tomography for the evaluation of stent patency after left main coronary artery stenting: a comparison with conventional coronary angiography and intravascular ultrasound. Circulation 2006;114(7):645-53.
17. Flohr TG, McCollough CH, Bruder H, et al. First performance evaluation of a dual-source CT (DSCT) system. Eur Radiol 2006;16(2):256-68.
18. Austen WG, Edwards JE, Frye RL, et al. A reporting system on patients evaluated for coronary artery disease. Report of the Ad Hoc Committee for Grading of Coronary Artery Disease, Council on Cardiovascular Surgery, American Heart Association. Circulation 1975;51(4 Suppl):5-40.
19. Mollet NR, Cademartiri F, van Mieghem CA, et al. High-resolution spiral computed tomography coronary angiography in patients referred for diagnostic conventional coronary angiography. Circulation 2005;112(15):2318-23.
20. Foley DP, Escaned J, Strauss BH, et al. Quantitative coronary angiography (QCA) in interventional cardiology: clinical application of QCA measurements. Prog Cardiovasc Dis 1994;36(5):363-84.
21. Bossuyt PM, Reitsma JB, Bruns DE, et al. Towards complete and accurate reporting of studies of diagnostic accuracy: The STARD Initiative. Ann Intern Med 2003;138(1):40-4.
22. Leber AW, Knez A, von Ziegler F, et al. Quantification of obstructive and nonobstructive coronary lesions by 64-slice computed tomography: a comparative study with quantitative coronary angiography and intravascular ultrasound. J Am Coll Cardiol 2005;46(1):147-54.
23. Smith PJ, Hadgu A. Sensitivity and specificity for correlated observations. Stat Med 1992;11(11):1503-9.
24. Zellweger MJ, Weinbacher M, Zutter AW, et al. Long-term outcome of patients with silent versus symptomatic ischemia six months after percutaneous coronary intervention and stenting. J Am Coll Cardiol 2003;42(1):33-40.
25. Sharma SK, Choudhury A, Lee J, et al. Simultaneous kissing stents (SKS) technique for treating bifurcation lesions in medium-to-large size coronary arteries. Am J Cardiol 2004;94(7):913-7.
26. Hoffmann U, Shapiro M. Coronary multidetector computed tomography: a new standard for preoperative risk assessment? J Am Coll Cardiol 2006;47(10):2025-6.
27. Morin RL, Gerber TC, McCollough CH. Radiation dose in computed tomography of the heart. Circulation 2003;107(6):917-22.

18

Clinical Value of Dual-Source CT Coronary Angiography in Symptomatic Patients after Previous Percutaneous Coronary Stent Implantation.

Carlos A.G. Van Mieghem[1,2], Annick C. Weustink[1,2], Francesca Pugliese[1,2], W. Bob Meijboom[1,2], Nico R. Mollet[1,2], Gabriel P. Krestin[2], Myriam G. Hunink[2,3], Ron van Domburg[1], Majanka H. Heijenbrok-Kal[2,3], Patrick W. Serruys[1], Pim J. de Feyter[1,2]

From the departments of Cardiology[1], Radiology[2], Epidemiology and Biostatistics[3], Erasmus MC, Rotterdam, the Netherlands

Submitted .

ABSTRACT

Objectives

We sought to evaluate the diagnostic performance of a traditional work-up as compared to CT coronary angiography (CTCA) in symptomatic patients after previous percutaneous coronary stent implantation.

Background

Patients with recurrent chest pain after percutaneous coronary intervention (PCI) are traditionally investigated using exercise electrocardiography (ex-ECG), myocardial perfusion imaging (MPI) and dobutamine-stress echo (DSE) or by direct referral for a conventional coronary angiogram (CCA).

Methods

Fifty-one consecutive symptomatic patients underwent dual-source cardiac CT and CCA in addition to a traditional work-up consisting of ex-ECG, MPI, DSE. All angiograms were evaluated for in-stent restenosis and the presence of disease progression at non-PCI sites.
Significant disease was defined by quantitative coronary angiography (QCA) as the presence of ≥ 50% lumen diameter stenosis.

Results

According to QCA, 40/51 patients (78%) presented with restenosis (11 patients) or progression of native vessel disease (29 patients). On a patient level, the sensitivity of CTCA (98%, 95%CI 93-100%) was significantly higher ($P < 0.05$) than that of the traditional work-up (65%, 95%CI 50-80%) whereas specificity was identical (55%, 95%CI 25-84%; P=NS).
Revascularization was performed in 36 of the 40 patients with angiographically significant disease.

A negative CTCA reliably excluded the need for revascularization. By contrast, in the presence of a negative or inconclusive functional test, the probability of revascularization was as high as 60%.

Conclusions

CTCA improves the traditional diagnostic work-up of symptomatic patients with previous percutaneous coronary stent implantation. Ideal candidates for CTCA prior to CCA are patients with a negative or inconclusive stress test.

INTRODUCTION

Percutaneous coronary intervention (PCI) for symptomatic patients with coronary artery disease is a well established therapy.(1) Currently, more than 90% of PCIs involve the implantation of a coronary stent.(2) Drug-eluting stents are increasingly being used and actually comprise ~50% of the stenting procedures because of their increased efficacy to reduce in-stent restenosis (ISR).(3) The recurrence of symptoms in patients, requiring additional coronary intervention at 5 years follow-up in 20%, after an initial successful PCI may either be caused by progression of atherosclerotic disease in non-stented segments or from ISR.(4)

Current ACC/ AHA guidelines advocate exercise stress testing, preferably combined with nuclear or echocardiographic imaging, for the initial work-up of symptomatic patients after previous PCI.(5) Due to its costs and invasive nature, catheter-based coronary angiography (CCA) is ideally restricted to patients with an abnormal functional test result. CT coronary angiography (CTCA) has emerged as a potentially useful alternative for CCA to assess coronary anatomy and larger stents (≥ 3mm). (6,7)

In a consecutive cohort of 51 symptomatic patients after previous stent-based PCI, we sought to evaluate the diagnostic performance of CTCA as compared to a traditional approach using either: exercise electrocardiography (ex-ECG), myocardial perfusion imaging (MPI), dobutamine-stress echocardiography (DSE), or direct referral for CCA. We also compared the therapeutic decision based on this traditional work-up with CTCA.

METHODS

Patient population

Between August 2006 and December 2007, we prospectively enrolled 51 consecutive patients who experienced recurrence of anginal symptoms after previously successful PCI and who were scheduled to undergo a CCA. The majority of the patients was recruited in referring community hospitals and underwent most of the diagnostic work-up, including CCA, in the referring hospital. The CTCA was performed in our institution on an outpatient basis, within a 3-week period prior to CCA. Patients with prior coronary artery bypass graft surgery, previous PCI using small-diameter stents (stent diameter < 3mm), previous PCI for ISR with a resulting double layer of stents, and previously implanted tantalum, titanium or gold-coated stents were excluded, as well as women of childbearing age. Exclusion criteria for CTCA were: an irregular heart rhythm, inability to breath hold for 15 seconds, contraindications for heart-rate lowering drugs and IV contrast media (history of prior contrast allergy, renal insufficiency defined as

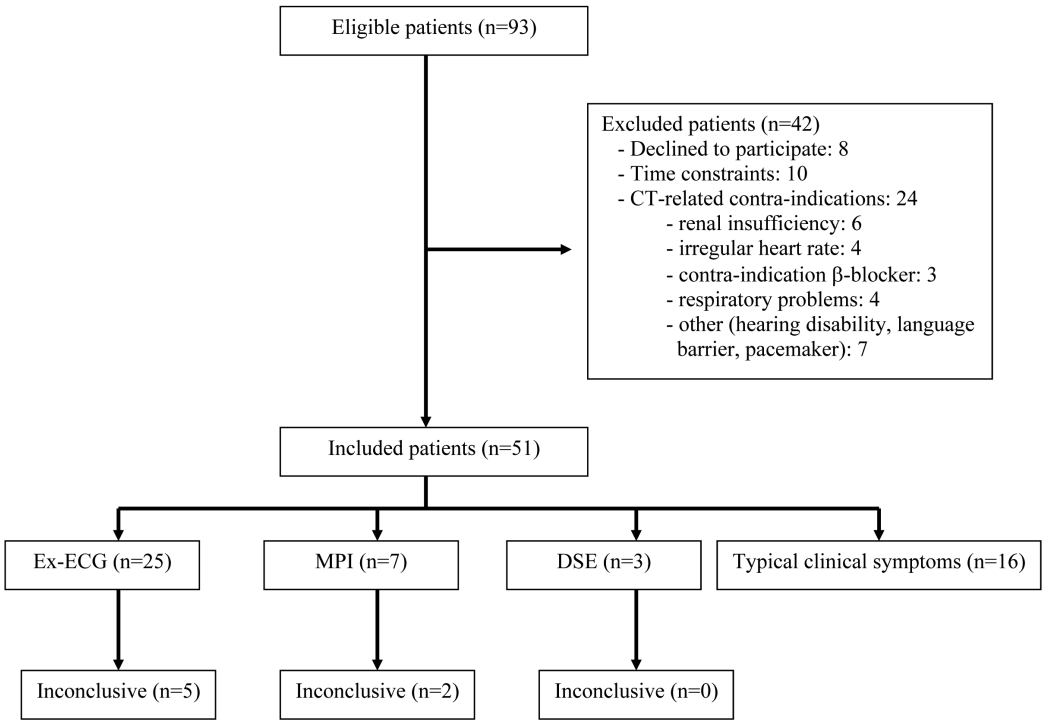

Figure 1. Flow diagram of the study.

the presence of a creatinine clearance < 60 ml/min, as calculated with the Cockroft formula), and the presence of an implanted pacemakers or defibrillator. A flow diagram of the study is presented in Figure 1. The institutional ethical review board approved the study protocol. All participating patients gave informed consent.

CT based strategy: CT scan protocol and image reconstruction

Patients with a resting heart rate above 80 beats per minute (bpm) received oral beta-blockers (metoprolol 50-100 mg) 1 hour before the scan. For patients with astma we used an oral calcium-antagonist (diltiazem 60-120 mg). An additional IV bolus of metoprolol (5-10 mg) was administered where the heart rate remained above 80 bpm. Nitrates were given sublinguallu (0.4 mg) to all patients 5 to 10 minutes before initiation of the scan.

The examination was performed using previously reported methodology.(8) In brief, all patients were scanned using a dual-source CT (DSCT) scanner (Somatom Definition, Siemens, Forcheim, Germany). A non-contrast-enhanced scan was not performed. The angiographic scan parameters were: individual detector collimation 32 x 2 x 0.6mm, gantry rotation time 330 ms, tube voltage 120 kV, current of 412 mAs per tube. Pitch values were adapted to heart

rate and estimated based on the last 10 heartbeats preceding the scan. Full x-ray tube current was limited to 25-70% of the RR-interval. The tube current was reduced to 20% of the maximum tube current outside the ECG pulsing window.

Contrast material (Ultravist® 370 mg of iodine per ml, Schering AG, Germany) was delivered intravenously with a flow rate of 5.5 ml/sec, followed by 40 ml of saline flush at 5.5 ml/s. A bolus tracking technique was used to monitor the appearance of contrast material in the aortic root cranial to the origin of the left coronary artery. Once the signal in the ascending aorta reached a predetermined density level of +100 Hounsfield units, CT acquisition was automatically started during an inspiratory breath hold. Images were reconstructed using ECG-gating to obtain optimal, motion free image quality.

The scan data were reconstructed with 0.75 mm slice thickness and 0.4 mm increment at various phases of the cardiac cycle using medium-to-smooth (B26f) and sharp (B46f) convolution kernel. Datasets with least motion artefact were selected for further analysis. The non-stented vessel segments were evaluated using images generated with medium-smooth kernel. The segments that contained stents were evaluated using both medium-smooth and sharp kernel datasets.

The effective radiation dose was calculated from the scan parameters using dedicated software (ImPACT CT Patient Dosimetry Calculator, version 0.99x), as described in the European Guidelines on Quality Criteria for Computed Tomography (Available at: http://www.drs.dk/guidelines/ct/ quality/index.htm).

CTCA image interpretation

Two experienced investigators (CVM, ACW), who were blinded to the patients' clinical history as well as the angiographic data, interpreted each CT study independently, and subsequently a consensus reading was performed. Cardiac CT data were analyzed off-line using a Leonardo workstation (Siemens Medical Solutions). All coronary segments, regardless of image quality, were visually scored for the presence of significant disease, which was defined as a diameter reduction of ≥ 50%, by evaluating the original transaxial images and by using oblique and curved multiplanar reconstructions. A significant narrowing within the stent, including the 5mm vessel borders proximal and distal to the stent, was considered as ISR. A significant stenosis outside these borders was considered as progression of native vessel disease. Vessel segments with poor image quality that precluded reliable assessment were considered as having significant disease.(9) Different window settings, including a window width/ window level setting of 1500 by 300 HU, were used for optimal stent assessment.

Traditional work-up

The traditional work-up was defined as referral to CCA on the basis of typical clinical symptoms and/or a positive result on functional testing, including ex-ECG, MPI or DSE (Figure 1). The decision whether or not to use a functional stress test before proceeding to CCA was left to the discretion of the treating physician. In general, direct referral to CCA is considered a valid option for patients with typical anginal symptoms that substantially limit exertion or when presenting with unstable symptoms.(10)

Exercise electrocardiography (ex-ECG)

The exercise test was performed on a bicycle ergometer beginning at a workload of 25W and increasing by 25W every 2 minutes. Heart rate and blood pressure were recorded at rest and at the end of each stage of exercise. A 12-lead electrocardiogram was obtained each minute and 3-channel monitoring of cardiac rhythm was performed continuously. The exercise test was considered 'positive' when one of the following events occurred: ≥1mm horizontal or downsloping ST-segment depression or elevation measured 80 ms after the J-point during exercise or recovery, or occurrence of typical angina.(11) An exercise test without accompanying ST-segment changes or anginal symptoms was classified as inconclusive when the patient did not reach at least 85% of the maximum predicted heart rate.

Dobutamine-stress echocardiography (DSE)

Dobutamine was used as the stress agent for this examination and was administered through a peripheral vein starting at a dose of 5 μg/kg/min, followed by a dose of 10 μg/kg/min and further increasing by 10 μg/kg/min every 3 minutes to a maximum of 40 μg/kg/min. The infusion was stopped when 85% of age-predicted heart rate was achieved. Otherwise, dobutamine infusion was continued and supplemented by atropine (up to a maximal dose of 1 mg). Echocardiographic images were acquired using the standard views at rest and during stress and recovery. The test was considered positive for significant coronary artery disease (CAD) if new or worsening wall motion abnormalities developed during stress.(12)

Myocardial perfusion imaging (MPI)

Myocardial perfusion single photon emission CT (SPECT) was carried out with symptom-limited bicycle exercise or pharmacologic (adenosine or dobutamine) stress. A two-day protocol was used with rest and stress images acquired on subsequent days. An intravenous dose of 370 MBq technetium-99m tetrofosmin was administered approximately 1 minute before the termination of the stress test. For resting studies, 370 MBq technetium-99m tetrofosmin was injected at least 24 hours after the exercise study. Images were obtained with a triple-head gamma camera system without attenuation or scatter correction. The interpretation of the scan was performed by visual analysis. A reversible perfusion defect was defined as a perfusion defect on stress images that partially or completely resolved at rest. A fixed perfusion

defect was defined as a perfusion defect on stress images that persisted on rest images. An abnormal study was indicated by the presence of a fixed or reversible perfusion defect (or both).(13) This was considered diagnostic of significant CAD.

Quantitative coronary angiography (QCA)

Invasive coronary angiograms were obtained in multiple projections after intracoronary nitrate administration with standard techniques. One experienced cardiologist (WBM), unaware of the results of the CT examination, identified all available coronary segments using a 17-segment modified American Heart Association classification.(14) All vessel segments with a reference diameter of at least 1.5mm were included for comparison with CTCA, except for segments distal to an occlusion. Stenoses were evaluated in the angiographic projection showing the most severe narrowing using validated, automated, quantitative software (CAAS II, Pie Medical, Maastricht, the Netherlands), and classified as significant if the lumen diameter reduction was $\geq$ 50%.

Statistical analysis

Continuous variables are presented as mean $\pm$ standard deviation. Categorical variables are presented as counts and percentages. The diagnostic performance of CTCA for the detection of a significant coronary artery stenosis was calculated per patient, per segment, and per stent using QCA as the reference test and is presented as sensitivity, specificity, and positive- and negative predictive values. The diagnostic performance of the traditional work-up was calculated per patient using QCA as reference test with a positive test defined as a positive result on a non-invasive functional test or the presence of typical symptoms.(15,16) Precision of the diagnostic parameters is presented using 95% confidence intervals. The pairwise McNemar's test was used to compare per-patient sensitivity and specificity of the traditional work-up and CTCA. For the analysis with revascularization versus no revascularization as outcome, the reference test used was a combination of QCA, fractional flow reserve and intravascular ultrasound. The predictive values of typical symptoms or the functional test result (i.e. the traditional work-up) versus CTCA for predicting the need for revascularization (revasc) were calculated. Interobserver variability in the interpretation of CTCA was calculated using kappa-statistics. A two-sided p-value of <0.05 was considered statistically significant. Statistical analysis was performed with SPSS, version 11.5 (SPSS Inc., Chicago, USA).

RESULTS

Patient characteristics are summarized in Table 1. Twenty percent of the patients received additional heart-rate lowering drugs resulting in an average heart rate of 64 $\pm$ 8.2 beats per minute during CT data acquisition. The mean effective CT radiation dose was estimated as 18.1

Table 1. Patient characteristics (n=51).

Variable	Value
Age, yrs	61.4 ± 9.5
Men, n (%)	41 (80)
Body mass index, kg/m2	23.2 ± 3.7
Clinical presentation, n (%)	
- stable angina	47 (92)
- acute coronary syndrome	4 (8)
Hyperlipidemia, n (%)	47 (92)
Arterial hypertension, n (%)	23 (45)
Diabetes mellitus, n (%)	7 (14)
Current cigarette smoking, n (%)	5 (10)
Medication, n (%)	
- Aspirin	51 (100)
- Beta-blocker	39 (76)
- Calcium-channel blocker	15 (29)
- Nitrates	18 (35)
- Statin	45 (88)
- ACE inhibitor or ARB	33 (65)
Creatinin clearance, ml/min	90.1 ± 26.7
Heart rate during CT scan, bpm	64 ± 8.2
Contrast amount during scan, ml	80.3 ± 9.9
Radiation dose estimate CTCA, mSv	18.1 ± 4

Values are mean ± SD, or number with percentage in parentheses. ACE denotes angiotensin converting enzyme, and ARB angiotensin-receptor blocker.

± 4 mSv. The amount of contrast media used for the CT scan was on average 80.3 ± 10 ml. All 51 patients successfully underwent CTCA without untoward side effects. The median time interval between CTCA and CCA was 1 day (range 0 to 20 days). The median time interval between PCI and CTCA was 522 days (range 16-2350 days).

A noninvasive functional test was available in 35 patients: 25 patients underwent a symptom-limited bicycle stress test, 7 patients underwent nuclear SPECT imaging and in 3 patients a dobutamine stress echocardiogram (DSE) was performed. Sixteen patients were directly referred for CCA because of severe stable angina (n=8), residual angina after primary percutaneous coronary intervention for myocardial infarction (n=5), or other forms of unstable angina (n=3).

Traditional work-up versus CT coronary angiography. Diagnostic performance.

According to QCA, 78% (40/51) of the patients presented with in-stent restenosis (11/51) or progression of native vessel dis-

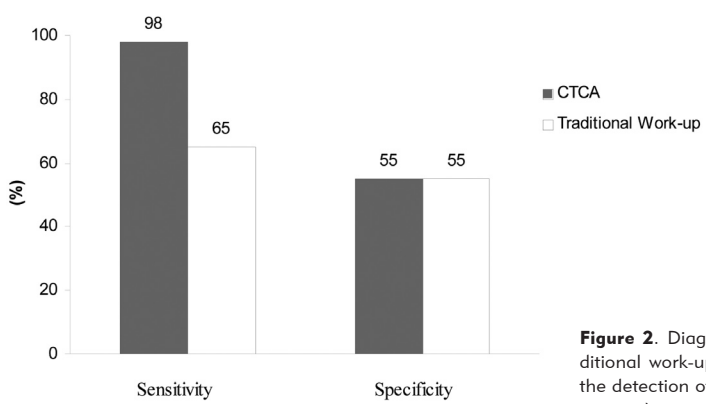

Figure 2. Diagnostic performance of CTCA versus a traditional work-up (functional test or clinical symptoms) for the detection of significant coronary artery disease (n= 51 patients).

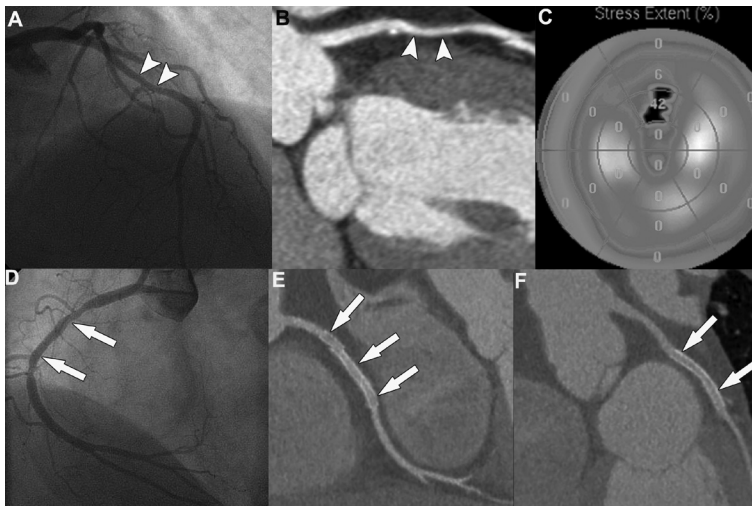

Figure 3. Patient with a 47% diameter stenosis in the LAD (A, arrowheads). Corresponding CTCA (B, arrowheads). Nuclear SPECT stress image showing a reversible perfusion defect in the anteroapical region (C). The stents in the RCA (D and E, arrows) and CX (F, arrows) were patent both on CCA (D) and CTCA (E and F). Measurement of the fractional flow reserve (FFR) across the lesion was within normal limits (value of 0.81). (A full color version of this illustration can be found in the color section).

ease (29/51). Five of the 11 patients with ISR also showed significant disease in non-PCI sites. The diagnostic performance of CTCA versus a traditional work-up is shown in Figure 2. The sensitivity of CTCA (98%, 39 of 40 patients, 95%CI 93-100%) was significantly higher ($P<0.05$) compared to the traditional work-up (65%, 26 of 40 patients, 95%CI 50-80%); specificity was identical (55%, 6 of 11 patients, 95%CI 25-84%; P=NS).

When we restrict the data to those 35 patients who had a functional test available before CCA, we found the following results (data not shown): sensitivity of 100% (28 of 28 patients, 95%CI 94-100%) versus 50% (14 of 28 patients, 95%CI 31-69%), specificity of 57% (4 of 7 patients, 95%CI 20-94%) versus 86% (6 of 7 patients, 95%CI 60-100%), for respectively CTCA and the traditional work-up.

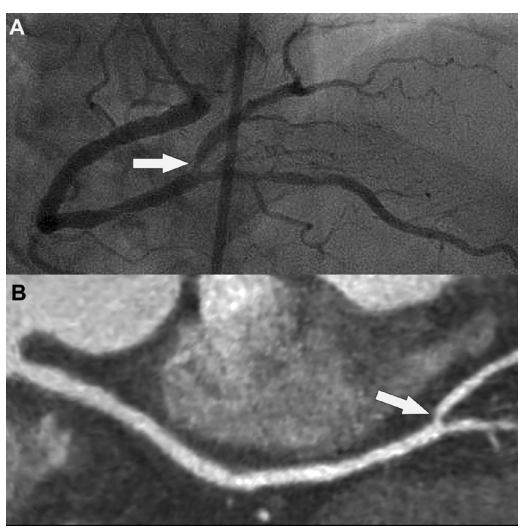

Figure 4a. Patient with a significant stenosis (52% by QCA, A, arrow) in the distal RCA. Corresponding CTCA showing a non-significant narrowing at the corresponding spot (B, arrow).

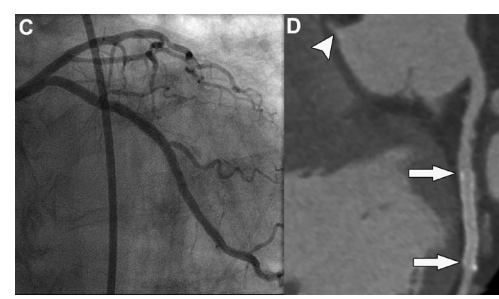

Figure 4b. The previously implanted stent in the CX artery was patent both on CCA(C) and CTCA (D, arrows). The take-off of the RCA is also visible on the CTCA (D, arrowhead).

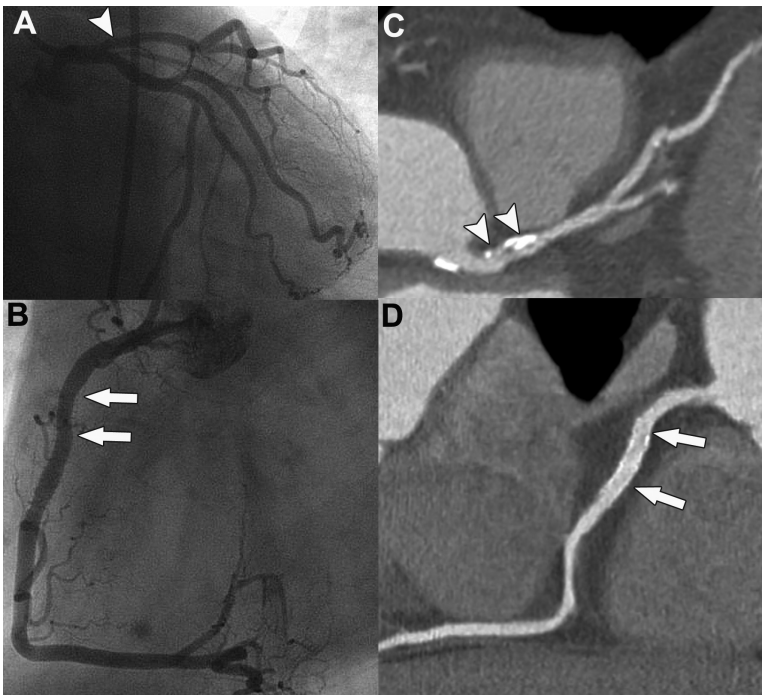

Figure 5. Patient with a functionally non-significant (fractional flow reserve value of 0.88) narrowing of the proximal LAD. The CCA shows minimal lumen narrowing (A, arrowhead). Corresponding CTCA showing a calcified plaque at this spot (C, arrowheads), which was evaluated as causing significant lumen narrowing. The previously implanted stent in the RCA was patent both on CCA (B, arrows) and CTCA (D, arrows).

Among the 15 patients with an incorrect functional test result, 10 were due to a false negative (n=7) or inconclusive (n=3) bicycle stress test, 4 were due to a false negative nuclear SPECT (n=2) or DSE (n=2), and 1 was due to a false positive nuclear SPECT (Figure 3). Six of the 51 patients were incorrectly classified by CTCA: 1 patient, in whom the severity of disease was underestimated, showed a significant stenosis distal to the take-off of the posterior descending branch of the right coronary artery (Figures 4a and 4b). Five patients with angiographically nonsignificant disease were classified as having significant disease by CTCA (Figure 5). The interobserver agreement in the interpretation of CTCA on a patient level was very good (kappa value of 0.81).

Diagnostic accuracy of DSCT coronary angiography: segment-based analysis.

Overall, 687 (of 867 theoretically available) segments were included for comparison with QCA. Sixty-nine segments were anatomically absent, 46 segments were located distal to an occlusion and 65 segments were smaller than 1.5mm. The sensitivity, specificity, positive and negative predictive values were 85% (71 of 84, 95% CI 77-92%), 96% (578 of 603, 95% CI 94-97%), 74% (71 of 96, 95% CI 65-83%) and 98% (578 of 591, 95% CI 97-99%), respectively. The severity of 13 significant coronary stenoses was underestimated or missed and classified as non-significant by CTCA. All of these false negative interpretations were due to lesions located in distal segments (n=5) or in side branches (n=8). The severity of 25 non-significant lesions

Table 2. Stent characteristics (n=87).

Variable	Value
Stents per patient, mean (range)	1.7 (1-6)
Single- / multi-vessel PCI, number of patients (%)	42 (82)/ 9 (18)
Stent diameter, mm (range)	3.3 (3-4.5)
Drug-eluting stent, n (%)#	60 (69)
Stent type, n (%)	
- Express 2*	18 (21)
- Liberté*	37 (42)
- Bx velocity*	11 (13)
- R-stent*	9 (10)
- NIR*	7 (8)
- Multi-link Vision§	4 (5)
- S-stent*	1 (1)

Drug-eluting stents that were implanted were the paclitaxel-eluting stent (n=51) using the Express 2 or Liberté stent platform, the sirolimus-eluting stent (n=4) using the Bx velocity stent platform, the everolimus-eluting stent (n=4) using the Multi-link Vision stent platform and the tacrolimus-eluting stent (n=1) using the S-stent platform.
* Material: stainless steel, strut thickness: 0.091-0.14 mm. § Material: Cobalt-chromium, strut thickness: 0.081 mm.

was overestimated by CTCA: false positive interpretations were mainly related to severe vessel wall calcifications (n=14) or stent related artefacts (n=2). The interobserver agreement in the interpretation of CTCA on a segment level was good (kappa value of 0.71).

Coronary stent analysis.

The stent characteristics are shown in Table 2. Seven different stent types were evaluated, most of them (69%) being drug-eluting stents. All stents had a diameter of ≥ 3mm (range 3 to 4.5mm) and the majority of the patients (82%) had undergone single-vessel PCI. By QCA, ISR was present in 22% (6 of 27) of the bare metal stents and in 13% (8 of 60) of the drug-eluting stents. The diagnostic performance of DSCT to detect ISR is summarized in Figure 6. The sensitivity, specificity, positive and negative predictive values were 100% (14 of 14, 95% CI 88-100%), 97% (71 of 73, 95% CI 94-100%), 87% (14 of 16, 95% CI 71-100%) and 100% (71 of 71, 95% CI 97-100%), respectively. All 14 stents with ISR were identified by CTCA, whereas two stents were incorrectly considered as having significant disease.

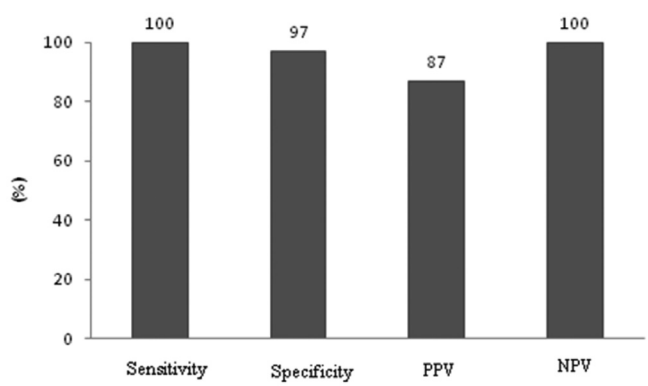

Figure 6. Diagnostic performance of CTCA to detect in-stent restenosis. (n= 87 stents)

Therapeutic decision.

Of the 40 patients with angiographically significant coronary artery disease (CAD), 36 underwent a repeat revascularization: 1 patient received coronary artery bypass graft surgery, the other 35 underwent PCI. In 10 patients additional information obtained by fractional flow re-

Table 3. Stratification of the CTCA data according to the final therapeutic decision.

	CTCA		
	Positive	**Negative**	**Total**
Therapeutic decision			
Revascularization	36	0	36
No revascularization	8	7	15
Total	44	7	51

A negative/ positive CTCA is determined as: the absence or presence of significant coronary artery disease.

Table 4. Stratification of the noninvasive functional and clinical data according to the final therapeutic decision.

	Noninvasive functional test/ typical clinical symptoms		
	Positive	Negative	Total
Therapeutic decision			
Revascularization	24	12	36
No revascularization	7	8	15
Total	31	20	51

A positive result on a "noninvasive functional test or typical clinical symptoms" is determined as: the presence of an abnormal functional test or typical anginal symptoms (in those patients in whom a functional test was not available). A negative result is determined as the presence of a normal or inconclusive functional test.

serve (n=9) or intravascular ultrasound (n=1) was necessary to guide the final therapeutic decision. A stratification of the CTCA data and those of the traditional work-up according to the final therapeutic decision, i.e. revascularization versus no revascularization, is shown in Tables 3 and 4. Importantly, a negative CTCA reliably excluded the need for revascularization (Table 3), or put in other words, all ultimately revascularized patients were identified by a CTCA based approach. Of the 8 patients in whom the CT-based result did not match with the therapeutic decision, 5 had a functional test available that in all cases did not show signs of ischemia (4 tests negative, 1 test inconclusive). By contrast, in the presence of a negative or inconclusive functional test, the probability of revascularization was as high as 60% (12/20) (Table 4). All these 12 patients were correctly identified based on CTCA. The presence of an abnormal functional test (n=15) was almost always indicative of angiographically significant CAD and sufficient reason to revascularize: only one of the patients with an abnormal nuclear test did not show anatomically important epicardial CAD.

DISCUSSION

Recent 64-slice CT technology has shown to be a robust non-invasive diagnostic modality to visualize the coronary arteries.(8,17) CTCA is recommended for symptomatic patients at intermediate pre-test risk of having CAD in whom the presence of significant CAD can reliably be excluded.(7) Today, firm evidence is lacking that CTCA may be clinically useful in patients who have undergone coronary stent implantation, because the stent lumen is often obscured by significant blooming effects of the stent struts. This artefact is less cumbersome in large-sized stents and hence CTCA is indicated only in selected patients.

The present study evaluated the value of dual-source CTCA in patients with recurrent angina after previous percutaneous coronary stent implantation. To provide a useful answer to this clinically relevant topic, we chose a study design that differed from previous reports by providing an assessment of the stented as well as the non-stented coronary artery segments and by comparing the diagnostic performance of CTCA with a traditional work-up that is currently used in routine clinical practice. Several conclusions can be drawn from this study.
First, after a median follow-up of 1.4 years post PCI, 67% of patients had symptom recurrence related to progression of native CAD. Second, the diagnostic performance of CTCA was better as compared to a traditional work-up. CTCA had high sensitivity to detect anatomically significant CAD in stented as well as non-stented segments, however non-invasive functional tests had better specificity. Third, CTCA correctly identified all patients who needed a repeat revascularization, however the low specificity resulted in 18% of patients in whom revascularization eventually was not deemed necessary. By contrast, the rather poor sensitivity of non-invasive functional tests resulted in significant underestimation of clinically relevant CAD and revascularization was deemed necessary in a fair number of patients who had a negative or inconclusive functional test result. Fourth, CTCA appears useful as it provides an alternative to CCA whenever further work-up is deemed necessary in case of a negative or inconclusive functional test.

Advancements in CT technology have improved stent assessability, but even when using current state-of-the-art 64-slice DSCT- technology, which provides the most optimal spatial and temporal resolution, factors such as stent size and material as well as strut thickness still have an important impact on the visualization of the stent lumen.(6,18-20) However, these studies have shown that diagnostic in-stent lumen visibility can be obtained for the majority of stents with a diameter of $\geq$ 3mm. Additional factors such as x-ray scattering in patients with high body-mass index, severe vessel wall calcifications and artefacts related to cardiac or respiratory motion, further hamper in-vivo imaging of coronary stents and are an important cause of non-diagnostic image quality.(21)

Limitations.

The current study only applies to a selected group of patients as we used stringent selection criteria: patients were only considered appropriate in case of a large stent diameter (≥ 3mm), with a relatively low metal density, and were treated with heart-rate lowering drugs despite the use of DSCT technology, to ensure optimal image quality. The decision to reduce the heart rate below 80 bpm, was based on our earlier experience with DSCT, where we demonstrated a higher proportion of non-diagnostic scans in patients with a heart rate above 80 bpm.(22) The effective radiation dose in our study was relatively high compared with previous reports, because we used a wide pulsing window (25% to 70% of the RR interval) in combination with the β-blocker induced lower heart rate, which results in a lower pitch and thus longer scan time.(23) A significant reduction in dose, well below 5 mSv, with preservation of optimal image quality can be achieved with newer 64-slice CT technology and also with very recent updated DSCT technology.(24) The design of our study could be criticized since not all patients had a functional test available before referral for a CCA. Some patients were instead referred to CCA because of the presence of typical symptoms, which in itself can be considered a positive test result given its high likelihood ratio.(16) In addition, most patients with a functional test were evaluated using ex-ECG instead of a functional imaging test, which may have caused the relatively low diagnostic performance of the traditional work-up. We chose not to select patients on the basis of the availability of a functional imaging test because of potential selection bias. Furthermore, we believe that the enrolment of a consecutive patient group fits most closely with current medical practice and therefore contributes to the generalizability of the results. Note that referral to CCA was based on the traditional work-up and not on the CTCA result implying that verification bias (=post-test referral bias) may have overestimated the sensitivity of the traditional work-up but not of CTCA.(25) In spite of this potential bias we still showed that the sensitivity of CTCA was far higher than that of the traditional work-up.

REFERENCES

1. Lenzen MJ, Boersma E, Bertrand ME, et al. Management and outcome of patients with established coronary artery disease: the Euro Heart Survey on coronary revascularization. Eur Heart J 2005;26:1169-79.
2. Serruys PW, Kutryk MJ, Ong AT. Coronary-artery stents. N Engl J Med 2006;354:483-95.
3. Ramcharitar S, Hochadel M, Gaster AL, Onuma Y, Gitt A, Serruys P. An insight into the current use of drug eluting stents in acute and elective percutaneous coronary interventions in Europe: a report on the EuroPCI Survey. EuroIntervention 2008;3:429-441.
4. Boden WE, O'Rourke RA, Teo KK, et al. Optimal medical therapy with or without PCI for stable coronary disease. N Engl J Med 2007;356:1503-16.

5. Gibbons RJ, Balady GJ, Bricker JT, et al. ACC/AHA 2002 guideline update for exercise testing: summary article: a report of the American College of Cardiology/American Heart Association Task Force on Practice Guidelines (Committee to Update the 1997 Exercise Testing Guidelines). Circulation 2002;106:1883-92.
6. Van Mieghem CA, Cademartiri F, Mollet NR, et al. Multislice spiral computed tomography for the evaluation of stent patency after left main coronary artery stenting: a comparison with conventional coronary angiography and intravascular ultrasound. Circulation 2006;114:645-53.
7. Schroeder S, Achenbach S, Bengel F, et al. Cardiac computed tomography: indications, applications, limitations, and training requirements: report of a Writing Group deployed by the Working Group Nuclear Cardiology and Cardiac CT of the European Society of Cardiology and the European Council of Nuclear Cardiology. Eur Heart J 2008;29:531-56.
8. Weustink AC, Meijboom WB, Mollet NR, et al. Reliable high-speed coronary computed tomography in symptomatic patients. J Am Coll Cardiol 2007;50:786-94.
9. Garcia MJ, Lessick J, Hoffmann MH. Accuracy of 16-row multidetector computed tomography for the assessment of coronary artery stenosis. Jama 2006;296:403-11.
10. Levine GN, Kern MJ, Berger PB, et al. Management of patients undergoing percutaneous coronary revascularization. Ann Intern Med 2003;139:123-36.
11. Gibbons RJ, Balady GJ, Beasley JW, et al. ACC/AHA guidelines for exercise testing: executive summary. A report of the American College of Cardiology/American Heart Association Task Force on Practice Guidelines (Committee on Exercise Testing). Circulation 1997;96:345-54.
12. Elhendy A, van Domburg RT, Bax JJ, et al. Optimal criteria for the diagnosis of coronary artery disease by dobutamine stress echocardiography. Am J Cardiol 1998;82:1339-44.
13. Elhendy A, Schinkel AF, Bax JJ, et al. Accuracy of stress Tc-99m tetrofosmin myocardial perfusion tomography for the diagnosis and localization of coronary artery disease in women. J Nucl Cardiol 2006;13:629-34.
14. Austen WG, Edwards JE, Frye RL, et al. A reporting system on patients evaluated for coronary artery disease. Report of the Ad Hoc Committee for Grading of Coronary Artery Disease, Council on Cardiovascular Surgery, American Heart Association. Circulation 1975;51:5-40.
15. Diamond GA, Forrester JS. Analysis of probability as an aid in the clinical diagnosis of coronary-artery disease. N Engl J Med 1979;300:1350-8.
16. Chun AA, McGee SR. Bedside diagnosis of coronary artery disease: a systematic review. Am J Med 2004;117:334-43.

17. Abdulla J, Abildstrom SZ, Gotzsche O, Christensen E, Kober L, Torp-Pedersen C. 64-multislice detector computed tomography coronary angiography as potential alternative to conventional coronary angiography: a systematic review and meta-analysis. Eur Heart J 2007;28:3042-50.
18. Maintz D, Seifarth H, Raupach R, et al. 64-slice multidetector coronary CT angiography: in vitro evaluation of 68 different stents. Eur Radiol 2006;16:818-26.
19. Pugliese F, Weustink AC, Van Mieghem C, et al. Dual source coronary computed tomography angiography for detecting in-stent restenosis. Heart 2008;94:848-54.
20. Sheth T, Dodd JD, Hoffmann U, et al. Coronary stent assessability by 64 slice multi-detector computed tomography. Catheter Cardiovasc Interv 2007;69:933-8.
21. Nieman K, Cademartiri F, Raaijmakers R, Pattynama P, de Feyter P. Noninvasive angiographic evaluation of coronary stents with multi-slice spiral computed tomography. Herz 2003;28:136-42.
22. Weustink AC, Mollet NR, Pugliese F, et al. Optimal electrocardiographic pulsing windows and heart rate: effect on image quality and radiation exposure at dual-source coronary CT angiography. Radiology 2008;248:792-8.
23. Stolzmann P, Scheffel H, Schertler T, et al. Radiation dose estimates in dual-source computed tomography coronary angiography. Eur Radiol 2008;18:592-9.
24. Husmann L, Valenta I, Gaemperli O, et al. Feasibility of low-dose coronary CT angiography: first experience with prospective ECG-gating. Eur Heart J 2008;29:191-7.
25. Hachamovitch R, Di Carli MF. Methods and limitations of assessing new noninvasive tests: part I: Anatomy-based validation of noninvasive testing. Circulation 2008;117:2684-90.

PART V

SUMMARY AND CONCLUSIONS

19

Summary and conclusions.

Ten years after its introduction as a new diagnostic technique, computed tomography coronary angiography (CTCA) is still undergoing technical improvements underscoring the need to further improve image quality of the coronary arteries. From a technical point of view, high temporal and spatial resolution are the key factors determining the validity of CTCA as a non-invasive alternative to conventional coronary angiography (CCA). This thesis uses as a foundation the optimisations in technique that have been achieved so far and focuses on the clinical applications that appear reasonable at the current stage.

Interventional cardiology is a discipline that relies on accurate imaging of the heart and coronary vasculature. The interventional cardiologist uses as a medium CCA, a catheter-based technique that allows selective contrast injection of the coronary arteries and " in the same run" a targeted therapeutic intervention where appropriate. Contrary to the general belief, CCA does not always prove to be the gold standard technique for the visualization of the coronary anatomy even in the hands of an expert angiographer. Indeed, the intrinsic limitations of an imaging technique that is inherently 2-dimensional make it sometimes impossible to accurately assess the presence or severity of a coronary narrowing especially where the anatomy is complex. Furthermore, the "catheter-handling" itself needs to be performed with attention for detail in order to obtain an adequate and reliable visualisation of the coronary arteries. In **chapter 2**, we comment on the limitations of CCA and demonstrate that the 3-dimensional properties of CTCA help to resolve complex coronary pathology. In addition, the unique information that is provided on the trajectory of a coronary artery or the composition of an atherosclerotic lesion may prove valuable in planning and guiding interventional procedures.

The emergence of CTCA is changing the basic image format we are using in daily practice to discuss on the subject of coronary artery disease (CAD). Instead of looking at the luminographic impact of atherosclerosis, we are now able to directly visualize the disease process in the vessel wall. As a result, the metrics we are using to describe CAD are being modified: a "significant coronary stenosis in the proximal LAD" is being rephrased as "the proximal LAD shows a noncalcified plaque causing significant lumen narrowing" or "the RCA has a normal appearance" becomes "the RCA shows a small calcified plaque in segment 2 without luminographic involvement". In this thesis we report on the Integrated Biomarker and Imaging Study (IBIS), which evaluates the feasibility to detect subclinical atherosclerosis using 16-slice CTCA in combination with the assessment of changes in plaque characteristics using invasive imaging modalities (**Chapter 3** and **4**). Compared with intravascular ultrasound (IVUS), CTCA can identify atherosclerotic plaque, in vessels with only minimal angiographic disease, with high sensitivity and moderate specificity. After 6 months of standard medical therapy, conventional imaging with quantitative coronary angiography and IVUS did not show significant changes in lumen or plaque dimensions of the atherosclerotic disease process. Similarly, plaque composition as assessed with IVUS echogenicity did not show temporal changes. However, significant

changes in plaque deformability or strain were evident on IVUS palpography. Studies like IBIS are indicative of the paradigm shift that has recently occurred linking the occurrence of acute coronary syndromes to plaque disruption of non-flow-limiting stenoses rather than to gradual progression to complete occlusion of fixed, high-grade stenoses. As a noninvasive imaging modality, CTCA has potential to facilitate the identification at a preclinical stage of those individuals that harbour atherosclerotic plaques that are deemed to carry a high risk for rupture and ensuing acute coronary event. These so-called vulnerable plaques are most often characterized by positive remodelling of the vessel wall, a large lipid-rich necrotic core covered by a thin fibrous cap and surrounding intense inflammatory activity. Preliminary clinical studies have reported on the feasibility to demonstrate compensatory vessel wall remodelling and plaque composition with CTCA. Novel invasive imaging modalities such as IVUS palpography, IVUS radiofrequency analysis and optical coherence tomography, have been developed to assess in more detail plaque biomechanical and compositional characteristics. Although promising, limitations in spatial resolution restrict the ability of CTCA to identify non-calcified plaques to larger advanced lesions that are located in proximal and middle coronary segments. Furthermore, the plaque density measurements obtained with CTCA are only a rough estimate of the true plaque composition as they correlate linearly with the amount of attenuation derived from intracoronary contrast material: this phenomenon is a consequence of partial volume and interpolation artefact. Both artefacts combined result in averaging of the different attenuation profiles of the various tissues present within one voxel, in stead of preserving and showing the attenuation profile of each tissue type separate. It remains to be demonstrated whether these new approaches to assess vulnerable plaques will impact on the occurrence of acute coronary events in patients at highest risk. **Chapter 5** illustrates the coronary plaque characteristics as assessed by CTCA in comparison to optical coherence tomography. **Interlude 1** demonstrates the feasibility of CTCA to visualize noninvasively the angiographic visible and non-visible aspects of native CAD as well as to evaluate the bypass grafts in the revascularized patient.

The assessment of coronary artery stenoses with CTCA was already demonstrated to be feasible with the early 4-slice and 16-slice CT scanners. In this thesis we report on the diagnostic accuracy with 64-slice CT, which was introduced in 2004 (**Chapters 6** and **7**). The increase in spatial and temporal resolution that accompanies this new generation of CT scanner, results in an improved diagnostic performance while at the same time reducing the percentage of unevaluable coronary segments to less than 5%. These results remain valid in patients presenting with acute coronary syndromes without ST-segment elevation (**Chapter 7**).

Conventional coronary angiography should remain the preferred imaging technique for symptomatic patients with a high pretest likelihood of significant coronary artery disease in whom anatomical assessment of the coronary vasculature is deemed necessary. As a new diagnostic

test, each new CT scanner version has been systematically validated against CCA, to assess for the presence or absence of obstructive CAD. By default, the patients that have been included in these validation studies almost invariably had a high pretest probability of significant CAD as all of them had an indication for CCA based on clinical grounds. Not unexpectedly, the value of a "normal" or "nonobstructive" scan result appears not rewarding in patients who based on clinical grounds already have a high pre-test probability of harbouring anatomically significant CAD, as the post-test probability of significant CAD in case of a negative CT scan remains as high as 17%. By contrast, the same CT scan result in symptomatic patients with a low-to-intermediate pre-test likelihood reveals a post-test probability of 0% and thus reliably rules out the presence of significant CAD (**Chapter 8**). A well defined patient group who may benefit from this "CTCA-first" approach before referral for CCA are those patients who need to undergo cardiac valve surgery. Obstructive CAD that is left untreated at the time of cardiac valve surgery worsens prognosis. As a result most patients above the age of 35 currently undergo a CCA to preoperatively assess coronary anatomy. The pre-test odds of having significant CAD is relatively low in this patient population, averaging around 30%. We found that CTCA could effectively be implemented as a gatekeeper for CCA in this patient group, as most of them turned out to have normal coronary arteries or non-obstructive CAD and the post-test odds of significant CAD were zero in case of a negative CTCA (**Chapter 9**).

The addition of CTCA, a noninvasive anatomical test, to the current armamentarium of diagnostic tests creates the need for a reassessment of currently used diagnostic algorithms in patients with suspected CAD. We made a first attempt to assess the possible value of 16-slice CTCA within the diagnostic work-up of patients presenting with stable angina who underwent an exercise stress test and subsequent CCA (**Chapter 10**). As expected the prevalence of significant CAD was high (74%) in this patient group. We demonstrated a much higher diagnostic accuracy with CTCA as compared to exercise electrocardiography, which in addition turned out to be inconclusive in 15% of the patients studied. The purpose of a test in this population entails more than just diagnosing the presence of significant CAD, which is highly likely already based on the clinical symptomatology. More important is how the diagnostic test result would impact on the subsequent management of the patient. An exercise stress test showing severe ST-segment changes or an important drop in systolic blood pressure carries a poor prognosis for the patient and is a clear indication for coronary angiography and eventual subsequent revascularization. Although not proven in the current study, CTCA might be useful for those patients with a negative or inconclusive exercise stress test result: considering its high diagnostic accuracy, particularly in large-calibre coronary segments, CTCA could become a useful tool towards the exclusion of high-risk coronary anatomy such as left main- or triple vessel CAD.

Coronary artery disease can be evaluated from an anatomical and/ or functional perspective. Both approaches are not mutually exclusive but are rather complementary since both ways of assessment have test-related limitations. Today, even the most advanced dual-source CT scanners still have suboptimal spatial resolution as compared to catheter-based coronary angiography (0.4mm versus 0.2mm). When quantifying the degree of coronary artery lumen narrowing in percent diameter stenosis for lesions with at least 50% diameter reduction, the limits of agreement vary by 27% when comparing 16-slice CTCA with quantitative coronary angiography, the reference standard. Indeed, considering a 3mm coronary artery the difference between a 50% and 70% diameter stenosis would not be evident for a 16-slice CT scanner that features a spatial resolution of 0.6mm in optimal circumstances. This difference in spatial resolution explains the relatively low specificity of CTCA as compared to CCA. More than a decade ago, it was demonstrated that the angiographic interpretation, using QCA, of intermediate type severity coronary artery stenoses, usually reported in the range of 40% to 70% narrowing, did not predict well the functional consequence of this type of stenosis, in other words whether a coronary narrowing significantly impairs coronary blood flow thereby causing myocardial ischemia. Using the same methodology, we demonstrated that an anatomically significant coronary stenosis as determined by CTCA poorly predicts its hemodynamic relevance (**Chapter 11**). Based on our observation and those of other investigators we recommend to use a combined approach with a functional test to decide upon further patient management whenever obstructive CAD is diagnosed on CTCA. In certain circumstances, invasively obtained functional information may be appropriate for this purpose (**Interlude 3**).

The angiographic assessment by CCA of patients with anatomically complex CAD sometimes yields insufficient diagnostic information to confidently decide upon further appropriate therapy. Often a repeat CCA, with the associated risks of an invasive procedure, is performed to determine the exact lesion anatomy. We demonstrated that CTCA might be an excellent alternative for CCA in patients presenting with coronary bifurcation lesions or chronic total occlusions (**Chapters 12** and **13**, **Interlude 4**). Chronic total occlusions (CTOs) are a frequent observation in patients found to have significant CAD on CCA. Because of failure rates as high as 40%, percutaneous coronary intervention (PCI) is often not attempted in this type of lesion. We demonstrated that evaluation of CTOs by means of CTCA offers a better description of its anatomical features as compared to CCA and predicts procedural success in patients referred for PCI. More specifically, the presence of severe calcification, i.e. calcium occupying >50% of the vessel cross-sectional area, as determined by CTCA is an independent predictor of procedural failure. We also showed that the radiation exposure and amount of contrast used during a PCI attempt is considerable (**Chapter 13**). The judicious use of a preprocedural CTCA therefore makes sense and might modify the approach in case PCI is attempted or could drive the physician's preference to an alternative therapeutic modality, i.e. medical treatment or bypass surgery. Magnetic navigation represents a novel technology that has been introduced

within the field of interventional cardiology with the aim to improve procedural success in coronary lesions with tortuous vessel anatomy and/or complex morphology. The incorporation of CT data into the magnetic navigation software allows to generate a detailed preprocedural pathway of the coronary artery to be treated, which facilitates the precise control of the direction of a guidewire in three-dimensional space (**Chapter 14**).

Percutaneous coronary intervention (PCI) using stents has become the dominant form of revascularization. Although the advent of drug-eluting stents significantly reduced the occurrence of in-stent restenosis (ISR), symptoms still recur as a result of ISR or more often due to progression of atherosclerotic disease in non-stented segments. Improvements in CT scan technology and utilisation of dedicated filters and window settings have progressively improved the assessability of the lumen inside the stent (**Chapter 15**). Still, ISR evaluation continues to be difficult with CTCA due to the extreme blooming effect of the stent material. The blooming effect is a fairly constant phenomenon and therefore less evident in large diameter stents (Chapter 17). We demonstrated that for stents implanted in the left main coronary artery, CTCA may be useful to exclude the presence of ISR (**Chapter 16**, **Interlude 5**). To be useful in clinical practice, the overall patient-related diagnostic performance including stented and non-stented segments needs to be sufficiently high. Using dual-source CTCA in symptomatic patients with previously implanted large-diameter stents (≥ 3.0 mm), we found CTCA to be clinically useful for patients with a negative or inconclusive stress test (**Chapter 18**).

Conclusions and future perspective

Current 64-slice and dual-source 64-slice CT coronary angiography has a high diagnostic performance and in particular, is highly reliable to rule out CAD. It is now recommended for use in symptomatic patients with a low-to-intermediate pre-test likelihood of CAD, where a negative CT scan reliably rules out the presence of CAD and prevents patients from referral to CCA. CTCA overcomes the limitations of 2-dimensional CCA and justifies its use in patients with coronary anomalies. The transition to the broader group of patients with complex CAD is already happening in cathlab centres that provide PCI facility as it avoids performing a repeat CCA in case the initial angiographic assessment is deemed to be suboptimal. In patients with CTOs, CTCA helps to predict the chances of success of a PCI attempt and therefore might be useful in deciding upon the most appropriate therapeutic modality. In the post-revascularization setting, CTCA currently provides only a niche application: after previous bypass surgery CTCA is useful to rule out obstructive disease in venous and arterial bypass grafts, evaluation of stenotic disease in native coronary arteries remains problematic. Post-PCI, CTCA may be useful in patients with larger stents (≥3.0 mm diameter); smaller stents cannot be reliably evaluated. Finally, the emergence of CTCA creates the need to reassess currently applied work-up strategies for patients with suspected CAD. Noninvasive access to coronary anatomy has become feasible and reinforces the importance of functional evaluation as a guide for

selection of therapy. Both approaches are not mutually exclusive but become rather complementary.

The clinical applications will benefit from further developments in CT technology. In particular, the challenges posed by extensive calcification or irregular cardiac rhythms will require novel technical approaches probably taking many years to be implemented in the in-vivo setting. For the time being, consolidating and conveying the knowledge already in existence, will help to embrace this fascinating new technology on a broader scale. We eagerly await the data of ongoing multi-center studies to see whether the results of highly performing research centres can be reproduced. Cost-effectiveness studies will be essential to establish the value of CTCA as compared to other diagnostic tests. The radiation risk is a matter of concern and is providing impetus for the development of dose-saving algorithms and new scanning protocols aiming at reducing the effective radiation dose to the level of CCA. Finally, the fast development of CTCA has been the result of a successful interaction between 2 specialties, the cardiology and radiology community. To maintain this high level of expertise, is critical to ensure that those performing it have adequate training in the technique and adhere to guidelines issued by professional societies.

Samenvatting en Conclusies

Tien jaar na haar introductie als een nieuwe diagnostische techniek, ondergaat CT coronair angiografie (CTCA) nog steeds technische verfijningen ten behoeve van verdere verbetering van de beeldkwaliteit van de coronair arteries. Een hoge temporele en spatiele resolutie zijn de voornaamste technische vereisten om CTCA te kunnen aanbieden als een niet-invasief alternatief voor conventionele coronair angiografie (CCA). Deze thesis bouwt voort op de verbeteringen in CT technologie die tot op heden werden gerealiseerd en focust op meest voor de hand liggende klinische toepassingen anno 2009.

Interventionele cardiologie is een discipline die steunt op accurate beeldvorming van het hart en de coronaire vasculatuur. De interventiecardioloog maakt als medium gebruik van CCA, een catheter-gebaseerde techniek waarbij contrastvloeistof selectief in de coronair arteries wordt geïnjecteerd en waarbij indien geïndiceerd in dezelfde sessie een therapeutische interventie kan worden gedaan. In tegenspraak met de gangbare opvatting is CCA niet de onomstreden "gouden-standaard" techniek voor visualisatie van de coronair arteries, zelfs wanneer ze wordt uitgevoerd door een expert in coronair angiografie. Het is inderdaad zo dat de 2-dimensionele eigenschappen van CCA soms een beperkende factor zijn om een coronaire stenose en de ernst ervan goed in beeld te brengen, zeker wanneer de coronair anatomie complex is. Ook de cathetermanipulatie dient omzichtig en precies te gebeuren zodat de coronair arteries adequaat en betrouwbaar in beeld worden gebracht. In **hoofdstuk 2** bespreken wij de beperkingen van CCA en tonen wij aan dat de 3-dimensionele eigenschappen van CTCA toelaten om complexe coronair pathologie precies in beeld te brengen. Bovendien geeft CTCA unieke informatie aangaande het verloop van een coronair arterie of de samenstelling van een coronaire stenose, hetgeen waardevolle informatie is bij de keuze van het type revascularizatie en de uitvoering van de revascularizatieprocedure zelf.

De implementatie van CTCA gaat gepaard met een verandering van het beeld "format" dat wij in de dagelijkse praktijk gebruiken bij discussie over het onderwerp coronaire atherosclerose. In plaats van te kijken naar de impact van coronaire atherosclerose op het lumen, is het nu mogelijk geworden het primaire ziekteproces in de vaatwand te visualiseren. Bijgevolg is ook de terminologie die wij gebruiken om coronaire atherosclerose te beschrijven aan verandering onderhevig: een "significante stenose in de proximale LAD" wordt nu omschreven als "de proximale LAD vertoont een niet-verkalkte plaque gepaard gaande met significante vernauwing van het lumen" of "de RCA heeft een normaal angiografisch aspect" wordt "de RCA vertoont een kleine gecalcifieerde plaque in segment 2 niet gepaard gaande met vernauwing van het lumen". In dit proefschrift bespreken wij de Integrated Biomarker and Imaging Study (IBIS). Deze studie onderzoekt de diagnostische accuraatheid van 16-slice CTCA voor de detectie van subklinische atherosclerose en evalueert de verandering in plaque karakteristieken over de tijd daarbij gebruik makende van invasieve beeldvormingsmodaliteiten (**Hoofdstuk 3** en **4**). In vergelijking met intravasculaire echografie (IVUS) heeft CTCA een

hoge sensitiviteit en matige specificiteit voor het aantonen van atherosclerotische plaque in bloedvaten met minimale angiografische afwijkingen. Na een standaard medicamenteuse therapie van 6 maanden, waren er geen veranderingen in lumen of plaque dimensies. Ook de plaque samenstelling bleef dezelfde bij evaluatie met IVUS "echogenicity". Er traden wel significante veranderingen op in de biomechanische eigenschappen van de plaque zoals met IVUS "palpography" kan worden aangetoond. Studies zoals IBIS zijn een verdere uitwerking de huidige nieuwe inzichten in de pathogenese van atherosclerose, namelijk dat een acuut coronair syndroom meestal optreedt als gevolg van plaque ruptuur ter plaatse van niet-significante vernauwingen in de vaatwand, in plaats van het progressief verder vernauwen van een significante stenose totdat er een occlusie optreedt. Mede omwille van haar niet-invasieve karakter, is CTCA een veelbelovende techniek om in het pre-klinische stadium individuen te identificeren die plaque karakteristieken vertonen die gecorreleerd zijn aan een hoger risico voor ruptuur en daaraan geassocieerd optreden van een acuut coronair syndroom.

Deze "vulnerabele plaques" worden meestal gekenmerkt door: positieve remodelling van de bloedvatwand, een grote vet-rijke kern die overdekt wordt door een dunne fibreuse laag, en de aanwezigheid van veel inflammatoire cellen voornamelijk in de rand van de lipidenrijke kern. In een aantal preliminaire klinische studies werd aangetoond dat het mogelijk is met CTCA de remodelling van de bloedvatwand en de samenstelling van de plaque in beeld te brengen. IVUS palpography, IVUS radiofrequentie analyse en "optical coherence tomography" zijn vrij nieuwe invasieve beeldvormingstechnieken die werden ontwikkeld om de biomechanische eigenschappen en samenstelling van de plaque te kunnen bestuderen. CTCA heeft beperkingen in spatiële resolutie met als gevolg dat de techniek in hoofdzaak kan worden gebruikt voor de evaluatie van niet-verkalkte plaques in het proximale- of midden segment van de coronair arteries. Bovendien is het zo dat de densiteitsmetingen van de plaque door middel van CTCA slechts een ruwe inschatting toelaten van de reëele plaque compositie, aangezien de gemeten densiteitswaarde een lineaire correlatie vertoont met de mate van contrastvloeistofattenuatie: dit fenomeen is een gevolg van 2 artefacten die optreden met CT, namelijk "partial volume" artefact en interpolatie artefact. De combinatie van beide artefacten resulteert in een densiteitsmeting per voxel dat een gemiddelde is van elk van de weefselspecifieke attenuatieprofielen die in deze voxel aanwezig zijn, in plaats van ieder weefsel met zijn eigen densiteitsprofiel afzonderlijk weer te geven. Het dient nog te worden aangetoond dat deze nieuwe methoden om vulnerabele plaques te bestuderen het optreden van acute coronaire syndromen bij hoog-risico patiënten op een gunstige manier kunnen beïnvloeden. In **hoofdstuk 5** vergelijken we de plaque karakteristieken van CTCA met deze van "optical coherence tomography". **Tussenhoofdstuk 1** is een illustratie van de mogelijkheid om met CTCA bij een gerevasculariseerde patient de angiografisch zichtbare- en niet-zichtbare aspecten van natief coronarialijden evenals de bypass greffen niet-invasief in beeld te brengen.

Reeds met de 4-slice en 16-slice CT scanners was het mogelijk om met CTCA coronair stenoses te beoordelen. In dit proefschrift rapporteren wij de diagnostische accuraatheid van de 64-slice CT scanner, die werd geïntroduceerd in 2004 (**Hoofdstukken 6** en **7**). Deze scanner zorgde voor een belangrijke verbetering van de spatiële en temporele resolutie met als gevolg een betere diagnostische performantie en een afname van het percentage niet-beoordeelbare coronair segmenten, tot minder dan 5%. Dezelfde resultaten worden bekomen bij evaluatie van patiënten die zich presenteren met een acuut coronair syndroom, zonder ST-segment elevatie (**Hoofdstuk7**).

Conventionele coronair angiografie blijft de voorkeurstechniek bij symptomatische patiënten met een hoge vooraf-kans op significant coronarialijden wanneer anatomische evaluatie van de coronair arteries noodzakelijk is. Aangezien het een nieuwe techniek betreft werd iedere nieuwe CT-scanner versie steeds opnieuw gevalideerd ten opzichte van CCA, de referentietechniek, voor de beoordeling van de aanwezigheid of afwezigheid van significant coronarialijden. Per definitie hadden al de patiënten die werden geïncludeerd in deze validatiestudies een hoge vooraf-kans op significant coronarialijden aangezien er voor iedere patiënt een klinische indicatie bestond voor het uitvoeren van een CCA. Het is bijgevolg geen verrassing dat een CT scan die als "normaal" of "niet-significant" wordt geprotocolleerd relatief weinig waardevol is bij patiënten die puur op basis van klinische symptomatologie reeds een hoge vooraf-kans op anatomisch significant coronarialijden vertonen, aangezien de waarschijnlijkheid van significant coronarialijden in geval van een "normale of niet-significante CT scan" nog steeds 17% bedraagt. Dezelfde CT scan uitslag bij symptomatische patiënten met een lage-tot-intermediaire vooraf-kans gaat gepaard met een post-test waarschijnlijkheid van 0% en sluit bijgevolg op betrouwbare wijze significant coronarialijden uit (**Hoofdstuk 8**). Een geschikte doelgroep voor een initiële benadering met CTCA in plaats van CCA zijn patiënten die hartklepchirurgie dienen te ondergaan. Obstructief coronarialijden dat niet wordt behandeld op het moment van hartklepchirurgie heeft een nadelige invloed op de prognose van de patiënt. Dientengevolge ondergaat de meerderheid van de patiënten die ouder zijn dan 35 jaar en in aanmerking komen voor hartklepchirurgie een CCA om pre-operatief de coronair anatomie te beoordelen. De vooraf-kans op significant coronarialijden is evenwel laag in deze patiëntengroep en bedraagt ongeveer 30%. CTCA zou in deze patiëntengroep effectief als sluitstuk kunnen worden geïmplementeerd vooraleer over te gaan tot CCA, aangezien het merendeel van de patiënten normale coronair arteries of niet-significant coronarialijden blijkt te vertonen en de post-test waarschijnlijkheid van significant coronarialijden 0 is in het geval van een "negatieve" CT scan (**Hoofdstuk 9**).

De beschikbaarheid van CTCA als een niet-invasieve anatomische test binnen het bestaande arsenaal van diagnostische modaliteiten, maakt het noodzakelijk de diagnostische algoritmes die actueel worden gebruikt voor de evaluatie van patiënten met vermoeden van coronariali-

jden te herevalueren. In **hoofdstuk 12** evalueren wij de mogelijke waarde van 16-slice CTCA bij de diagnostische work-up van patiënten met stabiele angina pectoris die een inspannings stress test en vervolgens een CTCA ondergingen. Zoals verwacht was de prevalentie van significant coronarialijden hoog (74%) in deze patiëntengroep. De diagnostische accuraatheid van CTCA was hoger in vergelijking met inspanningselectrocardiografie, die bovendien inconclusief was bij 15% van de patiënten. Het doel van een diagnostische test in deze populatie behelst evenwel meer dan enkel de diagnose van significant coronarialijden, aangezien deze reeds zeer waarschijnlijk is voortgaande op de symptomatologie van de patiënt. Belangrijker is de impact van de diagnostische test op het therapeutisch beleid van de patiënt. Een inspanningselectrocardiogram dat gepaard gaat met uitgesproken deviatie van het ST-segment of belangrijke daling van de systolische bloeddruk is van slechte prognostische waarde voor de patiënt en vormt een duidelijke indicatie voor het uitvoeren van een coronair angiografie en eventueel revascularisatie. Hoewel dit niet wordt aangetoond in de huidige studie, is het uitvoeren van een CTCA mogelijks zinvol voor de evaluatie van patiënten met een negatief of inconclusief inspanningselectrocardiogram: de hoge diagnostische accuraatheid van CTCA, in het bijzonder voor de grotere segmenten van de coronair arteries, maakt deze techniek mogelijks waardevol voor het uitsluiten van significant hoofdstam- en/of 3-vatslijden, met andere woorden prognostisch relevante coronair pathologie.

Ziekte van de kransslagaders kan geëvalueerd worden vanuit een anatomische en functionele invalshoek. De ene benadering sluit de andere niet uit maar zijn eerder complementair aangezien beide evaluatiemethoden beperkingen hebben. De meest performante CT technologie die actueel beschikbaar is, met name de dual-source CT scanner, vertoont een spatiële resolutie die inferieur is aan CCA (0.4mm versus 0.2mm). Bij quantificatie van de hoeveelheid diameter reductie in geval van een coronaire lesie met minstens 50% diameter stenose, bestaat er een variatie van 27% wanneer 16-slice CTCA wordt vergeleken met de referentietest, namelijk quantitatieve coronair angiografie. Met een 16-slice CT scanner is het inderdaad niet mogelijk in een coronair arterie met een referentiediameter van 3mm het onderscheid te maken tussen een stenose die varieert tussen 50% en 70% diameter reductie, aangezien de spatiële resolutie van deze scanner in optimale omstandigheden 0.6mm bedraagt. Dit verschil in spatiële resolutie verklaart de relatief lage specificiteit van CTCA in vergelijking met CCA. Reeds meer dan 10 jaar geleden werd aangetoond dat de quantitatieve angiografische evaluatie van een coronaire stenose met een diameter reductie die varieert tussen 40 en 70% geen goede predictie toelaat van de functionele weerslag van deze graad van stenose, met andere woorden of deze stenose de coronaire flow op significante wijze beïnvloedt en als gevolg hiervan leidt tot myocardischemie. Uitgaande van dezelfde methodologie hebben wij aangetoond dat een stenose die bij CTCA als anatomisch significant wordt ingeschat geen goede inschatting toelaat van de hemodynamische weerslag ervan (**Hoofdstuk 11**). Uitgaande van onze bevindingen en deze van andere onderzoekers, stellen wij voor

een functionele test uit te voeren wanneer obstructief coronarialijden wordt gediagnosticeerd door middel van CTCA om zodoende het verder therapeutisch beleid te kunnen bepalen. In een aantal omstandigheden is invasief verkregen functionele informatie hiervoor het meest aangewezen (**Tussenhoofdstuk 3**).

Voornamelijk bij patiënten met anatomisch complex coronarialijden, levert CCA soms onvoldoende diagnostische informatie op om een gefundeerde therapeutische beslissing beleid te kunnen nemen. Niet onfrequent wordt een nieuwe CCA uitgevoerd, hetgeen opnieuw een risico voor de patiënt inhoudt omwille van het invasieve karakter van de procedure, om de anatomische kenmerken van de stenose beter te kunnen beoordelen. Bij patiënten met bifurcatiepathologie of chronische totale occlusies biedt CTCA een uitstekend alternatief voor CCA (**Hoofdstukken 12** en **13**, **Tussenhoofdstuk 4**). Chronische totale occlusies (CTOs) zijn een frequente bevinding bij patiënten die significant coronarialijden vertonen bij CCA. Aangezien het succes percentage van een percutane coronaire interventie (PCI) voor CTOs niet optimaal is, met name tot 40% ervan kunnen percutaan niet gerevasculariseerd worden, wordt een PCI dikwijls niet uitgevoerd bij dit type van coronair pathologie. CTCA laat een betere beschrijving toe van de anatomische karakteristieken van een CTO in vergelijking met CCA en voorspelt bij welke patiënten de kans op een succesvolle PCI het hoogst is. In het bijzonder blijkt dat de aanwezigheid van ernstige calcificaties op CTCA, met name calcium dat >50% van het cross-sectionele oppervlak van het bloedvat in beslag neemt, een onafhankelijke voorspeller is van een niet-succesvolle procedure. Bovendien is de stralingsbelasting voor de patiënt en de gebruikte hoeveelheid contrastvloeistof aanzienlijk bij het uitvoeren van een PCI (**Hoofdstuk 13**). Het oordeelkundig gebruik van een CTCA vóór het uitvoeren van een eventuele PCI lijkt daarom zinvol en kan de behandelstrategie bijsturen in het geval dat een PCI wordt ondernomen of kan een argument voor de behandelend arts zijn om te kiezen voor een andere therapeutische optie, met name medicamenteuse therapie of coronaire bypass chirurgie. Magneet navigatie is een nieuwe technologische ontwikkeling die recent binnen het domein van interventiecardiologie werd geïntroduceerd. Met behulp van deze techniek beoogt men bij coronair stenoses met tortueuse bloedvat anatomie of andere complexe coronair pathologie de kansen op succes van de PCI te vergroten. De incorporatie van CT data in de magneet navigatie software biedt de mogelijkheid vóór de procedure een gedetailleerd pad van de te behandelen coronair arterie uit te werken: in combinatie met het magnetisch veld dat rondom de patiënt wordt gecreëerd, wordt het zodoende mogelijk de richting van de draad heel precies in 3 dimensies te sturen(**Hoofdstuk 14**).

Percutane coronaire interventies waarbij gebruik wordt gemaakt van stents is de meest frequent toegepaste vorm van coronaire revascularisatie. Het beschikbaar worden van drug-eluting stents is gepaard gegaan met een significante reductie van het voorkomen van instent restenose (ISR), doch niet tot een volledige eliminatie van dit probleem. Patiënten die

opnieuw klachten ontwikkelen na een eerdere succesvolle PCI vertonen inderdaad soms ISR, doch meer frequent progressie van ziekte in bloedvat segmenten die nog niet werden gestent. Verbeteringen in CT scan technologie en het gebruik van speciale filters en "window settings" hebben de visualisatie van het lumen binnenin de stent progressief beter gemaakt (**Hoofdstuk 15**). Het aantonen van de aanwezigheid van ISR blijft evenwel moeilijk met CTCA als gevolg van de metaal component van de stent die gepaard gaat met artefact vorming, het "blooming effect", waardoor het stent materiaal in belangrijke mate wordt uitvergroot. Het "blooming effect" is een relatief constant fenomeen en bijgevolg minder uitgesproken in stents met een relatief grote diameter (**Hoofdstuk 17**). CTCA kan worden gebruikt voor het uitsluiten van ISR bij patiënten die gestent werden in de hoofdstam (**Hoofdstuk 16**, **Tussenhoofdstuk 5**). Toepassing van CTCA in de dagelijkse praktijk is evenwel enkel mogelijk indien de diagnostische accuraatheid op "patiënt-niveau", waarbij zowel de gestente als niet-gestente bloedvat segmenten worden geïncludeerd, voldoende hoog is. Bij patiënten die opnieuw symptomen vertonen na eerdere implantatie van stents met grote diameter (≥ 3.0 mm) en geëvalueerd worden met een dual-source CT scanner, blijkt CTCA klinisch waardevol te zijn in de patiëntengroep met een negatieve of inconclusieve stress test (**Hoofdstuk 18**).

Conclusies en toekomstperspectief

De huidige 64-slice en dual-source 64-slice CT scanner vertoont een hoge diagnostische performantie en is met name uiterst geschikt voor het uitsluiten van de aanwezigheid van kransslagaderziekte. CTCA kan worden gebruikt als diagnostische modaliteit bij de evaluatie van symptomatische patiënten met een lage-tot-intermediaire vooraf-kans op coronarialijden: een "negatieve" CT scan sluit op betrouwbare wijze coronarialijden uit en doet de noodzaak voor het uitvoeren van een CCA afnemen. CTCA is niet onderhevig aan de 2-dimensionele beperkingen van CCA en is bijgevolg een waardevolle techniek voor de evaluatie van patiënten met coronaire anomaliëen. In hartcatheterisatiecentra met PCI faciliteiten wordt CTCA meer en meer gebruikt voor evaluatie van de bredere groep van patiënten met complexe vormen van coronair lijden: CTCA laat een goede beoordeling toe van patiënten waarbij de initiële angiografische evaluatie suboptimaal was en maakt een nieuwe CCA overbodig. Bij patiënten met CTOs biedt CTCA de mogelijkheid de slaagkans van een PCI op voorhand in te schatten en kan deze informatie zinvol zijn bij de uiteindelijke therapiekeuze. Bij patiënten die voorheen werden gerevasculariseerd biedt CTCA op dit moment enkel een niche applicatie: na bypass chirurgie is CTCA waardevol ter uitsluiting van obstructief vaatlijden in de veneuse en arteriële greffen, de evaluatie van stenotisch vaatlijden in de natieve bloedvaten blijft problematisch. Bij patiënten na PCI is CTCA waardevol voor evaluatie van stents met een relatief grote diameter (≥3.0 mm diameter); kleine stents kunnen niet betrouwbaar worden beoordeeld. De beschikbaarheid van CTCA maakt het noodzakelijk de diagnostische algoritmes die actueel worden gebruikt voor de evaluatie van patiënten met vermoeden van coronaria lijden te herevalueren. De niet-invasieve toegang tot coronair anatomie is nu mogelijk en bekrachtigt het belang van

functionele evaluatie om de meest geschikte therapiekeuze te kunnen maken. Beide benaderingswijzen sluiten elkaar niet uit maar zijn eerder complementair.
Nieuwe ontwikkelingen in CT technologie zullen de klinische toepassingen van CTCA verder verbreden. Uitgesproken calcificaties en een onregelmatig hartritme zijn momenteel een belangrijke beperking voor CTCA en vereisen unieke technische oplossingen die wellicht verscheidene jaren in beslag zullen nemen vooraleer implementatie mogelijk is in de in-vivo setting. De belangrijkste uitdaging op dit moment is de consolidatie en overdracht van de kennis die reeds voorhanden is. Dit zal bijdragen tot een implementatie op bredere schaal van deze nieuwe fascinerende technologie. De data van een aantal lopende multi-center studies zullen aantonen of de resultaten van hoog-performante research centra kunnen worden gereproduceerd. Studies die de kosten-effectiviteit van CTCA beoordelen zijn noodzakelijk om de waarde van CTCA te kunnen vergelijken met andere diagnostische tests. De stralingsbelasting van CTCA is een nadeel maar tegelijkertijd een krachtige impuls die actueel leidt tot de ontwikkeling van protocollen en algoritmes die de stralingsdosis in belangrijke mate reduceren tot op het niveau van CCA. Tot slot dient vermeld te worden dat de snelle ontwikkeling van CTCA heeft kunnen plaats vinden door een succesvolle interactie tussen de deelspecialismen cardiologie en radiologie. Om dit hoge niveau van expertise te kunnen behouden is het essentieel dat de specialisten die zich met deze techniek zullen bezig houden op een goede manier worden opgeleid en zich houden aan de richtlijnen die worden opgesteld door de betreffende beroepsgroepen.

Acknowledgements

Deze thesis zou niet volledig zijn zonder de personen te bedanken die cruciaal geweest zijn om dit project tot een succesvol einde te brengen. Ik richt mij in de eerste plaats tot mijn vrouw, Tine, die gedurende 5 jaar de kracht en het geduld heeft gehad mij te blijven steunen en op eender welk moment de ruimte te geven om zodoende de optimale omstandigheden te creëren voor het schrijven van een manuscript of voorbereiden van een voordracht. Menige weekends ben jij met de kinderen naar België getrokken om mij mijn werk te kunnen laten doen. Steeds was er je luisterend oor en je praktische hulp bij om het even welk probleem. Bovendien maakte je je eigen carrière ondergeschikt aan mijn eigen ambitie. Zonder je onbaatzuchtige houding had ik deze thesis niet rond gekregen.

Onze 2 kinderen, Alexander en Victor, wil ik vermelden voor de vreugde die zij mij iedere dag opnieuw brengen. Lieve jongens, ik ben fier op de eerste plaats jullie papa te zijn!

Mijn papa wil ik als volgende bedanken. Je ambitie en enthousiasme waren voor mij reeds van kinds af aan aanstekelijk en hebben een belangrijke impact gehad op mijn eigen professionele ontwikkeling. An en Frans, mijn schoonouders, wil ik bedanken voor hun levensvisie en fantastische betrokkenheid op velerlei vlak.

In augustus 2003 begon ik in het Thoraxcentrum, Rotterdam, aan dit hoofdstuk in mijn carrière, waarvan dit proefschrift de resultante is. Tijd om terug te blikken op een unieke en fantastische ervaring. In deze paragraaf wil ik van de gelegenheid gebruik maken mijn promotoren, copromotor, opleiders en andere naaste medewerkers die ieder op hun manier hebben bijgedragen tot dit proefschrift te bedanken.

Professor de Feyter, beste Pim, jij verenigt op een unieke manier als wetenschapper en als arts een aantal kwaliteiten die mij zeer bevielen. Zowel in het cathlab als in het geschreven woord ben je steeds in staat de zaken tot hun essentie te herleiden. Je subtiele maar tegelijkertijd doortastende aanpak en gedrevenheid zullen mij steeds bijblijven.

Professor Patrick Serruys, mijn andere promotor en opleider, U heeft mij de mogelijkheden en vrijheid gegeven om de opleiding tot interventiecardioloog te combineren met de wereld van niet-invasieve cardiale beeldvorming. Ik kijk met veel genoegen terug op de vele leermomenten binnen en buiten het cathlab. Bovendien heeft U mij de kans gegeven mezelf waar te maken op het internationale podium. Uw aanbod om aan de universiteit te blijven was voor mij een lastige afweging. Voor mijn familie is mijn huidige keuze evenwel de juiste.

Nico Mollet, mijn copromotor, jij hebt gezorgd voor mijn technische bekwaming op het vlak van de cardiale CT en hebt in belangrijke mate bijgedragen tot een succesvolle afronding van deze thesis. De noodzakelijke basis is gelegd voor een verdere goede samenwerking. Je

recente verhuis naar het uiterste zuiden van het land getuigt van goede smaak: Nederlander van origine maar doordrenkt met een Belgisch parfum.

Dr de Jaegere, beste Peter, jij gaf mij je onvoorwaardelijke steun en was van bij het begin mijn grote supporter. Hartelijk dank. Ik kijk uit naar een verdere samenwerking, zij het in een andere setting. De bergtocht in de Alpen heb je nog van mij te goed.

Eugène McFadden, thank you for being my paranymph, but most of all for the sincere friendship, training in the cathlab and help in reviewing some of my manuscripts.

Professor van der Giessen, beste Wim, ik herinner mij nog goed mijn trainingssessies met jou in het cathlab: doordacht, rustig in alle omstandigheden en steeds voorzien van een vleugje droge humor.

George Sianos, you are an extremely gifted interventional cardiologist who teached me the necessary tips and tricks I could not find in the textbooks. You were right: the moment you don't feel the need to look back anymore in the cathlab, the fellow becomes independent as an operator. Thanks a million and keep in touch.

Evelyn Regar, combining a research career with the tasks of a mother must be extremely difficult. Wish you all the best and try to keep the balance.

Martin van der Ent, jij combineert 2 unieke specialismen die mij nauw aan het hart liggen, interventiecardiologie en intensieve zorgen. Succes met je verdere carrière.

Robert-Jan van Geuns en Eric Duckers, onze min of meer gezamenlijke opleiding in het cathlab was een aangename tijd samen: de drempel om ervaringen uit te wisselen was onder elkaar steeds lager dan aan tafel met de "seniors". Veel succes met jullie nieuwe positie als "senior" in het cathlab.

Professor Gabriel Krestin, als hoofd van de afdeling radiologie wil ik U bedanken voor uw interesse, het faciliteren van mijn werkzaamheden op de afdeling radiologie en het ten dienste stellen van de afdeling grafische vormgeving. Het is een hele eer voor mij U te hebben in de kleine leescommissie. Ook Professor Ton van der Steen en Professor Wiro Niessen wil ik bedanken voor de bereidwilligheid te willen optreden als lid van de kleine leescommissie.

De leden van de grote leescommissie zijn ter gelegenheid van mijn thesisverdediging speciaal uit België afgekomen en wil ik ieder afzonderlijk bedanken. Dr William Wijns, expert in interventiecardiologie en cardiale beeldvorming, het is voor mij een eer dat U mee zetelt in de PhD

commissie. Professor Peter Sinnaeve en Professor Steven Dymarkowski, jaargenoten van mij toen wij nog in Leuven studeerden en nu beiden een belangrijke positie innemend als staflid aan de Katholieke Universiteit Leuven, dank u wel om mijn thesis mee te beoordelen. Ik kon het niet beter treffen twee deskundigen op respectievelijk het vlak van cardiologie en radiologie hier aan tafel te krijgen.

De andere medewerkers van het cathlab wil ik ook hartelijk bedanken voor de steun die ik op velerlei manier mocht ontvangen. Ik hoop dat ik niemand vergeet op te noemen. De verpleging en technici van het cathlab wil ik alle respect toebedelen omwille van hun toewijding en expertise: Marjo, stuwende kracht, organisator en veel flair, Tineke, "mater familias" met een geweldig oog voor detail, Dick, schitterende kerel en vol humor, Nico, steeds goed gezind en een gezonde eetlust, Marianne, enorme interesse en op korte tijd reeds veel expertise, Elza, veel potentie als leidinggevende, Caroline, invoelend en veel inzet bij de organisatie van het cathlab, Kim, nog heel jong maar eveneens enorme inzet en reeds veel expertise, Marieke, veel succes met je nieuwe carrière, Fiona, jammer dat je overgegaan bent naar een ander ziekenhuis, je was steeds aangenaam gezelschap, Jeanine, het voelt goed aan een "oude bekende" van het Thoraxcentrum te hebben in mijn nieuwe werkomgeving, Sandy en Evelyn, twee "diamanten" zowel in het werk als daarbuiten, Karen, een beetje timide maar steeds veel inzet, Dennis, steeds goed gezind en essentieel voor de goede organisatie van het cathlab. De technici van het cathlab: Jurgen, onbaatzuchtig en een geweldige leermeester op het gebied van IVUS, Gio en gedurende een korte periode Emile, ik heb veel opgestoken van jullie technische expertise, Anne-Marie, John en Elco, eveneens veel expertise en veel dank voor de hulp bij het aanleveren van "beeldjes" voor voordrachten en artikels. Max en Maaike, veel succes met jullie nieuwe carrière.

De collega's en medewerkers van de afdelingen cardiologie en cardiochirurgie wil ik eveneens bedanken voor alle geboden kansen. In het bijzonder wil ik vermelden: Professor Maarten Simoons, diensthoofd van de afdeling cardiologie, dank u wel voor de interesse en steun voor het proefschrift. Ron van Domburg en Eric Boersma, dank u wel voor de adviezen op het gebied van statistiek. Nico Bruining, jij bent een enorme bron van kennis op het gebied van medische beeldvorming waar ik veel van heb kunnen gebruik maken, bovendien ben jij steeds in staat op heel korte termijn zaken af te werken. Johannes Schaar, geweldige researcher en essentiële schakel bij het tot stand brengen van de IBIS studie. Paul en Arno, beiden onvermoeibaar bij het in goede banen leiden van de verschillende studies, Paul, bedankt voor de eerste lessen in powerpoint etcetera. Jan Tuin wil ik bedanken voor de fantastische hulp bij het voorbereiden van de posters, bovendien kon ik op die momenten steeds mee genieten van je uitgebreide jazz collectie. Annet Louw, charmante vrouw, dank u wel voor de begeleiding bij de laatste loodjes voor het proefschrift. Maria, Jolanda, Cecile, Maarten en Stijn, dank u wel voor alle praktische steun bij de verschillende studies. Titia, Mieke en Sjaan, het heeft mij even

tijd gekost om jullie mee te krijgen maar de hulp die ik van jullie gekregen heb bij het inplannen van patiënten voor het cathlab en cardiale CT en opvragen van medische gegevens was van goudwaarde. Marijke, Denise en later Jeanette, dank u wel om steeds op korte termijn Professor de Feyter te "strikken" om mijn manuscripten te kunnen bespreken. Anja, op een of andere manier ben jij in staat de agenda van Professor Serruys in goede banen te leiden, ik heb je manier van werken leren appreciëren. Elles en Edith, dank u wel voor de steun zij het meer op de achtergrond. Ellen en Ymtje, de 2 verpleegkundigen van het hartfalen team, wil ik bedanken om buiten hun eigen werkzaamheden mij te willen helpen bij de voorbereiding van een groot aantal patiënten bij de verschillende CT studies.

De IBIS studie was niet mogelijk geweest zonder de input van het core lab, Cardialysis, onder de goede begeleiding van Gerrit-Anne van Es en andere medewerkers. Het was een intensieve maar zeer leerzame periode.

De CT laborantengroep kan ik niet genoeg bedanken. Marcel Dijkshoorn, jij hebt een enorme kennis op het gebied van MSCT waar ik veel van heb opgestoken. Bovendien kon jij steeds mijn klinische vraagstelling omzetten in een technisch goed onderbouwd advies en/of scan protocol. Berend, Marieke en Ronald, bedankt voor jullie inzet en flexibiliteit bij het scannen van de vele "cardiac" patiënten.

Ton Everaers en Eric-Jan Schoonen, jullie bijdrage in dit proefschrift is eveneens essentieel geweest. Dank u wel voor de geboden faciliteiten en vormgeving van het boek. Het is van hoge kwaliteit en beantwoordt volledig aan wat ik ervan verwacht had.

De fellows van het Thoraxcentrum en de afdeling radiologie waarmee ik heb samengewerkt vormen een apart hoofdstuk. Zij zijn de rijkdom van het centrum en een unieke groep van mensen die mijn eigen fellowship een enorme persoonlijke meerwaarde hebben gegeven. Ik wil ze in min of meer chronologische volgorde van commentaar voorzien. Pedro Lemos, een briljant persoon die intellectuele bagage combineert met een enorme werklust. Zijn PhD was van 'outstanding quality', ik heb het voorrecht gehad met hem mijn eerste artikel in Rotterdam te schrijven. Francesco Saia, een vriendelijk persoon met veel flair, slaagde erin in minder dan 2 jaar een PhD rond te krijgen. Akis Arampatzis, de fellow uit Griekenland waarmee ik de kamer deelde op 1200, jij hebt mij in de begin periode van mijn fellowship enorm gesteund met databases en ander computerwerk. De IBIS-3 en IBIS-5 presentaties waren memorabel. Wij delen een gezamenlijke interesse in muziek en wijn, voor beiden moet ik evenwel onderdoen. Best regards to Vicky and the children! Andrew Ong, from Australia, combineert intellect met een nooit eerder geziene kennis van 'faits divers', culturele bagage en beleefdheid. We will keep in touch. Angela Hoye, from the UK, het was niet evident een klinisch fellowship te combineren met een PhD. Jij bracht beide projecten evenwel tot een schitterend einde!

Marco Valgimigli, mijn nieuwe kamergenoot na het vertrek van Akis, eveneens een briljant persoon, de database van patiënten met PCI van de hoofdstam had niet in betere handen kunnen terechtkomen. I wish you all the best in Italy. Gaston Rodriguez Granillo, from Argentina, ik hield van je enthousiasme en openheid. I wish you all the best with your future career. Sophia, jij was één van de eerste fellows die ik zelf mee mocht opleiden in het cathlab. Ik hoop dat je de positie die je beoogde in Athene hebt kunnen verkrijgen. Hector Garcia, aangename en zeer behulpzame collega uit Mexico, de gezamenlijke studie over de waarde van CT bij patiënten met een CTO heeft veel tijd gekost maar was de moeite waard. Succes met de laatste loodjes voor je eigen PhD! Joost Daemen, enorm gedreven, jij hebt op korte tijd een prachtig PhD geproduceerd. Jiro, Keichii, Shuzou en Masato, de 4 opeenvolgende fellows uit Japan, jullie vriendelijkheid en werkijver is bij momenten onnavolgbaar. All the best with your future careers. Steve Ramcharitar, the guy from the UK, we wrote some nice papers together. Above all, I liked your company inside and outside the cathlab and had the opportunity to meet your wonderful wife from Belgium, Véronique. All the best back in London and keep in touch. Neville Kukreja en Anne-Louise Gaster, wishing you all the best in the future.

Ook de afdeling radiologie kenmerkt zich door een ambitieuse groep van fellows. Koen Nieman, ondertussen teruggekeerd als staflid cardiologie, jij bent één van de pioniers van "multislice cardiac CT" en hebt veel troeven in handen om het baanbrekende werk dat tot op heden werd verricht met blijvend succes voort te zetten. Filippo Cademartiri, beheerst volledig het domein van cardiovasculaire beeldvorming. All the best with your own cardiac CT department in Parma. Bob Meijboom, mijn "sparring partner" ten tijde van de 64-slice CT, wij hebben een aantal zeer succesvolle projecten kunnen uitwerken, ik heb het meest genoten van de "FFR-paper". Succes met je opleiding tot cardioloog. Annick Weustink, de discussies met jou waren steeds pittig en boeiend. Je bent een vrouw met karakter, daar hou ik van. Bedankt voor je input en hulp, ook buiten het werk, en succes met de laatste loodjes voor je eigen proefschrift. Francesca Pugliese, dedicated person and fine colleague, I appreciate the work we did together that resulted in a few successful papers. I hope you soon find the position you are looking for in the UK. Niels van Pelt, collega van Nieuw-Zeeland, we had more or less the same interests in cardiology, in particular the clinical part of it, it is a pity you left already within one year. Tot wederhoren. Timo Baks, plezante collega, de cardiale MRI was jouw domein en om deze reden was er weinig tijd voor interactie. Geniet van je opleidingstijd als cardioloog. Sharon Kirschbaum, eveneens een heel aangename en kleurrijke collega, ik geloof in jouw toekomst als expert cardiale beeldvorming. Eleni Vourvouri, echtgenote van George Sianos, charmant en zeer gedreven. All the best with your career and the family.

Mijn collega's van de maatschap cardiologie van het Maasstad ziekenhuis, wil ik hartelijk bedanken voor de ruimte die ik gekregen heb om de laatste hoofdstukken van mijn thesis te kunnen voltooien. Verder kijk ik uit naar een succesvolle uitwerking van het cardiale CT project

met de collega's van de afdeling radiologie, naar analogie met het model dat in het Erasmus MC wordt gebruikt.

De collega's van mijn vrouw in het Oogziekenhuis Rotterdam wil ik bedanken voor de faciliteiten die ik er mocht gebruiken om te schrijven: wat een fantastische werkplek!

Tot slot wil ik mij richten tot de vrienden en kennissen uit de naaste omgeving. Carolien en Olivier, vrienden van het eerste uur, ik ben er eindelijk klaar mee met het "boek". Dank u wel voor het geduld en blijvende support. Olivier, bedankt om mij te ondersteunen als paranymph. Valentine en Guy, Ida en Marie, ik kan jullie niet genoeg bedanken steeds klaar te staan voor de personen die mij het meest dierbaar zijn, mijn vrouw en 2 kinderen.

List of publications

ARTICLES IN PEER-REVIEWED JOURNALS

1. **Van Mieghem CAG**, Dens J, Herregods MC, Desmet W. Left ventricular wall hematoma complicating PCI using IIb/IIIa receptor antagonists. J Interv Cardiol 2003; 16: 381-384.
2. **Van Mieghem CAG**, Sabbe M, Knockaert D. The clinical value of the electrocardiogram in non-cardiac conditions. Chest 2004; 125: 1561-1576. Review article.
3. Lemos PA, **Van Mieghem CAG**, Arampatzis CA, Hoye A, Ong AT, McFadden E, Sianos G, van der Giessen WJ, de Feyter PJ, van Domburg RT, Serruys PW. Post-sirolimus-eluting stent restenosis treated with repeat percutaneous intervention: late angiographic and clinical outcomes. Circulation 2004; 109: 2500-2502.
4. Valgimigli M, **Van Mieghem CAG**, Ong AT, Aoki J, Granillo GA, McFadden EP, Kappetein AP, de Feyter PJ, Smits PC, Regar E, van der Giessen WJ, Sianos G, de Jaegere P,van Domburg RT, Serruys PW. Short- and Long-term Clinical Outcome after Drug-Eluting Stent Implantation for the Percutaneous Treatment of Left Main Coronary Artery Disease: insights from the Rapamycin-Eluting and Taxus Stent Evaluated At Rotterdam Cadiology Hospital registries (RESEARCH and T-SEARCH). Circulation 2005; 111: 1383-9.
5. Agostoni P, Valgimigli M, **Van Mieghem CAG**, Rodriguez Granillo GA, Aoki J, Ong AT, Tsuchida K, McFadden EP, Ligthart JM, Smits PC, de Jaegere P, Sianos G, van der Giessen WJ, de Feyter P, Serruys PW. Comparison of early outcome of percutaneous coronary intervention for unprotected left main coronary artery disease in the drug-eluting stent era with versus without intravascular ultrasonic guidance. Am J Cardiol 2005; 95: 644-647.
6. Ong AT, Hoye A, Aoki J, **Van Mieghem CAG**, Rodriguez-Granillo GA, Sonnenschein K, Regar E, McFadden EP, Sianos G, van der Giessen WJ, de Jaegere PP, de Feyter P, van Domburg RT, Serruys PW. Thirty-day incidence and six-month clinical outcome of thrombotic stent occlusion after bare-metal, sirolimus, or paclitaxel stent implantation. J Am Coll Cardiol 2005; 45: 947-53.
7. Ong AT, Serruys PW, Aoki J, Hoye A, **Van Mieghem CAG**, Rodriguez-Granillo GA, Valgimigli M, Sonnenschein K, Regar E, van der Ent M, de Jaegere PP, McFadden EP, Sianos G, van der Giessen WJ, de Feyter P, van Domburg RT. The unrestricted use of paclitaxel- versus sirolimus-eluting stents for coronary artery disease in an unselected population: one-year results of the Taxus-Stent Evaluated at Rotterdam Cardiology Hospital (T-SEARCH) registry. J Am Coll Cardiol 2005; 45:1135-41.
8. Hofma SH, Ong AT, Aoki J, **Van Mieghem CAG**, Rodriguez-Granillo GA, Valgimigli M, Regar E, de Jaegere PP, McFadden EP, Sianos G, van der Giessen WJ, de Feyter PJ, van Domburg RT, Serruys PW. One-year clinical follow-up of paclitaxel-eluting stents for acute myocardial infarction compared to sirolimus-eluting stents. Heart 2005; 91:1176-80.

9. Hoye A, **Van Mieghem CAG**, Ong ATL, Aoki J, Rodriguez-Granillo GA, Valgimigli M, Tsuchida K, Sianos G, McFadden EP, van der Giessen WJ, de Feyter PJ, van Domburg RT, Serruys PW. Treatment of de novo bifurcation lesions: comparison of Sirolimus- and Paclitaxel-eluting stents. EuroInterv 2005; 1:24-30.
10. **Van Mieghem CAG**, Bruining N, Schaar J, McFadden E, Mollet N, Cademartiri F, Mastik F, Ligthart JMR, Rodriguez-Granillo GA, Valgimigli M, Sianos G, van der Giessen WJ, Backx B, Morel MA, van Es GA, Sawyer JD, Kaplow J, Zalewski A, van der Steen A, de Feyter P, Serruys P. Rationale and methods of the Integrated Biomarker and Imaging Study (IBIS): Combining Invasive and Non-Invasive Imaging with Biomarkers to Detect Subclinical Atherosclerosis and Assess Coronary Lesion Biology. Int J Cardiovasc Imaging 2005; 21:425 441.
11. **Van Mieghem CAG**, McFadden E, de Feyter P, Bruining N, Schaar J, Mollet N, Cademartiri F, Goedhart D, de Winter S, Rodriguez-Granillo GA, Valgimigli M, Mastik F, van der Steen A, van der Giessen WJ, Sianos G, Backx B, Morel MA, van Es GA, Kaplow J, Zalewski A, Serruys PW. Non-invasive Detection of Subclinical Coronary Atherosclerosis Coupled With Assessment, Using Novel Invasive Imaging Modalities, of Changes in Plaque Characteristics Over Time: The IBIS Study (Integrated Biomarker and Imaging Study). J Am Coll Cardiol. 2006; 47:1134-42.
12. Mollet NR, Cademartiri F, **Van Mieghem CAG**, Runza G, Mc Fadden EP, Serruys PW, Krestin GP, de Feyter PJ.High-resolution Spiral CT Coronary Angiography in Patients Referred for Diagnostic Conventional Coronary Angiography. Circulation 2005; 112:2318-23.
13. Rodriguez-Granillo GA, Valgimigli M, Garcia-Garcia HM, Ong AT, Aoki J, **Van Mieghem CAG**, Tsuchida K, Sianos G, McFadden E, van der Giessen WJ, van Domburg RT, de Feyter P, Serruys PW. One-Year Clinical Outcome after Coronary Stenting of Very Small vessels Using 2.25 mm Sirolimus- and Paclitaxel-Eluting Stents: a comparison between the RESEARCH and T-SEARCH Registries. J. Invasive Cardiol. 2005;17:409-12.
14. Aoki J, Ong AT, Rodriguez-Granillo GA, **Van Mieghem CAG**, Daemen J, Sonnenschein K, McFadden E, Sianos G, van der Giessen W, de Feyter P, van Domburg R, Serruys PW.The efficacy of sirolimus-eluting stents versus bare metal stents for diabetic patients undergoing elective percutaneous coronary intervention. J Invasive Cardiol. 2005; 17: 344-348.
15. Tsuchida K, Ong AT, Aoki J, **Van Mieghem CAG**, Rodriguez-Granillo GA, Valgimigli M, Sianos G, Regar E, McFadden EP, van der Giessen WJ, de Feyter PJ, de Jaegere PP, van Domburg RT, Serruys PW.Immediate and one-year outcome of percutaneous intervention of saphenous vein graft disease with Paclitaxel-eluting stents. Am J Cardiol.2005;96:395-8.

16. Ong AT, Aoki J, **Van Mieghem CAG**, Rodriguez-Granillo GA, Valgimigli M, Tsuchida K, Sonnenschein K, Regar E, van der Giessen WJ, de Jaegere PP, Sianos G, McFadden EP, de Feyter P, van Domburg RT, Serruys PW. Comparison of Short- (One Month) and Long- (Twelve Months) Term Outcomes of Sirolimus- Versus Paclitaxel-Eluting Stents in 293 Consecutive Patients With Diabetes Mellitus (from the RESEARCH and T-SEARCH Registries).Am J Cardiol. 2005;96:358-62.
17. Rodriguez-Granillo GA, Aoki J, Ong AT, Valgimigli M, **Van Mieghem CAG**, Regar E, McFadden E, de Feyter P, Serruys PW. Methodological considerations and approach to cross-technique comparisons using in vivo coronary plaque characterization based on intravascular ultrasound radiofrequency data analysis: insights from the Integrated Biomarker and Imaging Study (IBIS). Int J Cardiovasc Intervent. 2005;7:52-8.
18. Hoye A, **Van Mieghem CAG**, Ong AT, Aoki J, Rodriguez-Granillo GA, Valgimigli M, Tsuchida K, Sianos G, McFadden EP, van der Giessen WJ, de Feyter PJ, van Domburg RT, Serruys PW. Percutaneous therapy of bifurcation lesions with drug-eluting stent implantation: the Culotte technique revisited. Int J Cardiovasc Intervent. 2005;7(1):36-40.
19. Rodriguez-Granillo GA, Serruys PW, McFadden EP, **Van Mieghem CAG**, Goedhart D, Bruining N, Sianos G, van der Steen A, Margolis P, Vince DG, Kaplow J, Zalewski A, de Feyter P. First in man prospective evaluation of temporal changes in coronary plaque composition by in vivo intravascular ultrasound radiofrequency data analysis: an integrated biomarker and imaging study (IBIS) substudy. EuroInterv. 2005; 3: 282-288.
20. Rodriguez-Granillo GA, Serruys PW, Garcia-Garcia HM, Aoki J, Valgimigli M, **Van Mieghem CAG**, McFadden E, de Jaegere PP, de Feyter P. Coronary artery remodelling is related to plaque composition. Heart 2006; 92:388-91.
21. **Van Mieghem CAG**, Ligthart JMR, Cademartiri F. Spontaneous dissection of the left main coronary artery in a patient with Osler-Weber-Rendu disease (Images in Cardiology). Heart 2005; 92: 394.
22. Rodriguez-Granillo GA, Valgimigli M, Ong AT, Aoki J, **Van Mieghem CAG**, Hoye A, Tsuchida K, McFadden E, de Feyter P, Serruys PW.Paclitaxel eluting stents for the treatment of angiographically non-significant atherosclerotic lesions. Int J Cardiovasc Intervent 2005;7:68-71.
23. Hoye A, Ong ATL, Aoki J, **Van Mieghem CAG**, Rodriguez-Granillo GA, Valgimigli M, Sianos G, van der Giessen WJ, de Feyter PJ, van Domburg RT, Serruys PW. Drug-eluting stent implantation for chronic total occlusions: comparison between the sirolimus- and paclitaxel-eluting stent. EuroInterv 2005; 1:193-197.
24. Aoki J, Ong AT, Rodriguez-Granillo GA, McFadden EP, **Van Mieghem CAG**, Valgimigli M, Tsuchida K, Sianos G, Regar E, de Jaegere PP, van der Giessen WJ, de Feyter P, van Domburg RT, Serruys PW. "Full metal jacket" (stented length ≥ 64 mm) using drug-eluting stents for de novo coronary artery lesions. Am Heart J. 2005; 150:994-999.

25. Pugliese F, Mollet NR, Runza G, **Van Mieghem CAG**, Meijboom WB, Malagutti P, Baks T, Krestin GP, de Feyter PJ, Cademartiri F. Diagnostic accuracy of non-invasive 64-slice CT coronary angiography in patients with stable angina pectoris. Eur Radiol 2006;16:575-82.
26. Rodriguez-Granillo GA, McFadden EP, Aoki J, **Van Mieghem CAG**, Regar E, Bruining N, Serruys PW. In vivo variability in quantitative coronary ultrasound and tissue characterization measurements with mechanical and phased-array catheters. Int J Cardiovasc Imaging 2006; 22:47-53.
27. Valgimigli M, Malagutti P, Aoki J, Garcia-Garcia HM, Rodriguez Granillo GA, McFadden EP, **Van Mieghem CAG**, Ligthart JM, Ong AT, Sianos G, Regar E, van Domburg RT, Kappetein AP, de Feyter PJ, Smits PC, van der Giessen WJ, de Jaegere P, Serruys PW. Sirolimus-eluting versus paclitaxel-eluting stent implantation for the percutaneous treatment of left main coronary artery disease: a combined RESEARCH and T-SEARCH long-term analysis. J Am Coll Cardiol 2006; 47:507-14.
28. Valgimigli M, Malagutti P, **Van Mieghem CAG**, Vaina S, Ligthart JM, Sianos G, Serruys PW. Persistence of neointimal growth 12 months after intervention and occurrence of delayed restenosis in patients with left main coronary artery disease treated with drug-eluting stents. J Am Coll Cardiol 2006; 47:1491-4.
29. Rodriguez-Granillo GA, McFadden EP, Valgimigli M, **Van Mieghem CAG**, Regar E, de Feyter PJ, Serruys PW. Coronary plaque composition of nonculprit lesions, assessed by in vivo intracoronary ultrasound radio frequency data analysis, is related to clinical presentation. Am Heart J. 2006; 151:1020-24.
30. Hoye A, Iakovou I, Ge L, **Van Mieghem CAG**, Ong AT, Cosgrave J, Sangiorgi GM, Airoldi F, Montorfano M, Michev I, Chieffo A, Carlino M, Corvaja N, Aoki J, , Rodriguez-Granillo GA, Valgimigli M, Sianos G, van der Giessen WJ, de Feyter PJ, van Domburg RT, Serruys PW, Colombo A. Long-term outcomes after stenting of bifurcation lesions with the "crush" technique: predictors of an adverse outcome. J Am Coll Cardiol 2006;47:1949-58.
31. Pugliese F, Cademartiri F, **Van Mieghem CAG**, Meijboom WB, Malagutti P, Mollet NR, Martinoli C, de Feyter PJ, Krestin GP. Multidetector CT for visualization of coronary stents. Radiographics 2006; 26:887-904.
32. **Van Mieghem CAG**, Cademartiri F, Mollet NR, Malagutti P, Valgimigli M, McFadden EP, Ligthart JMR, Runza G, Bruining N, Smits PC, Regar E, van der Giessen WJ, Sianos G, van Domburg RT, de Jaegere PPT, Krestin GP, Serruys PW, de Feyter P. Multislice Spiral Computed Tomography for the Evaluation of Stent Patency after Left Main Coronary Artery Stenting: a Comparison with Conventional Coronary Angiography and Intravascular Ultrasound. Circulation 2006; 114:645-53.

33. Rodriguez-Granillo GA, Garcia-Garcia HM, Valgimigli M, Vaina S, **Van Mieghem CAG**, Regar E, de Jaegere P, van der Ent M, van Geuns RJ, de Feyter P, Serruys PW. Global characterization of coronary plaque rupture phenotype using 3-vessel intravascular ultrasound radiofrequency data analysis. Eur Heart J 2006; 27: 1921-7.
34. Meijboom WB, Mollet NR, **Van Mieghem CAG**, Kluin J, Weustink AC, Pugliese F, Vourvouri E, Cademartiri F, Bogers AJJC, Krestin GP, de Feyter PJ. Preoperative computed tomography coronary angiography to detect significant coronary artery disease in patients referred for cardiac valve surgery. J Am Coll Cardiol 2006; 48:1658–65.
35. Malagutti P, Nieman K, Meijboom WB, **Van Mieghem CAG**, Pugliese F, Cademartiri F, Mollet NR, Boersma E, de Jaegere PP, de Feyter PJ. Use of 64-slice CT in symptomatic patients after coronary bypass surgery: evaluation of grafts and coronary arteries. Eur Heart J 2006; 28:1879-85.
36. **Van Mieghem CAG**, Van der Ent M, de Feyter PJ. Percutaneous coronary intervention for chronic total occlusions: value of preprocedural MSCT guidance (Images in Cardiology). Heart 2007; 93:1492.
37. **Van Mieghem CAG**, Sianos G, Meijboom B, Vourvouri E, Serruys PW, de Feyter PJ. Reliable angiographic evaluation by 64-slice computed tomography after trifurcation stenting of the left main coronary artery. Image in cardiology. EuroInterv 2006; 1: 482-483.
38. Papafaklis MI, Sianos G, Cost B, Vaina S, Manginas A, Dardas PS, Tsikaderis D, **Van Mieghem CAG**, Michalis LK, Serruys PW. Clinical and angiographic follow-up after overlapping implantation of polytetrafluoroethylene covered stents with drug eluting stents. EuroInterv 2006; 2: 218-223.
39. Sianos G, Papafaklis MI, Vaina S, Daemen J, **Van Mieghem CAG**, Van Domburg RT, Michalis LK, de Jaegere P, Serruys PW. Rheolytic thrombectomy in patients with ST-elevation myocardial infarction and large thrombus burden: the Thoraxcenter experience. J Invasive Cardiol 2006;18 Suppl C:3C-7C.
40. Daemen J; **Van Mieghem CAG**. Twenty years of stenting at the Thoraxcenter: a patient's perspective. EuroInterv 2006; 2: 399-401.
41. Patterson MS, Schotten J, **Van Mieghem CAG**, Kiemeneij F, Serruys PW. Magnetic navigation in percutaneous coronary intervention. J Interv Cardiol 2006; 19: 558-565. Review.
42. Meijboom WB, Mollet NR, **Van Mieghem CAG**, Weustink AC, Pugliese F, van Pelt N, Cademartiri F, Vourvouri E, de Jaegere P, Krestin GP, de Feyter PJ. 64-slice computed tomography coronary angiography in patients with non-ST elevation acute coronary syndrome. Heart 2007; 93:1386-92.
43. Mollet NR, Cademartiri F, **Van Mieghem CAG**, Meijboom B, Pugliese F, Runza G, Baks T, Dikkeboer J, Mc Fadden EP, Freericks MP, Kerker JP, Zoet SK, Boersma E, Krestin GP, de Feyter PJ. Adjunctive value of CT coronary angiography in the diagnostic work-up of patients with typical angina pectoris. Eur Heart J 2007; 28:1872-8.

44. **Van Mieghem CAG**, Thury A, Meijboom WB, Cademartiri F, Mollet NR, Weustink AC, Sianos G, de Jaegere PPT, Serruys PW, de Feyter PJ. Detection and characterization of coronary bifurcation lesions with 64-slice computed tomography coronary angiography. Eur Heart J 2007; 28:1968-76.
45. Sianos G, Papafaklis MI, Daemen J, Vaina S, **Van Mieghem CAG**, Van Domburg RT, Michalis LK, Serruys PW. Angiographic stent thrombosis after routine use of drug-eluting stents in ST-segment elevation myocardial infarction: the importance of thrombus burden. J Am Coll Cardiol 2007; 50:573-83.
46. Weustink AC, Meijboom WB, Mollet NR, Otsuka M, Pugliese F, **Van Mieghem CAG**, Malago R, van Pelt N, Dijkshoorn ML, Cademartiri F, Krestin GP, de Feyter PJ. Reliable high-speed coronary computed tomography in symptomatic patients. J Am Coll Cardiol 2007; 50:786-94.
47. García-García HM, Kukreja N, Daemen J, Tanimoto S, **Van Mieghem CAG**, Gonzalo N, van Weenen S, van der Ent M, Sianos G, de Feyter P, Serruys PW. Contemporary Treatment of Patients with Chronic Total Occlusion: Critical Appraisal of Different State-of-the-art Techniques and Devices. EuroInterv 2007; 3: 188-96.
48. de Feyter PJ, Meijboom WB, Weustink A, **Van Mieghem CAG**, Mollet NR, Vourvouri E, Nieman K, Cademartiri F. Spiral multislice computed tomography coronary angiography: a current status report. Clin Cardiol. 2007; 30:437-42.
49. Pugliese F, Weustink AC, **Van Mieghem CAG**, Alberghina F, Otsuka M, Meijboom WB, Van Pelt N, Mollet NR, Cademartiri F, Krestin GP, Hunink MG, de Feyter PJ. Dual-source coronary computed tomography angiography for detecting in-stent restenosis. Heart 2008; 94: 848-54.
50. Meijboom WB, **Van Mieghem CAG**, Mollet NR, Pugliese F, Weustink AC, Van Pelt N, Cademartiri F, Nieman K, Boersma E, de Jaegere P, Krestin GP, de Feyter PJ. 64-slice computed tomography coronary angiography in patients with high, intermediate or low pre-test probability of significant coronary artery disease. J Am Coll Cardiol 2007; 50:1469-75.
51. García-García HM, Daemen J, Kukreja N, Tanimoto S, **Van Mieghem CAG**, van der Ent M, van Domburg RT, Serruys PW. Three-year clinical outcomes after coronary stenting of chronic total occlusion using sirolimus-eluting stents: Insights from the rapamycin-eluting stent evaluated at rotterdam cardiology hospital-(RESEARCH) registry. Catheter Cardiovasc Interv 2007; 70:635-639
52. Meijboom WB, Weustink AC, Pugliese F, **Van Mieghem CAG**, Mollet NR, Van Pelt N, Cademartiri F, Nieman K, Vourvouri E, Regar E, Krestin GP, de Feyter PJ. Comparison of diagnostic accuracy of 64-slice computed tomography coronary angiography in women versus men with angina pectoris. Am J Cardiol. 2007; 15:100:1532-1537.

53. Pugliese F, Mollet NR, Hunink MG, Cademartiri F, Nieman K, van Domburg RT, Meijboom WB, **Van Mieghem CAG**, Weustink AC, Dijkshoorn ML, de Feyter PJ, Krestin GP. Diagnostic performance of coronary CT angiography by using different generations of multisection scanners: single-center experience. Radiology 2008; 246: 384-93.
54. **Van Mieghem CAG**, Ramcharitar S, Barlis P, Oosterhuis W, Kik C, de Feyter P, Serruys P. Myocardial infarction in a patient with sickle cell trait. Treatment dilemmas and imaging findings at follow-up. EuroInterv 2008; 3: 627-634.
55. Ramcharitar S, Patterson MS, van Geuns RJ, **Van Mieghem CAG**, Serruys PW. Technology Insight: magnetic navigation in coronary interventions. Nat Clin Pract Cardiovasc Med 2008;5:148-56.
56. de Visser RN, **Van Mieghem CAG**, van Pelt NC, Weustink AC, Kerker JP, Galema TW. Papillary fibroelastoma of the aortic valve and coronary artery disease visualised by 64-slice CT. Nat Clin Pract Cardiovasc Med 2008; 5: 350-3.
57. Meijboom WB, **Van Mieghem CAG**, van Pelt N, Weustink A, Pugliese F, Mollet NR, Boersma E, Regar E, van Geuns RJ, de Jaegere PJ, Serruys PW, Krestin GP, de Feyter PJ. Comprehensive assessment of coronary artery stenoses: computed tomography coronary angiography versus conventional coronary angiography and correlation with fractional flow reserve in patients with stable angina. J Am Coll Cardiol 2008; 52: 636-43.
58. Bruining N, Tanimoto S, Otsuka M, Weustink A, Ligthart J, de Winter S, **Van Mieghem CAG**, Nieman K, de Feyter PJ, Serruys PW. Quantitative multi-modality imaging analysis of a bioabsorbable poly-L-lactic acid stent design in the acute phase: a comparison between 2- and 3D-QCA, QCU and QMsCT-CA. EuroInterv 2008; 4: 285-291.

BOOK CHAPTERS:

1. **Van Mieghem CAG**, Mollet NR, de Feyter PJ. OCT plaque characterization- comparison to multislice computed tomography. In: Optical Coherence Tomography in Cardiovascular Reasearch. Editors- Evelyn Regar, Ton G van Leeuwen, Patrick W Serruys. ISBN: 1841846112. Informa Healthcare, 2007.
2. **Van Mieghem CAG**. CT assessment of coronary stents. In: Computed Tomography of the Coronary Arteries, Second Edition. Editors- Pim J de Feyter and Gabriel P Krestin. ISBN: 9781841846576. Informa Healthcare, 2008.
3. **Van Mieghem CAG**. CT pre-PCI assessment (chronic total occlusions, magnet navigation). In: Computed Tomography of the Coronary Arteries, Second Edition. Editors- Pim J de Feyter and Gabriel P Krestin. ISBN: 9781841846576. Informa Healthcare, 2008.

ABSTRACT PRESENTATIONS:

1. Ong ATL, Lemos PA, Hoye A, Arampatzis CA, Saia F, Aoki J, **Van Mieghem CAG**, Hofma SH, Smits PC, van der Giessen WJ, Sianos G, McFadden E, de Feyter PJ, Serruys PW Safety and feasibility of paclitaxel-eluting stents in the treatment of ST-elevation acute myocardial infarction. Presented at the American College of Cardiology- 53rd Annual Scientific Sessions, 2004, New Orleans, USA.
2. Hoye A, Lemos PA, Tanabe K, Arampatzis C, Saia F, Degertekin M, Ong ATL, **Van Mieghem CAG**, Hofma SH, Sianos G, Smits PC, van der Giessen W, McFadden E, de Feyter PJ, Serruys PW. Low repeat revascularization rates following drug-eluting stent implantation in de novo bifurcation lesions. Presented at the American College of Cardiology- 53rd Annual Scientific Sessions, 2004, New Orleans, USA.
3. Ong ATL, Lemos PA, Hoye A, Arampatzis CA, Saia F, Aoki J, **Van Mieghem CAG**, Hofma SH, Smits PC, van der Giessen WJ, Sianos G, McFadden E, de Feyter PJ, Serruys PW. Comparative incidence of angiographically proven early stent thrombosis in unselected sirolimus- and paclitaxel-eluting stent populations. Presented at the American College of Cardiology- 53rd Annual Scientific Sessions, 2004, New Orleans, USA.
4. Hoye A, Ong ATL, Lemos P, Arampatzis C, Saia F, Aoki J, **Van Mieghem CAG**, Rodriguez-Granillo G, van der Giessen G, Sianos G, Hofma S, McFadden E, de Feyter PJ, Serruys PW. Incidence of angiographically proven subacute stent thrombosis in 1750 patients treated with drug-eluting stents. Presented at the British cardiac society, 2004, United Kingdom.
5. Ong ATL, Hoye A, Aoki J, **Van Mieghem CAG**, Rodriguez-Granillo G, Smits PC, van der Giessen WJ, de Feyter P, McFadden E, Serruys PW. Safety and feasibility of paclitaxel-eluting stents in the treatment of ST-elevation acute myocardial infarction. Presented at the 52nd annual scientific meeting of the cardiac society of Australia and New Zealand, 2004.
6. Ong ATL, Hoye A, Aoki J, **Van Mieghem CAG**, Rodriguez-Granillo G, Lemos PA, van der Giessen WJ, de Feyter P, McFadden E, Serruys PW. Comparative incidence of angiographically proven early stent thrombosis in unselected sirolimus- and paclitaxel-eluting stent populations. Presented at the 52nd annual scientific meeting of the cardiac society of Australia and New Zealand, 2004.
7. Ong ATL, Hoye A, Aoki J, **Van Mieghem CAG**, Rodriguez-Granillo G, van der Giessen WJ, de Feyter P, McFadden EP, Serruys PW. Unrestricted "real-world" paclitaxel-eluting stent implantation in a consecutive series of patients. Insights from the Taxus-Stent Evaluated At Rotterdam Cardiology Hospital (T-SEARCH) registry. Presented at the 52nd annual scientific meeting of the cardiac society of Australia and New Zealand, 2004.

8. **Van Mieghem CAG**, McFadden E, de Feyter P, Serruys P, Schaar J, Bruining N, Disco C, de Winter S, Mollet N, Cademartiri F, Rodriguez-Granillo G, Mastik F, van der Steen A, van der Giessen W, Sianos G, Backx B, Morel MA, van Es GA, Sawyer J, Kaplow J, Zalewski A. The IBIS-study: invasive and non-invasive investigations in high-risk coronary lesions. Presented at the European Society of Cardiology, 2004, Munich, Germany.
9. Aoki J, Ong AT, Hoye A, **Van Mieghem CAG**, Rodriguez-Granillo GA, Valgimigli M, Tsuchida K, Sonnenschein K, Regar E, van der Giessen WJ, de Jaegere P, Sianos G, McFadden EP, de Feyter PJ, van Domburg RT, Serruys PW. Comparison of unrestricted utilization of paclitaxel and sirolimus eluting stents in consecutive unselected diabetic patients. Presented at the European Society of Cardiology, 2004, Munich, Germany.
10. Ong ATL, Hoye A, Aoki J, **Van Mieghem CAG**, Rodriguez-Granillo G, Lemos PA, van Domburg RT, Serruys PW. Pacitaxel-eluting stent implantation in an unselected consecutive cohort of patients with de novo lesions. Medium term results from the Taxus-Stent Evaluated At Rotterdam Cardiology Hospital (T-SEARCH) registry. Presented at the European Society of Cardiology, 2004, Munich, Germany.
11. Hoye A, **Van Mieghem CAG**, Ong ATL, Aoki J, Valgimigli M, Rodriguez-Granillo G, Sianos G, McFadden E, van der Giessen WJ, de Feyter PJ, van Domburg RT, Serruys PW. Clinical and angiographic outcomes following "crush" bifurcation stenting with drug-eluting stents. Presented at the American Heart Association 2004, Annual Scientific sessions, New Orleans, USA.
12. Aoki J, Lemos PA, Hoye A, Ong AT, Rodriguez-Granillo G, **Van Mieghem CAG**, Valgimigli M, van Domburg RT, de Feyter PJ, Serruys PW. The efficacy of sirolimus-eluting stents versus bare metal stents for diabetic patients undergoing percutaneous coronary intervention. Presented at the American Heart Association 2004, Annual Scientific sessions, New Orleans, USA.
13. Hoye A, **Van Mieghem CAG**, Ong ATL, Aoki J, Rodriguez-Granillo GA, Valgimigli M, Tsuchida K, Sianos G, McFadden EP, van der Giessen WJ, de Feyter PJ, van Domburg RT, Serruys PW. Percutaneous coronary intervention of de novo bifurcation lesions: therapy with sirolimus-eluting stents is associated with fewer major adverse cardiac events and target lesion revascularizations compared with paclitaxel-eluting stent implantation. Presented at the American College of Cardiology- 54rd Annual Scientific Sessions, 2005, Orlando, USA.
14. Mollet NR, Cademartiri F, **Van Mieghem CAG**, Runza G, Baks T, Mc Fadden EP, Krestin GP, de Feyter PJ. Noninvasive 64-slice multidetector CT coronary angiography of the entire coronary tree in patients with stable angina pectoris or an acute coronary syndrome. Presented at the American College of Cardiology- 54rd Annual Scientific Sessions, 2005, Orlando, USA.

15. **Van Mieghem CAG**, McFadden E, de Feyter P, Serruys P, Schaar J, Bruining N, Disco C, de Winter S, Mollet N, Cademartiri F, Rodriguez-Granillo G, Mastik F, van der Steen A, van der Giessen W, Sianos G, Backx B, Morel MA, van Es GA, Sawyer J, Kaplow J, Zalewski A. Integrating Biomarkers with invasive and non-invasive coronary plaque imaging: the IBIS study (Integrated biomarker and imaging study). Presented at the American College of Cardiology- 54rd Annual Scientific Sessions, 2005, Orlando, USA.
16. **Van Mieghem CAG**, Cademartiri F, Mollet NR, Malagutti P, Valgimigli M, McFadden EP, Ligthart JMR, Runza G, Krestin GP, Serruys PW, de Feyter P. Comparison of Multislice Computed Tomography with Conventional Coronary Angiography for the Detection of In-stent Restenosis in the Left Main Coronary Artery. Presented at the American College of Cardiology- 54rd Annual Scientific Sessions, 2005, Orlando, USA.
17. Aoki J, Ong ATL, Rodriguez-Granillo GA, **Van Mieghem CAG**, Valgimigli M, K Tsuchida, Hector Garcia, Eugene McFadden, de Feyter PJ, van Domburg RT, Serruys PW. Full metal jacket for de novo coronary artery lesions in the drug-eluting stent era. Presented at the American College of Cardiology- 54rd Annual Scientific Sessions, 2005, Orlando, USA.
18. Regar E, Schaar J, Mc Fadden E, van der Giessen W, Rodriguez-Granillo GA, **Van Mieghem CAG**, de Feyter P, Serruys PW. Clinical application of real-time, high-resolution optical coherence tomography. Can we detect features of vulnerable plaque? Presented at the German Society of Cardiology, 2005, Mannheim, Germany.
19. Regar E, Ong ATL, Hoye A, Aoki J, **Van Mieghem CAG**, Rodriguez-Granillo GA, Sonnenschein K, Mc Fadden EP, Sianos G, van der Giessen WJ, de Jaegere PP, de Feyter P, van Domburg RT, Serruys PW. 30-day incidence of thrombotic stent occlusion following bare metal, sirolimus or paclitaxel stent implantation. Presented at the German Society of Cardiology, 2005, Mannheim, Germany.
20. Ong ATL, Aoki J, **Van Mieghem CAG**, Rodriguez-Granillo GA, Valgimigli M, Tsuchida K, Garcia-Garcia HM, Serruys PW. Short- and long-term (1-year) outcomes of sirolimus and paclitaxel-eluting stents in 293 consecutive all-comers diabetic patients- insights from the RESEARCH and T-SEARCH Registries. Presented at the European Society of Cardiology Congress, 2005, Stockholm, Sweden.
21. Rodriguez-Granillo GA, Garcia-Garcia HM, Aoki J, Valgimigli M, **Van Mieghem CAG**, Tsuchida K, Ong ATL, Serruys PW.Vulnerable plaque detection using ultrasound radio frequency data analysis. Presented at the European Society of Cardiology Congress, 2005, Stockholm, Sweden.
22. Garcia-Garcia HM, Rodriguez-Granillo GA, Valgimigli M, Aoki J, **Van Mieghem CAG**, Ong ATL ,Tsuchida K, Serruys PW. One year clinical outcome after coronary stenting of very small vessels using 2.25 mm sirolimus and paclitaxel-eluting stents: a comparison between the Research and T-search registries. Presented at the European Society of Cardiology Congress, 2005, Stockholm, Sweden.

23. Rodriguez-Granillo GA, Garcia-Garcia HM, Aoki J, Valgimigli M, **Van Mieghem CAG**, Ong ATL, Tsuchida K, Serruys PW. Coronary artery remodelling is related to plaque composition. Presented at the European Society of Cardiology Congress, 2005, Stockholm, Sweden.
24. Mollet NRA, Cademartiri F, **Van Mieghem CAG**, Runza G, Freericks MP, Kerker J, Krestin GP, de Feyter PJ. Clinical value of CT coronary angiography in patients with a high prevalence of coronary artery disease. Presented at the European Society of Cardiology Congress, 2005, Stockholm, Sweden.
25. Regar E, Schaar J, Mc Fadden E, van der Giessen WJ, **Van Mieghem CAG**, Rodriguez-Granillo GA, de Jaegere PPT, Serruys PW. Real-time, high-resolution optical coherence tomography (OCT)- a potential tool to detect features of vulnerable plaque in-vivo? Presented at the European Society of Cardiology Congress, 2005, Stockholm, Sweden.
26. Ong ATL, Polad J, Jewbali L, Aoki J, **Van Mieghem CAG**, Rodriguez-Granillo GA, Valgimigli M, Serruys PW. Long-term clinical and angiographic outcome of repeat drug-eluting stent implantation in drug-eluting stent failures. Presented at the European Society of Cardiology Congress, 2005, Stockholm, Sweden.
27. Rodriguez-Granillo GA, Valgimigli M, Mc Fadden E, **Van Mieghem CAG**, Aoki J, Ong ATL, de Feyter PJ, Serruys PW. Coronary plaque composition assessed by in vivo intracoronary Ultrasound radiofrequency data analysis, is related to clinical presentation and circulating biomarkers of vulnerability. Presented at the European Society of Cardiology Congress, 2005, Stockholm, Sweden.
28. Hoye A, Iakovou I, Ge L, **Van Mieghem CAG**, Ong ATL, Cosgrave J, Sangiorgi G, Airoldi F, Montorfano M, Michev I, Chieffo A, Carlino M, Corvaja N, Aoki J, Rodriguez Granillo GA, Valgimigli M, Sianos G, van der Giessen WJ, de Feyter PJ, Serruys PW, Colombo A. Bifurcation stenting with the crush technique: 9-month clinical and angiographic outcome. Presented at the seventeenth annual symposium, Transcatheter Cardiovascular Therapeutics, 2005, Washington, USA.
29. Hoye A, Iakovou I, Ge L, **Van Mieghem CAG**, Ong ATL, Cosgrave J, Sangiorgi G, Airoldi F, Montorfano M, Michev I, Chieffo A, Carlino M, Corvaja N, Aoki J, Rodriguez Granillo GA, Valgimigli M, Sianos G, van der Giessen WJ, de Feyter PJ, Serruys PW, Colombo A. Bifurcation stenting with the crush technique is associated with a high adverse event rate if used to treat the distal left main stem. Presented at the seventeenth annual symposium, Transcatheter Cardiovascular Therapeutics, 2005, Washington, USA.
30. **Van Mieghem CAG**, Mollet NRA, Cademartiri F, Serruys PW, Krestin GP, de Feyter PJ. Adjunctive value of CT coronary angiography in the diagnostic work-up of patients with stable angina pectoris. Presented at the Belgian Society of Cardiology, 2006, Brussels, Belgium.

31. Malagutti P, Nieman K, Meijboom WB, Pugliese F, **Van Mieghem CAG**, Palumbo AL, La Grutta L, Cademartiri F, Mollet NR, Krestin GP, de Jaegere PPT, de Feyter PJ. 64-slice computed tomography angiography detects grafts and coronary artery stenosis in patients with previous coronary artery bypass graft surgery. Presented at the American College of Cardiology- 55td Annual Scientific Session, 2006, Atlanta, USA.
32. Meijboom WB, **Van Mieghem CAG**, Kluin J, Pugliese F, Mollet NR, Cademartiri F, Malagutti P, Bogers AJ, Krestin GP, de Feyter PJ. Comparison of computed tomography coronary angiography with conventional coronary angiography for the detection of significant coronary lesions in the preoperative valve surgery patient. Presented at the American College of Cardiology- 55td Annual Scientific Session, 2006, Atlanta, USA.
33. Meijboom WB, **Van Mieghem CAG**, Pugliese F, Kluin J, Mollet NR, Cademartiri F, Krestin GP, de Feyter PJ. Preoperatieve computed tomography coronary angiography to detect significant coronary artery stenosis in patients referred for valve surgery. Presented at the European Society of Cardiology Congress, 2006, Barcelona, Spain.
34. Sianos G, Papafaklis MI, Daemen J, Vaina S, **Van Mieghem CAG**, Van Domburg RT, Michalis LK, Serruys PW. Incidence and predictors of stent thrombosis in patients treated with precutaneous coronary intervention and drug-eluting stent implantation for acute ST elevation myocardial infarction. Presented at the European Society of Cardiology Congress, 2006, Barcelona, Spain.
35. Sianos G, Papafaklis MI, Vaina S, Daemen J, **Van Mieghem CAG**, Van Domburg RT, Michalis LK, Serruys PW. Impact of baseline thrombus on the clinical outcome in patients with ST-segment elevation myocardial infarction. Validation of a pre-existing and proposition of a new simplified classification. Presented at the European Society of Cardiology Congress, 2006, Barcelona, Spain.
36. **Van Mieghem CAG**, Cademartiri F, Mollet NR, Meijboom WB, Krestin GP, Serruys PW, de Feyter PJ. Multislice spiral computed tomography for the evaluation of stent patency after left main coronary artery stenting: a comparison with conventional angiography and intravascular ultrasound. Presented at the European Society of Cardiology Congress, 2006, Barcelona, Spain.
37. Malagutti P, Nieman K, Meijboom WB, **Van Mieghem CAG**, Pugliese F, Cademartiri F, Mollet N, de Feyter P. Diagnostic performance of 64-slice CT in symptomatic patients with in patients with previous coronary bypass surgery: evaluation of grafts and coronary arteries. Presented at the European Society of Cardiology Congress, 2006, Barcelona, Spain.
38. **Van Mieghem CAG**, Thury A, Meijboom WB, Cademartiri F, Mollet NR, Krestin GP, Serruys PW, de Feyter PJ. Assessment of coronary bifurcation lesions with 64-slice computed tomography coronary angiography. Presented at the European Society of Cardiology Congress, 2006, Barcelona, Spain.

39. Garcia-Garcia HM, Daemen J, Tsuchida K, **Van Mieghem CAG**, Tanimoto S, van der Ent M, de Feyter P, Serruys PW. Three-year clinical and angiographic outcomes after coronary stenting of chronic total occlusion using sirolimus-eluting stents: insights from the RESEARCH registry. Presented at the European Society of Cardiology Congress, 2006, Barcelona, Spain.
40. Sianos G, Papafaklis MI, Daemen J, Vaina S, **Van Mieghem CAG**, van Domburg RT, Michalis LK, Serruys PW. Incidence and predictors of angiographic stent thrombosis in patients treated with drug-eluting stent implantation for ST segment elevation myocardial infarction. Presented at the eighteenth annual symposium, Transcatheter Cardiovascular Therapeutics, 2006, Washington, USA.
41. **Van Mieghem CAG**, Thury A, Meijboom WB, Cademartiri F, Mollet NR, Krestin GP, Serruys PW, de Feyter P. Assessment of coronary bifurcation lesions with 64-slice computed tomography coronary angiography. Presented at the eighteenth annual symposium, Transcatheter Cardiovascular Therapeutics, 2006, Washington, USA.

42. **Van Mieghem CAG**, Cademartiri F, Mollet N, Meijboom B, Pugliese F, de Feyter P. Multislice spiral computed tomography for the evaluation of stent patency after left main coronary artery stenting: a comparison with conventional angiography and intravascular ultrasound. Presented at the Radiological Society of North America, 92nd Assembly and Annual Meeting, 2006, Chicago, USA.
43. Meijboom WB, Mollet N, **Van Mieghem CAG**, Pugliese F, Weustink A, Vourvouri E, Cademartiri F, Malago R, Alberghina F, Bogers A, Krestin G, de Feyter P.Preoperative computed tomography coronary angiography to detect significant coronary artery disease in patients referred for cardiac valve surgery. Presented at the Radiological Society of North America, 92nd Assembly and Annual Meeting, 2006, Chicago, USA.
44. Meijboom WB, Mollet N, **Van Mieghem CAG**, Weustink A, Pugliese F, Vourvouri E, Cademartiri F, Malago R, Alberghina F, Krestin G, de Feyter P. Diagnostic accuracy of 64-slice computed tomography versus conventional coronary angiography: results of 180 consecutive patients. Presented at the Radiological Society of North America, 92nd Assembly and Annual Meeting, 2006, Chicago, USA.
45. Nieman K, Malagutti P, Meijboom WB, Pugliese F, Weustink A, Mollet N, Cademartiri F, Vourvouri E, **Van Mieghem CAG**, Krestin G, de Feyter P.Diagnostic performance of 64-slice CT in symptomatic patients with previous coronary bypass surgery: evaluation of grafts and coronary arteries. Presented at the Radiological Society of North America, 92nd Assembly and Annual Meeting, 2006, Chicago, USA.
46. Pugliese F, Cademartiri F, Alberghina F, Malago R, Mollet N, **Van Mieghem CAG**, Dijkshoorn M, de Feyter P, Krestin G. Complex lesion stenting techniques in coronary arteries: non-invasive imaging with 64-slice CT coronary angiography. Presented at the Radiological Society of North America, 92nd Assembly and Annual Meeting, 2006, Chicago, USA.

47. **Van Mieghem CAG**, Meijboom WB, Cademartiri F, Mollet NR, Pugliese F, Weustink A, Sianos G, de Jaegere PPT, Serruys PW, de Feyter P. Detection and characterization of coronary bifurcation lesions with 64-slice computed tomography coronary angiography. Presented at the Belgian Society of Cardiology, 2007, Brussels, Belgium.
48. **Van Mieghem CAG**, Meijboom WB, Mollet NR, Kluin J, Weustink A, Pugliese F, Vourvouri E, Cademartiri F, Bogers A, Krestin GP, de Feyter PJ. Preoperative computed tomography coronary angiography to detect significant coronary artery disease in patients referred for cardiac valve surgery. Presented at the Belgian Society of Cardiology, 2007, Brussels, Belgium.
49. Weustink AC, Mollet NR, Meijboom WB, Otsuka M, Pugliese F, **Van Mieghem CAG**, Malago R, van Pelt N, Cademartiri F, Krestin GP, de Feyter PJ. Diagnostic accuracy of dual source coronary tomography coronary angiography in patients referred for conventional angiography. Presented at the American College of Cardiology- 56td Annual Scientific Sessions, 2007, New Orleans, USA.
50. Meijboom WB, Mollet NR, **Van Mieghem CAG**, Weustink AC, Pugliese F, Cademartiri F, Vourvouri E, Otsuka M, Nieman K, van Pelt N, Krestin GP, de Feyter PJ. Diagnostic accuracy of 64-slice computed tomography versus conventional coronary angiography: results on 300 consecutive patients. Presented at the American College of Cardiology- 56td Annual Scientific Sessions, 2007, New Orleans, USA.
51. Meijboom WB, **Van Mieghem CAG**, Weustink AC, Pugliese F, Mollet NR, Vourvouri E, Cademartiri F, Otsuka M, van Pelt N, Nieman K, Krestin GP, de Feyter PJ. Diagnostic accuracy of 64-slice computed tomography coronary angiography in patients with unstable angina and non-ST segment elevation myocardial infarction. Presented at the American College of Cardiology- 56td Annual Scientific Sessions, 2007, New Orleans, USA.
52. Meijboom WB, Mollet NR, **Van Mieghem CAG**, Pugliese F, Weustink AC, Van Pelt N, Nieman K, Cademartiri F, Krestin GP, de Feyter PJ. 64-slice computed tomography coronary angiography in patients with high, intermediate or low pre-test probability of significant coronary artery disease. Presented at the European Society of Cardiology Congress, 2007, Vienna, Austria.
53. Patterson M, Hoeks SE, Tanimoto S, **Van Mieghem CAG**, Ramcharitar S, Van Domburg RT, Serruys PW. A simple score for predicting prolonged crossing times to select patients who would benefit from a magnetic percutaneous coronary intervention. Presented at the European Society of Cardiology Congress, 2007, Vienna, Austria.
54. Van Pelt N, Meijboom WB, **Van Mieghem CAG**, Weustink AC, Mollet NR, Pugliese F, Nieman K, Krestin GP, de Feyter PJ. Can CT coronary angiography determine the significance of coronary artery stenosis: a comparison with invasive fractional flow reserve management. Presented at the European Society of Cardiology Congress, 2007, Vienna, Austria.

55. Meijboom WB, Weustink AC, Pugliese F, **Van Mieghem CAG**, Mollet NR, Van Pelt N, Nieman K, Cademartiri F, Krestin GP, de Feyter PJ. Diagnostic accuracy of 64-slice computed tomography coronary angiography in women. Presented at the European Society of Cardiology Congress, 2007, Vienna, Austria.
56. Meijboom WB, Mollet NR, **Van Mieghem CAG**, Pugliese F, Weustink AC, Van Pelt N, Nieman K, Cademartiri F, Krestin GP, de Feyter PJ. 64-slice computed tomography coronary angiography in patients with high, intermediate or low pre-test probability of significant coronary artery disease. Presented at the American Heart Association 2007, Orlando, USA.
57. **Van Mieghem CAG**, Weustink AC, Meijboom WB, Pugliese F, Krestin GP, de Feyter P, Mollet NR. Clinical value of CT coronary angiography in symptomatic patients after percutaneous coronary intervention. Presented at the Radiological Society of North America, 93nd Assembly and Annual Meeting, 2007, Chicago, USA.
58. Mollet NR, Meijboom WB, Weustink AC, **Van Mieghem CAG**, van Pelt N, Pugliese F, Krestin GP, de Feyter P. Sixty-four slice computed coronary angiography in patients with high, intermediate or low pre-test probability of significant coronary artery disease. Presented at the Radiological Society of North America, 93nd Assembly and Annual Meeting, 2007, Chicago, USA.
59. Weustink AC, **Van Mieghem CAG**, Mollet NR, Matheijssen N, de Feyter P, Krestin GP. Radiation exposure, procedure time and contrast load in patients referred for coronary angiography: head-to-head comparison of Dual Source CT with conventional coronary angiography. Presented at the Radiological Society of North America, 93nd Assembly and Annual Meeting, 2007, Chicago, USA.
60. Weustink AC, Nieman K, **Van Mieghem CAG**, van Pelt N, Pugliese F, Meijboom WB, Mollet NR, de Feyter P, Krestin GP. Dual source CT in symptomatic patients after coronary bypass surgery: evaluation of grafts and distal coronary run-offs. Presented at the Radiological Society of North America, 93nd Assembly and Annual Meeting, 2007, Chicago, USA.
61. Kedhi E, Wassing JGP, **Van Mieghem CAG**, Sheik Joesoef K, McFadden EP, Smits PC. Compare-AMI: preliminary results of 30 day follow-up, comparing the everolimus-eluting stent, Xience V, with the paclitaxel-eluting stent, Taxus LiberteTM, in patients with ST-elevation myocardial infarction. Presented at the NVVC-Voorjaarscongres, 2008, Amsterdam, The Netherlands.
62. García-García HM, **Van Mieghem CAG**, Gonzalo N, Meijboom WB, Weustink AC, Onuma Y, Mollet NR, Schultz CJ, Meliga E, van der Ent M, Goedhart D, den Boer A, de Feyter P, Serruys PW. Computed tomography in totally occluded lesions (CTTO Registry): Focus on conventional angiography and computed tomography angiography predictors of success and radiation exposure. Presented at the European Society of Cardiology Congress, 2008, Munich, Germany.

63. Kedhi E, **Van Mieghem CAG**, Wassing JGP, Sheik Joesoef K, McFadden EP, Smits PC. Compare-AMI: preliminary results of 30 day follow-up, comparing the everolimus-eluting stent, Xience V, with the paclitaxel-eluting stent, Taxus LiberteTM, in ST-elevation myocardial infarction. Presented at the European Society of Cardiology Congress, 2008, Munich, Germany.
64. Meijboom WB, Meijs, Schuijf J, Cramer, Mollet N, **Van Mieghem CAG**, Bax J, Doevendans P, Krestin G, de Feyter P. Diagnostic accuracy of 64-slice computed tomography coronary angiography: a prospective multicenter, multivendor study. Presented at the European Society of Cardiology Congress, 2008, Munich, Germany.

PhD Portfolio Summary

SUMMARY OF PHD TRAINING AND TEACHING ACTIVITIES

Name PhD student: Carlos van Mieghem
Erasmus MC Department: Cardiology
Research School: COEUR

PhD period: 2003-2008
Promotors: Prof PJ de Feyter, Prof PW Serruys

1. PHD TRAINING	Year	Workload (ECTS)
General academic skills - Biomedical English Writing and Communication	2005	2.0
Research skills - Statistics NIHES - Methodology	2004	3.0
In-depth courses (e.g. Research school, Medical Training)		
- PhD Courses at COEUR (10x)	2003-2008	15.0
- Basic Science PhD Courses Papendal (3x)	2003-2008	6.0
Presentations		
International conferences - Ten Symposia and congresses	2004-2006	12.6 ECTS
Seminars and workshops **10 COEUR research seminars**	2004-2008	3.0 ECTS
Didactic skills		
Other		
2. TEACHING ACTIVITIES	**Year**	**Workload (Hours/ECTS)**
Lecturing	2004-2007	10 ECTS
Supervising practicals and excursions		
Supervising Master's theses		
Total		51.6 ECTS

Curriculum Vitae

Carlos A.G. Van Mieghem was born in Wynberg, Cape Town, South Africa on February 5th 1971. He obtained his medical degree in 1996 at the Catholic University of Leuven, Belgium.

He completed his training in internal medicine and cardiology at the University Hospital Gasthuisberg, Leuven from 1996 to 2002 and obtained a certificate in Emergency medicine in 2000. From 2002 to 2003 he completed a training in intensive care medicine at the University Hospital Gasthuisberg, Leuven and became registered as specialist in Intensive Care Medicine in 2005. From August 2003 to September 2007, he worked as a research fellow at the department of Interventional Cardiology and Radiology, Erasmus MC, Rotterdam, The Netherlands, under the supervision of Professor Pim J. de Feyter, Professor Patrick W. Serruys and Professor Gabriel P. Krestin. In September 2007 he assumed his current position as staff member of the department of Cardiology, Maasstad Hospital, Rotterdam, The Netherlands.

Carlos Van Mieghem is a member of the Dutch Society of Cardiology, of the European Association of Percutaneous Cardiovascular Interventions, of the European Working Group on Acute Cardiac Care, titular member of the Belgian Society of Cardiology and Fellow of the European Society of Cardiology.

Color Section

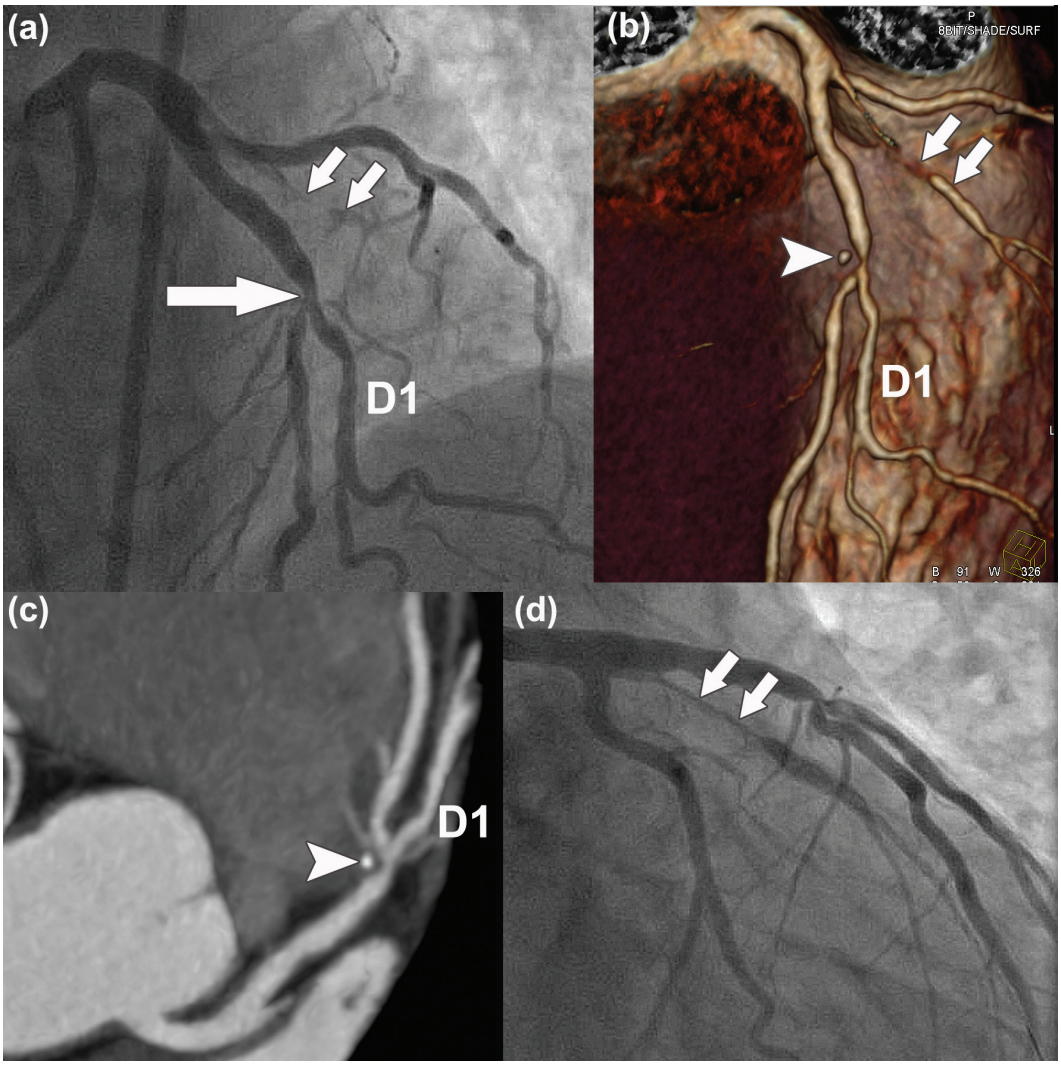

Chapter 2, page 32, Figure 9

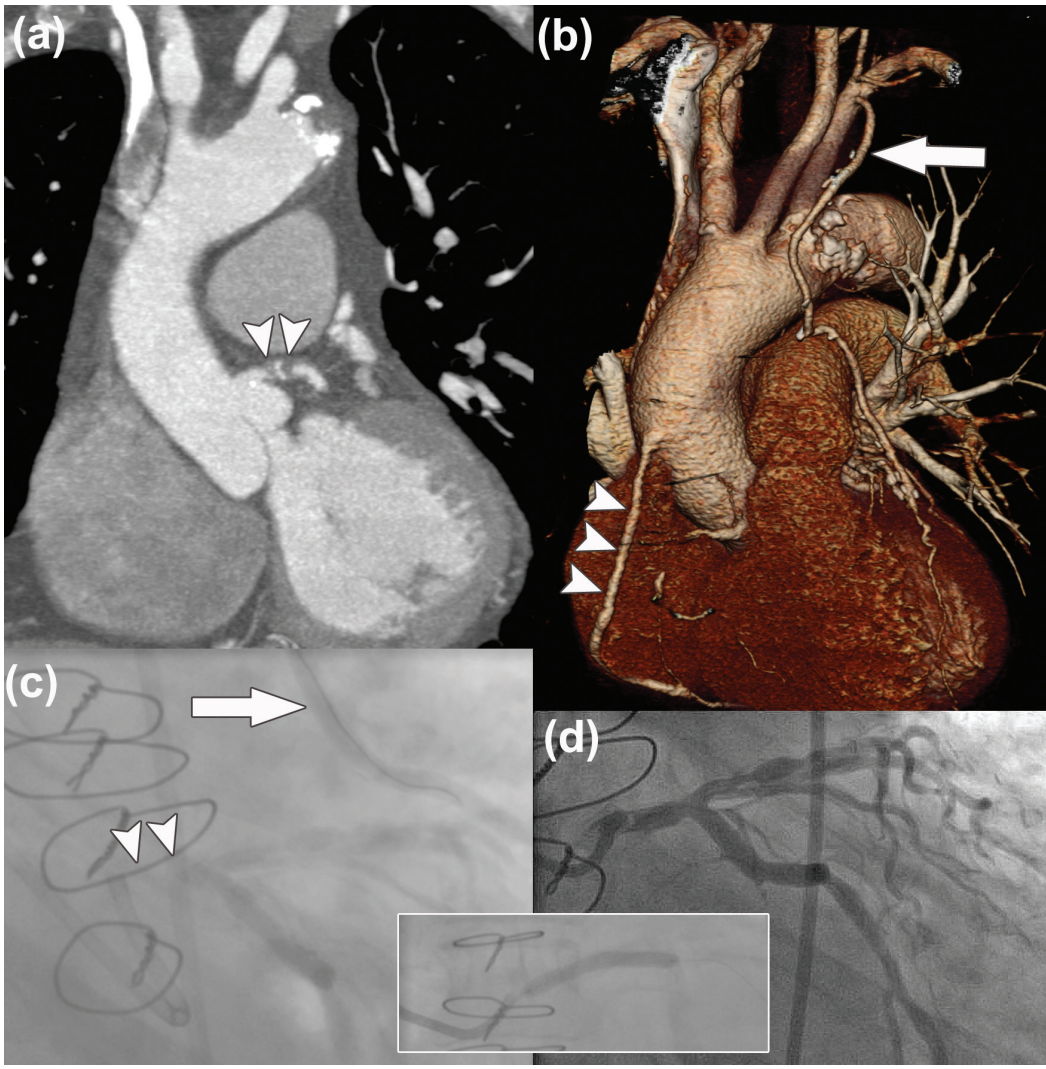

Chapter 2, page 33, Figure 11

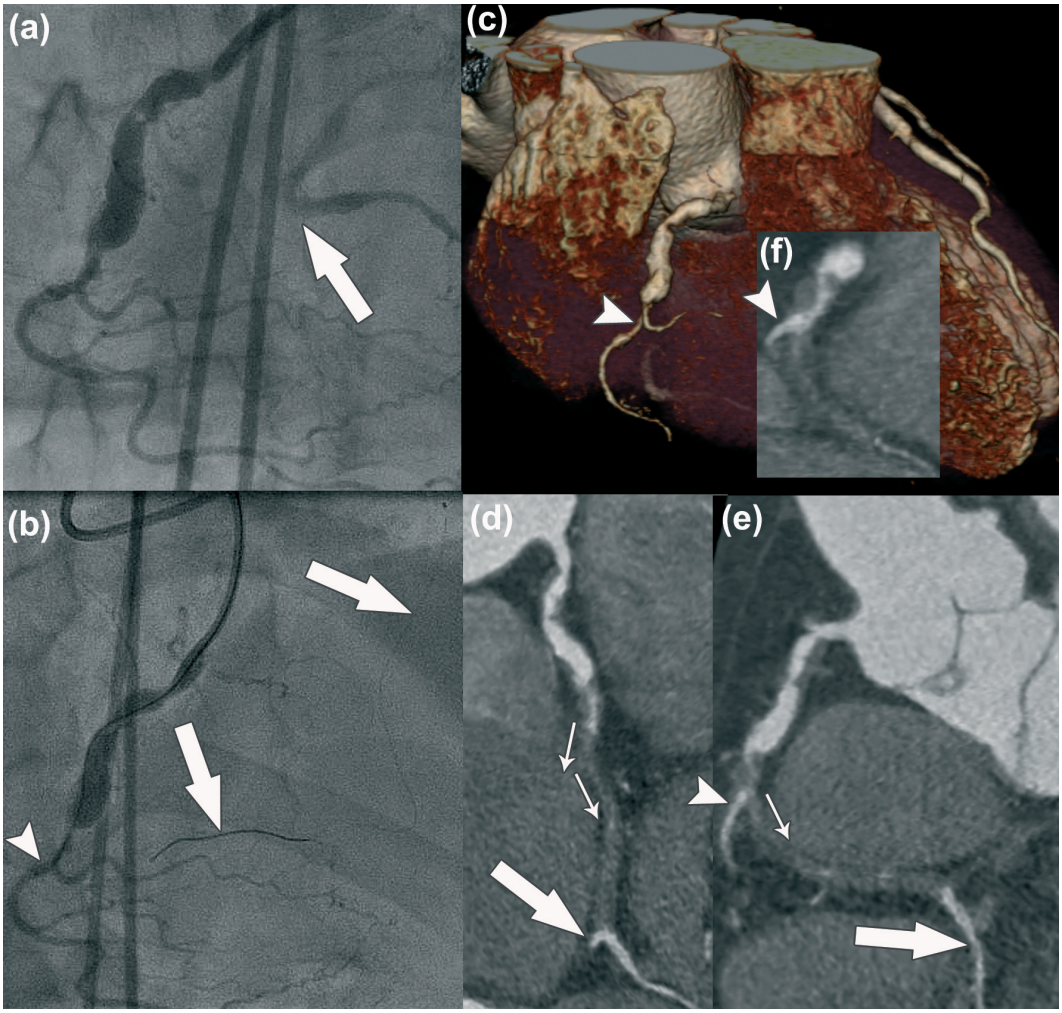

Chapter 2, page 34, Figure 12

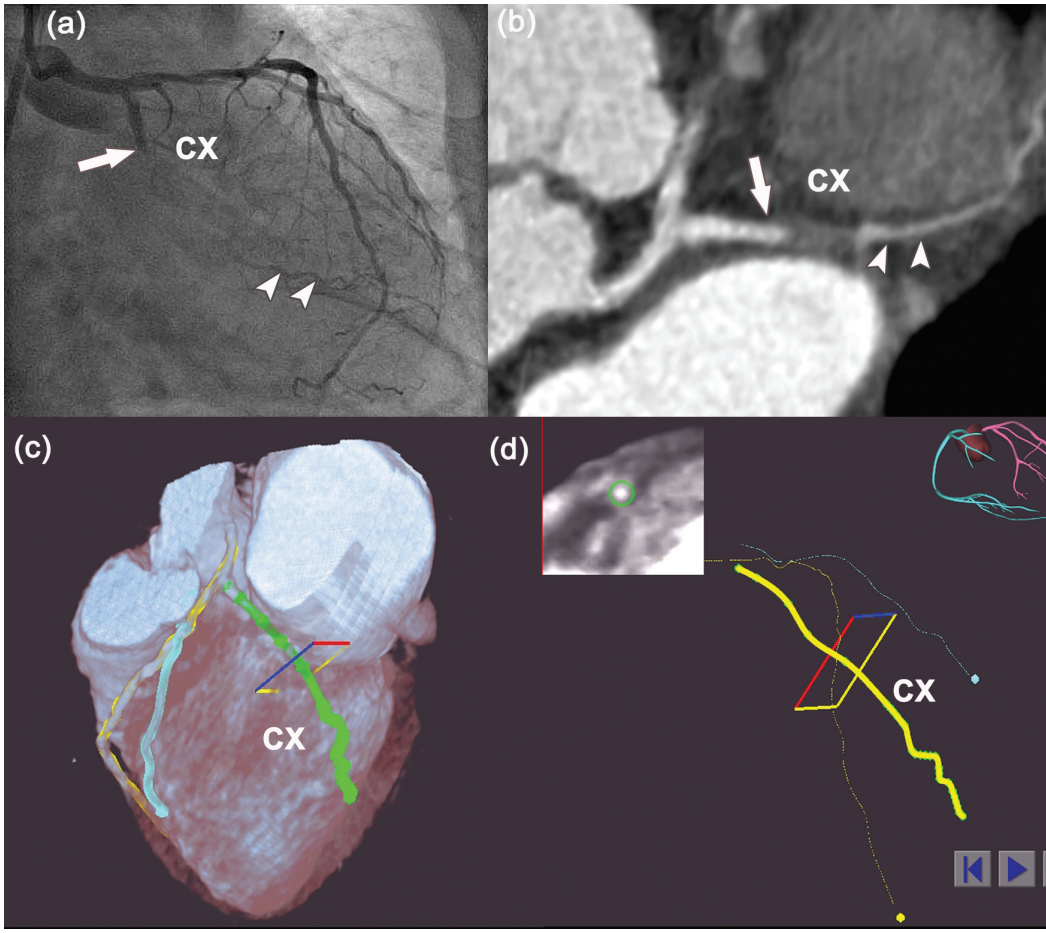

Chapter 2, page 35, Figure 14

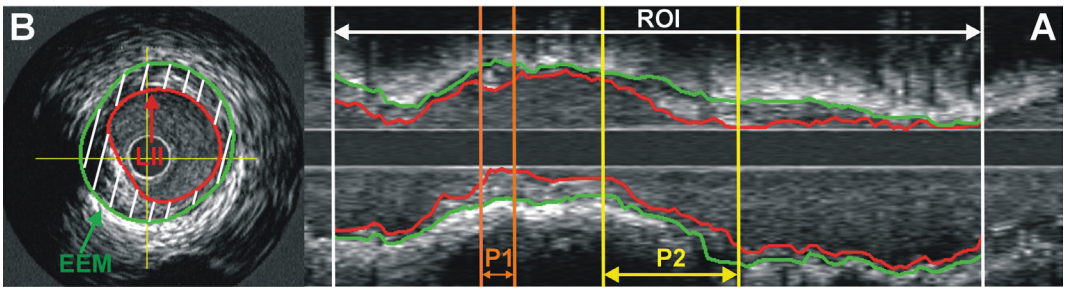

Chapter 3, page 55, Figure 2

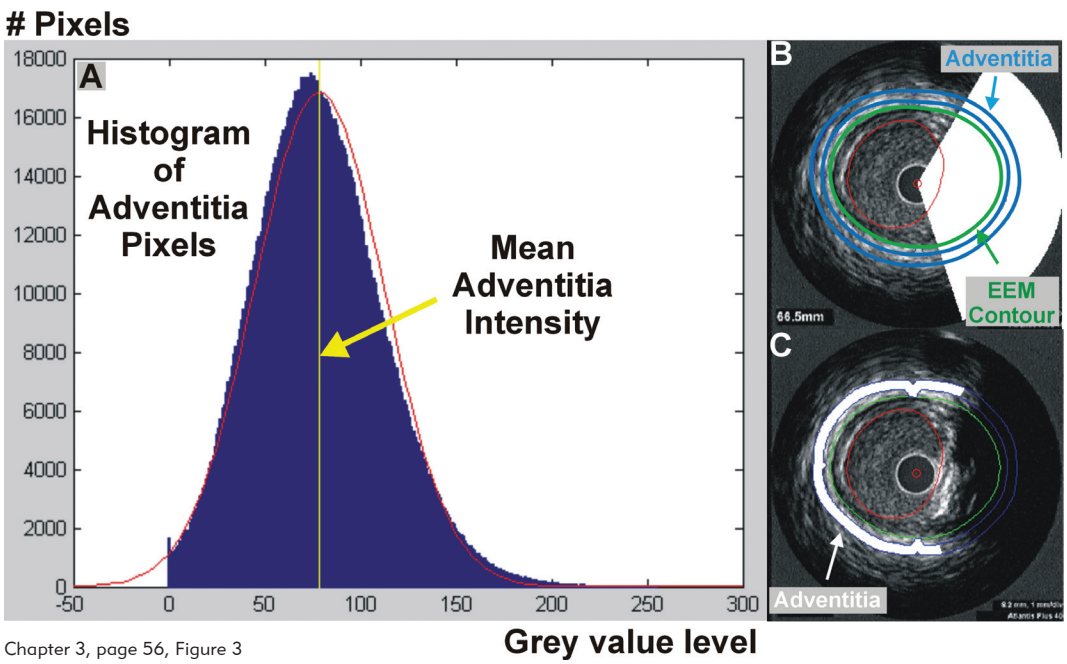

Chapter 3, page 56, Figure 3

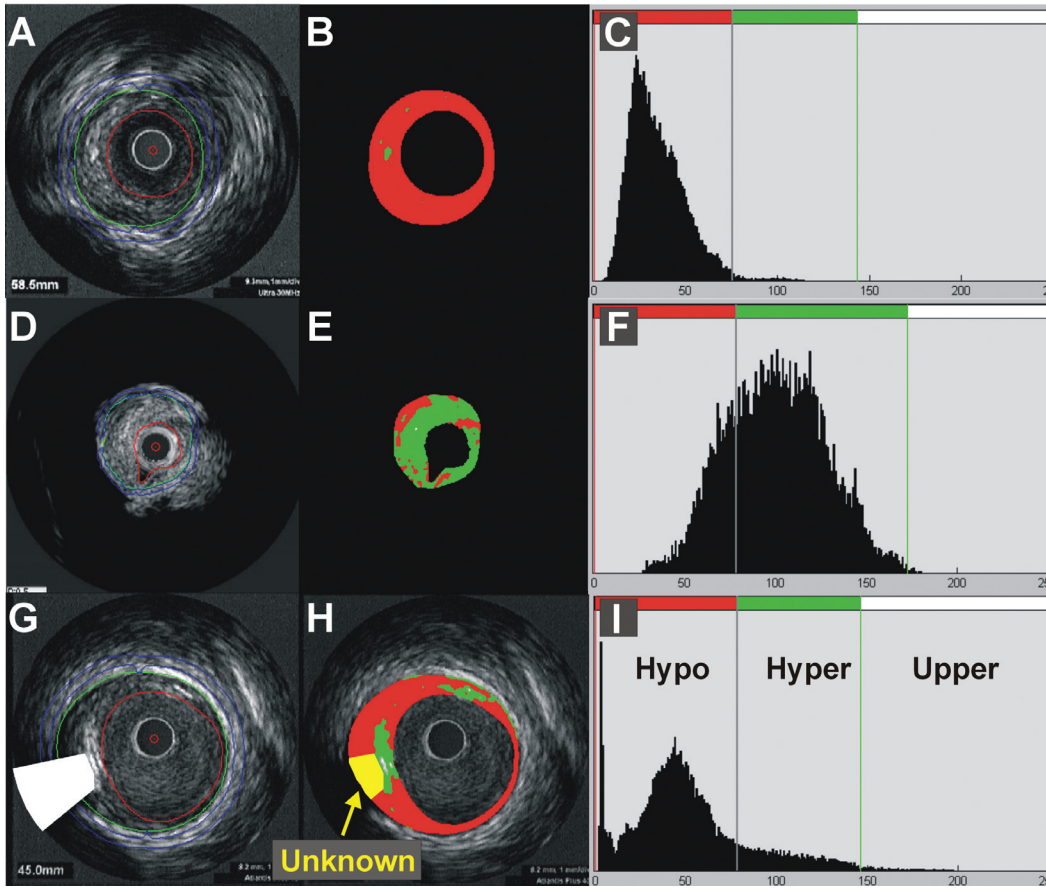

Chapter 3, page 57, Figure 4

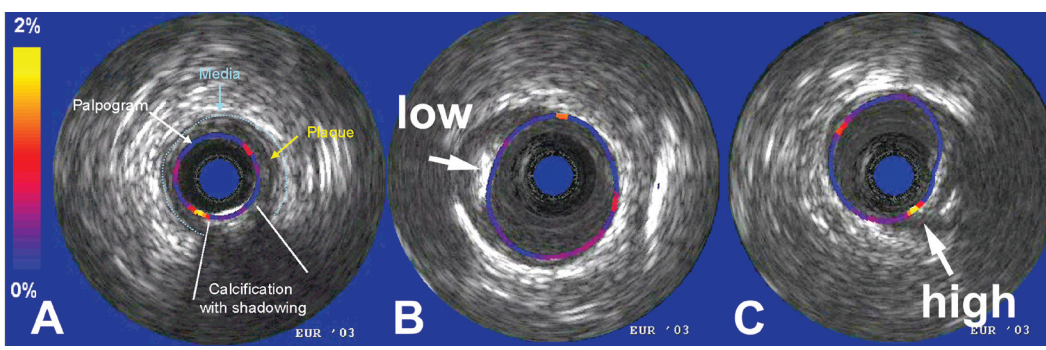

Chapter 3, page 57, Figure 5

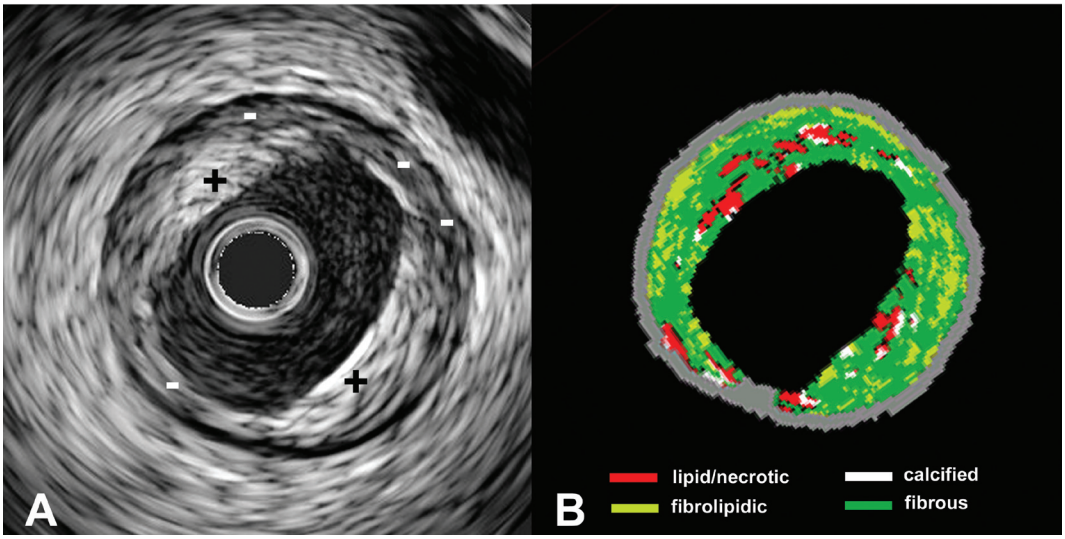

Chapter 3, page 60, Figure 7

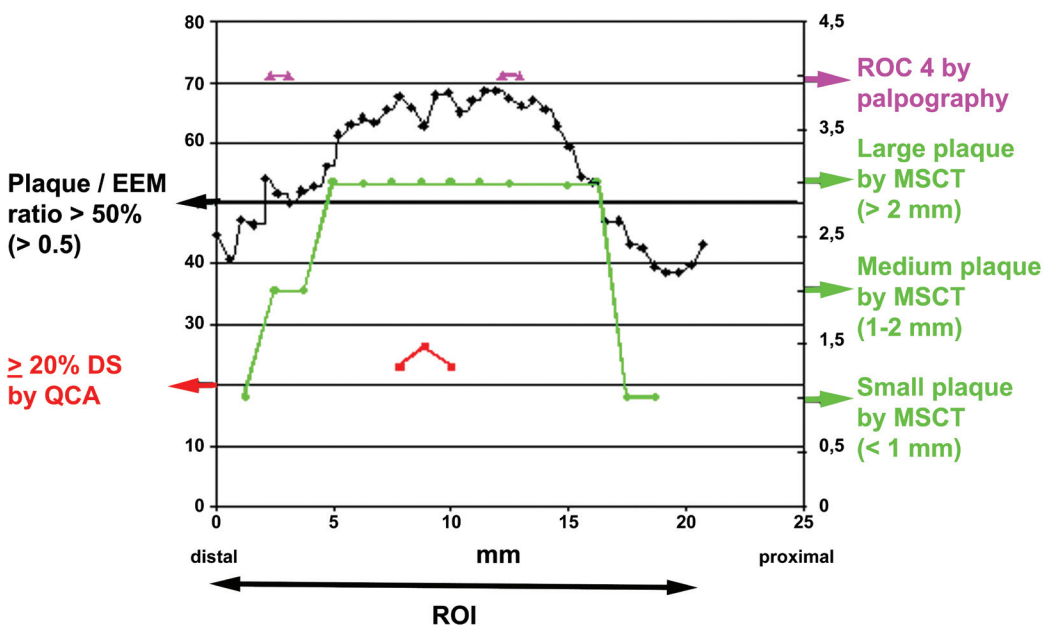

Chapter 3, page 62, Figure 8

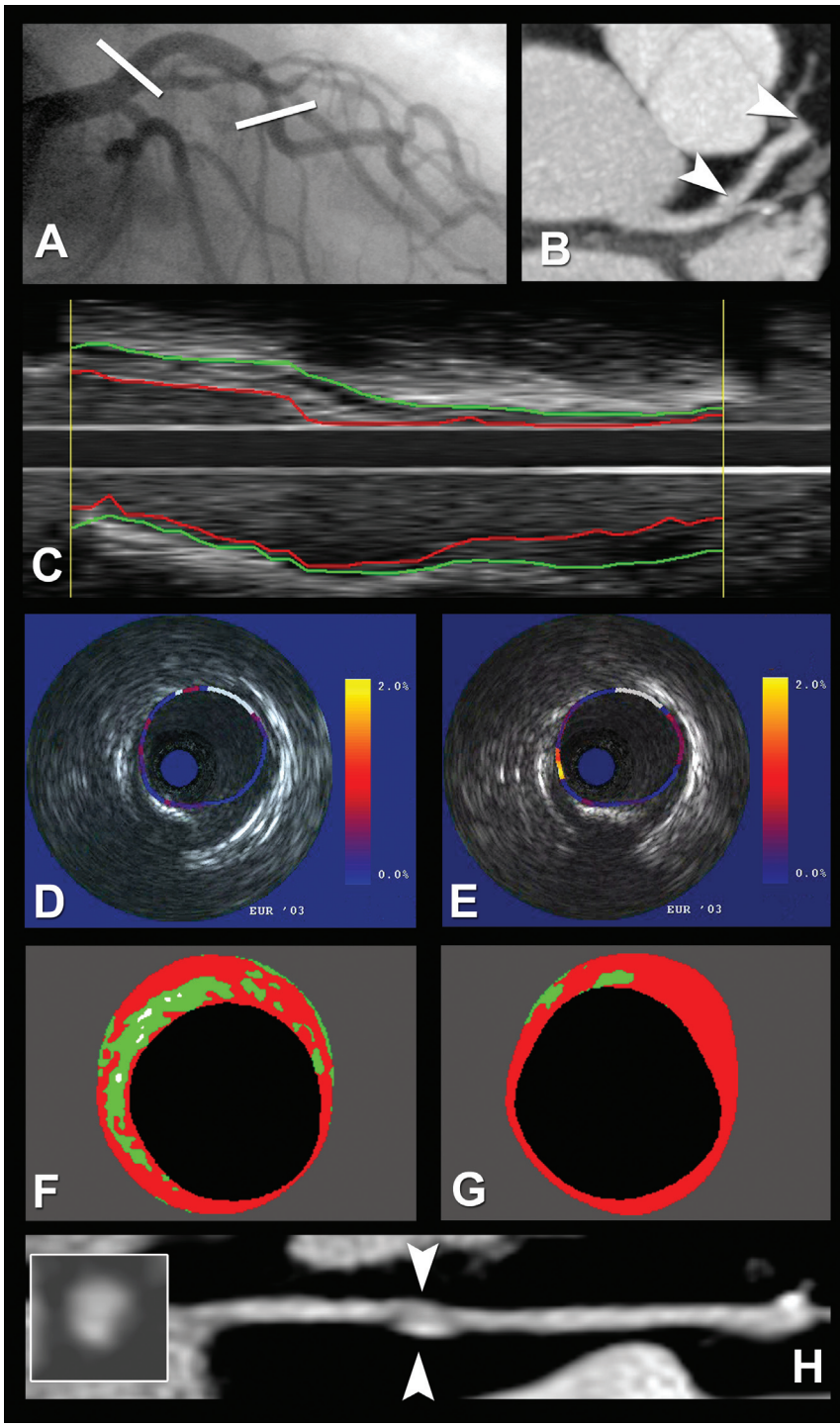

Chapter 4, page 84, Figure 3

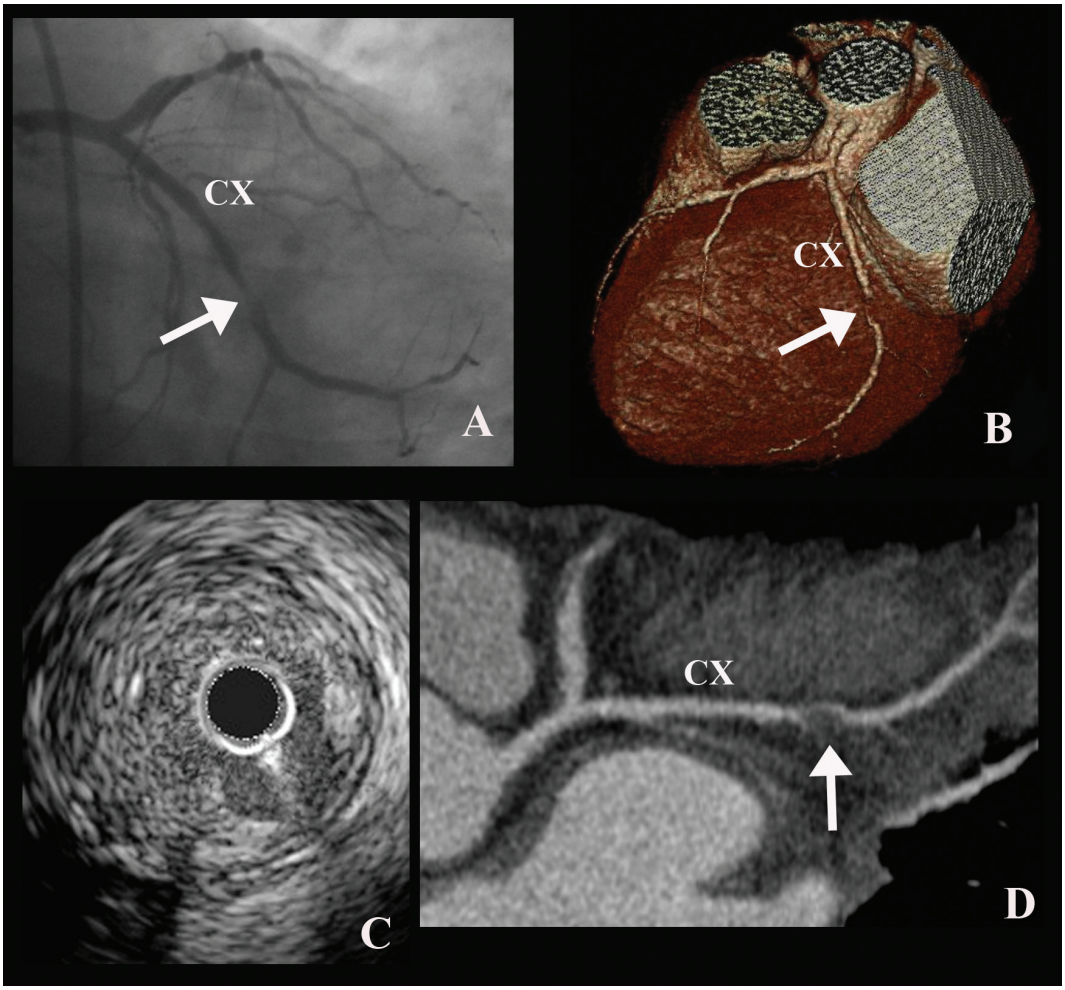

Chapter 5, page 94, Figure 2

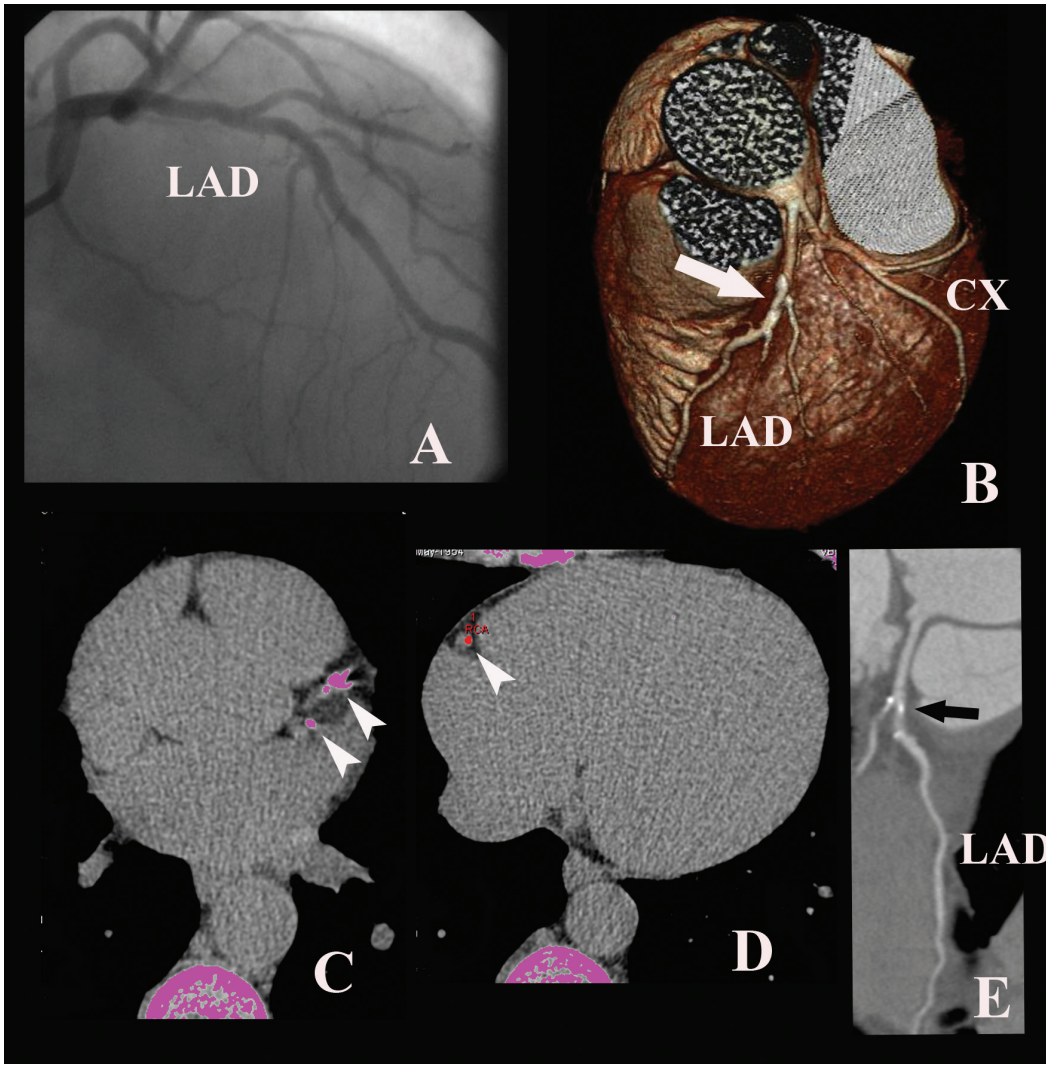

Chapter 5, page 95, Figure 3

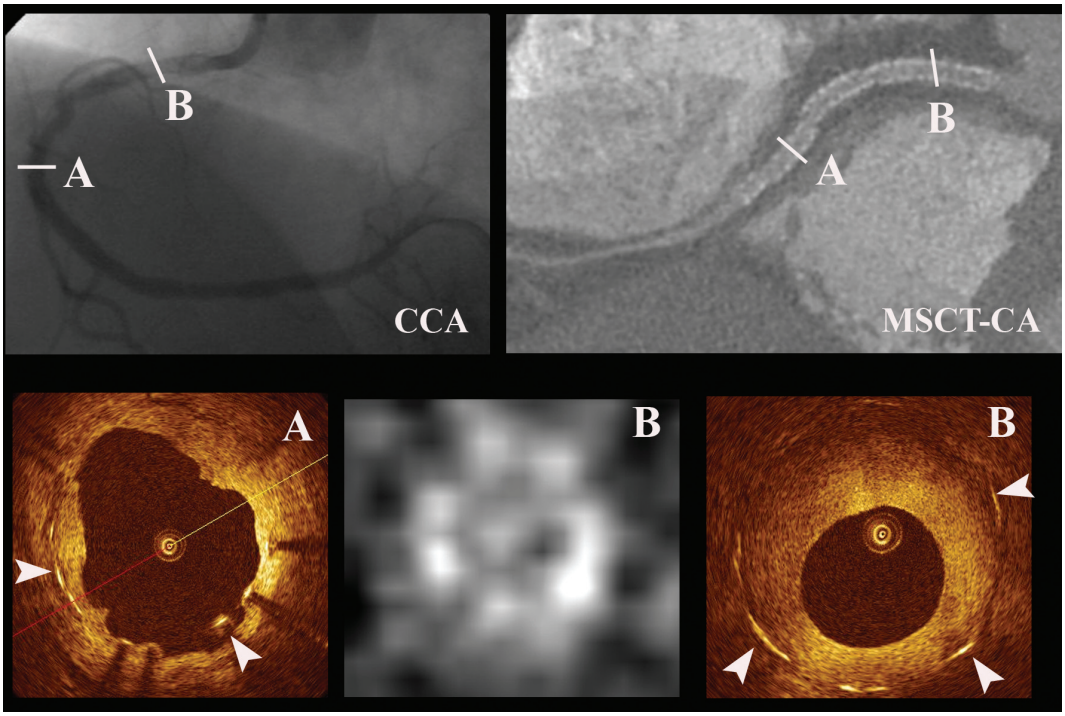

Chapter 5, page 96, Figure 6

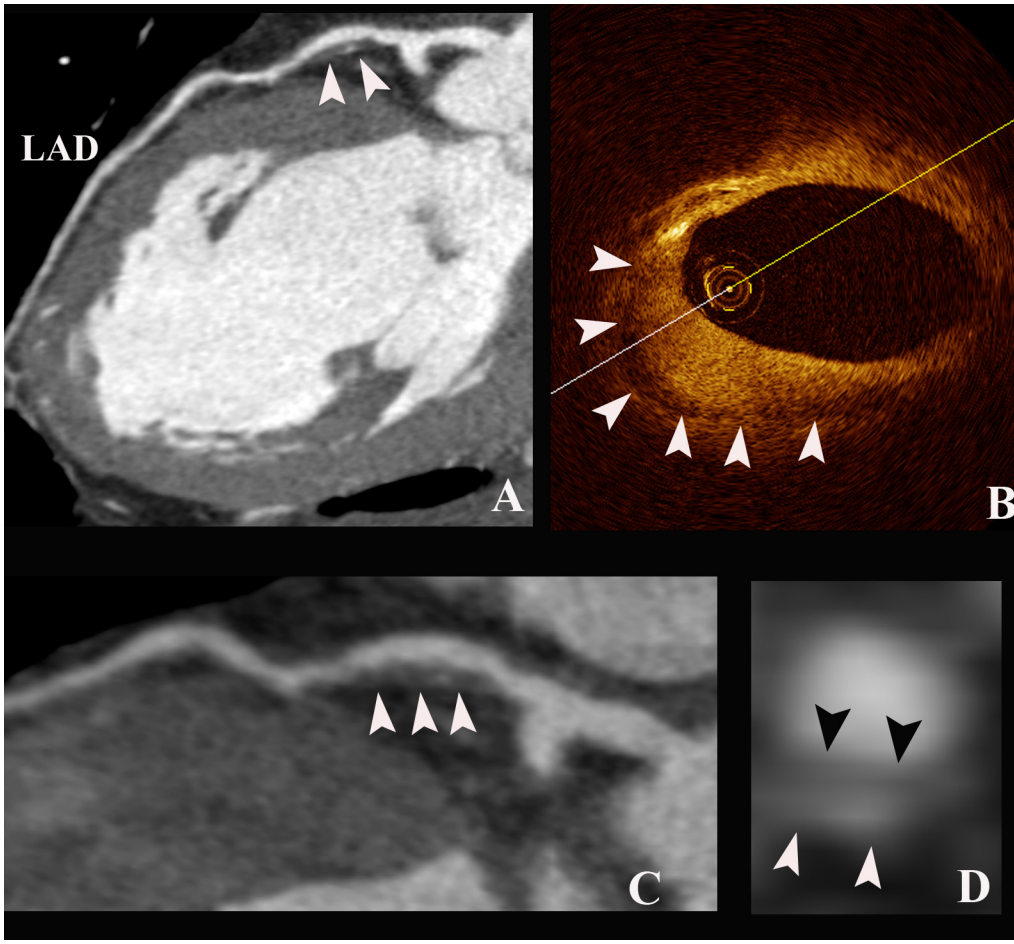

Chapter 5, page 97, Figure 7

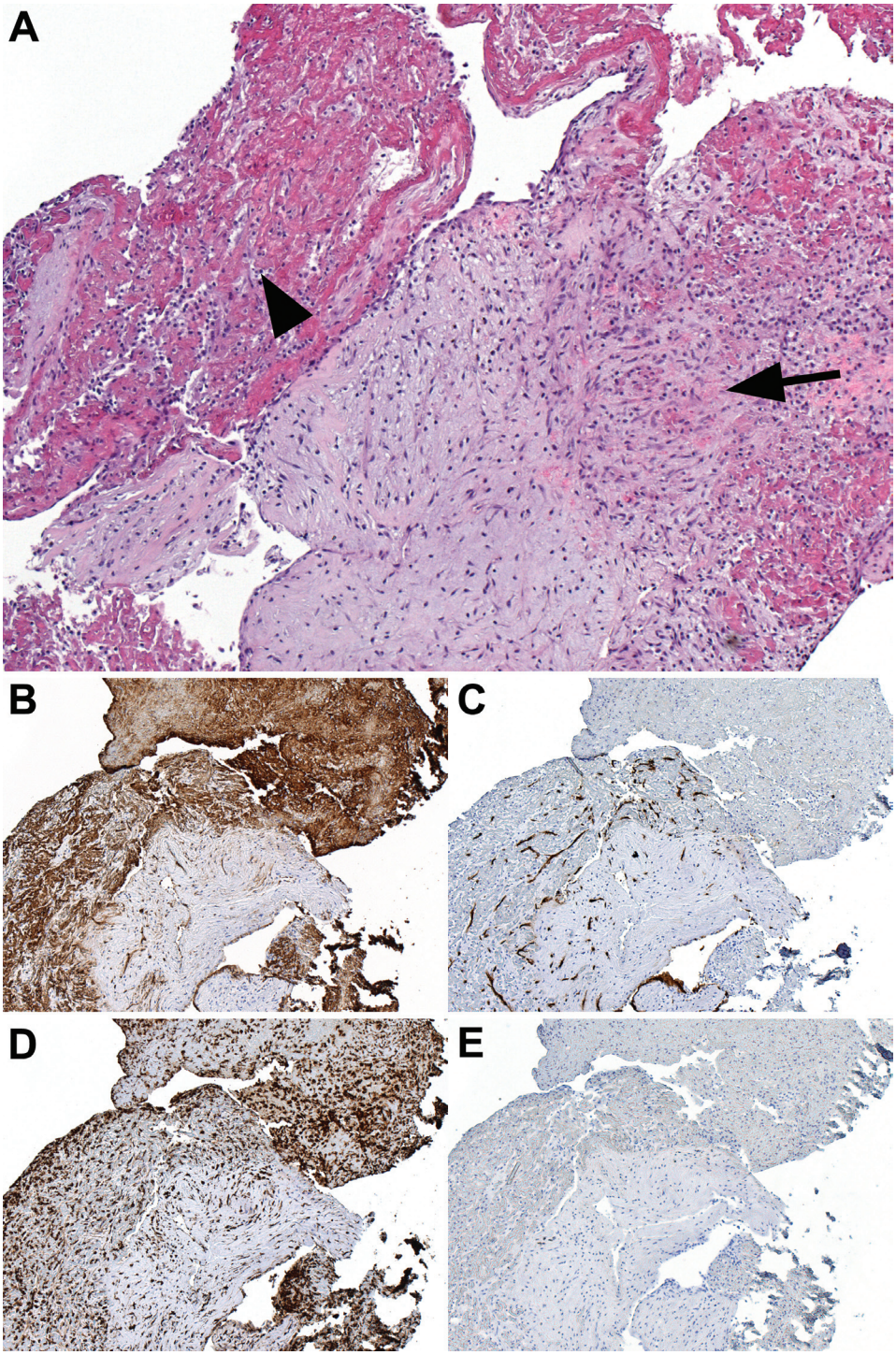

Interlude 1, page 109, Figure 3

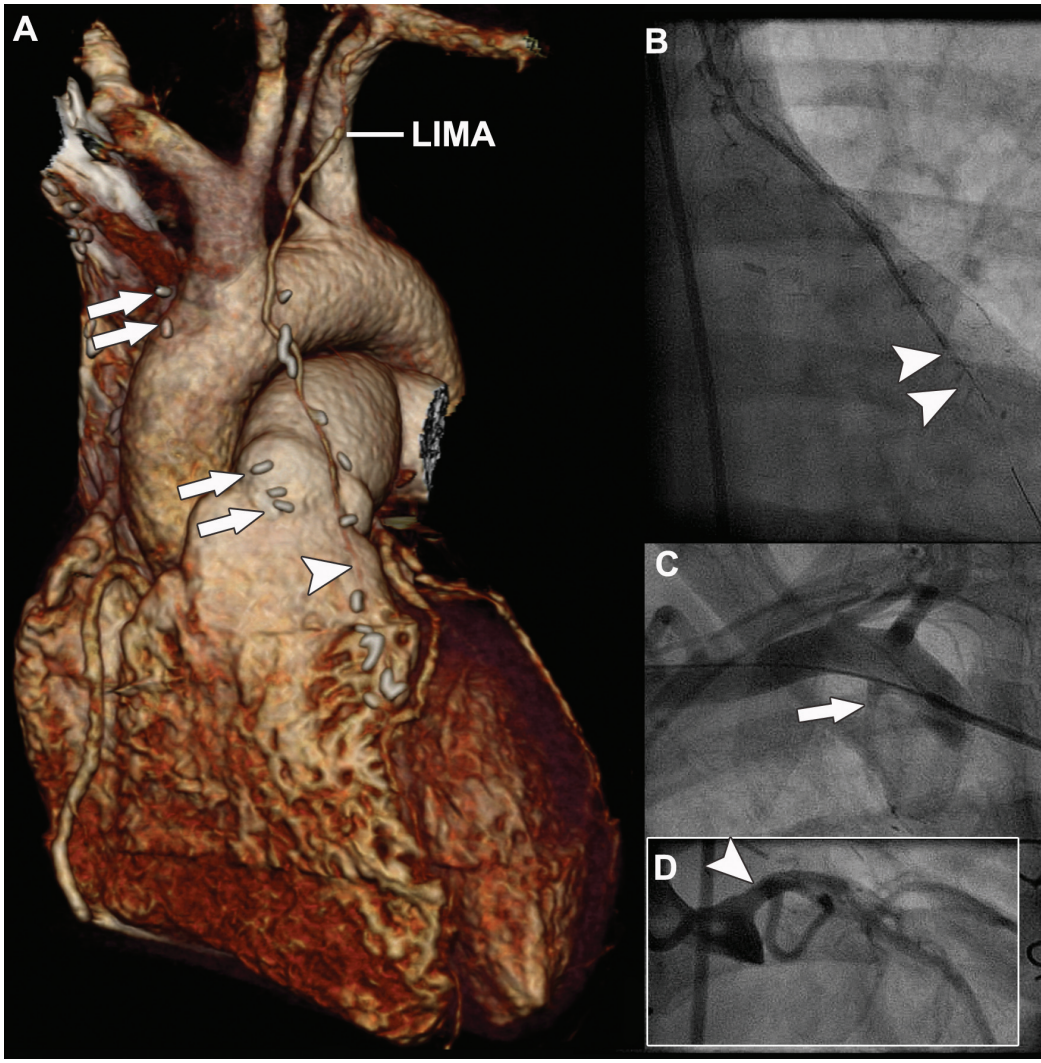

Interlude 1, page 109, Figure 4

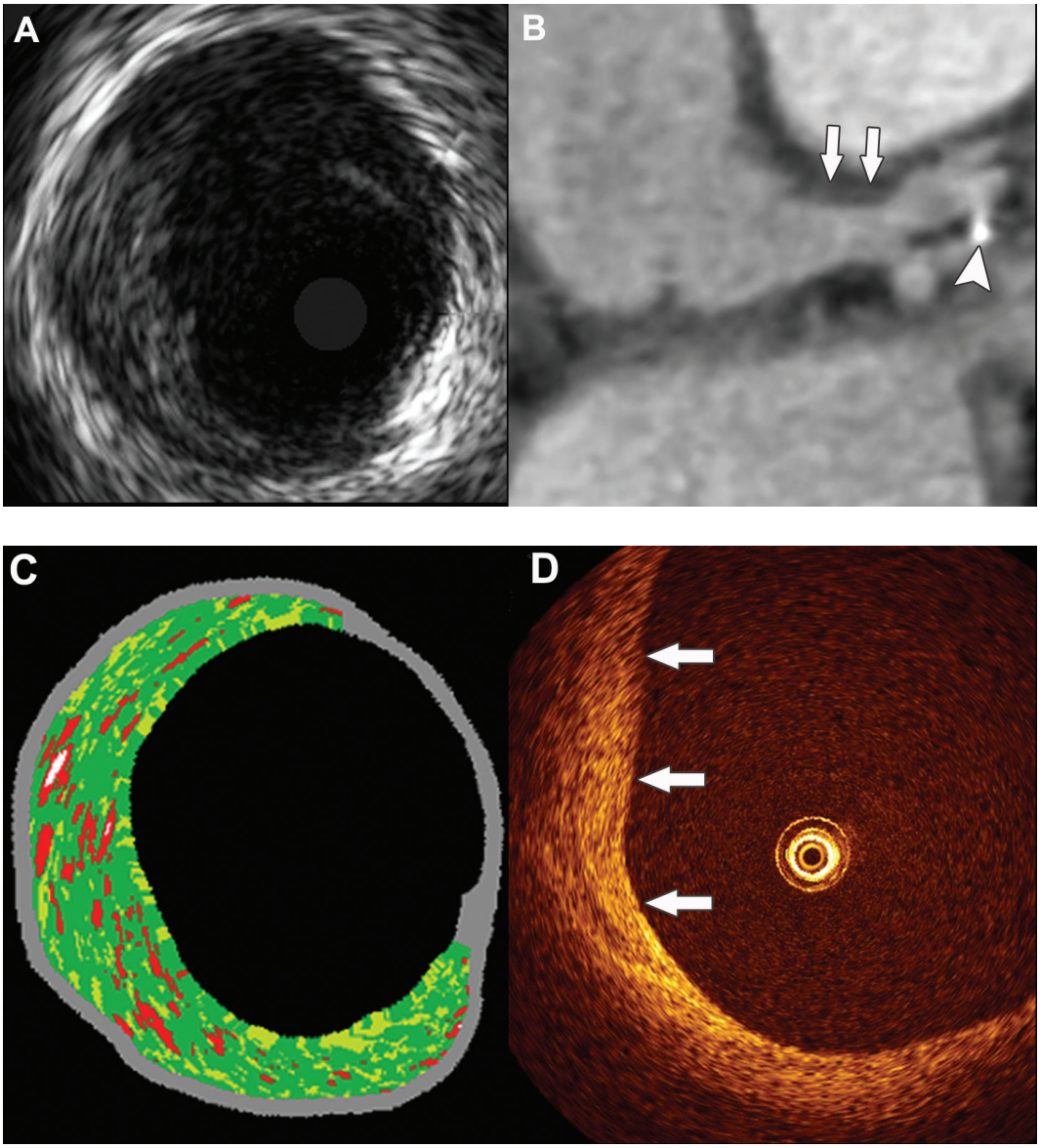

Interlude 1, page 110, Figure 5

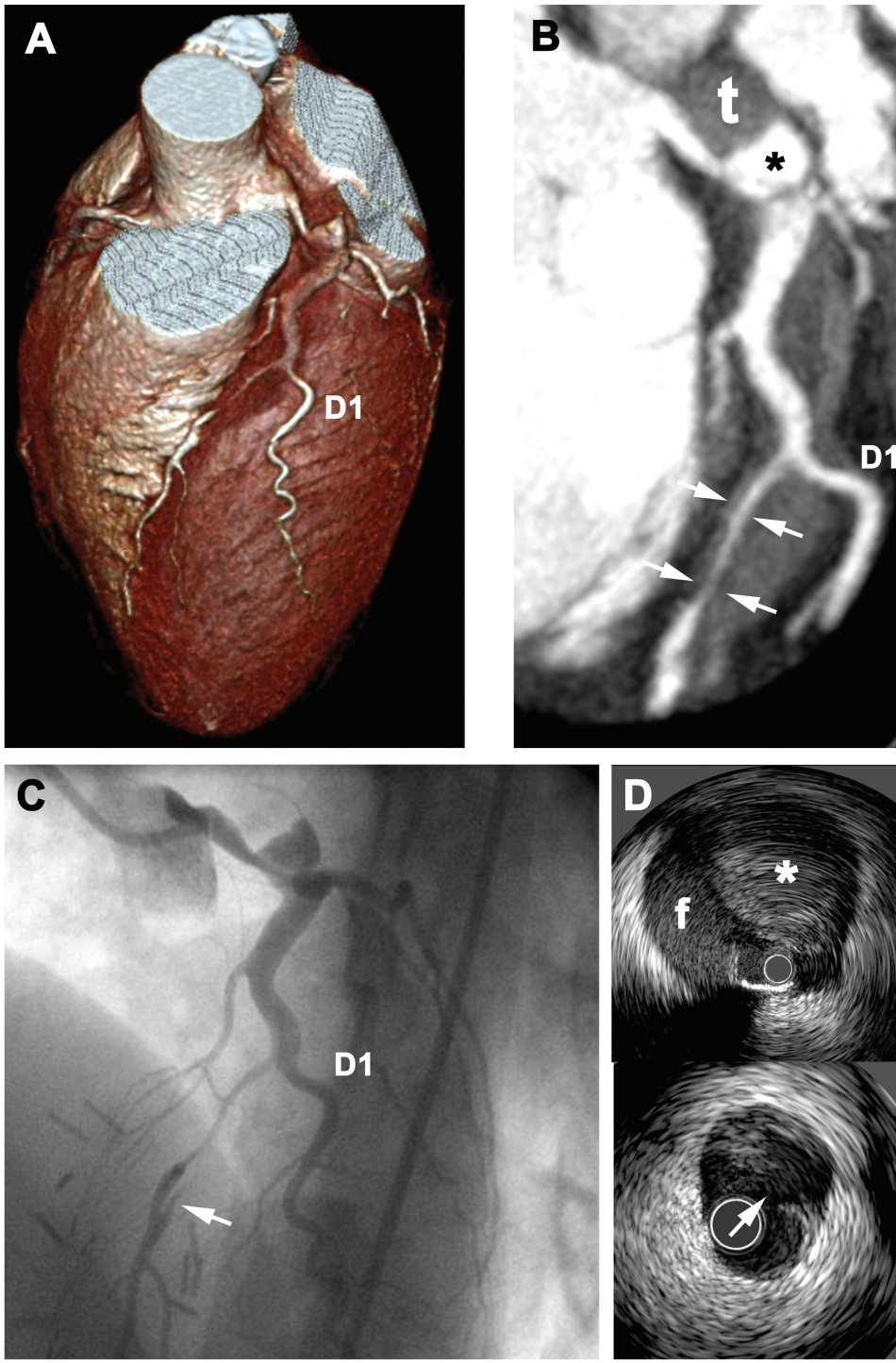

Interlude 2, page 152, Figure

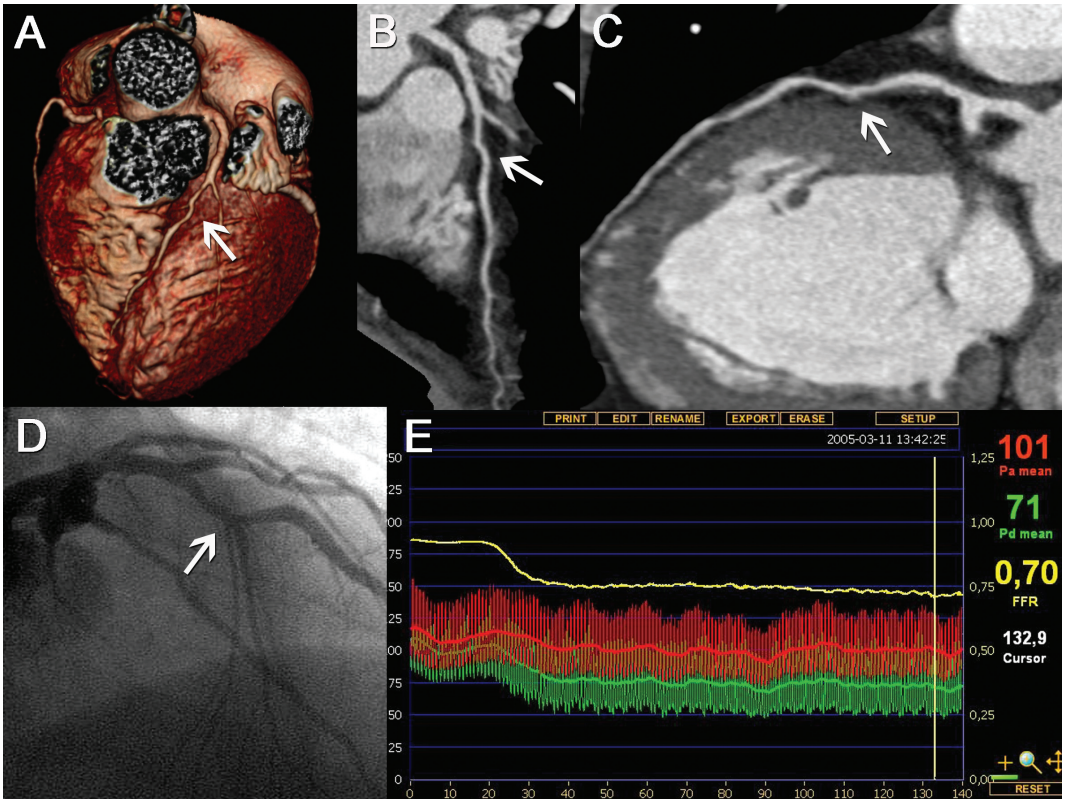

Chapter 11, page 201, Figure 2

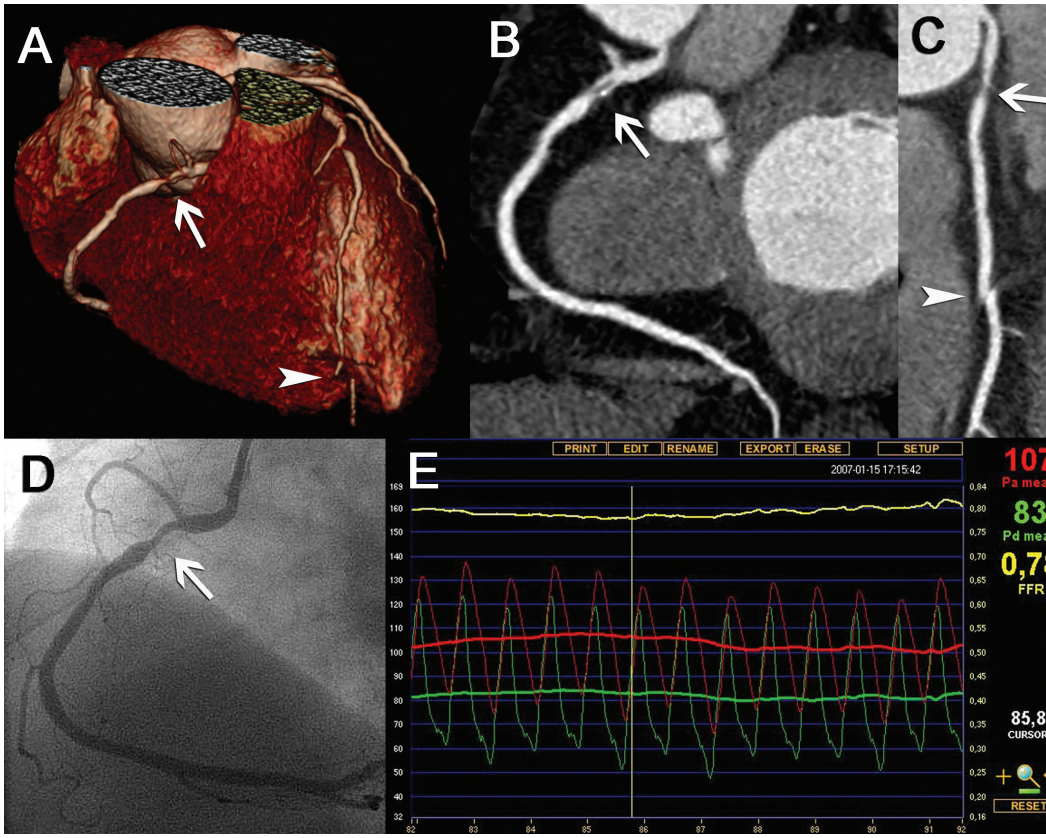

Chapter 11, page 201, Figure 3

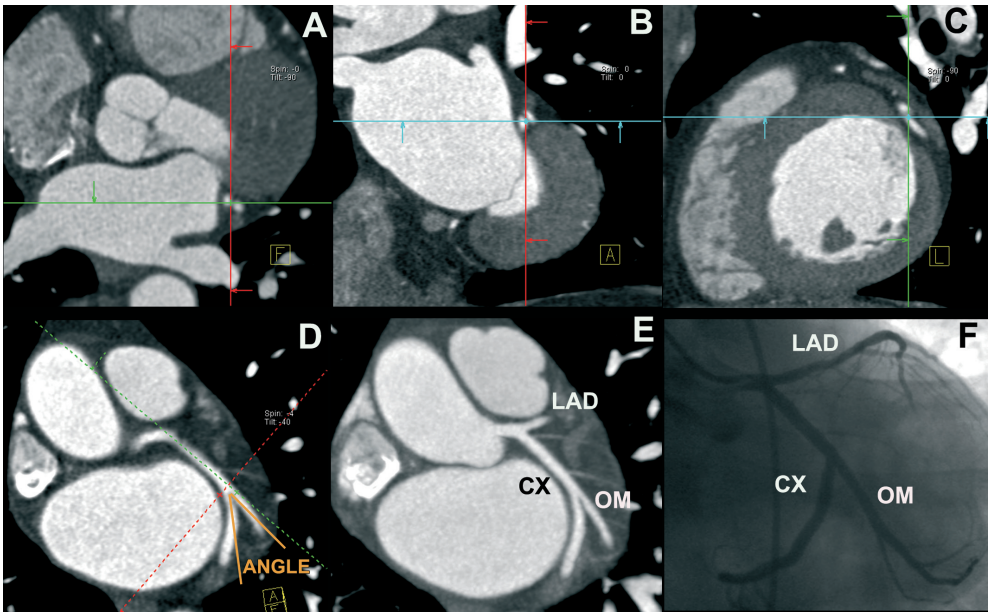

Chapter 12, page 219, Figure 1a

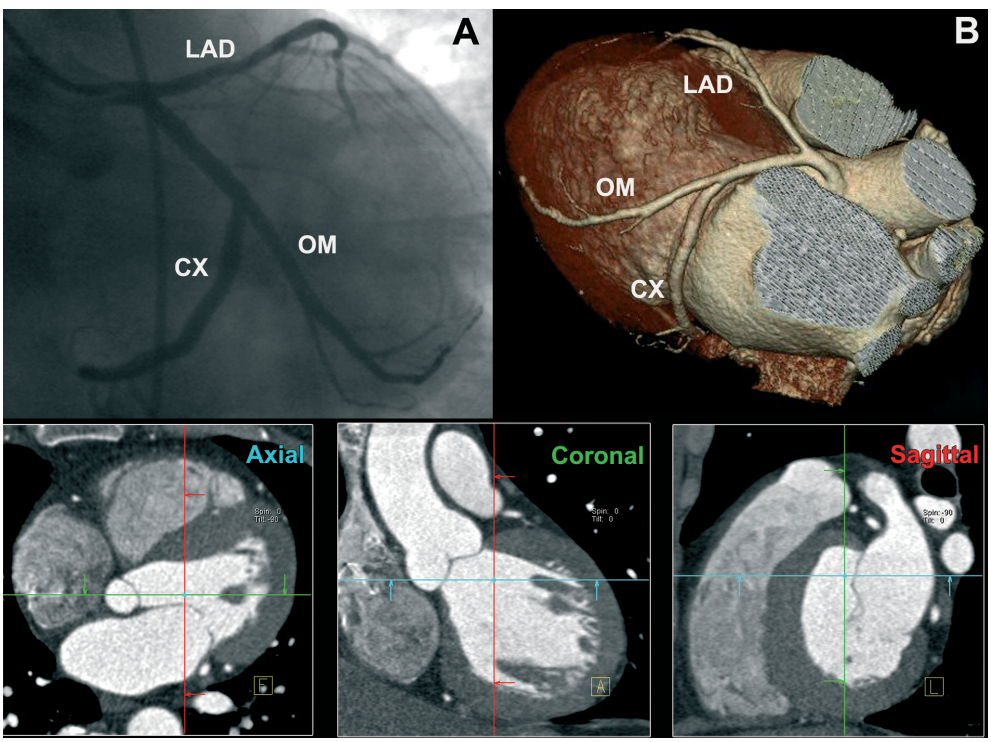

Chapter 12, page 219, Figure 1b

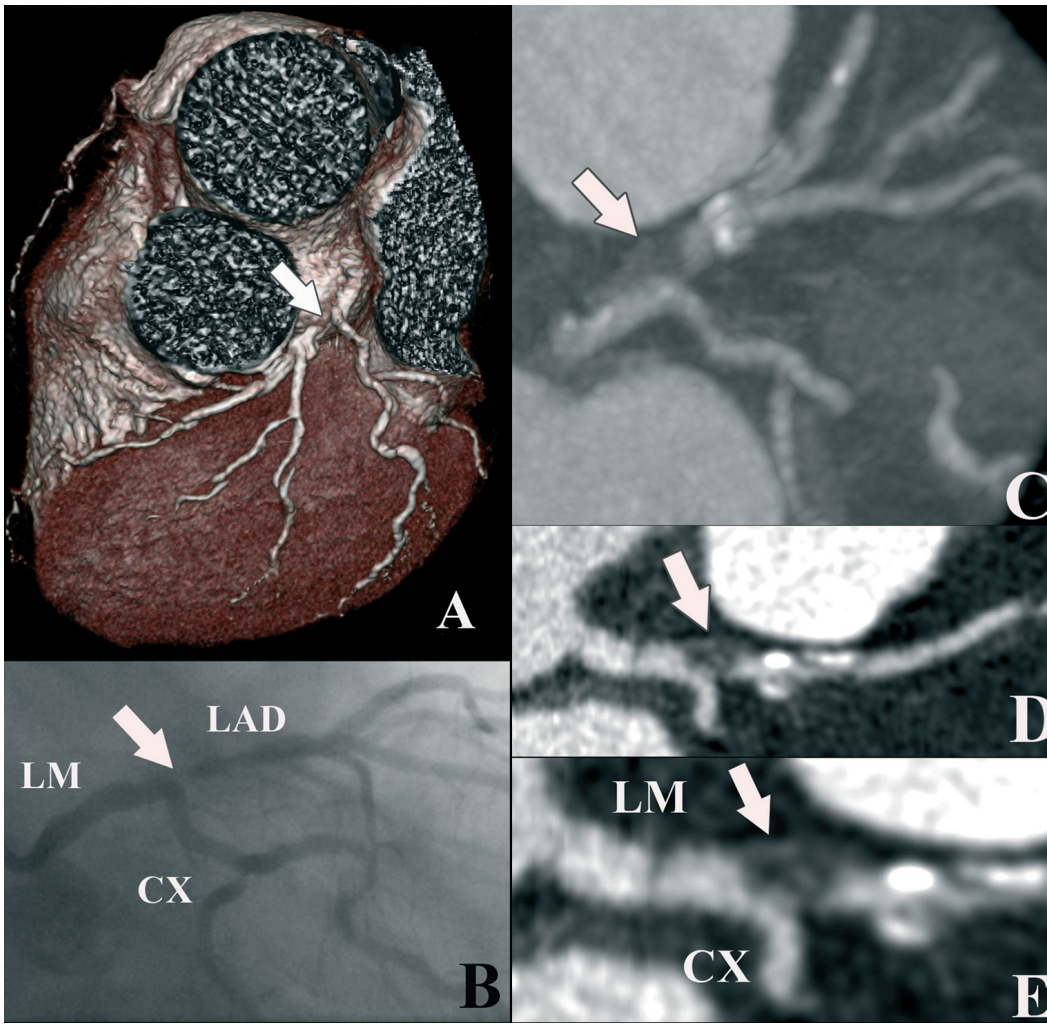

Chapter 12, page 225, Figure 3

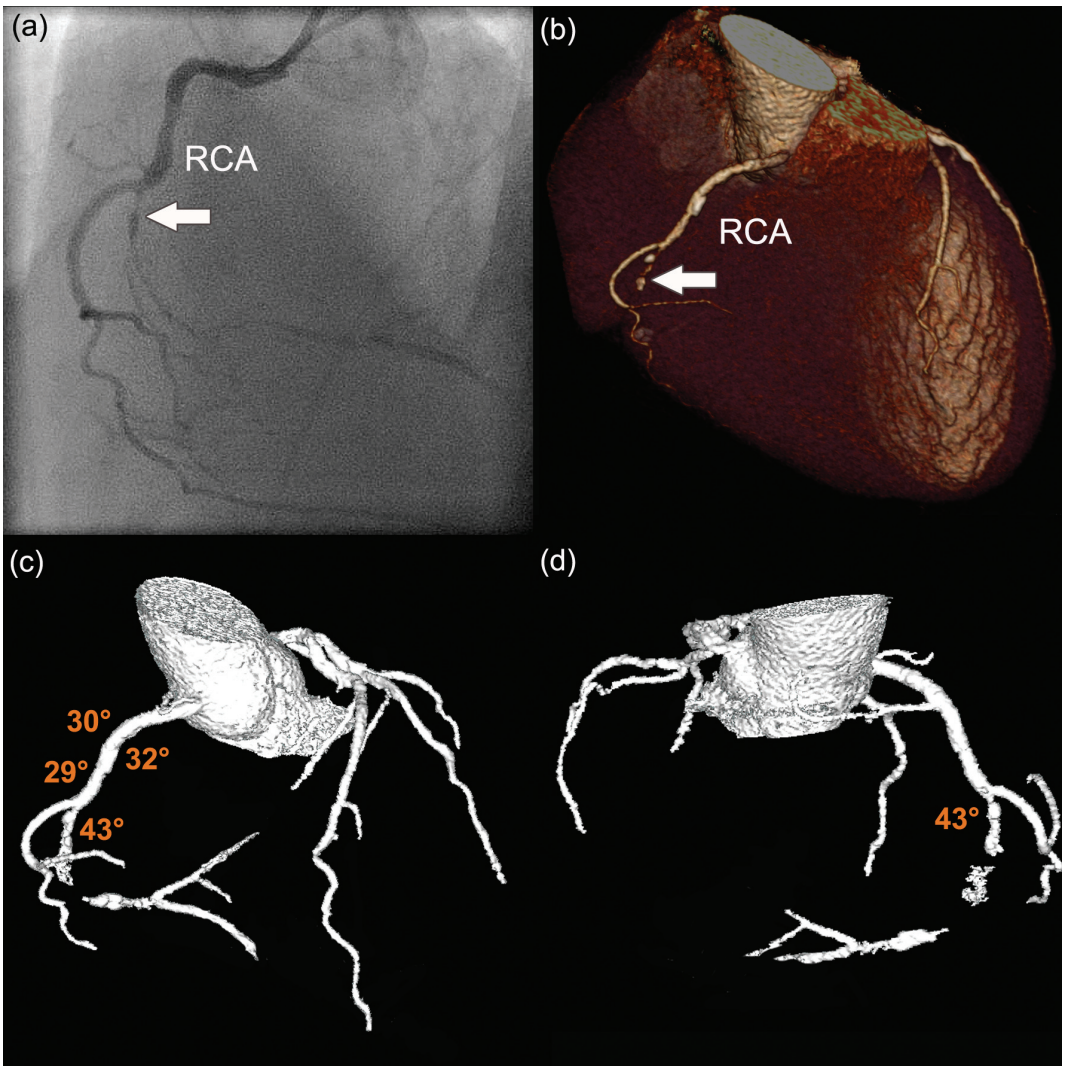

Chapter 13, page 235, Figure 1

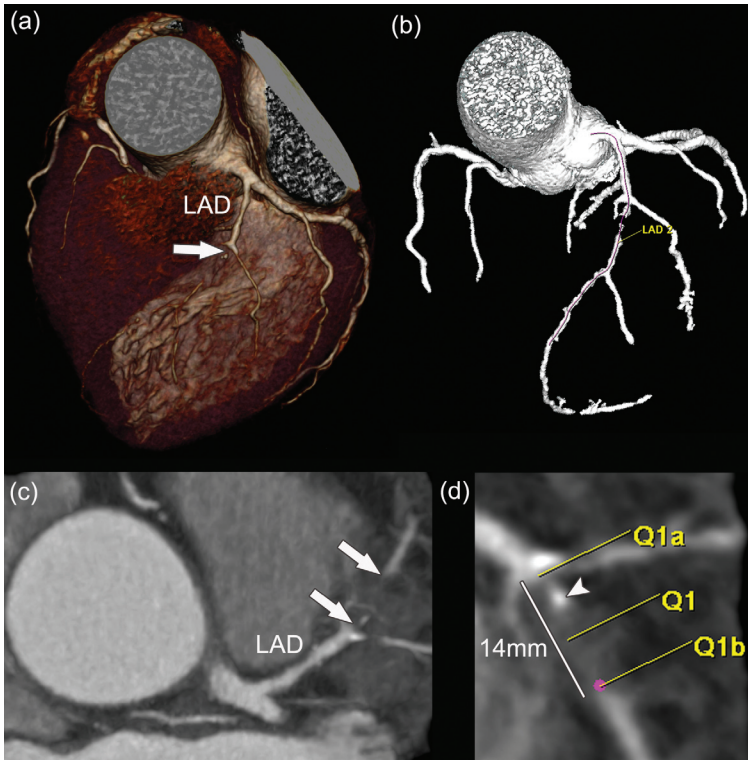

Chapter 13, page 239, Figure 3

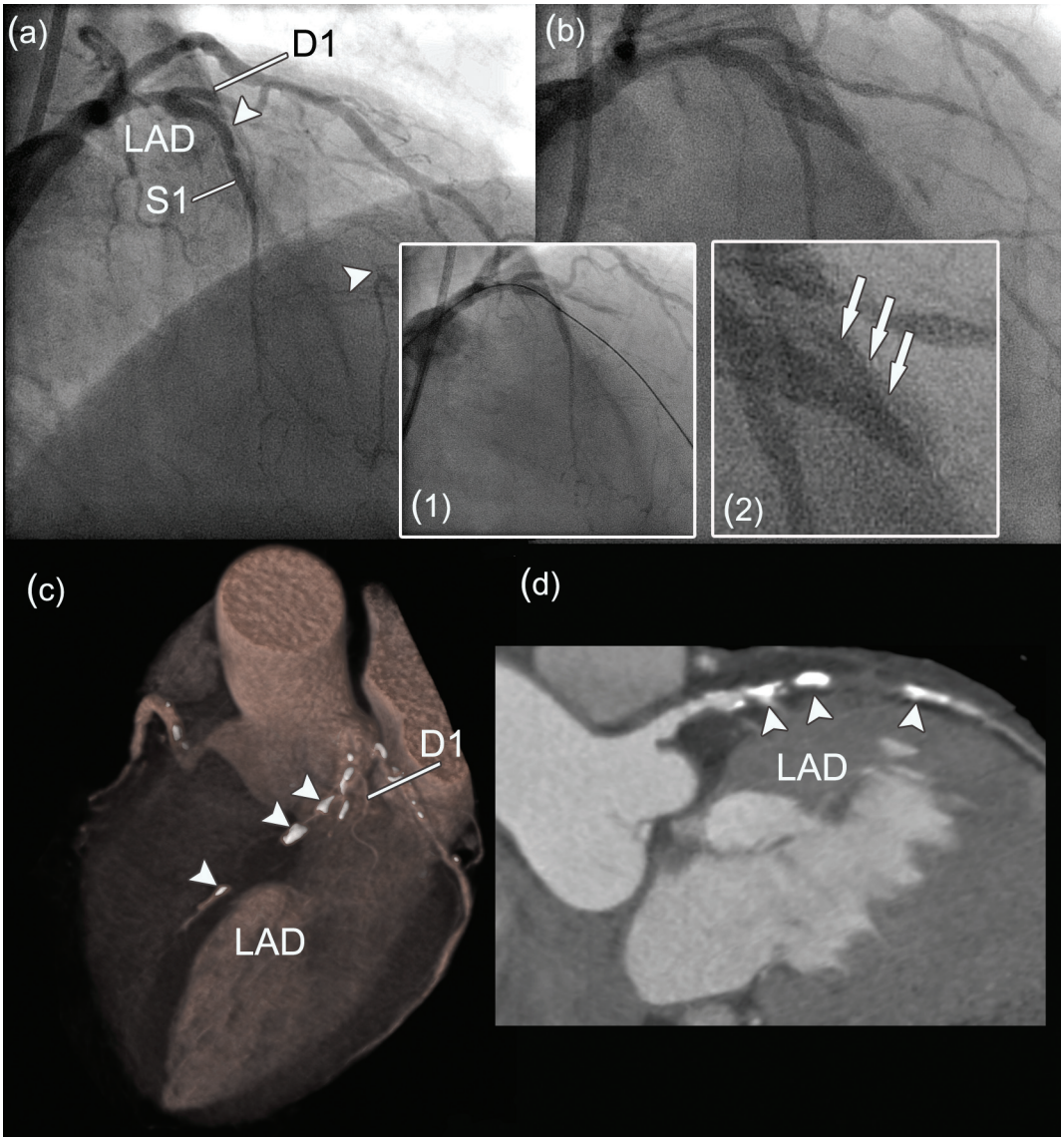

Chapter 13, page 244, Figure 4

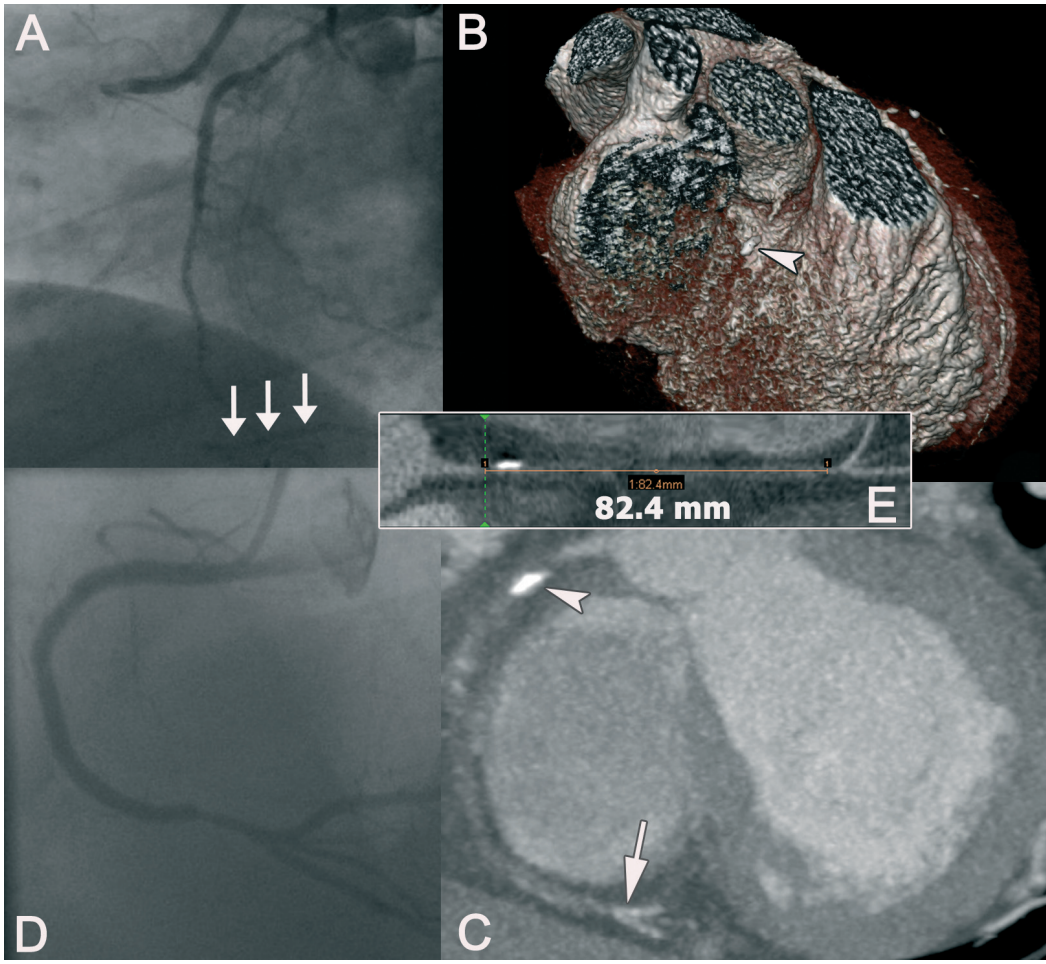

Interlude 4, page 253

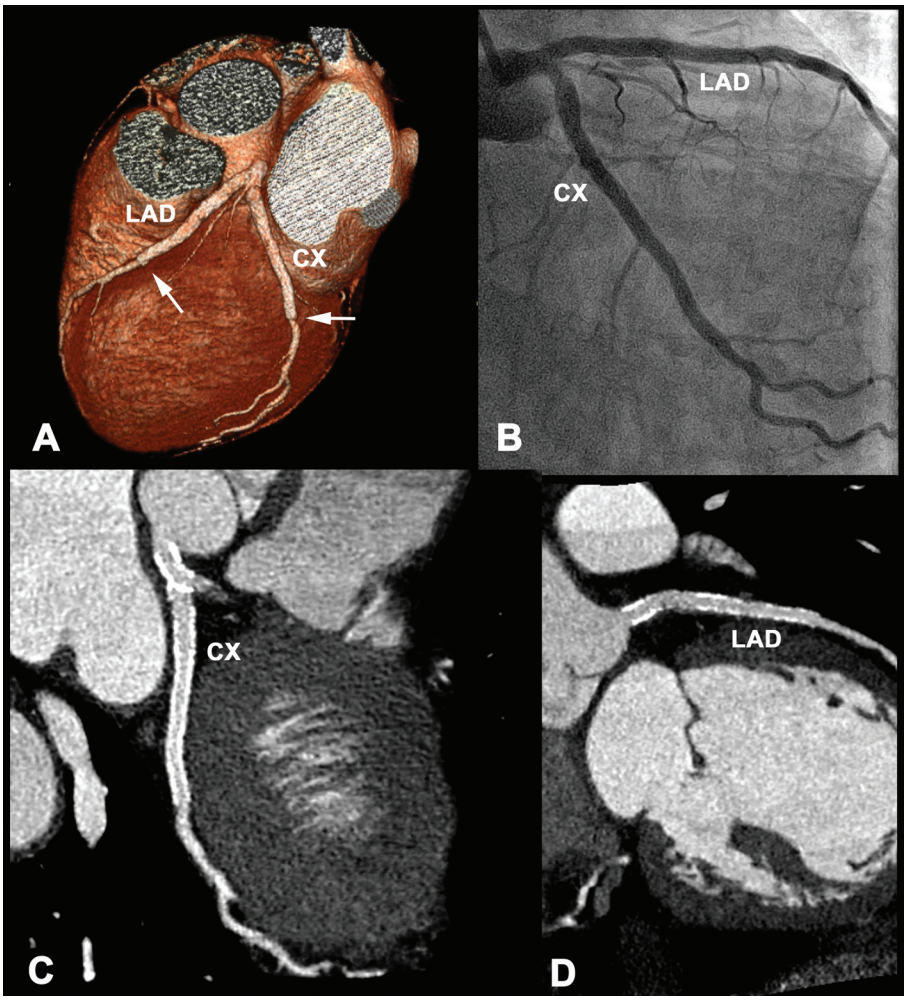

Chapter 16, page 305, Figure 1

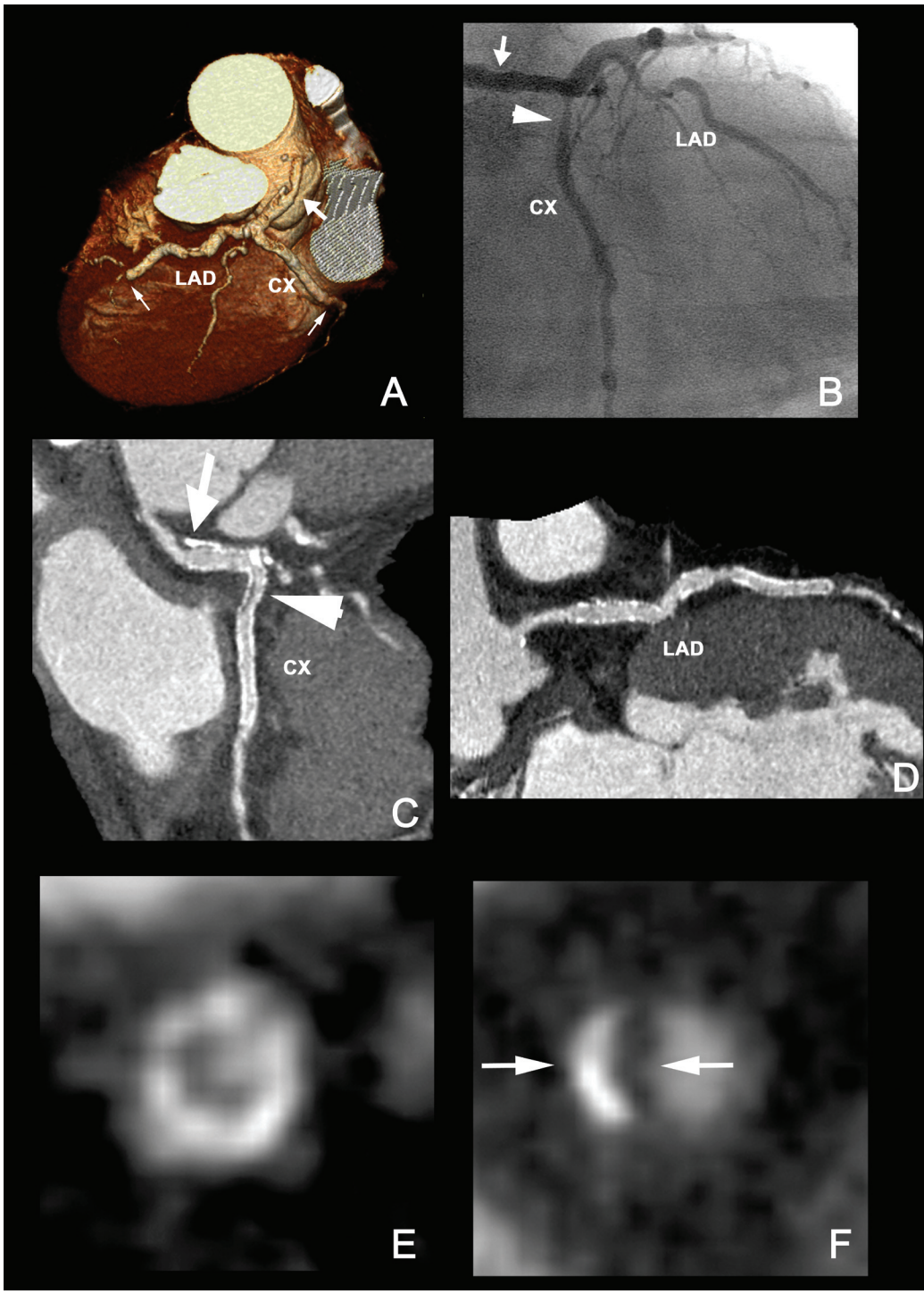

Chapter 16, page 305, Figure 2

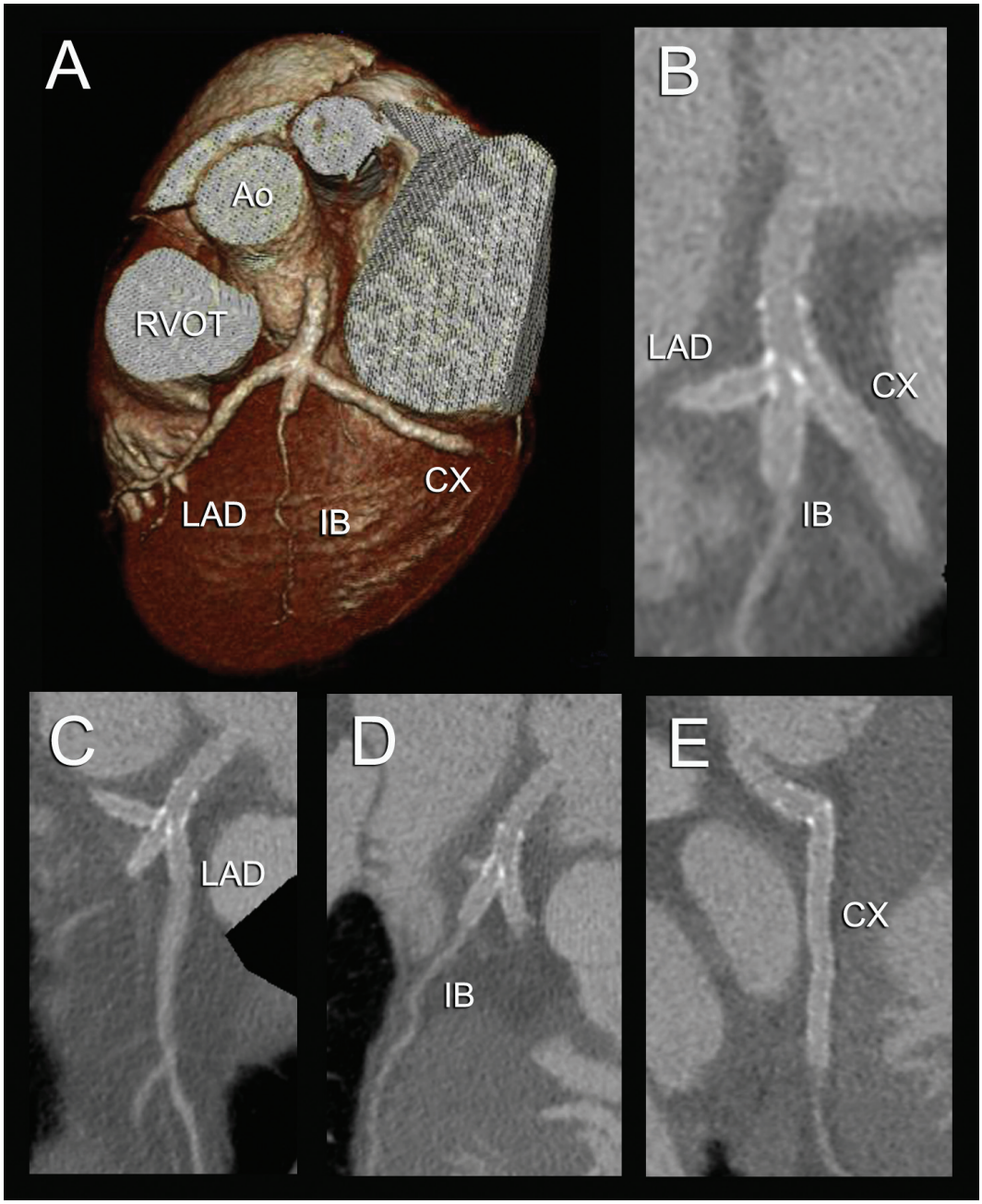

Interlude 5, page 317, Figure 2

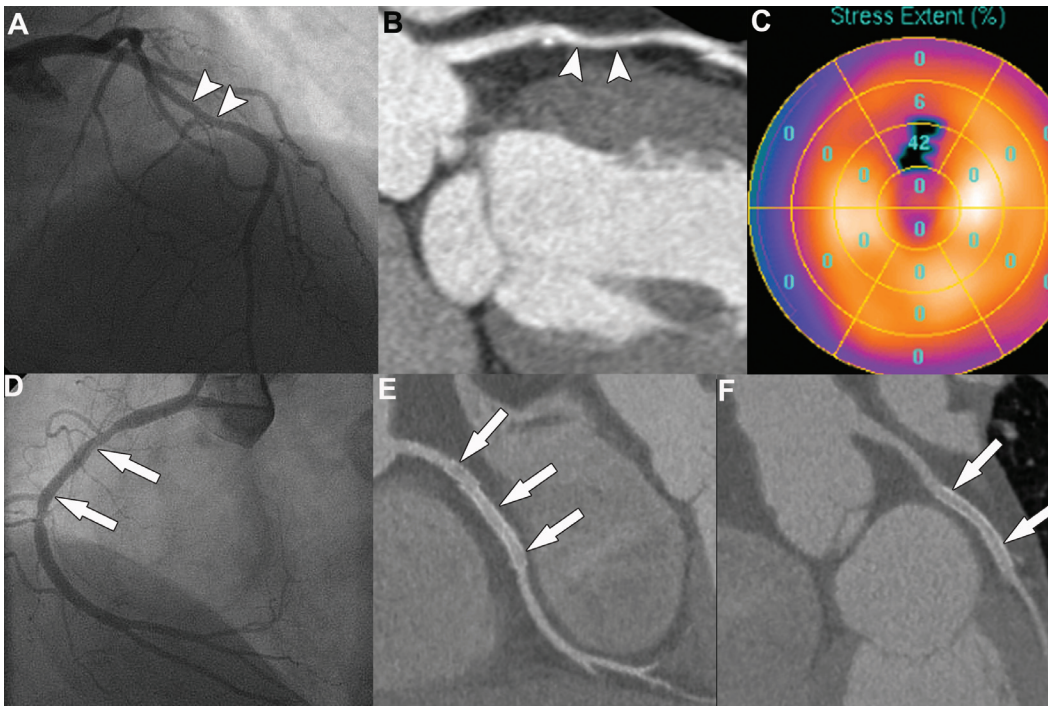

Chapter 18, page 343, Figure 3

Foto achterzijde proefschrift:
bronzen beeld door Frank Stoopman. "Geen hindernis te hoog".
Geschonken door Tine, Alexander en Victor.